

Lancaster
University



Sustainable Reductive Aminations
Catalysed by Triaryl Borane Frustrated
Lewis Pairs

By

Noah Wright

A dissertation submitted to Lancaster University

for the degree of Doctor of Philosophy

School of Chemistry

June 2024

Declaration

I hereby declare that this thesis represents my own work which has been done after registration for the degree of Doctor of Philosophy at Lancaster University and has not been submitted in support of an application for another degree at this or any other university. It is the result of my own work and includes nothing that is the outcome of work done in collaboration except where specifically indicated. Many of the ideas in this thesis resulted from discussion with my supervisor Dr Julien Doulcet.

Noah Wright MSc

Lancaster University, UK

Abstract

Over the past 18 years, frustrated Lewis pairs (FLPs) have advanced significantly from concept to catalysis, however their broad use, for example in reductive aminations has been hampered by their moisture sensitivity and the lack of efficiency for asymmetric catalysis. The work described in this thesis aimed to expand the scope of FLP catalysed reductive amination reactions using moisture tolerant boranes. For this, two axes of focus were chosen: 1) application of FLP-borane catalysed reductive amination to novel substrates, which offer the opportunity for asymmetric reactions; 2) development of continuous flow conditions suitable for reductive amination reactions using hydrogen (this aim was further encouraged by the collaboration with Autichem Ltd. who produces flow reactors).

The initial part of this project, described in chapter two, focused on the synthesis of three known moisture tolerant FLP-boranes. The three boranes were obtained in multigram quantities following adaptation of literature procedures. The moisture tolerant boranes synthesised were used to catalyse reductive aminations (and imine reductions) using silanes and hydrogen in batch (chapter three) and using hydrogen in continuous flow (chapter four). Focusing on novel reductive aminations to produce 2-substituted pyrrolidines. Chapter four focused on the development of a proof-of-concept reductive amination system in continuous flow using hydrogen, and despite issues with metal contamination of the flow equipment used, the work performed confirmed that FLP-boranes do catalyse imine reduction in flow. To the best of our knowledge this is the first example of such a reaction performed in flow using hydrogen.

Finally, chapter five focused on the synthesis of a novel FLP-borane using an azide-alkyne click route. It was envisaged that upon demonstrating the feasibility of this synthetic route, it could be applied to the synthesis of solid supported boranes. Synthesis of the click-borane proved complex; an impure product, assumed to be the desired borane, was obtained but it could not be further purified and further attempts to synthesise it were unsuccessful. Nonetheless, the catalytic activity of the obtained product was demonstrated, and synthesis of an intermolecular analogue demonstrated that triazoles can be effective Lewis bases for imine reduction using hydrogen.

Acknowledgements

First and foremost, I want to express my deep gratitude to Dr Julien Doulcet, my supervisor, for his guidance and support over the past three and a half years. The last four to five years have been an incredible journey for both of us, and I feel fortunate to have witnessed the beginning of his journey as a lecturer as well as to have benefitted from your pivotal role in my own. I am certain that my experience at Lancaster would have been entirely different without your presence, and for that, I will be forever grateful.

I would also like to thank my former supervisor, Professor Joe Sweeney, for giving me the opportunity to join his research group for my Master's degree many years ago. Being part of the group alongside postdocs and PhDs was a pivotal moment in my research career. Being welcomed as an equal by the group was truly inspirational for me, especially since I felt like a small fish in a very big pond. Dr Susannah Coote, also deserves thanks, whilst the work using her H-cube[®] for flow chemistry was challenging, I would not have had the opportunity to do it without her lending the equipment to me. A huge thank you to both Dr Rachel Platel and Dr Nathan Halcovitch for allowing and training me to use their gloveboxes.

I want to give special thanks to Dr Geoffrey Akien for his continued support with all things NMR related especially all the VT NMR spectroscopic analysis. Without people like Geoff a chemistry department simply cannot run. Likewise, my journey would not have been the same without Dr Anthony Ball, who is a king of the COSHH form and now holds a senior position at Charnwood Discovery, where he rightfully belongs. I also want to acknowledge Pete Wilson, the "Master Yoda" of chemistry, who has been a crucial part of my research journey. I consider myself extremely fortunate to have met and worked alongside someone who had been with Pfizer for as long as I have been alive. Your tips and tricks have been passed on to the future inhabitants of C21, and the spirit of the "cowboy chemist" will continue to inspire me wherever I work in the future.

On that note I want to express my gratitude to my colleagues at C21, both past and present. From festive Christmas meals and summer BBQs to PGR seminars, it's been a great experience. I especially want to thank Matt, Steven, and the triathlon crew - Josh,

Sean, and Adam. You have all made my time here much more enjoyable by offering valuable advice on chemistry, being great training partners, providing companionship at conferences, and entertaining lunchtime discussions.

Josh deserves his own shout out, having been in the PhD trenches with me from day one we will be lifelong friends. We've attended catalysis summer schools, workshops, and practiced numerous presentations together, fine-tuning posters and talks down to the second. In addition to our academic work, we've also gone hiking, golfing (maybe a bit too much at times), and holidaying together. Note to self: camping in Scotland in April is still a great idea even if it's 4 °C and there are 40 mph winds! Maz and I consider you part of our inner circle, and we have no intention of Lett.ing you go.

Importantly I am proud of myself. Throughout my PhD, I've had the opportunity to attend and present at numerous conferences and workshops. One memorable experience was at Sygnature Discovery's medicinal chemistry workshop for exceptional PhD students and postdocs, held at the conference centre in Alderley Park. Four years earlier, during my master's program, I attended my first meeting with my sponsor company, Apex Molecular, also based in Alderley Park. I vividly remember feeling terrified as I delivered my first-ever presentation to Stuart and Gabe from Apex. Fast forward four years, during the Sygnature Discovery workshop, we were split into breakout rooms, and by luck, I found myself in the same meeting room where I had presented my research four years earlier. Standing there, I realised that not only had I become a confident and capable research chemist, but I was also more comfortable and content in myself as an individual. My experiences throughout my PhD have shaped me into who I am today.

Finally, I would like to thank my family (Mum, Mil and Grandma) for putting up with me. There were numerous times during my PhD journey where I felt I might explode, and you were always there for me. I also want to acknowledge my amazing partner, Maz. You have been my rock throughout this experience, and I look forward to the adventures that lie ahead. Thank you for standing by me during the toughest moments and bringing light into my darkest days over the past eight and a half years.

Above all else, this PhD is dedicated to my father (Martin Ian Wright). Whilst you may not be here to see me doff the cap, you are the only reason I ever could.

Table of Contents

Declaration	ii
Abstract	iii
Acknowledgements	iv
I. List of Abbreviations	ix
II. List of Publications	xiii
Chapter One: General Introduction	1
1.1 Background, Context and Aims	1
1.1.1 Funding	1
1.1.2 Hydrogen and Hydrogenations	1
1.1.3 The Importance of Amines and Reductive Aminations	2
1.1.4 Sustainable Catalysis and the Role of FLPs	4
1.1.5 Thesis Aims	6
1.2 Introduction to Frustrated Lewis Pairs	8
1.2.1 Historical Discovery	8
1.2.2 Types of Frustrated Lewis Pairs	10
1.2.3 Activation of Hydrogen	12
1.2.4 Conclusion	18
1.3 Borane-containing Frustrated Lewis Pairs (FLP-boranes) for Hydrogenation Reactions ...	19
1.3.1 Catalyst Design	19
1.3.2 Scope and Limitations of FLP-borane Catalysed Hydrogenations	25
1.3.3 Borane Moisture Sensitivity	34
1.3.4 Asymmetric FLP-borane Reactions	39
1.4 FLP-borane Hydrogenations in Continuous Flow	49
1.4.1 General Introduction to Flow Chemistry	49
1.4.2 Advantages to Hydrogenations in Flow	50
1.4.3 Solid-supported Catalysts in Flow	52
1.4.4 Boranes in Flow Catalysed Reactions	53
1.5 Conclusions	57
Chapter Two: Synthesis of Known Moisture-tolerant Boranes	58
2.1 Introduction	58
2.1.1 Context and Aims	58
2.1.2 Choice of Target Moisture-tolerant Boranes	59
2.1.3 Brief Overview of Triaryl Borane Synthesis	60

2.2 Results and Discussion	62
2.2.1 Synthesis of Known Triaryl Boranes	62
2.3 Outlook and Conclusions	77
Chapter Three: Application of Synthesised Moisture Tolerant Boranes to Batch Reductive Aminations	78
3.1 Introduction and Aims.....	78
3.2 Results and Discussions.....	81
3.2.1 Intermolecular Reductive Aminations Using Silanes.....	81
3.2.2 Intramolecular Reductive Amination: Synthesis of Cyclic Amines	89
3.2.3 Batch Reactions Using Hydrogen	102
3.3 Outlook and Conclusions	110
Chapter Four: Application of Synthesised Moisture-tolerant Boranes to Flow Reductive Aminations	114
4.1 Introduction.....	114
4.1.1 General Introduction Aims of the Chapter.....	114
4.1.2 Aims of the Chapter	116
4.1.2 Important Preface to Chapter Four Results.....	118
4.2 Results and Discussion	119
4.2.1 General Reaction Setup.....	119
4.2.2 Preliminary Results.....	123
4.2.3 Reaction Optimisation with PTFE Filter	128
4.2.4 Optimisation without the PTFE Filter	139
4.2.3 Catalyst Cartridge	147
4.3 GISMO Funding and Autichem Ltd. Collaboration	149
4.4 Outlook and Conclusions	150
Chapter Five: Synthesis of Novel Moisture-tolerant Boranes	151
5.1 Introduction.....	151
5.1.1 General Aims	151
5.1.2 Literature Precedents for the Synthesis of Solid Supported Boranes	151
5.1.3 Our Approach to Solid Supported Triaryl Boranes	156
5.2 Results and Discussion	160
5.2.1 Work Towards the Synthesis of Novel Intramolecular Borane 76	160
5.2.2 Analysis and Characterisation of 76 by Understanding the Intermolecular Analogue 92	176
5.2.3 Preliminary FLP Reactivity of Novel Inter-/Intramolecular Adducts 92 and 94	185
5.5 Outlook and Conclusions	188
Chapter Six: Conclusions	191

Chapter Seven: Experimental Details and Characterising Data.....	194
7.1 General Methods	194
7.2 Experimental Details for Chapter Two	196
7.2.1 Synthetic Route 1: FLP-borane Synthesis by Sequential Grignard Addition to $\text{BF}_3 \cdot \text{OEt}_2$	196
7.2.2 Synthetic Route 2: FLP-borane Synthesis via Potassium Aryltrifluoroborate Salts (ArBF_3K)	197
7.2.3 NMR Spectra	204
7.3 Experimental Details for Chapter Three.....	213
7.3.1 General Procedures.....	213
7.3.2 Synthesis of <i>N</i> -(<i>para</i> -Methoxyphenyl) Pyrrolidinone (103b) ²²⁸	220
7.3.3 Compound Characterisation Data	221
7.4 Experimental Details for Chapter Four.....	240
7.4.1 General Procedures.....	240
7.5 Experimental Details for Chapter Five.....	246
7.5.1 General Procedures.....	246
7.5.2 Preliminary FLP Reactivity of Novel Inter-/Intramolecular FLPs 92 and 94	250
7.5.3 Synthesis of Diazide 100 for Potential Future Asymmetric FLP Borane Scaffold	252
7.5.4 Compound Characterisation Data	253
7.5.5 Intermolecular FLP 92 Characterisation and VT NMR Spectroscopy	274
References.....	282
Appendices.....	298
Appendix A Palladium-catalysed Hydro arylation for the Synthesis of 3-aryl Pyrrolidines... 298	
A.1 Introduction and Previous Work	298
A.2 Results and Discussion	299
A.2.2 Substrate Scope Expansion	299
A.2.3 Application to Drug Compound Synthesis	302
A.3 Outlook and Conclusion.....	303
Appendix B C-C Bond Formation by Dual Pyrrolidine and Nickel Catalysis: Allylation of Ketones by Allylic Alcohols	304

I. List of Abbreviations

°C	degrees Celsius
Ac	acetyl, $-\text{COCH}_3$
AN	acceptor number
API	active pharmaceutical ingredient
atm	atmosphere
BCF	$\text{B}(\text{C}_6\text{F}_5)_3$
BDC	1,4-benzenedicarboxylate
ArBF_3K	potassium aryltrifluoroborate salt
Bn	benzyl
Boc	<i>tert</i> -butyloxycarbonyl
C-C	carbon-carbon
CSTR	continuous stirred-tank reactor
Cu	copper
CuAAC	Cu(I)-catalysed azide-alkyne 1,3-dipolar cycloaddition
DABCO	1,4-diazabicyclo[2.2.2]octane
DCB	dichlorobenzene
DCM	dichloromethane
de	diastereomeric excess
DFT	density functional theory
DME	dimethoxyethane
DMSO	dimethylsulfoxide
DOSY	diffusion ordered spectroscopy

EDG	electron donating group
ee	enantiomeric excess
EPC	electrophilic phosphonium cation
EPR	electron paramagnetic resonance
Eq	equivalent
EtOAc	ethyl acetate
EWG	electron withdrawing group
FDA	U.S. Food and Drug Administration
FG	functional group
FLP	frustrated Lewis pair
FRP	frustrated radical pair
GSK	GlaxoSmithKline
HPLC	high-performance liquid chromatography
hr(s)	hour(s)
HRMS	high-resolution mass spectrometry
HOESY	heteronuclear overhauser effect spectroscopy
HOMO	highest occupied molecular orbital
K_B	binding equilibrium constant
LA	Lewis acid
LB	Lewis base
LP	Lewis pair
LUMO	lowest unoccupied molecular orbital
M	molar

MAO	methylaluminoxane, trimethylaluminum
Me	methyl, CH ₃
MeCN	acetonitrile
MeOH	methanol
Mes	mesityl, C ₆ H ₂ Me ₃
MOF	metal-organic framework
m	meta
MS	molecular sieves
MTBE	methyl <i>tert</i> -butyl ether
NHC	N-heterocyclic carbene
NMR	nuclear magnetic resonance
P	para
PG	protecting group
PMHS	polymethylhydrosiloxane
POC	proof-of-concept
PTA	phosphotungstic acid, H ₃ PW ₁₂ O ₄₀
PTFE	polytetrafluoroethylene
RBF	round-bottom flask
SPOS	solid-phase organic synthesis
TBA	tetrabutylammonium
TBAF	tetrabutylammonium fluoride, <i>n</i> Bu ₄ N ⁺ F ⁻
TBAOH	tetrabutylammonium hydroxide, <i>n</i> Bu ₄ N ⁺ OH ⁻
TBTA	tris(benzyltriazolylmethyl)amine

<i>t</i> Bu	<i>tert</i> -butyl, $-\text{C}(\text{CH}_3)_3$
TES	triethylsilane
THF	tetrahydrofuran
Ti	titanium
TIBAL	triisobutylaluminum
TMs	transition metals
TMS	trimethylsilane
TMSCl	trimethylchlorosilane
TMSOTf	trimethylsilyl trifluoromethanesulfonate, $(\text{CH}_3)_3\text{SiO}_3\text{SCF}_3$
Trip	2,4,6-triisopropylphenyl, $\text{C}_6\text{H}_2\text{-}2,4,6\text{-}i\text{Pr}_3$
VT	variable temperature
X_c	chiral auxiliary
Xyl	xylene, dimethylbenzene (<i>o</i> , <i>m</i> , or <i>p</i>)

II. List of Publications

1. Article in Chemicals Northwest non-peer-reviewed Elements magazine: *FLP catalysis: the smart new approach to hydrogenation?*, Noah Wright, *Elements Autumn*, 2021, 12, (<https://www.cia.org.uk/chemicalsnorthwest/Elements-Magazine/?PageNo=1>) (Chapter One and Chapter Four)
2. C-C Bond Formation by Dual Pyrrolidine and Nickel Catalysis: Allylation of Ketones by Allylic Alcohols, Noah Wright, Bara Townsend, Steven Nicholson, Joshua Robinson, Geoffrey Akien, Anthony K. Ball, Joseph B. Sweeney, Julien Doulcet, *Adv. Synth. Catal.*, **366**, 2024, 3833-3838 (Appendix B)
3. Reductive Heck paper, Josh Robinson, Noah Wright, Joe Sweeney and Julien Doulcet, 2024 [Manuscript submitted for publication] (Appendix A)
4. Main-group Catalysed Intramolecular Reductive Amination of Functionalised Aminoketones for the Synthesis of Cyclic Amines Using Silanes as the Reductant, Noah Wright, Julien Doulcet, 2024 [Manuscript in preparation] (Chapter Three)

Chapter One: General Introduction

1.1 Background, Context and Aims

1.1.1 Funding

My project was funded by the Greater Innovation for Smarter Materials Optimisation (GISMO)¹ project, which was itself a body under the Lancaster University Materials Science Institute, funded by the European Region Development Fund (ERDF). GISMO's purpose was to provide access to university researchers for small or medium-sized enterprises (SMEs) in the Cheshire and Warrington area. The GISMO project focused on three themes (chemicals and hydrogen, surfaces and coatings, and additive manufacturing) and was supported by three research associates as well as several PhD students (including my project which was part of the chemicals and hydrogen theme).

1.1.2 Hydrogen and Hydrogenations

The hydrogenation of unsaturated organic substrates is ubiquitous in chemical industrial processes including materials science, polymers, pharmaceuticals, agrochemicals, and foodstuffs.² It is reported that hydrogenation accounts for 10 – 15% of reactions in the chemical industry, with half of all of the hydrogen produced being used in the Haber-Bosh process to make ammonia for fertilisers (Figure 1. **A**). The hydrogenation transformation can be achieved using stoichiometric reductants such as LiAlH_4 or NaBH_4 , transfer hydrogenation, biocatalysis, organocatalysis and the addition of hydrogen mediated by transition metals.³⁻⁵

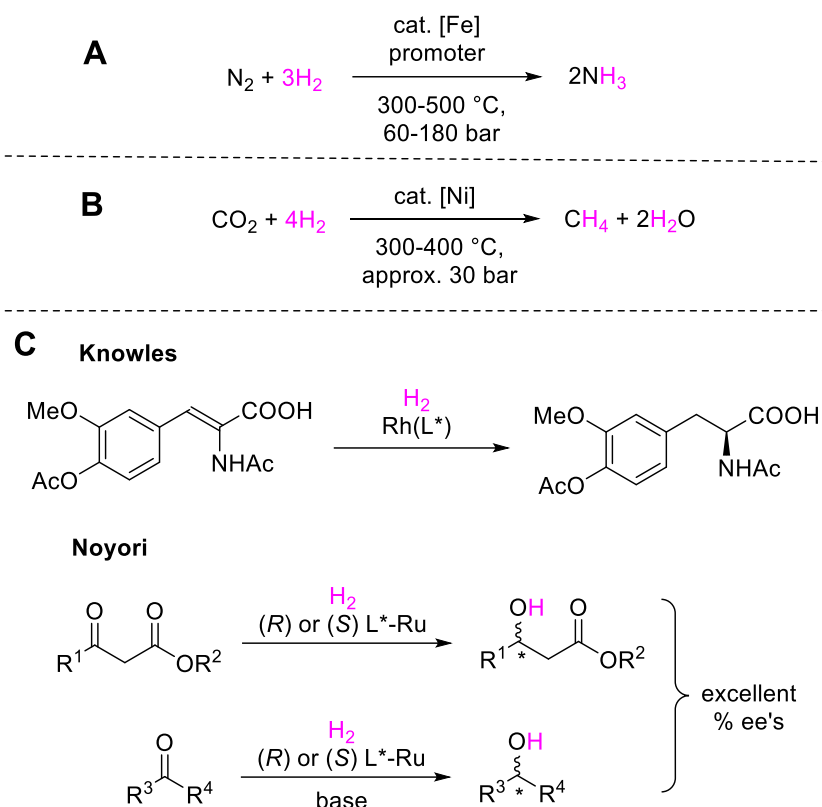


Figure 1. **A.** Haber-Bosch hydrogenation process. **B.** Sabatier seminal Nobel prize-winning hydrogenation. **C.** Knowles and Noyori Nobel prize-winning asymmetric hydrogenation systems.

Following the first catalytic hydrogenation using transition metals (TMs) by Sabatier in 1897 (Figure 1. **B**),⁶ the 20th century saw ground-breaking developments in hydrogenation chemistry. These works include that of Grignard in 1912, the later development of this organometallic chemistry in the 1960s and 70s and Knowles and Noyori Rh- and Ru-based enantioselective hydrogenation catalysts which have both led to Nobel prize awards all using metal-based catalysts (Figure 1. **C**).⁷⁻⁹ Ultimately this meant that chemists turned almost exclusively to metals to activate hydrogen for the past 100 years.¹⁰

1.1.3 The Importance of Amines and Reductive Aminations

Amines represent highly privileged chemicals which are extensively applied in different areas of chemistry.¹¹ Notably, amines and functional groups built from amines are present in the majority of drugs.¹² They are commonly found in many drugs, with approximately 90% of the top 200 selling drugs in 2022 containing amine and/or nitrogen components (Figure 2).¹³ Saturated cyclic amines, especially 5- and 6-membered systems,¹⁴ are also significant structural motifs in pharmaceuticals. Piperidine and

pyrrolidines, in particular, have been the focus of extensive studies in drug discovery.¹⁵ Taylor and co-workers' recent analysis of rings present in clinical trials and drugs found that piperidine and pyrrolidines appeared as the 3rd and 8th most frequently used ring systems within small molecule drugs listed in the FDA orange book before January 2020.¹⁶

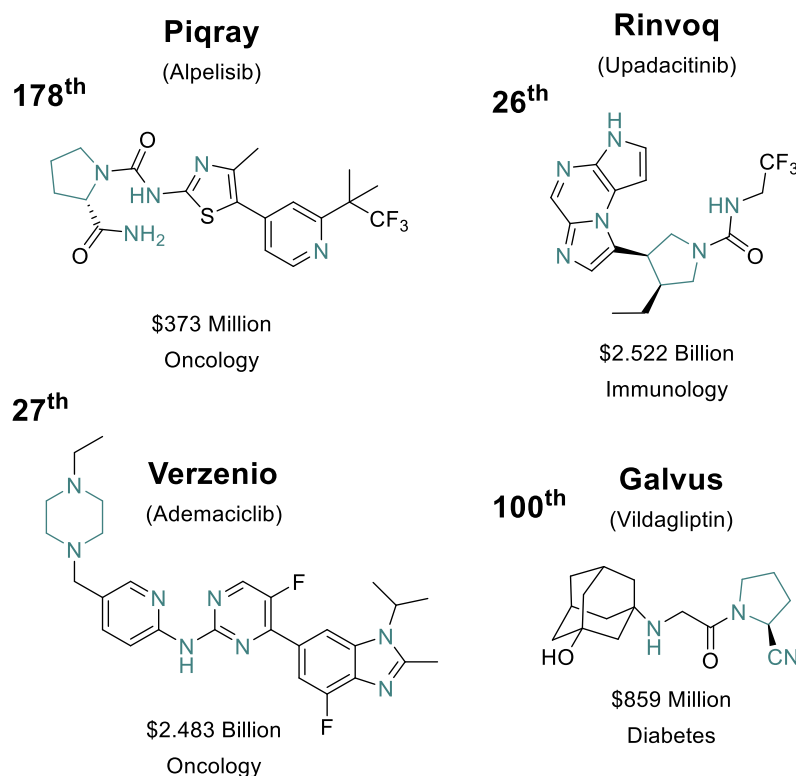
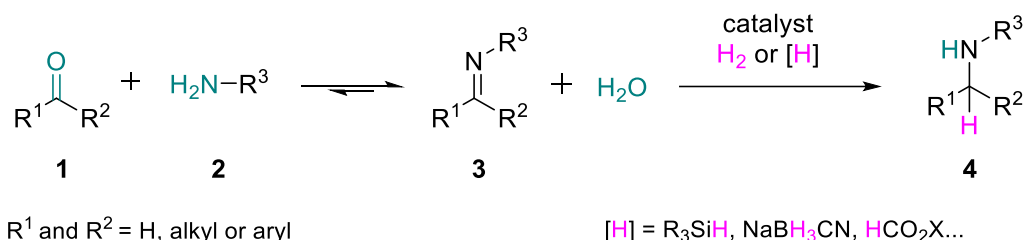


Figure 2. Select examples of drugs containing amine and/or nitrogen components from the top 200 small molecule drugs sold in 2022.¹³

Recently, there has been a push for using cyclic amines in medicinal chemistry to create more saturated and three-dimensional drug-like compounds.^{17,18} Chiral cyclic amines are important as building blocks for auxiliaries and as key structures in biologically active substances. It is suggested that having a higher fraction of sp^3 hybridised centres will lead to more successful drug candidates.¹⁹

Reductive aminations make up a significant portion of C-N bond-forming reactions in the pharmaceutical industry, accounting for about a quarter of them.²⁰ As a result, they are highly valuable tools in the medicinal chemist's toolbox. In the reductive amination process, carbonyl compounds such as ketones and aldehydes react with ammonia or amines using suitable catalysts in the presence of molecular hydrogen or stoichiometric

reducing agents (Scheme 1).^{21,22} These reactions are widely used to prepare primary, secondary, and tertiary amines. Direct asymmetric reductive amination of ketones is one of the most efficient methods for creating chiral amines, increasing the likelihood of successful drug candidates.^{19,23}



Scheme 1. Reductive aminations proceeding via the catalytic reduction of an in situ generated imine to produce valuable amine products.

Reductive aminations require a hydride source such as H₂, silanes, or reducing agents.^{12,24} Hydrogen is preferable because this reagent is abundant, inexpensive, and atom economical.^{25,26} In contrast, stoichiometric reducing agents such as metal borohydrides, formic acid, formates, and silanes generate significant waste products, some of which are hazardous and difficult to handle.¹¹ Therefore, catalytic reductive aminations utilising molecular hydrogen are more appropriate for the sustainable and cost-effective synthesis of amines. Transition metals are traditionally used to catalyse these reductive aminations and asymmetric reductive aminations are often performed using precious metals such as rhodium (Rh), ruthenium (Ru), and iridium (Ir); thus, more sustainable alternatives are required.²³

1.1.4 Sustainable Catalysis and the Role of FLPs

Since the turn of the century, the costs, toxicity, and rarity of precious metals, have led, to the development of new metal-free systems to catalyse hydrogenations.⁹ For example, the emergence of iron- and manganese-based catalysts for hydrogenations exemplifies the evolving field of research to provide inexpensive and sustainable alternatives to precious metals.²⁷

Main-group elements have also proved to be a valid alternative to TMs and provide a greener and more sustainable approach to hydrogenation catalysis. Recently, frustrated Lewis Pairs (FLP) have appeared as suitable catalysts for hydrogenation reactions. Among

the several FLP designs that have been reported in the past two decades, FLP catalytic systems using boranes as the Lewis acids component have been the focus the synthetic FLP community due to their relative ease of synthesis and tunability of Lewis acidity / reactivity.

Despite the rapid developments in FLP boranes in the past 18 years, their broad application to hydrogenation reactions has been hampered by limitations such as moisture sensitivity of the borane catalyst and the lack of efficiency for asymmetric catalysis. There have been multiple attempts to improve moisture tolerance, notably the 'size-exclusion' principle, which we intend to employ and will be discussed in section 1.3.3.3. We do not believe that the current set of boranes, which have been labelled moisture tolerant, have been fully exploited for their full potential as FLP catalysts.

FLP boranes, have also been developed for application as catalysts for reductive aminations.¹² There are many examples of borane-catalysed reductive aminations, with the vast majority using silanes as reductants because they are much more reactive hydride sources which do not require the forcing conditions that would be needed for H₂ splitting.²⁸⁻³³ The development of moisture-tolerant boranes has been crucial in the use of FLPs as catalysts in reductive aminations as the reaction must proceed in the presence of super-stoichiometric amounts of water, which is a by-product of imine formation and therefore cannot be avoided (Scheme 1).²⁸

However, despite these developments, there are some limitations to FLP-borane catalysed reductive aminations. Notably the substrate scope is still limited, with alkyl amines often being sluggish substrates in FLP-borane catalysed reductive amination reactions using hydrogen.³⁴ Also, there are very limited examples of asymmetric reductive aminations,^{35,36} which is reflective of the FLP-field as a whole. Additionally, forcing conditions can often be required, particularly using hydrogen where pressures of up to 80 bar have been used.³⁷ Finally, FLPs have not been employed in continuous flow for hydrogenation purposes including reductive aminations. Given the forcing conditions required, performance of FLP-borane reductive aminations in continuous flow could be extremely valuable to the FLP field.

1.1.5 Thesis Aims

The first aim of this project would be to expand the scope of FLP boranes catalysed reductive amination reactions, with a particular focus on the synthesis of chiral 2-substituted cyclic amines. If progress were sufficient for the efficient synthesis of chiral 2-substituted cyclic amines, attempts at asymmetric reactions using chiral boranes or chiral Lewis bases would be attempted.

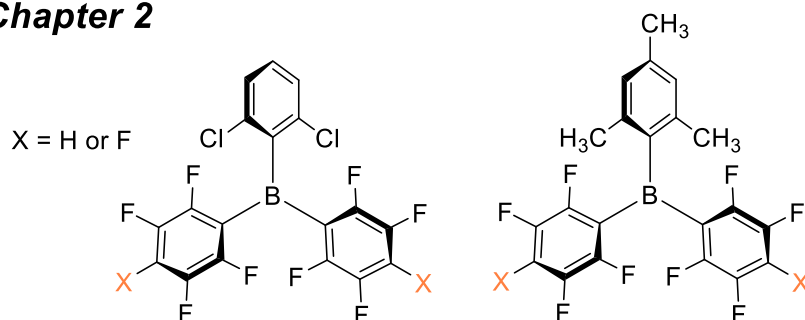
As part of the GISMO funding, a major goal was to collaborate with companies from the Cheshire and Warrington area in order to support their needs with regards to hydrogenation chemistry. The article published in the Chemicals Northwest non-peer-reviewed Elements magazine garnered interest from Autichem Ltd. a flow chemistry company based in Cheshire specialising in the production of custom flow reactors for use in scale-up reactions.³⁸ They were interested in collaborating on our project and have experience working with 'challenging' catalysts in flow.³⁹

Our discussions with Autichem reinforced the potential for both homogenous and heterogeneous FLP catalysis in continuous flow. As a result, the second aim of this thesis would be to investigate FLP-borane catalysed reductive amination reactions in continuous flow using hydrogen.

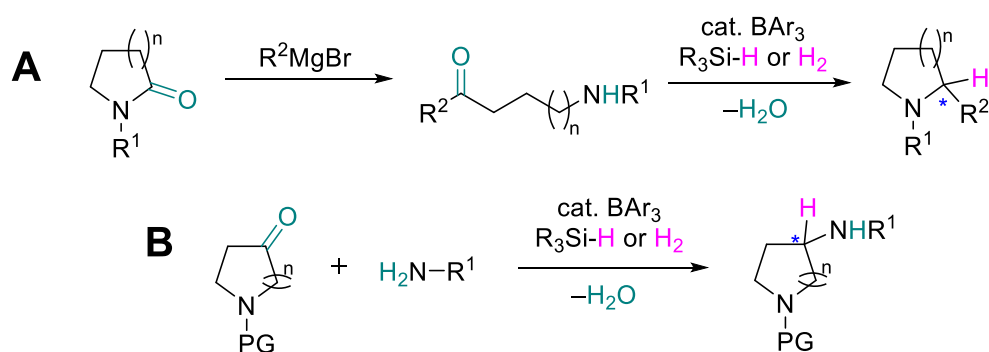
In order to achieve the above aims, the following objectives will be pursued and will constitute chapters 2, 3, 4 and 5 of this thesis (Scheme 2):

- Chapter 2: Synthesis of a range of known moisture-tolerant triaryl boranes.
- Chapter 3: Use the moisture tolerant boranes synthesised to perform reductive amination in batch on novel substrates using silanes and hydrogen (with the ultimate ambition of developing an enantioselective reaction).
- Chapter 4: Use the moisture tolerant boranes synthesised to perform FLP-borane catalysed reductive aminations in continuous flow.
- Chapter 5: Synthesis of novel moisture-tolerant triaryl borane.

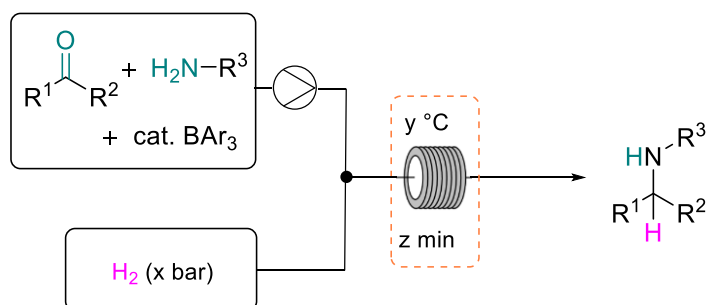
Chapter 2



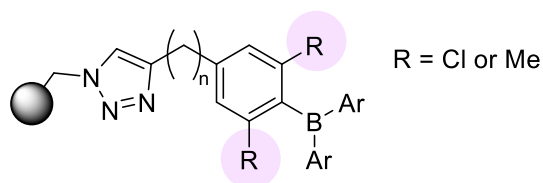
Chapter 3



Chapter 4



Chapter 5



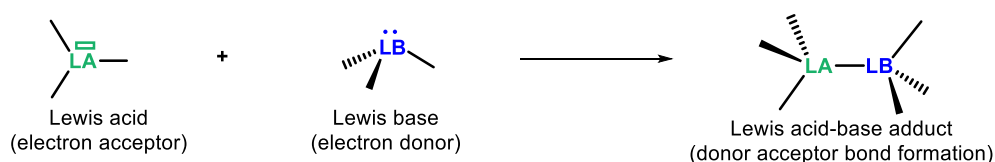
Scheme 2. Objectives to be pursued in: **Chapter 2.** Synthesis of known boranes. **Chapter 3.** Novel reductive aminations performed in batch. **A.** Adaptation of synthetic route to functionalised pyrrolidines via a hypothetical borane-catalysed reductive amination cyclisation.⁴⁰ **B.** Example of cheap and commercially available pyrrolidinones and piperidinones used to access valuable substrates through reductive aminations. **Chapter 4.** Application of FLP-borane catalysed reductive aminations in continuous flow. **Chapter 5.** Novel moisture tolerant FLP borane synthesis.

1.2 Introduction to Frustrated Lewis Pairs

1.2.1 Historical Discovery

Although the concept of sterically encumbered Lewis acid and base pairs had been known since 1942,^{41–43} the major stepping stone in the creation of this field came when Douglas Stephan and co-workers developed a metal-free reversible hydrogen activation system using $(\text{C}_6\text{H}_2\text{Me}_3)_2\text{P}(\text{C}_6\text{F}_4)\text{B}(\text{C}_6\text{F}_4)_2$ **5** (Figure 5).⁴⁴ This sterically encumbered phosphine and borane combination with the inability to quench one another is the reason for naming them ‘frustrated’ Lewis pairs (FLPs).⁴⁴ It was quickly realised that the reactivity could be generalised to other LA/LB combinations (often borane/phosphine) given the steric constraints are sufficient to prevent adduct formation (Figure 3).

Standard Lewis acid/base interactions



Frustrated Lewis pair interactions

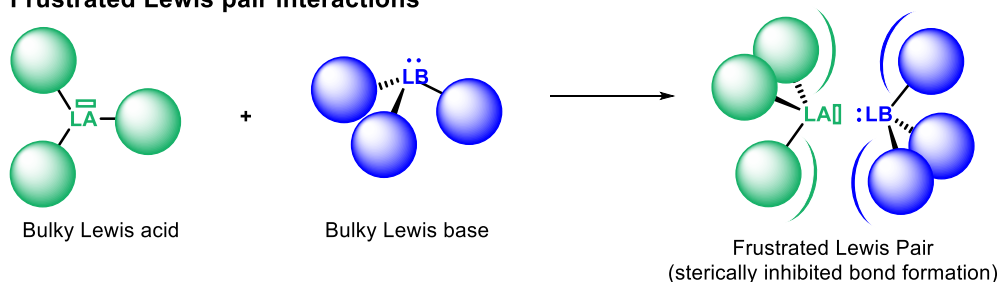


Figure 3. Concept of Frustrated Lewis pairs compared to a classical Lewis adduct.^{9,44}

The catalytic ability of transition metals (TMs) to activate hydrogen is due to their electronic structures, allowing for simultaneous nucleophilic/Lewis base (LB) and electrophilic/Lewis acid (LA) frontier orbitals on the same atom (Figure 4. **A**). Similarly, frustrated Lewis pairs (FLPs) can emulate TM electronic interactions to activate hydrogen (Figure 4. **B**).⁴⁵ In a seminal Science paper, Stephan *et al.* reported the formation of a zwitterionic phosphonium borohydride salt, exemplifying TM-like interaction to cleave H_2 reversibly (Figure 5).⁴⁴

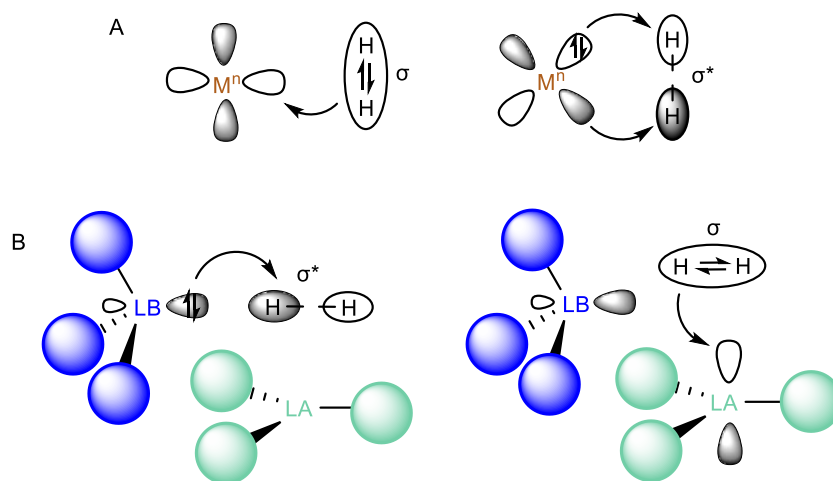


Figure 4. Frontier molecular orbital interactions for hydrogen activation by (A) transition metals and (B) an example of a frustrated Lewis pair.^{9,44}

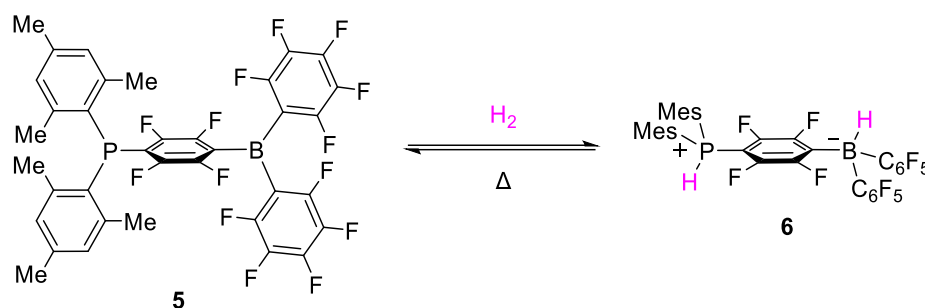
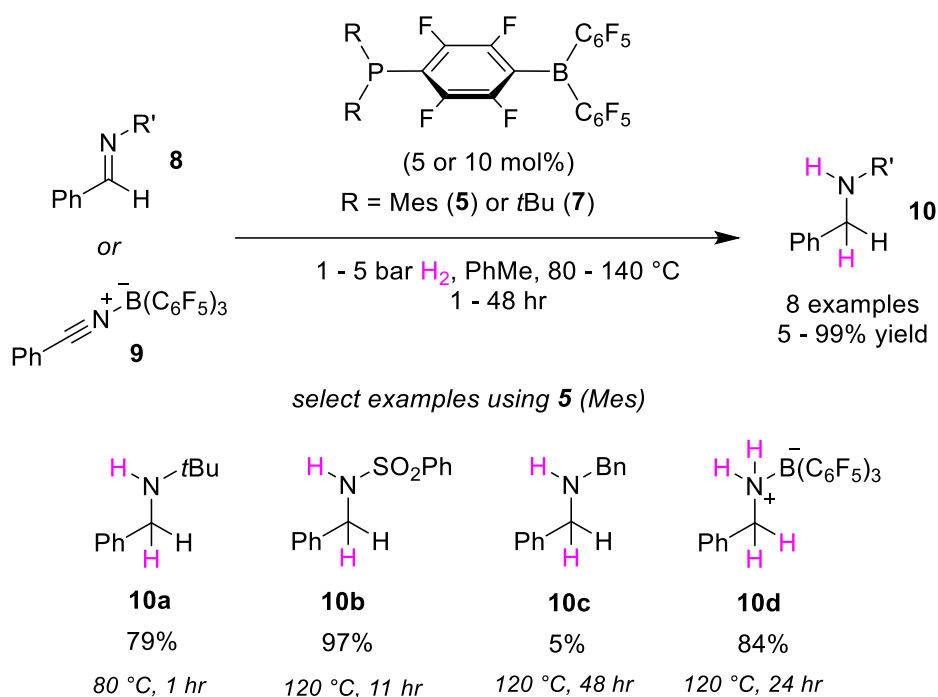


Figure 5. Reversible H_2 activation by a phosphine/borane intramolecular FLP.⁴⁴

Within two years the Stephan group used this system for the first FLP catalysed hydrogenation of imines, nitriles, and aziridines to produce amines in high yields under mild conditions (Scheme 3). They used the phosphonium borates $(R_2PH)(C_6F_4)BH(C_6F_5)_2$ ($R = \text{Mes}$ (**5**) and $t\text{Bu}$ (**7**)) as catalysts, achieving fair to excellent yields (57 – 99%) at elevated temperatures (80 – 140 °C) and low H_2 pressures (1 – 5 bar). They also found that less sterically demanding imines and nitriles are not effectively reduced, but by using a more active catalyst they were able to reduce nitriles to the corresponding primary amine-borane adduct.

The relative rates of imine reduction led Stephan and co-workers to better understand the mechanism for the catalytic reduction. They found that sterically hindered and electron-rich imines were reduced quickly, while sterically hindered, electron-poor imines took longer. Stephan claimed that imine reduction first undergoes proton transfer from the phosphine to the nitrogen, rather than borohydride attack. While imines and

nitriles were efficiently reduced catalytically, aldehydes only reacted stoichiometrically due to their lower basicity compared to nitrogen.^{44,46–48}



Scheme 3. The first reported FLP-catalysed hydrogenation of imines was also applicable to nitriles and aziridines.⁴⁶

1.2.2 Types of Frustrated Lewis Pairs

1.2.2.1 Classification of FLPs

Many LA/LB combinations have been employed in their role as FLP catalysts and can be categorised in a variety of ways (Figure 6). Primarily, LA/LB combinations can be inter- or intramolecular. The latter of which have the LA and LB covalently connected and are therefore, both part of one single molecule, and would be expected to react at a faster rate due to the reduced entropic penalty that has to be overcome to form the active catalytic intermediate.

It should be noted that the activity of intramolecular FLP catalysts suffer from being extremely sensitive to the nature of the linker used to connect LA to the LB. For example, Erker *et al.* observed that polymethylene-linked FLP catalysts $\text{Mes}_2\text{B}(\text{CH}_2)_n\text{P}(\text{C}_6\text{F}_5)_2$ were active when $n = 2$ and 4 but unreactive towards H_2 when $n = 3$.⁴⁹ Similar observations have been made for other intramolecular systems.⁵⁰

On the other hand, intermolecular FLPs are composed of two distinct components, a LA and a LB that, as discussed in the previous section, must be held together in an 'encounter complex' before H₂ activation can occur. Intermolecular FLPs can themselves be split again in two categories depending on whether they are sterically or thermally frustrated (Figure 6). Sterically frustrated FLPs, like the prototypical systems such as the *t*Bu₃P/B(C₆F₅)₃ (BCF) pair, cannot interact due to the steric bulkiness around both components. Conversely, both the 2,6-lutidine/BCF and 1,4-dioxane/BCF are examples of thermally frustrated FLPs. Thermally frustrated FLPs form a strong adduct at room temperature but dissociate when heated allowing them to activate H₂. The final type is 'LA-only' systems, which require the substrate to be sufficiently basic so that it can act as an auxiliary LB. Imine hydrogenation can often be categorised as 'LA-only' systems.^{45,51}

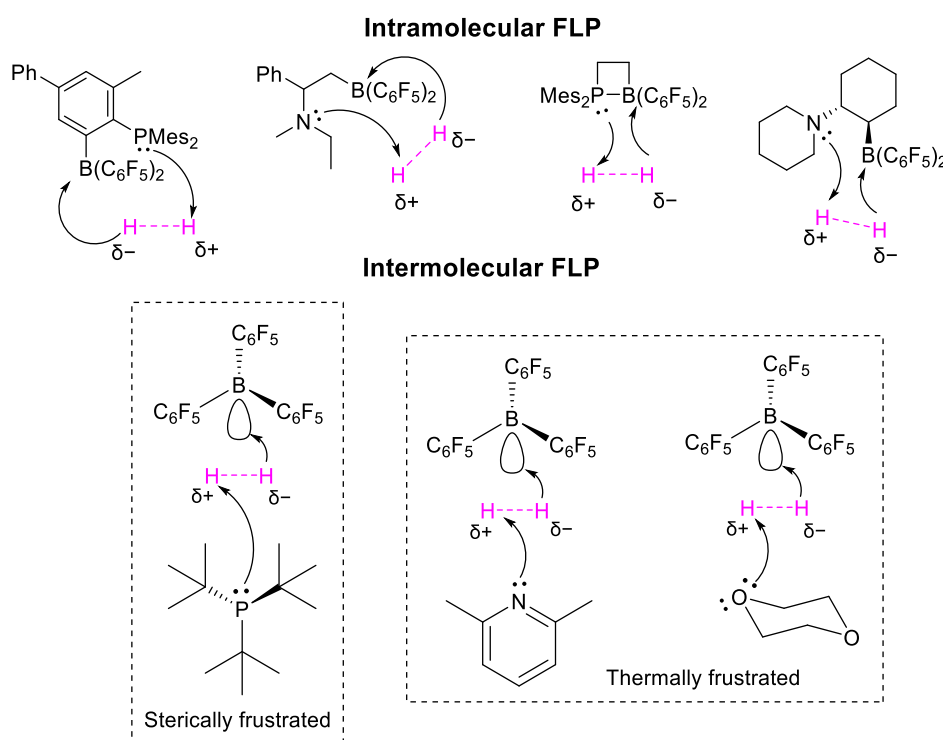


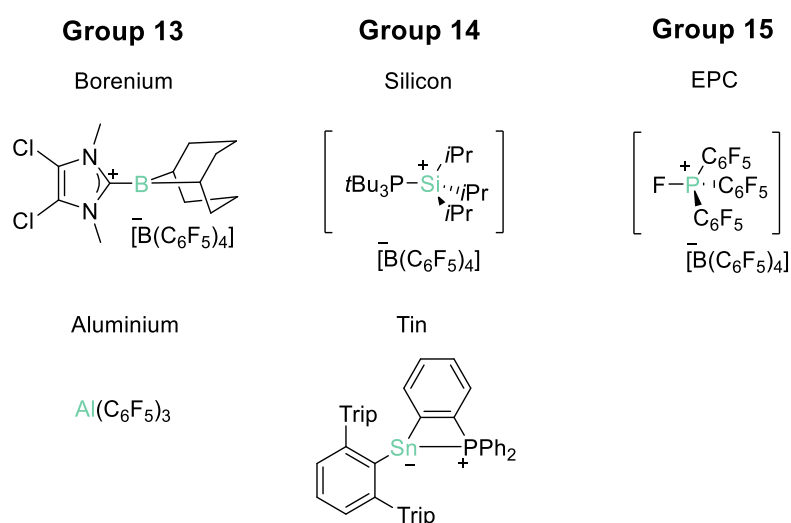
Figure 6. FLP types and how they can activate H₂.⁵²

1.2.2.2 Lewis Acidic and Lewis Basic Components of FLPs

Typical FLP systems usually employ a sterically hindered boranes (LA) and phosphines (LB). There has been limited utilisation of other Lewis acids, with the majority of work

employing perfluorinated electrophilic boranes, particularly using the prototypical borane. However, there have been studies to explore the used of less conventional main-group Lewis acids from group 13, 14, and 15.^{53,54} Such examples include but are not limited to borenium,⁵⁵ aluminium,⁵⁶ silicon,⁵⁷ tin,⁵⁸ and electrophilic phosphonium cation (EPC)⁵⁹ based Lewis acids (Figure 7). On the other hand, numerous Lewis bases have been employed in FLP chemistry, including but not limited to alkyl amines,⁶⁰ *N*-heterocycles,⁶¹ phosphines,⁴⁹ ethers,⁶² carbenes⁶³ and more exotic bases such as silylenes.^{53,64}

Lewis Acids



Lewis Bases

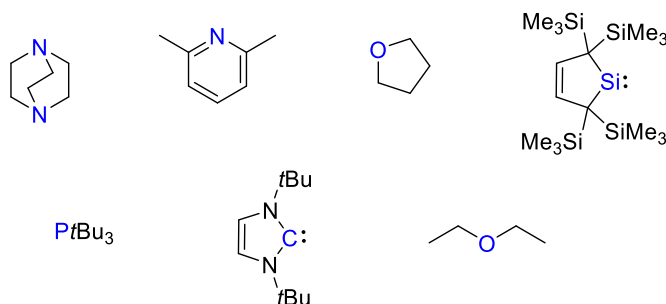


Figure 7. Select examples of alternative Lewis acids and bases employed in FLPs.^{53,64}

1.2.3 Activation of Hydrogen

Since their discovery in 2006, FLPs have played a major role in filling the metal-free catalyst hole.⁴⁴ LA/LB combinations have been employed in their role as FLP catalysts

and can be categorised in a variety of ways; primarily, LA/LB combinations can be inter- or intramolecular (Figure 8). The latter of which has the LA and LB covalently connected and are, therefore, both part of one single molecule whilst the former are two distinct components, LA and LB. Since the initial finding of H₂ activation by FLPs, their electronics have been exploited for the activation of a range of other substrates including CO₂,⁶⁵ N₂O,⁶⁶ SO₂,⁶⁷ R₃SiH,⁶⁸ THF,⁶⁹ alkenes, and alkynes⁷⁰ (Figure 9).⁵³

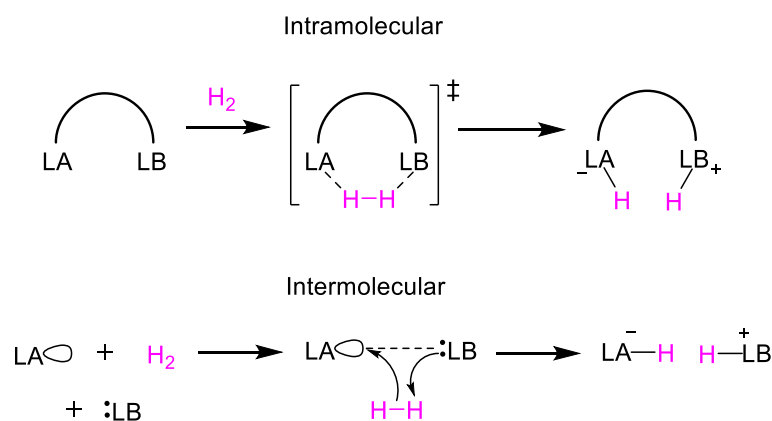


Figure 8. H₂ activation and heterolytic cleavage step-in mechanism by intra- and intermolecular FLPs. The intermolecular following a termolecular reaction step which is kinetically allowed by the formation of an ‘encounter complex’ between the LA/LB before H₂ addition.⁴⁵

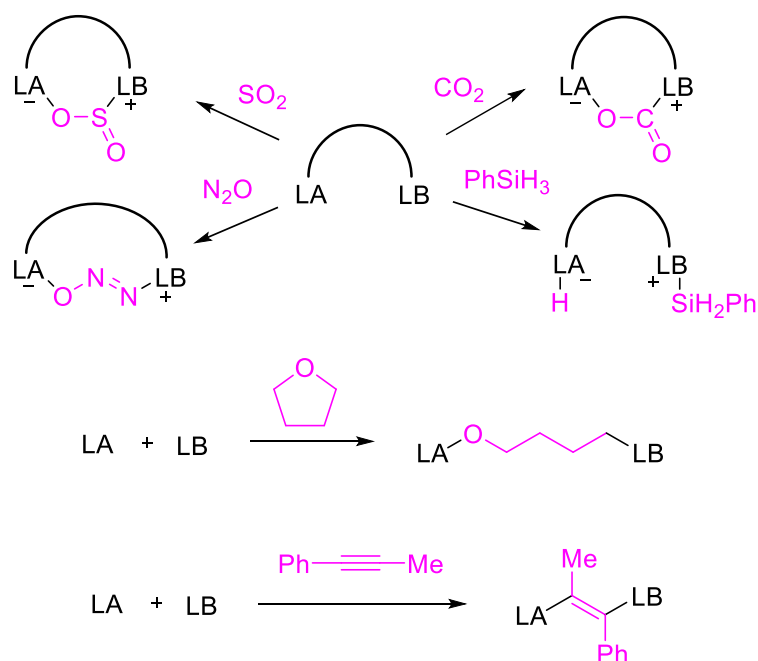
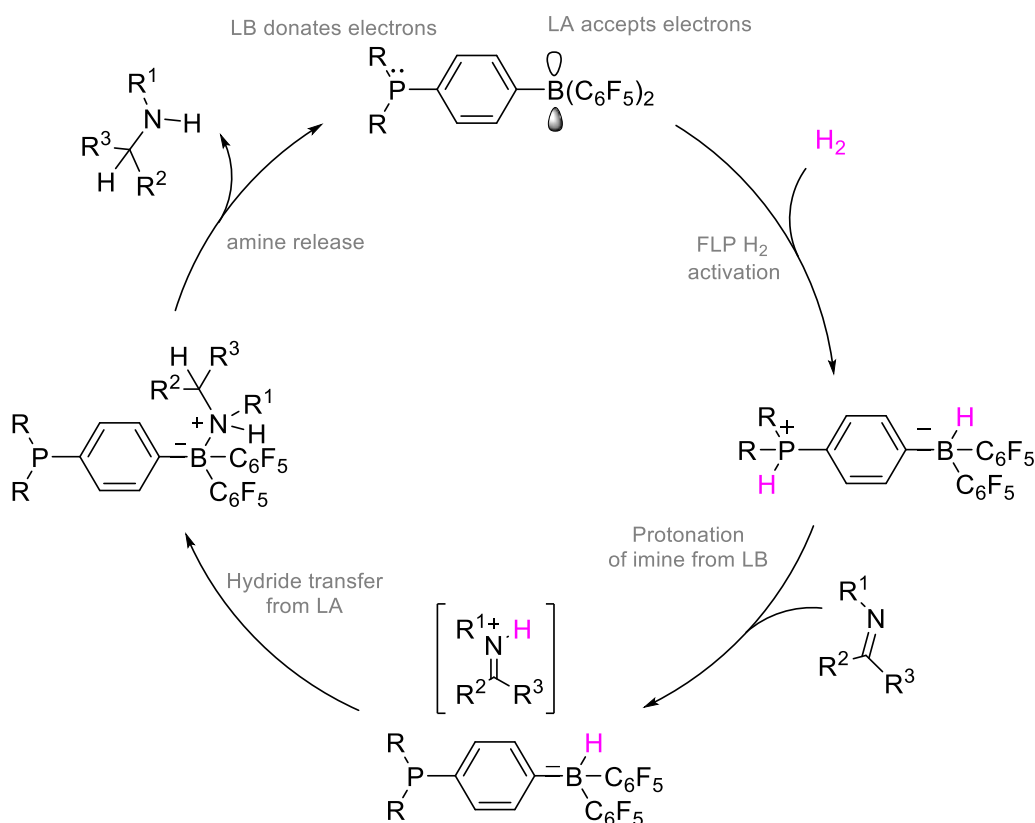


Figure 9. General schematic showing intra- and intermolecular FLP activation of other substrates/ small molecules.^{65–70} (Figure adapted from Scott 2016)⁷¹

The accepted mechanism, proposed by Stephan and co-workers for their intramolecular FLP catalyst system for the hydrogenation of imines (Scheme 4), follows 4 key steps. The first step in the mechanism is H-H bond activation/cleavage by the FLP catalyst. It is believed to occur by the simultaneous interaction with both LA/LB. For intermolecular FLP-catalysed reactions this simultaneous interaction implies an entropically unfavourable intermolecular step (Figure 8). As a result, there must be an interaction between two components prior to interaction with the third to kinetically access the bond cleavage step.⁴⁵ Studies by Soós *et al.* suggest an 'encounter complex' in which the LA/LB in intermolecular FLP catalysts are held together by weak intermolecular interactions, in such a way that they are preorganised for subsequent H₂ activation. This was observed through the intermolecular ¹H/¹⁹F correlations via 2D HOESY NMR (Figure 10).⁷²



Scheme 4. Initially proposed mechanism for imine hydrogenation by an intramolecular FLP.⁴⁶

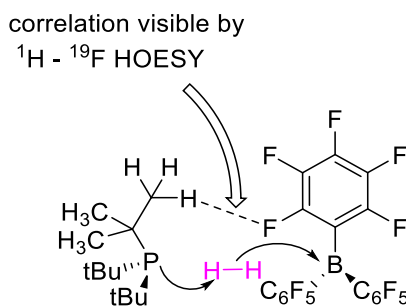
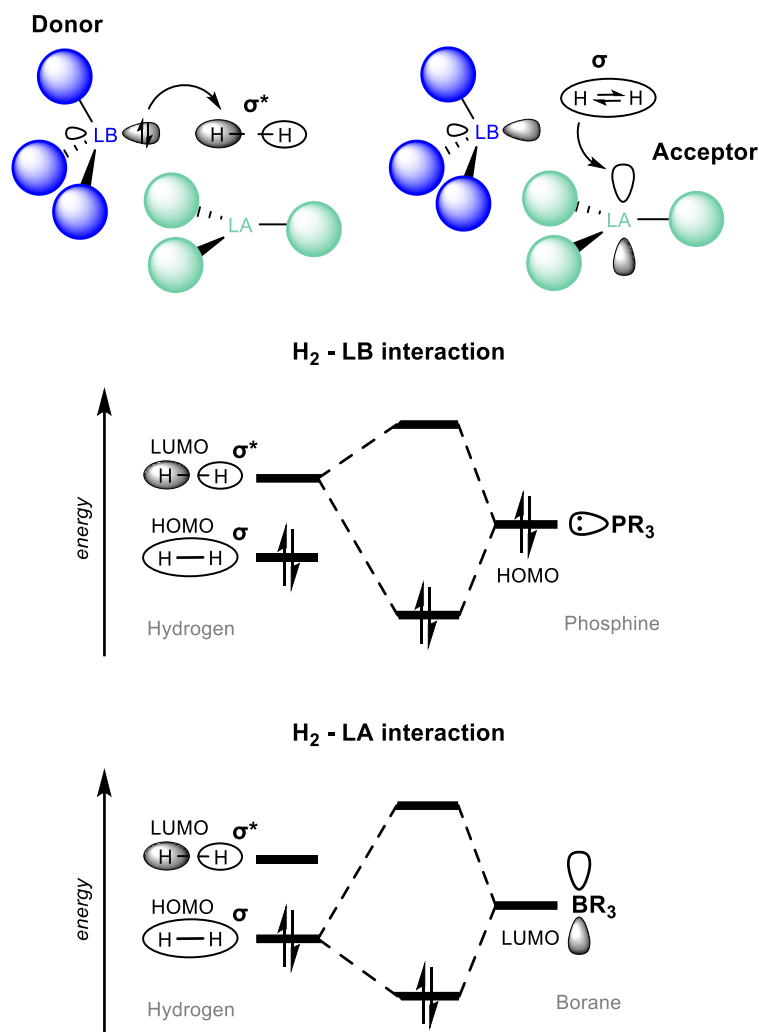


Figure 10. Example of NMR spectroscopic evidence to suggest the formation of an 'encounter complex' between the LA/LB before H_2 addition. Correlation is visible between all fluorine environments but only shown between one for simplicity.^{52,72}

Computational studies have suggested that the encounter complex is responsible for a degree of pre-polarisation in the H_2 molecule before FLP interaction.⁷³ The orbital interactions can be attributed to the concomitant interactions of the donation of electron density from the lone pair on the LB [highest occupied molecular orbital (HOMO)] to the $\sigma(\text{H}_2)^*$ orbital of the H_2 [lowest unoccupied molecular orbital (LUMO)], as well as the decrease of electron density in the $\sigma(\text{H}_2)$ orbital (HOMO) by interaction with the empty orbital on the LA (LUMO) (Scheme 5).^{72,74,75} These interactions lead to the heterolytic splitting of hydrogen whether the FLP was inter- or intramolecular. In some more recent publications, there has been some debate as to whether intermolecular FLPs react in an intra- or intermolecular fashion.⁷⁶ Early computational experiments suggested that the term 'frustration' with regards to the FLPs, should refer to not only steric effects but also an implied strain, which can be utilised for bond activation. The frustration energy of an FLP vs. a classical Lewis pair (LP) lowers the activation barrier to heterolytic H_2 bond cleavage.⁷² It is, however, clear that the activation of H_2 by FLPs is a cooperative process which cannot occur without the availability of relevant empty and filled orbitals which would not be available in the prototypical LB-LA quenched adduct.

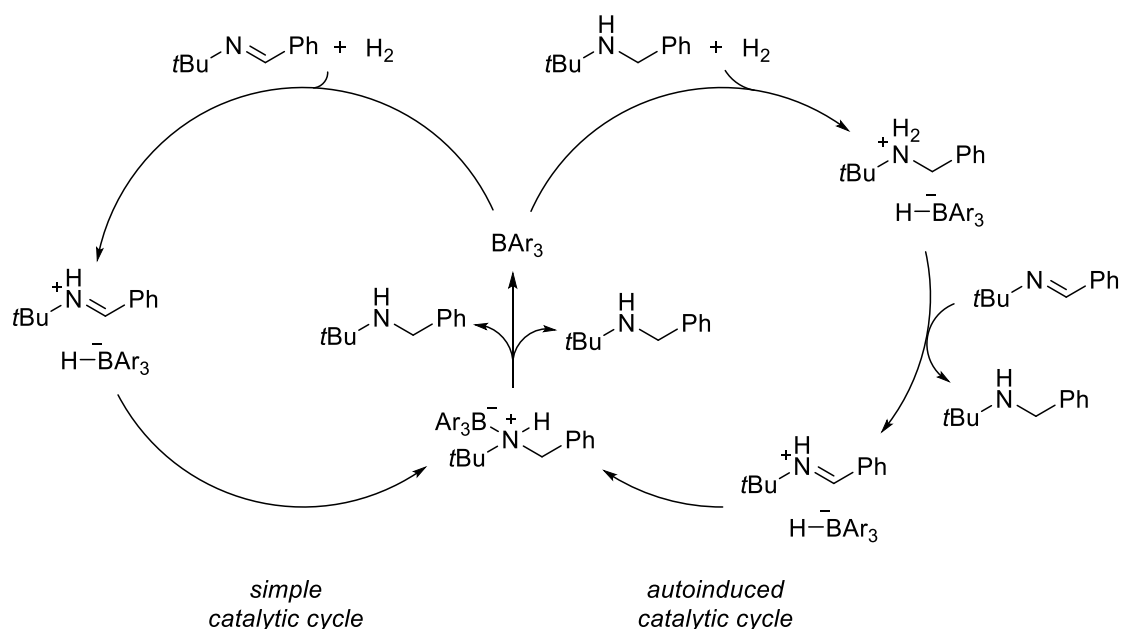


Scheme 5. The orbital interactions in H₂ activation with FLPs including frontier molecular orbital (FMO) diagrams.^{74,77}

Following H₂ activation, hydrogenation requires the transfer of the resultant H⁺ and H⁻ to the substrate being reduced. In most examples, and in this case, when imines are the substrate, the mechanism is believed to follow protonation of the substrate first, which activates the substrate for the subsequent hydride transfer. This is attributed to the mass use of boranes with electron-withdrawing groups (EWGs) resulting in relatively stable [Ar₂RBH]⁻ or [Ar₃BH]⁻ adducts after H₂ activation and themselves are not powerful enough hydride donors to reduce the unactivated substrates. After protonation from the LB, the substrate becomes electrophilic enough for hydride transfer from the LA (most commonly boranes) to yield the reduced substrate, in this case, as an amine-borane adduct. Thermal dissociation of this adduct yields the reduced substrate (amine) and regenerates the free FLP catalyst that can enter the catalytic cycle again.^{45,78,79}

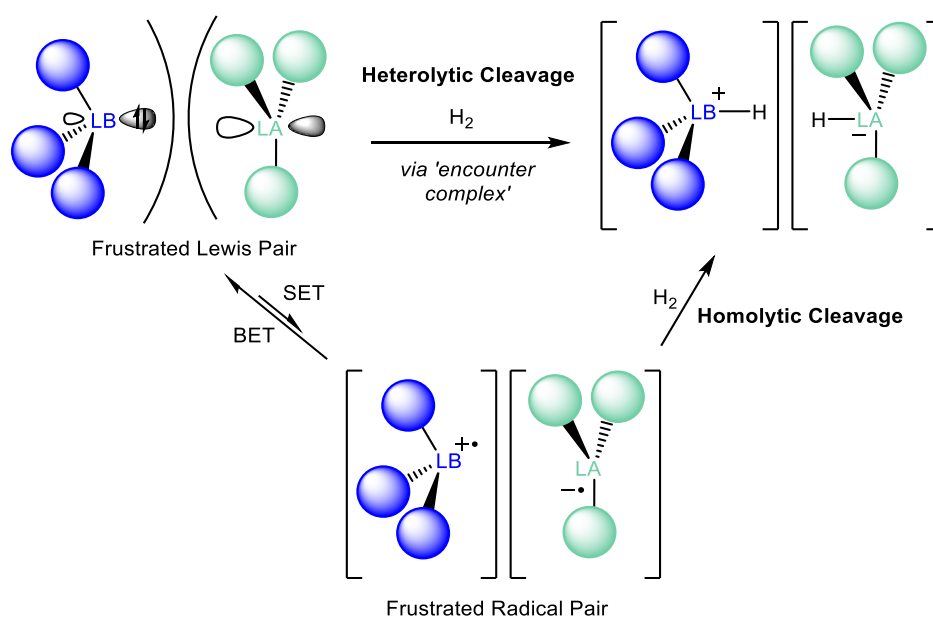
The example above discusses the mechanism for the reduction of imines with the first FLP $(C_6H_2Me_3)_2P(C_6F_4)B(C_6F_4)_2$. As previously introduced, this is an intramolecular FLP and therefore, contains a LB in the form of a phosphine. Following Stephan's seminal 2007 paper, it was quickly established that for imine reduction the LA could operate in concert with the imine to activate H_2 , which is dependent on the strength of the LA strength of the borane used. This alleviates the need for an external catalytic LB such as a phosphine as the imine can perform this role.

One important milestone for FLPs was the hydrogenation of *N*-tbutylimines. Paradies *et al.* performed a detailed kinetic study of $B(C_6F_5)_3$ (BCF), $B(2,4,6-C_6F_3H_2)_3$ or $B(2,6-C_6F_2H_3)_3$ as catalysts for imine hydrogenation (Scheme 6). BCF was able to activate H_2 in cooperation with the imine following a simple catalytic cycle. Conversely, the weaker Lewis acidic boranes [$B(2,4,6-C_6F_3H_2)_3$ or $B(2,6-C_6F_2H_3)_3$] and imines operate through an auto-induced cycle where the amine product from the simple catalytic cycle acts as the LB to activate H_2 with the borane.^{80–82} This was a major step in establishing the structure–reactivity relationship for imine hydrogenations with clear mechanistic differences through relatively discreet changes to LA strength and the electronic nature of the LB.



*Scheme 6. Reaction mechanism of the auto-induced catalytic hydrogenation of N-tbutylimines with boranes (BCF , $B(2,4,6-C_6F_3H_2)_3$ or $B(2,6-C_6F_2H_3)_3$). **Left cycle:** H_2 activation with imine as the LB. **Right cycle:** H_2 activation with amine as the LB.⁴¹*

An alternative mechanism originally proposed by Piers *et al.* in 2011 has recently seen major development and involves single-electron transfer (SET) from the Lewis base to the acid to generate a frustrated radical pair (FRP) which can subsequently react with substrates (Scheme 7). Notably, the FRP can be converted back to the FLP system via back electron transfer (BET).^{83–85} In 2020, Slootweg *et al.* showed that radical-ion pairs of the archetypal frustrated Lewis pair (FLP) systems $\text{PMe}_3/\text{B}(\text{C}_6\text{F}_5)_3$ and $\text{PtBu}_3/\text{B}(\text{C}_6\text{F}_5)_3$ can be accessed by visible-light-induced single-electron transfer. This contrasts the conventional FLP mechanism. FRPs are proposed to cleave the H_2 bond homolytically (Scheme 7). Recent work, probing the FLP system, $\text{PMe}_3/\text{B}(\text{C}_6\text{F}_5)_3$ system showed that the reactivity with H_2 had no light dependence. It was observed that even in the dark the phosphonium hydridoborate salt, $[\text{Mes}_3\text{PH}]^+[\text{HB}(\text{C}_6\text{F}_5)_3]^-$, could still be detected. This suggests that in the case of H_2 activation, the FRP mechanism does not play a significant role, and instead, activation follows proven polar, heterolytic pathways.^{83,86,87}



Scheme 7. Plausible Mechanisms of H_2 activation by FLPs via the established heterolytic path or by the proposed homolytic cleavage of H_2 via a SET process.⁸⁵

1.2.4 Conclusion

In conclusion, FLPs provide a powerful alternative to TMs for small molecule activation, particularly hydrogen. Since their discovery over two decades there has been a major expansion to their capabilities. Whilst there have been major efforts to develop

alternative Lewis acids and bases the prototypical system still centres around borane-containing frustrated Lewis pairs (FLP-boranes), with the majority of systems having been developed using BCF. For this reason, my project will also focus on the application of FLP-boranes as hydrogenation catalysts but with a view to expanding the gaps in the literature which will be discussed in more detail throughout chapter one.

1.3 Borane-containing Frustrated Lewis Pairs (FLP-boranes) for Hydrogenation Reactions

1.3.1 Catalyst Design

1.3.1.1 FLP-Borane Structures

FLP-boranes which are used as catalysts for hydrogenations are typically triaryl boranes. The geometry of triaryl boranes is typically trigonal planar, with an empty p orbital perpendicular to the compound's plane. The aryl groups are arranged into a paddlewheel-type structure to reduce steric hindrance (Figure 11).^{88,89} This leads to increased protection of the empty p orbital, making triaryl boranes ideal for FLP hydrogenation catalysis.

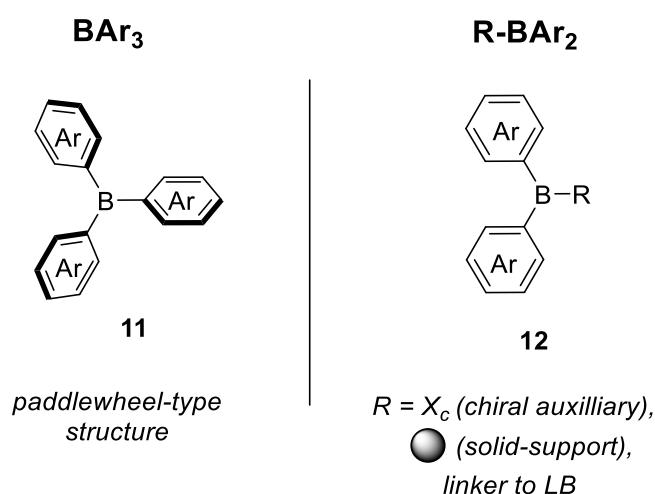


Figure 11. General FLP-borane structures. **Left.** Triaryl boranes and, **Right.** Diaryl boranes.

Alternatively, in order to incorporate a synthetic scaffold, such as an intramolecular linker to a LB, chiral auxiliary or solid support, it is not uncommon to find diaryl boranes (**12**, Figure 11). These diaryl boranes are commonly synthesised by hydroboration between

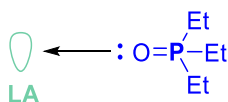
Piers' borane ($\text{HB}(\text{C}_6\text{F}_5)_2$) or the respective HBAr_2 and a synthetic scaffold containing an alkene or alkyne.⁹⁰ The moieties surrounding a borane centre control the steric hinderance and the Lewis acidity of the FLP-borane.

1.3.1.2 Lewis Acidity in FLP-boranes

1.3.1.2.1 Determination of Lewis Acidity for FLP-boranes

The concept of Lewis acidity, which involves accepting an electron pair and reacting with a Lewis base to form a Lewis adduct, was introduced by Lewis in 1923.⁹¹ Despite its universal understanding, the ability to measure Lewis acidity on a large scale remains unestablished. Thankfully, there are a few techniques that are widely used to determine Lewis acidity within the FLP field.

The Gutmann-Beckett method is the first well-established technique used to determine Lewis acidity (Figure 12).^{92,93} The technique includes an acceptor number (AN) system for scaling a range of LAs, mainly boranes against one another. It is a simple technique in which a LA is mixed with an excess of triethyl phosphine oxide, which forms a LP adduct, resulting in a signal shift in the ^{31}P NMR spectrum. This shift is directly related to the strength of the LA in its ability to draw electron density into its empty orbital. The use of simple Equation 1 shows how the AN is derived in relation to the ^{31}P NMR signal shift. The higher the AN determined, the greater the Lewis acidity.⁹⁴ These experiments are usually performed in an NMR tube making them easy practical methods to similarly determine the Lewis acidity of any new boranes that are synthesised.



Gutmann-Beckett method
 ^{31}P NMR

Figure 12. Gutmann-Beckett method for Lewis acidity determination.^{92,93}

$$AN = 2.21 \times (\delta_{\text{sample}} - 41.0) \quad (1)$$

Equation 1. The equation used to determine the AN of a given LA.^{92,93}

The second most common method is the Childs method (Figure 13).⁹⁵ This method relies on monitoring the chemical shift of the H³ proton in crotonaldehyde within the ¹H NMR spectrum. Again, this method relies upon the complexation of a compound, in this case, crotonaldehyde with a LA. However, for the Childs method, Lewis acids are compared to a 0.3 M solution of boron tribromide and hexane in dichloromethane (DCM) at -20 °C. In this case, the boron tribromide was assigned a value of 1.00 as a strong acid ($\delta^1\text{H}$ of H³ = 8.47 ppm) whilst hexane was assigned a value of 0 ($\delta^1\text{H}$ of H³ = 6.89 ppm). The relative Lewis acidity of new LAs which are being determined or compared can be calculated using Equation 2.

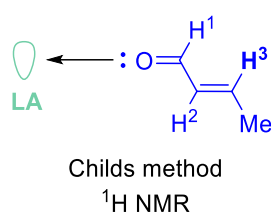


Figure 13. Childs method for Lewis acidity determination.⁹⁵

$$\text{Relative acidity} = \frac{\Delta^1\text{H LA crotonaldehyde adduct}}{\Delta^1\text{H BBr}_3 \text{ crotonaldehyde adduct}} \quad (2)$$

Equation 2. The equation used to determine the relative acidity of given LA in comparison to BBr₃.⁹⁵

The experimental methods to determine Lewis acidity are convenient to perform however, there is often an inconsistency between them due to the different NMR probes used. Solvent effects have also been shown to influence Lewis acidity calculations between experiment runs, as well as experimental setup errors, with concentration being extremely influential on chemical shifts and human error in reading the NMR spectrum. For example, in 2013 Sivaev *et al.* collated measurements from multiple sources using the Gutmann-Beckett method to determine the Lewis acidity of various boranes.⁹⁶ The compiled ANs calculated for just the prototypical FLP borane, BCF, ranged from 76.0 - 82.0 across 15 different measurements. Only 4 different solvents were used across these different readings. As a result, major efforts have also been placed into determining the Lewis acidity of borane through computational methods.

Although the Gutmann-Beckett method initially used AN to compare Lewis acidity, the FLP field has since moved away from it. Nowadays, in research comparing Lewis acidity

in FLP boranes, the Lewis acidity of the prototypical borane, BCF, is often defined as 100%, and then the Lewis acidity of other boranes is compared to this benchmark.⁹⁷ As a result, relative Lewis acidity is often expressed as a percentage that can be greater than 100%, less than 100%, or equal to 100% (Figure 14), depending on the measurements calculated using the Gutmann-Becket method. This terminology has intriguing implications in experiments, as it could potentially reduce some of the inaccuracies in measuring AN. When comparing a new or chosen borane to the archetypal and commercially available BCF, the aim is not necessarily to match an exact literature number but to compare the Lewis acidity directly across two samples that have hopefully been consistently set up.

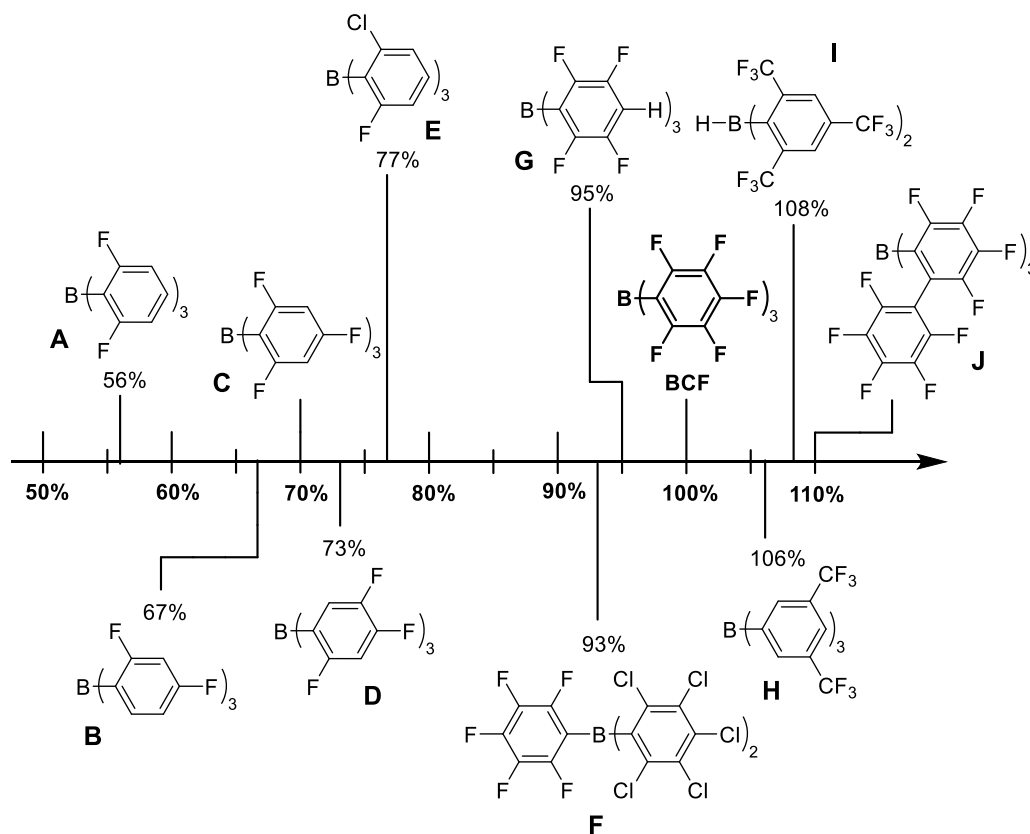


Figure 14. Lewis acids **BCF** and **A-J** are used for H_2 activation. % included corresponding to the Lewis acidity referenced to **BCF** (100%, Gutmann-Becket method or Childs method)⁹⁷. **BCF**⁹⁸, **A**⁹⁹, **B**¹⁰⁰, **F**¹⁰¹, **G**¹⁰², **H**¹⁰¹, **I**¹⁰³, **J**¹⁰⁴.

1.3.1.2.2 Influence of Lewis Acidity on Catalytic Activity of FLP-boranes

The strength of the $\sigma(\text{H}_2)$ orbital interaction is determined by the inherent Lewis acidity of the LA used (Scheme 5).⁹⁷ As discussed in the hydrogenation mechanism using FLPs (Scheme 4), the borane/LA gains the hydride and produces a borohydride, while the Lewis base gains the proton. If the borane is highly Lewis acidic, such as BCF, the activation of hydrogen is easier, but the subsequent hydride delivery is slower.^{74,97}

When choosing a Lewis acid for hydrogenations, it is important to consider how increased Lewis acidity will affect the nucleophilicity (hydride affinity) of the generated hydride. Using strong Lewis acids may appear to enhance the H_2 activation step; however, this may lead to reduced nucleophilicity of the borohydride species. However, whilst hydride affinity is a crucial factor it should be balanced with the Lewis acidity as the H_2 activation is predominantly the rate-determining step in hydrogenation reactions, whereas the proton and hydride transfers from the to the substrates generally have a much smaller barrier respectively.^{78,105,106}

Understanding the impact of modifying aryl groups on Lewis acidity is crucial. The Lewis acidity of triaryl boranes increases when strongly EWGs are incorporated into the borane aryl rings.⁹⁴ Other methods for altering Lewis acidity include increasing the number of fluorine atoms, replacing fluorine with heavier halogens,^{100,101,107} substituting aryl rings with perfluoronaphthyl or perfluorobiphenyl moieties,^{108,109} and preparing heteroleptic triaryl boranes.^{100,101,107} The general trends in the modification of Lewis acidity are summarised in Figure 15.

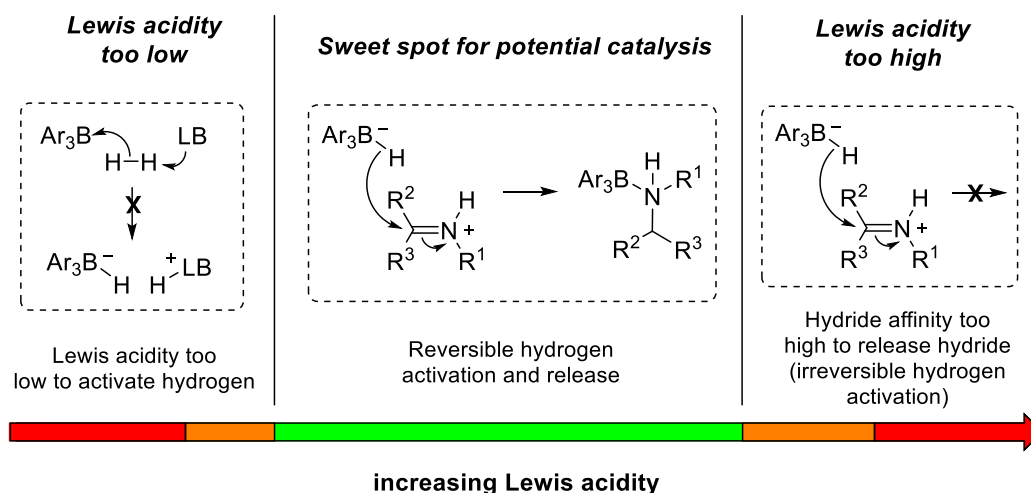


Figure 15. Qualitative representation of how FLP-borane Lewis acidity can affect the catalytic success/activity.

Ultimately, in catalyst design, it is necessary to balance various characteristics. The moieties that surround the LA centre can be considered analogous to ligands that surround a metal centre in traditional TM chemistry. These moieties provide precise control over Lewis acidity, hydride affinity, electronics, and steric hindrance. However, in the case of FLPs, these moieties need to be incorporated from the start, while varied ligands are usually added to metals *in situ*.

1.3.1.3 Influence of Steric Hindrance on Catalytic Activity of FLP-boranes

Another major factor that must be tailored for FLPs is steric hindrance, because it influences the interaction with both hydrogen and the target substrate being reduced. With too little steric bulk, classical LA/LB adducts can be formed. In other words, LA and LB are too strongly interacting for H₂ activation. With too high steric bulk, the [LA-H]⁻ will be too sterically congested to interact with the substrate and perform the reduction. The sweet spot for successful FLP hydrogenation catalysis lies somewhere in the middle where thermally and sterically frustrated FLPs must both have lower steric hindrance to allow for bulkier substrates and inversely have greater steric bulk for less bulky substrates (Figure 16). Thermally induced FLP typically have lower steric bulk as they can form an adduct at low temperatures but dissociate upon heating. This understanding can

help determine which type of catalyst would be expected to achieve the most efficient hydrogenation with a chosen substrate given the bulky nature of said substrate.

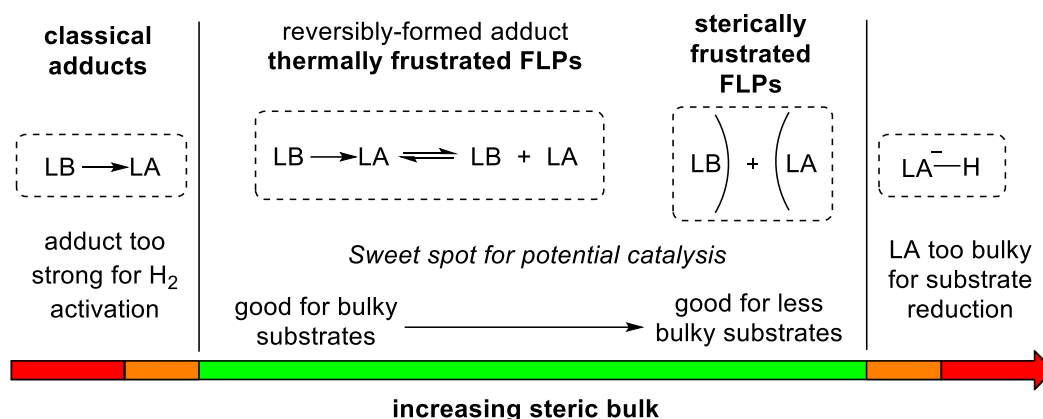


Figure 16. Qualitative representation of how FLP-borane steric bulk can affect catalyst activity.

(Figure reproduced from Ashley et al.)⁵²

1.3.2 Scope and Limitations of FLP-borane Catalysed Hydrogenations

1.3.2.1 Substrate Scope

Several examples of FLP catalysed transformations have been developed and include: hydrosilylation, transfer hydrogenation, hydroboration, amination, hydroarylation, C–H borylation, polymerisation, CO_2 reduction and C–F derivatisation.^{110–112} Although these FLP-catalysed transformations are not relevant to this body of work, these developments support the strength and potential of FLP catalysis to compete on an industrial level with TM catalysts with a wide range of applications.⁵¹

This project will focus on hydrogenation. Therefore, H_2 activation FLP systems developments are of the utmost interest. Many excellent reviews have been written in recent years, highlighting the rapid growth in the scope of hydrogenation substrates.^{9,45,51} The scope of functional groups that have been reduced by various optimised FLP systems include oximes, hydrazones, imines, nitriles, aziridines, enamines, alkenes, allenes, *N*-heterocycles, ketones, aldehydes, enones, ynones, polyaromatics, alkynes, and amides (Figure 17).^{51,113,114}

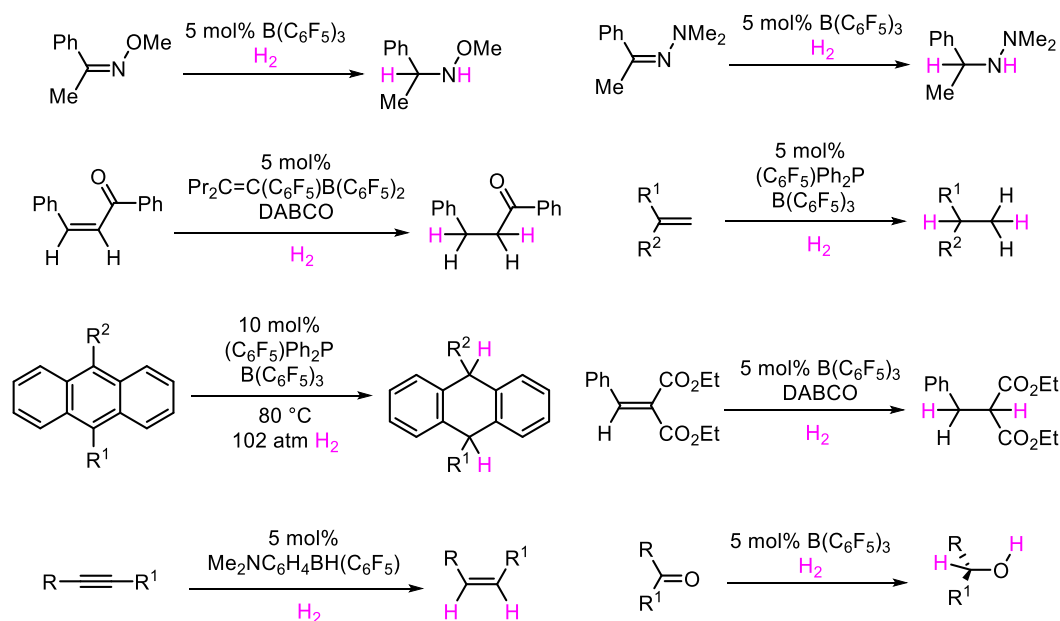


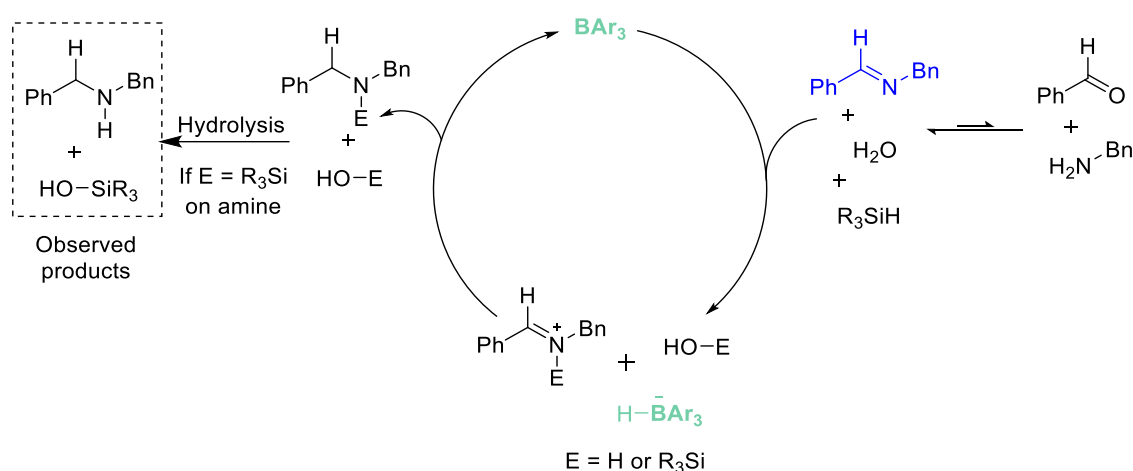
Figure 17. Select examples of the functional scope broadening.⁵¹

1.3.2.2 FLP-Borane Catalysed Reductive Aminations

Prior to the first FLP-borane catalysed reductive amination reaction reported in 2016 by Ingleson (see below),¹¹⁵ imine reduction had been extensively studied.^{116–119} These studies had revealed that most imines could be reduced conveniently using either hydrogen or silanes. Performing FLP-borane catalysed reductive amination rather than stepwise imine formation and hydrogenation can be more desirable, providing a more direct access to amine products, but has proven a more complex task since the borane catalyst is exposed to one equivalent of water formed as a by-product of imine formation in the reaction.

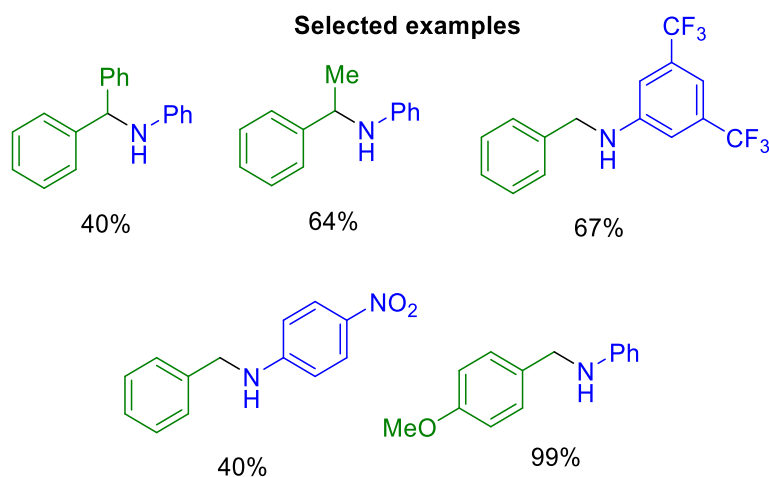
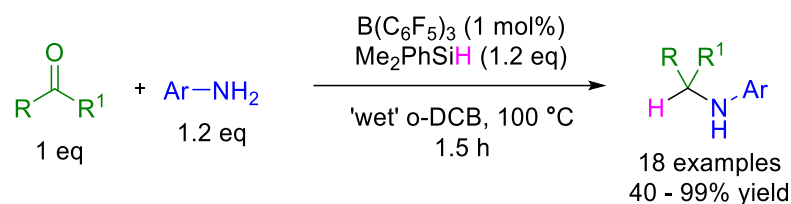
Since 2016, the development of FLP-catalysed reductive amination systems using H₂ and silanes has been established by a few key research groups. These FLP catalysts/systems have been designed directly for reductive aminations, where the LA aids with the imine formation, enables hydrogenation activation, and delivers the hydride for the subsequent imine reduction. Soós and co-workers (Budapest, Hungary),^{120,121} Ingleson and co-workers (Edinburgh, UK)^{28,122,123} and Hoshimoto *et al.* (Osaka, Japan)^{33,124,125} have all made excellent contributions to reductive amination using FLP catalysts and it is select examples from these works which will be discussed in this section.

Currently the majority of FLP-borane catalysed reductive aminations use silanes as reductants because they are much easier to handle (relative to hydrogen) and do not require the forcing conditions that would be needed for H₂ splitting.^{28–33} Like TMs, LAs, such as FLP-boranes, can also be used for the activation of H₂ and Si-H bonds (in the case of silanes) and therefore act as catalysts for reductive amination.¹²⁶ The resulting [Ar₃BH]⁻ adducts formed can reduce the iminium cation by hydride transfer in a very similar mechanism to that shown in regular FLP reactivity for imines (Scheme 4 and Scheme 8).



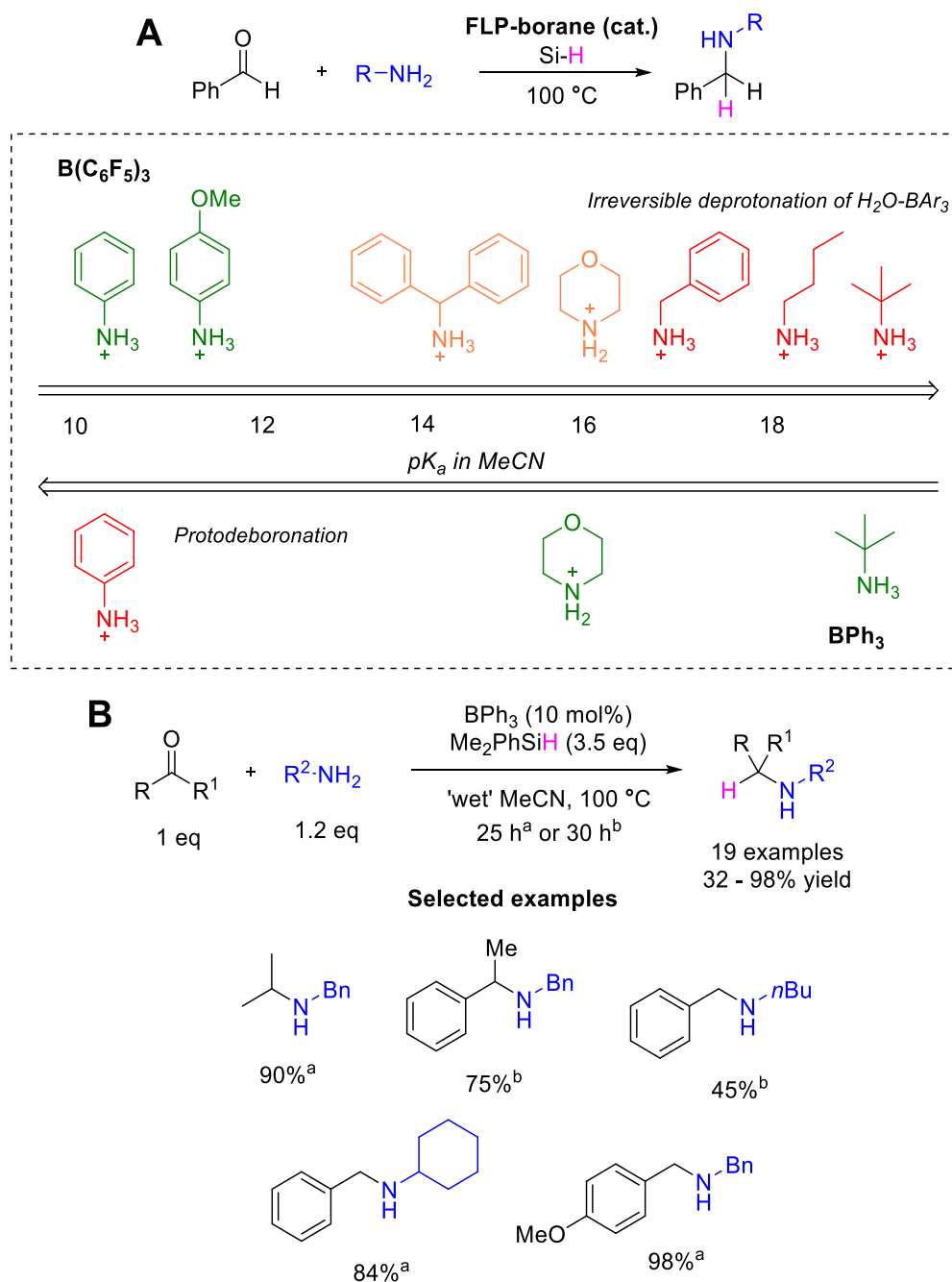
Scheme 8. Feasible catalytic cycle proposed by Ingleson et al. for the borane-catalysed reductive aminations using silanes of benzylamine and benzaldehyde.²⁸

Early work on reductive aminations using B(C₆F₅)₃ and silanes was reported by Ingleson *et al.* in 2016.²⁹ They used BCF (1 mol%), Me₂PhSiH (1.2 eq), and non-dried ('wet') *o*-dichlorobenzene (*o*-DCB) (Scheme 9). 18 Secondary amines were obtained from a range of simple aldehydes, ketones and primary aryl amines used to explore the electronic requirements of the system. The yields were mostly good to excellent (60 – 99%) with two examples below 50%. Notably, the system did not tolerate alkyl amines, and the two moderately sterically encumbered carbonyls screened, (benzophenone and acetophenone), gave fairly low yields compared to the rest of the substrate scope (40% and 64% respectively). Similarly, electron deficient amines gave lower yields, presumably due to the lower nucleophilicity and the subsequent impact on the imine equilibrium.¹²²



Scheme 9. Early work on BCF catalysed reductive aminations using silanes, with selected examples showing the initial challenges to FLP-catalysed reductive aminations.¹²²

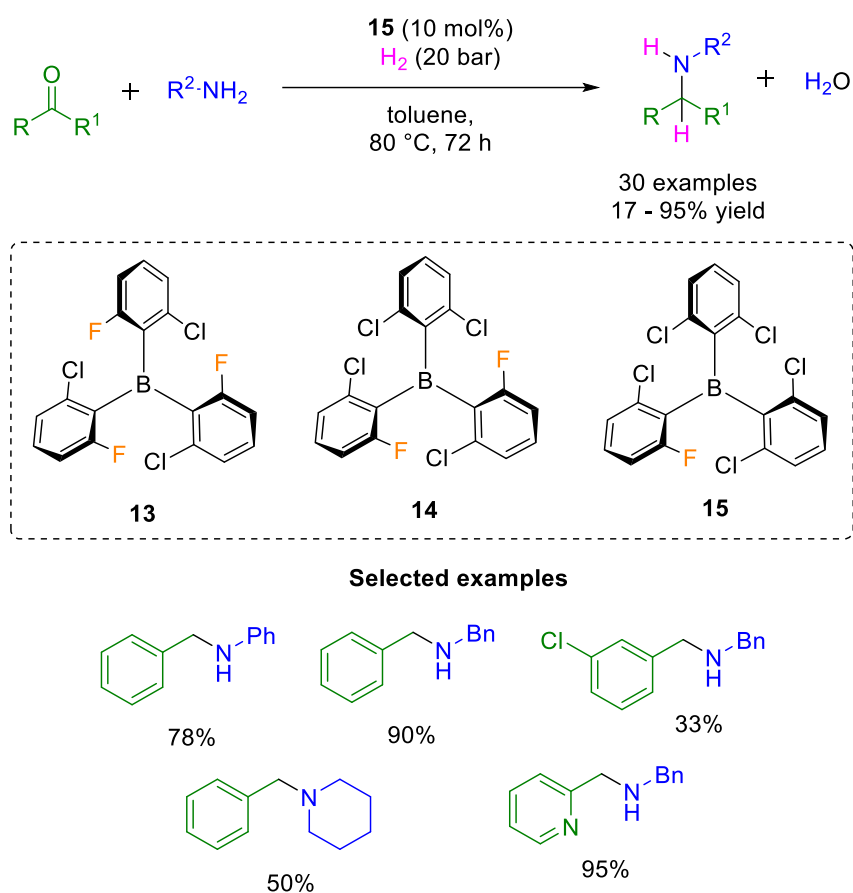
In a separate report, Ingleson and co-workers explored the shortcomings of FLP borane water tolerance in the presence of various amines when performing reductive aminations (Scheme 10. **A**).²⁸ Whilst BCF is a viable catalyst for aryl amines (conjugate acids $pK_a < 12$ in MeCN) it is not for alkylamines (conjugate acids $pK_a > 16$ in MeCN). The increased Brønsted basicity of alkyl amines leads to irreversible deprotonation of $\text{H}_2\text{O}-\text{BAr}_3$ through the decomposition path **A** (Scheme 14).^{28,127} Conversely they were able to optimise a reductive amination system catalysed by BPh_3 , which was capable of catalysing alkylamines (Scheme 10. **B**). 17 Secondary amines and 2 tertiary amines were obtained from a range of simple aldehydes and ketones. The yields were mostly good to excellent (70 – 98%) including alkyl amines, with high Brønsted basicity ($pK_a \geq 16$) such as *t*butyl amine and hexyl amine. Conversely to BCF and other highly Lewis acidic FLP-boranes, aryl amines were not tolerated.



Scheme 10. **A.** Amine substrate scope tolerance under reductive amination reaction conditions for BCF (FLP-boranes with high Lewis acidities) vs BPh₃. **B.** BPh₃ catalysed reductive amination system.²⁸

A similar approach was employed by Soós and co-workers who developed an FLP-catalysed reductive amination with H₂ as a reductant. Soós *et al.* proposed that both electronic and steric tuning would be required and therefore, screened a series of boranes with gradual changes to their steric environments. They found that chlorine atoms at the *ortho*-position on the aryl substituents provided sufficient bulk to limit

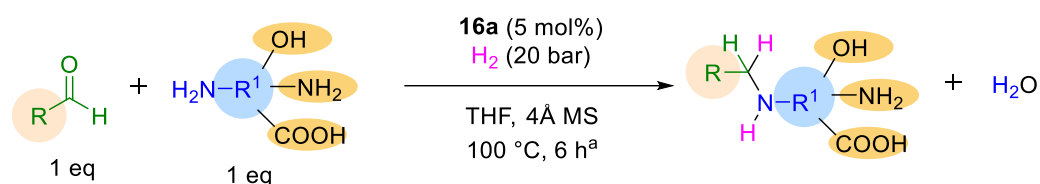
water coordination. The most suitable catalyst **15** was able to carry out the reductive amination of aryl and alkyl amines using a 1:1 ratio between the carbonyl and the amine, 10 mol% **15**, 20 bar of H₂ and using toluene as the solvent (80 °C, 72 hours) (Scheme 11).¹²⁸ 24 Secondary amines and 6 tertiary amines from a wide array of aldehydes and a limited selection of ketones. Whilst the yields ranged from poor to excellent (17 – 95%), the FLP-borane catalyst were obtained from a range of simple aldehydes and ketones was shown to be capable of performing reductive aminations with alkyl and arylamines.



Scheme 11. Water tolerant FLP catalyzed reductive amination of carbonyl compounds.¹²⁸

A more recent breakthrough in reductive amination was achieved by Hoshimoto and co-workers. They aimed to enhance the reactivity of boranes towards substrates that were previously challenging, such as bulky aldehydes, while also incorporating functional groups like alcohols, amines, and carboxylic acids. These functional groups also add value as they act as synthetic handles for future diversity-orientated synthesis. Of the five boranes tested, borane **16a** proved to be superior due to its incorporation of bulky *ortho*-chlorines. They were able to optimise a set of conditions and achieve their goals,

screening a broad range of aldehydes and mostly aryl amines with ten examples bearing COOH/OH/NH₂ groups (Scheme 12).¹²⁴ Ketones were not screened and only 3 of the 21 amines screened were alkyl amines. Whilst benzylamine attained only 34% the two other alkyl amines screened attained excellent yields (91 and 99%). To achieve this, the team used THF and MS to remove the water produced *in situ* (a method initially developed by Stephan *et al.*).^{124,129}



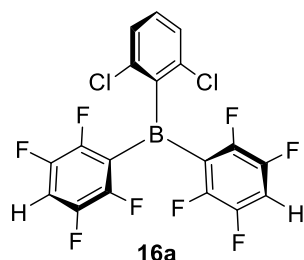
14 examples of aldehydes (29-99% isolated yield)

21 examples of amines (34-99% isolated yield*)

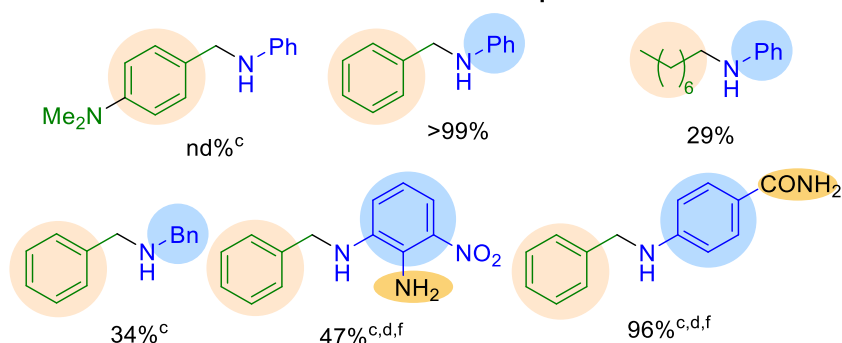
*one compound yield estimated by NMR

other conditions were sometimes required

(2 h^b. At 80 bar H₂^c. 10 mol% **16a**^d. 15 mol% **16a**^e. 15 h^f. 18 h^g.)

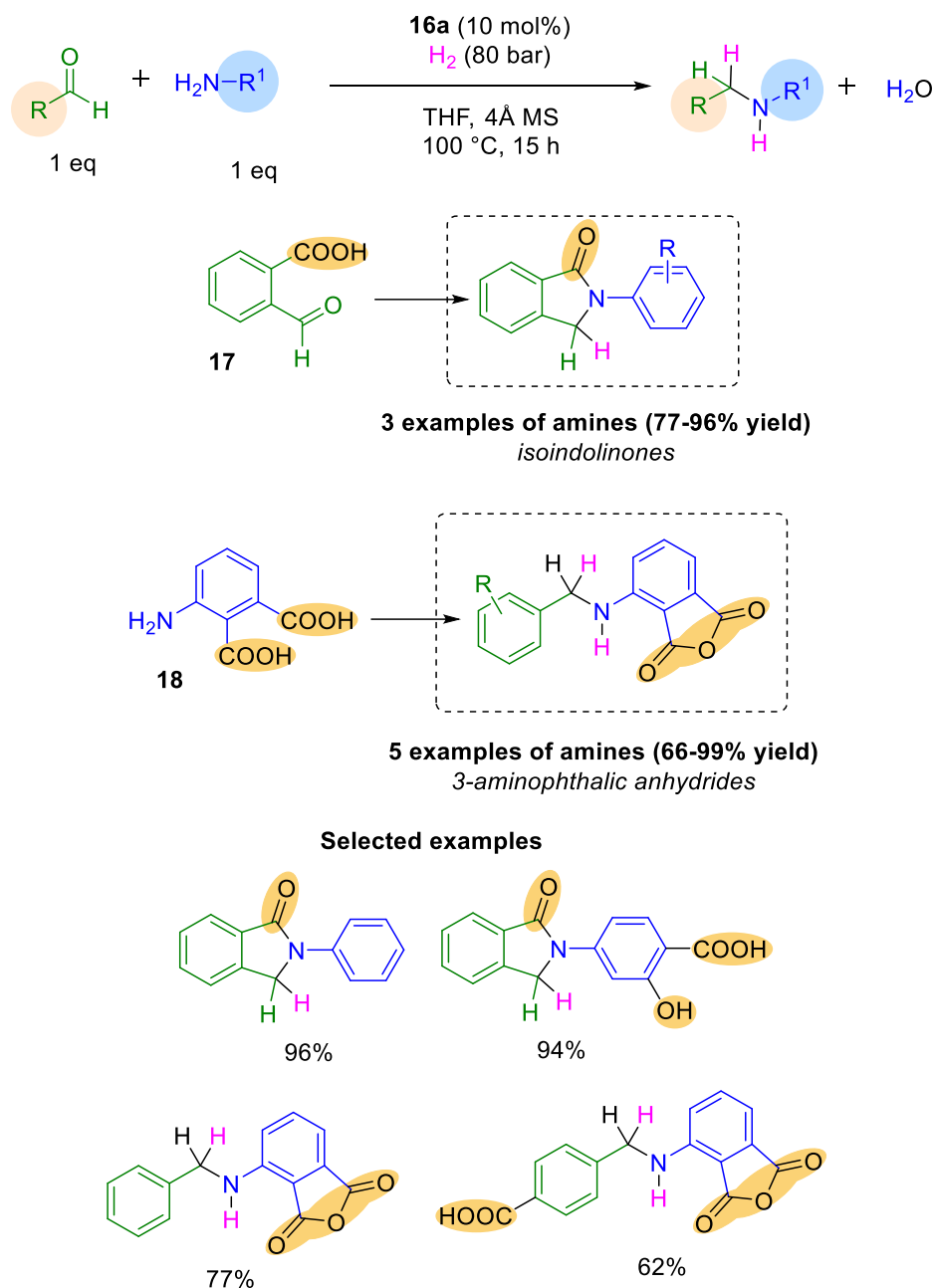


Selected examples



Scheme 12. Moisture-tolerant FLP-catalysed reductive amination using H₂.¹²⁴

Hoshimoto *et al.* optimised the conditions further to develop a system that can perform a reductive amination and subsequent cyclisation. This system produces isoindolinones from aldehyde **17** and 3-aminophthalic anhydrides from amine **18** (Scheme 13). This research is an excellent example of what FLPs can offer in terms of reductive aminations.



*Scheme 13. Application of FLP-catalysed reductive amination system producing isoindolinones from **17** and 3-aminophthalic anhydrides from **18**.¹²⁴*

1.3.2.3 FLP-borane Catalysed Reductive Amination: Conclusions

In the past two decades, significant progress has been made in FLP chemistry. However, challenges remain, such as the lower reactivity and stereoselectivity compared to TM catalysts. These general limitations are also valid for reductive aminations as well as other FLP applications. Recent developments aim to address these limitations by enabling FLP systems to operate using silanes or hydrogen at room temperature with

catalyst loadings as low as 0.1 mol%. Additionally, efforts have been made to develop asymmetric versions of FLP-catalysed reactions. These advancements aim to bring FLP systems closer to TM-like levels of reactivity and enantioselectivity, however, it is clear there are still a requirement for further improvement in these areas.

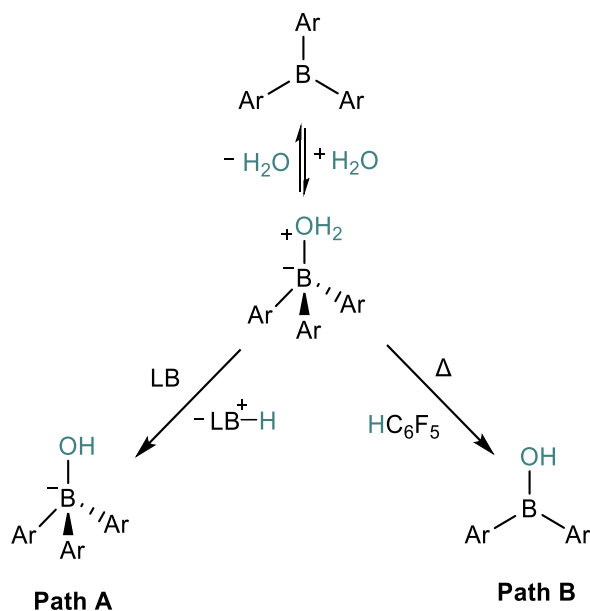
The development of moisture-tolerant boranes has been crucial in the use of FLPs as catalysts in reductive aminations as the reaction must proceed even in the presence of a super-stoichiometric amount of water, which is derived from imine formation and therefore cannot be avoided (Scheme 8).²⁸ Alkylamines represent a major challenge for FLP-borane catalysed reductive aminations due to their increased Brønsted basicity compared to arylamines, which have seen much greater success.³⁴ FLP-borane catalysed reductive aminations have also seen very limited substrate exploration, often producing simple disubstituted amines with limited functionality or attention to relevant medicinal motifs. Although Hoshimoto and co-workers recent developments have started to shift this focus (Scheme 12 and Scheme 13), there are areas which have yet to be exploited. These include the synthesis and functionalisation of cyclic amines, which is a transformation often performed via reductive amination in 'fine' chemical synthesis.¹³⁰ In this vein, limited progress has been made towards the use of ketones in FLP-borane catalysed reductive aminations, which is something that should be addressed.

1.3.3 Borane Moisture Sensitivity

1.3.3.1 Decomposition Pathways

Perhaps the largest limitation for FLP-borane catalysed reactions is moisture tolerance. Boranes exhibit high oxophilicity due to their strong inherent Lewis acidity. Therefore, water can be a major issue for BAr_3 /Lewis base catalysed reactions where coordination to the borane leads to a $[\text{Ar}_3\text{B}-\text{OH}_2]$ adduct, which precludes the binding of other small molecules.⁵¹ These water-adducts have pK_a comparable to strong Brønsted acids (e.g. HCl) and as a result, they can protonate the LB component of the FLP system (Scheme 14. Path **A**).^{123,131} Importantly this proton transfer is often irreversible and kills the FLP catalyst stopping H_2 activation.

Even in the absence of a LB, the forcing conditions (high temperatures) that most FLP systems require, have been reported to lead to intramolecular proton transfer (protodeboronation) from the bound water to one of the aryl substituents of the LA (Scheme 14. Path **B**). It should be noted that in the presence of an alcohol (ROH), the same issues arise and end in FLP catalyst deactivation.¹²³



Scheme 14. Deactivation pathways of BAr_3 (LA) in the presence of water. **Path A**: Irreversible protonation of LB by $\text{LA}-\text{OH}_2$ adduct. **Path B**: Intramolecular proton transfer from water to one of the aryl substituents of the LA (hydrolysis).¹²³

Whilst solvent drying and purification are commonplace in a research laboratory, major improvement in impurity tolerances is a major goal for FLP developments to allow these catalysts to replace their TM alternatives in industrial processes. The H₂O binding itself, although preventing H₂ activation, is reversible. Thus, efforts to develop water tolerance has played a major role in FLP research.

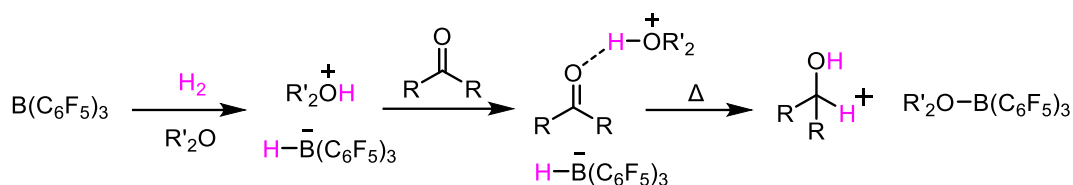
It is important to differentiate between water tolerance and moisture tolerance, even though they are often used interchangeably in the FLP field. Water tolerance is the more commonly used term, as it has a broader definition. In the context of FLPs, water tolerance refers to the ability of an FLP catalyst to tolerate any amount of water. This can include bench-top stability, water spiking in experiments, or using non-anhydrous solvents. However, this definition is somewhat ambiguous, so the field has adopted the more specific term 'moisture-tolerant', which will be used more frequently in this thesis. Moisture tolerance refers to the ability to tolerate the presence of more than one equivalent of water relative to the borane while still exhibiting catalytic activity.^{45,100,132–}

134

1.3.3.2 Methods to Achieve Water Tolerance: Use of Weakly Coordinating Lewis Basic Solvents

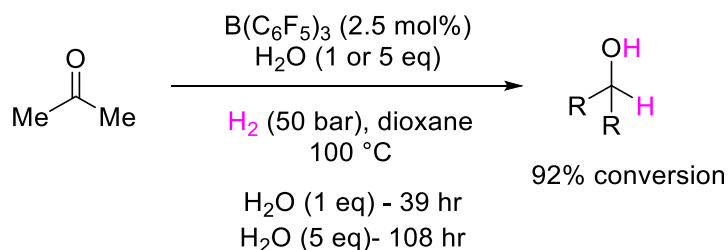
As discussed, the first FGs to be reduced by FLPs that were reported following 2006 included imines, enamines, aromatics, aziridines, alkenes and alkynes. However, up until 2014, the catalytic hydrogenation of C=O (aldehydes and ketones) had not been achieved. This challenging reduction was attributed, in intermolecular FLP systems, to alcohol-borane adducts followed by protodeboronation upon heating as mentioned (Scheme 14. Path **B**), leading to HC₆F₅ and an alkoxyborate.

This was overcome by both the Stephen and Ashley groups by using weakly coordinating solvents as the base.^{135,136} Both Et₂O and 1,4-dioxane are better nucleophiles than carbonyls and the protonated ethers are also much more acidic than phosphines/amines (pK_a Et₂OH⁺ = 0.2 in MeCN)¹³⁷. Therefore, they promote carbonyl activation through hydrogen bonding, followed by the hydride transfer from the LA⁻-H (Scheme 15).



Scheme 15. FLP catalysed hydrogenation of carbonyls setup under ambient conditions using etheral solvents.^{123,138}

The Ashley group were eventually able to perform carbonyl hydrogenation setup under ambient conditions (open air, technical grades solvents and no Schlenk line or glovebox use). In this case, the presence of water did not kill the catalyst as the solvent was not basic enough to deprotonate the LA-OH₂ adduct. It is important to note that the presence of water in the reaction mixture led to significantly longer reaction times to achieve the same high conversion as the reaction under anhydrous conditions. Using 2.5 mol% of the B(C₆F₅)₃ catalyst at 100 °C and 50 bar H₂ the reaction took 39 hours with 1 equivalent of water and 108 hours with 5 equivalents of water to achieve the same 92% conversion (Scheme 16).⁶²

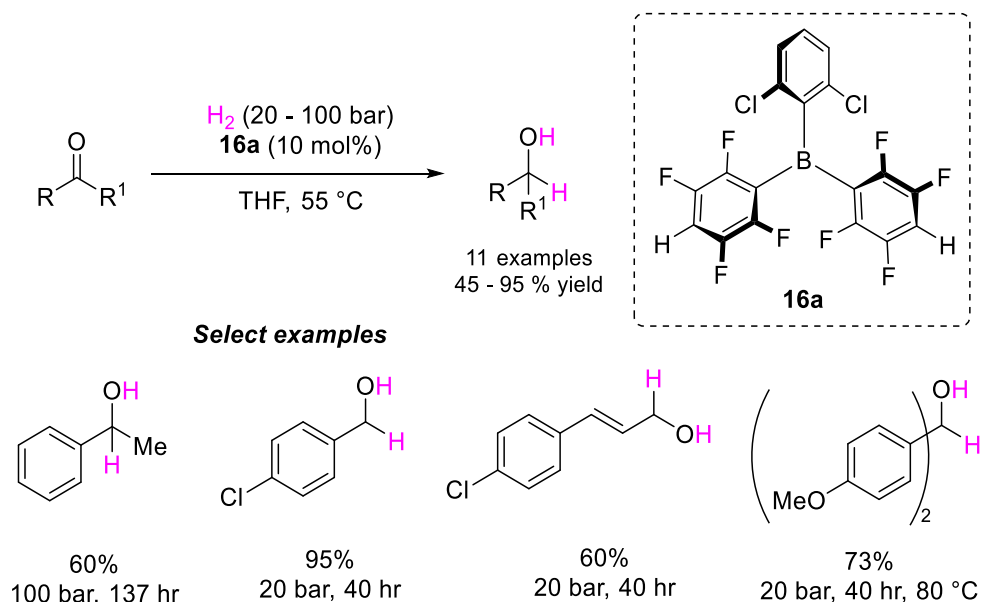


Scheme 16. Hydrogenation of acetone in the presence of various amounts of water.⁶²

1.3.3.3 Methods to Achieve Water Tolerance: The Size-Exclusion Principle

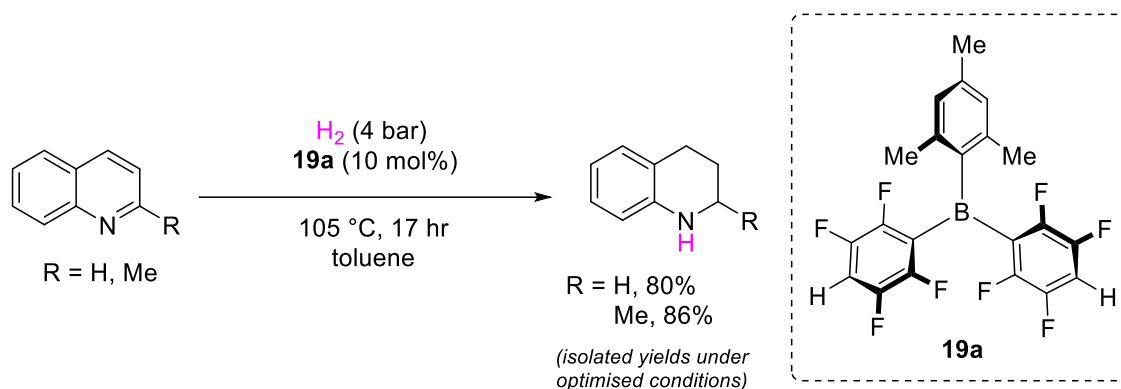
Alternatively, using the 'size-exclusion' principle to sterically block the LA centre, Soós and co-workers were able to develop a carbonyl hydrogenation system in etheral solvent (THF) by utilising (2,6-Cl₂C₆H₃)B(4-HC₆F₄)₂ (**16a**) (Scheme 17). Again, the reaction could be performed under ambient conditions. However, the presence of water significantly slowed the reaction and higher H₂ pressures (20 to 50 bar) were required for effective hydrogenations. The 'size-exclusion' principle was a term coined by Soós *et al.* that has become an established technique in FLP catalyst design.^{107,134,139} The principle is based on increased congestion at the boron (LA) centre and still allows for H₂

activation. The incorporation of large *ortho*-chlorines (relative to *ortho*-fluorines) substantially decreases water complexation. Use of the weak coordinating, low basicity ethereal solvent THF also helps with water tolerance.^{100,134,139,140}



Scheme 17. Carbonyl hydrogenation using moisture tolerant catalyst **16a**.¹³⁴

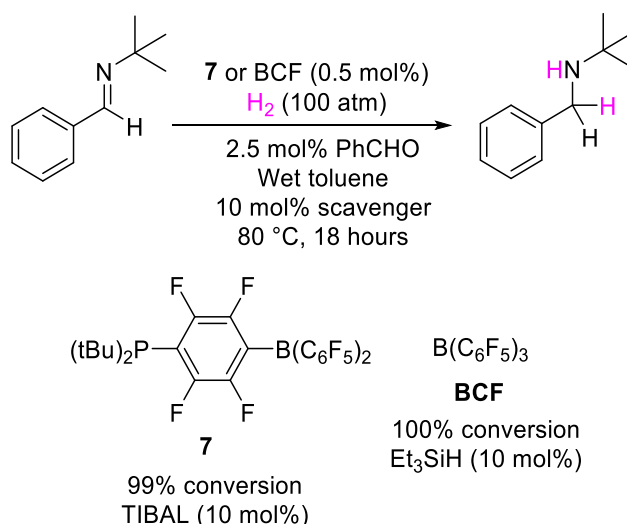
As part of their research, Soós *et al.* also explored the use of *ortho*-methyl groups by employing mesityl moieties as one of the aryl rings in a heteroleptic triaryl borane. Soós *et al.* successfully synthesised catalyst **19a** to achieve air and moisture stability and catalyse the reduction of quinoline derivatives. Under anhydrous conditions, catalyst **19a** can hydrogenate quinoline in a 99% conversion with 10 mol% catalytic loading (Scheme 18). Using the standard catalyst BCF the yield is heavily reduced when exposed to air (3% conversion) whilst the **19a** catalyst benefits from improved moisture sensitivity. Using catalyst **19a**, which had been exposed for 30 minutes to air (43% humidity and 24 °C), increasing the temperature to 105 °C led to 84% conversion. This provided extremely promising evidence for the improved moisture tolerance using the steric hindrance of the mesityl substituent over the standard B(C₆F₅)₃ catalyst.¹³⁹



Scheme 18. Quinoline reductions with BCF and moisture tolerant catalyst **19a**.¹³⁹

1.3.3.4 Methods to Achieve Water Tolerance: Chemical Scavengers

An alternative method for water tolerance was developed in 2013 and took advantage of inexpensive poison scavengers to allow for economical and practical scale-up for FLP catalytic hydrogenation. These cheap chemical scavengers remove water and aldehyde impurities from commercial-grade solvents, substrates and gases. Chase *et al.* in collaboration with FLP pioneer Douglas Stephan, found that the scavengers also regenerated the poisoned catalysts, increasing turnover numbers and lengthening catalyst lifetimes. They screened a range of scavengers (1 mol% loading) that had proven useful in industrial ethylene polymerisation (such as MAO) and a variety of silanes, based on the work of the Piers group using BCF to catalyse the dehydrogenative silylation of alcohols with silanes. The best three scavengers TIBAL (triisobutylaluminum), Et_3SiH and MAO achieved excellent conversions (86 – 98%) for imine reductions with both catalysts **7** and BCF (Conditions: 100 atm H_2 , 25 °C for 2 hours). Additionally, they found that even with 2.5 mol% benzaldehyde and wet toluene (solvent), under the established optimised conditions, 0.5 mol% of **7** and 10 mol% of TIBAL achieved a 99% conversion whilst using 0.5 mol% BCF and 10 mol% Et_3SiH attained 100% conversion (Scheme 19). The ability to employ low catalyst loadings using inexpensive scavengers should greatly simplify the implementation of these FLP catalysts into industrial-scale processes for hydrogenation and other small molecular FLP activation processes.³

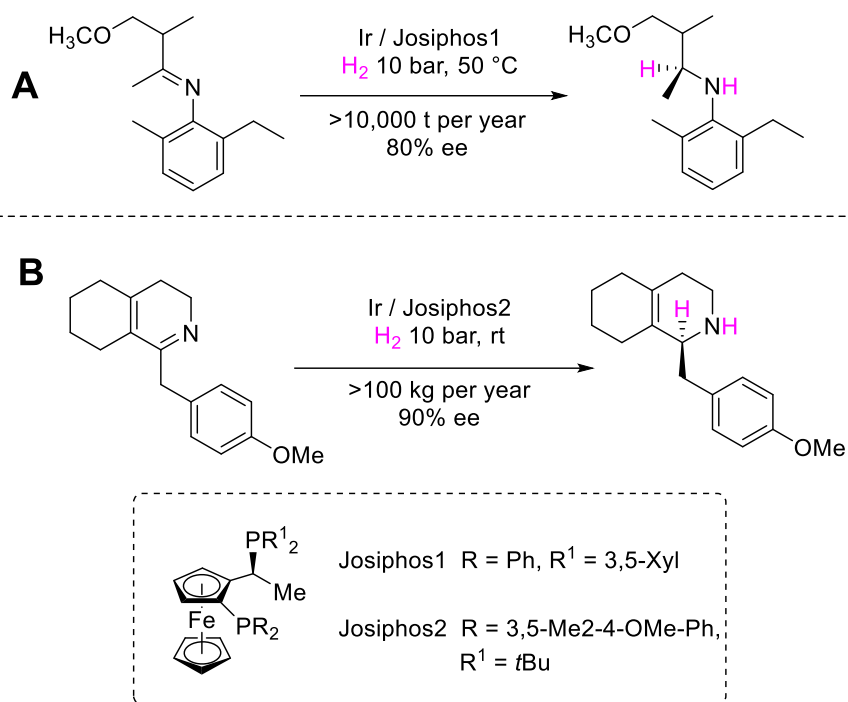


Scheme 19. FLP catalyzed the hydrogenation of imines under demanding conditions using scavengers to remove impurities and regenerate poisoned catalysts.³

1.3.4 Asymmetric FLP-borane Reactions

One major drive for the use of FLP catalysis is to replace TMs in industrial-scale enantioselective hydrogenation for “fine” chemical production. Knowles’ Nobel Lecture review in 2001 stated that asymmetric hydrogenations made up 50% of production scale, 90% of pilot scale and 74% of bench scale catalytic enantioselective processes in industry.¹⁴¹ Now, two decades later, although these percentages may no longer be valid, they do represent the industrial dependence on asymmetric hydrogenations. Asymmetric hydrogenations are often performed using rhodium (Rh), ruthenium (Ru) and iridium (Ir). In addition to the high cost of these rare metal catalysts, it is also well known that the removal of TM catalyst residue from pharmaceutical products constitutes a significant cost for the drug industry. Development of systems to replace valuable asymmetric TM catalyzed hydrogenations with an optimised FLP catalyst would be excellent for reducing industrial catalyst costs, toxicity and purification costs.

For example, two valuable intermediates, synthesised by the asymmetric imine hydrogenations, are the herbicide intermediate (S)-metolachlor¹⁴² (Scheme 20. **A**) and the antitussive drug intermediate dextromethorphan¹⁴³ (Scheme 20. **B**). The former is made on a >10,000 t per year scale and the latter >100 kg a year.¹⁴⁴



Scheme 20. Industrial-scale intermediate compounds are accessible through FLP asymmetric imine hydrogenations. A. Industrial scale synthesis of herbicide intermediate (S)-metolachlor by iridium catalysed asymmetric hydrogenation of an imine.¹⁴² B. Industrial scale synthesis of the drug intermediate dextromethorphan via asymmetric imine hydrogenation.¹⁴³

Over the last 10 years efforts have been focused on enantioselective FLP catalysed hydrogenation and hydrosilylations using chiral FLPs. A fairly wide array of unsaturated compounds, including imines, enamines, *N*-heteroarenes, silyl enol ethers, ketones, and enones have all seen varying degrees of successful asymmetric hydrogenation and/or hydrosilylation (Figure 18).^{145–148}

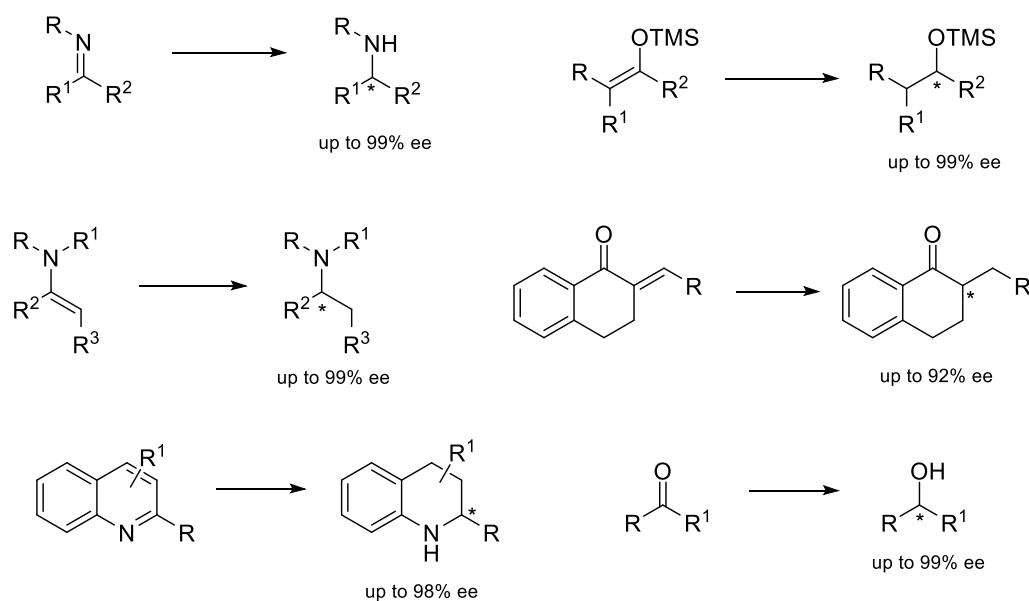
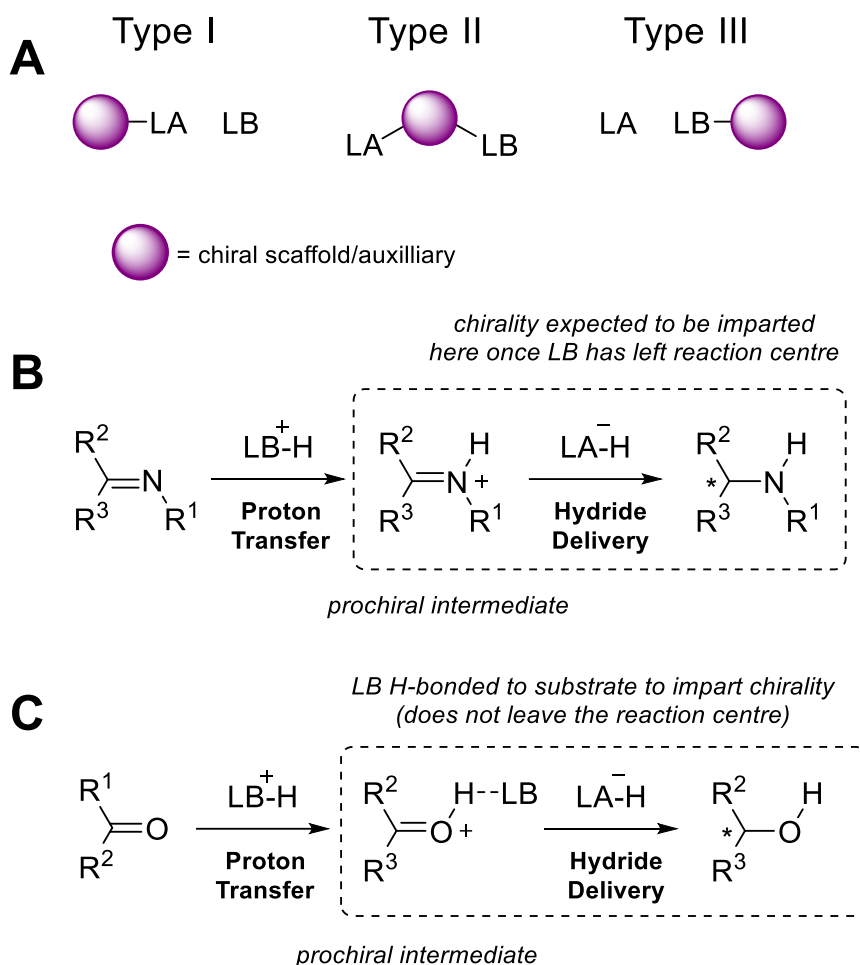


Figure 18. Select examples of substrates which have been asymmetrically hydrogenated by FLPs. (Figure adapted from Du 2023)¹⁴⁸

Chiral FLPs can be categorised in three ways: I) intermolecular FLPs containing a chiral LA and achiral LB, II) chiral intramolecular FLPs, and conversely III) intermolecular FLPs containing an achiral LA and a chiral LB (Scheme 21). The latter type III is by far the least developed, despite the relatively high number of chiral LBs, whilst conversely type I and II asymmetric catalysts have seen significant advances in the last 10 years. It is noteworthy that for the majority of substrates reported (imines and carbonyls) the proton transfer step does not create a chiral centre (Scheme 21). As a result, it is not clear whether a chiral LB would create high enantioselectivity for imines, which could explain its underdeveloped research.⁵¹



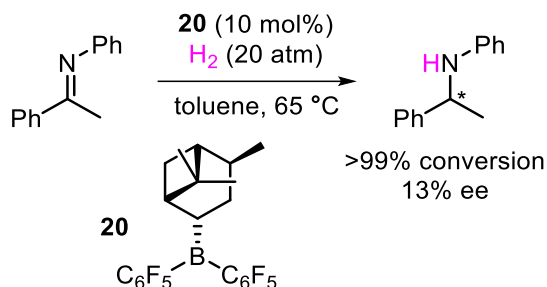
Scheme 21. A. General three categories of Chiral FLPs. B. General mechanism for the reduction of imines to impart enantioselectivity through the LA component. C. General mechanism for the reduction of ketones to impart enantioselectivity through the LB and/or LA component^{148,149}

There are two excellent recent reviews on asymmetric FLP reductions^{148,149} and whilst there are too many individual systems/catalysts to discuss, a selection of reports will be discussed here. This aims to highlight the three types of chiral FLP as well as the progression from limited to greatly improved enantioselectivity for various substrates.

Type I – Chiral LA

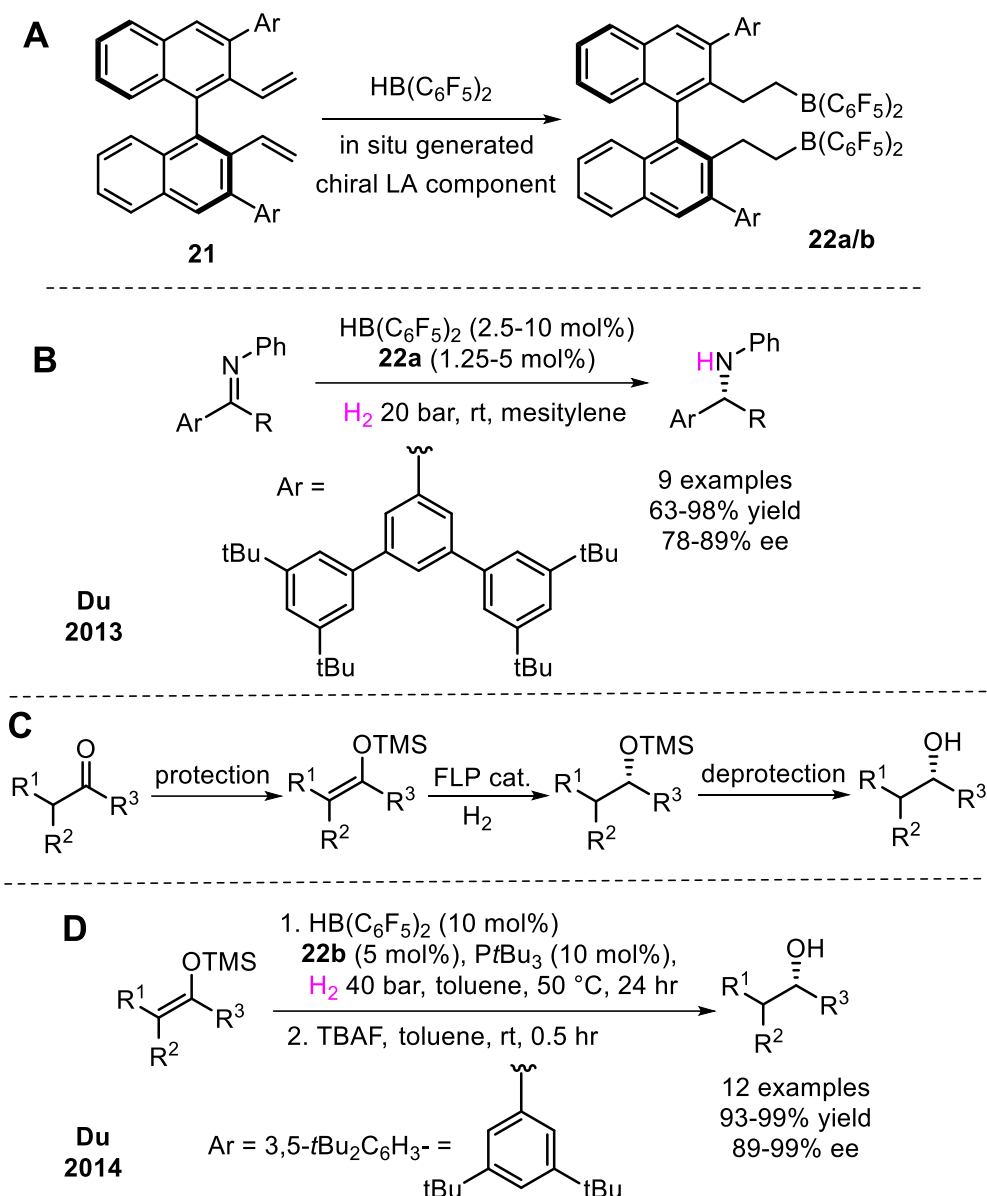
The first asymmetric hydrogenation using FLPs was reported in 2008, the same year as the first catalytic hydrogenation system. The asymmetric reaction involved the reduction of an imine to a chiral amine. Unfortunately, despite quantitative conversion, the reaction only proceeded with 13% ee. However, the poor enantioselectivity obtained

with catalyst **20** prepared from (+)- α -pinene presented the promising possibility of asymmetric hydrogenation (Scheme 22).¹⁵⁰



Scheme 22. First FLP catalysed asymmetric hydrogenation (catalysed by the chiral borane **20**).¹⁵⁰

Since this initial report, the majority of enantioselective FLP catalysis has involved developing chiral LAs. Type I systems in which the LA is bound to a chiral scaffold, have been dominated by R^*BAR_2 (where the aryl moieties are most often C_6F_5 or $p\text{-C}_6\text{F}_4\text{H}$). These type I chiral LAs have been synthesised by hydroboration between Piers' borane ($\text{HB}(\text{C}_6\text{F}_5)_2$) or the respective ($p\text{-C}_6\text{F}_4\text{H}$)₂ and a chiral auxiliary containing an alkene or alkyne.⁹⁰ One example of this came in 2013, when Du *et al.* developed an elegant way of screening new chiral FLP catalysts, which allowed them to explore a range of large sterically hindering aryl groups at the 3,3' positions of a chiral diene scaffold **22a/b** for the asymmetric hydrogenation of imines and silyl enol ethers (Scheme 23).^{151,152} This system interestingly formed the chiral LA borane component in situ, through hydroboration of the chiral diene scaffold with $\text{HB}(\text{C}_6\text{F}_5)_2$. They were able to use catalyst **22a** to successfully hydrogenate some aryl amines asymmetrically (9 examples). The yields obtained were good to excellent (63 – 98%) and the enantioselectivities were also good relative to the rest of the FLP field (78 – 98% ee). Du proposed using silyl enol ethers instead of ketones was a clever detour, which required protection/deprotection on either side of the hydrogenation. This catalytic system was extremely successful, and 12 examples of secondary alcohols were produced with excellent yields (93 – 99%) and very good enantiomeric excesses (89 – 99% ee).¹⁵²

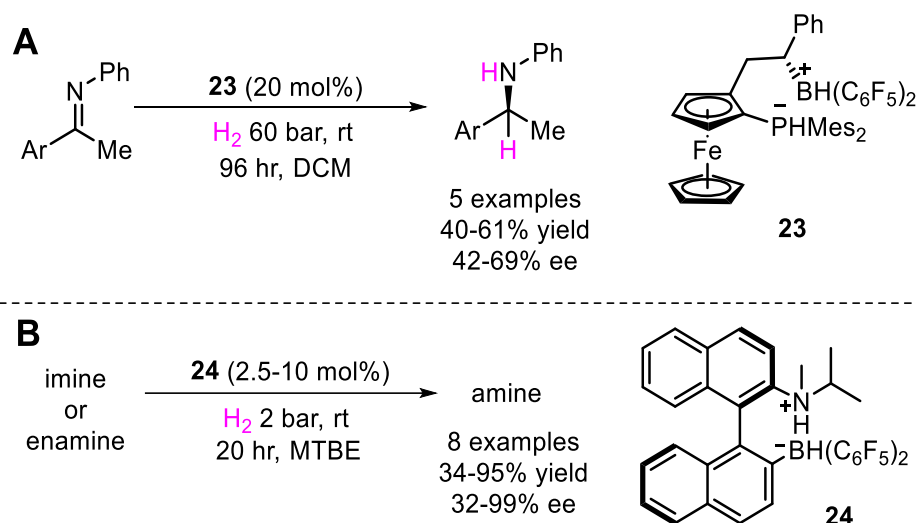


Scheme 23. **A.** General schematic of in situ generated chiral LA catalyst **22a/b**, **B.** Asymmetric hydrogenation of imines using chiral diene **22a**, **C.** Asymmetric hydrogenation of ketones via silyl enol ethers, **D.** Asymmetric hydrogenation of silyl enol ethers using chiral diene **22b**.^{151,152}

Type II – Chiral Intramolecular FLPs

Type II asymmetric catalysts, based on intramolecular FLPs, have also been developed (Scheme 24). These have been relatively successful in their achievement of asymmetric imine reduction. For example, the intramolecular chiral ferrocene based FLP catalyst **23** achieved moderate yields (40 – 61%) and moderate enantiomeric excesses (42 – 69%) (Scheme 24. **A**).^{153,154} Another intermolecular asymmetric FLP catalyst developed is the chiral aminoborane **24** built off a binaphthyl chiral scaffold (Scheme 24. **B**), similar to the

previously mentioned dienes screened by Du *et al.* This catalyst was able to hydrogenate 8 compounds which were a mix of imines and enamines with varying levels of success from poor to excellent yields (34 – 95%) and similarly varying enantiomeric excesses (32 – 99%).¹⁵⁵



Scheme 24. **A.** Asymmetric hydrogenation of imines using a ferrocene based intramolecular FLP catalyst^{153,154}, **B.** Asymmetric hydrogenation of imines/enamines using a chiral intramolecular aminoborane FLP catalyst.¹⁵⁵

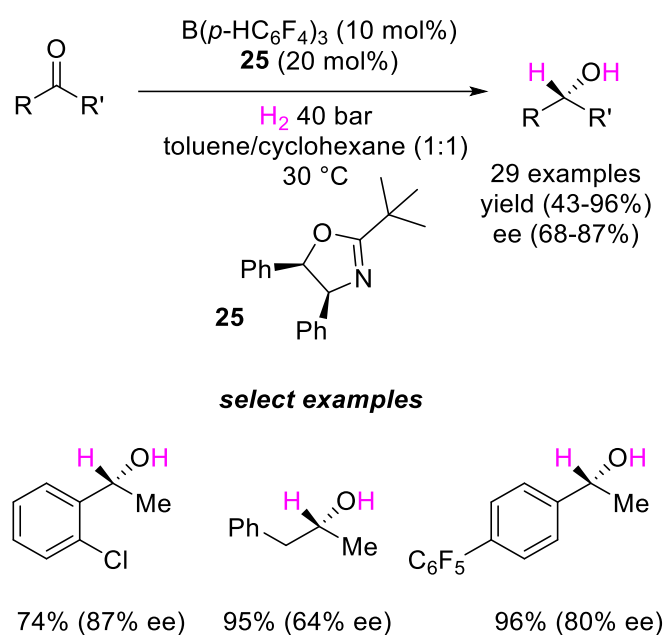
Type III – Chiral LB

For type I and II asymmetric FLP catalysts, chiral induction is highly controlled by the LA chirality. The challenging synthesis of these chiral LA components and the lack of chiral scaffolds currently exhibiting moisture tolerance restrict their use.

Chiral Lewis bases (LBs) are highly stable and commonly used as chiral ligands or catalysts for asymmetric catalysis in both academic and industrial settings. When it comes to type III catalysts, there are two primary challenges to consider. First, the outcome is dependent on the substrate, specifically whether the LB component is the lone pair of electrons on the substrate or an additional chiral LB. If the substrate is the active LB, then the chiral Lewis basic additive will not be involved, and the product will be racemic. The second challenge is related to the mechanism. In cases where the proton transfer occurs first, the LB may be released from the reaction centre, leading to minimal impact on the asymmetric induction. Ideally, the proton/hydride transfer should either be concerted,

the LB would not be released from the reaction centre through favourable intermolecular interactions (Scheme 21) or the proton delivery does create a chiral centre.

One of the few asymmetric hydrogenations achieved using type III chiral FLP catalysts is the recent publication by Du *et al.* in 2020. The group screened various chiral oxazolines (which are relatively weakly Lewis basic), to convert ketones to secondary alcohols. Through the use of chiral LB oxazoline **25** and $B(p\text{-HC}_6\text{F}_4)_3$ 29 alcohols were obtained in generally good yields (43 – 96%) and moderate to good enantioselectivity (68 – 87% ee) (Scheme 25). They found that ketones bearing electron-donating substituents at either the aryl group or heteroaryl-substituted ketones were not tolerated in the system catalytic system, whilst electron withdrawing group were well tolerated. It is noteworthy that whilst dialkyl ketones were tolerated the enantioselectivity appeared to drop marginally compared to aryl-alkyl ketones (50 – 75% ee).^{147,156}

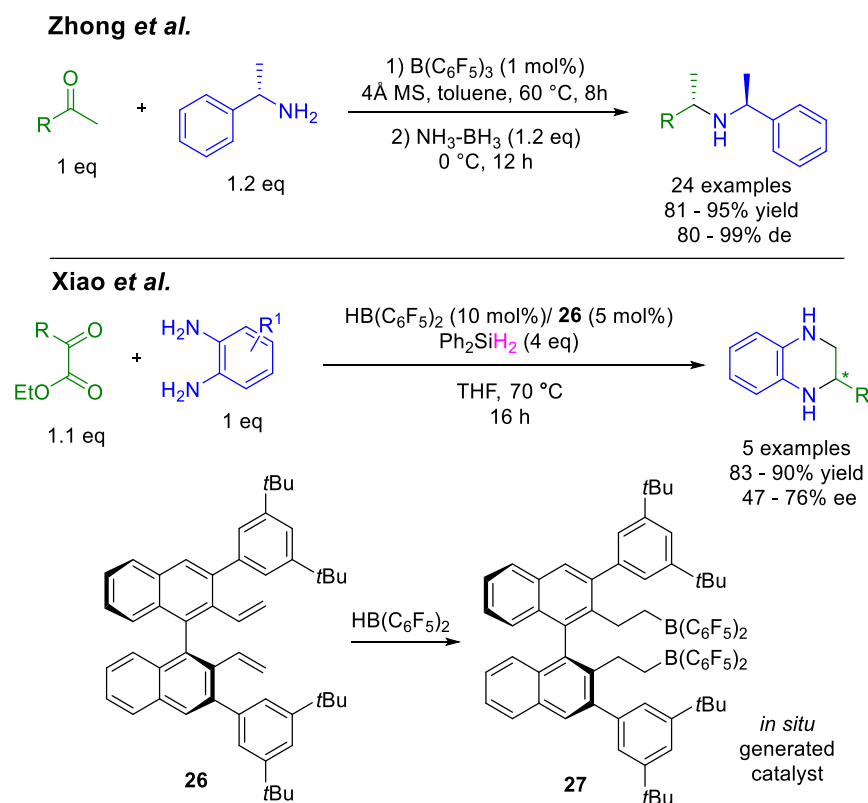


Scheme 25. Asymmetric hydrogenation of ketones using a chiral LB oxazoline **25** and $B(p\text{-HC}_6\text{F}_4)_3$.^{147,156}

Enantioselective Reductive Aminations

Limited work has taken place to develop asymmetric reductive amination examples. Zhong and co-workers reported using ammonia borane (NH_3BH_3) as the reductant to

perform a BCF-catalysed diastereoselective reductive amination of ketones using α -methylbenzylamine (α -MBA) (Scheme 26). The system showed a broad substrate scope tolerance with excellent yields for both aryl-methyl ketones and alkyl-methyl ketones (81 – 95% yield, 80 – 99% de).¹⁵⁷ Xiao and co-workers who had reported a racemic synthesis of tetrahydroquinoxalines (Scheme 26), adapted their previous work to allow for the use of *in situ* generated chiral borane **27**.³⁵ Their system tolerated a small range of alkyl substituents on the α -ketoester however, the best enantioselectivity was achieved with the one aryl substituent (R = Ph, 83% yield, 76% ee). Unlike Zhong *et al.* this system used silanes as the reductant. At the time of writing, an asymmetric FLP catalysed reductive amination using hydrogen has not been achieved.



Scheme 26. Examples of asymmetric reductive aminations catalysed by FLPs. Zhong *et al.* employed the chiral auxiliary, α -methylbenzylamine (α -MBA), using ammonia borane as the reductant.¹⁵⁷ Xiao *et al.* devised a system for the asymmetric synthesis of 2-substituted-1,2,3,4-tetrahydroquinoxalines via FLP-catalysed reductive amination using silanes as a hydride

source.^{145,151}

Future Developments for Asymmetric FLP Catalysis

Overall, the FLP chemistry discussed provides a promising approach for metal-free asymmetric reduction of unsaturated compounds. Despite these advances, the substrate scope for asymmetric FLP borane catalysed hydrogenation remains limited (most developments so far have been limited to imines as substrates with some select examples expanding research into ketones and some heterocycles), and the level of asymmetric induction could be improved. Further advances could be achieved by synthesis of more moisture tolerant chiral boranes, more systematic screening of chiral Lewis bases or the combined use of chiral boranes and chiral LB. Nevertheless, the current pioneering work lays the foundations and presents the potential for improved asymmetric FLP hydrogenation catalysis, which will ultimately remain a major aim in the field.¹⁴⁵

It has been hypothesised by multiple established chemists in the field that the goal is to develop an FLP system where both the LA and the LB are chiral.^{83,90} The purpose of this is to create a chiral pocket between the two sites which will enable high degrees of enantioselectivity (Figure 19).⁹⁰

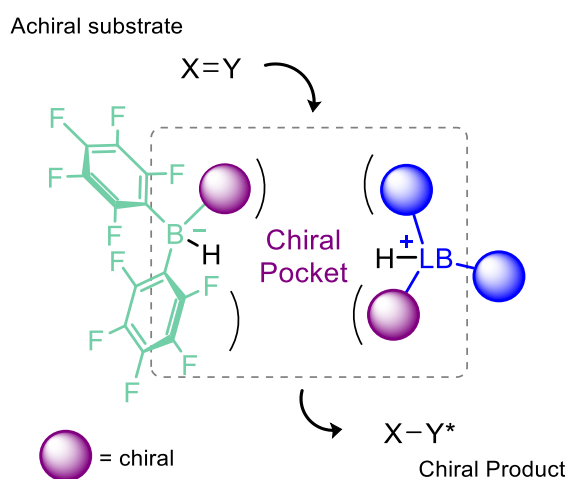


Figure 19. Graphical representation of the proposed chiral pocket that would be created through the cooperative use of a chiral LA and chiral LB leading to high enantioselectivity.

(Figure reproduced from Melen et al.)⁹⁰

1.4 FLP-borane Hydrogenations in Continuous Flow

1.4.1 General Introduction to Flow Chemistry

Continuous flow chemistry is an alternative approach to performing chemical reactions. It is a technique that has gained significant attention in recent years, particularly in industry, due to its ability to facilitate automation and scale-up.^{158–160} A typical continuous flow system consists of various basic and complex components, which can be installed or removed in a telescoped process, with endless customisation for extremely bespoke systems (Figure 20).

A basic system will contain one or more stock solutions, which can allow starting materials, catalysts and other reagents to be stored separately. Each stock solution will be delivered to the flow system typically by an individual pump. The stock solutions will first reach a mixer which is the opportunity for gas to be introduced, should it be required, and for the stock solutions to be mixed. These mixers can be staggered if reagents need to be added sequentially and the time between additions can be staggered through altering the length of tubing in between. Once the reaction mixture has been created through the mixing of respective stock solutions and the possible introduction of gas, the mixture will be passed through the flow reactor under the desired reaction conditions. These will be controlled by a heater/cooler whilst pressure, where gas has been introduced, will be controlled by back pressure regulation. In basic systems the reaction mixture can be collected at the end of the flow system for analysis and purification.^{161,162} Flow chemistry is a complex field that can be a costly and time-consuming process to optimise and perform. Therefore, it must be significantly advantageous to carry out a transformation in flow rather than batch to justify the investment.¹⁶⁰

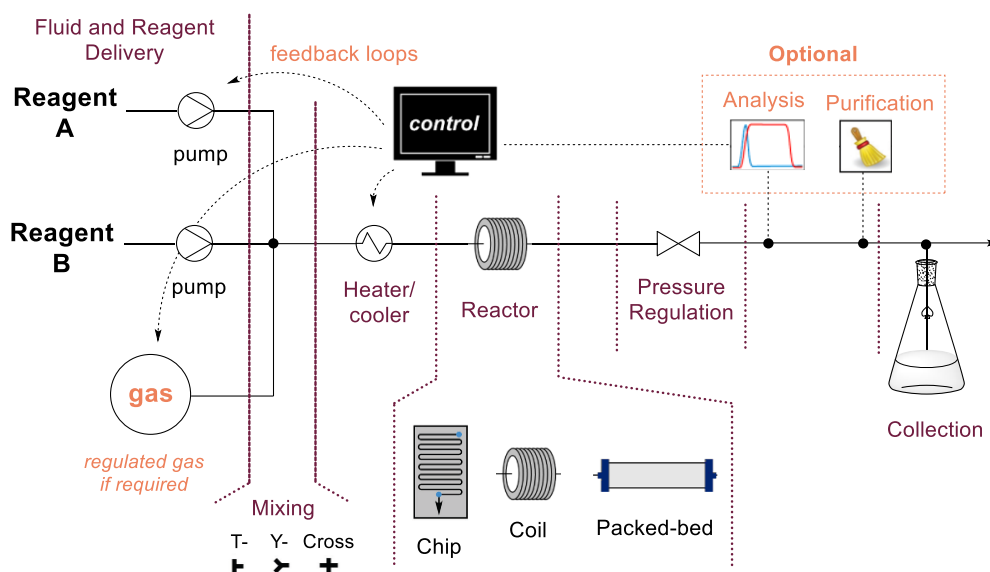


Figure 20. Breakdown of the basic components that can be used in a bespoke continuous flow system including some optional parts.^{159,160,162}

For reactions performed in flow, it is important to note that the traditional term "reaction time" is not the correct way to determine the progress of the reaction. Instead, the term "residence time," which is calculated using Equation 3 should be used. In flow chemistry, longer residence times (and therefore longer reaction times) can be achieved by either decreasing the flow rate of reagents or by increasing the length of the system. The length of the system can be increased simply; by increasing the length of tubing in between the components of the flow system or using larger reactors with increased volume. The progression of the reaction is no longer based on time, but rather on the point at which the reagents are located in the telescoped flow system.

$$\text{residence time} = \frac{\text{volume of the system}}{\text{flow rate of the system}} \quad (3)$$

Equation 3. The equation to calculate residence time in a flow system.¹⁶⁰

1.4.2 Advantages to Hydrogenations in Flow

Flow chemistry hydrogenation is well established as a tool for "fine" chemical synthesis of industrially targeted compounds (Figure 21), which include active pharmaceuticals, agrochemicals, electronic chemicals and fragrances.^{158,163–169} In hydrogenation the hydrogen is delivered either by gas cylinder or from electrolysis of water. It is then subsequently mixed in with the stream of the respective substrate(s) (Figure 20).¹⁶⁰ Flow

chemistry hydrogenations possess many advantages over their batch counterparts. For example, flow chemistry hydrogenations are often favoured as they have superior gas-liquid contact compared to traditional hydrogenations which are limited by the gas diffusion rate into the reaction solvent.¹⁶⁴ In flow reactions, the ratio of headspace to solvent is lower. By pressurising the reactor, the solubility of the gas in the solution is increased. Small-scale pressurised batch reactions are possible and are standard in academic labs, but it is sometimes not possible or safe to conduct preparative-scale reactions in batch.¹⁶⁰ Hydrogen is also highly flammable and has the potential for exothermic detonation, which makes it a significant safety risk. As most hydrogenations require high pressures, the risk is significantly increased.¹⁷⁰ This safety concern multiplies exponentially when scaling up reactions in batch especially, whilst the continuous flow safety concerns remain constant.¹⁷¹

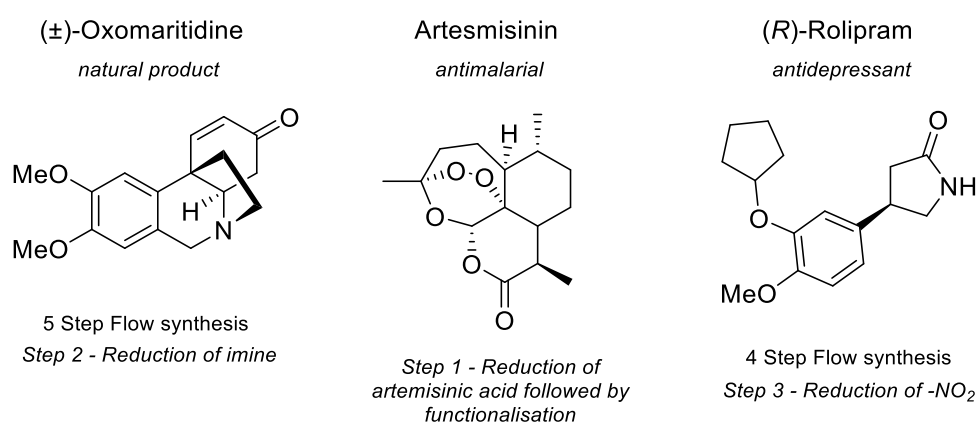
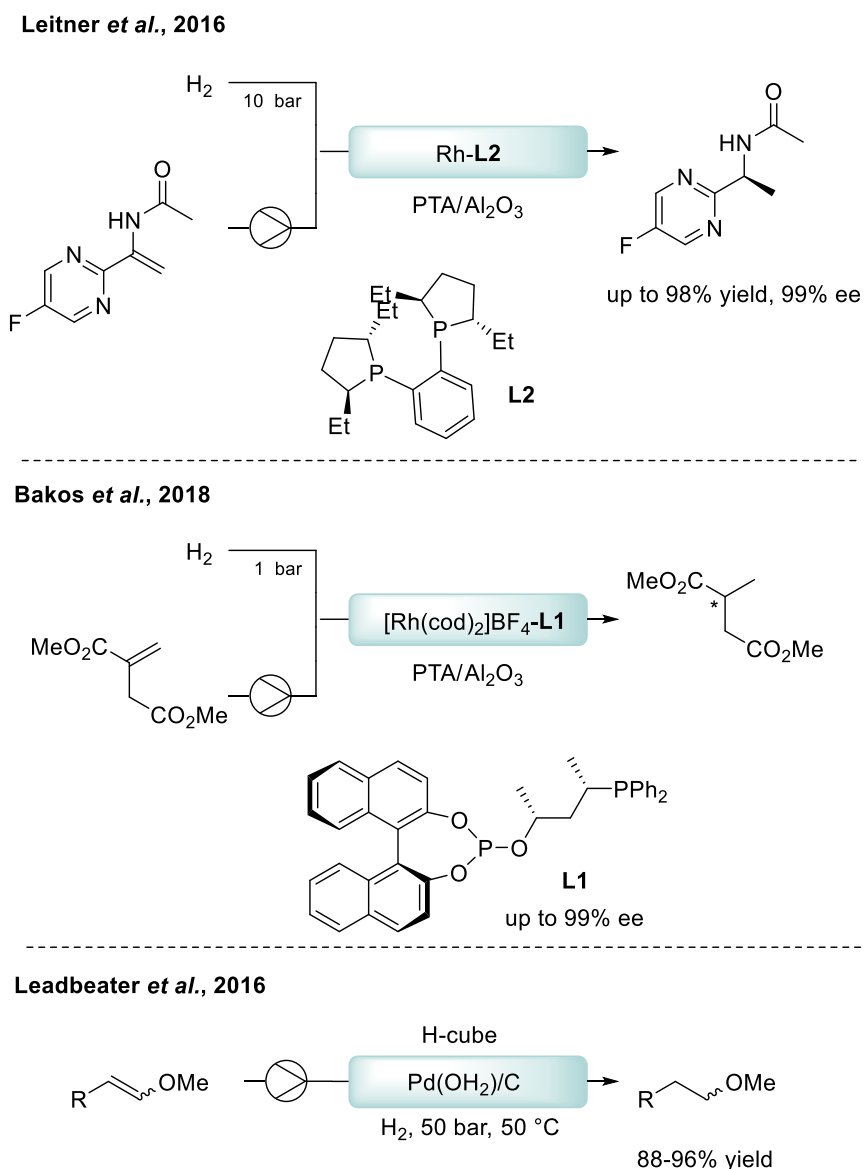


Figure 21. Select examples of industrially relevant “fine” chemical compounds produced completely by flow chemistry and incorporating a hydrogenation step.¹⁷²

Flow chemistry offers several other advantages over batch chemistry. Firstly, it provides better reproducibility since it involves little external manual interaction. Secondly, reactions can be faster because high temperatures and pressure can be reached and maintained, thereby increasing the reaction kinetics, and accessing the forcing conditions often required for hydrogenations. Flow chemistry can also ensure high chemoselectivity because it allows for precise control over temperature-dependent products by maintaining narrow temperature windows throughout the flow reactor. It also provides a broad range of access to *in situ* and in-line reaction monitoring. Lastly, it allows for the integration of niche-enabling technologies such as photochemistry and electrochemistry.^{159,160,173}

1.4.3 Solid-supported Catalysts in Flow

The use of heterogeneous catalysts in continuous flow is also a well-established practice (Scheme 27). In flow chemistry, packed bed reactors are commonly used when working with heterogeneous/ solid-supported catalysts (Figure 20). This type of reactor is perhaps one of the most important advantages to flow chemistry hydrogenations over batch. Firstly, it provides a significantly higher effective molarity of the catalyst/reagent, which decreases residence times. Secondly, the catalyst/reagent is contained within a column, which eliminates the need for a subsequent separation step of the reaction mixture from the catalyst.^{160,169} However, continuous heterogeneous catalysis in a packed bed reactor can be challenging, especially for immobilised transition-metal catalysis, where leaching of the catalytic material can occur, resulting in contamination of the product and deactivation of the column.^{160,174} The scope of flow chemistry hydrogenations has also been expanded to include the use of immobilised asymmetric catalysts for enantioselective hydrogenations (Scheme 27). This is extremely valuable to industry as extremely time and resource-expensive catalysts can be easily separated from your product and recycled.^{158,175}



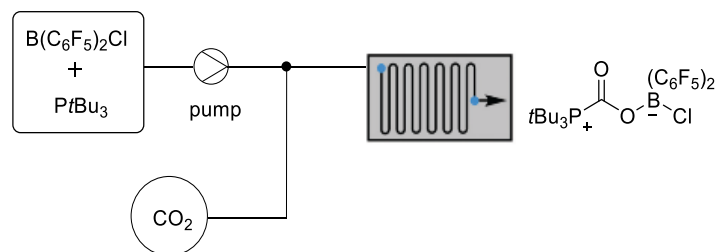
Scheme 27. Select examples of heterogeneous hydrogenation systems optimised in continuous flow.¹⁷⁶ Top. The enantioselective reduction of API enamide.¹⁷⁷ Middle. The enantioselective reduction of dimethyl 2-methylenesuccinate.¹⁷¹ Bottom. The reduction of aryl vinyl ethers.¹⁷¹

1.4.4 Boranes in Flow Catalysed Reactions

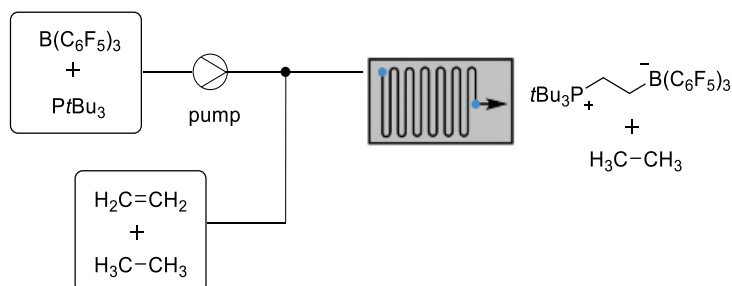
Boranes also have the potential to be embedded into a solid support within a packed bed reactor or catalyst cartridge and as a result, LA-catalysed reactions in flow could occur heterogeneously. There are numerous examples of heterogeneous and homogeneous general LA-catalysed transformations such as Diels-Alder reactions and Friedel-Crafts acylations which have been carried out in flow.^{178–181}

However, there are much fewer examples of boranes application as FLP catalysts in flow. So far and to the best of our knowledge, there are only 3 examples^{182–184} of homogenous borane catalysis applied in flow and as a result, there is a definite requirement for more research into this area for it to become efficient and versatile.¹⁸⁵ Stephan and Kumacheva reported the first proof-of-concept example of FLP chemistry in continuous flow in 2014. They investigated the capture of CO₂ by the FLP PtBu₃/ClB(C₆F₅)₂ in continuous flow and reported that the use of flow chemistry was beneficial due to *in situ* monitoring and the improved control over gas–liquid interfaces, something which is extremely challenging and time consuming to control in batch reactors. Stephan *et al.* were able to employ a microfluidic platform with well-defined interfacial areas achieved in gas–liquid segmented flows to ensure the best control over CO₂ diffusion in a far superior way to what is possible in batch.¹⁸⁶ A year later the same collaborative team reported a similar seminal system using the FLP a PtBu₃/B(C₆F₅)₃ to separate ethane from ethylene under continuous flow conditions. This is because of the FLP's ability to react with ethylene whilst it is unreactive towards the alkane (ethane) (Scheme 28).^{187,188}

Kumacheva and Stephan *et al.* 2014



Kumacheva and Stephan *et al.* 2015



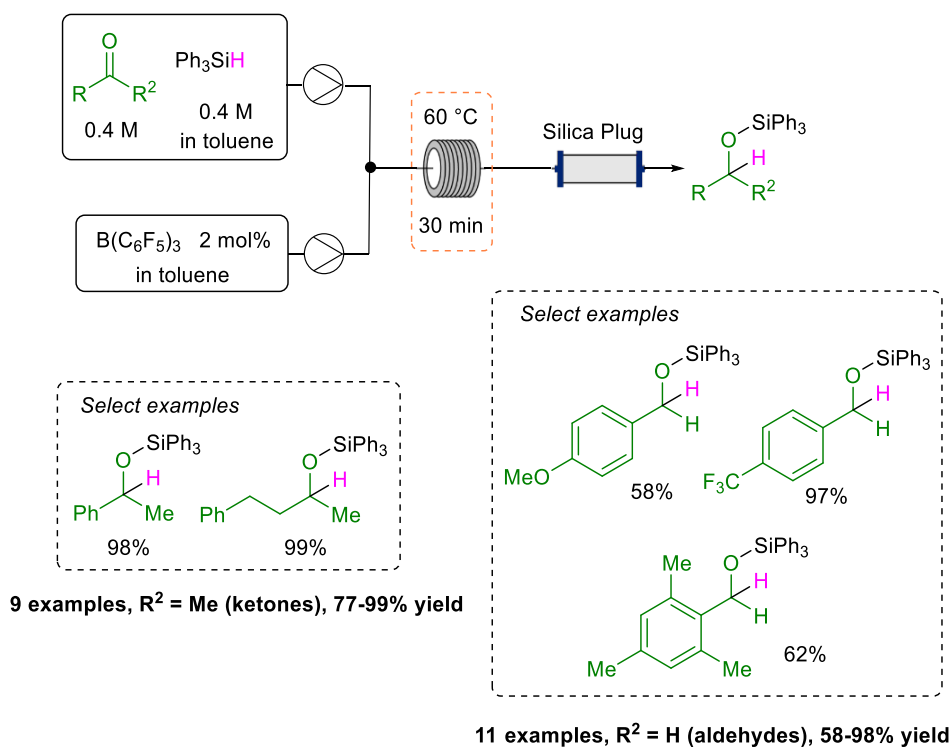
Scheme 28. The first examples of FLP catalysed small molecule activation in continuous flow.^{186–}

188

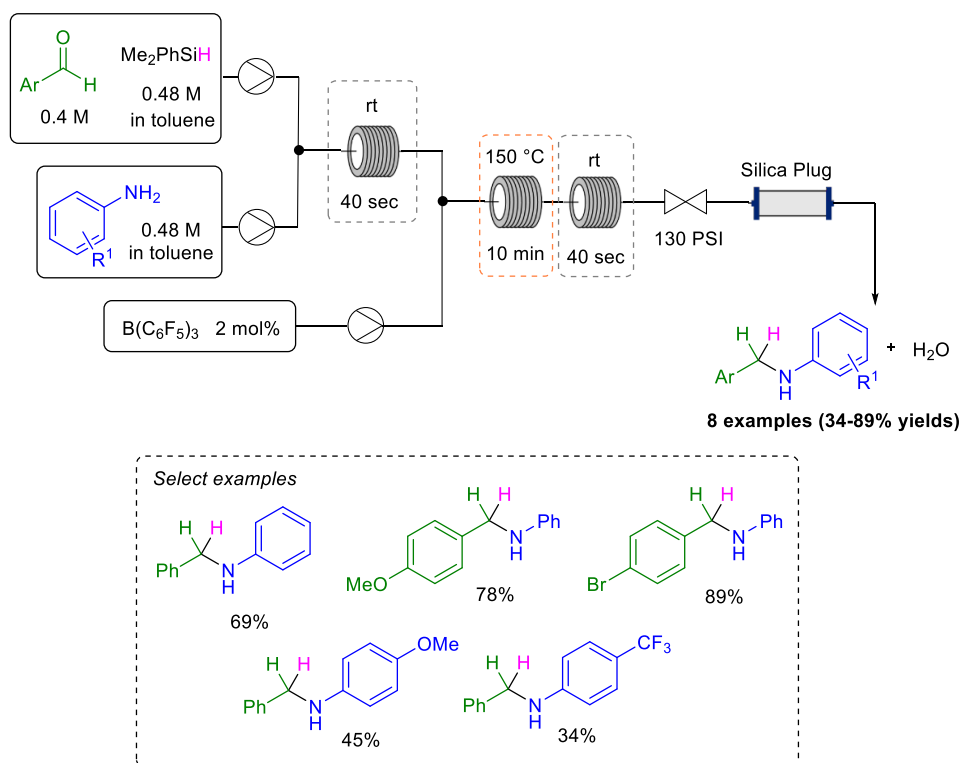
Collaboration is key when combining two complex fields such as FLPs and flow chemistry. As a result, the only other reported publication using FLPs as catalysts in continuous flow

arose from the collaboration between Melen and Browne groups in 2017. This seminal piece of work provided optimised conditions to perform BCF-catalysed hydrosilylations of aldehydes and ketones (20 examples, 58 – 99% conversion, Scheme 29). Whilst the majority of aldehydes and ketones progressed in excellent conversions relatively low conversion were observed for the respective ketone and aldehyde featuring the activating *p*-MeOC₆H₄ on the aryl group. They claimed that this is further evidence that a deactivated aldehyde or ketone is beneficial to facilitate effective hydride transfer.¹⁸⁴

Crucially as part of this work, Melen *et al.* reported an optimised system to perform reductive aminations using silanes also catalysed by BCF (2 mol%) (Scheme 30). Here an imine, synthesised through a condensation reaction between the aldehyde with an aryl amine, was telescoped towards a BCF-catalysed reduction at 150 °C. They were able to monitor 8 secondary amines in poor to excellent conversion (34 – 89%). The system particularly struggled with strongly electron withdrawing or donating groups on the aniline reagent (*p*-OMe = 45%, *p*-CF₃ = 34%). When comparing the synthesis of one of the secondary amines produced by this reaction in batch the yield after thirty minutes was only 17%, whilst the optimised flow system could yield the product in a 78% yield in only 15 minutes.¹⁸⁴



Scheme 29. BCF-catalysed hydrosilylations of aldehydes and ketones in continuous flow.

Scheme 30. BCF-catalysed reductive amination using silanes performed in continuous flow.¹⁸⁴

At the time of writing, FLP-catalysed hydrogenation using H_2 as the reductant in continuous flow has not been achieved. However, this presents a great opportunity for the advantages of flow chemistry to be utilised, and these two fields will likely combine

in the near future. I believe that the application of FLP-catalysed hydrogenations in continuous flow is crucial for the industrial use of FLPs. This is especially true if the metal or organic LA catalysts developed could be applied in a heterogeneous manner within a packed bed reactor.

1.5 Conclusions

In this introduction, I have described Frustrated Lewis Pairs from their discovery in 2006 to the most recent advances such as asymmetric reactions and reactions performed in flow. This review of the field, with a particular focus on FLP-boranes (the prototypical FLP system), evidenced that FLP-boranes can compete in some instances with transition metals, but also that some further advances are required for FLP to be adopted in industrial processes. Most significant limitations include moisture sensitivity, poor asymmetric induction, and lack of development of flow hydrogenation reactions.

My work on this project will aim to provide some of these necessary advances mentioned above. Initial focus will aim to apply known moisture tolerant boranes to perform novel reductive amination reactions. I aim to expand the scope of FLP-catalysed reductive aminations to include alkyl amines and cyclic substrates, with a specific focus on producing α -substituted pyrrolidines.

The second aim will be to develop the first proof-of-concept reductive amination in continuous flow using hydrogen. My work in batch will help us establish conditions for a reductive amination using hydrogen, which is valuable for catalyst comparison allowing us to select the most appropriate catalyst for creating a continuous flow system.

My final aim will be to synthesise novel moisture tolerant boranes for application in flow or batch. Examples of heterogeneous FLP boranes are extremely limited due to their challenging synthesis. Unfortunately, the heterogeneous FLPs that have been made are often moisture sensitive, leading to low conversions. Therefore, there is a significant demand for progression in this area of FLP research. As a result, my novel moisture tolerant FLP boranes will employ the size-exclusion principle and will be designed for potential future adherence to a heterogeneous / solid-support.

Chapter Two: Synthesis of Known Moisture-tolerant Boranes

2.1 Introduction

2.1.1 Context and Aims

As highlighted in section 1.3.1 a successful borane based FLP hydrogenation is a complex balancing act of steric and electronic modifications. Moreover, aiming to perform reductive amination reactions, which generate one equivalent of water as by-product, the use of moisture tolerant FLP boranes as catalysts seemed obvious.^{115,189} For example, at 1 mol% borane catalyst loading, there would be as much as 100 equivalents of water with respects to the borane catalyst and as a result, it is crucial that the boranes chosen should be able to perform under these conditions. The key properties of boranes which must be finely tuned to attain optimal reactivity can be summarised as:

- *Hydride affinity*: both allowing for the activation of hydrogen but also crucially the subsequent delivery to a substrate.
- *Moisture tolerance for catalytic reactivity and bench stability*: balancing steric hinderance for protection from decomposition with substrate scope compatibility.
- *Incorporation of synthetic handles*: to further functionalise the organoborane and allow for post-modification to incorporate intramolecular FLP character or adhere the catalyst to a solid support.

Since FLP catalysis is such a young field of research the shift to improve synthetic routes has been broad and is far from completely established. Triaryl boranes have the potential for greatly improved water resistance and greater reactivity due to the fine-tuning of steric and electronics properties in three aryl moieties. This project has focused on the synthesis of triaryl boranes, which have been developed for reductive aminations with moisture tolerance in mind.

2.1.2 Choice of Target Moisture-tolerant Boranes

Our initial goal was to select known moisture-tolerant boranes for synthesis, aiming to gain hands-on experience and replicate existing literature. FLP catalysis is challenging due to their oxophilic nature, requiring excellent mastering of synthetic techniques. Replicating literature synthesis methods would help us improve our skills and explore new synthetic routes, which could then be applied to the synthesis of novel FLP borane.

Significant progress has been made in developing moisture-tolerant triaryl boranes that have proven suitable for reductive aminations in the presence of water. Two main strategies have been employed since 2012: mitigating electron deficiency from the boron centre and using a size exclusion approach to hinder binding to the LA boron centre. The introduction of large *ortho*-chlorines has been particularly effective in satisfying steric requirements. Work from Soós and co-workers,^{190–193} Stephan *et al.*,^{194–196} Ingleson *et al.*,^{34,197} and Hoshimoto *et al.*³⁷ on expanding water tolerant FLP has explored the varied aryl substituents electronic and steric effects leading to a range of moderate to successful water tolerance, with multiple ‘bench stable’ catalysts. These literature readings led to a choice of four known water-tolerant boranes **16a/b**^{37,190} and **19a/b**¹⁹⁸ (Figure 22).

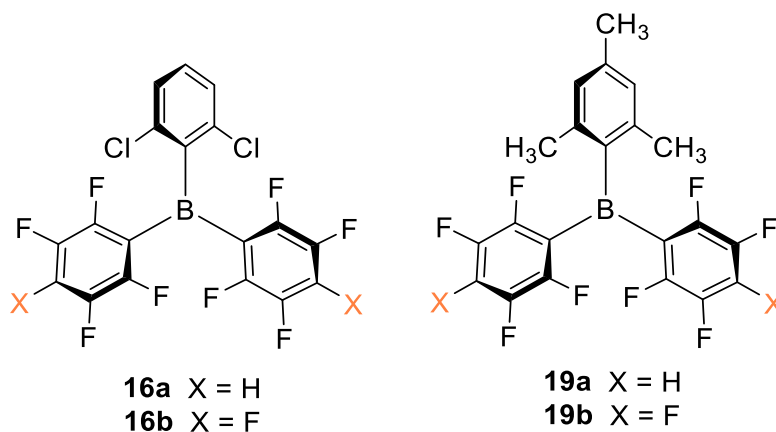


Figure 22. Chosen known moisture-tolerant boranes to be synthesised as part of this project.

The boranes selected are considered to be the best catalysts for reductive aminations/imine reductions. They are easily accessible from common and affordable starting materials and allow for the comparison of the ‘size-exclusion’ principle using *ortho*-chlorines or methyl groups. Minor changes in electronics, such as altering the

para-positions (H or F), can impact catalytic activity. Similar minor changes were found to have an impact of up to 5% in the measurement of Lewis acidity, as discussed in section 1.3.1.2.

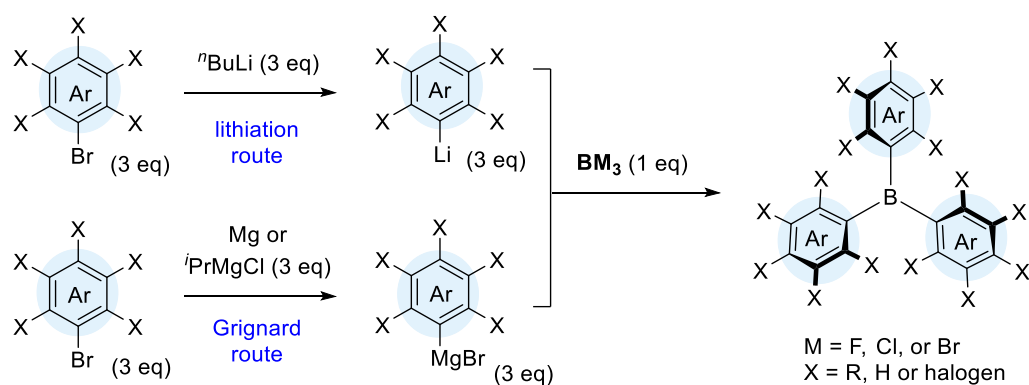
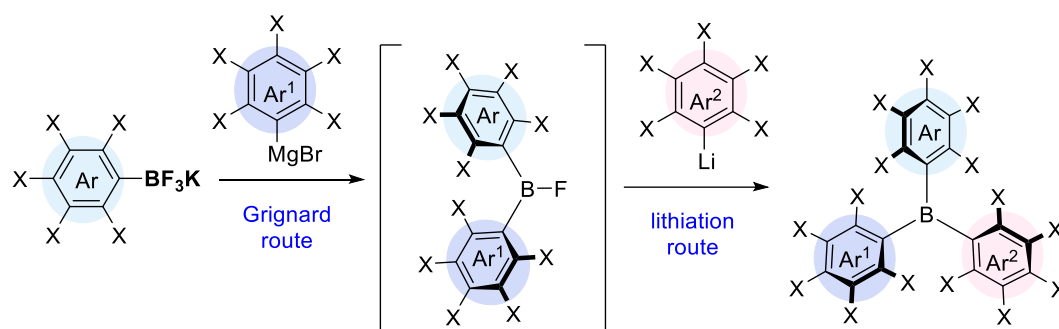
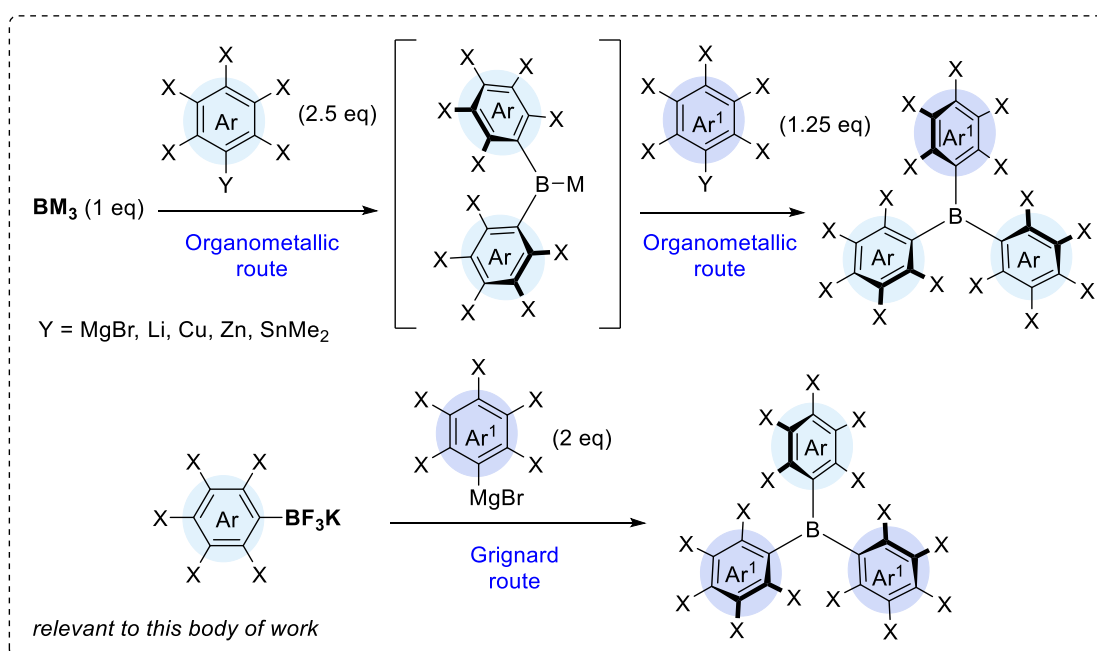
2.1.3 Brief Overview of Triaryl Borane Synthesis

Various synthetic routes have been probed for the synthesis of triaryl boranes since the first reported synthesis in 1885.¹⁹⁹ The synthetic methods to make halogenated triaryl boranes were covered extensively in two key reviews.^{94,200} Triaryl boranes can be classified as homoleptic, where all the aryl rings are identical, or heteroleptic, where the aryl rings are not identical. Our chosen triaryl boranes, **16a/b** and **19a/b**, are examples of heteroleptic triaryl boranes.

The synthesis of homoleptic triaryl boranes is very well reported and has been dominated by the reaction of BM_3 ($M = F, Cl, \text{ or } Br$) with analogous aryl lithium or Grignard species (Scheme 31).²⁰¹ This metal-boron exchange is the most widely used method to synthesise triaryl boranes, especially using BF_3 as the boron source with Grignard or organolithium reagents. There are also examples of nickel, mercury, zinc, copper, silicon and tin reagents having been employed for triaryl borane synthesis.²⁰²

This method can be adapted for the synthesis of heteroleptic triaryl boranes through the sequential addition of varied aryl organometallic reagents in their desired equivalents (Scheme 31). Our first attempt to synthesise our chosen moisture-tolerant boranes was an attempt to follow this synthetic approach.

Alternatively, aryltrifluoroborates ($ArBF_3K$ salts) can be employed as boron sources (Scheme 31), a method which quickly became a popular due to its simplicity, scalability, and potential for high yields. This methodology has also become a favoured synthetic route in the FLP field to provide rapid libraries of various heteroleptic borane derivatives on a large scale from easily accessible fluoroborates and commercially available halogenated arenes.^{120,190,192,203}

Homoleptic triaryl boranes**Heteroleptic triaryl boranes**Scheme 31. Established synthetic routes for homoleptic and heteroleptic triaryl boranes.^{201,202}

2.2 Results and Discussion

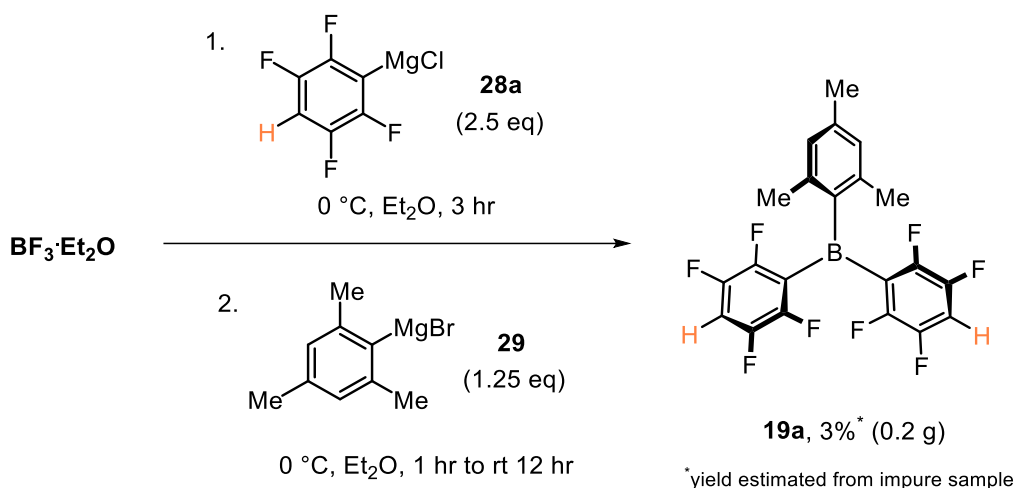
2.2.1 Synthesis of Known Triaryl Boranes

2.2.1.1 General Information for Triaryl Borane Synthesis and Purification

Due to the water sensitivity of the triaryl borane products, all reactions were performed under an inert atmosphere using Schlenk line apparatus. Solvents were removed under vacuum using a trap and Schlenk line apparatus. Oven-dried glassware, and anhydrous solvents were essential, and all products were placed under inert atmosphere and then stored in a glove box. Manipulation of the products, such as weighing, and NMR sample preparation was carried out in a glovebox and anhydrous solvent/J-Young NMR tubes were used for all samples unless stated otherwise. It can be assumed that the techniques employed have been acquired through trial and error following *The Schlenk Line Survival Guide*, which has been an invaluable resource for me in this project,²⁰⁴ especially as the glovebox used during this project was only available for storage and weighing. This is something that is too often not discussed in FLP papers and supporting information, where access to a glovebox is taken for granted or the creative ways required to overcome challenging purifications are not discussed. Section 2.2.1 will contain findings that have allowed me to establish procedures for application to novel boranes and will hopefully provide help for future project students in my research group.

2.2.1.2 Initial attempts

The successful synthesis of mesityl-substituted boranes, **19a/b**, was first achieved in 2012 by Soós *et al.* Following the sequential addition of 2.5 equivalents of Grignard **28a** and 1.25 equivalents of **29** to boron trifluoride etherate ($\text{BF}_3 \cdot \text{OEt}_2$), Soós was able to isolate **19a** in yields ranging from 20 to 30%.¹⁹⁸ Unfortunately, poor yields (1 – 3%) of impure **19a** were obtained on our first attempts at this route (Scheme 32).



Scheme 32. First attempted synthetic route to mesityl substituted borane **19a** following the sequential Grignard route.

Initially, these yields were equated to our inexperience and/or poor technique. Particularly we believed this was due to our inexperience in performing hot decantations with hexanes via cannula filtration.²⁰⁴ Without access to custom glassware, containing sintered glass frits, we were forced to be more creative with our filtration and decantation steps (Figure 23). Whilst these techniques are known and established, they do require experience to be performed effectively and to extract optimal yield. I found, however, that much of our yield was being lost after this decantation.

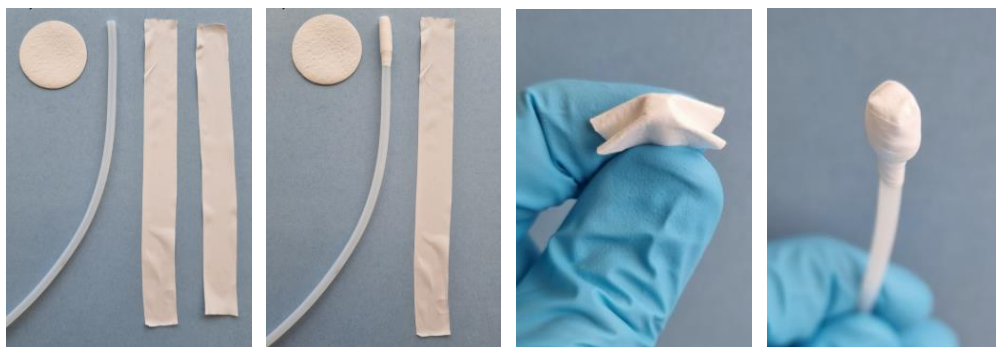


Figure 23. General preparation of a filter cannula using PTFE tape and filter paper.²⁰⁴ (Note: Metal cannulas were more often used during this project so they could be oven-dried and purged with Argon whilst cooling)

Following hot decantation, the filtrate was then concentrated to approximately 10% of its volume, by which point a white precipitate crashed out of the yellow solution. This yellow solution was then filtered off and the white solids were washed with further hexanes with the aim of furnishing the pure product after drying under vacuum. At this stage, it was found that, the majority of the desired product was being lost in the hexane

washes, as **19a** appeared to be extremely soluble in hexanes (even when cooled to 0 °C). As a result, too many washes removed much of our product, whilst conversely too few washes left behind quenched or homo-coupled unreacted Grignard as well as the decomposed borane side product ($\text{Ar}_2\text{B-OH}$), which could be seen in the ^{19}F and ^{11}B NMR spectra respectively (Figure 24). Ultimately, after some repeated attempts the best efforts gave an impure sample (200 mg) of borane **19a** in ~3% yield (with 8% by weight $\text{Ar}_2\text{B-OH}$ considered). At this point, I decided to abandon this route and explore an alternative option to access our chosen catalysts.

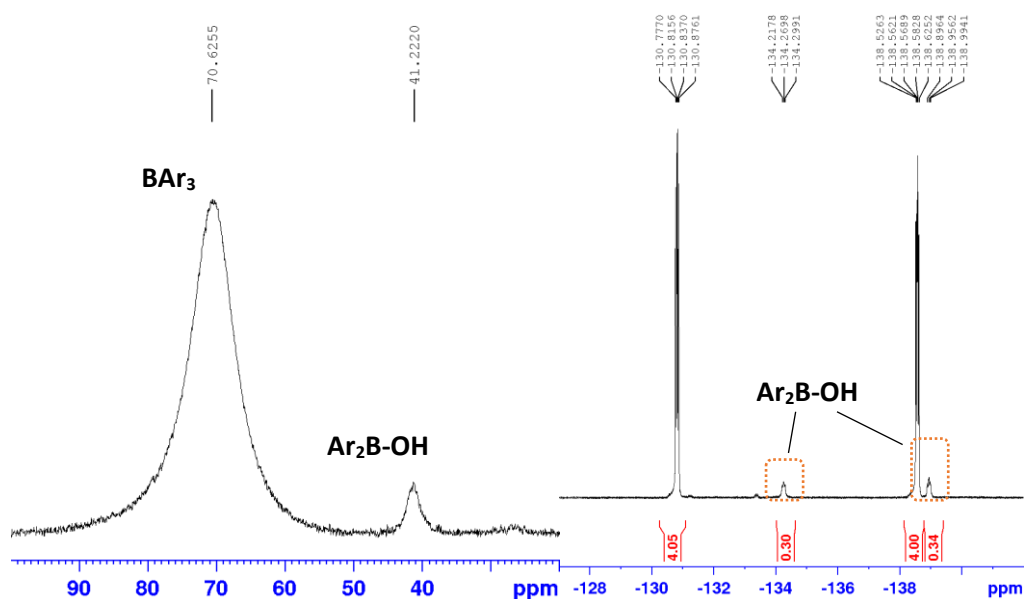
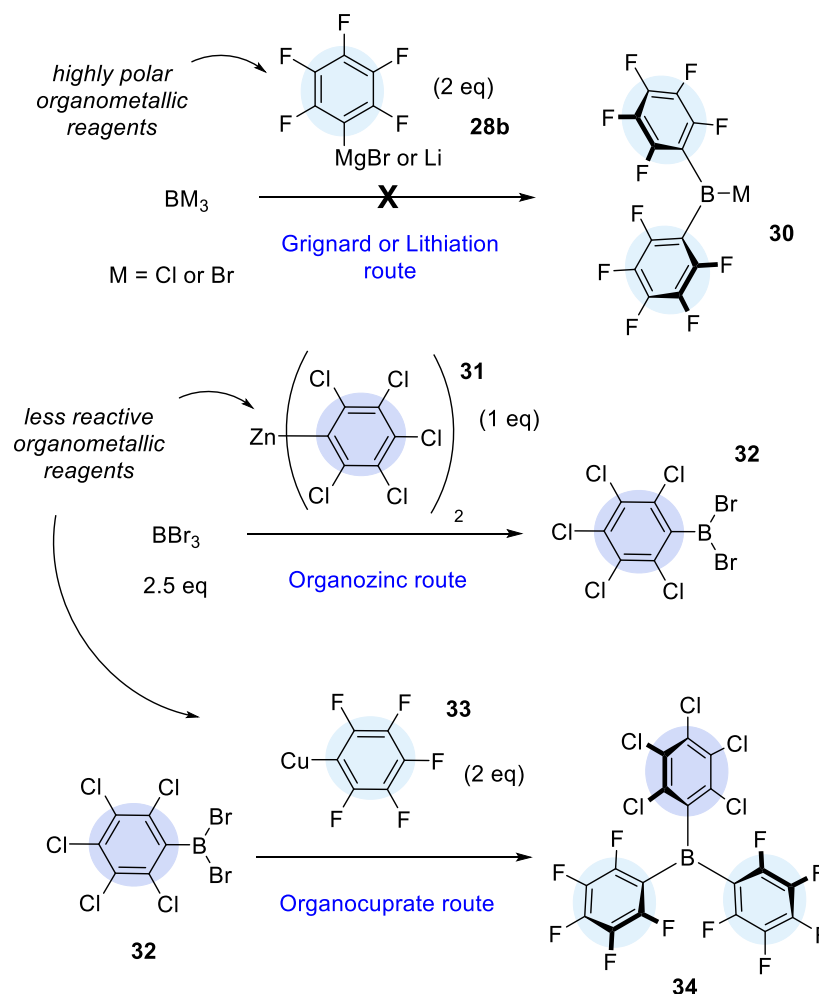


Figure 24. Best ^{11}B NMR spectrum (Left) and ^{19}F NMR spectrum (Right) of 'pure' **19a** after hexane washes. Further washes removed more product than decomposition side product.

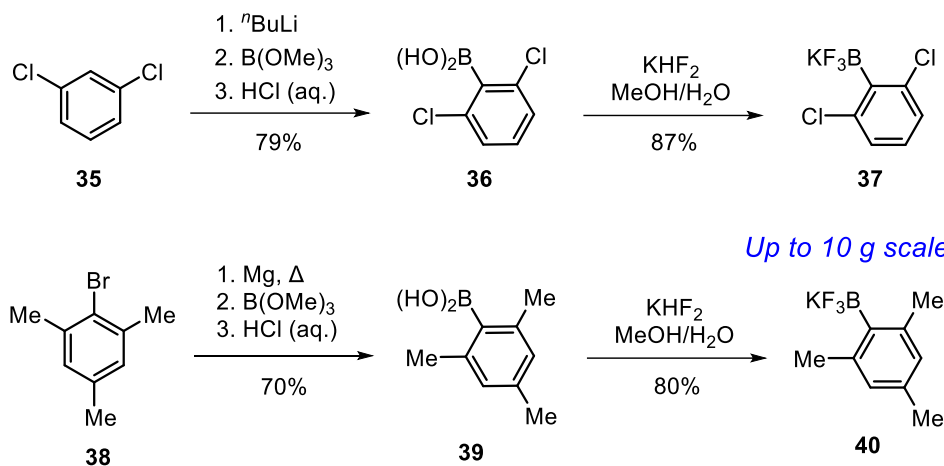
2.2.1.3 Synthesis of Triaryl Boranes Potassium Aryltrifluoroborate Salts as Boron Sources

In 2011, Ashley and O'Hare found that producing heteroleptic boranes through the use of organolithium or Grignard intermediates was unselective due to their high reactivity (Scheme 33). They found that less reactive organozinc and organocuprate species were required for the successful synthesis of heteroleptic borane **34**.²⁰⁵



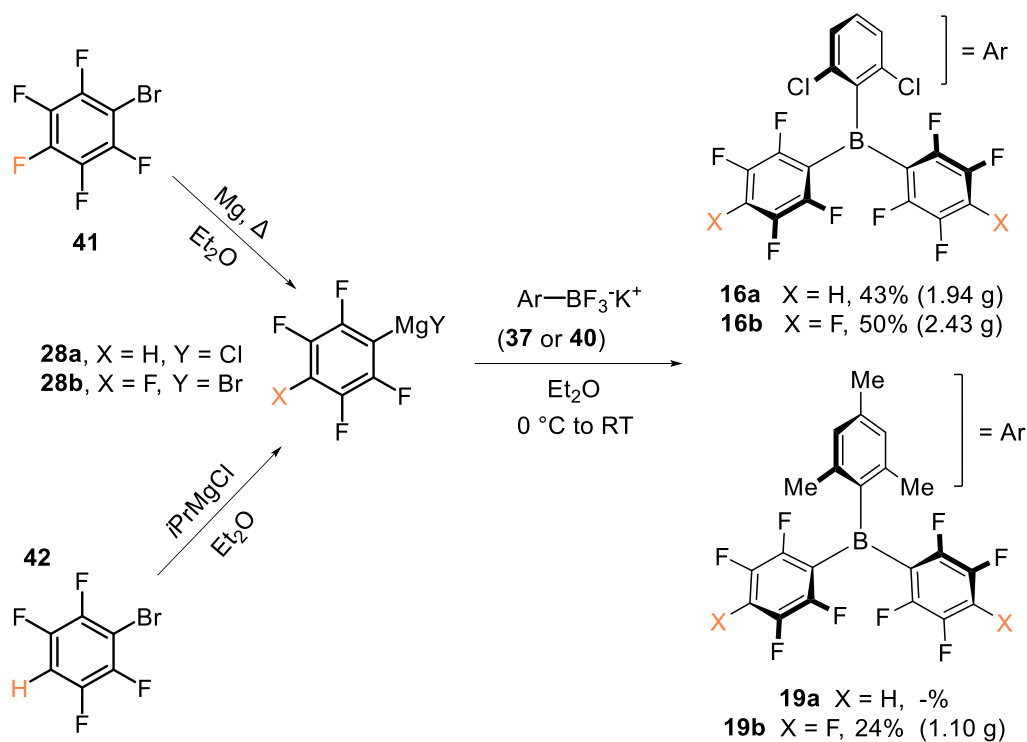
Scheme 33. Synthesis of heteroleptic triaryl boranes with less reactive and more selective organometallic reagents after unsuccessful synthesis via traditional Grignard and organolithium reagents.²⁰⁵

However, rather than pursue these more niche metal-boron exchange routes the second synthetic approach explored was the use of stable potassium aryl trifluoroborates (ArBF_3K salts) as boron sources (Scheme 31 and Scheme 34). ArBF_3K salts **37** and **40** were prepared in a two-step synthesis from aromatic precursors **35** or **38**. The first step provides the corresponding boronic acids **36** and **39** in good yields (79 and 70% respectively). These boronic acids, when treated with potassium bifluoride, yielded ArBF_3K salts **37** and **40** in good overall yields (87% and 80% respectively) on multigram scale (Scheme 34).^{120,190,192}

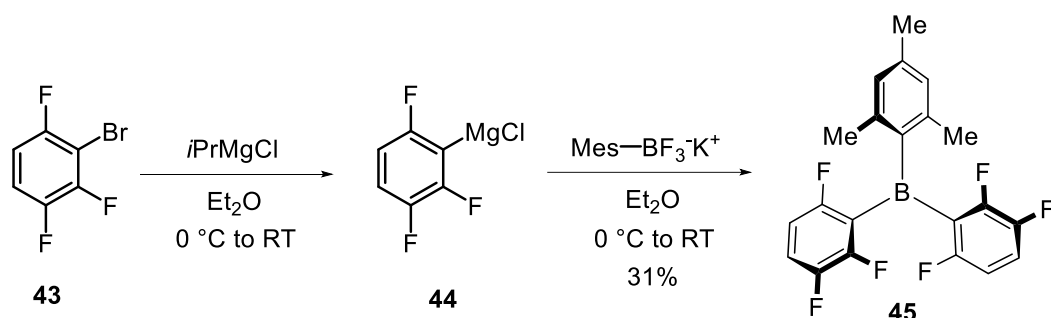


Scheme 34. Synthetic routes to potassium (2,6-dichlorophenyl) trifluoroborate (**37**) and potassium (2,4,6-trimethylphenyl) trifluoroborate (**40**).^{120,190,192}

Synthesis of the desired boranes (**16a/b** and **19a**) was achieved by reacting respective trifluoroborate salts with Grignard reagents **28a/b**. The Grignard reagents **28a/b** were obtained following standard literature procedures and were then added dropwise to a suspension of the relevant ArBF₃K salt in diethyl ether at 0 °C which yielded the desired boranes (**16a/b**) in yields (43 and 50% for **16a** and **16b**) comparable to the ones previously reported (43 – 68% respectively, Scheme 35). Although, **19b** had never been made via the ArBF₃K salt route, a similar analogue (**45**) was synthesised by Soós *et al.* previously (31% yield, Scheme 36), comforting us in our approach.⁶⁰ Using this route, **19b** was obtained in 24% yield (Scheme 35).



Scheme 35. Synthetic route to target triaryl boranes using potassium aryltrifluoroborate salts as the boron source.^{37,60,120,192,206}

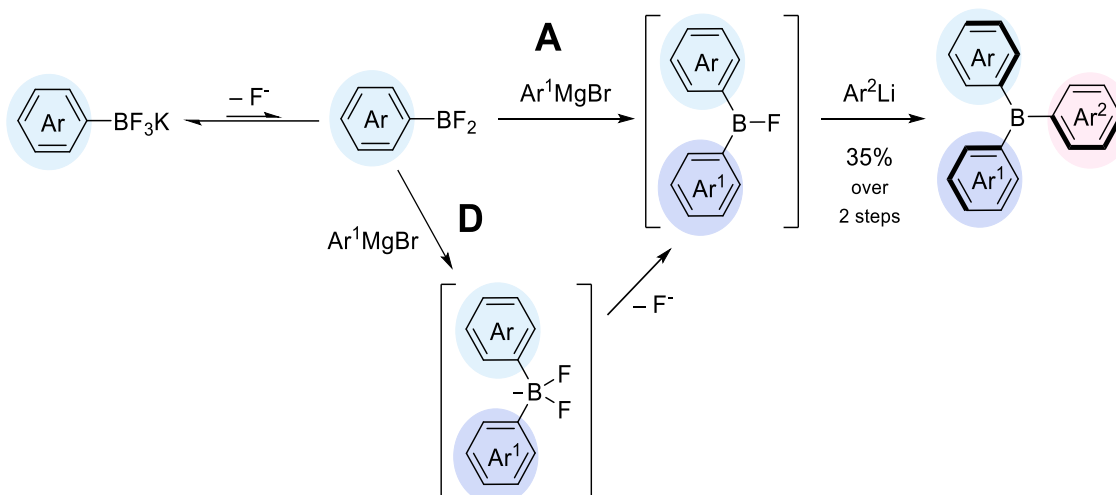


Scheme 36. Synthesis of similar mesityl analogue triaryl borane **45** by ArBF_3K salt method.⁶⁰

I have found that using ArBF_3K salts resulted in higher yields than directly attacking boron trihalides (e.g. $\text{BF}_3\cdot\text{Et}_2\text{O}$) with organometallic compounds. This method allowed us to produce three pure moisture-tolerant heteroleptic triaryl boranes on a gram scale for use as catalysts (1.10 - 2.43 g). Due to challenges in purifying **19b**, which will be discussed in more detail in the section 2.2.1.5, the previous inability to isolate a pure sample of **19a**, and initial results of batch reactions, where **19b** appeared to be less reactive for our intended application, I abandoned the synthesis of **19a**.

2.2.1.4 Plausible Mechanism for Triaryl Borane Synthesis Using ArBF_3K salts

It could seem peculiar to see ArBF_3K salts as electrophilic boron sources as the boron does not have an empty p -orbital making it a poor electrophile. ArBF_3K salts have been known since the 1960s and are commonly employed in cross-coupling reactions where the boron motif is lost.^{202,207,208} It is also counterintuitive that fluoride would be a leaving group and it is clear, therefore, that B-F bond cleavage is most likely the critical factor in this reaction. Whilst the exact mechanism of triaryl borane synthesis from trifluoroborate salts is unknown, several reports suggest initial dissociation of F^- is essential and some mechanistic pathways have been postulated (Scheme 37).



Scheme 37. Postulated mechanism for the synthesis of heteroleptic triaryl boranes using ArBF_3K salts which can proceed via an **A**. associative or **D**. dissociative pathway.²⁰⁹

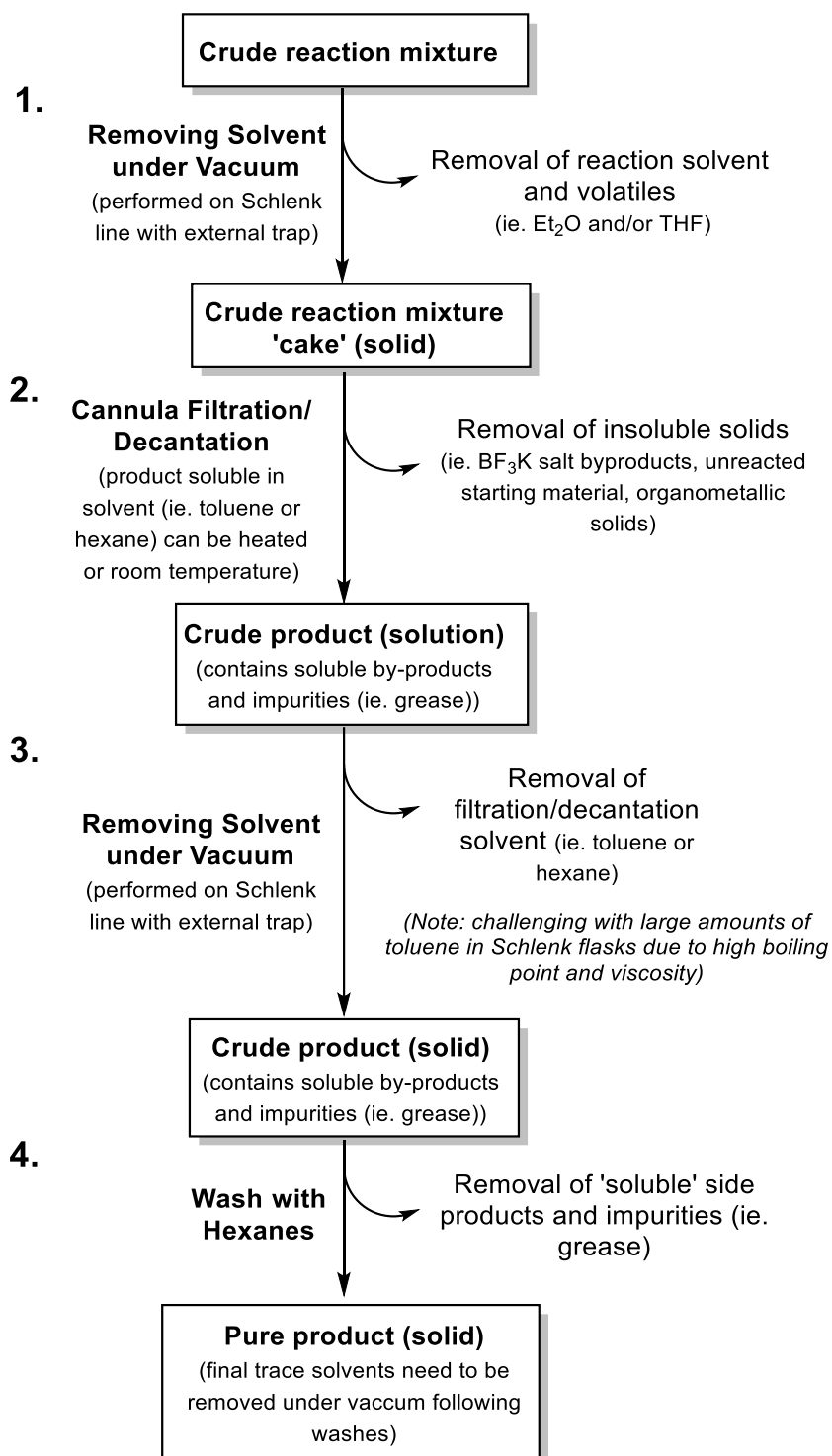
Marder and his colleagues offered some mechanistic insight, suggesting that the loss of a fluoride ion through dissociation leads to the formation of the short-lived ArBF_2 species *in situ*.²⁰⁹ The ArBF_2 species can be attacked with one equivalent of Grignard reagent. The resulting $\text{ArBF(Ar}^1\text{)}$ species reacts with another organometallic species to produce the heteroleptic target product $\text{ArB(Ar}^1\text{)Ar}^2$. The more reactive organolithium species was required to overcome steric hindrance around the boron centre, as all the aryl species synthesised by Marder contained the 2,6-dimethyl moiety. Whilst the use of LA's usually increases the rate of fluoride dissociation using TMSCl did not increase the formation of ArBF_2 , and the yield obtained was 35% over two steps.²⁰⁹ The mechanism for organometallic addition when using $\text{BF}_3\cdot\text{Et}_2\text{O}$ is very similar, without the initial F^-

dissociation. BF_3 is commonly used as an electrophilic source of boron in the synthesis of BODIPY dyes.^{210,211} These dyes contain a stable boron difluoride (BF_2) group similar to the ArBF_2 and dissociative intermediate $[\text{ArBAr}^1\text{F}_2]^-$.

2.2.1.5 Improvements to the Purification Procedure and Problem-Solving

2.2.1.5.1 Purification procedure

The greatest challenge in working with air/moisture sensitive products is often the purification. This is also true for triaryl borane synthesis which follows the same general 4-step purification pathway (Step 1. Solvent removal under vacuum, Step 2. Hot cannula filtration/decantation, Step 3. Solvent removal under vacuum, and Step 4. Wash with hexanes), shown in Scheme 38, regardless of the synthetic route chosen. This purification pathway will be referred to throughout this section (section 2.2) as well as in chapter 5 where much of our time has been spent problem-solving the challenging purification of our target boranes.



Scheme 38. General 4-step purification pathway for triaryl boranes.

2.2.1.5.2 Purification of **19b**

During our initial attempts to synthesise **19a** (discussed in section 2.2.1.2), large portions of the desired product had been lost after performing hexane washes. After this experience, when purifying **19b** the hexane washes (Step 4, Scheme 38) were combined and the solvents were removed under vacuum. NMR spectroscopic analysis of **19b**, solids from step 4 which would be expected to be 'pure', and of the material obtained from evaporation of combined hexane washes from step 4, confirmed the challenging purification of mesityl analogue triaryl boranes was due to their solubility in hexane. The NMR spectra revealed that the 'pure' sample contained a significant amount of an undesired diaryl borinic acid impurity in the ^{11}B NMR spectrum (Figure 25.A (orange)) at ~ 40.0 ppm whilst the material obtained from hexane contained mostly the desired product (~ 70.0 ppm) and only a small amount of the borinic acid side product (Figure 25.A (black)). The borane impurity observed at ~ 40.0 ppm is presumed to be the Ar_2BOH which has been identified by other FLP researchers monitoring triaryl borane decomposition.²¹² I have often observed this decomposition impurity for **16a/b** but it can usually be removed in the hexane washes. Unfortunately, the solubilities are too similar for **19b** making purification extremely challenging.

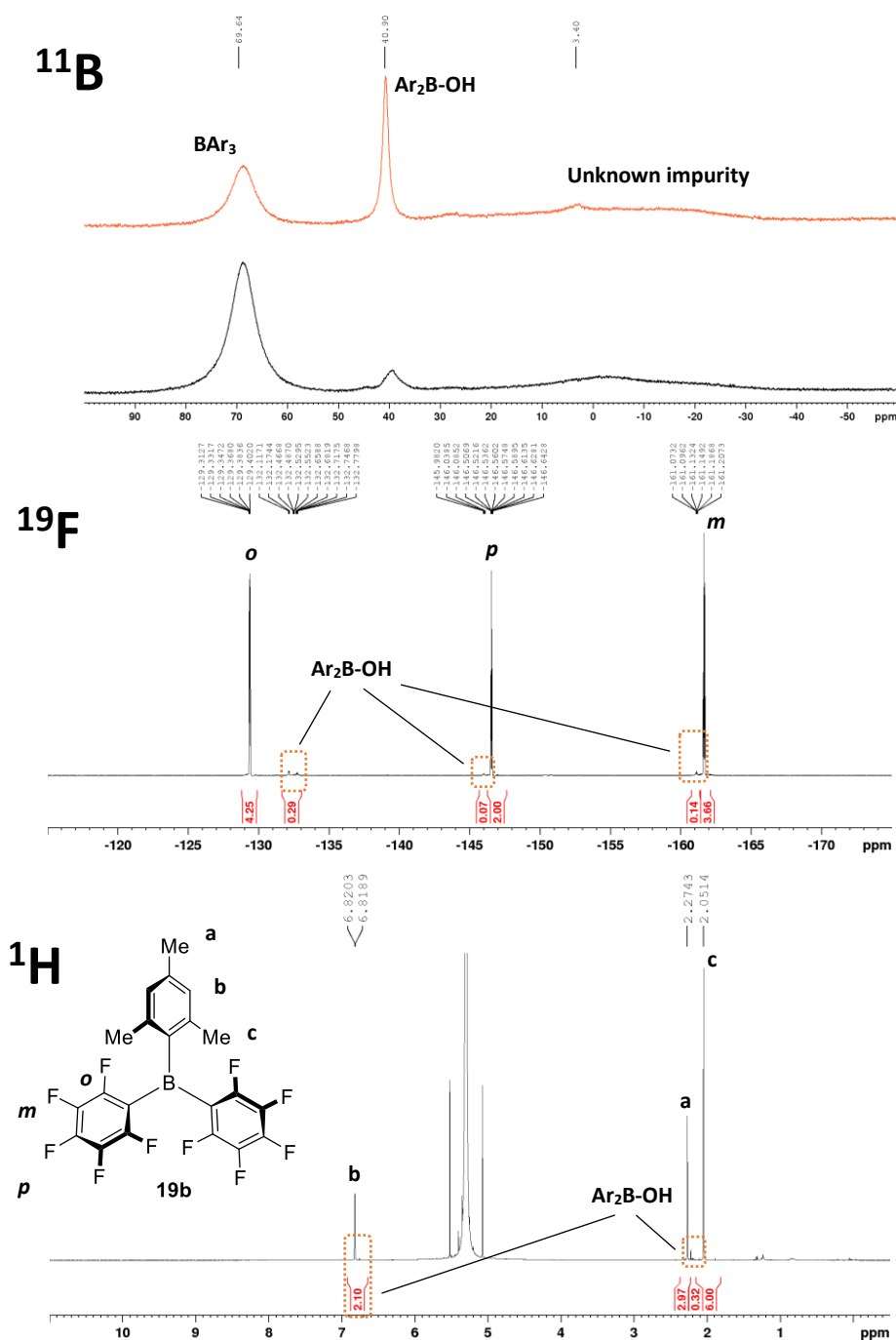


Figure 25. ^{11}B NMR spectra, in DCM, of **19b** post hexane washes which would be expected to be 'pure' (orange) vs. combined hexane washes containing significantly more **19b** (black). ^{19}F NMR and ^1H NMR spectra, in DCM, of combined hexane washes

Thankfully, literature delving revealed a new purification route, which is much more specific than the hexane washes usually described in FLP experimental sections.²¹³ After the reaction solvent is removed extraction can be carried out using 3:1 toluene-hexane and sonication. The resulting suspension is allowed to settle, and the solvent layer is syringed out and filtered. The filtered solvent layer then has the solvent removed under

vacuum before the final stage in the purification, which is a recrystallisation from ether and hexane at $-30\text{ }^{\circ}\text{C}$. Using this purification method, **19b** was isolated in moderate yield (1.1 g, 24%).²¹³

2.2.1.5.3 Other Insoluble Impurities

Upon making more concentrated NMR samples of **16a/b** and **19b** in anhydrous DCM, for more detailed analysis I noticed some fine insoluble impurities had been carried through the purification pathway with our product. After allowing the concentrated NMR sample to settle overnight a fine suspension appeared to settle in a layer at the bottom of the NMR tube (Figure 26).

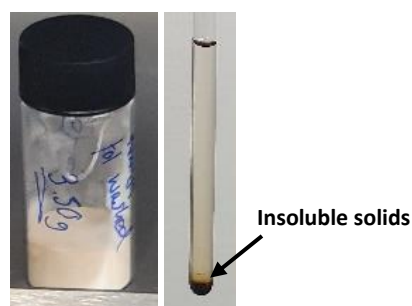


Figure 26. Left: Image of purified **16b** as a beige/ off-white powder. Right: NMR sample of purified **16b** in benzene after allowing to settle.

This problem had not been reported anywhere in the literature. Originally believing that this was our desired product crashing out after maximum borane saturation had been achieved, I carried out a simple solubility experiment. 10, 20 and 30 mg of **16b** (pure by NMR spectroscopy) were weighed into sample vials. 0.6 mL of benzene was added, and all 3 samples were transferred to the NMR tubes before being allowed to settle. After settling the same insoluble solids were observed in every sample (Figure 27). NMR spectroscopic analysis of all three solutions showed the product was 100% pure.

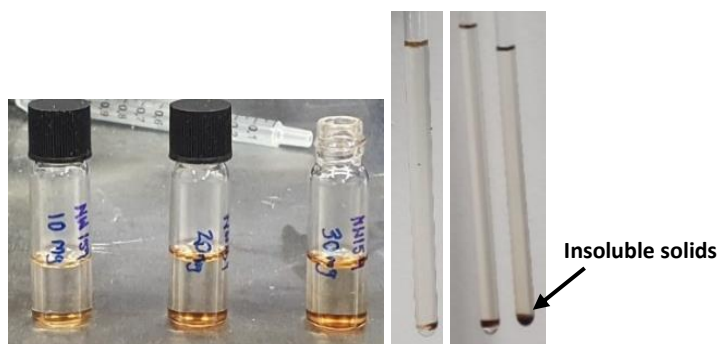


Figure 27. Solubility experiment: left to right 10, 20 and 30 mg samples of purified **16b** in benzene (0.6 mL) after being allowed to settle.

The 30 mg NMR sample was allowed to settle, and the benzene solution was removed using a syringe making sure to leave the solids behind. The benzene solution was dried under vacuum and were redissolved in DCM for NMR spectroscopic analysis. The solids were dried under vacuum, and likewise suspended in DCM for NMR spectroscopic analysis. NMR spectroscopic analysis confirmed the pure product was soluble in benzene and had been completely transferred; the remaining solids were not soluble in the DCM, toluene or benzene and did not contain any product (Figure 28).

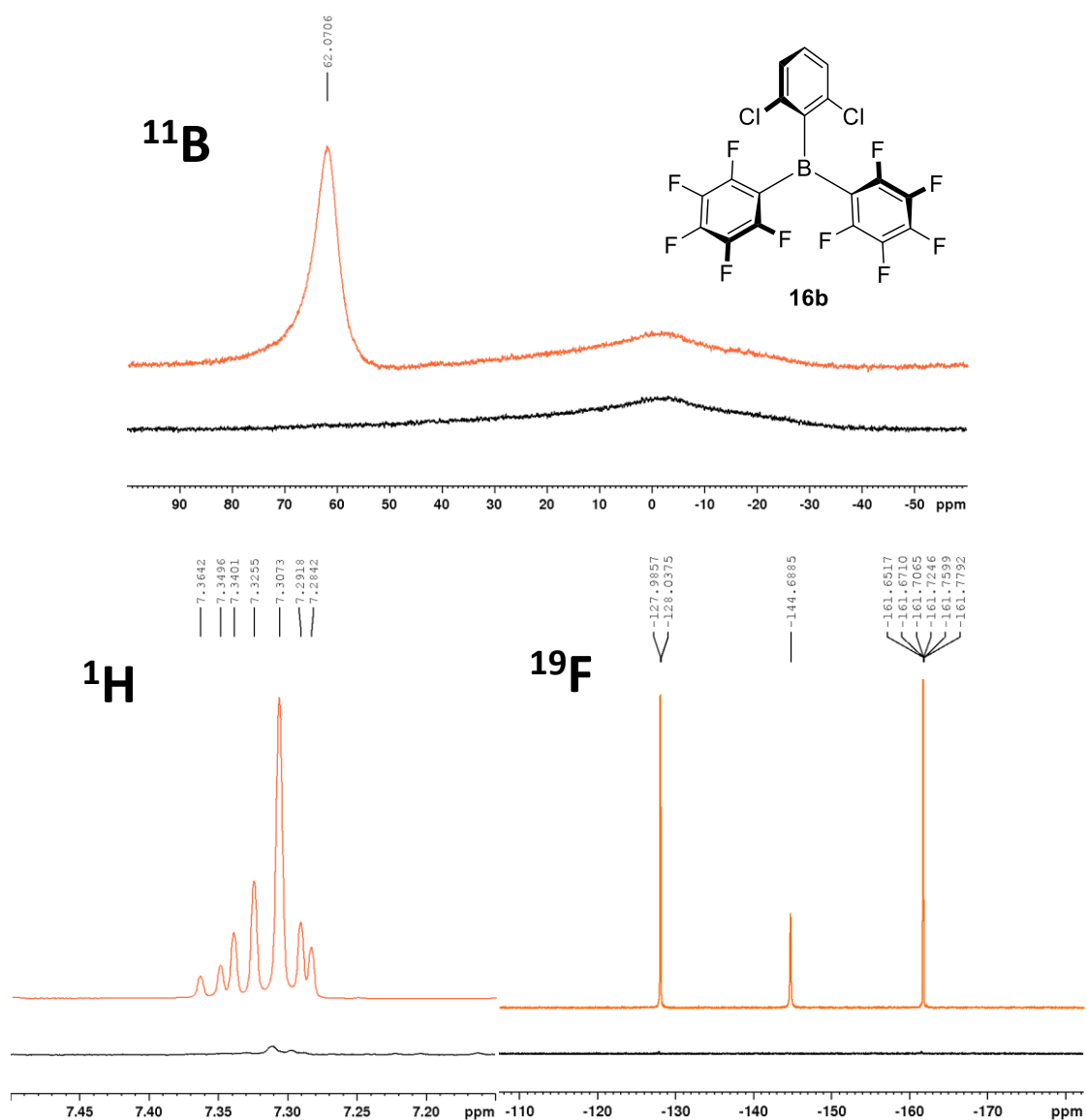
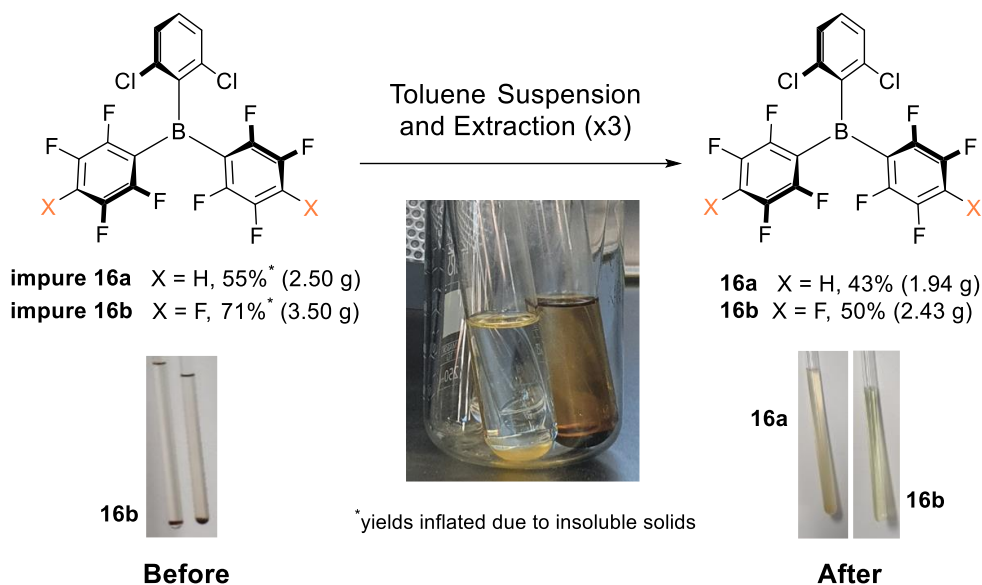


Figure 28. ¹¹B, ¹H, and ¹⁹F NMR spectra **16b**. Spectra in orange refer to the soluble product and spectra in black refer to insoluble solids after suspension and separation.

Before identifying the insoluble impurities as described above, **16a** and **16b** had been isolated in a 55% and 71% yield respectively, inflated by extra solids. Once this issue was identified, both impure boranes **16a/b** were purified to remove the insoluble solids, giving pure **16a** and **16b** in good yields of 43% and 50%, respectively. For this, impure boranes **16a/b** were suspended in toluene overnight and a syringe was used to transfer the solute, repeating this process two more times (Scheme 39). The addition of this extra

purification step has been essential for our boranes' planned application in reductive aminations and hydrogenations, allowing us to use accurate catalyst loadings.



Scheme 39. Scaled up toluene suspension and extraction to remove fine insoluble impurities from 16a/b.

Once they had been successfully removed from the pure product the insoluble solids were dried under vacuum to remove trace toluene. They were found to be soluble in DMSO. Unfortunately, NMR spectroscopic analysis of these solids in DMSO did not allow us to confirm the identity. However, their solubility in DMSO implies an inorganic/salt-like nature especially given that they were not soluble in DCM. Analysis of the ^{11}B NMR spectrum confirmed that the insoluble solids contained boron and that it was not the ArBF_3K salt starting material. The spectrum showed only one peak at -2.35 ppm for both **16a** and **b** insoluble solids, which is the same region as $\text{R}_3\text{B-LB}$ bound adducts. This is not surprising as DMSO is itself a LB and given its extreme excess as a solvent one could imagine any borane salt side product to be fully bound. The ^1H and ^{19}F NMR both imply some aryl functionality is present and as a result, it is plausible that the insoluble solids are an intermediate similar to the aryl difluoro borane (ArBF_2) and ArBFAR^1 species discussed in Scheme 37. Regardless it was deemed not worth the time to determine accurately what the insoluble solids were, especially as I now had a method to remove them.

2.3 Outlook and Conclusions

In conclusion, we have successfully synthesised and purified gram quantities of three known moisture-tolerant FLP-boranes (**16a/b** and **19b**). All three have been used in literature as moisture tolerant catalysts for reductive aminations and imine reductions. Each catalyst has been synthesised on a large enough scale to be used in our novel reductive aminations in batch and proof-of-concept continuous flow system.

Through attempted and successful synthesis, we have acquired the techniques and experience to produce moisture-tolerant triaryl boranes, aiding in our synthetic route and planned purification of our novel moisture-tolerant boranes.

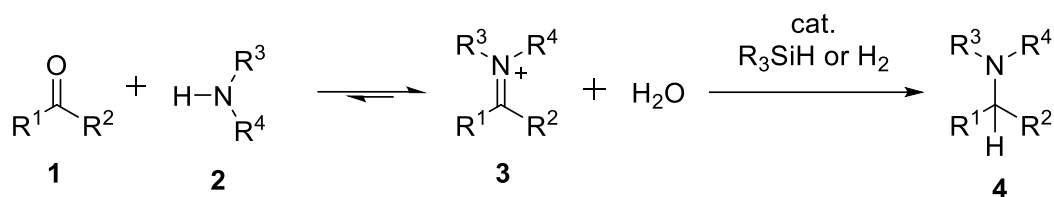
We encountered solubility issues while trying to purify **19a/b**. We believe these issues stem from the higher solubility imparted by the mesityl moiety, which enhances the solubility of **19a/b** in hexane to a point that the crucial final step of the purification (hexane extraction of side products) cannot be carried out efficiently.

In each of our attempts to synthesise our target moisture tolerant boranes, the decomposition side-product $\text{Ar}_2\text{B-OH}$ was observed. This side-product is produced due to water entering the reaction mixture. At higher temperatures, such as when solvents are removed under vacuum, water bound to the target borane ($\text{Ar}_3\text{B-OH}_2$) can undergo intramolecular proton transfer (protodeboronation) from the bound water to one of the aryl substituents. Fortunately, this has only been observed as a minor side-product and was successfully removed from our target FLP-boranes.

Chapter Three: Application of Synthesised Moisture Tolerant Boranes to Batch Reductive Aminations

3.1 Introduction and Aims

Reductive aminations, discussed in section 1.3.2, allow for the production of functionalised amines (Scheme 40) and are widely used reactions in the pharmaceutical industry.^{214,215}



$\text{R}^1, \text{R}^2, \text{R}^3$ and $\text{R}^4 = \text{H}, \text{alkyl}$ or aryl

Scheme 40. General scheme for catalysed reductive aminations using silanes or hydrogen to produce functionalised amine products.

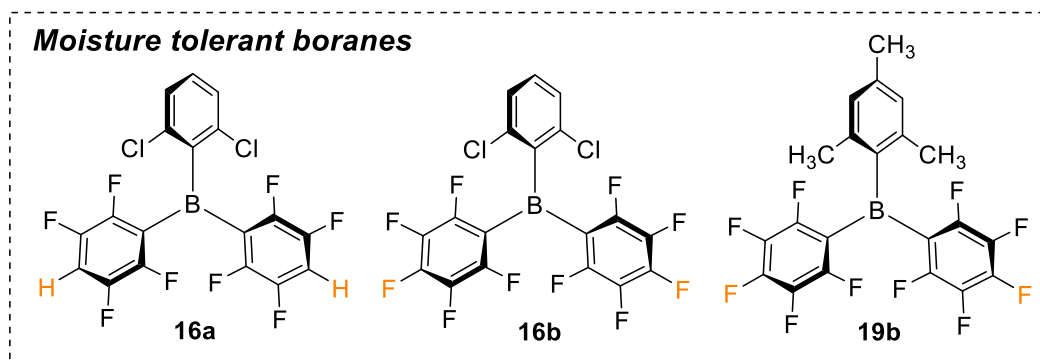
Whilst there is precedent for the use of FLP-boranes as catalysts for reductive aminations, there are limitations to these systems, as discussed in section 1.3.2. These limitations are generally regarding the substrate scope. Aliphatic and secondary amines as well as ketones, at the time of writing, have seen limited success. FLP-catalysed reductive aminations have similarly seen limited examples which have led to cyclisation, especially to form cyclic amines such as piperidines or pyrrolidines. Asymmetric versions of these reactions are also extremely limited, with both examples of asymmetric reductive aminations being discussed in section 1.3.4.

As discussed in introduction, some moisture tolerant boranes have been developed and seem particularly relevant for using in reductive amination as water is formed as a byproduct in the reaction (Scheme 40).²⁸ Despite these developments, these moisture tolerant boranes have not been used systematically to evaluate the scope in amine and carbonyls in reductive amination reactions. This will constitute the first objective of this chapter.

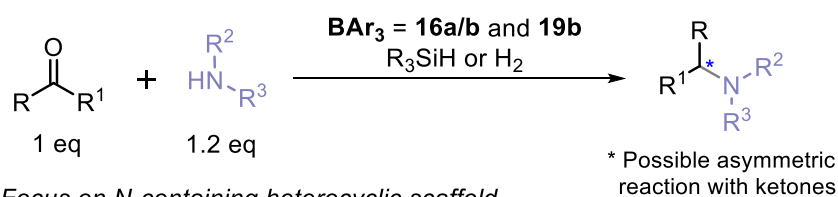
Established reductive amination systems, such as benzaldehyde and aniline (Scheme 41), will be used to benchmark our catalysts and set up. This will help determine which catalyst is most suitable for these transformations. Subject to the creation of a successful system, aliphatic amines, starting with benzylamine, will be screened to try to improve previous performances from FLP-boranes. Whilst reductive aminations with alkyl amines can be performed with BPh_3 , as was discussed in the introduction, this would not be adaptable to hydrogen and as a result, it is still important to provide effective FLP-borane catalysts which are not limited to aryl amines.

Given the importance of reductive aminations to the pharmaceutical industry, it is essential for FLPs to broaden their substrate scope to include catalytic systems that can produce similarly valuable products. As discussed in section 1.1.3 functionalised saturated cyclic amines, especially those in 5- and 6-membered rings, are widely present and crucial structures in biologically active and natural product.

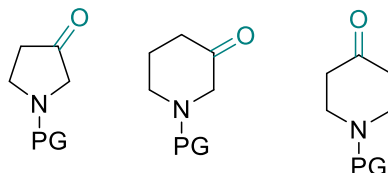
The use of FLP-catalysed reductive aminations for accessing saturated cyclic amines has not been investigated. Once basic trends have been established with well-studied systems, the results/conclusions will be applied to other reductive aminations affording more pharmaceutically relevant molecules like for example chiral cyclic amines such as pyrrolidines and piperidines (Scheme 41).³²



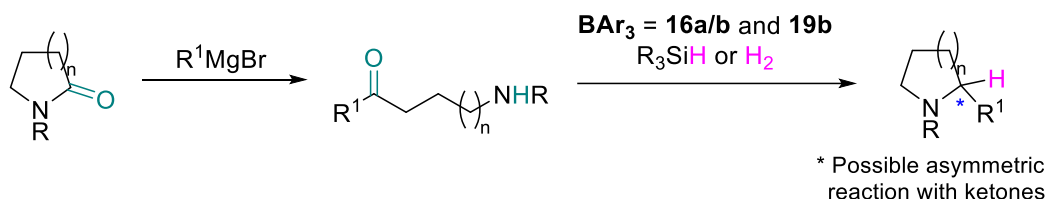
Intermolecular reductive amination



Focus on N-containing heterocyclic scaffold



Intramolecular reductive amination



Scheme 41. Cheap and commercially available pyrrolidinones and piperidinones are used to access valuable substrates through intermolecular reductive aminations. Adaptation of synthetic route to functionalised pyrrolidines via a hypothetical borane-catalysed intramolecular reductive amination cyclisation.³²

Subject to successful expansion of the substrate scope using silanes, the project will advance to reductive aminations using hydrogen in a Parr pressure vessel. Our optimised conditions for standard reductive aminations using hydrogen in batch will serve as the basis for comparison when developing our proof-of-concept reductive amination system in continuous flow (chapter four).

3.2 Results and Discussions

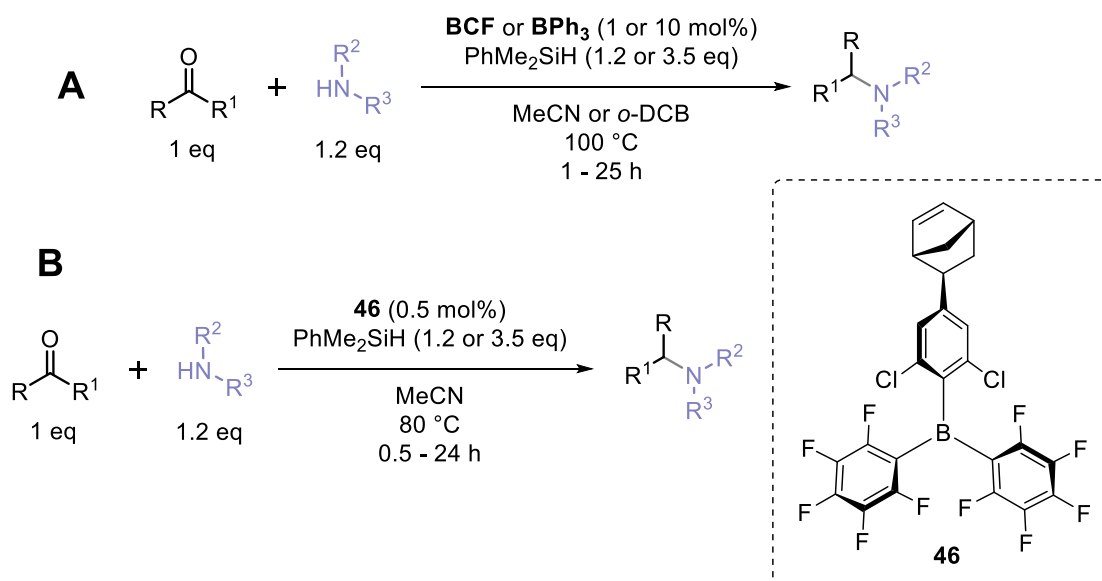
3.2.1 Intermolecular Reductive Aminations Using Silanes

3.2.1.1 Reaction Conditions

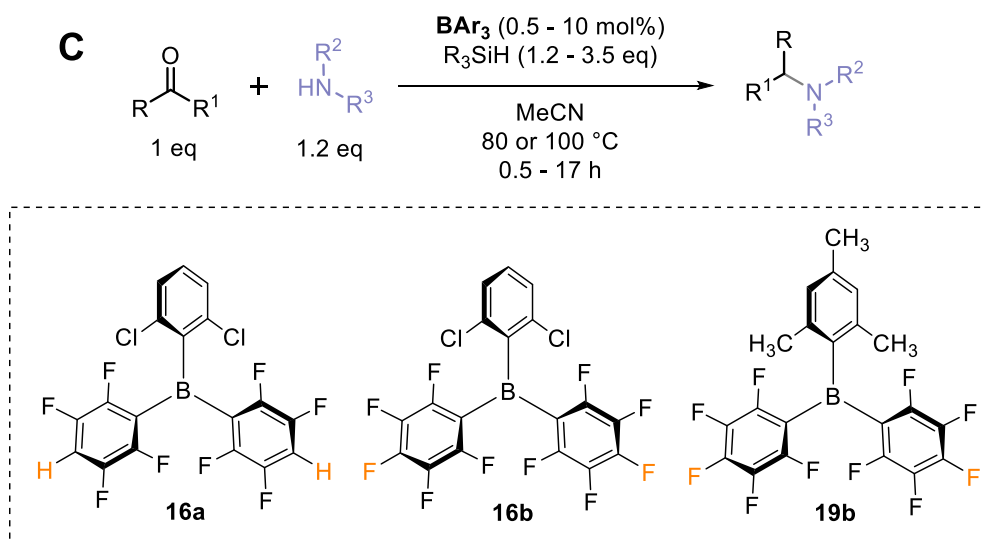
In 2017, Ingleson *et al.* developed two reductive amination systems using the prototypical FLP-borane BCF and BPh₃ (Scheme 42.A).^{34,115} They demonstrated the limitations of FLP-boranes and regular boranes catalysed reductive aminations, which were discussed in section 1.3.2 and 3.2.1. In 2020, Jäckle *et al.* optimised a similar reductive amination system using their novel FLP-borane **46** (Scheme 42.B), which was explored for its potential to produce a heterogeneous FLP-borane through polymerisation of the subunit **46**.²¹²

The known moisture-tolerant boranes **16a/b** and **19b** have been synthesised and used as catalysts for reductive aminations and imine hydrogenations with hydrogen.^{37,60,216} However, to the best of our knowledge, they have not been applied to reductive aminations using silanes. Combining Ingleson and Jäckle's reaction conditions provided a starting point to explore FLP-boranes' catalysis of reductive aminations using silanes (Scheme 42.C).

Previous work



This work



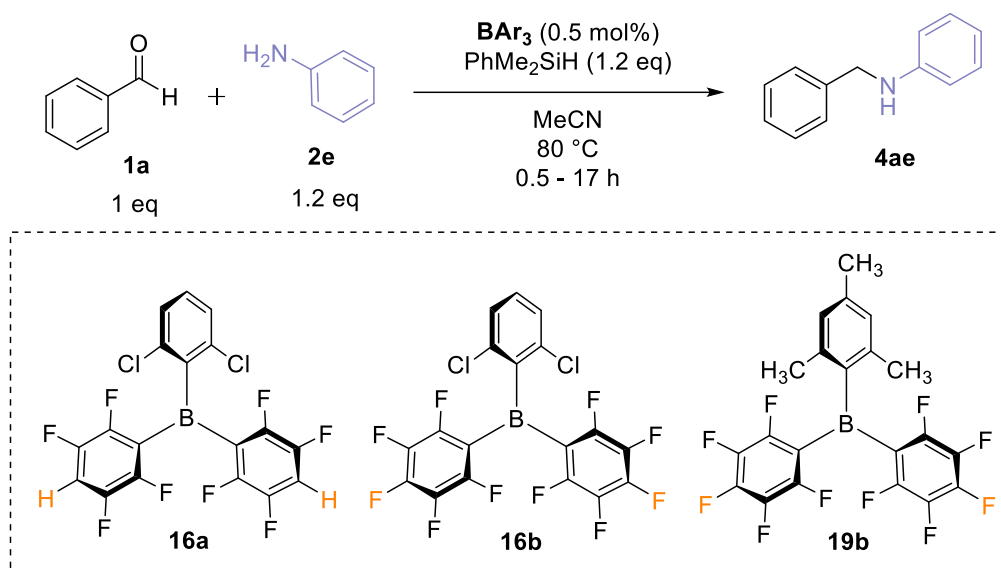
Scheme 42. Previous work (top and middle) reductive aminations catalysed by BCF^{115} , BPh_3^{34} and **46**²¹². This work (bottom) general scheme for reductive amination catalysed by known water tolerant FLP-boranes (**16a/b** and **19b**).

3.2.1.2 Initial Results

In our initial experiments, we used aniline and benzaldehyde to test the reactivity of known moisture-tolerant FLP boranes under basic reductive amination conditions (Table 1). **16b** (0.5 mol%) achieved a 98% yield within 30 minutes, while **16a** required 9 hours to achieve the same yield under the same conditions. However, **19b** only attained a 21% yield after 17 hours. The increased catalytic activity is consistent with the higher Lewis

acidity of **16b** compared to **19b** and **16a**. Using Ph_3PO , the Lewis acidity of **19b** and **16a** has been determined via the Gutmann-Beckett method to be 76% and 89% respectively relative to BCF (100%).¹⁹³ Although we couldn't find a literature source for the Lewis acidity of **16b**, it can be assumed to be higher than **16a** (89%) due to the addition of two extra fluorine atoms at the para-position.

Table 1. Catalyst comparison for basic reductive amination system.²¹²



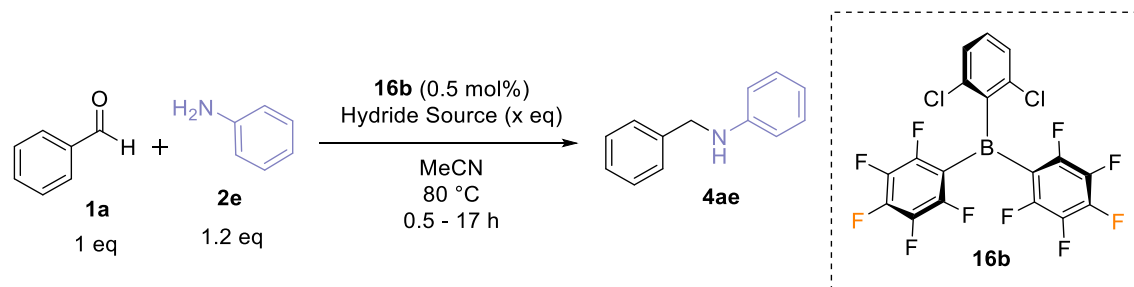
Entry	Catalyst (BAr_3)	Time (h)	Yield (%) [*]
1	16b	0.5	98
2	16a	9	98
3	19b	17	21
4 ^{**}	16b	17	98
5	-	17	-

^{*}determined by quantitative ^1H NMR spectroscopy and a mesitylene internal standard. ^{**}0.1 mol% catalyst loading

Whilst Ingleson and Jäckle optimised the hydride source to be PhMe_2SiH (1.2 or 3.5 equivalents) other hydride sources were explored including PhSiH_3 , Hantzsch ester and PMHS (polymethylhydrosiloxane, effective mass per hydride of 60 g mol^{-1}). The results from this screening, are shown in Table 2. Ultimately, 1.2 equivalents of PhMe_2SiH appeared to be optimal (Entry 1) to achieve the highest yield (98%) in the shortest reaction time (0.5 hours). However, it should be noted that all the hydride sources

screened achieved excellent yields (94 – 98%) after basic optimisation of the equivalents of hydride source and time.

Table 2. Hydride source screening for basic reductive amination system.²¹²

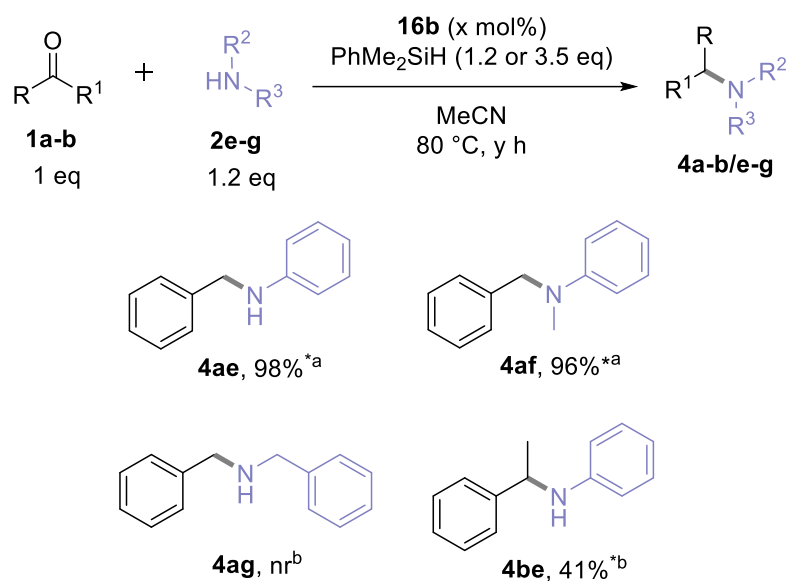


Entry	Hydride source	Equivalents (x)	Time (h)	Yield (%)*
1	PhMe ₂ SiH	1.2	0.5	98
2	PhSiH ₃	1.2	2	97
3	PhSiH ₃	0.4	2	94
4	Hantzsch ester	1.2	2	96
5	PMHS	1.2	17	67
6	PMHS	3.5	17	98

*determined by ¹H NMR spectroscopy and a mesitylene internal standard.

3.2.1.3 Substrate Scope Exploration

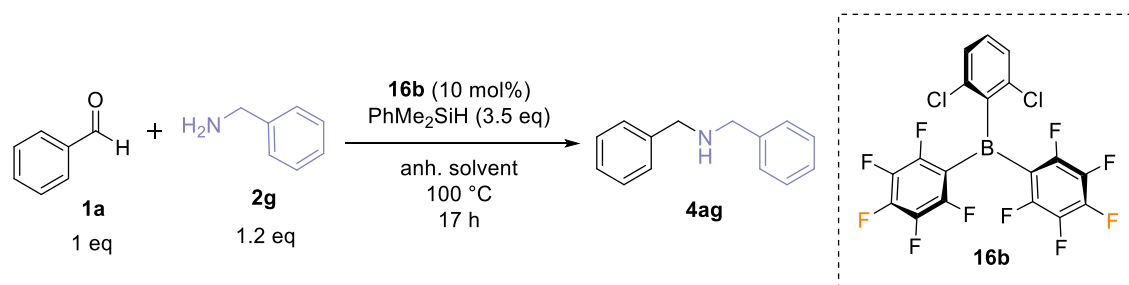
The optimal FLP-borane catalyst (**16b**) and hydride source (PhMe₂SiH) were used to explore a limited range of substrates (Scheme 43). Basic optimisation of conditions was carried out for the substrates screened which revealed 2 sets of conditions (0.5 or 1 mol% **16b**, 1.2 or 3.5 equivalent Silane, and 0.5 or 17 hours). Initially, using acetonitrile as the solvent aniline (**2e**) and secondary aryl amine *N*-Me aniline (**2f**) proceeded with in excellent yield with benzaldehyde (**1a**) (98% and 96% respectively). Unfortunately, the alkyl amine benzylamine (**2g**) was not tolerated. Similarly, the alkyl-aryl ketone acetophenone (**1b**) only obtained a 41% yield with aniline (**2e**), even under slightly more forcing conditions (1 mol% **16b**, 3.5 equivalent silane, and 17 hours).



Scheme 43. Substrate scope for FLP-borane **16b** catalyzed reductive aminations in MeCN. (^a**16b** (0.5 mol%), silane (1.2 eq), MeCN, 80 °C, 0.5 hr. ^b**16b** (1 mol%), silane (3.5 eq), MeCN, 80 °C, 17 hr.)

Inspired by previous reports using alternative solvents with FLPs,^{62,115,184} the reductive amination of benzaldehyde (**1a**) with benzylamine (**2g**) which had not been tolerated in acetonitrile was used to screen other solvents (Table 3). The reductive amination of alkyl amines such as benzylamine (**2g**) is known to be sluggish when using electron deficient FLP-borane catalysts (best yield at the time of writing is 60%).^{34,212} The solvent screening was performed testing anhydrous THF, dioxane, EtOAc, DCE, toluene and MeCN using 10 mol% catalyst loading and 3.5 equivalents of silane at 100 °C for 17 hours (Table 3). We were extremely gratified to isolate **4ag** in 93% yield using THF. The optimal solvents were found to be EtOAc and THF. Whilst THF is an established FLP solvent,⁶² we were surprised to find EtOAc to be such an effective solvent, especially as it had not been previously reported to be successful for such a transformation.

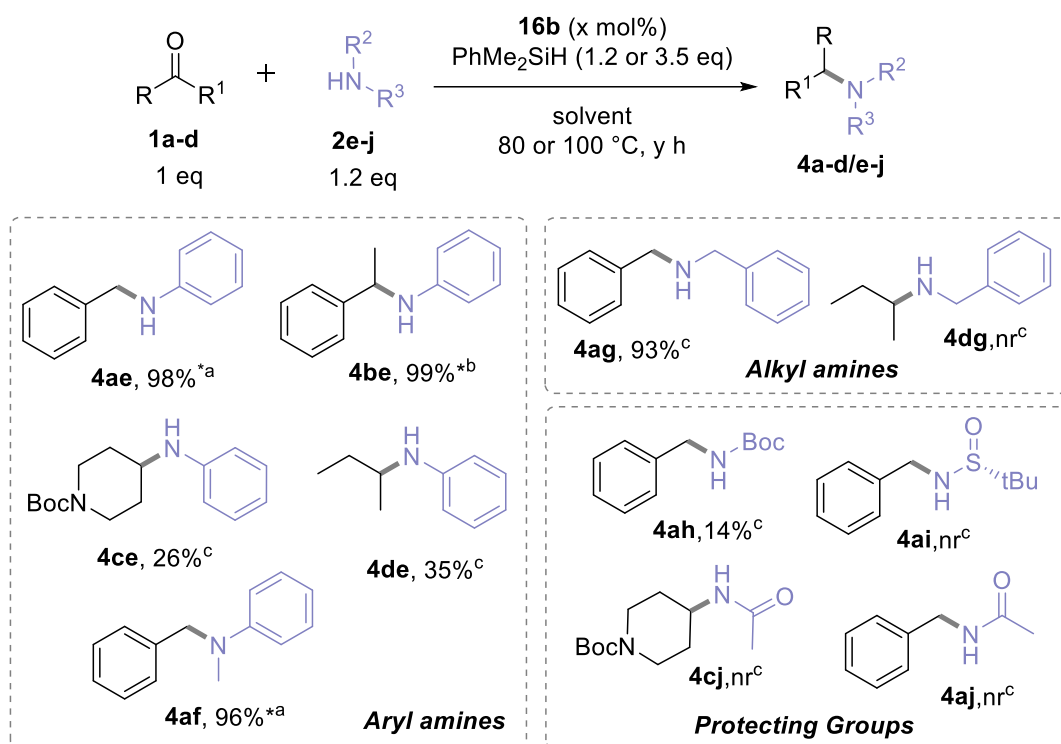
Table 3. Solvent screening for the reductive amination of alkyl amine, benzylamine (**2g**) catalysed by FLP-borane **16b**.



Entry	Solvent	Yield (%)*	Isolated Yield (%)
1	THF	98	93
2	Dioxane	21	-
3	EtOAc	93	83
4	DCE	11	-
5	Toluene	13	-
6	MeCN	24	-

*yields determined by ^1H NMR spectroscopy and a mesitylene internal standard.

These more enabling forcing conditions were then used to evaluate the scope of the reaction with varied amines and carbonyls (Scheme 44). Switching to THF or EtOAc we were pleased to find that as well as tolerating benzylamine (**2g**), the system obtained **4be**, from the reaction of aniline (**2e**) with acetophenone (**1b**) in excellent yield (99%). This was significantly improved from the 41% yield obtained in MeCN (Scheme 43), and similarly improved upon previously observed yields with acetophenone in similar reductive amination systems using electron deficient FLP-boranes (64%¹¹⁵ and 67%²¹² yield).



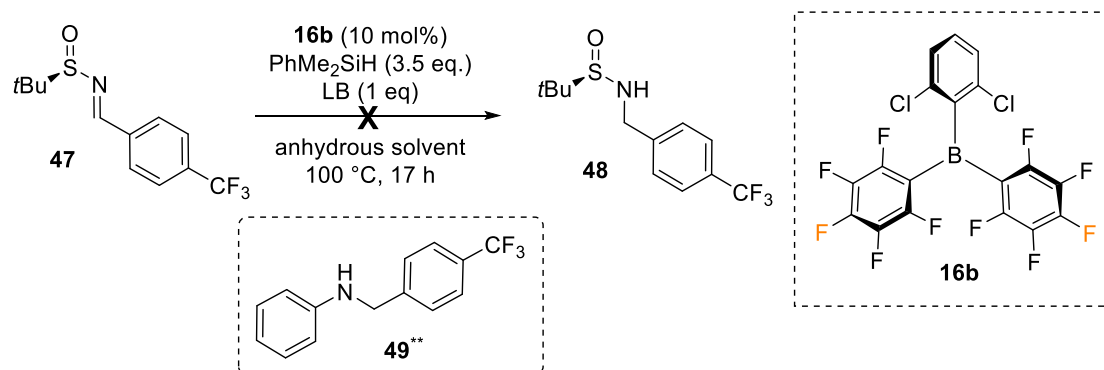
Scheme 44. Substrate scope for FLP-borane **16b** catalysed reductive aminations. ^a**16b** (0.5 mol%), silane (1.2 eq), THF or EtOAc, 80 °C, 0.5 hr; ^b**16b** (1 mol%), silane (3.5 eq), THF or EtOAc, 80 °C, 17 hr. ^c**16b** (10 mol%), silane (3.5 eq), THF or EtOAc, 100 °C, 17 hr. * yields determined by ¹H NMR spectroscopy and a mesitylene internal standard.

Unfortunately, despite creating a set of optimised forcing conditions we had limited success applying these conditions to other challenging substrates. For example, low isolated yields were obtained for the alkyl ketones *N*-Boc-4-piperidone (**1c**) and 2-butanone (**1d**) even with the aryl amine aniline (**2e**) (26% and 35% yield respectively).

Unfortunately, whilst we were hopeful that reduction of Ellman's type *N*-sulfinyl imines could lead to an asymmetric reduction,^{217,218} the screening of the amides, acetamide (**2j**) and *tert*-butylsulfonamide (**2i**) was ultimately unsuccessful. This was attributed to the lack of nucleophilicity of both amide components, as no imine was observed in the crude ¹H NMR spectra before or after reaction. Various alterations were made to the reaction conditions including the direct reduction of the *N*-sulfinyl aldimine intermediate (**47**) (Table 4), but we were unable to achieve successful reduction.

After obtaining these results, we were satisfied with the low isolated yield (14%) achieved when reacting *tert*-butylcarbamate (**2h**) with benzaldehyde (**1a**). Despite its slightly increased nucleophilicity compared to the amides (**2j** and **i**), we believe that the yield is impacted by the stability of the subsequent Boc-protected amine under the reaction conditions. We observed significant decomposition in the Boc region of the crude ¹H NMR spectra for both **4ce** and **4ah**.

Table 4. Attempts at the reduction of *N*-sulfinyl imine **47** catalysed by FLP-borane **16b** using silanes.



Entry	LB	Solvent	Yield (%) [*]	Conversion (%) [*]
1	-	MeCN	0	10
2	-	THF	0	100
3	Aniline	MeCN	92 ^{**}	100
4	DABCO	MeCN	0	100

^{*}yields determined by quantitative ¹H and ¹⁹F NMR spectroscopy and a mesitylene internal standard.

^{**}isolated 92% yield of **49**, by substitution of *N*-sulfinyl aldimine intermediate by aniline and subsequent reduction.

3.2.1.4 Conclusions

Whilst the scope explored was limited, the mild conditions already established (Table 2) were applicable for primary and secondary aryl amines (**4ae** and **5af**) achieving 98% and 96% yield respectively. Slightly more forcing conditions (1 mol% **16b**, 3.5 equivalents of silane, a change in solvent to THF or EtOAc, and an increased reaction time of 17 hours) were required for the reductive amination of the alkyl-aryl ketone (**4be**) achieving a 99% yield. More forcing conditions again (10 mol% **16b**, 3.5 equivalents of silane, THF or

EtOAc, 17 hours, and an increased in reaction temperature to 100 °C) allowed for the reduction of alkyl amines (**4ag**) which was obtained in a 93% yield. The most forcing set of conditions were applicable to alkyl ketones (**4ce** and **4de**) as well as the *N*-Boc protected amine (**4ah**), however only poor yields could be obtained (26%, 35% and 14% respectively). Even in this limited range of substrates, we have demonstrated some of the key limitations to FLP-catalysed reductive aminations. Crucially for our aim to perform intramolecular reductive amination cyclisation reactions we have optimised conditions which are amenable to primary and secondary aryl amines as well as alkyl-aryl ketones using silanes. These substrates are analogous to the intramolecular reductive amination cyclisation we wish to perform.

At the time of performing these intermolecular reductive aminations using silanes, we did not yet have access to our Parr pressure vessel. As a result, we were not able to perform batch intermolecular reductive aminations using hydrogen for comparison to our results, with silanes. Our work in batch using hydrogen will be discussed further in section 3.2.2.

3.2.2 Intramolecular Reductive Amination: Synthesis of Cyclic Amines

3.2.2.1 Background, Context and Aims

The intramolecular reductive amination of functionalised aminoketones can be utilised to synthesise α -substituted cyclic amines. Figure 29 illustrates examples of valuable fine chemicals that can be obtained through this method. These examples all feature a chiral cyclic amine moiety, highlighting the potential of this FLP-borane catalysed reaction if it can be carried out in an enantioselective manner.

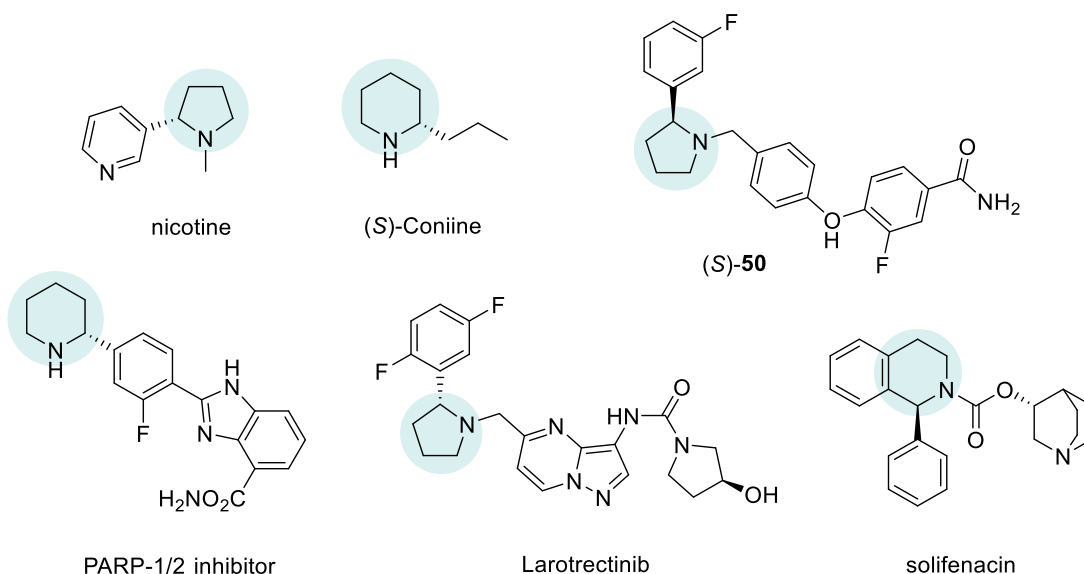
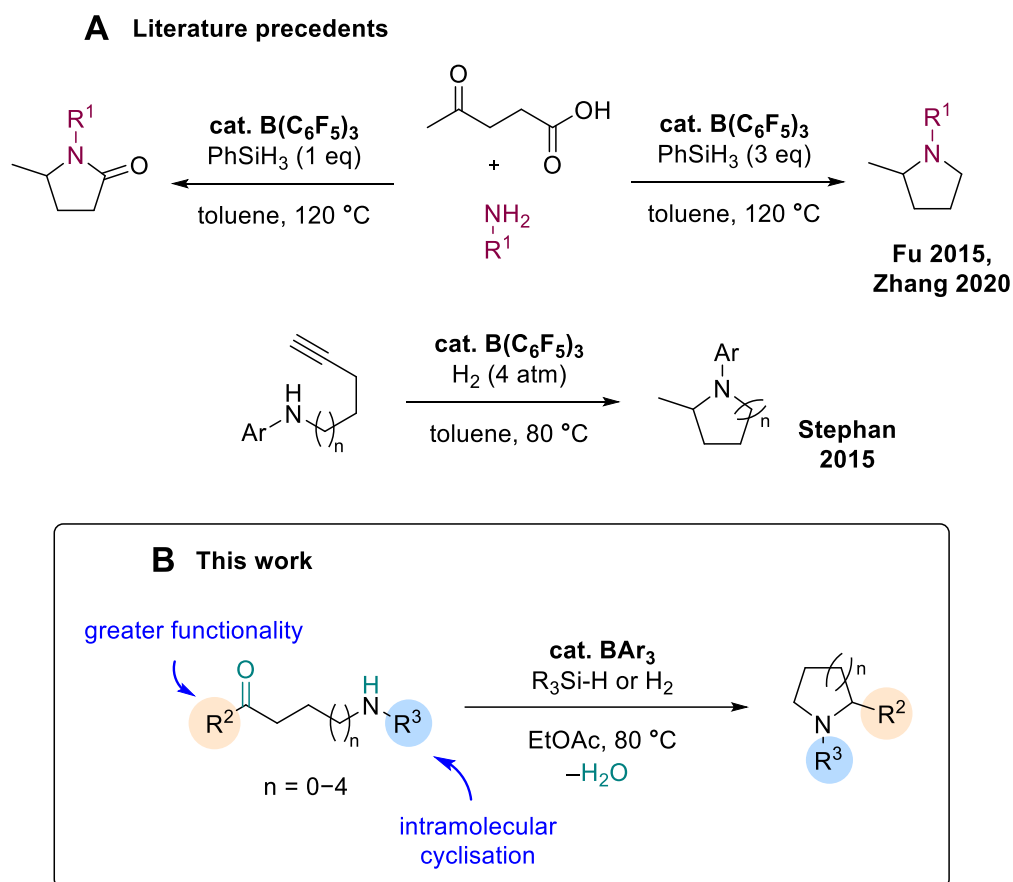


Figure 29. Select structures of biologically active compounds and pharmaceutical drugs containing the chiral cyclic amine moiety.^{219–221}

The prototypical FLP-borane, BCF, has been used to catalyse reductive amination systems which have produced α -substituted pyrrolidines from the renewable bio feedstock levulinic acid using the phenylsilane (PhSiH_3) (Scheme 45. A).^{222,223} They were able to selectively produce the pyrrolidinone or pyrrolidine with 1 or 3 equivalents of phenylsilane respectively. A range of amines were screened, and whilst good to excellent yields (64 – 93%) were obtained with aryl amines, alkyl amines, including benzylamine were unsuccessful.

In 2015, Stephan and co-workers developed a FLP-borane catalysed intramolecular hydroamination of terminal alkynes (Scheme 45. A).²²⁴ The substrates were limited to aryl amines only, but the reaction was able to synthesise 5, 6, and 7-membered rings in moderate to good yields (52 – 73%).

Whilst these FLP-borane catalyst systems provide valuable additions to the FLP field, they both only produce α -Me substituted cyclic amines. The development of a practical reductive amination system which enables direct access to highly functionalised cyclic amines is therefore, of high interest (Scheme 45. B).



Scheme 45. Previous work (top and middle): FLP-catalysed *N*-heterocycle forming reactions by reductive amination of levulinic acid with aniline and by intramolecular hydroamination;^{222–224} this work (inset below): Catalytic intramolecular reductive amination cyclisation for the preparation of α -substituted saturated cyclic amine.

3.2.2.2 Optimisation and Reaction Conditions

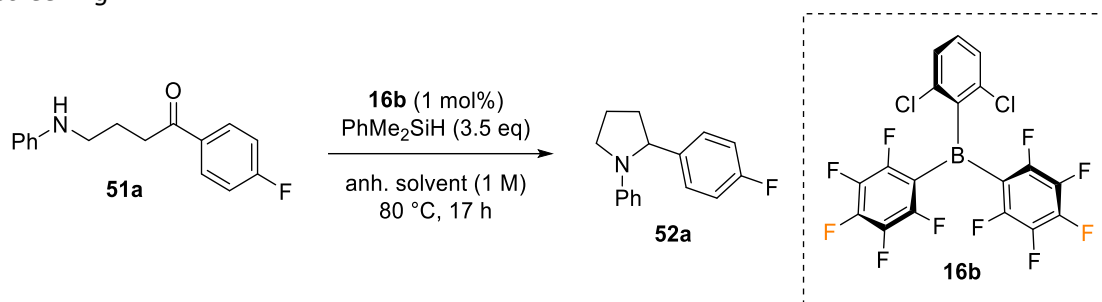
The intermolecular reaction we carried out previously, showed that aryl ketones were reactive (Scheme 44), therefore these previously established reaction conditions should be appropriate for our novel intramolecular reductive amination cyclisation of **51a**. Thus, our initial intramolecular cyclisation experiments used 1 mol% catalyst loading (**16b**) and 3.5 equivalents of PhMe₂SiH in anhydrous THF or EtOAc at 80 °C for 17 hours (Table 5, Entries 1 and 2). The conditions were the same as those optimised for the analogous reductive amination of the alkyl aryl ketone (acetophenone, **1b**) with a secondary aryl amine (*N*-methylaniline, **2f**) (Scheme 44, **4be** and **4af**).

Whilst we were confident that THF and EtOAc had been effective solvents for intermolecular reductive aminations, we did not want to overlook the possibility that our intramolecular may have required different conditions. As a result, we performed a

solvent screening, comparing 10 solvents which had been used previously in FLP-catalysed reductions (THF, MeCN, toluene and *o*-DCB), EtOAc and a selection of green solvents containing Lewis basic functionalities (TBME, CPME, anisole and 2-Me-THF). We were extremely pleased that even after performing a solvent screening (Table 5) both our initial experiments achieved excellent yields of the desired pyrrolidine **52a** (90% and 93%) in THF and EtOAc respectively. Similar to the analogous intermolecular reactions both THF and EtOAc appeared to be the optimal solvents. Whilst the screening of available greener solvents (CPME, anisole and 2-Me THF) was not successful, we chose to proceed with EtOAc as it was deemed a much more sustainable solvent than THF according to GSK's sustainable solvent guide.²²⁵

It is noteworthy that whilst reactions were set up under ambient conditions, anhydrous solvents were used during the solvent screening. Entries 10 and 11, show improved yield when the reaction was set up under anhydrous conditions in THF and EtOAc (99% and 98% respectively). The system also showed tolerance for 'wet' EtOAc (lab grade and undried, Entry 12), however, for comparable yields (90%) to those with anhydrous EtOAc the catalyst loading was increased to 2.5 mol%.

Table 5. Initial attempts at novel intramolecular reductive amination cyclisation and solvent screening.

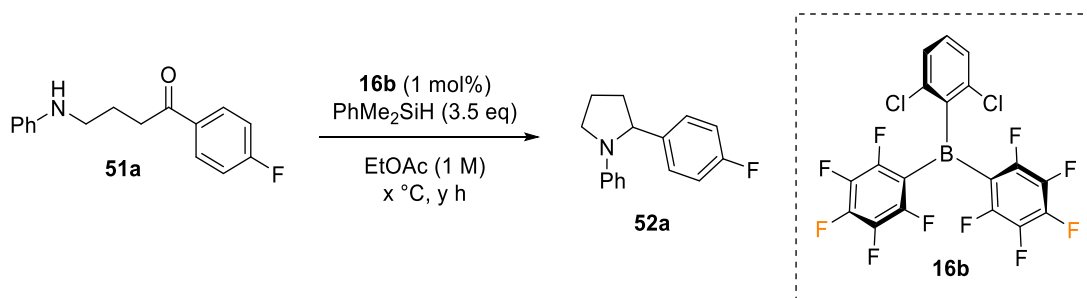


Entry	Solvent	Yield (%) [*]	Conversion (%) [*]
1	THF	90	100
2	EtOAc	93	100
3	MeCN	17	60
4	Toluene	27	53
5	<i>o</i> -DCB	7	50
6	TBME	29	55
7	CPME	2	45
8	Anisole	4	35
9	2-Me THF	43	60
10^a	THF	99	100
11^a	EtOAc	98	100
12^b	'wet' EtOAc	90	100
13 ^c	EtOAc	72	100

^{*}determined by ¹⁹F NMR spectroscopy using a 1,4-bis(trifluoromethyl)benzene internal standard.
^aanhydrous set up. ^b2.5 mol% **16b**. ^c4Å MS.

Reaction monitoring showed that the full 17 hours was required to achieve full conversion and 96% yield of **52a** (Table 6). After 6 hours, only 36% yield had been achieved. Similarly, 80 °C was also required as any reduction in temperature led to a significant drop in yield (Table 6, Entries 6 and 7).

Table 6. Reaction monitoring.

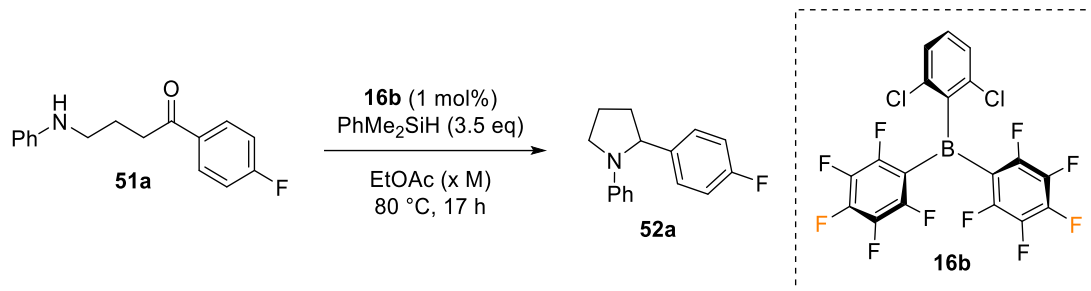


Entry	Time (y hours)	Temp. (x °C)	Yield (%) [*]	Conversion (%) [*]
1	1	80	10	48
2	3	80	27	66
3	6	80	36	77
4	17	80	96	100
5	17	80	96	100
6	17	60	41	72
7	17	40	5	19

^{*}determined by ¹⁹F NMR spectroscopy using a 1,4-bis(trifluoromethyl)benzene internal standard.

The concentration for our intermolecular reductive aminations had been 1 M (Scheme 44), following Jäckle *et al.* optimised conditions. We had been surprised when our initial reactions at this concentration had been so successful, as it appeared counterintuitive that an intramolecular cyclisation reaction would not require more dilute conditions. We were therefore, pleased that concentration appeared to have no impact on the yield of **52a** (Table 7). At 2 M and 0.5 M the reaction yield obtained was equivalent to the yield currently obtained at 1 M (95 – 96%). This was a promising finding for future practical scale up of this reaction.

Table 7. Concentration test.



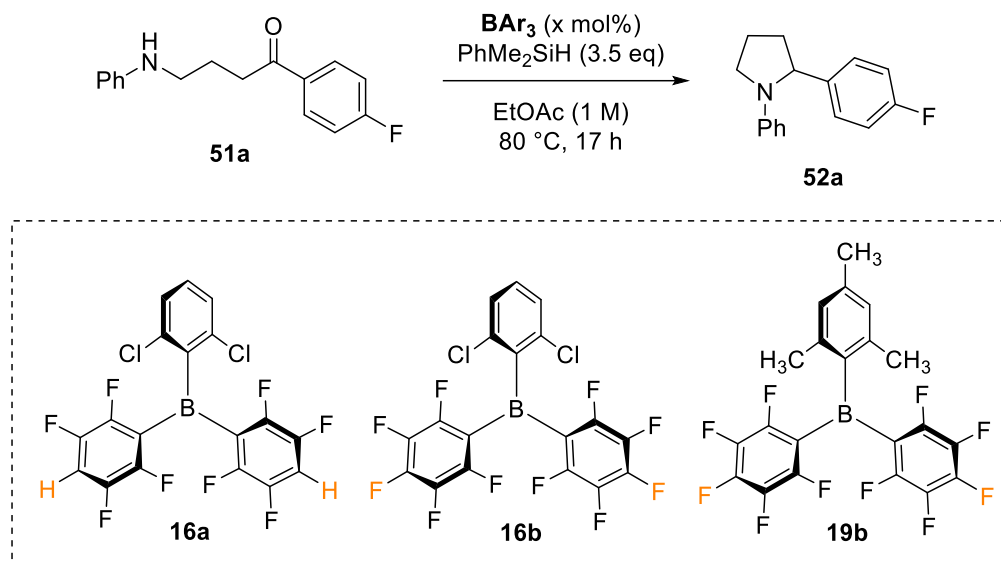
Entry	Conc. (x M)	Yield (%)*	Conversion (%)*
1	1	96	100
2	2	95	100
3	0.5	95	100

*determined by ^{19}F NMR spectroscopy using a 1,4-bis(trifluoromethyl)benzene internal standard.

With optimal conditions in hand, we explored the use of our alternative available borane catalysts. Unlike our intermolecular reductive amination catalyst comparison (Table 1), where **16b** had been considerably faster than **16a** (0.5 hour vs. 9 hours to achieve the same yield), **16a** and **16b** were indistinguishable, both achieving 96% yield of **52a** in 17 hours (Table 1, Entries 1 and 2); although it is possible that full conversion was achieved in shorter time with **16a**. As we had observed before, **19b** was significantly worse than **16a/b** attaining only 4% yield. We were surprised to find BPh_3 attained a 66% yield as Ingleson and co-workers seminal work in this area had shown BPh_3 to be poor at catalysing reductive aminations with aryl amines (35% yield after 24 hours).³⁴ We were similarly surprised to achieve a 97% yield using BCF (Table 8, Entry 4), as discussed in section 3.2.1, Ingleson *et al.* had found BCF to be less effective for alkyl-aryl ketones (achieving 64% with acetophenone) using silanes.¹¹⁵

Whilst the reaction was amenable to a reduction in the catalyst loading 0.5 mol% achieving 88% yield (Table 8, Entry 6), the drop in yield (8%) was not determined to be worth the borane saved on small scale (0.2 mmol). The system could not tolerate any further reduction below 0.5 mol% (Table 8, Entry 7).

Table 8. Catalyst comparison.



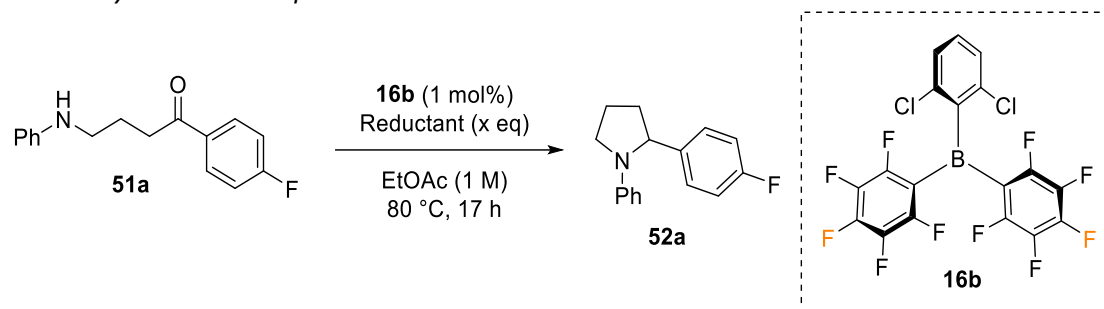
Entry	BAR ₃	Catalyst loading (x mol%)	Yield (%) [*]	Conversion (%) [*]
1	16b	1	96	100
2	16a	1	96	100
3	19b	1	4	60
4	BCF	1	97	100
5	BPh ₃	1	66	92
6	16b	0.5	88	96
7	16b	0.25	40	80
8	none	-	0	55

^{*}determined by ¹⁹F NMR spectroscopy using a 1,4-bis(trifluoromethyl)benzene internal standard.

The final variable which was screened was the hydride source. Seven hydride sources were screened including the silane PhMe₂SiH which had been used up until this point (Table 9). Both alternative silanes (PhSiH₃ and PMHS) proved to be less effective than PhMe₂SiH, even when 3.5 equivalents were used (Table 9, Entries 2 and 3).

Unfortunately, our initial attempt to perform the reaction with hydrogen proved to be unsuccessful (Table 9, Entry 6), as was the use of potassium formate. Further work to explore the use of hydrogen as the reductant for our novel reaction will be discussed in section 3.2.3.4.

Table 9. Hydride source optimisation.

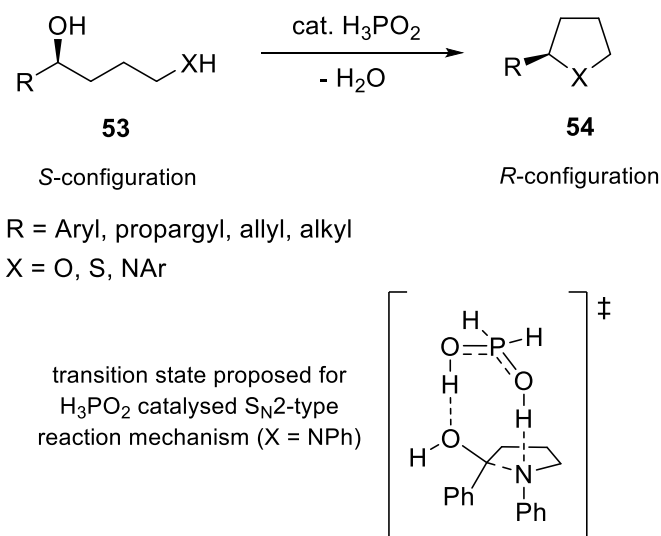


Entry	Reductant	Reductant equivalents (x)	Yield (%) [*]	Conversion [*] (%)
1	PhMe₂SiH	3.5	96	100
2	PhSiH ₃	3.5	67	100
3	PMHS	3.5	63	91
4	Hantzsch ester	3.5	99	100
5	HCO ₂ K	3.5	trace	2
6	H ₂ (20 bar)	-	0	58
7	PhMe ₂ SiH	2.5	93	100
8	PhMe₂SiH	2	91	100
9	PhMe₂SiH	1.2	10	42
10	HCO ₂ H	3.5	97	100
11	HCO ₂ H	1.2	96	100
12^a	HCO₂H	1.2	98	100
13 ^a	Hantzsch ester	3.5	52	78
14	none	-	0	28

^{*}determined by ¹⁹F NMR spectroscopy using a 1,4-bis(trifluoromethyl)benzene internal standard. [°]0 mol% catalyst.

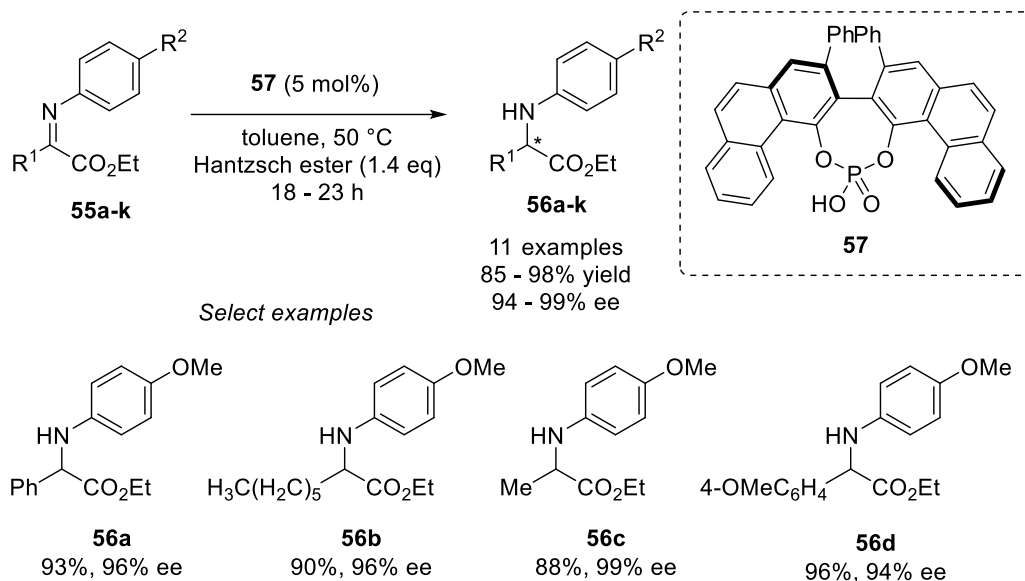
Having seen that formic acid (HCO₂H) could be used as a reductant in metal and metal-free reductive aminations,^{219,226,227} we were interested to explore the possibility of using it with our own system. We were therefore, extremely gratified to find that 97% yield of **52a** could be achieved using 3.5 equivalents of HCO₂H, and that the reaction was amenable using only 1.2 equivalents, still producing 96% yield of the desired product **52a** (Table 9, Entries 2 and 3). Unfortunately, whilst looking into the literature to find NMR spectra for our subsequent substrate scope expansion, we came across an intramolecular phosphinic acid catalysed cyclisation system, which proceeded via S_N2-type substitution of the hydroxyl group in **53** as shown in Scheme 46.^{228,229} Concerned

that our own system was proceeding via a similar simultaneous Brønsted acid/aasic transition state (Scheme 46), we performed a reaction without our optimised FLP-borane **16b** (Table 9, Entry 12). Without any FLP-borane and using 1.2 equivalents of HCO₂H, we still obtained 98% yield of **52a**. This reaction, using only formic acid as both catalyst and reductant was robust enough to withstand the addition of up to 5 equivalents of water without a reduction in yield. After further literature delving, we realised that we had found a novel intramolecular Leuckart type cyclisation to produce α -substituted pyrrolidines.^{227,230} Leuckart reactions are usually catalyst-free reductive alkylation of primary and secondary amines using HCO₂H as the reductant. Whilst the manner in which the hydride moiety is transferred to the iminium intermediate is unknown, it is clear that the subsequent release of CO₂ would be a favourable driving force.^{230,231}



Scheme 46. Phosphonic acid catalysed nucleophilic substitution of hydroxyl group to perform intramolecular cyclisation.^{228,229}

It is possible that Hantzsch ester may also be able to achieve the same yield observed without the presence of the FLP-borane catalyst. As a result, a reaction was performed without any FLP-borane using 1.2 equivalents of Hantzsch ester which obtained only 52% yield (Table 9, Entry 13). This intramolecular Leuckart type cyclisation is something that should be explored in the future for potential asymmetric synthesis of α -substituted cyclic amines, similar to Antilla *et al.* chiral phosphoric acid-catalysed asymmetric reduction of α -imino esters (**55a-k**) using Hantzsch ester (Scheme 47).²³²

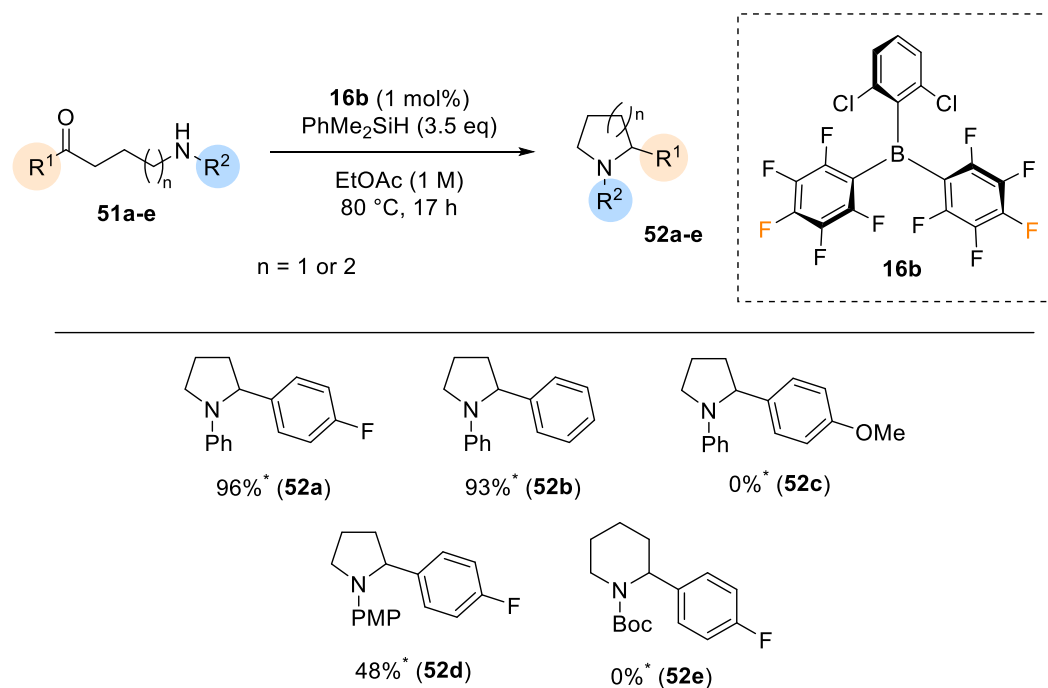


Scheme 47. Chiral phosphoric acid-catalysed asymmetric reduction of α -imino esters (**55a-k**) using Hantzsch ester.²³²

As a result, 3.5 equivalents of PhMe_2SiH ultimately still appeared to be the optimal hydride source. Whilst 2 equivalents of PhMe_2SiH still provided product **52a** in an excellent 91% yield (Table 9, Entry 8), further reduction to 1.2 equivalent proved to be insufficient for effective reductive amination reducing the yield significantly to 10% (Table 9, Entry 9).

3.2.2.3 Substrate Scope

With the optimised reaction conditions in hand, a limited substrate scope (due to lack of time) was explored (Scheme 48). Each starting material was synthesised through the addition of 1.1 equivalents of the respective aryl Grignard to the analogous pyrrolidinone.²²⁹ The simple reductive aminations of alkyl aryl amines and alkyl aryl ketones (**51a** and **51b**) were highly effective, achieving 93% and 96% yield respectively. Using a *para*-methoxy phenyl (PMP) aryl group that would allow for potential subsequent deprotection, led to a significant decrease in the yield of the desired product **52d** (48%). Similarly, use of the Boc protected amine was unsuccessful, with the crude ^1H and ^{19}F NMR spectra showing mostly untouched starting material **51e**.



Scheme 48. Substrate scope for α -substituted saturated cyclic amines. (*determined by ^1H and ^{19}F NMR using a mesitylene or 1,4-bis(trifluoromethyl)benzene internal standard.)

The range of starting materials we explored was extremely limited but allowed to suggest significant impact of the electronics on the aryl ketone functionality (R^1). Comparing the reaction of **51a** and **51c**, shows that electron-donating methoxy substituent (**51c**) appear to entirely prevent the reaction from occurring. This could simply be rationalised by the impact of the electron donation of the methoxy group which would make the ketone significantly less electrophilic, however further studies (about the influence of steric hindrance and electronics) would be required to draw definitive conclusions on this phenomenon.

3.2.2.4 The Limitation of Reductive Aminations with Silanes

The use of FLP-boranes to catalyse reductive aminations has been accomplished mainly using hydrosilanes. However, these reactions suffer from the high price of hydrosilanes relative to other hydride sources and particularly the copious amounts of silyl ethers and siloxane side products especially when large excesses of silane are required (3.5 equivalents).²²⁶ These wasted side products are not atom economical and can be extremely challenging to remove when purifying desired products. Silyl ethers in

particular were a significant side product from our novel intramolecular reductive amination cyclisation reactions (Scheme 48) and were part of the motivation to trial other hydride sources such as formic acid.

When high yields (>80%) were achieved during our intramolecular reductive amination optimisation, no PhMe_2SiH could be observed in the crude ^1H NMR spectrum (Figure 30). Instead, all leftover hydrosilane had been converted to the respective silyl ether, 2 $\text{PhMe}_2\text{Si-OEt}$ (**58**) or $\text{PhMe}_2\text{Si-OnBu}$ (**59**) through hydrosilylation of EtOAc or THF (Figure 30). Whilst these transformations are known to be catalysed by FLP-boranes in the presence of hydrosilanes,^{71,233} we were surprised to observe 100% conversion of the excess hydrosilane as we had not observed this silyl ether side product in any of our intermolecular reductive amination screenings (for example crude **4ag** (Scheme 44), also shown in Figure 30). Due to the challenging purification of target pyrrolidines (**52a**, **b** and **d**) from the silyl ether side products (**58** and **59**) and lack of time, further expansion of the substrate scope was abandoned with a view to optimising an intramolecular reductive amination system using hydrogen, where no side products would be formed.

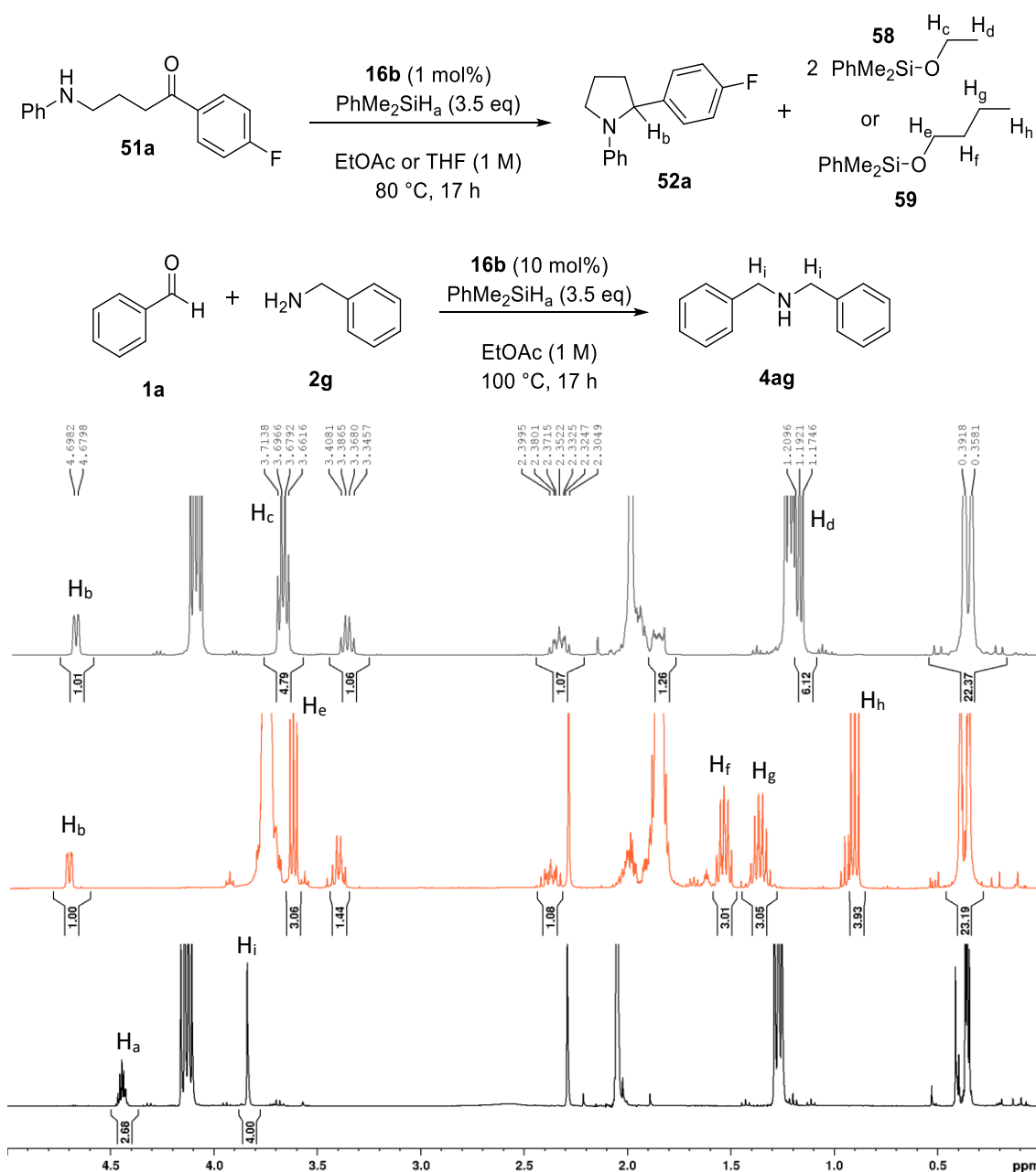


Figure 30. Crude ¹H NMR spectra of intramolecular reductive amination cyclisation using EtOAc (top, grey), THF (middle, orange) and intermolecular reductive amination under similar conditions (bottom, black).

3.2.3 Batch Reactions Using Hydrogen

3.2.3.1 Preface to Work Using Hydrogen

Due to departmental inexperience, the equipment, training and safe operating procedures were not available or approved until partway through this project. As a result, reactions performed using the Parr pressure vessel with hydrogen, were used as

a complimentary technique. In this regard, 'complimentary' means that the reactions performed using hydrogen were done to provide a baseline and for comparison, for example between batch and flow (see chapter four). It is important to note that, due to the delays in accessing the Parr pressure vessel, the work towards our proof-of-concept reductive amination system in continuous flow (which will also be discussed in chapter four) was performed before conducting any batch reaction with hydrogen.

3.2.3.2 The Importance of Reaction Setup and Preliminary Results

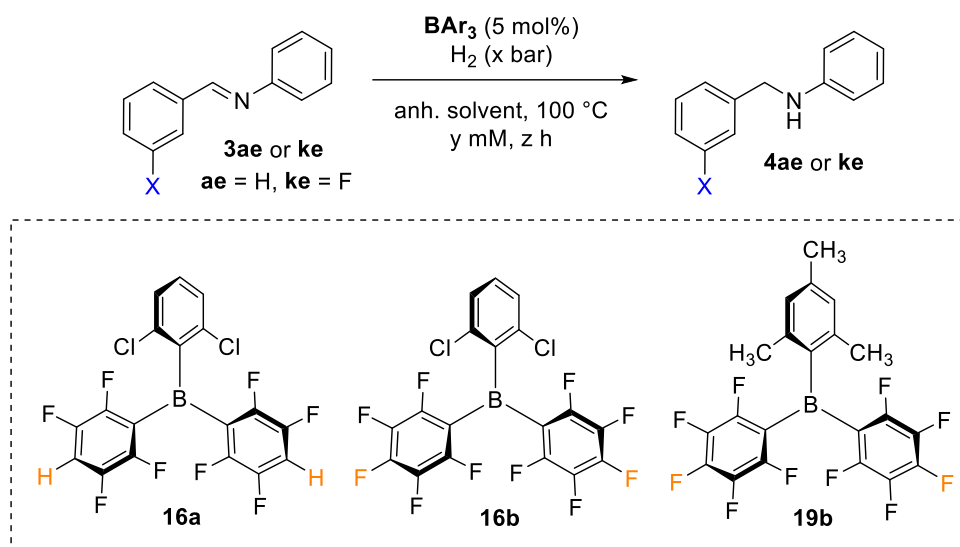
The results presented in Table 10 showcase our initial FLP-borane catalysed imine reductions performed in batch using hydrogen as a reductant. The reaction conditions initially were the same as the final optimised conditions used in the proof-of-concept continuous flow system (chapter four, Table 15). EtOAc had been as successful as THF when using silanes (see sections 3.2.1 and 3.2.2) and due to its greener credentials, we were keen to try and use EtOAc with hydrogen as well. Unfortunately, under these conditions (5 mol% **16a**, dilute concentration (5 mM), H₂ (40 bar), anhydrous EtOAc) only 16% yield was achieved (Table 10, Entry 2). After minor alterations to the reaction conditions, we were able to improve the yield to 67% with 60 bar hydrogen pressure and increasing the reaction time to 18 hours.

Before moving forward with our EtOAc system we decided to first replicate Hoshimoto and coworker's reductive amination results, which also uses catalyst **16a**.³⁷ Our initial attempts using Hoshimoto's optimised conditions in THF are shown in Entries 6 and 7. We were disappointed that our yields (32%) did not match those attained by Hoshimoto (>99%).

The supporting information for batch hydrogenations often lacks experimental setup details, such as where and how an autoclave pressure vessel was loaded and sealed. Some autoclaves can be degassed under vacuum before pressurising with hydrogen, but ours cannot. We were concerned that Hoshimoto's experiments might have been degassed or prepared and sealed in a glovebox. Catalyst and reagents used in entries 1-7 were weighed and prepared within a glovebox, where the catalysts and reagents were stored. However, the Parr pressure vessel was sealed outside of the glovebox. As a result,

when the vessel was pressurised with hydrogen (20 bar), it is possible that 1 atm of air was already inside. We proposed that this was the cause for the significant decrease in yield for Entries 6 and 7.

The reaction setup was changed so that the Parr pressure vessel was sealed within the glovebox, which resulted in excellent yields (92 – 99%) that were consistently reproducible (Table 10, Entries 8 – 10). However, despite the improved setup, EtOAc proved to be a much less effective solvent than THF, yielding only 8% under the same reaction conditions (compare Table 10, Entries 11 with 8 and 9). Some limited adjustments (Entries 12 and 13) were made to improve the yield in EtOAc giving respectively 12% and 32% in, but we eventually decided to stop further batch imine reductions using hydrogen with EtOAc.

Table 10. Preliminary imine reductions in batch.³⁷

Entry	X	BAr ₃	Solvent	Conc. (y mM)	H ₂ (x bar)	Time (z hours)	Yield (%) [*]
1	F	-	EtOAc	5	40	18	0
2	F	16a	EtOAc	5	40	2	16
3	F	16a	EtOAc	5	40	24	16
4	F	16a	EtOAc	5	60	18	67
5	F	16a	EtOAc	5	20	18	35
6 ^a	F	16a	THF	50	20	2	32
7 ^a	F	16a	THF	50	20	6	32
8 ^a	H	16a	THF	50	20	2	99
9 ^a	H	16a	THF	50	20	2	99
10 ^a	F	16a	THF	50	20	2	92
11 ^a	H	16a	EtOAc	50	20	2	8
12 ^a	H	16a	EtOAc	10	30	18	12
13 ^a	H	16a	EtOAc	5	80	2	32
14 ^a	H	16b	THF	50	20	2	99
15 ^a	H	19b	THF	50	20	2	2
16 ^a	H	BCF	THF	50	20	2	0
17 ^a	H	BPh₃	THF	50	20	2	0

^{*}determined by ¹H and ¹⁹F NMR using a mesitylene or 1,4-bis(trifluoromethyl)benzene internal standard.

^a4Å MS

Under the optimal reaction conditions, a catalyst comparison was performed with our available known moisture tolerant FLP-boranes (**16a/b** and **19b**) and the commercially available BCF and BPh₃. The synthesised moisture tolerant FLP-boranes (**16a** and **b**) were found to be effective catalysts for imine hydrogenation, both achieving a 99% yield with hydrogen (Table 10, Entries 9 and 14). In contrast, the commercially available triaryl boranes (BCF and BPh₃), as had been observed by Hoshimoto *et al.* were ineffective,³⁷ with a 0% yield for both (Table 10, Entries 16 and 17), validating the synthetic efforts put into the moisture tolerant FLP-boranes (**16a/b**). Unfortunately, under the given reaction conditions, **19b**, with its mesityl functionality, also proved to be ineffective, yielding only 2% (Table 10, Entry 15).

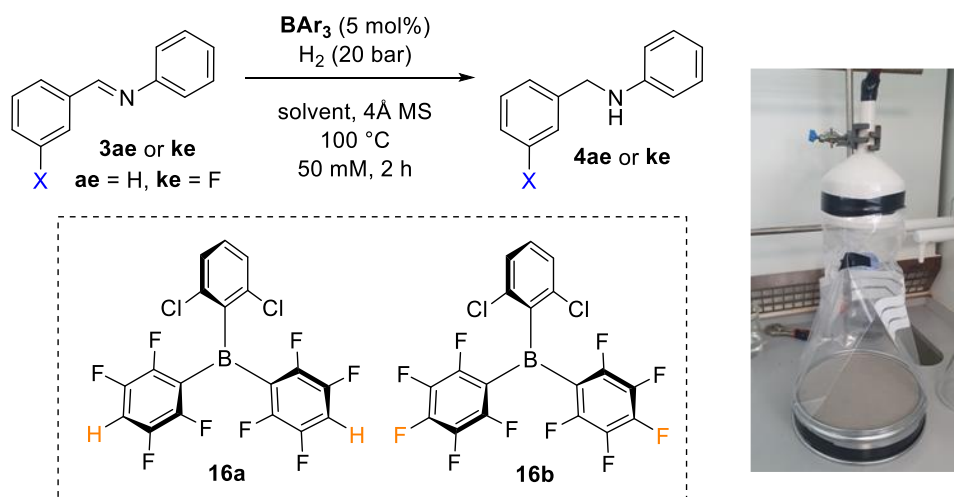
We were interested in creating a system which could be set up outside the glovebox. The high cost and bespoke nature of the required equipment have been major obstacles in advancing FLP-borane catalysed reductions using hydrogen. To make the reaction set up more practical (and also allow for faster screening of reaction conditions), we sought to create a reaction setup that could be reliably carried out using more readily available alternatives.

Table 11 displays select data from our batch imine hydrogenation experiments using hydrogen, which were conducted outside the glovebox. All reagents were weighed under normal atmospheric conditions and then placed in a Parr pressure vessel. To create an inert atmosphere, we covered the vessel with an upturned funnel attached to an argon tap line within a fume hood (see Table 11). After adding the anhydrous solvent (THF, 2-Me THF, or propylene carbonate), the pressure vessel was sealed and pressurised with hydrogen (20 bar) before heating to 100 °C.

We found that it was crucial to ensure that the system, at the point of hydrogen pressurisation, contained 1 atm of inert argon instead of air. This adjustment led to significantly improved yields (97 – 99%) in our reactions compared to our initial trials, in which the presence of air appeared to have caused low yields. We were pleased to achieve similar yields with our new reaction setup (Table 11, Entries 1 and 2) as those optimised in Table 10 (92 – 99%).

In contrast to Hoshimoto's system, we were able to achieve a 97% yield for both **16a** and **16b** (Table 11, Entries 5 and 6) without using molecular sieves. Similarly, a 99% yield was still possible when conducting a reductive amination without molecular sieves, using 1 equivalent of 3-F benzaldehyde and aniline, instead of the preprepared imine **3ke**.

Table 11. Imine hydrogenation and reductive amination using hydrogen setup outside the glovebox.³⁷



Entry	X	BAR_3	Solvent	Yield (%) [*]
1	H	16a	THF	99
2	F	16a	THF	97
3	F	16a	2-Me THF	13
4	F	16a	Propylene carbonate	2
5 ^a	F	16a	THF	97
6 ^a	F	16b	THF	97
7 ^{a,b}	F	16b	THF	99

^{*}determined by ^1H and ^{19}F NMR using a mesitylene or 1,4-bis(trifluoromethyl)benzene internal standard.

^ano 4Å MS. ^b1 eq 3-F benzaldehyde and 1 eq aniline

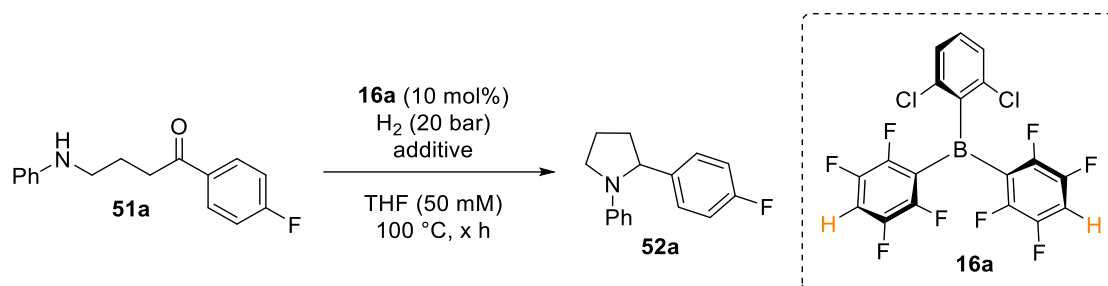
3.2.3.3 Intramolecular Reductive Amination

As alluded to in the previous section, the initial attempt to carry out the novel intramolecular reductive amination cyclisation using hydrogen was unsuccessful (Table 9, Entry 6). For this initial attempt, the reaction conditions were the same as those optimised for the use of silanes as the reductant. These conditions included 1 mol%

catalyst loading (**16b**) and were performed in EtOAc at a relatively high concentration (1 M) compared to those optimised for hydrogen (typically 50 mM). The reaction mixture was pressurised with hydrogen (20 bar) and then heated to 80 °C. Using reaction conditions previously optimised for reductive amination reactions using hydrogen (Table 11, Entry 7), the reductive amination of compound **51a** was attempted (Table 12, Entry 1).

Table 12 displays our attempts at conducting intramolecular reductive amination cyclisation using hydrogen. We applied our optimised hydrogenation reaction conditions and setup from (Table 11). Whilst **16a** and **16b** exhibited similar catalytic performance in our tests, there was more literature support for the use of FLP-borane **16a** with hydrogen.^{37,190} As a result, we opted to use **16a** and increased the loading to 10 mol%.

Table 12. Limited attempts to perform intramolecular reductive amination cyclisation using hydrogen.



Entry	Time (x h)	Additive	Yield (%) [*]	Conversion (%)
1 ^a	2	4Å MS	0	100
2 ^b	2	-	0	25
3	2	-	0	58
4	24	TMSOTf (10 mol%)	0	100
5	24	TMSOTf (1 eq)	0	100

^{*}determined by ¹⁹F NMR using a mesitylene or 1,4-bis(trifluoromethyl)benzene internal standard. ^anon fluorinated SM. ^bcontrol/blank (no catalyst)

We were disappointed that our initial attempt resulted in a 0% yield, despite achieving 100% conversion of the starting material **51a** (Table 9, Entry 6). We reintroduced molecular sieves in the hope that the condensation equilibrium would be favoured by removing the water byproduct. Although molecular sieves are supposed to be inert, we

were concerned that their use might be increasing the instability of our starting material **51a**. Stephan *et al.* suggested that molecular sieves, through their embedded oxygens, can act as heterogeneous Lewis bases. In 2015, they developed an FLP-borane-catalysed hydrogenation and deoxygenation of aryl alkyl ketones using molecular sieves as the Lewis basic component. Regardless, the crude ^1H NMR spectrum from Table 12, Entry 1 was a complex mixture, containing no starting material.

In order to demonstrate the instability of our amino ketone starting material **51a** under the relatively harsh conditions, we conducted a control reaction without any catalyst. After 2 hours, we observed a 25% conversion (Table 12, Entry 2).

Our final attempts, we investigated the use of trimethylsilyl trifluoromethanesulfonate (TMSOTf) as an additive. TMSOTf is often used as a silylating agent and a Lewis acid activator in organic synthesis.²³⁴ We hypothesised that the hydrosilane (PhMe₂SiH) in our cyclisation system may have served a dual purpose, acting as both the hydride source and activating the ketone for cyclisation as shown in Figure 31. However, we obtained a 0% yield when TMSOTf was added catalytically and stoichiometrically. Consequently, and due to the lack of time, we decided to abandon further work on developing this intramolecular cyclisation using hydrogen.

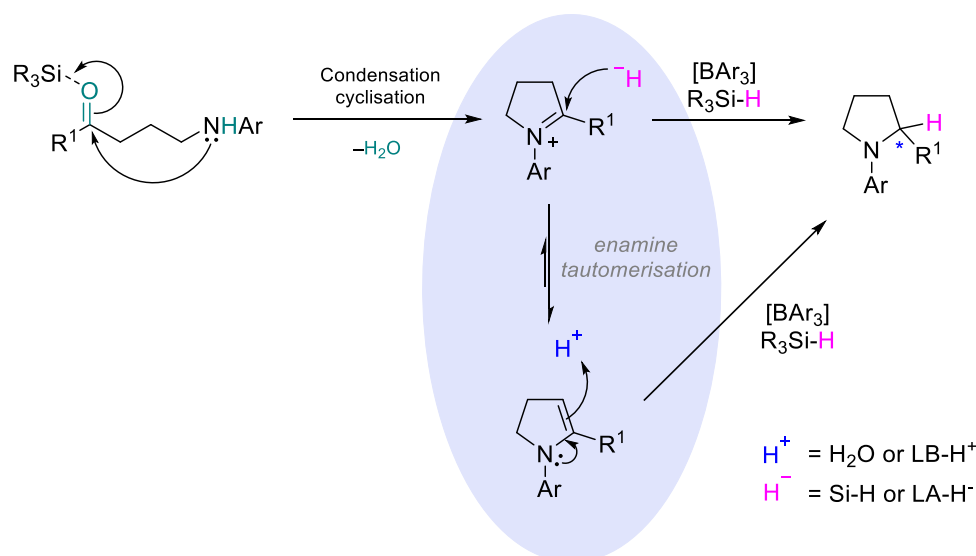


Figure 31. Plausible mechanism for the FLP-borane catalysed intramolecular reductive amination cyclisation of amino ketones using silanes.

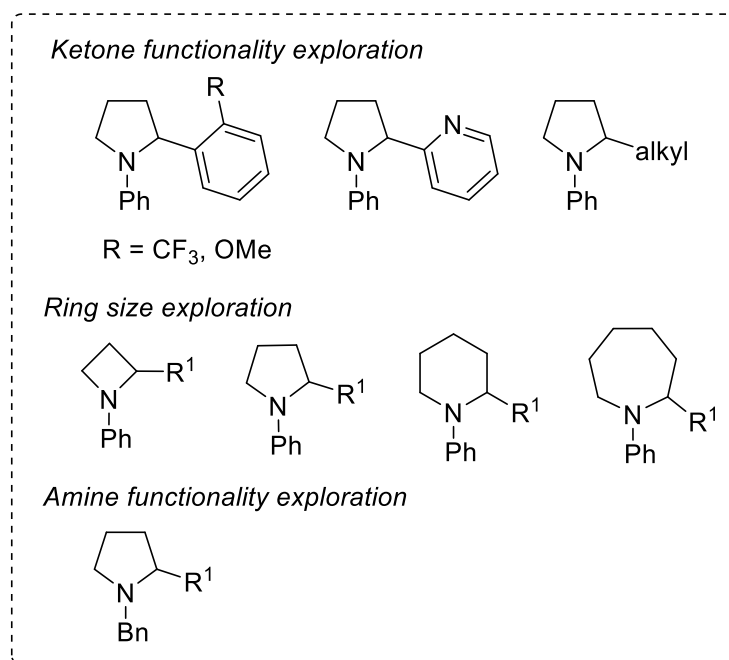
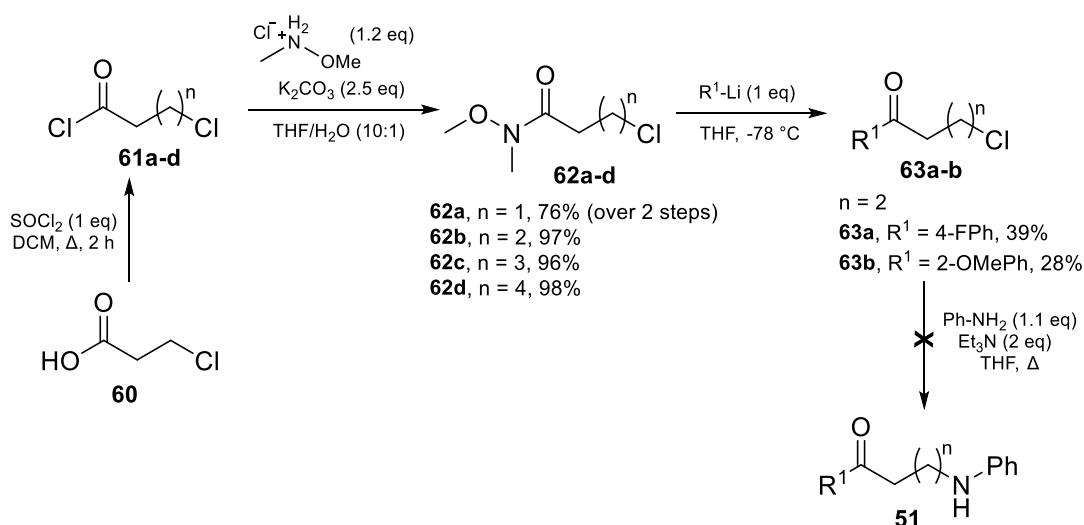
3.3 Outlook and Conclusions

In summary, we investigated the use of three moisture-tolerant FLP-boranes for catalysing reductive aminations/imine hydrogenations using silanes and hydrogen. Whilst all three FLP-boranes (**16a/b** and **19b**) were previously used for reductive amination reactions, until now they have not been directly compared to each other and to commercially available BCF or BPh₃. FLP literature rarely compares results obtained with new boranes to ones obtained with BCF or BPh₃ and we were pleased to see our catalysts outperformed commercially available ones in most cases. Our work with silanes and hydrogen revealed that high Lewis acidity and adherence to the size exclusion principle are crucial for effective catalysis. We found that **19b**, which is substituted with the bulky mesityl functionality, consistently showed significantly less effectiveness as a catalyst for both inter and intramolecular reductive aminations using silanes and hydrogen. Although the steric hindrance from the mesityl substituent may improve the catalyst's moisture tolerance, it also leads to a reduction in Lewis acidity (76%) compared to the similarly sterically hindered 2,6-dichlorophenyl-substituted **16a/b** ($\geq 89\%$), which significantly slowed down hydrogen and silane activation in our systems.

Using our most effective catalyst **16b**, we were able to perform intermolecular reductive aminations with 11 examples through the optimisation of multiple sets of conditions. Whilst there were a limited number of examples, the substrate scope was able to provide a fair reflection of the strengths and limitations to FLP-catalysed reductive aminations incorporating primary and secondary aryl amines, alkyl amines, *N*-protecting groups, aldehydes, alkyl-aryl ketones and alkyl ketones. We were also able to overcome some of these limitations. By changing the solvent to EtOAc or THF and using more forcing conditions (1 or 10 mol% catalyst loading, 3.5 equivalents silane, 80 or 100 °C and 17-hour reaction time) we were able to improve upon literature precedents for some FLP-catalysed reductive aminations. These improvements included: obtaining dibenzylamine **4ag** in 93% yield which had previously been obtained using electron deficient FLP-boranes in moderate yield (60%), as well as, using the alkyl-aryl ketone acetophenone (**1b**), to obtain **4be** in 99% yield which had similarly only been obtained by electron deficient FLP-boranes in moderate yield (67%).

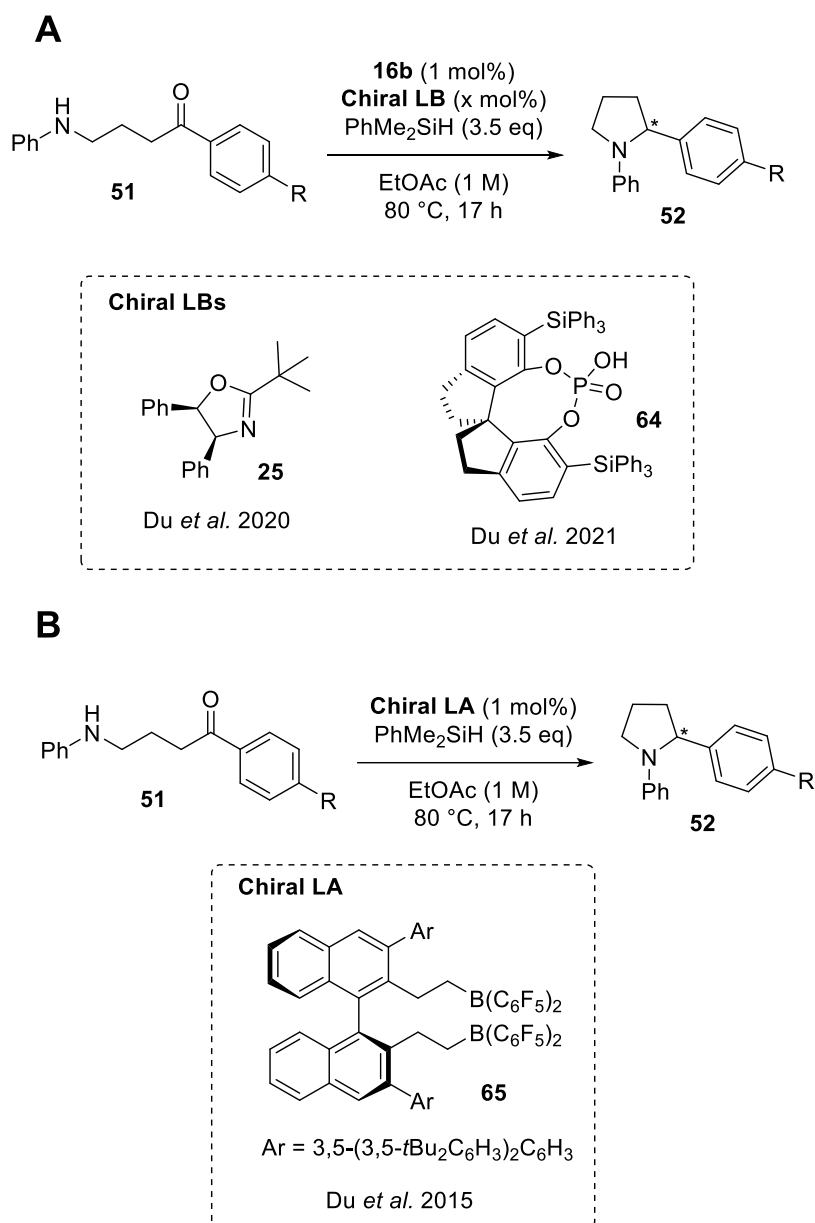
Through optimisation of reaction conditions, a system was developed for the novel FLP-borane catalysed intramolecular reductive amination of functionalised aminoketones, used for the synthesis of 3 examples of α -substituted pyrrolidines (48 – 93% yield). The system has been optimised and EtOAc has been shown to be effective solvent for the system when using silanes. Using EtOAc is not something that, to the best of our knowledge, has been shown to be an effective solvent in FLP-catalysed reductions. Although attempts to further develop this system by incorporating the use of hydrogen as the reductant were unsuccessful, there is potential for future expansion of the limited substrate scope of the novel cyclisation. At present, multiple intermediates have been produced for expanding the substrate scope (Scheme 49). These intermediates could produce starting materials which explore increasing/decreasing the ring size (4, 6, and 7-membered), alternative ketone functionalisation such as (hetero)aryl and alkyl groups in the future, and alternative amine functionalisation (particularly with a removable deprotecting group) (Scheme 49).

Synthesis of alternative starting materials



Scheme 49. Future planned expansion of intramolecular reductive amination substrate scope, including intermediates for the future starting materials which have already been synthesised.

Crucially, future work should aim to develop an asymmetric version of the reaction. Unfortunately, due to a lack of time we could not investigate the use of chiral LBs (**25**²³⁵ and **64**²³⁶) to perform our intramolecular cyclisation asymmetrically, as we had intended (Scheme. **A**). In the future, an asymmetric version on our system could also be achieved through the adaptation of currently established asymmetric imine hydrosilylations (such as exploiting the chiral LA **65** shown in Scheme. **B**).²³⁷



Scheme 50. Future work: **A.** Application of established chiral LBs to intramolecular cyclisation.^{235,236} **B.** Application of established chiral LA to intramolecular cyclisation.²³⁷

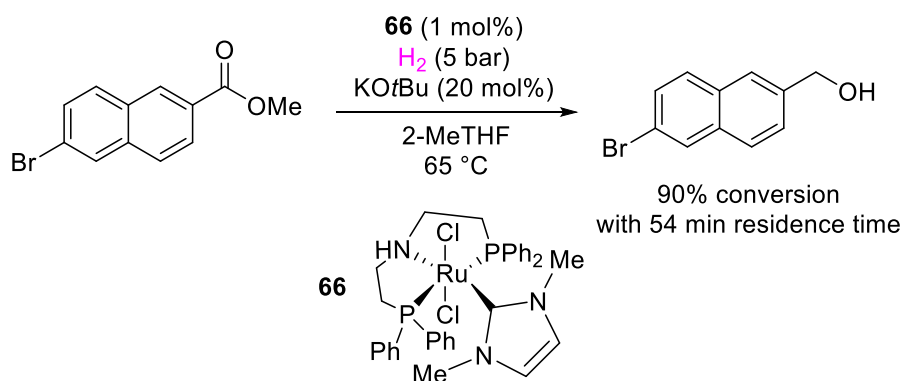
Chapter Four: Application of Synthesised Moisture-tolerant Boranes to Flow Reductive Aminations

4.1 Introduction

4.1.1 General Introduction Aims of the Chapter

My project was funded by ERDF with the aims to develop collaborations with local industrial partners. We were fortunate to be able to collaborate with Autichem Ltd. following the article published in the Chemicals Northwest non-peer-reviewed Elements magazine.³⁸ Autichem Ltd. is a company based in Cheshire developing innovative flow reactors (production of custom Continuous Stirred-Tank Reactor (CSTR)). The Autichem DART reactors specialise in using agitators to mobilise slurries leading to a greater tolerance for solids and more efficient gas-liquid contact.

Thankfully, Autichem Ltd. has experience working with 'challenging' catalysts in flow.³⁹ In a previous collaboration with GlaxoSmithKline Pharmaceuticals (GSK) and the University of Strathclyde, a custom CSTR (Continuous stirred-tank reactor) flow reactor was used to scale up reductions of two pharmaceutically relevant esters, both in continuous flow under relatively mild conditions (hydrogen 5 bar). Crucially for our work, the ruthenium pincer complex, **66**, that was used to catalyse their hydrogenations was used as a heterogeneous slurry under anhydrous conditions (Scheme 51).³⁹



*Scheme 51. Catalytic reduction of pharmaceutically relevant ester in a bespoke Autichem Dart flow reactor using heterogeneous ruthenium catalyst **66**.²³⁸*

Following more detailed discussion about our project, Autichem were interested in demonstrating the utility of their reactors using sustainable catalysts such as our FLP boranes. Ideally this would include developing solutions for a heterogeneous FLP catalysis system using their reactor. This collaboration is one of the reasons for our novel moisture tolerant FLP catalysts to be designed with the potential to be incorporated into a heterogeneous support. Working in this design principle would allow our catalyst to eventually be employed heterogeneously (this will be discussed in chapter 5). Our meetings and discussions with Autichem Ltd. have reinforced the potential for both homogenous and heterogeneous FLP catalysis in continuous flow. Whilst both provide excellent value to the FLP academic space, heterogeneous FLP catalysis using their reactor could allow for the collection and recycling of our heterogeneous borane catalyst.

The DART-DM[®] CSTR flow reactors, which Autichem produces are available in many different forms, with sizes ranging from 1 mL to 100 L. As they are designed to be adaptable and versatile, DART reactors can be manufactured using a wide range of chemically resistant robust materials including glass for photochemical reactors.²³⁹ At the time of our initial discussions, we were organising a loan of a custom 160 mL DART-DM flow reactor with CSTR mixing. However, unfortunately Autichem Ltd. was unable to provide us with a custom reactor due to the COVID-19 pandemic. The shortage of the corrosion-resistant nickel-alloy, Hastelloy, which is used to produce their custom flow reactors capable of handling high pressures, meant that we would not have access to a custom reactor until later in the project. Additionally, we thought it would be reasonable to explore the capabilities of boranes in simpler flow conditions using Thalesnano H-cube[®] available at Lancaster University.

The H-cube[®] is an example of ready-built “click-in reactors” capable of performing both homogeneous and heterogeneous hydrogenations in continuous flow.¹⁵⁸ Usually the H-cube[®] is used for traditional hydrogenations using easily switchable catalyst cartridges (CatCarts[®]) to allow for the use of standard heterogeneous metal catalysts. The H-cube[®] mini is primarily used for its simple and broad hydrogenation applications once the required cartridges have been purchased from their library. It is not typically employed as a method development system, although there are cases where people have used it

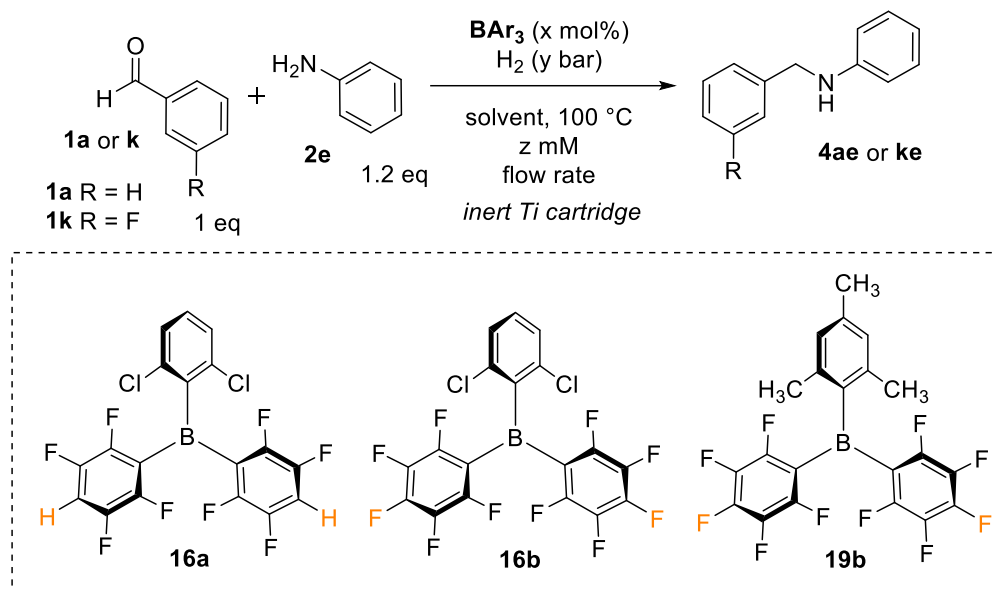
for this purpose. In these instances, individuals are usually performing novel transformations requiring standard TM cartridges,^{240–242} or testing their custom catalyst cartridges,²⁴³ which Thalesnano can develop and provide if you supply them with sufficient heterogeneous catalysts.

However, the H-cube[®] also can be fitted with inert catalyst cartridges made from quartz or titanium which would enable to collect preliminary homogeneous catalysis data, using stock solutions of FLP catalysts. With access hydrogen pressures (1 – 100 bar) and temperatures (25 – 100 °C) which may be required to enable efficient hydrogenation using FLPs,¹⁶⁴ it presents the perfect opportunity to test a range of conditions for our homogenous boranes in continuous flow with hydrogen for comparison with our results obtained in batch. The H-cube[®] does, however, have some limitations for our goals, which we were aware of before undertaking this research. Namely, the reactor volume of the H-cube[®] is extremely small (3 – 4 mL), which means with a minimum flow rate of 0.1 mL/min the residence time for the reaction mixture is estimated to be approximately 30 – 40 minutes (this will be discussed more in the H-cube[®] reaction setup in section 4.2.1). To overcome residence time limitations, reagent solutions used with H-cubes can be cycled so that full conversion are achieved.

4.1.2 Aims of the Chapter

With all this in mind, the initial aim of the work presented in chapter four is first to develop proof-of-concept (POC) examples of reductive amination reactions in flow using the H-cube[®] and homogeneous FLP-borane catalysts. It is clear, from the examples discussed in section 1.4, that hydrogenations in continuous flow possess many advantages over batch reactions. Although there have only been a few instances of FLP-catalysed systems developed in continuous flow,^{186,187,244} there is enough evidence to suggest that it is only a matter of time before a FLP-catalysed hydrogenation using hydrogen is achieved in flow. However, as there is very little literature precedent for FLPs in continuous flow, we decided to start our flow hydrogenations using our known boranes as catalysts. We have also chosen the reductive amination shown in Scheme 52,

due to our experience with this system which has been discussed in chapter three. Our experience with this reaction in batch will also allow us to establish whether these reductive aminations can benefit from performance in continuous flow.



Scheme 52. Reductive amination reaction chosen for proof-of-concept system development using the known moisture tolerant boranes synthesised.

Subject to the success of our POC system, the second aim is the application of our POC in a custom reactor from our partner company using homogenous catalysis initially. Since residence time can easily be controlled in CSTR flow reactors we would expect vast improvement of the results obtained in the POC example using H-cube[®]. Moreover, since catalyst immobilisation is one of the things Autichem Ltd. were also interested in, development of heterogenous catalysts capable of application under our POC flow conditions would also be an ultimate goal from this part of the project and this will be discussed in more details in chapter 5. The sheer novelty of this research means that both known and novel FLPs with heterogeneous potential provide great value to the FLP field. It is crucial therefore, that we can establish a POC system from our work with the H-cube[®].

4.1.2 Important Preface to Chapter Four Results

We spent a lot of time and resources investigating the use of FLPs as catalysts for reductive aminations in a continuous flow using the H-cube[®]. However, we encountered a problem that raised doubts about the reliability of the results obtained using this equipment. We aimed to carry out truly anhydrous reactions, but the stock solution inlet of the standard H-cube[®] was not suitable for this purpose, as it could only draw one stock solution through a PTFE filter. To create a custom inlet that would allow us to perform the anhydrous reactions, fresh tubing and a Y-junction was used, and the PTFE filter was excluded. However, unfortunately, after obtaining poor results using this system setup and troubleshooting, we found that the yield significantly dropped when the PTFE filter was not used. We eventually discovered that the lack of reproducibility was likely due to metal leaching, a well-known problem in heterogeneous catalysis systems.^{161,174,240} The H-cube[®] is a popular piece of equipment used in both academic and industrial labs because of its simplicity when it comes to reducing a product. To reduce a desired functional group within a target molecule, a heterogeneous catalyst cartridge with established conditions is chosen. When full conversion of starting material is not achieved, it is customary to recycle the stock solution back through the inlet until the desired conversion to the required product is achieved. Unfortunately, before we started using the equipment, this protocol must have led to significant metal leaching, which we believe has sedimented and been trapped within some of the tubing and filter frits within the machine. We propose that this metal sedimentation was helping catalyse our reductions and introduced a lack of reproducibility in the results, we obtained. We suspect that the sedimentation has been particularly bad within the PTFE filter, which should have been completely inert but has led to significantly increased yields when used. How we discovered these problems and what we have done to support our hypotheses will be discussed in detail in section 4.2.4.

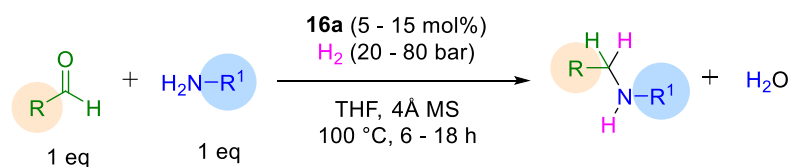
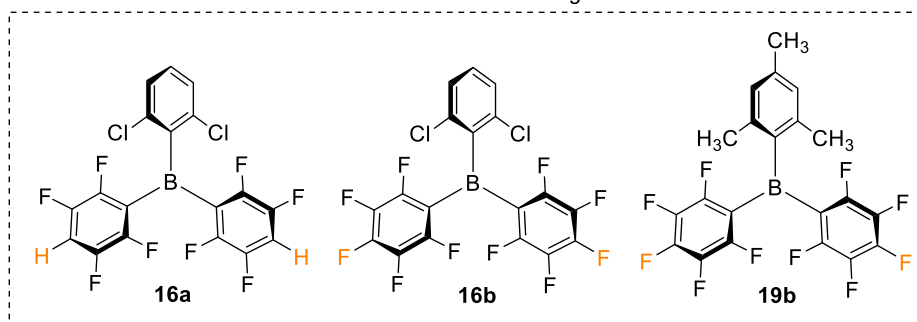
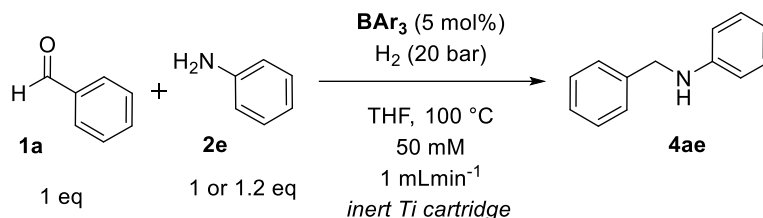
Despite these problems, I have given below an overview of the results we obtained using the H-cube[®] as we believe many of the trends we observed, and the problem-solving required to make changes to the experimental setup are valuable and would prove useful for future work. However, it is important to note that the absolute values of yields and conversions reported in this section are flawed and therefore we have focused analysis

on trends observed when varying parameters rather than specific yields obtained. This section was included as a preface to the results because, I wanted the reader to keep this in mind while reading this chapter and interpreting the observations, results, and discussions.

4.2 Results and Discussion

4.2.1 General Reaction Setup

As stated above in the aims, we have chosen to develop a POC system for the reductive amination reaction shown in Scheme 52. We have experience performing this reaction in batch by ourselves (section 3.2.3) which will provide a perfect opportunity for comparison. We will also be able to compare our POC system results to those in reported literature systems. Particularly useful was the established batch conditions from Hoshimoto and co-workers in their reductive amination system using hydrogen and **16a** (Scheme 53).³⁷ This work was discussed in more detail within section 1.3 but regardless adaptation of their conditions with our own discoveries provides the foundational starting point for our POC flow system.

A Hoshimoto *et al.* 2018**B** Starting conditions

Scheme 53. A. Established reductive amination batch system using hydrogen.³⁷ B. Chosen starting conditions for of proof-of-concept reductive amination system in flow using hydrogen.

The H-cube[®] employs a HPLC-like platform for substrate delivery. For simple reactions set up under ambient conditions (non-anhydrous/bench stable), the inlet contains a PTFE filter which is submerged in a stock solution of the reaction mixture (Figure 32 and Figure 33).¹⁶⁸ From here a piston pump delivers the reaction mixture into the system where it is mixed with the generated hydrogen gas, before passing over a cartridge which in our case is packed with inert titanium (Ti) or quartz. The particle size within the Ti cartridge is kept between 630 and 800 μm , to allow uniform flow and pressure through the catalyst column. The quartz CatCarts[®] are filled with quartz sand ranging from 100 – 800 μm particle size (no sieving is applied). Crucially, the reaction mixture can be heated up to 100 °C and pressurised up to 100 bar (Figure 34). The flow rate of the reaction mixture can be selected in the range of 0.1 – 3 mL/min via the touchscreen and is communicated to the external pump.^{168,245}

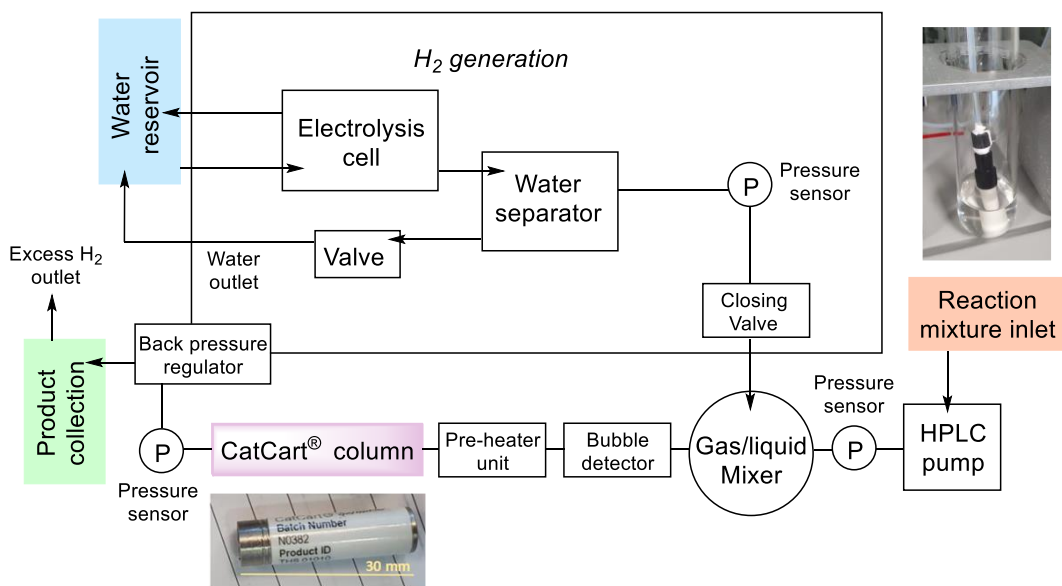


Figure 32. Schematic design of the H-cube[®], with highlighted images of the PTFE filter inlet and an inert titanium CatCart[®].²⁴⁶

Once a chosen pressure and flow rate is set, the system must be allowed to run for a few minutes to pressurise itself and equilibrate. The machine should be equilibrated with the same solvent, under the same conditions as the reaction will be performed. Most likely this solvent will also differ from the conditions required for storage of the H-cube[®]. Once the machine reports that it is 'stable', excess hydrogen bubbles should be coming out of the end of the device (Figure 34). At this point, the inlet line can be transferred to the reaction mixture solution. The reaction takes place in the heated cartridge and the H-cube[®] CatCarts[®] we had access to were 30 mm in length.

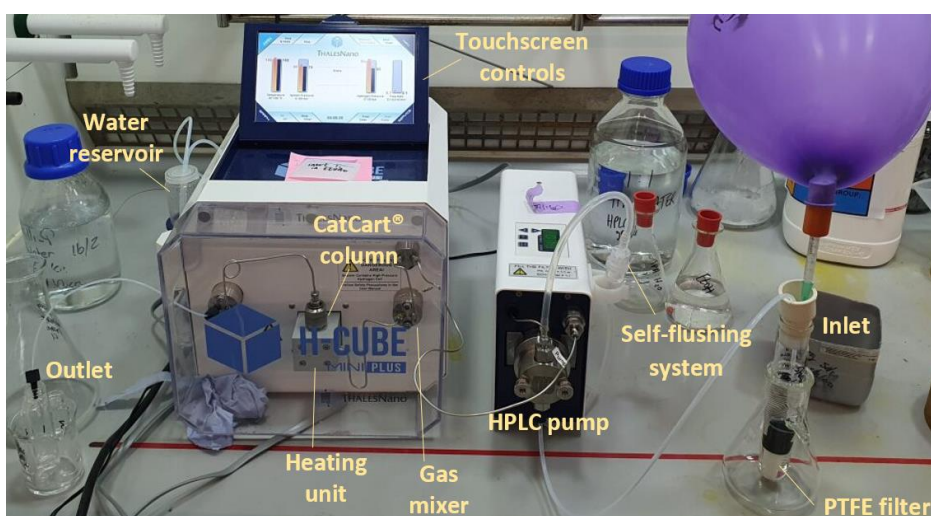


Figure 33. Labelled image of the H-cube[®] and typical preliminary reaction setup.

The system's total volume has been determined by us to be approximately 4 mL, with our 30 mm cartridge. With the lowest flow rates of 0.1 mL/min, the maximum residence time is around 40 minutes. However, since the reaction conditions are not introduced until after the gas mixer and upon reaching the heating unit, the estimated residence time under reaction conditions is only a fraction of the total 40 minutes (Figure 33).¹⁷¹ We were aware of this when we proposed using the H-cube[®] to collect preliminary results.

The system volume, and as a result, total residence time is significantly impacted by alteration of the reaction mixture inlet. As the H-cube[®] is a complete flow platform, we never changed the any tubing in the flow path after the HPLC pump. Only the cartridge was ever altered after this point. Any modifications to the set up discussed will be mentioned where appropriate in the subsequent sections. However, as can be seen in Figure 32 and Figure 33, the HPLC-like platform allows for modification of the reaction mixture inlet and associated tubing prior to the HPLC pump. For example, switching the reaction inlet to more standard flow tubing, with a smaller diameter (1 mm) and no PTFE filter we noticed the total system volume drop significantly from 4 mL to 2.75 mL. This 31% decrease in system volume has all been lost prior to the HPLC pump and is further evidence estimated residence time under the desired reaction conditions is only a fraction of the total system volume/residence time. Throughout this section, every modification to the general system setup described above, will be discussed in context to how that modification altered the system conditions and total system volume. It is important to note that as we will never modify the system setup after the HPLC pump, the system volume and therefore, residence time desired under reaction conditions ('post-pump') will always remain the same for all reactions as long as equivalent flow rates are used.



Figure 34. Touchscreen control panel for the H-cube®, showing the system running with pressure set to 100 bar H₂ at 100 °C and a flow rate of 0.1 mL/min. The system is 'stable' and therefore is ready for the reaction.

4.2.2 Preliminary Results

The preliminary results (Table 13), were collected using the general set-up described above. The respective solvent was used to flush the system and establish reaction conditions. Whilst the reaction conditions were stabilised the reaction mixture was prepared by the addition of anhydrous tetrahydrofuran (THF) to an oven dried Schlenk tube (under argon) containing benzaldehyde, aniline and pre-weighed borane catalyst (taken from the glovebox). The mixture was allowed to briefly stir before it was transferred to an oven-dried test tube that would be used as the vessel to contain the inlet solution. Although it is challenging to achieve truly anhydrous conditions with this reaction set up (which uses the PTFE filter for the inlet solution), a balloon of argon was pierced through a customised Suba seal to ensure an argon blanket could be maintained over the anhydrous setup solution (shown in Figure 33). The use of a balloon over a stock solution at an intake to a flow machine is not unheard of and as a result, we were fairly confident this setup could limit the excess water ingress from our hygroscopic reaction mixture throughout the reaction.¹⁶⁹

The total system volume was determined through a trial reaction using our general reaction setup. In order to determine a precise system volume (approximate system volume was 3 – 4 mL), we collected aliquots at 5-minute intervals from 20 – 50 minutes whilst using a 0.1 mL/min flow rate. The aliquots were collected in sample vials each containing approximately 0.5 mL of solvent. Because of the dilute concentrations used,

solvent was removed from each aliquot under reduced pressure and were redissolved in CDCl_3 for NMR spectroscopic analysis. Aliquots contained nothing but solvent until 40 – 45 minutes and as a result, it was determined that the system volume was ~ 4 mL. For every reaction after inserting the PTFE filter into stock solution the first 4 mL was collected as the 'dead-zone' containing the solvent that was already within the system before the reaction was commenced.

For our first reaction (Table 13, Entry 1), where the flow rate was so high (1 mL/min), the first 3 aliquots were collected 1 minute apart, with each aliquot being 1 mL in size. However, as we very quickly transitioned to the slowest available flow rate (0.1 mL/min) for standard reactions, and until stated otherwise, aliquots were taken every 10 minutes after the system volume ('dead-zone') (4 mL) had passed. At 0.1 mL/min this resulted in aliquots which were approximately 1 mL in volume. In general, 3 aliquots were taken for every reaction between 40 and 70 minutes. The reaction yield was monitored by quantitative ^1H NMR spectroscopy. After removing solvent from each aliquot, the crude oil would be dissolved in CDCl_3 for NMR spectroscopic analysis. Whilst the yield for each aliquot was determined, for comparison only the first aliquot is reported. The determination of the NMR spectroscopic yields was based on the benzylic protons attached to the α -carbon in the product ($\sim\delta = 4.36$ ppm) compared to the aldehyde ($\sim\delta = 10.06$ ppm) and imine protons ($\sim\delta = 8.49$ ppm). For a successful reaction a typical ^1H NMR spectrum of an aliquot is shown in Figure 35.

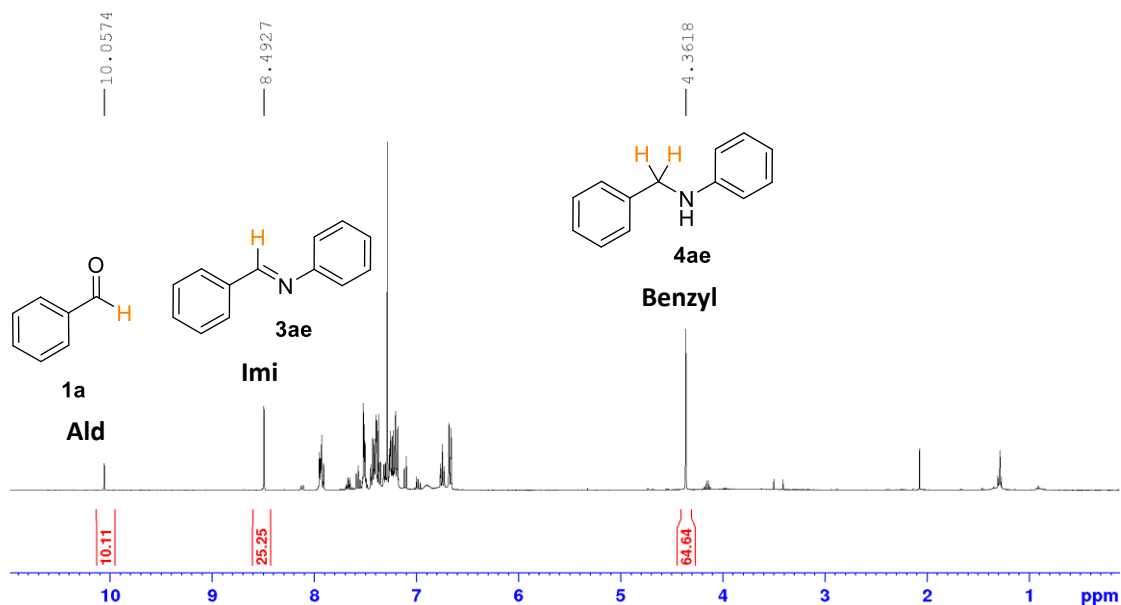
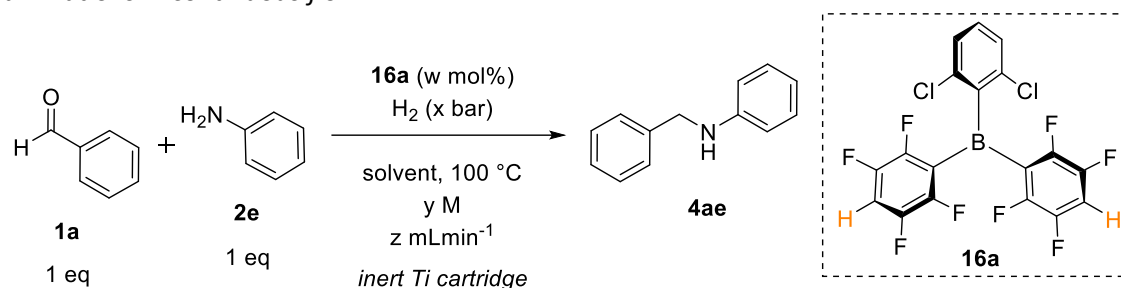


Figure 35. Typical ^1H NMR spectrum of a successful flow reaction aliquot used to estimate yield.

The first conditions tested (Table 13, Entry 1) were based on the work done by Hoshimoto *et al.* in batch introduced in section 1.3.2.¹²⁴ Unfortunately, the standard 1 mL/min flow rate appeared to be too fast, and no product was observed. To increase the residence time, the flow rate was dropped to the minimum achievable, 0.1 mL/min (Table 13, Entry 2), which led to a 2% yield. We proposed that given the short residence time, even at 0.1 mL/min, 20 bar H_2 pressure was not forcing enough conditions, considering Hoshimoto and co-workers' work had been optimised to take two hours for their synthesis of **4ae**. As a result, we were extremely gratified to find that increasing the H_2 pressure to 60 bars led to a 22% yield (Table 13, Entry 3).

Table 13. Select preliminary results, using the H-cube® to perform borane-catalysed reductive aminations in continuous flow.



Entry	Solvent	Catalyst/ loading (w mol%)	H ₂ pressure (x bar)	Conc. (y mM)	Flow rate (z mL/min)	Yield (%) [*]
1	THF	5	20	50	1	0
2	THF	5	20	50	0.1	2
3	THF	5	60	50	0.1	22
4	THF	5	60	5	0.1	26
5	THF	10	60	50	0.1	5
6	THF	10	80	50	0.1	7
7	THF	10	80	50	0.1	11
8 ^{**}	THF	5	60	50	0.1	6
9 [*]	MeCN	5	60	50	0.1	1

^{*}determined by ¹H NMR spectroscopy using a mesitylene internal standard. ^{**}1.2 eq aniline

Despite these positive improvements, subsequent changes such as lowering the concentration, increasing catalyst loading, increasing the pressure, repeats, and changing the solvent did not lead to an improvement in the yield (Table 13, Entries 5-9). The yields dropped as more reactions were performed. We decided to investigate the reaction set up to determine what was causing the drop in yield observed.

Unfortunately, our poor yields could be traced to the leakage of the self-flush solution (50:50 EtOH/water). ¹H NMR data of aliquots taken showed during reactions showed significant amounts of water and ethanol (an example of spectrum is shown in Figure 35). The amount of self-flushing solution that we observed leaking into the system was considerable, and as a result completely inhibiting the borane catalytic activity.

The HPLC pump installed as part of the H-cube® employs a self-flushing pump head. This provides continuous washing of the inner piston surface. The flushing solution washes

away any buffer salts or starting materials that have precipitated onto the piston. If these were not removed the precipitates would abrade the high-pressure seal resulting in seal failure, leakage and possible damage to the pump. The self-flush solution is similarly vital for volatile solvents such as THF. These volatile solvents dry rapidly behind the seal, and without the use of the self-flush solution, will dry and degrade the seal. The self-flush system is attached to the HPLC pump (Figure 33) and should be refilled with 20 – 50% EtOH/water mix or 20 – 50% IPA/water mix before each use of the system. Fortunately, a new set of seals could be ordered and installed.

At this point, we also decided to swap the self-flush solution to 50:50 IPA/water, which would make it easier to diagnose leaks in the future. Checking flush aliquots for IPA in the future would be a much simpler way to determine if the seals are failing, without any competing complications. This is because at the end of every day the H-cube[®] is flushed with EtOH and therefore, trace EtOH could come from this process whereas IPA would only appear from the self-flush solution with this change. We are still uncertain whether the seal degradation was caused or exacerbated using THF following improper use by previous work performed on the H-cube[®]. The H-cube[®] had been used by other groups in our research lab, and it was unclear whether the use of highly concentrated stock solutions and poor maintenance of the self-flush system, or even simply ageing of H-cube[®] components could have led to the seal's degradation with THF pushing it over the edge. Whilst THF is a compatible solvent with the H-cube[®] according to the manual, anyone with experimental experience using THF could easily imagine that prolonged use could damage a rubber seal. Nevertheless, after changing the seals and priming the pumps, we decided, as we did not want to stall the project further, that we would find an alternative to THF and maintain the self-flush solution appropriately. Over a hundred reactions have been carried out since the seals were changed (with other solvents than THF), and we have never observed the self-flushing solution leak since our preliminary studies. However, more tests would need to be performed to prove the responsibility of THF for the seal degradation.

It is important to note, ethanol also acts as the storage solvent for the H-cube[®]. As a result, when reactions are complete the H-cube[®] must be flushed with ethanol and stored under these conditions. Therefore, trace ethanol is another factor that must be

monitored in future experiments when performing solvent flushes to prime the system before reactions occur.

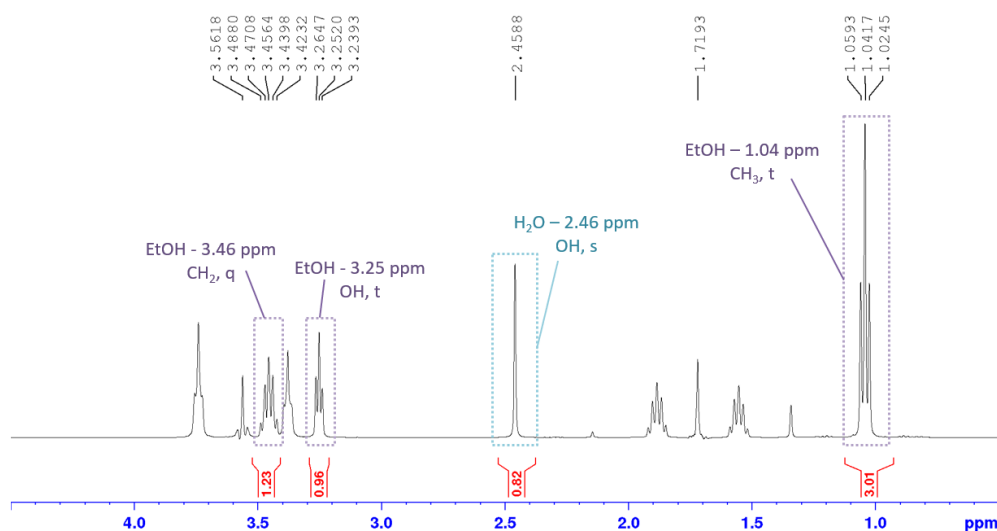


Figure 36. Example NMR spectrum from an aliquot collected after excess THF (40 mL) had been flushed through the system with clear presence of large quantities of EtOH and H₂O visible in the spectrum.

4.2.3 Reaction Optimisation with PTFE Filter

4.2.3.1 Introduction

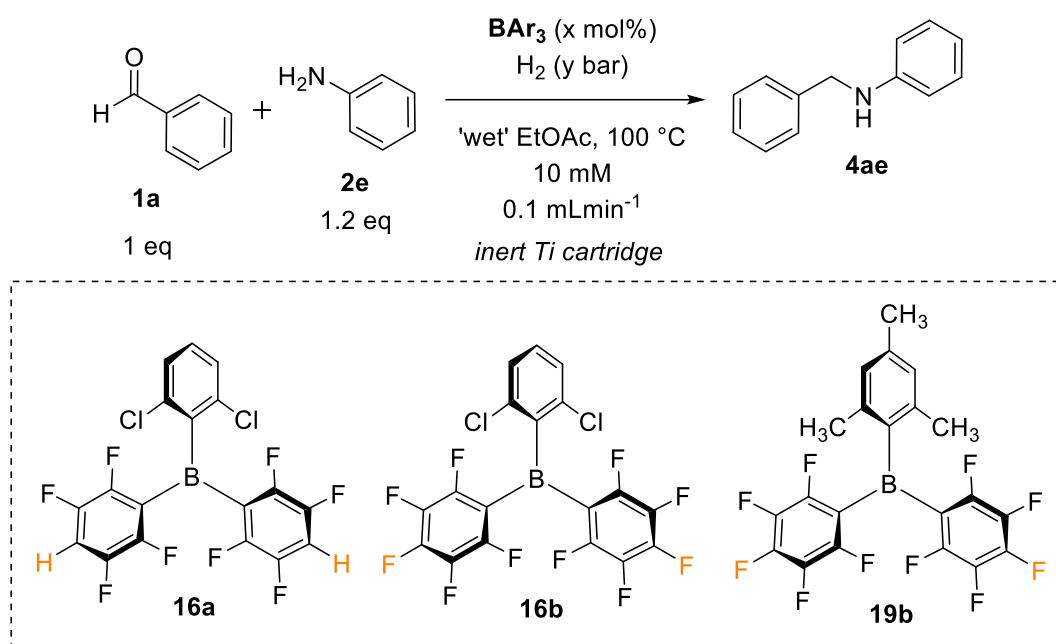
The optimisation attempts discussed in this section 4.2.3 were set up using the general reaction setup, employing the regular PTFE filter and test-tube stock solution inlet. However, all reactions herein were performed post-seal change and therefore, no self-flushing solution (alcohol/water) was observed leaking into the reaction mixture. We also switched the concentration after replacing the seals from 5 mM to 10 mM.

4.2.3.2 Initial Results

As we had decided to no longer use THF as a solvent we needed to explore the use of another solvent. We decided to explore the use of ethyl acetate (EtOAc), a solvent which we had previously observed to be of equal reactivity to THF in our reductive aminations work using silanes (section 3.2.1). It should be noted that chronologically, our work with the H-cube[®] occurred before we had access to the Parr pressure vessel, as was discussed

in section 3.2.3. As a result, we had not yet determined that THF is a significantly more effective solvent for FLP-catalysed reductions using hydrogen.

Select experiments from our initial reactions performed using the new HPLC pump seals are recorded in Table 14. Our first yield of 51% using lab grade ('wet') EtOAc under the best yielding conditions from our preliminary results (Table 14, Entry 1), left us very positive for what could be achieved with further optimisation of this system. Changing the catalyst did not seemingly lower the yield significantly (Table 14, Entries 4 – 8). We were surprised to find that **19b** and commercially available BCF achieved similar yields to **16a** and **16b** at 60 bar H₂ pressure given the major impact, we had observed in altering the Lewis acidity of the borane catalyst in batch using silanes (section 3.2.1, Table 1). Importantly, our work since then with hydrogen had shown that reducing Lewis acidity had slowed the reaction significantly, using **19b**, had led to only 2% yield, whilst **16a/b** had both achieved 99% yield under the same conditions (see section 3.2.3, Table 10, Entries 8, 14 and 15). We were similarly perplexed when we altered catalyst loading (compare Table 14, Entries 1, 9, and 10). Increasing the catalyst loading from 10 to 20 mol% led to a decrease in the yield by over 10% (Table 14, Entry 10). Whilst this was initially confusing, after a quick NMR spectroscopic experiment, we observed that increasing borane concentration pushed the imine equilibrium towards the aldehyde, which on the short timescale of the reaction could be responsible for the observed decrease in yield observed. We were gratified to find that the yield did not drop significantly when lowering the catalyst loading to 5 mol% (Table 14, Entry 9). Nevertheless, **16a** (10 mol%) still appeared to be the marginally superior, thus 10 mol% catalyst loading was used for attempts at further optimisation.

Table 14. Initial reactions for catalyst comparison and probing H_2 pressure (bar).

Entry	Catalyst	BAr_3 (x mol%)	H_2 pressure (y bar)	Yield (%)*
1	16a	10	60	51
2	16a	10	80	55
3	16a	10	100	44
4	16b	10	60	46
5	16b	10	100	47
6	16a	10	40	52
7	BCF	10	60	42
8	19b	10	60	48
9	16a	5	60	45
10	16a	20	60	40

*determined by 1H NMR spectroscopy using a mesitylene internal standard

4.2.3.3 Influence of Hydrogen Pressure

In an attempt to optimise our reductive amination system, we evaluated the influence of H_2 pressures (9 data points ranging from 5 to 100 bar, Figure 37) on the formation of product **4ae**. The experiments showed that increasing the H_2 pressure beyond 40 bar did not result in any significant increase in yield. Although, the highest yield was observed

at 80 bar, it was only 3% higher than the yield at 40 bar, a plateau was observed between 40 and 80 bar; and further increasing the H₂ pressure to 100 bar resulted in a decrease in the yield by approximately 10%. Thus, we decided to proceed with the less forcing conditions (40 bar hydrogen) for further optimisations, knowing that the pressure could be increased in the future if required.

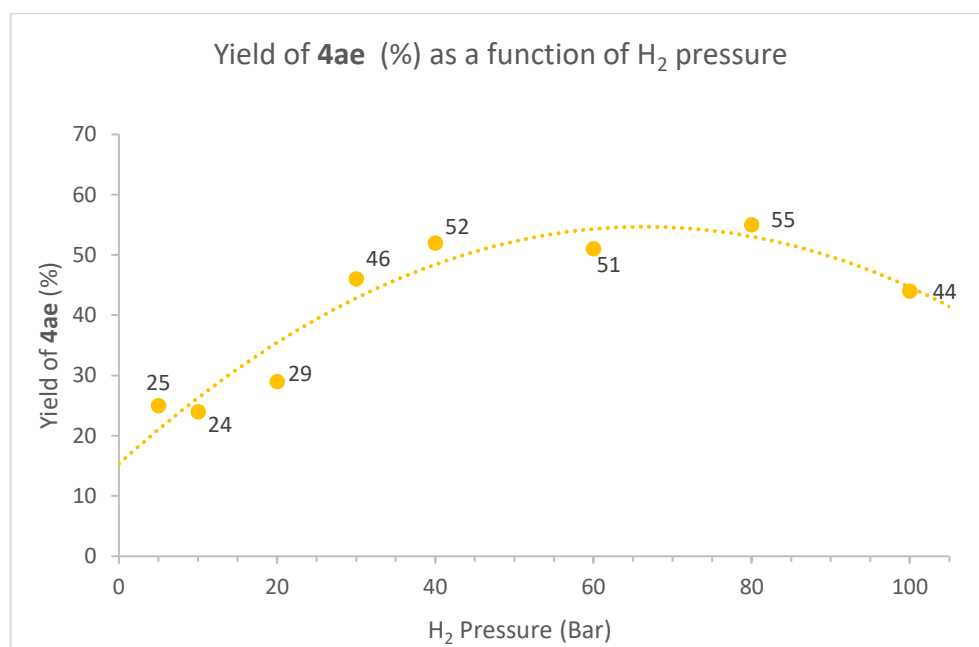
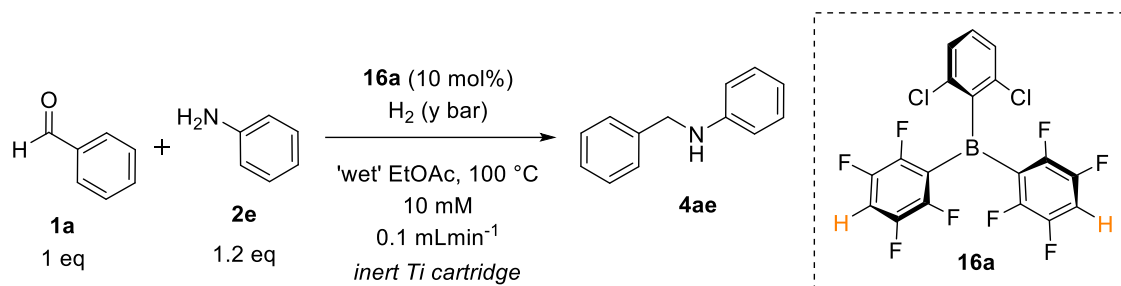


Figure 37. Graph showing Yield of **4ae** (%) vs. H₂ pressure (bar) for **16a** catalysed reductive amination.

4.2.3.4 Solvent Screening

Although our experience with silanes in batch had guided us to use EtOAc as a solvent we wanted to explore other solvents (Scheme 54). We took inspiration from GSK's green solvent list²⁴⁷ and similar reports^{248–250} to probe greener and more sustainable alternatives particularly to the traditional dipolar aprotic (MeCN), chlorinated (*o*-DCB, chlorobenzene), aromatic (toluene) and ethereal solvents (THF, dioxane etc.) often employed for FLP reactions. Greener and more sustainable solvents included in these

reports are chosen based on their availability, biodegradability, volatility, and toxicity. A scaling system is often employed to rank them.²⁴⁷

The solvent screening coincided with our switch to using 3-F benzaldehyde. We conducted some T_1 relaxation NMR spectroscopic experiments and found that we needed a 28 – second relaxation time for quantitative fluorine NMR spectroscopic analysis in EtOAc. Following advice from our NMR technician the relaxation delay (D_1) was set to 60 seconds to ensure we did not need to conduct T_1 experiments for every solvent. A T_1 experiment could be performed once an optimum solvent was determined to give us more optimal NMR spectroscopic analysis conditions.²⁵¹ The switch to include a fluorine tag was an essential development for the solvent screening to estimate the yield (Figure 38), as many of the solvent peaks would overlap with the benzylic protons of the product in the ^1H NMR spectra. Within the ^{19}F NMR spectrum, only the aldehyde, imine, and reduced amine product were observed.

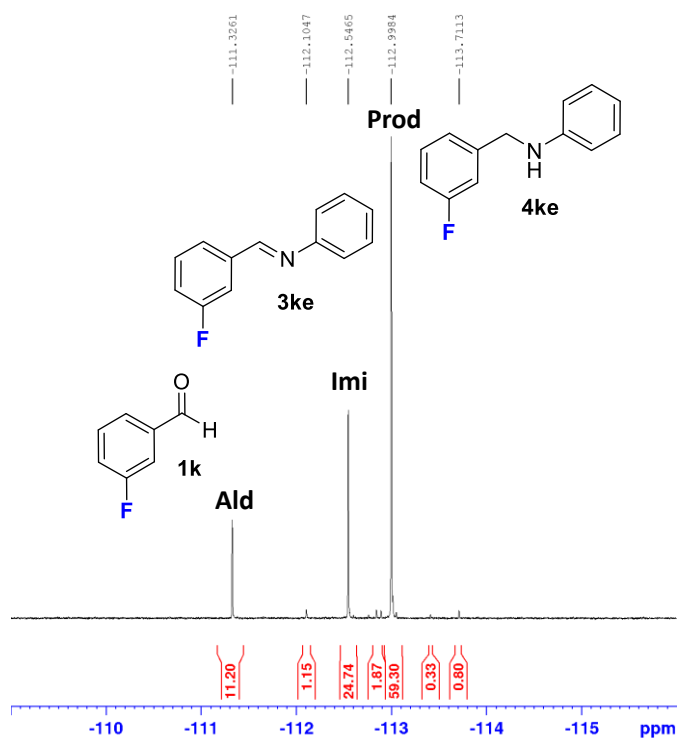
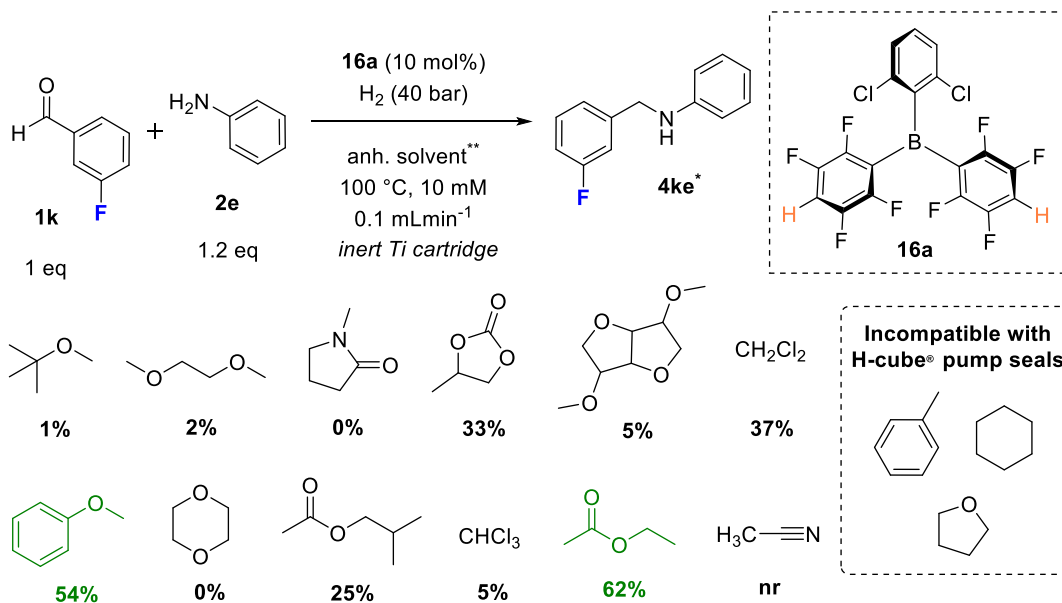


Figure 38. Typical quantitative ^{19}F NMR spectrum of a crude aliquot used to estimate yield.

Alcohols and water were not included in the screening due to their known incompatibility with borane catalysts (of GSK's approved solvents, 8 were alcohols, accounting for 40% of the total)²⁴⁷. Other solvents which are not green alternatives were

also selected. The less commonly found green solvents that were screened were chosen as they were commercially available at a reasonable cost.



*Yields estimated by ¹⁹F NMR spectroscopy, **Using anhydrous solvents

Scheme 54. Solvent screening for the FLP catalysed reductive amination of 3-F benzaldehyde and aniline. Anhydrous solvents screened include: **Top (left to right):** methyl tert-butyl ether, dimethoxyethane, 1-Me-2-pyrrolidinone, propylene carbonate, isosorbide dimethylether, dichloromethane. **Bottom (left to right):** anisole, dioxane, isobutyl acetate, chloroform, ethyl acetate, and acetonitrile. Not included were: toluene, cyclohexane, and tetrahydrofuran as these are not compatible with the pump seals.

With multiple papers discussing minor changes in Lewis basicity leading to significant changes in H_2 activation,^{45,132,252} we were extremely interested to see the results of our oxygen-containing (LB component) solvents. There is great precedent for weakly Lewis basic ethereal solvents such as THF and dioxane being employed as solvents. Ashely *et al.*, used dioxane as a solvent for BCF catalysed reduction of ketones in batch, and observed reduced catalytic activity which was attributed to dioxane's reduced basicity and polarity compared to THF which makes H_2 activation much less favourable.¹³² As a result, despite not being able to screen THF again due to seal compatibility concerns it was not a complete surprise that dioxane was not a successful solvent. It was a surprise however, that dioxane achieved 0% yield, as we had expected some conversion. Similarly to dioxane we observed poor yields (1 – 5%) with most ethereal, solvents screened including methyl tert-butylether (MTBE), dimethoxyethane (DME), and isosorbide

dimethyl ether (the only GSK approved green ethereal alternative) with the exception of anisole (see further below). Peculiarly a relatively reasonable yield of 37% with dichloromethane was observed, whilst chloroform only managed to yield 5% product. It is not surprising that acetonitrile, despite being used successfully in our batch with silanes reactions proved to be unsuitable. Instead, reduction of the acetonitrile to ethyl amine was observed. Similarly, toluene and cyclohexane are not recommended solvents for the H-cube[®] as they are known to interact with the HPLC pump sealing. Considering our experience with THF, toluene and cyclohexane were not screened.

As our only solvent in the aromatics category, we were pleased to find that anisole also gave us a comparable yield to those that had previously achieved with 'wet' EtOAc (54%). We were also extremely happy as anisole is one of the highest recommended solvents in GSK's sustainability guide.²⁴⁷ GSK's report offers multiple green ester alternatives; however, the commercially available isobutyl acetate gave us a much lower yield than EtOAc.²⁴⁷

Ultimately, we came across something we previously observed with silanes wherein EtOAc proved to be an optimal solvent. The yield had increased a further 10% by switching to now anhydrous EtOAc. Although, all solvents had been dried using 3Å MS and the same setup method, other impurities had not been accounted for. Notably in the case of both of the esters used, the respective alcohols (*isobutanol* and ethanol) could both be observed in the NMR spectra of the pure solvents (Figure 39). These respective alcohols will be expected to inhibit catalyst performance and as a result, lowering their potential yields despite being anhydrous.

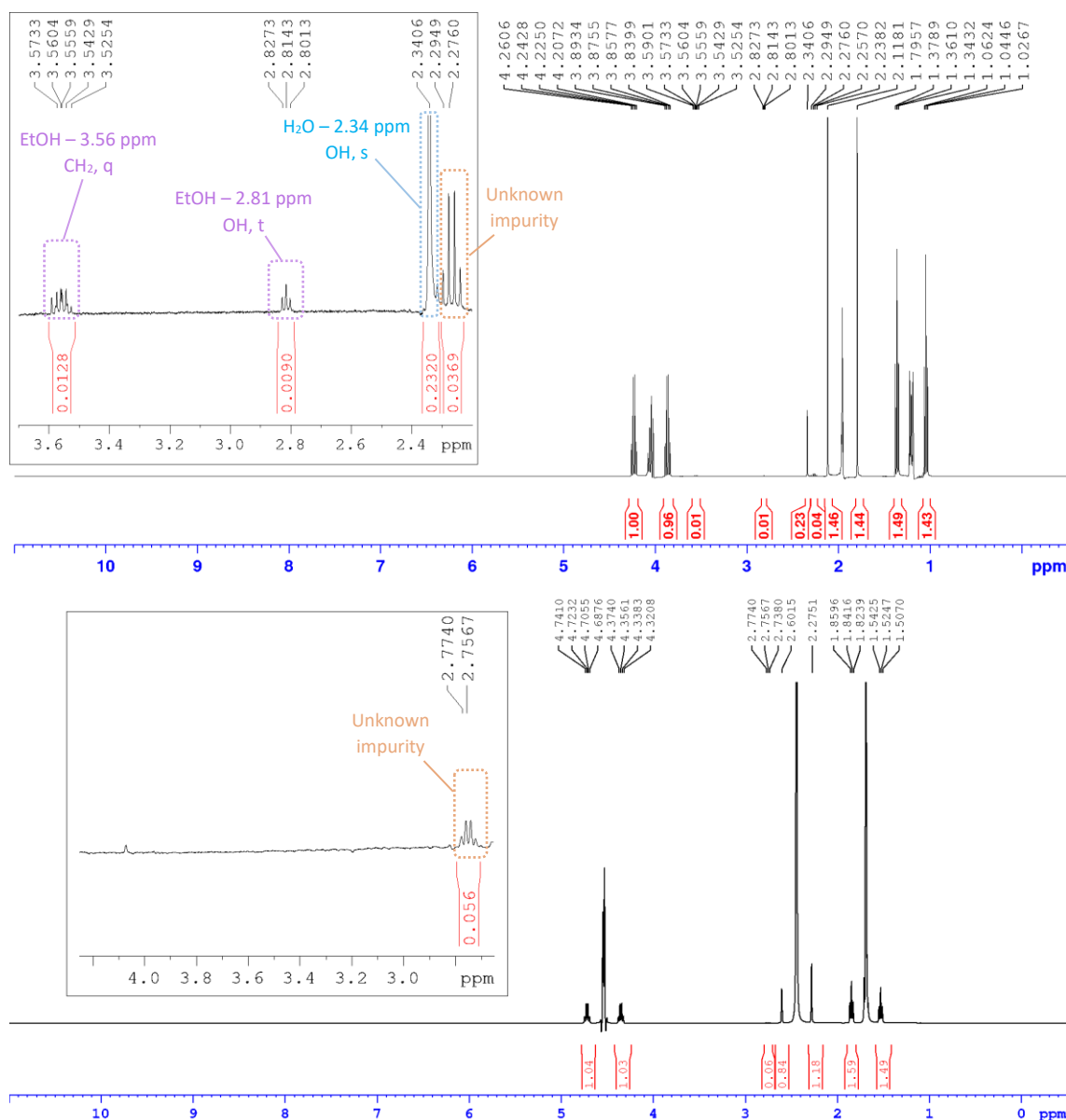


Figure 39. Top. Solvent suppressed quantitative ^1H NMR spectrum of anhydrous HPLC grade EtOAc, commercially available, and dried over 3\AA molecular sieves. Bottom. Solvent suppressed quantitative ^1H NMR spectrum of anhydrous EtOAc dried over 4\AA molecular sieves to remove EtOH.

Ethanol and acetic acid are known to be the two most common impurities in EtOAc. EtOAc is made from the esterification of these two compounds. However, whilst ethanol can be removed by storing EtOAc over activated 4\AA MS it is still commonplace for commercially available anhydrous EtOAc to be dried over 3\AA MS.²⁵³

After drying EtOAc over activated 4\AA MS in an oven-dried J-Youngs tap round-bottom flasks (RBFs) for three days the ethanol was successfully removed (Figure 39). Unfortunately, whilst water and ethanol could be removed from EtOAc using 4\AA MS, the

4Å pore size was not enough to remove *isobutanol* from *isobutyl acetate*. As a result, further use of the alternative green solvent was halted. The results, of switching to anhydrous EtOAc dried over 4Å MS will be discussed at the start of section 4.2.4 attempts to optimise the concentration were carried out (see section 4.3.2.5) before the switch from 3Å to 4Å MS was made.

It is important to note that, whilst the optimisation attempts have so far been discussed in chronological order with regards to how these results impacted the project decisions, no concrete conclusions can be taken from the solvent effects. In hindsight, considering the likelihood of metal leaching being responsible for high yields, it is plausible that individual solvents were superior at solubilising metal catalysts that had leached into the system. Overall, no clear trends were observed, however, EtOAc dried over 4Å MS was now used instead of lab-grade EtOAc.

4.2.3.5 Concentration

The final general trend which will be discussed in this section is the attempts to optimise the reaction concentration (Figure 40). Six concentrations between 2.5 and 100 mM were tested and three aliquots (40 – 60, 60 – 80 and 80 – 100 minutes) were collected at each concentration. It was expected that the yield would reach a single maximum however, this was not observed. In aliquot 1, yields were very similar with concentrations ranging from 5 – 40 mM (63 – 69% yield), but a significant drop in yield was obtained at 100 mM (54%).

In all cases yields significantly reduced in aliquots 2 and 3 which is perhaps unexpected but could be explained by the increased catalyst decomposition which was observed in the ^{11}B and ^{19}F NMR spectra. The drop off in yields, between aliquot 1 and 2, were more significant at higher concentration (40 and 100 mM), possibly confirming decomposition of the catalyst by the reagents as well as, possible water by-product from imine formation and not by air/moisture. Regardless the optimum concentration was found to be 5 mM in all three aliquots.

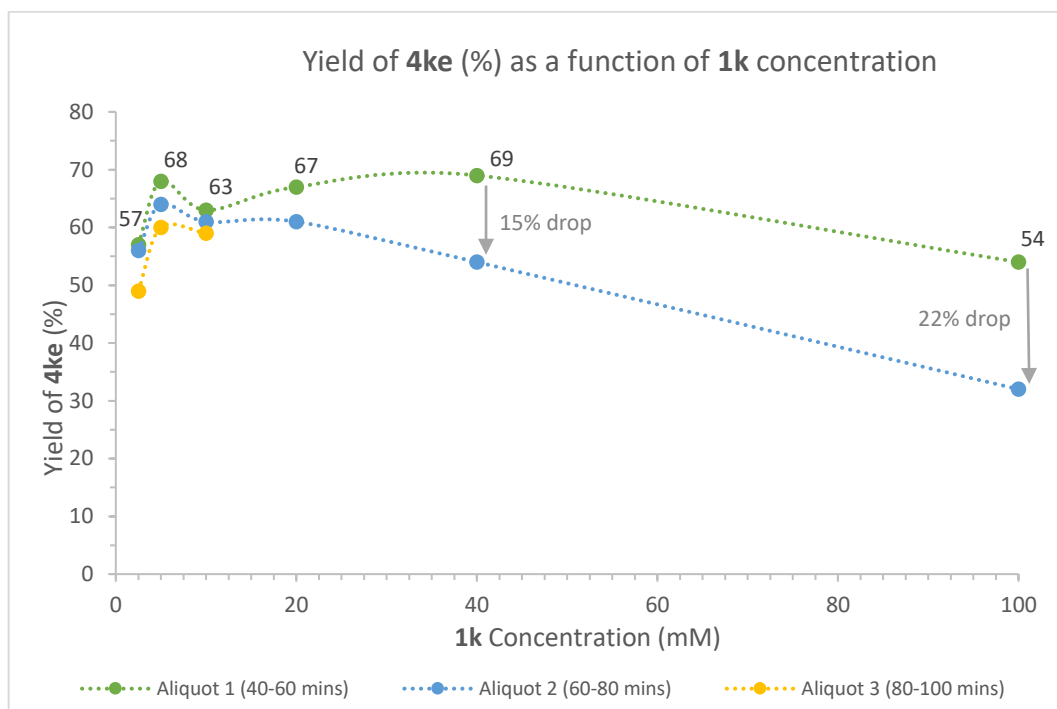
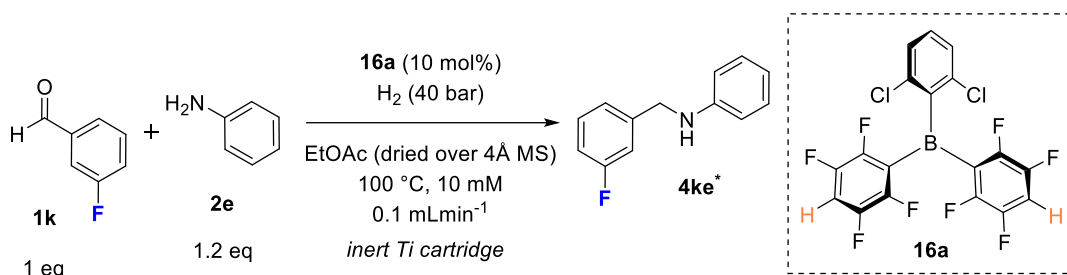
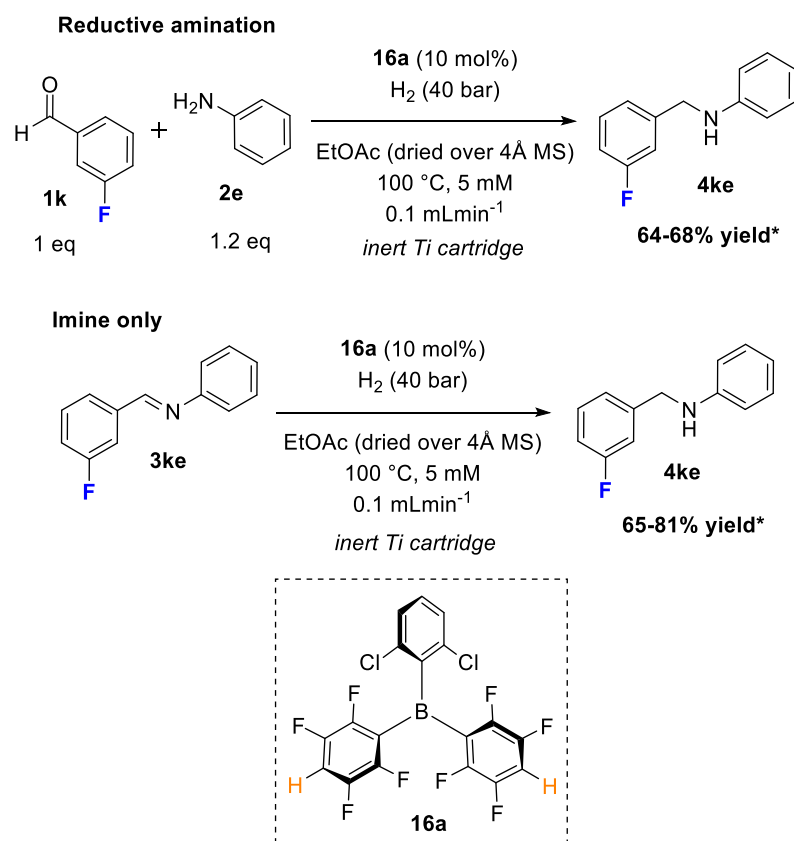


Figure 40. Graph showing Yield of **4ke** (%) vs. **1k** concentration (mM) for **16a** catalysed reductive amination using EtOAc in continuous flow. (*Yields determined by ^{19}F NMR spectroscopy)

4.2.3.6 Imine Reduction Compared to Reductive Amination

The requirement for a truly anhydrous reaction setup became clear when we switched from 3Å to 4Å MS anhydrous EtOAc. 4Å MS were used to remove EtOH from EtOAc, which resulted in an increased yield of the reductive amination from 63% to 68% (Scheme 55). Encouraged by this improvement, an imine-only reaction was attempted using the same 4Å MS drying method for the solvent. However, reproducibility issues were encountered when a completely dry reaction mixture stock solution was used, which revealed flaws in the general reaction setup using a PTFE filter (Figure 33). Up until this point, the results attained had been fairly consistent when repeated (64 – 68% yield for reductive amination system, Scheme 55). In the general reaction setup of the

experiment the inlet and PTFE filter are briefly exposed to air, also the lack of a perfect seal between the inlet stock solution and the atmosphere means air could penetrate the reaction vessel; we suspected both these factors could be responsible for the introduction of H₂O in the reagent stock solution which would lead to alteration of the imine equilibrium and decomposition of the borane catalyst. In our traditional aldehyde and amine (reductive amination conditions), typical imine equilibrium values were 2:1 (imine:aldehyde). This was a contributing factor to the switch to using 1.2 equivalents of amine, which increased this imine equilibrium to 3:1 (imine:aldehyde). In the 'imine-only' reactions, ¹⁹F NMR spectroscopic analysis of the stock solution showed a massive improvement in the imine equilibrium was > 10:1 (imine:aldehyde). As a result, water ingress would be expected to severely impact the 'imine-only' equilibrium and could be responsible for the more noticeable lack of reproducibility. The range of yields for the imine-only variant fluctuated between 65 – 81% for 6 repeats (Scheme 55), and whilst improved from the reductive amination system, we hoped these reproducibility issues could be resolved using a set up allowing for more thorough exclusion of moisture.



*yields estimated by ^{19}F NMR spectroscopy from aliquot 1 (40-50 mins)

Scheme 55. Comparison between the range of yields achieved for reductive amination vs. 'imine-only' set-up.

4.2.4 Optimisation without the PTFE Filter

4.2.4.1 Air/moisture Free Setup

We determined that there was 0.06 mol% water in the solution in our 'HPLC grade 99.5% EtOAc' before drying, which, at the concentration used (5 mM), is just over 11 equivalents of water with respect to the amount of borane present. Since even a small amount of water in the solution can affect the yield of such a dilute solution (5 mM), we set out to develop a truly anhydrous setup using the H-cube[®]. The goal was to use a different inlet without the PTFE filter and employ two separate stock solutions, one containing the catalyst and one containing the reagents to lower the risk of borane decomposition before reaching the reactor.

To develop this truly anhydrous system we went through various iterations of the reaction setup. Elaboration on these will be excluded for brevity but the challenges can be summarised by a brief description of our eventual two-stock solution anhydrous

setup (Figure 42). One of these stock solutions would contain our borane catalyst (**16a**), whilst the other would contain the imine (**3ke**). Both solutions would be prepared in the glovebox using anhydrous EtOAc (dried over 4Å MS) before being added to our two-oven dried stock solution vessels. Prior testing of both the imine and borane had shown that they were both relatively stable separately in anhydrous EtOAc over 3 days (Figure 41) and therefore, we were confident they would last the length of the reaction.

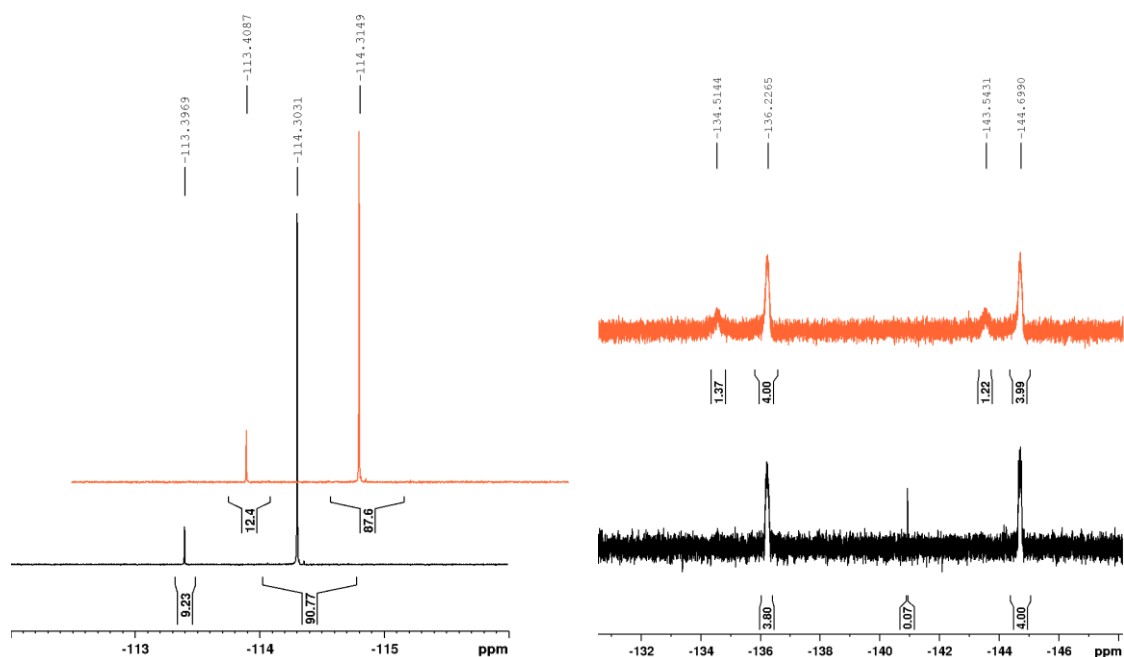
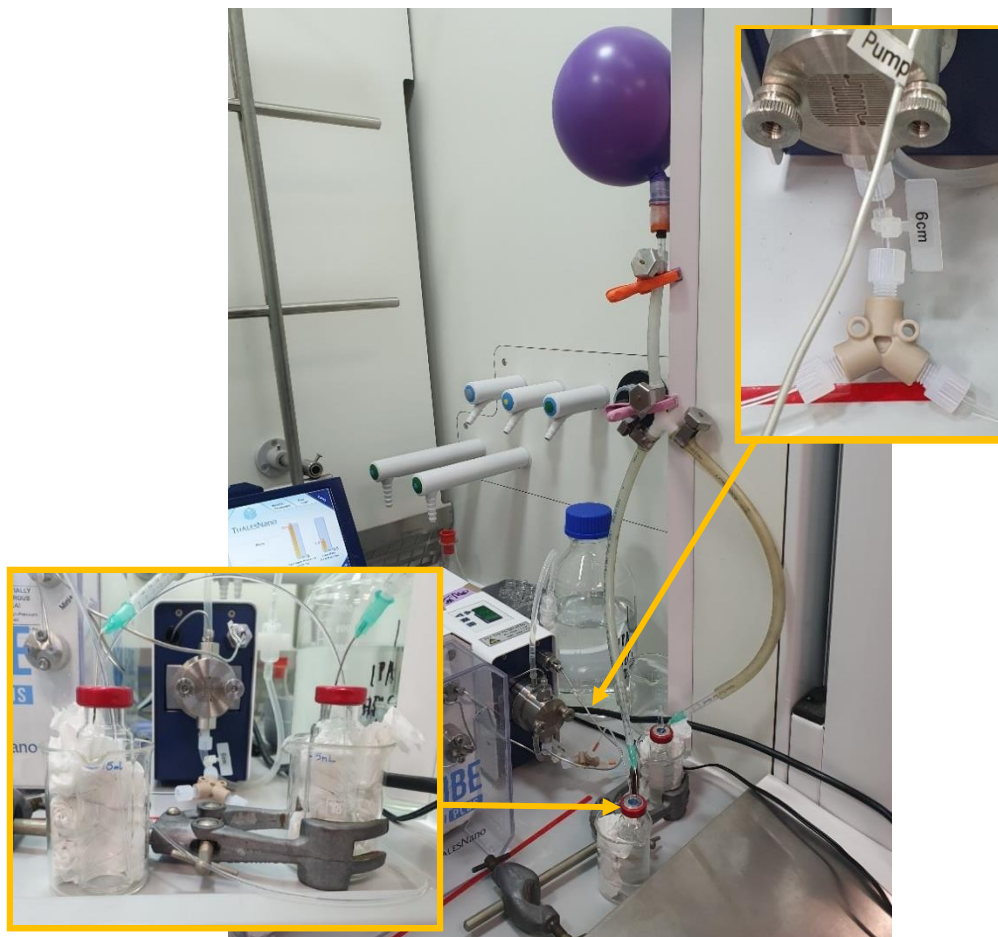


Figure 41. ^{19}F NMR spectra comparing **Left**: imine equilibrium in a 10 mM stock solution immediately (black) and after 3 days (orange). **Right**: borane stability in a 1 mM stock solution immediately (black) and after 3 days (orange).

All alterations to the system were made prior to the HPLC pump and as a result, the total system volume was altered but the residence time under reaction conditions was not. The PTFE filter was removed along with the wide tubing that connected it directly to the HPLC pump. This allowed tubing to be run directly into oven-dried, anhydrous and sealed containers under an inert atmosphere.

To draw from two stock solutions firstly, a new Y-mixer was used (Figure 42). The new tubing that we were using for the reaction mixture inlet was much smaller (1 mm diameter) than the previous tubing used with the PTFE inlet. Therefore, we were confident that the system volume would be reduced from the 4 mL we had determined for our general reaction setup. We used the same aliquot method we had employed

previously, passing a crude reaction mixture through the system, to determine the new system volume in our anhydrous setup to be 2.75 mL. As a result, for every reaction after commencing the reaction, the first 2.75 mL would be collected as a 'dead-zone' aliquot.



*Figure 42. Anhydrous system setup for reaction performed in continuous flow with two stock solutions using a H-cube® mini and Y-mixer before the pump. **Left:** Oven-dried MW vials used as anhydrous vessels for two stock solutions. Both vessels are filled with the same amount of respective stock solutions, kept level with each other, and kept under an equivalent positive pressure of argon. **Right:** The Y-mixer is employed to allow the mixing of the two stock solutions before they pass through the HPLC pump and into the H-cube®.*

We eventually established the use of crimp cap vials, due to their practical and more importantly consistent size (Figure 42). As part of our problem solving, we had established that for equal mixing both stock solutions had to be equidistant from the pump. This also meant that both vessels had to contain the same amounts of stock solution, be kept at the same height, and be under equivalent pressures from our inert atmosphere balloon source. If any of these were not adhered to, we observed that one

of the two stock solutions would be pushed from one vessel to another and vice versa to equilibrate the pressure in each vessel. One other complication we encountered was a result of our low flow rate (0.1 mL/min).

Initially tubing, with needles attached and pierced through the vial seal had been employed. Unfortunately, the needle diameter was too wide and as a result, the surface tension was not enough for the stock solutions to be pulled out of the two vessels given the flow rate was so low. Thankfully the use of 1 mm diameter clear tubing had the required surface tension to stop any backflow due to their capillary-like size.

4.2.4.2 Initial Results using the Air/Moisture Free Setup

With these significant efforts placed into this anhydrous two-stock solution setup, we were, therefore, extremely disappointed when after several attempts we could not get the yields to improve beyond 12% (Figure 43). Although the possibility of poor mixing of the two stock solutions cannot be discounted, we were reluctant to believe that other factors were not the cause of the significant drop.

Whilst only 12% yield was observed, the yield remained stable (approximately 10%) over a three-hour period which is in stark contrast with what was observed in our previous set up (Figure 43) possibly confirming our hypothesis that water ingress in the stock solution had been responsible for yield decrease over time. NMR spectroscopic analysis of both stock solutions showed that the borane remained undecomposed, and the imine equilibrium had only dropped from 91% to 87% imine which is within experimental error.

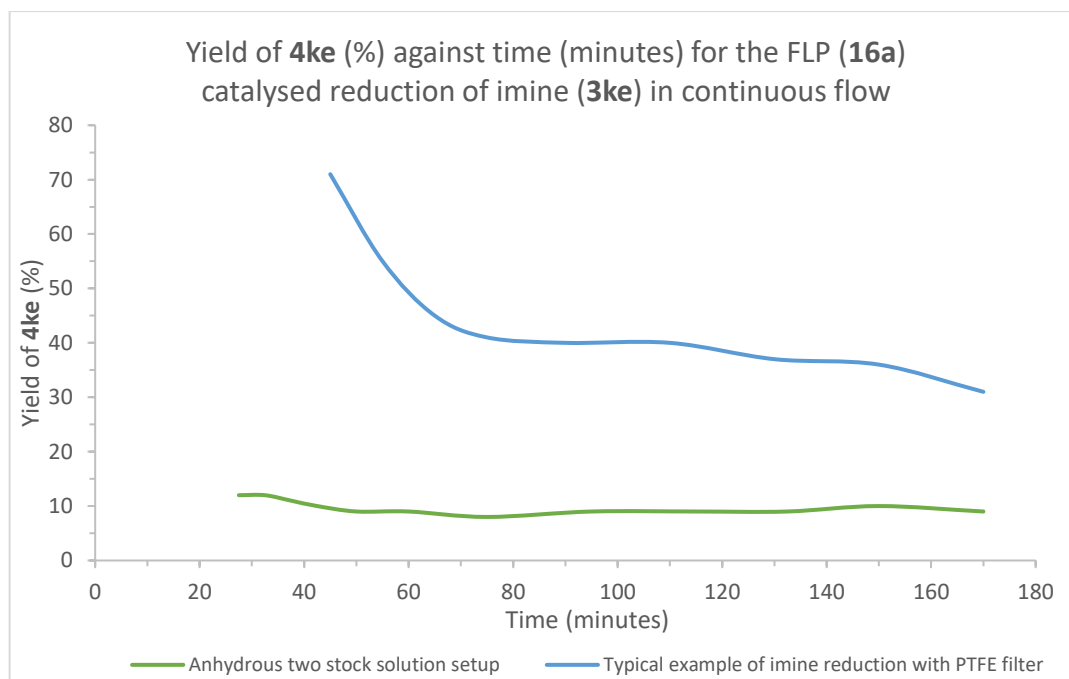
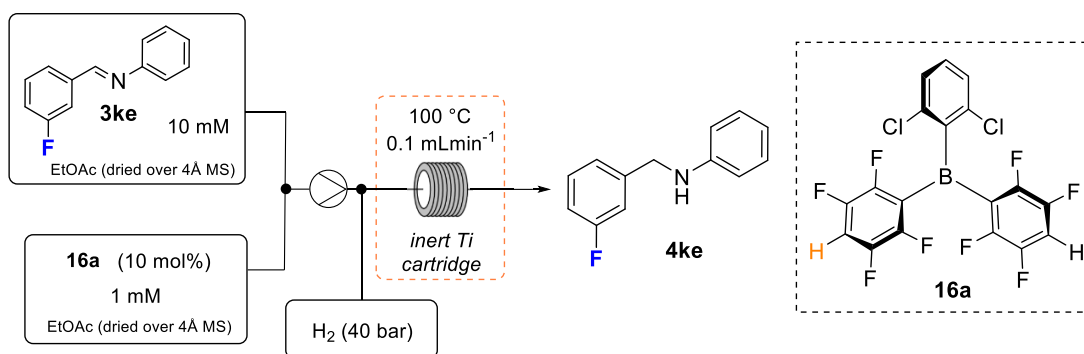


Figure 43. Graph showing Yield of **4ke** (%) vs. time (minutes) for **16a** catalysed reductive of imine (**3ke**) in continuous flow. Comparison of the general reaction set up using PTFE filter vs. anhydrous two stock solution set up.

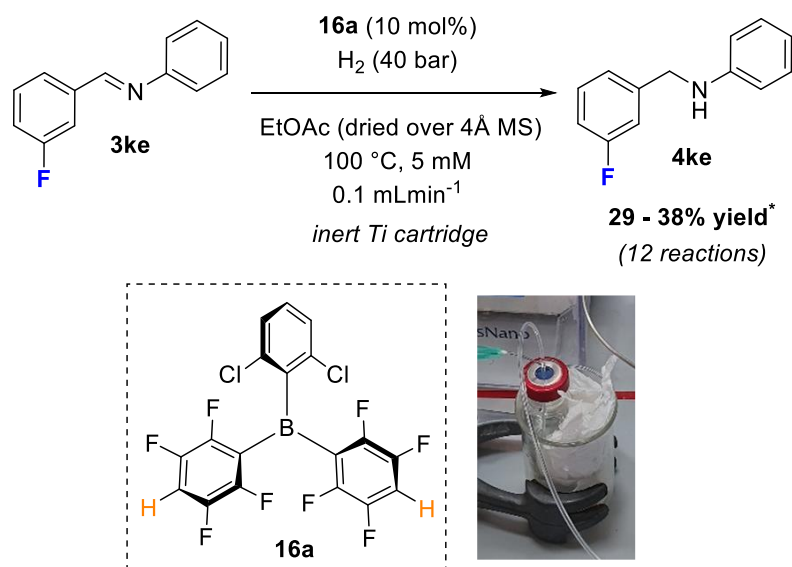
4.2.4.3 Simpler Reaction Setup

To remove any doubt around sufficient mixing a simpler setup would be used which only employed one reaction mixture stock solution. The simpler anhydrous reaction set up is shown in Figure 44 and uses the same 1 mm diameter tubing used for the two-stock solution anhydrous set up, but only one reaction mixture stock solution was employed inside of a crimp cap vial under inert conditions (Figure 44). Without the Y-mixer and extra tubing the system volume was again reduced and was determined to be 2 mL.



Figure 44. Simpler reaction setup for performing anhydrous reactions using one stock solution with a H-cube®.

Due to blockage of the previous catalyst cartridge, a new inert Ti cartridge was used for these reactions and with the one stock solution set up, promising results were obtained (up to 38% yield); these were tentatively attributed to improved mixing, either of borane and reagents because of the use of a single stock solution or of the reagents and hydrogen due to the new cartridge being used. Unfortunately, high variability was observed in the initial 10-minute aliquot (29 – 38% yield) over 12 reactions, Scheme 56.

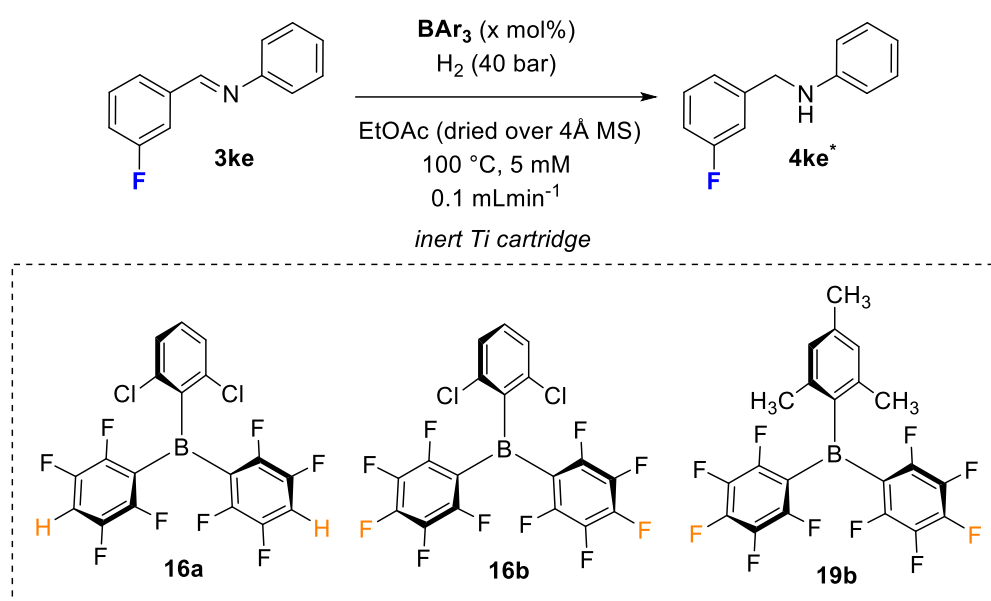


*yields estimated by ^{19}F NMR spectroscopy from aliquot 1 (20-30 mins)

Scheme 56. Hydrogenation reactions performed using the simplified anhydrous reaction setup with a new inert titanium cartridge.

It was decided that collecting one combined aliquot (20 – 60 minutes), would give more reproducible results and reveal more trustworthy trends could be observed when varying reaction parameters. Table 15, shows select attempts to perform borane catalysed imine reductions in flow using our simplified anhydrous setup and determining the yield through the collection of one combined aliquot. Collecting a larger aliquot (40 min compared to 10 min) gave reduced 24% yield but these could be reproduced.

Table 15. FLP-Borane catalysed imine **3ke** reduction using the simplified anhydrous setup (single stock solution).



Entry	Catalyst (BAR ₃)	BAR ₃ (x mol%)	Yield (%) [*]
1	16a	10	24
2	None	-	10-13 ^a
3 ^b	None	-	14
4	16a	5	23-24 ^c
5	16b	5	16
6	19b	5	23
7	BCF	5	8
8	BPh₃	5	4

^{*}Yield determined by ¹⁹F NMR spectroscopic analysis from combined 20 – 60-minute aliquot. ^aThree repeats ^binert quartz cartridge. ^c2 repeats

However, 10 – 14% yield were obtained using no catalyst (Table 15, Entries 2 and 3). Since the PTFE filter at the reaction inlet was not used, this indicates that trace metals are present in other part of the flow system, for example within filter frits located throughout the system.

Comparing the catalytic activity of several boranes (Table 15, Entries 4 – 8) showed that **16a** still appeared to be the superior catalyst used (Entry 4), although we could not explain why some catalysts gave lower yields than the one obtained with no catalyst (compare for example entries 2 and 8).

4.2.4.4 Conclusions

Despite the promising optimisation, using the PTFE filter system setup, including pressure (H₂ 40 bar), solvent (4Å MS EtOAc), concentration (5 mM), as well as adaptation of the H-cube[®] to use one or two stock solutions in an air/moisture free setup, further work using the H-cube[®] had to be halted as none of the trends or results could now be trusted. Since the control reaction with no catalyst gave us significant conversion to the product, further work to try to achieve better results would require full cleaning of the apparatus which was not possible. Also, since the residence time is very low, it is likely that we have already reached the best that could be achieved with this system. Nonetheless, and although having to be taken with precautions, this work represents a proof-of-concept that could be built on, using a flow reactor with higher residence time. Using THF instead of EtOAc would be also likely to allow for improved results. Unfortunately, no blank reaction had been performed until this point. Had we observed yield, from the start, when no catalyst was present, we would not have invested the time into 'optimising' this reaction in the H-cube[®].

4.2.3 Catalyst Cartridge

4.2.3.1 Cartridge Blockage

Whilst we were investigating the drop in yields when not using the PTFE filter, we blocked the cartridge. The H-cube[®] manual describes that the most common place for a blockage to occur is in the catalyst cartridge (CatCart[®]) because inside this reaction chamber new compounds are formed which might precipitate. It is also possible for micro particles of dust or ground-down molecular sieves to get through the PTFE and build up in the tightly packed CatCart[®], these are well-established in industrial engineering and flow chemistry and are often called fines. The CatCart[®]'s are sold in packs of 6 as consumable items so although we have a lot of measures in place to reduce the likelihood of blockages they can still occur. Using a standard 30 mm CatCart[®] the system pressure when pumping solvent at 1 mL/min should not exceed 10 bar. With our used inert titanium cartridge, the pressure was however 14-15 bar. When we changed out the inert titanium CatCart[®] and replaced it with the inert quartz variant the system pressure at 1 mL/min dropped significantly to 5 bar. This test clearly showed we had a blockage in our system and unfortunately located it to be in the CatCart[®]. New inert titanium catalyst cartridges were ordered, and it was proposed the general reaction setup should return, reintroducing the PTFE filter tubing to avoid any damage to the inert quartz CatCart[®]. Figure 45, shows the new unused titanium cartridge compared to the old one which contains a blockage.



Figure 45. **Left:** New unused inert titanium cartridge. **Right:** Heavily used titanium which contained a blockage.

4.2.3.2 Catalytic Activity of the “Inert” Cartridge Testing in Batch

In an attempt to determine if the metal sedimentation was present in the cartridges or just the PTFE filter and system filter frits, both the used ‘blocked’ cartridge and a brand new ‘inert’ titanium were dismantled in a glovebox (Figure 46). As shown in Figure 46, the cartridges contain inert titanium particles of uniform size (630 and 800 μm) which are packed and contained within the cartridge by two thin filter frits on opposing ends.

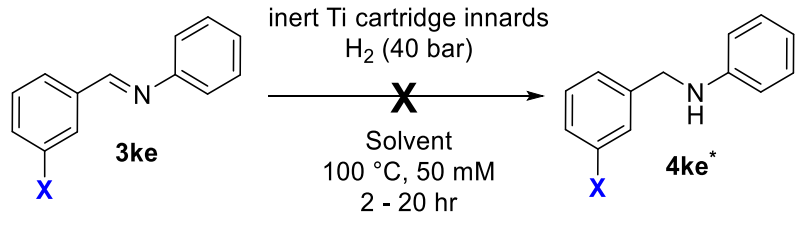


Figure 46. Select images of dismantled inert titanium catalyst cartridges inside the glovebox.


Left: View straight through cartridge after filter frits and titanium innards are removed. **Middle:** Comparison of used and unused cartridge innards. **Right:** Close-up view of the inert titanium particles as well as broken pieces of the filter frit.

Visually, the cartridge which was blocked during previous work appeared no different from a completely new and unused cartridge which was also dismantled. We were extremely gratified to find that subjecting both the used and unused cartridge innards, including some of the filter frit, to batch hydrogenation conditions led to 0% yield (Table 16). This is evidence that the metal sedimentation had not occurred in our inert cartridges and thus not been the cause of inflated and nonreproducible yields. The culprits were clearly elsewhere in the system and reaction setup.

Table 16. Batch imine hydrogenations performed using the new and used inert titanium cartridge innards from the H-cube®.



Reaction scheme showing the hydrogenation of imine **3ke** to secondary amine **4ke**. Reagents: inert Ti cartridge innards, H₂ (40 bar). Conditions: Solvent, 100 °C, 50 mM, 2 - 20 hr. A large 'X' is placed over the reaction arrow.



Entry	X	Inert Ti cartridge	Solvent	Time (hrs)	Yield (%)*
1	H	New	EtOAc	2	0
2	H	Used	EtOAc	2	0
3	F	New	THF	2	0
0	F	Used	THF	20	0

*determined by ¹H or ¹⁹F NMR spectroscopy, **Conditions adapted from those performed in flow as well as optimised in batch based on Hoshimoto et al. 2018.³⁷

4.3 GISMO Funding and Autichem Ltd. Collaboration

My project was fully funded by the Greater Innovation for Smarter Materials Optimisation (GISMO) project, which was itself a body under the Lancaster University Materials Science Institute, funded by the European Region Development Fund (ERDF). GISMO was dissolved during the second year of my PhD (2022) which made our collaboration with Autichem more challenging. Unfortunately, whilst Autichem were still willing to collaborate they still did not have a reactor available. This meant that we would not get access to a custom reactor to trial my POC system during my project. However, contact with Autichem Ltd. and another flow chemistry company, Stoli Chem, is promising for future collaboration in the group.

4.4 Outlook and Conclusions

In conclusion, the attempt to use the H-cube® to develop suitable reaction conditions achieving high yielding reductive amination reactions catalysed by FLP-boranes in continuous flow was unsuccessful. However, we can consider that a proof-of-concept example was established, and reduction of imine **3ke** was achieved, albeit in low yields. Although the absolute values of these yields cannot be trusted, we demonstrated that the reaction proceeded more successfully in the presence of FLP-borane catalysts. The presence of imine reduction products in control reactions when no catalyst was used, led us to conclude that metals (from solid supported catalyst cartridges previously used in the H-cube®) must have leached into the system (pipes, frits, etc.), which we assume were responsible for the background catalytic activity observed.

Despite conducting over 100 reactions, little confidence can be placed in the observed trends (catalyst loading, solvent, hydrogen pressure, concentration) due to challenges encountered. While some groundwork was laid for potential future FLP-catalysed hydrogenation in flow, the data collected on reductive amination is largely inconclusive due to issues with metal leaching from the equipment.

On a more positive side, we have successfully developed a method to carry out anhydrous reactions using a H-cube® from multiple stock solutions. Since many industrial and academic labs have a H-cube® but lack a custom continuous flow setup, this could be valuable to other researchers performing hydrogenation reactions. Also, this research has allowed us to increase our understanding in obtaining "anhydrous" ethanol-free EtOAc.

For further work to have been attempted with the H-cube®, a fully uncontaminated system would have been required (new machine, or full decontamination of the one used), which was not possible in this project. During this part of the project, I received advice from Professor Anna Slater (Liverpool University) through informal correspondence which was really helpful for troubleshooting issues with the flow system setup. In the future, I believe that collaboration with research groups with expertise in flow chemistry would be beneficial to bring this work from proof-of-concept to the identification of suitable reaction conditions.

Chapter Five: Synthesis of Novel Moisture-tolerant Boranes

5.1 Introduction

5.1.1 General Aims

As mentioned in the chapter one, flow hydrogenation offers advantages over batch reactions in terms of scalability and safety. From the beginning of this project, we were keen on utilising FLP borane-catalysed hydrogenation reactions using flow technology. Our collaboration with Autichem Ltd., a manufacturer of flow reactors, further supported this approach. Although soluble catalysts can be used in flow, it is more desirable to use solid-supported catalysts. Therefore, we aimed to obtain a heterogeneous FLP catalyst for hydrogenations and sought to leverage our experience in synthesising soluble water-tolerant triaryl boranes to access solid-supported triaryl boranes. Since many water-tolerant FLP systems use solvents such as THF as the Lewis base, we chose to develop polymer-supported triaryl boranes rather than focusing on supporting the Lewis base component.

5.1.2 Literature Precedents for the Synthesis of Solid Supported Boranes

The purpose of this brief introduction is to highlight the challenges that we faced in our project regarding heterogeneous catalysis. Examples of organic-derived heterogeneous FLP boranes are extremely limited due to their challenging synthesis. To achieve our goal of synthesising novel triaryl boranes, we needed to explore potential synthetic routes that would allow us to append these boranes to a solid support.

Across the varied FLP research in the last 15 years, the vast majority involve homogenous catalytic systems. This provides benefits for studying novel reactions and has allowed for *in situ* monitoring of the reaction progress. However, for the future applications of FLP catalysts, it must be noted that over 90% (by volume) of the chemicals manufactured globally are synthesised using heterogeneous catalysts.²⁵⁴ Heterogeneous catalysts are

employed in industry due to their increased stability, recyclability, and simplified catalyst-product separation.

As a part of our collaboration with Autichem Ltd., one of our objectives was to design catalysts that could be solid supported for potential application in flow chemistry. Packed bed reactors require heterogeneous reagents or catalysts, which is why we aim to achieve heterogeneity in organic-derived solid-supported catalysts.^{255,256}

The synthesis and utilisation of heterogeneous FLP catalysts have been split into two avenues; semi-immobilised FLP catalysts where the LA or LB components have been attached to a solid-support or fully immobilised where both the LA and LB components are attached to or within a range of materials.^{51,257,258} The semi-immobilised systems are typically easier to access, however, due to one of the components being soluble in the solvent, they can suffer from workup/purification issues and recyclability.

Some interesting examples of these semi-immobilised systems include the silica LA-supported catalyst using $-B(C_6F_5)_2$ bound to silica with soluble $P(tBu)_3$ (LB) dissolved in solution²⁵⁹ (**67**) (Figure 47. A) as well as the two LB immobilised organic polymer networks using phosphine²⁶⁰ (**68a/b**) (Figure 47. B) and amines²⁶¹ (**69**) (Figure 47. C) respectively.

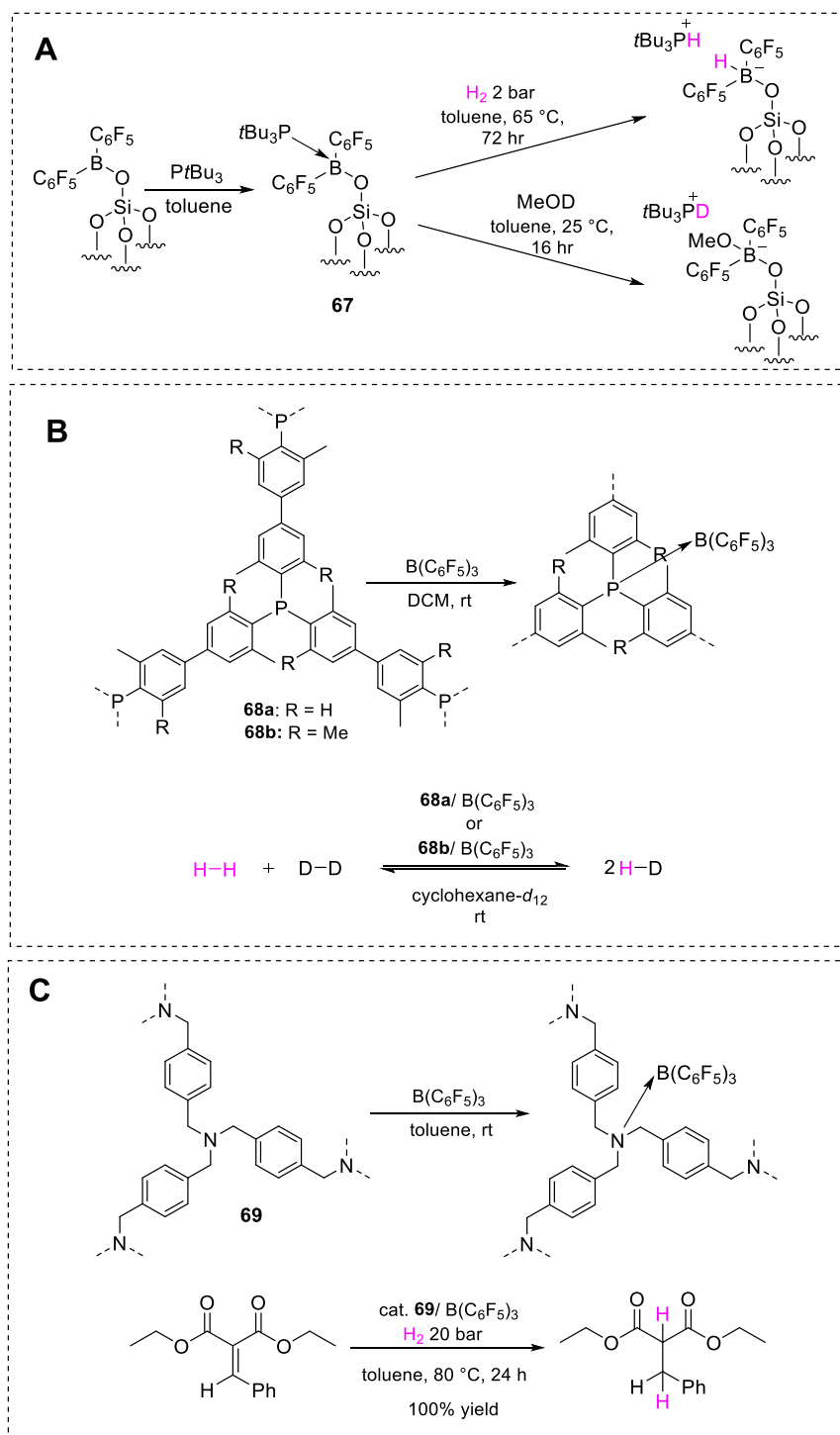
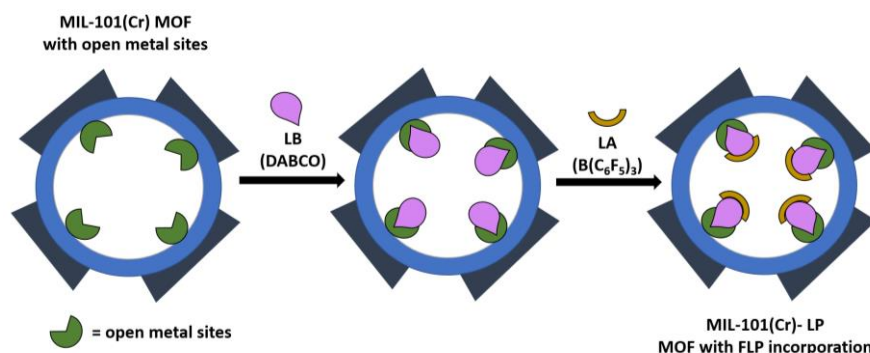


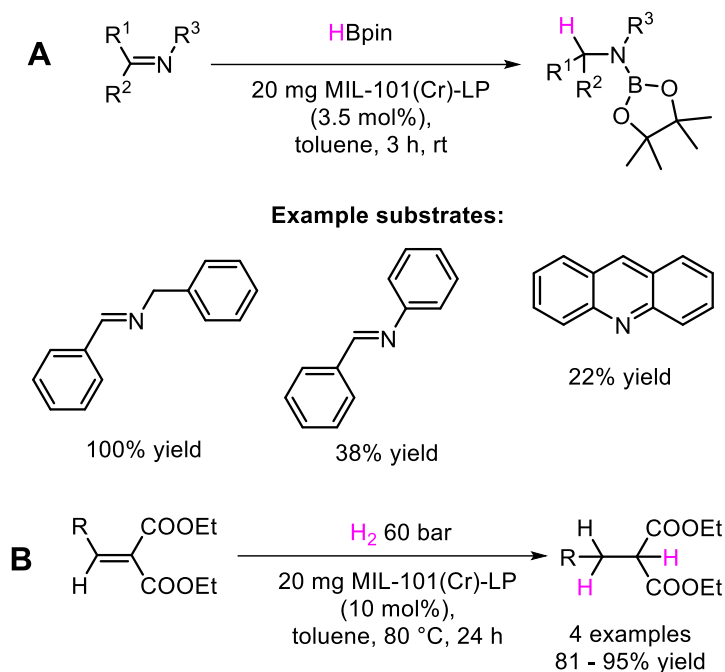
Figure 47. **A.** Solid-supported LA and semi-immobilised FLP **67** able to stoichiometrically activate H_2 and MeOD,²⁵⁹ **B.** Semi-immobilised LB FLP catalysts **68a** and **68b** with impregnated $B(C_6F_5)_3$ in a phosphine polymer network applied to stoichiometric isotopic scrambling to provide evidence of H_2 activation,²⁶⁰ and **C.** Polyamine organic framework with impregnated $B(C_6F_5)_3$ to force semi-immobilised FLP catalyst **69** for the catalytic reduction of diethyl benzylidenemalonate.²⁶²

On the other hand, the fully immobilised FLP catalysts tend to have increased catalyst stability and recyclability. Some of these systems have been supported on a range of solids including silica²⁵⁹, zeolites, metal-organic frameworks (MOFs)^{263,264}, polyoxometalate clusters²⁶⁵, metal oxides and graphene.

In 2018 by Ma and co-workers developed a partially organic derived heterogeneous FLP catalyst for hydrogenation. The dehydrated MOF MIL-101(Cr), $\text{Cr}_3(\text{OH})\text{O}(\text{BDC})_3$ (BDC = 1,4-benzenedicarboxylate), which was selected for its stability and large pore size relative to other MOFs was exposed to a solution of DABCO (1,4-diazabicyclo[2.2.2]octane). The DABCO bound itself to the chromium metal in the open pores of the MOF and subsequent $\text{B}(\text{C}_6\text{F}_5)_3$ exposure incorporated the LA similarly into the MOF (Scheme 57). Crucially Ma went on to employ MIL-101(Cr)-LP with the FLP bound as a catalyst for imine reduction (Scheme 58. A). The catalyst was also recyclable, with NMR spectroscopic studies showing no FLP leaching from the MOF and recovered MIL-101(Cr) was reused with the same performance through 7 cycles.^{266,267}



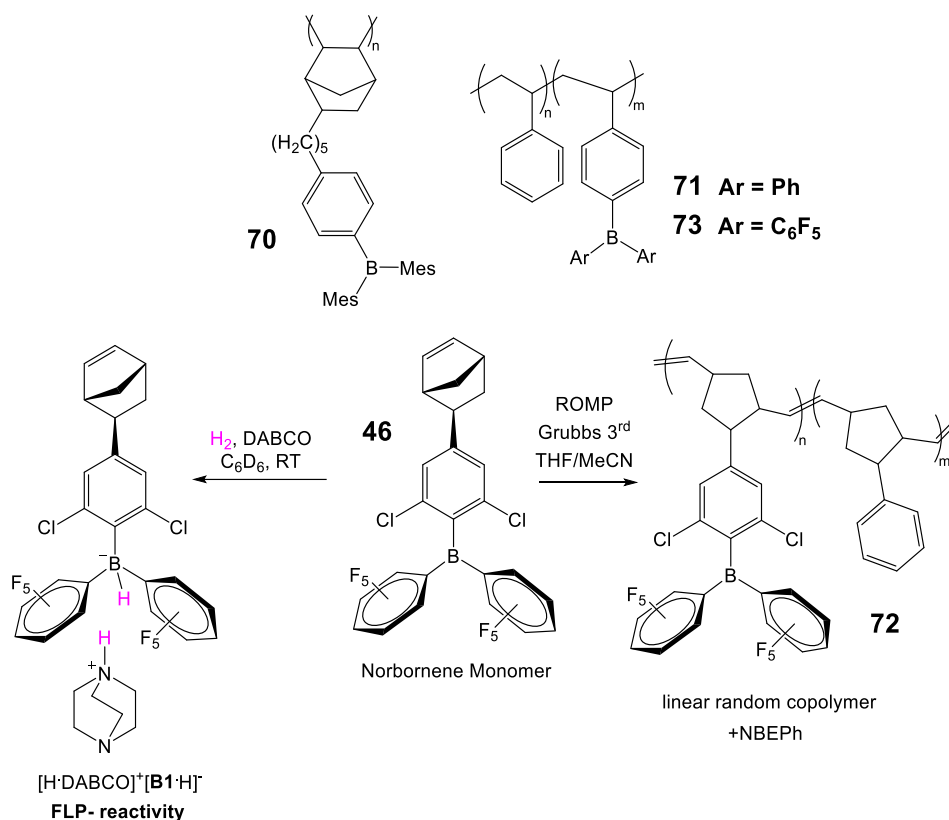
Scheme 57. Schematic representation of the incorporation of DABCO and $\text{B}(\text{C}_6\text{F}_5)_3$ into a pore within MIL-101(Cr) to form MIL-101(Cr)-LP.^{266,267}



Scheme 58. Reduction of imines (**A**) and alkylidene malonates (**B**) catalysed by MIL-101(Cr)-LP MOF.²⁶⁶

A powerful method for the synthesis of solid-supported boranes is through the functionalisation of polymers. The functionalisation of polymers with boranes can be split into two categories:²⁶⁸ monomer functionalisation and polymer functionalisation.^{269,270}

In recent years there have been a few examples of poly(triaryl boranes)s that were synthesised by functionalisation of their monomers followed by polymerisation (Scheme 59). At this time polymer supported boranes have been used as fluoride sensors (**70**),²⁷¹ self-healing responsive gels (**71**),²⁶⁸ as catalysts for reductive aminations (**72**)²¹² as well as for the formylation of a range of amines (**73**)²⁷². Even more promising for our goals is the most recent application of the borane functionalised monomer **46** showing full FLP reactivity to heterolytically split hydrogen with DABCO being used as the LB.²¹² To the best of our knowledge there are still no published examples of poly(triaryl boranes) being used to catalyse hydrogenations.



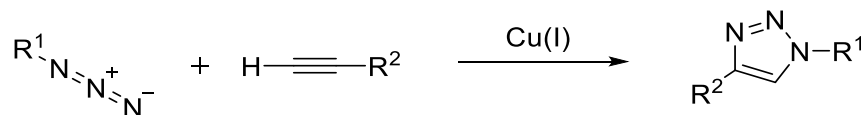
Scheme 59. Poly(triaryl boranes) **70**²⁷¹, **71**²⁶⁸, **72**²¹² and **73**²⁷² synthesised by functionalisation of their respective monomers before polymerisation. Also shown is the functionalised monomer **46** showing FLP reactivity to heterolytically split hydrogen.²¹²

5.1.3 Our Approach to Solid Supported Triaryl Boranes

We decided to focus on polymers as our solid-state material of choice. We were inspired by the research on polymer-bound boranes and aimed to find an alternative method to attach a monomeric borane catalyst unit to a solid support. The examples **70**, **71**, **72**, and **73** were all created through the polymerisation or copolymerisation of their respective monomer units.

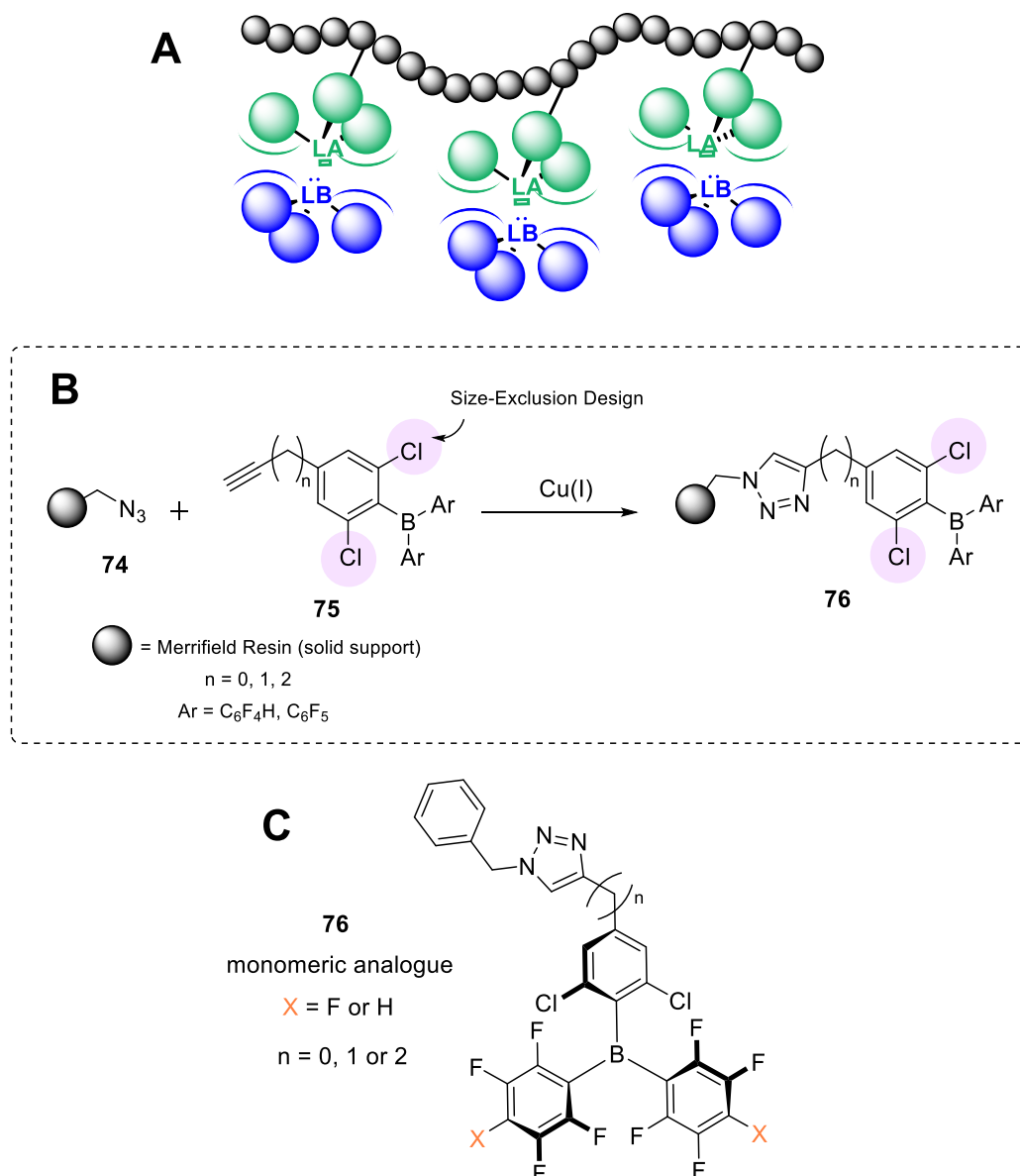
Merrifield Resin is a cross-linked polystyrene resin, which won Merrifield the 1984 Nobel Prize for its contribution to the field of solid-phase organic synthesis (SPOS).^{273,274} Due to its chloromethyl group, it can efficiently be functionalised through sequential step-by-step reactions in a single reaction vessel with limited and simple purification as the desired product is covalently bound to a solid support. The concept of SPOS has become the established method in peptide synthesis^{275–277} however, since its conception many other organic reactions have benefited through employing these solid supports to

address new synthetic problems.^{278,279} In the 21st century, the 1,2,3-triazole has emerged as an alternative bioisostere to replace amide bonds in peptides because of the stability of triazole scaffolds.²⁸⁰ 1,2,3-Triazoles are formed by the Cu(I)-catalysed azide-alkyne 1,3-dipolar cycloaddition (CuAAC) (Scheme 60), also known as ‘click’ chemistry because of its high yields, wide scope, selectivity and simple operation with limited purification required.^{281,282}



Scheme 60. Cu(I)-catalysed azide-alkyne 1,3-dipolar cycloaddition (CuAAC).²⁷³

The application of click chemistry to form functionalised materials using solid supports such as Merrifield resin is well established. Similarly, the use of a triazole group to adhere an organocatalyst to a solid support for application in flow has also been explored before.²⁸³ Trimesityl boranes bearing azide and triazole functionalities have also been developed for use as fluorophores and fluoride ion sensors.^{284,285} Whilst these triaryl boranes were not developed for, or tested as, FLP catalysts this work shows plausible functional group tolerance between triaryl boranes and azide/triazole moieties. Inspired by this research, we envisaged the functionalisation of commercially available Merrifield Resin to form azido methyl polystyrene (**74**)²⁸⁶ which could undergo a click reaction with our theorised borane functionalised alkyne monomer (**75**), to create a heterogeneous poly(triaryl borane) (**76**) potentially capable of FLP catalysis (Scheme 61.B). This combination of two established and Nobel Prize-winning pieces of chemistry appeared to be an extremely powerful set of tools to provide a novel answer to the heterogeneous FLP problem. Synthesis of the monomeric analogue (**77**, Scheme 61.C) of our hypothesised heterogeneous poly(triaryl borane) (**76**) would be crucial to test the synthetic plausibility of our target as well as compare its reactivity with boranes we have already synthesised (**16a/b** and **19b**) in homogenous catalysis.



Scheme 61. A. General structure of solid supported borane (LA) to a heterogeneous polymer (Merrifield Resin). B. Hypothesised ‘click’ chemistry used to adhere FLP borane to Merrifield Resin (solid support). C. Monomeric analogue for target synthesis to test reactivity of target FLP catalyst homogeneously.

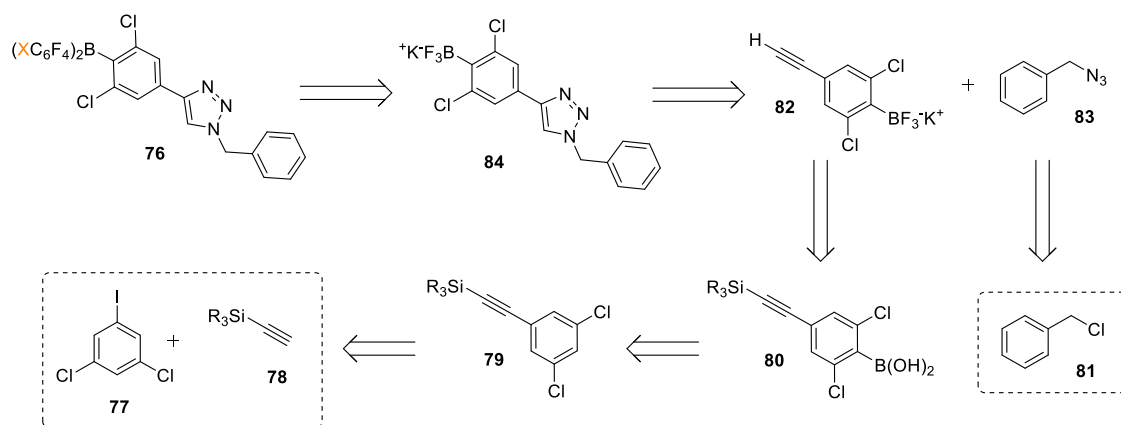
Whilst there is great promise in this idea there were, however, still some questions before starting to explore this path further:

1. How would we make the key borane functionalised alkyne monomer intermediate **75** (Scheme 61.B) and would our synthetic route to produce triaryl boranes be compatible with alkyne functionalisation?
2. How would we analyse the subsequent heterogeneous product and importantly determine catalyst loading? Whilst Merrifield Resin can be

bought with a known loading (x mmol/g) we would need to find a method to determine if every available site had been functionalised.

3. *How would a triazole unit impact the catalyst activity?*
 - a. *1,4-disubstituted 1,2,3-triazoles are known hydrogen bond acceptors and Lewis bases through the 3-position.²⁷⁹ They are likewise used as ligands in metal chemistry and as a result, will they form a classical Lewis adduct with our boranes or will they be sufficiently sterically hindered?*
 - b. *1,4-disubstituted 1,2,3-triazoles are also known to be weak electron withdrawing groups (EWGs) with respects to the electronics of the substituent at the 4-position.²⁸⁷ As a result, if no linker is used between the alkyne tether ($n = 0$, Scheme 61.B) and the aryl ring attached the borane, how will the electronics of the resulting triaryl borane be impacted?*

Nevertheless, we have devised a plausible retrosynthetic route (Scheme 62) to produce the monomeric analogue **76** of a potential heterogeneous FLP. We considered alternative routes that could have enabled us to produce a compound with an increased linker ($n = 1$ or 2) between the alkyne unit and adjoining aryl borane moiety. However, we ultimately decided to explore the route with the fewest synthetic steps in the hopes of producing a functioning catalyst as quickly as possible. This would allow us time to test and determine if it was necessary to synthesise other analogues. Synthesising this monomeric analogue **76** would provide us with the opportunity to test its catalytic activity before adapting this route to functionalise Merrifield Resin. It's important to note that our plan has a slight flaw, as it would be difficult to use the same route for the synthesis with the Merrifield resin. If this monomeric analogue is successful, we will have to adapt the route to functionalise the borane centre before performing the CuAAC (Scheme 62).



Scheme 62. Plausible retrosynthetic route to produce the monomeric analogue **76** of a potential heterogeneous FLP.

5.2 Results and Discussion

5.2.1 Work Towards the Synthesis of Novel Intramolecular Borane **76**

5.2.1.1 First Synthesis Attempt

The first step of the synthetic route was the Sonogashira cross-coupling of 3,5-dichloriodobenzene (**77**) with the silyl protected acetylene (**78a**) (Step 1. Scheme 63). Whilst following a literature procedure the first reaction was performed a 5 mmol scale test reaction (91% yield) before scaling up to 50 mmol (94% yield).²⁸⁸ Although the large scale reaction proceeded in excellent yield, the purified material contained a small amount of an impurity (9%) which was then identified to be the homo-coupled, diTES diacetylene **85a** (Scheme 63), which had coeluted on the column. Initially we were perplexed to isolate 14.79 g of the 'pure' product as this would be equivalent to 104% yield if all the isolated orange oil had been product. ^{13}C NMR spectroscopic analysis and quantitative ^1H NMR spectroscopy helped us to determine and quantify the culprit for the inflated yield (Figure 48). The literature procedure used 1.5 equivalents of the TES acetylene starting material **78a**. Whilst the homo-coupled side product was of no concern for the next step and could be removed in future purifications, reducing the equivalents of **78a** for future reactions might prevent formation of this undesirable side product.

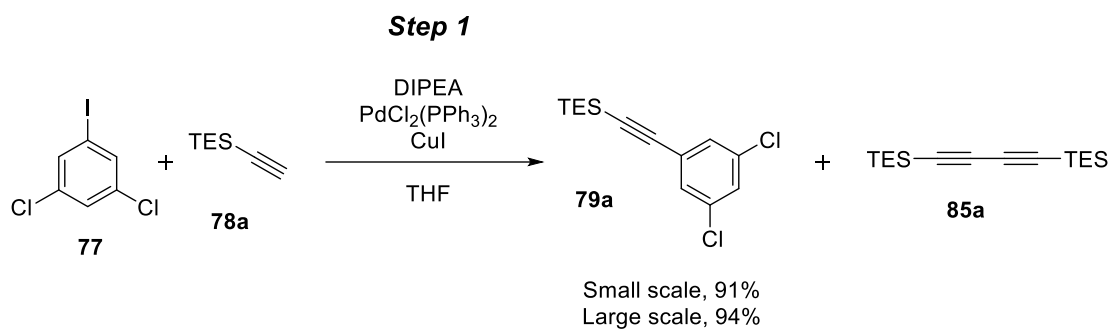
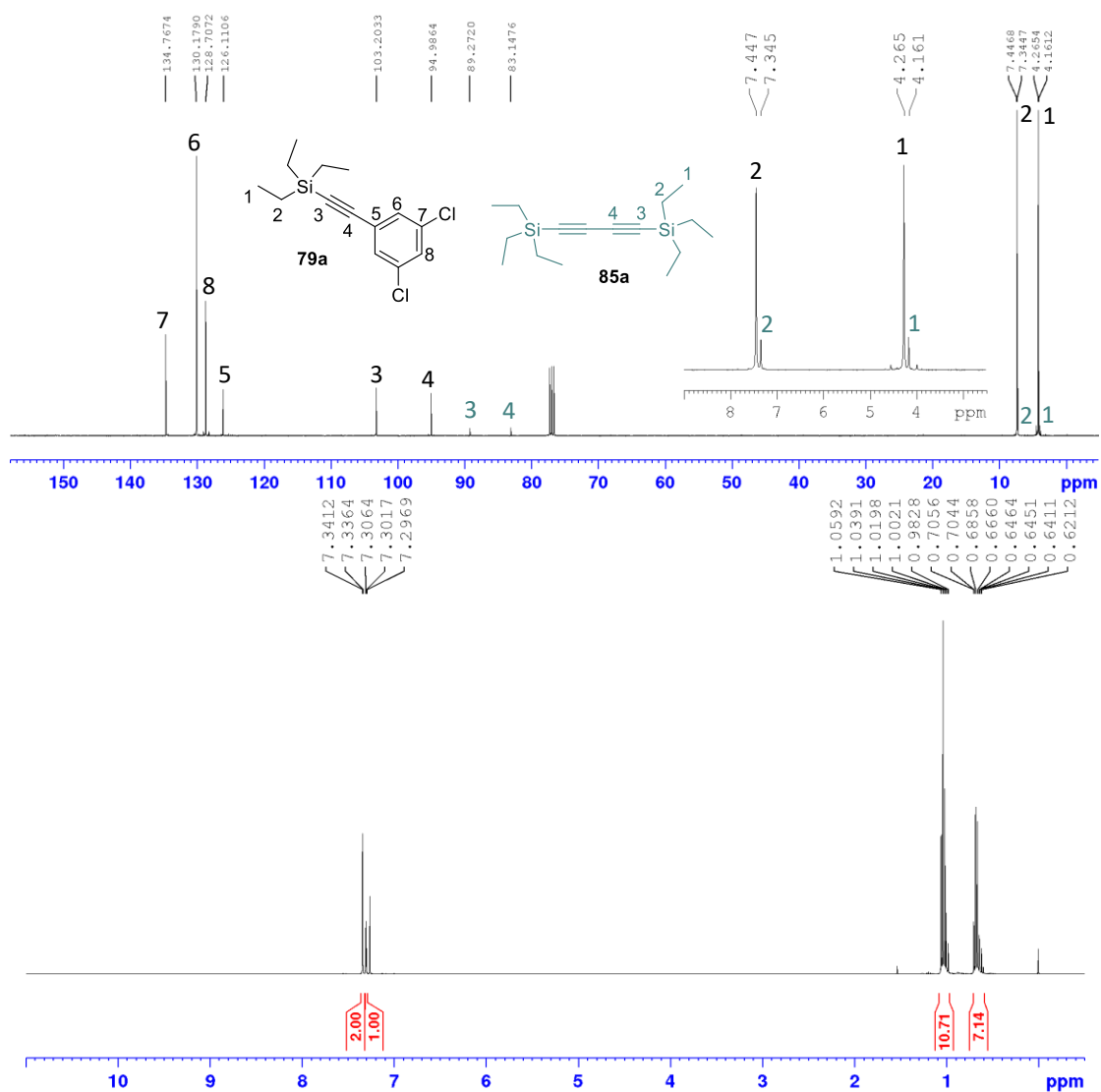
Scheme 63. **Step 1.** Sonogashira cross coupling.

Figure 48. Top. ^{13}C NMR spectrum of purified **79a** containing homo-coupled diTES diacetylene (**85a**). Bottom. Quantitative ^1H NMR spectrum to determine yield and amount of homo-coupled starting material (**85a**).

The second step in the synthetic route is the formation of a boronic acid **80a** (Step 2. Table 17). Initially, this step followed the same procedure adapted from our previous

triaryl borane synthesis for **16a/b**. This strategy relies upon the formation of an organolithium species through the deprotonation of the acidic proton at the 4-position (ortho to both chloro substituents) within compound **79a**. Subsequent addition of trimethyl borate to the organolithium species and quenching with water affords the desired boronic acid. A select number of the early attempts to form the boronic acid **80a** are shown in Table 17.

Unfortunately, as can be seen in Table 17, this proved to be a challenging step in the synthetic route with only two successful attempts (Table 17, Entry 1, 12% yield and Entry 4, 57% yield). Following a regular aqueous workup as well as removal of the solvent under vacuum the crude product for all successful reactions is a viscous orange oil.

In our previous experience with the analogous aryl boronic acids (**36** and **39**, Scheme 34) the crude compound crashes out as a white solid which can be triturated with hexane to yield the pure product. However, the crude boronic acid product **80a** is a viscous orange oil which is partially soluble in hexane. Presumably, this solubility is either due to decreased product formation or presence of the TES protecting group. As a result, purification of the pure boronic acid **80a** (which is still a white solid) is achieved by recrystallisation. Unfortunately, the yields from the recrystallisation's are very poor as is reflected in Table 17. Our early attempts at this synthetic route resulted in best yield of 57% (Table 17, Entry 4). In chapter two, we had obtained the analogous boronic acid **36** in 79% yield, as a result whilst a 22% drop in isolated yield was not perfect it was adequate for our initial attempts. We were able to isolate a total 2.18 g of pure boronic acid **80a** by performing a large scale recrystallisation on the combined filtrates from previous poor yielding recrystallisation attempts.

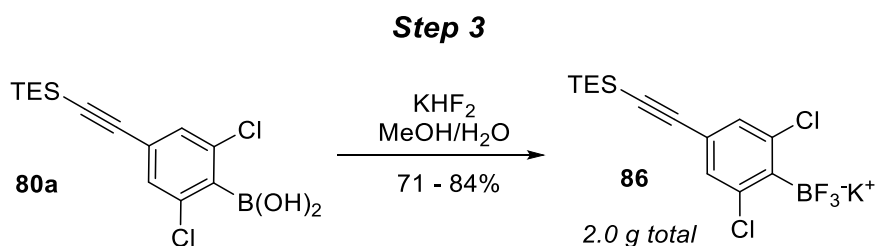
Table 17. Select early attempts to form boronic acid **80a** (Step 2).

Step 2

Entry	ⁿ BuLi (eq)	Organolithium rxn time (hrs)	B(OMe) ₃ (eq)	Conc. (M)	Isolated mass (g)	Isolated yield (%)
1*	1.1	2	2.2	0.2	0.04	12
2*	1.2	2	1.2	0.4	-	-
3*	1.2	2	2.2	0.7	-	-
4**	1.5	1	3.5	0.1	0.65	57

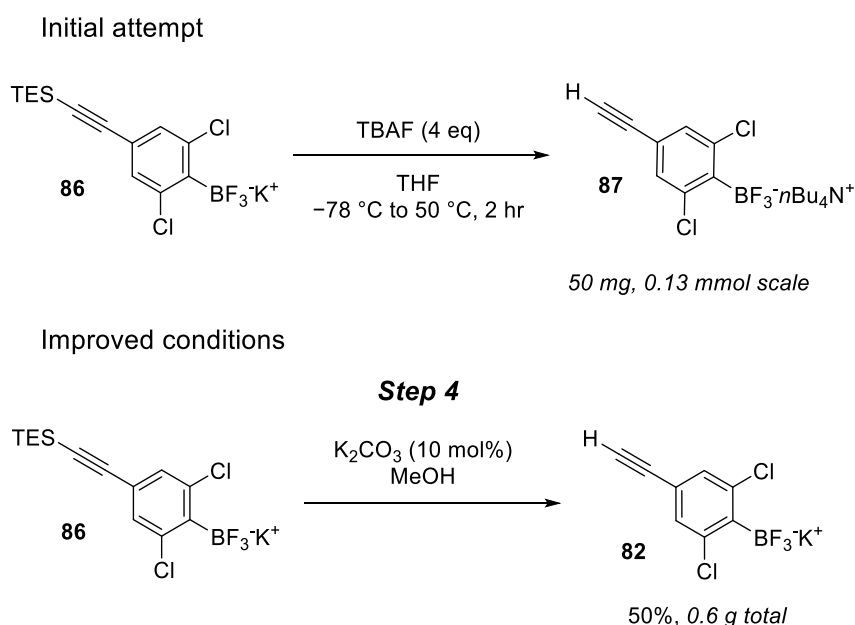
*following adapted synthetic route previously used in section 2.2.1 from Soós et al. 2015.¹⁹⁰ **following procedure from Lee et al. 2021.²⁸⁹

The third step in the synthetic route is the transformation of the boronic acid **80a** into the ArBF_3K salt **86** using potassium bifluoride (Step 3. Scheme 64). Like Step 2, this step followed the same procedure adapted from our previous triaryl borane synthesis for **16a/b**. Gratifyingly, this proved relatively straightforward and ArBF_3K salt **86** was obtained in good yield (71 – 84%, 2.0 g total).

Scheme 64. Step 3. ArBF_3K salt formation.

We were surprised to find that the TES group had not been deprotected by the KHF_2 . Either the fluoride ion in KHF_2 , which is in major excess (4.5 equivalents), is not dissociated enough under these conditions to deprotect the TES group, or the TES group is robust enough to remain untouched. Regardless this resulted in the requirement of subsequent deprotection of the silyl protecting group.

Our first attempt to deprotect the silyl protecting group (TES) was made using the standard silyl deprotecting reagent tetrabutylammonium fluoride (TBAF) (Scheme 65).²⁹⁰ Unfortunately, whilst the deprotection was successful with 100% conversion, the resulting desired product **82** underwent counter-ion exchange to produce the ArBF_3TBA salt analogue **87** which could not be isolated from the other TBA salts used for deprotection. This counter ion exchange is known and is employed often to improve ArBF_3K salt solubility for C-C cross coupling reactions.²⁹¹ After counter ion exchange the resulting tetraalkylammonium salts are soluble in less polar organic solvents such as dichloromethane (DCM), whilst ArBF_3K salts are only soluble in more polar solvents such as THF, MeOH, DMSO and water. Attempts to isolate the pure BF_3TBA salt analogue **87** by trituration's and by aqueous workup were both unsuccessful.

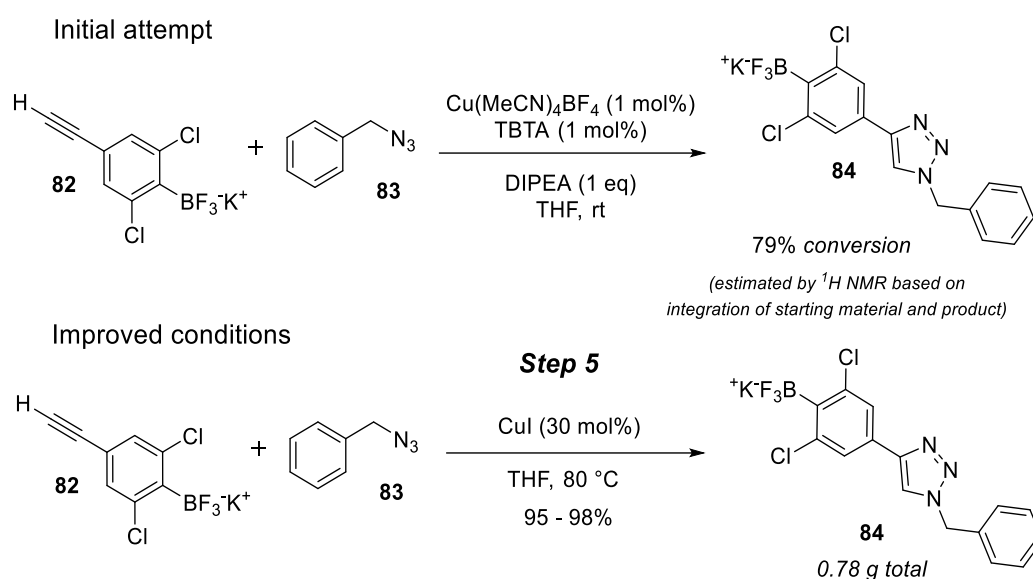


Scheme 65. First attempted deprotection of TES protecting group using TBAF and Step 4.

Improved deprotection of TES protecting group.

Further reading of the literature revealed an alternative mild set of conditions for the deprotection of less hindered silyl protected alkynes such as TES and TMS protecting groups.^{292,293} Using K_2CO_3 (10 mol%) and MeOH at room temperature overnight (Step 4, Scheme 65), successfully allowed for the production of our key alkyne intermediate **82**, albeit in moderate yield 50% after purification. Whilst we were not pleased with this yield, the loss of product was attributed to poor purification through suspension in MeCN. This yield equated to 0.69 g of **82** to proceed on to Step 5.

Step 5 was also relatively straight forward. The initial attempt was unsuccessful (Scheme 66)²⁹⁴, as incomplete conversion of the starting material alkyne was observed. Precedents for CuAAC of molecules bearing a ArBF₃K group exist in the literature.²⁹⁵ Adapting these literature conditions to our substrate, using a solvent (THF) that would both solubilise our reagents and could easily be separated from the click product, we isolated our target ‘clicked’ triazole ArBF₃K salt **84** in excellent yield (98%). Gratifyingly the more successful second attempt required much simpler reaction conditions as can be seen in Step 5, Scheme 66.

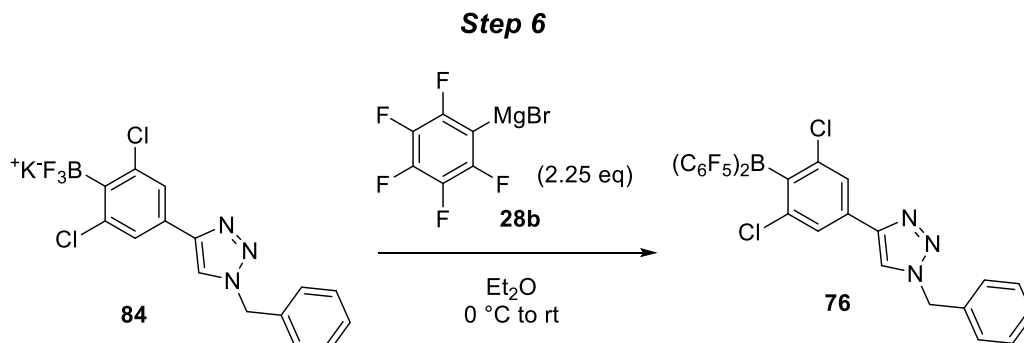


Scheme 66. First attempt at CuAAC ‘click’ reaction to form target triazole ArBF₃K salt **84**.²⁹⁴

With the ‘clicked’ ArBF₃K salt **84** in hand we were optimistic that we could finally synthesise the target triaryl borane **76** however, due to the challenging purification of the boronic acid, the wasted material from the TBAF deprotection as well as the trial ‘click’ reaction and general mass lost for analysis only, 0.59 g of **84** was available for the final step (Step 6, Scheme 67).

Like Step 2 and 3, Step 6 followed the same procedure adapted from our previous triaryl borane synthesis for **16a/b**.⁶⁰ For our first attempt we chose to use functionalise the ArBF₃K salt **84** with the pentafluoro phenyl Grignard **28b** as shown in Step 6, Scheme 67. Unfortunately, a tap got knocked off on my Schlenk line whilst this final step was left overnight and as a result, we were concerned that all or much of our desired product may have decomposed to the Ar₂B-OH adduct we had observed in our previous

experiences. We followed the same purification pathway discussed in Scheme 38, hot toluene decantation, solvent removal under vacuum and hexane washes to produce the crude product.



Scheme 67. Step 6. Final synthesis of triaryl borane 76 from potassium aryl trifluoroborate salt.

The same insoluble solids as for the synthesis of **16a/b** were observed and following an extra toluene suspension (developed for the synthesis of known FLP-boranes in chapter two, Scheme 39) we were able to isolate 86 mg (10% yield) of what we believed to be pure triaryl borane **76** (Figure 49). Figure 49 shows the isolated purified product **76** in a small Schlenk after toluene suspension. Unfortunately, NMR spectroscopic analysis of the purified product proved to be much more complex than we had experienced for the known triaryl boranes. The ^{11}B and ^{19}F NMR spectra showed signs of the desired product and the believed $\text{Ar}_2\text{B-OH}$ decomposition side product suggesting the purification pathway had been unsuccessful. The analysis of **76** will be discussed in detail in section 5.2.2. A summary for the first attempt at the 6-step synthesis of impure triaryl borane **76** is shown in Scheme 68.

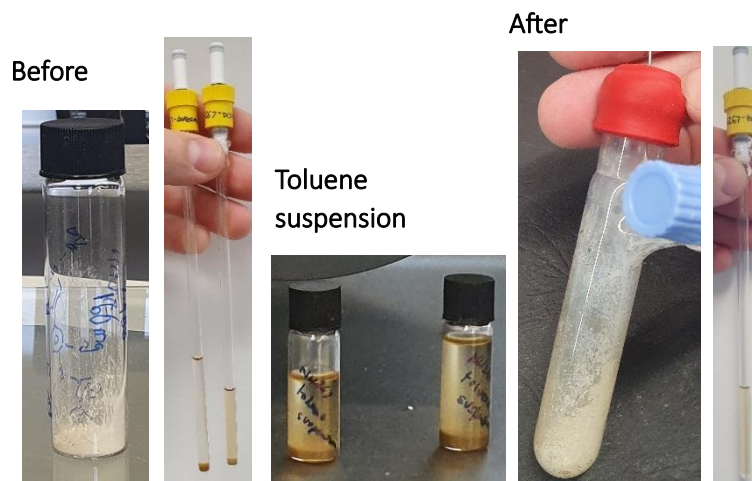
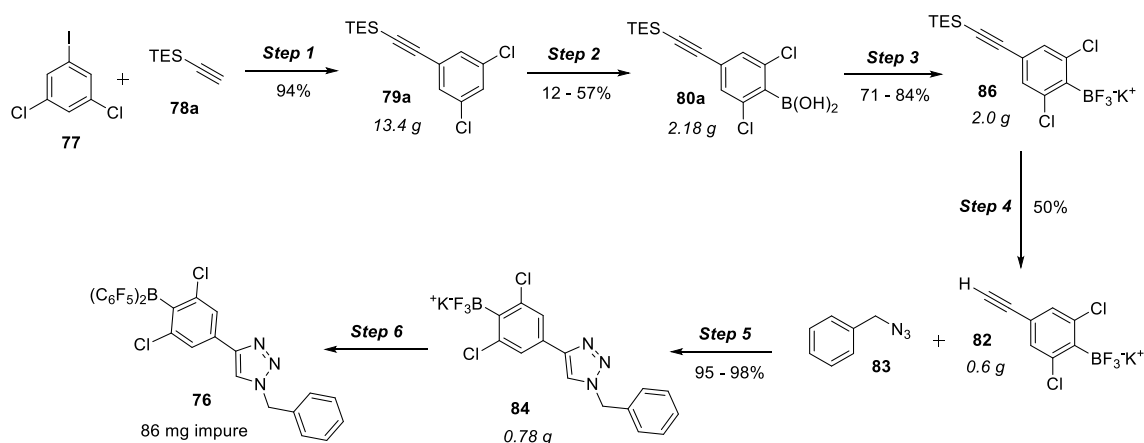


Figure 49. First attempted synthesis of monomeric novel borane analogue **76**. Left. Before toluene suspension. Middle. Toluene suspension on small scale. Right. After toluene suspension to produce 'pure' product.



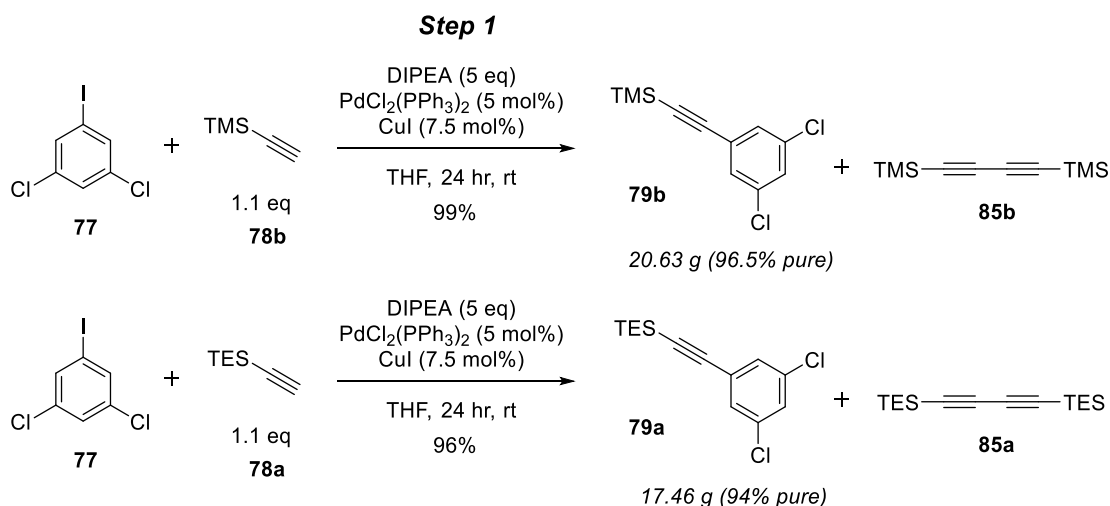
Scheme 68. Summary of 6-step synthesis of impure triaryl borane **76**.

5.2.1.2 Second Synthesis Attempt, Improvements and Scale-up

Attempts at reductive amination reactions using impure triaryl borane **76** had shown promising results (discussed in section 5.2.3.1), so we decided to repeat the synthetic route outlined in the previous section (section 5.2.1.1). As our previous attempt had not led to enough mass for further purification, adequate analysis and limited reactivity testing we chose to improve/partially optimise the synthetic route to be performed on larger scale. We were optimistic that this would lead to the best chance at an improved yield from the final step and produce pure product isolated from the Ar₂B-OH impurity. To improve the yield for Step 2 (boronic acid **80** formation), we proposed that using the trimethyl silyl (TMS) protecting group would lead to an improved recrystallisation due to

its less greasy nature compared to TES. We decided to run both protecting groups (TES and TMS) in parallel.

Similarly to our first attempt, the Sonogashira reaction proved straightforward with both the TES and TMS analogues (**79a** and **79b**). The amount of the respective silyl protected acetylene was reduced to 1.1 equivalents and although the homo coupled diTES/TMS diacetylene could be observed again after purification, it was present much lower amounts than our previous attempts (3.5% diTMS diacetylene **85b** in product **79b**). Regardless, we were able to produce 20.63 g of crude **79b** (96.5% pure) in 99% yield if accounting for the homo-coupled impurity) (Scheme 69). Likewise, 17.47 g of **79a** (96% yield, 94% purity) was isolated with 6% diTES diacetylene **85a**.

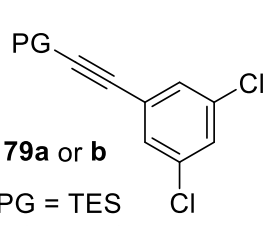


Scheme 69. Step 1. Straightforward Sonogashira cross coupling reaction TMS- and TES-acetylene with 3,5-dichloriodobenzene.

With ample material of both **79a** and **79b** (57.4 and 81.9 mmol respectively) we set out to try to improve Step 2 in our synthetic route. In our first pass synthesis of novel triaryl borane **76**, the boronic acid had been the one of the lowest yielding steps (57%). As a result, we aimed to optimise the yield for the boronic acid formation in Step 2 and determine the most effective purification method. The previous best conditions (Table 18, Entry 4) for the TES silyl protected compound **80a** achieved a 57% isolated yield. This yield had been achieved through multiple exhaustive recrystallisations where the subsequent recrystallisation solutions required cooling to $-20\text{ }^\circ\text{C}$ in a freezer for multiple days to extract maximum yield. Table 18 shows the limited optimisation performed on Step 2.

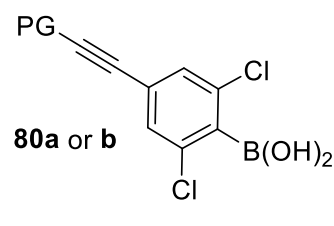
Table 18. Limited optimisation of boronic acid formation (**Step 2**).²⁸⁹

Step 2



79a or b
79a, PG = TES
79b, PG = TMS

1. BuLi (1.5 eq),
THF, -78 °C, 0.75 - 3 hr
 2. B(OMe)₃ (x eq)
 3. HCl or NH₄Cl (aq)



80a or b

Entry	PG	Organolithium rxn time (hrs)	B(OMe) ₃ (x eq)	Conc. (M)	Isolated mass (g)	Isolated yield (%)
1	TES	1	4	0.1	0.4	24
2	TMS	1	4	0.1	0.76	53
3*	TMS	3	1.3	0.7	-	-
4	TMS	1	3	0.1	1.34	45
5	TMS	1	3	0.1	2.0	54
6	TMS	0.75	3	0.1	12.76	64

*following adapted synthetic route from Jäckle et al. 2020.²¹²

Our initial attempts (Entries 1 and 2) exemplify the difference between silyl protecting groups. Both compounds **80a** (Entry 1) and **80b** (Entry 2) underwent a single overnight recrystallisation. Figure 50 shows both these recrystallisations set up simultaneously and is further evidence that our hypothesis was correct. The TMS silyl protected **80b** is significantly less soluble in hexane than **80a** and immediately began to crash out of the pale-yellow solution as a fine white solid. As a result, after only one pass recrystallisation Entry 2 for **80b** attained a 53% yield compared to the 24% yield for **80a**.



Figure 50. Comparison of boronic acids **80a** (TES, left) and **80b** (TMS, right) in hexane during recrystallisation as well as purified boronic acid **80b** (white solid) after recrystallisation.

After repeating this reaction (Step 2) several times, we noticed another trend. When using the similar 2,6-dichloro boronic acid analogue of **36** (Scheme 34), the typical intermediate organolithium species would crash out of solution as a white precipitate. However, in successful reactions with boronic acids **80a/b**, the organolithium intermediate would turn the clear THF solution instantly yellow upon addition of ${}^n\text{BuLi}$. With continued dropwise addition of ${}^n\text{BuLi}$, the solution would slowly turn golden orange (Figure 51). This colour would be lost once trimethyl borate was added, changing from golden orange to yellow to clear.



Figure 51. Left to right: Organolithium species immediately after addition of ${}^n\text{BuLi}$ (yellow solution). Clear solution of **80a** dissolved in THF before ${}^n\text{BuLi}$ addition. Organolithium species after being stirred at $-78\text{ }^\circ\text{C}$ for 1 hr (golden orange solutions). Reaction mixture after organolithium species is quenched with trimethylborate.

In our initial attempts (Entries 1 and 2), we identified the main impurity in the crude ${}^{11}\text{B}$ NMR spectra (Figure 52). After our workup, we found our desired product as the major

resonance at 28.6 ppm and a significant amount of boric acid ($B(OH)_3$) at 20.2 ppm.²⁹⁶ This was expected due to the large excess of trimethyl borate (4 equivalents). It was crucial to prevent this impurity from carrying over into Step **3**, as it could be similarly affected by KHF_2 , making it very difficult to remove.

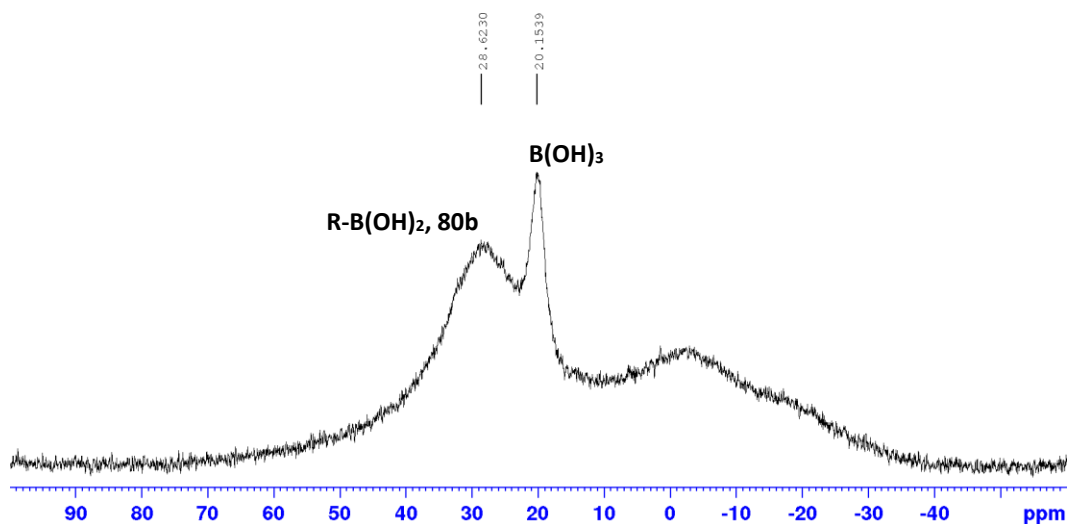


Figure 52. Crude ^{11}B NMR spectra containing boronic acid **80b** and boric acid ($B(OH)_3$).

We attempted to reduce the amount of trimethyl borate used to 1.3 equivalents (Table 18, Entry 3). Following Jäckle and co-workers' approach, we left the organolithium solution stir for 3 hours and observed a deep black solution.²¹² No visual change occurred upon adding the trimethyl borate (Figure 53). After isolation, we found mostly the homocoupling starting material **80b**. Whilst this is a side product, we observed in minor quantities within all attempts shown in Table 18, suggesting it had been formed by leaving the reactive organolithium species stirring for too long.

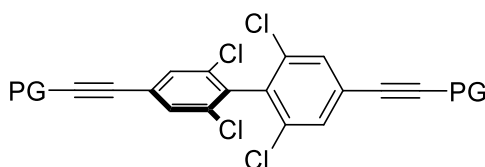
**88a/b****88a**, PG = TES**88b**, PG = TMS

Figure 53. Above: Image of Entry 3, Table 18 after borate had been added. The solution had turned black during the 3 hours the organolithium species was left. Below: Homo coupled starting material **88a/b**, formed when the organolithium species is left too long.

Entries 4 and 5, reverted to our best conditions and 3 equivalents of trimethyl borate were added at $-78\text{ }^{\circ}\text{C}$ from Entry 4 onwards. However, the yields were only 45% and 54% respectively after recrystallisation. We suspected that boric acid was too soluble in DCM and as a result, our aqueous washes to remove the boric acid were less effective. Combining the crude recrystallisation filtrates from entries 1, 2, 4, and 5, we removed the solvent and dissolved the crude oil in Et_2O . After washing exhaustively with water, we isolated an additional 3.86 g of crude product, with the boric acid completely removed. The minor impurities present (unreacted starting material **79b** and homo coupled **79b** (**88b**)) were not a concern for the next step in our synthesis.

The optimisation resulted in Entry 6, where on large scale (split into 3 reaction vessels) 12.76 g (64% yield) of pure product was isolated after Et_2O washes and subsequent recrystallisation, which had been proven to be much more effective with the TMS analogue **80b**.

Table 19 described the attempts performed for the formation of the ArBF_3K salt using either TMS or TES protected starting materials. In contrast to our first pass synthesis the purpose here was to compare the TMS and TES silyl protecting groups. Previously it had

been surprising when KHF_2 had not furnished the deprotected terminal alkyne product **82**, from our **80a** analogue (Step 3, Scheme 64), and as a result, silyl deprotection had been required (Step 4, Scheme 65).²⁹² Whilst relatively straightforward, we were hoping we would not need to perform this extra step for our **80b** analogue. We were, therefore, extremely gratified to observe only the deprotected key alkyne intermediate **82**, when the TMS protecting group was employed (Table 19, Entries 1 – 3). Our best yield, 94%, was achieved on the largest scale (Entry 3) to produce 11.54 g of terminal alkyne **82**.

Table 19. Comparison of ArBF_3K salt formation (Step 3) using TMS or TES silyl protecting groups.¹⁹⁰

Step 3

80a or b
80a, PG = TES
80b, PG = TMS

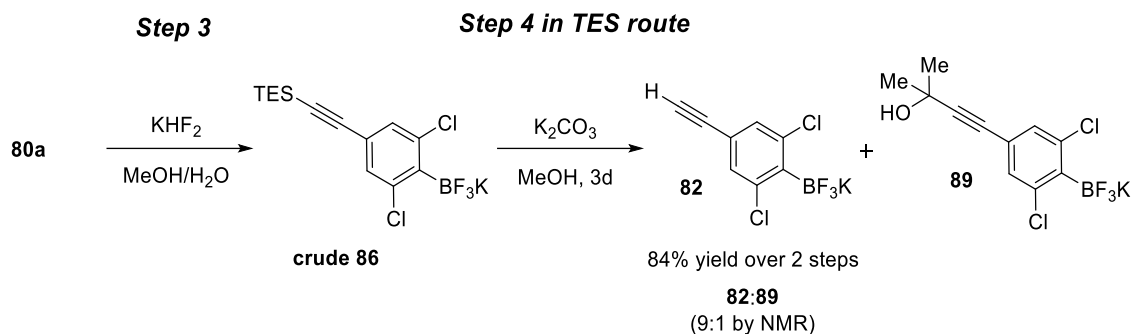
Entry	PG	Isolated mass (g)	Yield of 86 (%)	Isolated yield of 82 (%)
1	TMS	1.66	-	86
2	TMS	1.74	-	90
3	TMS	11.54	-	94
4 ^a	TES	8.76	65 [*]	11 [*]
5 ^{a,b}	TES	7.26	-	84 [*]

^{*}determined by ^1H NMR spectroscopy. ^ayield determined over two steps as **80a** was used crude without recrystallisation. ^bcrude carried straight through into K_2CO_3 deprotection. Pure product could not be isolated from impurity and material had to be abandoned.

Conversely, over two steps, Entry 4, employing crude **80a**, yielded 65% of the expected product **86** but, unlike our previous attempts, also produced 11% of the deprotected key alkyne **82**. We were pleased to find that Entry 5, using the TES protecting, was obtained in 84% yield. This was determined over two steps as crude **80a** was carried on into Step 3 after aqueous washes rather than performing the poor yielding recrystallisation.

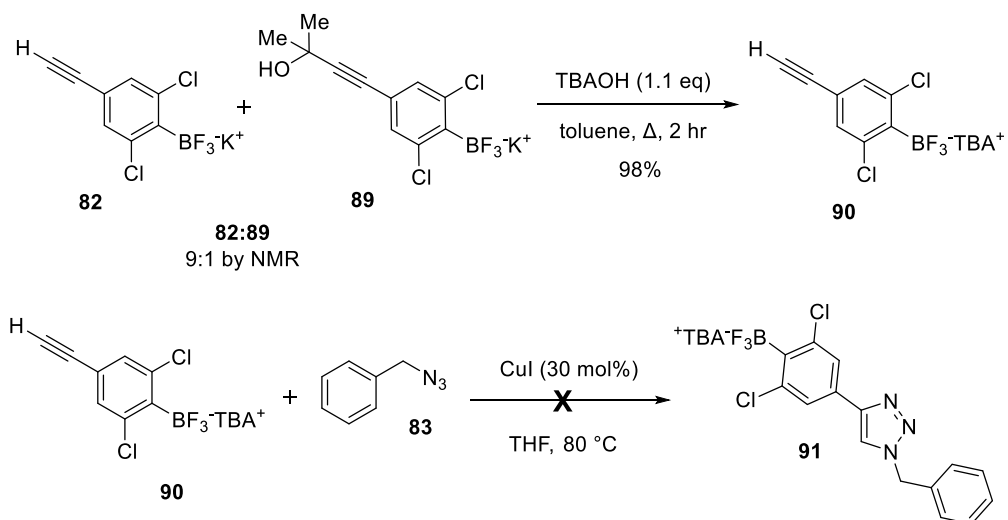
Unfortunately, Entry 5, was also carried on into Step 4, however the reaction mixture was stirred for 3 days under the deprotection conditions (Scheme 70). The reaction

yielded the desired product **82** in 84% yield, but also an acetylenic alcohol product **89** was also formed (10%).



Scheme 70. 2 step ArBF₃K salt formation and subsequent TES deprotection directly from crude ArBF₃K intermediate **86**.

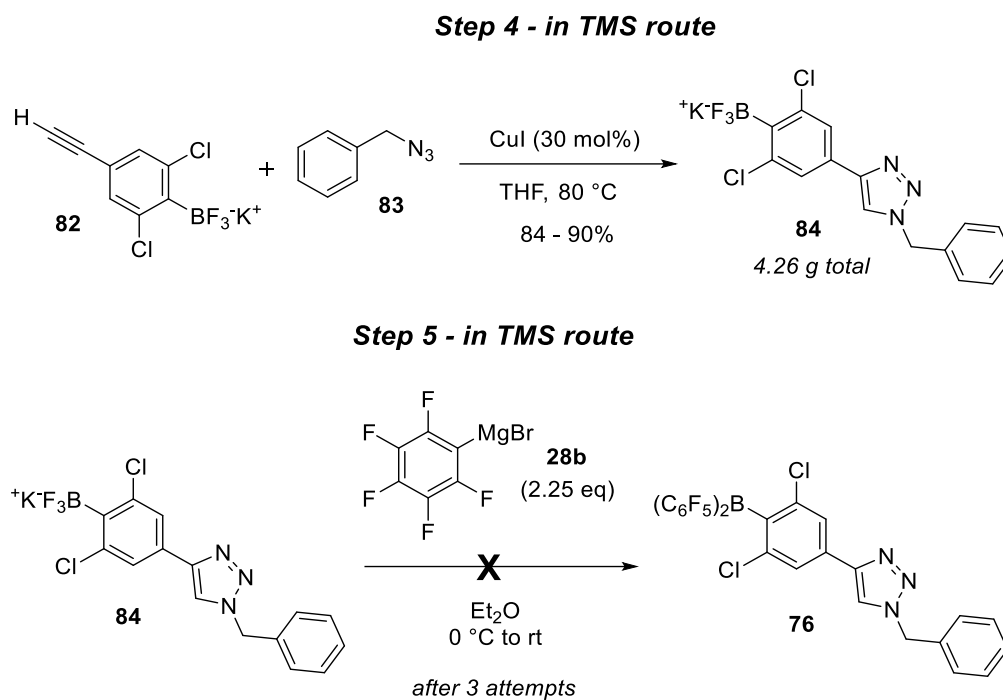
Whilst we performed a successful one pot deprotection of the hydroxyl isopropyl group as well as counter ion-exchange using tetrabutylammonium hydroxide (TBAOH), the subsequent BF₃TBA salt would not undergo successful click reaction (Scheme 71). As a result, further work with this compound containing the impurity was abandoned.



Scheme 71. Above. Successful deprotection of hydroxy isopropyl group and subsequent counter ion exchange. Below. Unsuccessful CuAAC click reaction using BF₃TBA salt, **90**.

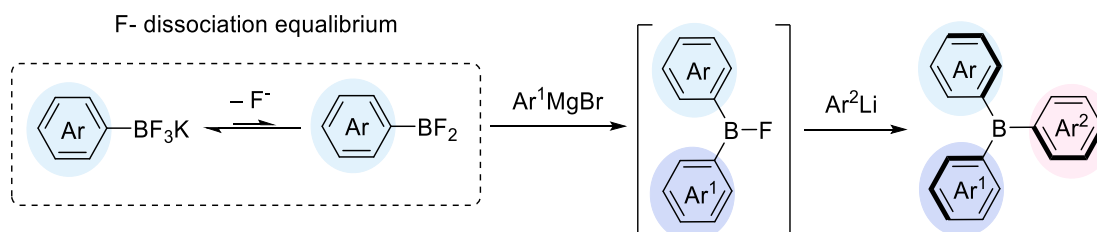
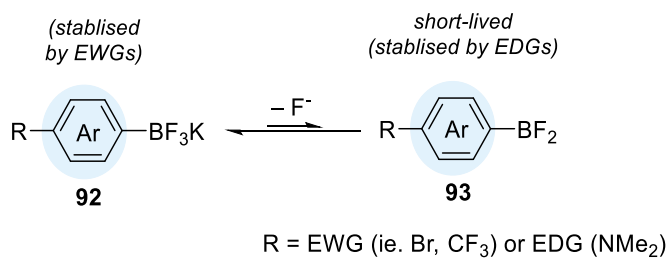
Overall, the clicked ArBF₃K salt **82** was produced with improved yield over 4 steps using the TMS protected synthetic route. After combining multiple reactions, we obtained 4.26 g of **82** in Step 4 of Scheme 72. Despite making improvements, we were unsuccessful in our final synthesis of triaryl borane **76** in Step 5 of Scheme 72. After multiple attempts on different scales, we were able to isolate various solids, including a promising 0.63 g

of a beige powder, however, analysis of the product by ^1H , ^{19}F and ^{11}B NMR spectroscopy did not show any signs of successful synthesis.



Scheme 72. Step 4. Click reaction, and Step 5. Unsuccessful Grignard addition to ArBF_3K salt **84**.

The unsuccessful synthesis of **76** may be due to the electron-withdrawing nature of the triazole unit.²⁸⁷ In previous work by Marder, discussed in section 2.2.1.4, the mechanism of triaryl borane synthesis using ArBF_3K salts as the boron source was explored, providing more information about the importance of the F^- dissociation equilibrium.²⁰⁹ Marder argued that regardless of whether the mechanism is associative or dissociative, the first fluoride dissociation step would benefit energetically from an electron-donating group (EDG) at the para position in the ArB_3K salt (Scheme 73). Conversely, an EWG, as would be present in our clicked ArBF_3K salt **84**, would hinder F^- dissociation.^{297,298} They showed that using the *N,N*-dimethylamino group at the para position (**92**), the short-lived ArBF_2 species **93** could be more favourable and attacked with one equivalent of Grignard reagent.²⁰⁹ As a result, future synthesis may need to incorporate a linker unit between the triazole unit and the ArBF_3K salt to avoid possible hinderance to the initial fluoride dissociation.



Scheme 73. Synthesis of triaryl boranes, with focus on the impact of electronics on the initial fluoride dissociation.^{209,297,298}

The non-triazole functionalised triaryl borane **16b** can be synthesised by adding 2.25 equivalents of Grignard reagent **28b** to the non-triazole functionalised ArBF₃K salt **37** (Scheme 35). However, it is possible that the triazole functionalised ArBF₃K salt **84** may require a more reactive organometallic reagent to install the second aryl moiety. Marder discovered that the steric hindrance caused by the 2,6-dimethyl aryl functionality on each of the 3 aryl rings made it too difficult to add 2 equivalents of the Grignard reagent. Instead, a more reactive organolithium species was needed for the addition of the second aryl moiety. Although our triazole functionalised ArBF₃K salt **84** does not have the same steric hindrance, it would be beneficial in the future to consider using an organolithium species for the addition of the second aryl ring.

5.2.2 Analysis and Characterisation of **76** by Understanding the Intermolecular Analogue **92**

The initial attempt to synthesise triazole-borane **76**, possibly gave us a small amount of impure material. Analysis of the NMR spectroscopic data obtained suggested that that despite the steric bulk around our borane centre the triazole unit was able to act coordinate and form a classical Lewis pair adduct at ambient temperature. The ¹¹B NMR spectrum shows completely bound adduct (Ar₃B-N, **94**) at -3.68 ppm as well as the

proposed $\text{Ar}_2\text{B-OH}$ decomposition product at 42.15 ppm (Figure 54). This matches well with the $\text{Ar}_2\text{B-OH}$ decomposition product (40.9 ppm) monitored by Jäckle *et al.* for decomposition experiments performed on the monomer **46** introduced in Scheme 59.²¹² As **46** shares the same triaryl borane motif as our own compound it is a fair assumption that the decomposition byproducts shall be observed in the same region. On the other hand, the ^1H and ^{19}F NMR spectra are too complex to confidently assign, due to the steric restrictions around the tetracoordinated borane centre (Figure 54). The complexity of the NMR spectra led us to synthesise the intermolecular analogue **92** prepared from **16b** and the triazole monomer **94** (Figure 54). With both **16b** and the triazole **94** isolated and analysed separately, when combined we were able to elucidate some of the complexity in our impure intramolecular compound **76**. The addition of excess borane **16b** (1.4 equivalents) to a solution of triazole **95** allowed us to see both the coordinated B-N adduct **92** and non-coordinated free borane **16b**. The ^{11}B NMR spectrum shows there is no free/uncoordinated triaryl borane in our novel compound **76**, whilst when excess **16b** is added in the intermolecular analogue, the excess uncoordinated borane **16b** can be observed at 62.9 ppm (Figure 54). The spectra also show that the B-N adduct **92**, for this combination of triaryl borane motif (**16b**) and 1H-1,2,3-triazole **95** appears at approximately -4.0 ppm. As $\text{Ar}_3\text{B-NR}_3$ adducts can come anywhere between 8 to -20 ppm,²⁹⁹ this is the most indicative piece of information to be confident in the successful synthesis of our target intramolecular analogue **76** and despite the $\text{Ar}_2\text{B-OH}$ present the whole borane was coordinated in a classical Lewis adduct with a triazole LB.

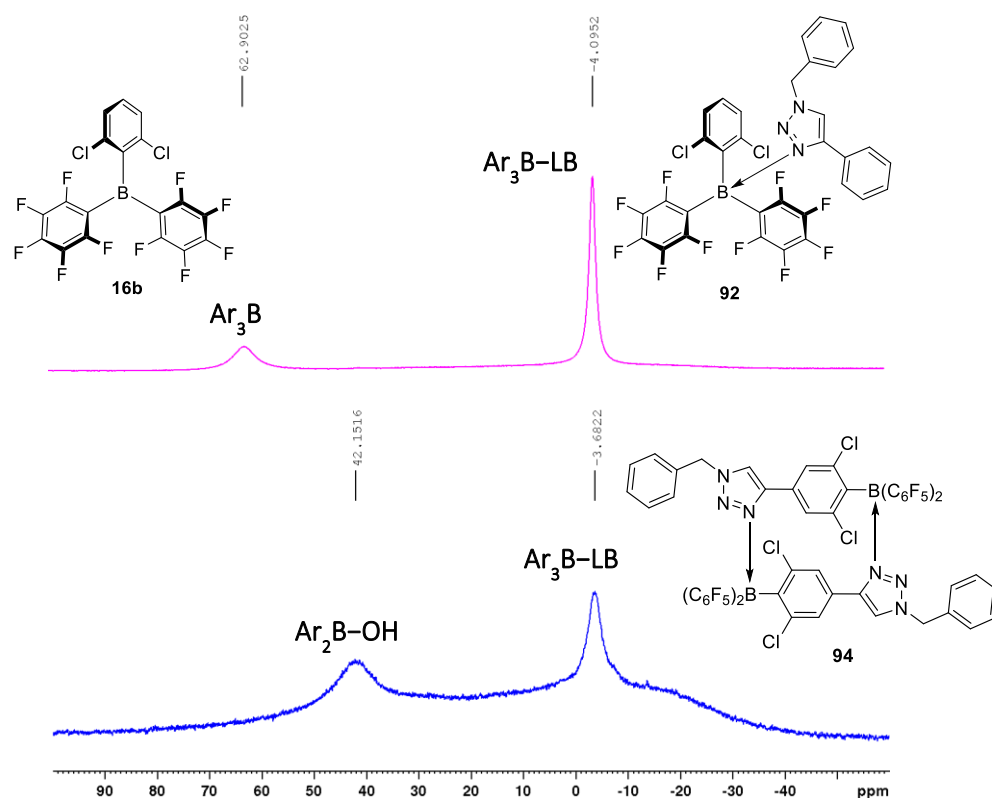


Figure 54. ^{11}B NMR spectra of novel intermolecular $\text{Ar}_3\text{B-N}$ adduct **92** (above) and intramolecular $\text{Ar}_3\text{B-N}$ adduct **94** (drawn as dimer for simplicity) containing decomposed $\text{Ar}_2\text{B-OH}$ byproduct impurity (below).

Observation of the B-N adduct was not a surprise considering triazoles are known to act as H-bond acceptors and LBs through the 3-nitrogen.²⁸⁰ Whilst there are many examples of FLP boranes coordinated to N-heterocycles, mostly the prototypical FLP BCF ,³⁰⁰ it is rare to find examples of labile B-N coordinated adducts. Dynamic dissociation of the B-N bond has been observed by Erker *et al.* in 2011 where the strongly LA borane **96** can form a labile intramolecular LP adduct with trialkyl amines (Figure 55).^{301,302} Due to facile exchange between the non-coordinated and the B-N coordinated conformation, **96** is still able to function as an FLP catalyst for hydrogen activation.³⁰¹ Similar labile coordination has been observed in less Lewis acidic boranes **97**³⁰³ as well as, in more sterically congested system **98**³⁰⁴ (Figure 55).

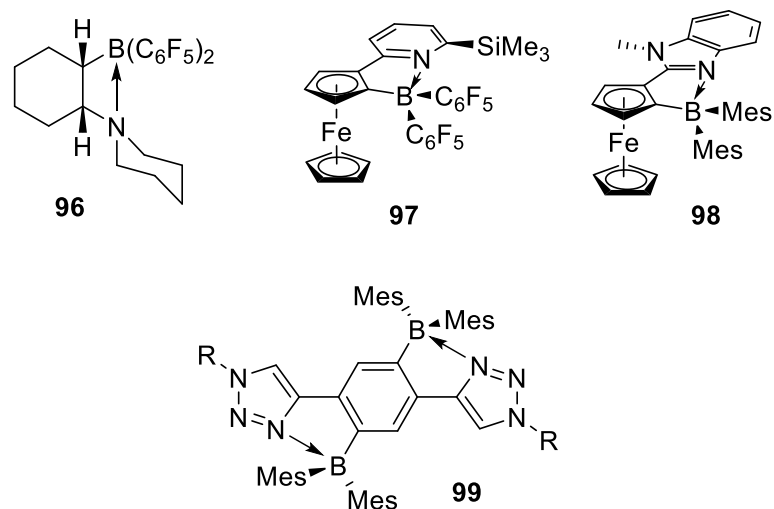


Figure 55. Examples of labile B-N adducts.^{301,303–305}

Triaryl boranes containing triazole appendages have also been synthesised before and commonly used as π -conjugated electronic materials. In most of these materials no B-N coordination is observed as all three triaryl moieties are mesityl analogues and the boron centre is too sterically congested for the classical LP adduct to form.^{209,284,306} However, in 2017 Pammer *et al.* synthesised a library of three intramolecular labile B-N coordinated compounds with the general structure **99** (Figure 55).³⁰⁵ These structures are the only similar evidence in the literature for 1*H*-1,2,3-triazoles forming labile adducts with triaryl boranes similar to ourselves. 1*H*-1,2,3-triazoles are significantly less basic than most common *N*-heteroarenes ($pK_aH = 1.2$). This includes 4*H*-1,2,4-triazoles ($pK_aH = 2.2$) and those employed by Jäckle (**97**, pyridyl, $pK_aH = 3.4$) and Wang (**98**, benzimidazolyl, $pK_aH = 5.7$).^{305,307} Pammer *et al.* claim that the N-B coordination in our own systems should be slightly weakened compared to the examples shown by **96**, **97** and **98** in Figure 55.³⁰⁵

With this in mind we were optimistic that variable temperature (VT) NMR spectroscopy could help us establish whether our system was labile and thus had potential for FLP catalysis. As alluded to, the 1H and ^{19}F NMR spectra were also extremely complex and practically unassignable for novel intramolecular FLP **76**. This is caused by the complex tetracoordinated borane adduct formed when a classical Lewis pair is formed. With the addition of unsymmetrical triaryl borane motif and unsymmetrical LB (triazole unit) it is of no surprise that no environments in the 1H or ^{19}F NMR spectra are equivalent at room temperature.

Unfortunately, crystal suitable for X-ray crystallography could not be isolated due to the small mass of **76** obtained. Therefore, the binding present in the intramolecular compound adduct is uncertain. We believe the adduct is formed through intermolecular coordination, which could be dimeric, polymeric, or a mixture of the two (Figure 56). We hoped that variable-temperature nuclear magnetic resonance spectroscopy of our less complex intermolecular adduct **92** would help us assign key environments by observing clear coordinated and uncoordinated adducts.

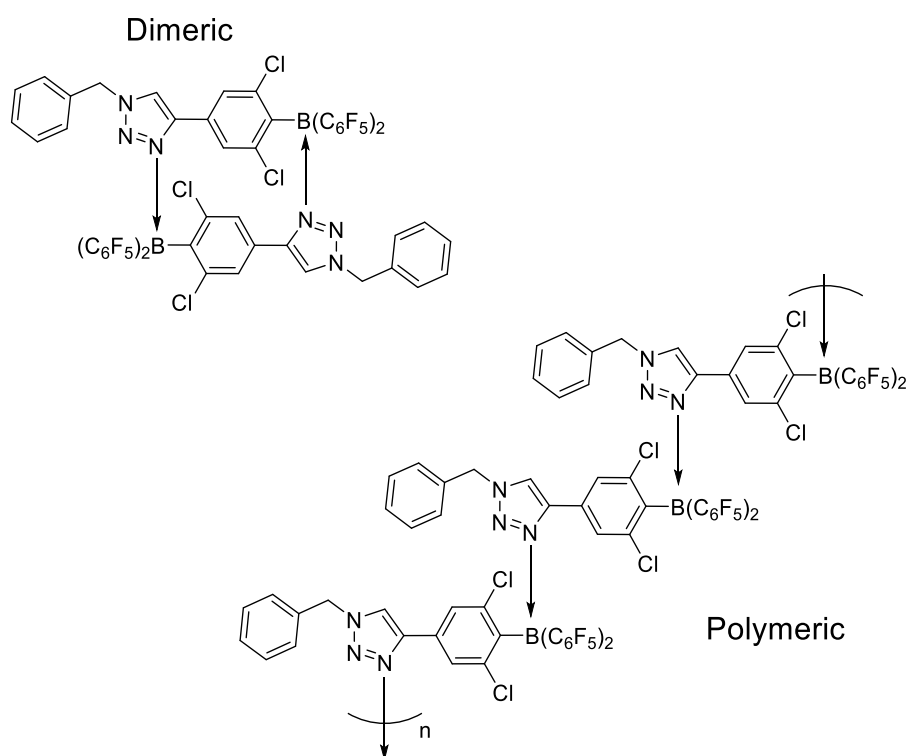


Figure 56. Two plausible modes of intermolecular adduct formation between our novel intramolecular Lewis pair subunits **76**.

Figure 57 shows the VT ^1H and ^{11}B NMR spectroscopic analysis of a 1:1 mixture of **16b** with **95** in deuterated toluene. At room temperature, the ^{11}B NMR spectrum shows a single resonance at -3.58 ppm, consistent with the tetra-coordinate B-N adduct. The observed resonance does not shift with decreased temperatures, although the peak becomes broader. As the temperature increases, in the ^{11}B NMR spectra becomes sharper until approximately 65 °C. After this point, the resonance begins to broaden significantly, indicating fast exchange between the bound and unbound species.

More information can be observed in the ^1H NMR spectra, where the resonances derived from benzylic protons H_b and triazole proton H_c are observed shifting downfield towards the resonance for the unbound triazole species **95** (Figure 57). Both H_b and H_c resonances become broader with increased temperature and converge at an average chemical shift between the bound (**92**, $\text{H}_b = 4.59, 4.31$ ppm and $\text{H}_c = 6.12$ ppm, at 298 K) and unbound (**95**, $\text{H}_b = 4.90$ ppm and $\text{H}_c = 6.95$ ppm) species.

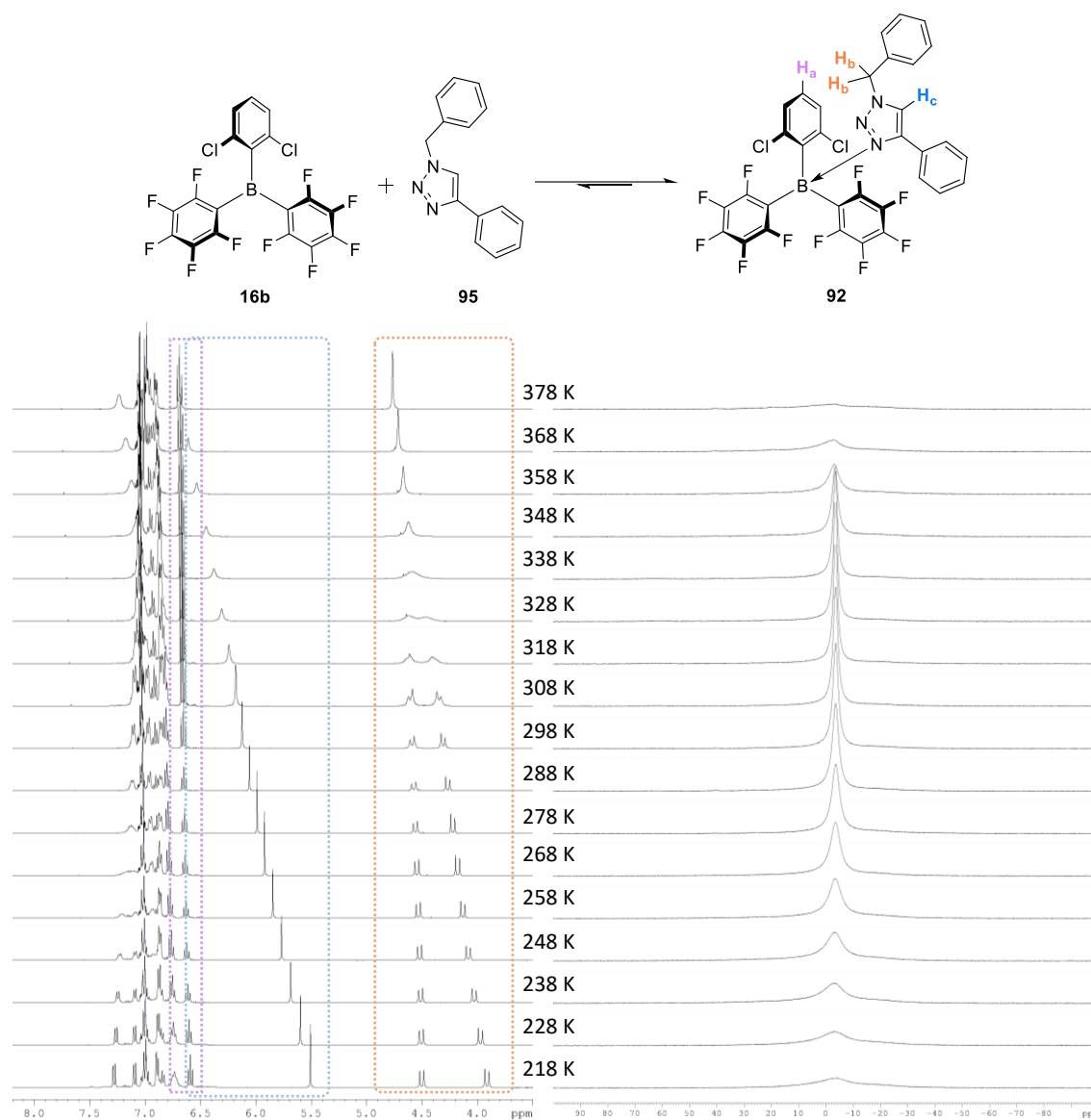
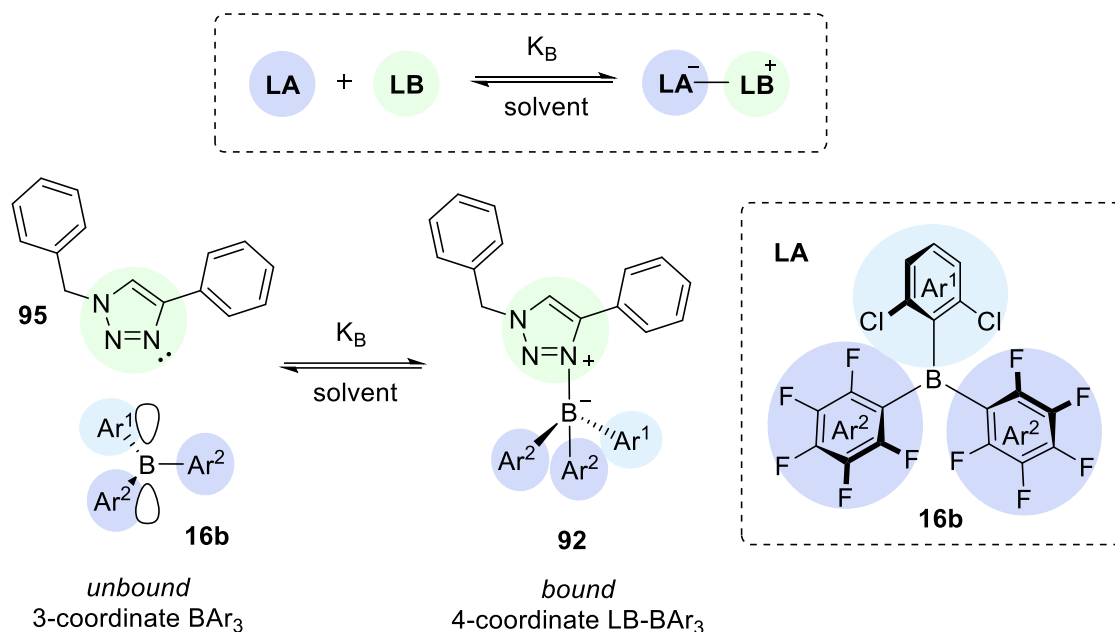


Figure 57. VT ^1H (Left) and ^{11}B (Right) NMR spectra for equimolar **16b/95** in toluene- d_8 .

In traditional thermally frustrated classified FLPs, we would expect the equilibrium to shift with temperature on the NMR timescale (Scheme 74). Typically, as temperature increases in VT NMR experiments, the equilibrium shifts towards the uncoordinated borane, resulting in a downfield shift in the ^{11}B NMR spectroscopic resonance (unbound

Ar_3B , 70 – 50 ppm).²⁹⁹ However, in this VT ^{11}B NMR spectra, this shift is not observable, indicating a high degree of binding character and fast exchange between the 3- and 4-coordinate species.



Scheme 74. Equilibrium for Lewis adduct formation by the reaction of an unsymmetrical heteroleptic borane **16b** with a triazole **LB 95**.³⁰⁸

In the process of transitioning from unbound to bound, the borane centre changes from being 3-coordinate to 4-coordinate (Scheme 74). This change in coordination is accompanied by a shift in geometry from trigonal planar (unbound) to tetrahedral (fully bound). This transition towards a tetrahedral geometry is also known as pyramidalisation. The strength of binding directly affects the degree of pyramidalisation experienced by the borane centre (Figure 58). Therefore, at high temperature, if the equilibrium shifts towards the uncoordinated borane, the degree of pyramidalisation decreases and vice versa.^{309–312}

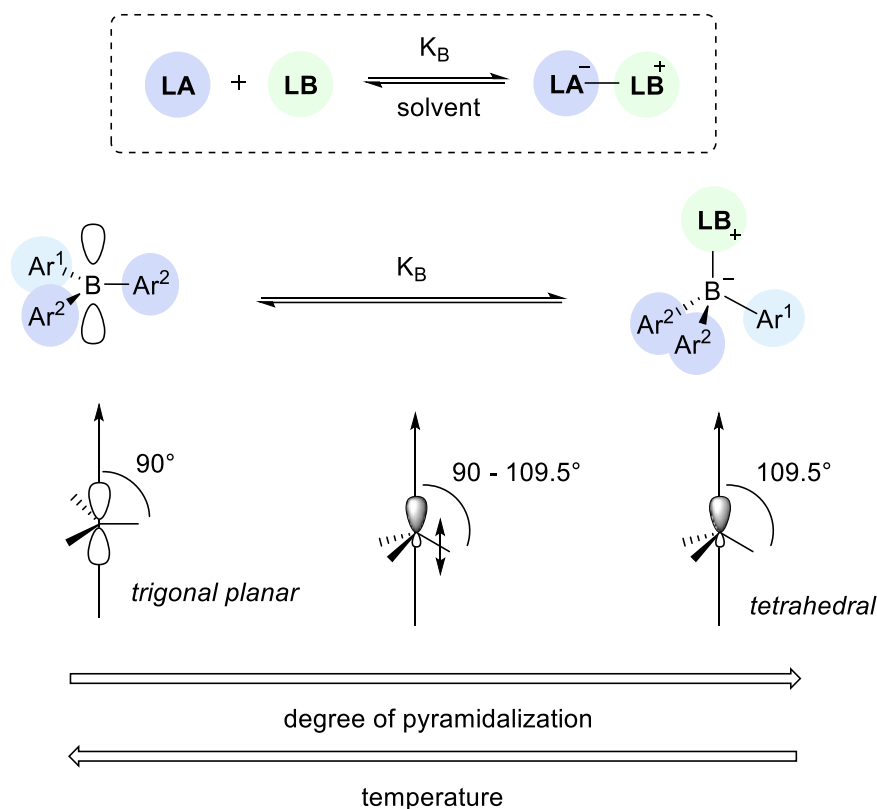


Figure 58. Impact of the binding equilibrium constant (K_B), between a triaryl borane (LA) and LB, on the degree of pyramidalisation in relation to temperature increase and decrease.^{309–312}

Due to pyramidalisation, it is very difficult to characterise the inter and intramolecular analogues obtained (**92** and **95**). Because the B-N adducts have a strong binding (high K_B) at room temperature, we can assume that they are both fully bound and therefore have a pyramidal (tetrahedral) geometry. This causes the unsymmetrical and sterically hindered aryl rings to be close together, creating non-equivalent chemical environments in the ^1H and ^{19}F NMR spectra (Figure 57 and Figure 59). Additionally, the unsymmetrical steric bulk introduced by our LB (**95**) compounds this effect.

Another observation caused by the degree of pyramidalisation in labile adducts can be seen in the ^{19}F NMR spectra (Figure 59). As temperature increases, in the VT ^{19}F NMR spectra we do not see a shift in for the para fluorine atom. In the ^{19}F NMR spectra the separation between the meta and para ^{19}F signals ($\Delta\delta$ meta, para ($\Delta\delta$ m,p)), which is large for 3-coordinate boron compounds, progressively decreases when going towards the 4-coordinate boron adducts due to the upfield shift of the para resonances, this results from the shielding caused by the increased electron density on the boron atom (Scheme 74 and Figure 58). For typical perfluorinated triaryl borane $\Delta\delta$ m,p \approx 20 ppm, whereas 4-

coordinate adducts show much lower $\Delta\delta_{m,p}$ (approx. 6 – 8 ppm).³¹³ At room temperature the $\Delta\delta_{m,p} = 7.55$ ppm and even at high temperatures (~ 105 °C), $\Delta\delta_{m,p}$ remains relatively the same (~ 6.90 ppm), which is indicative of a high degree of coordination between the LA **16b** and the triazole LB **95**. Similar to the VT ^1H and ^{11}B NMR spectra (Figure 57), the fluorine resonances broaden significantly with increased temperature.

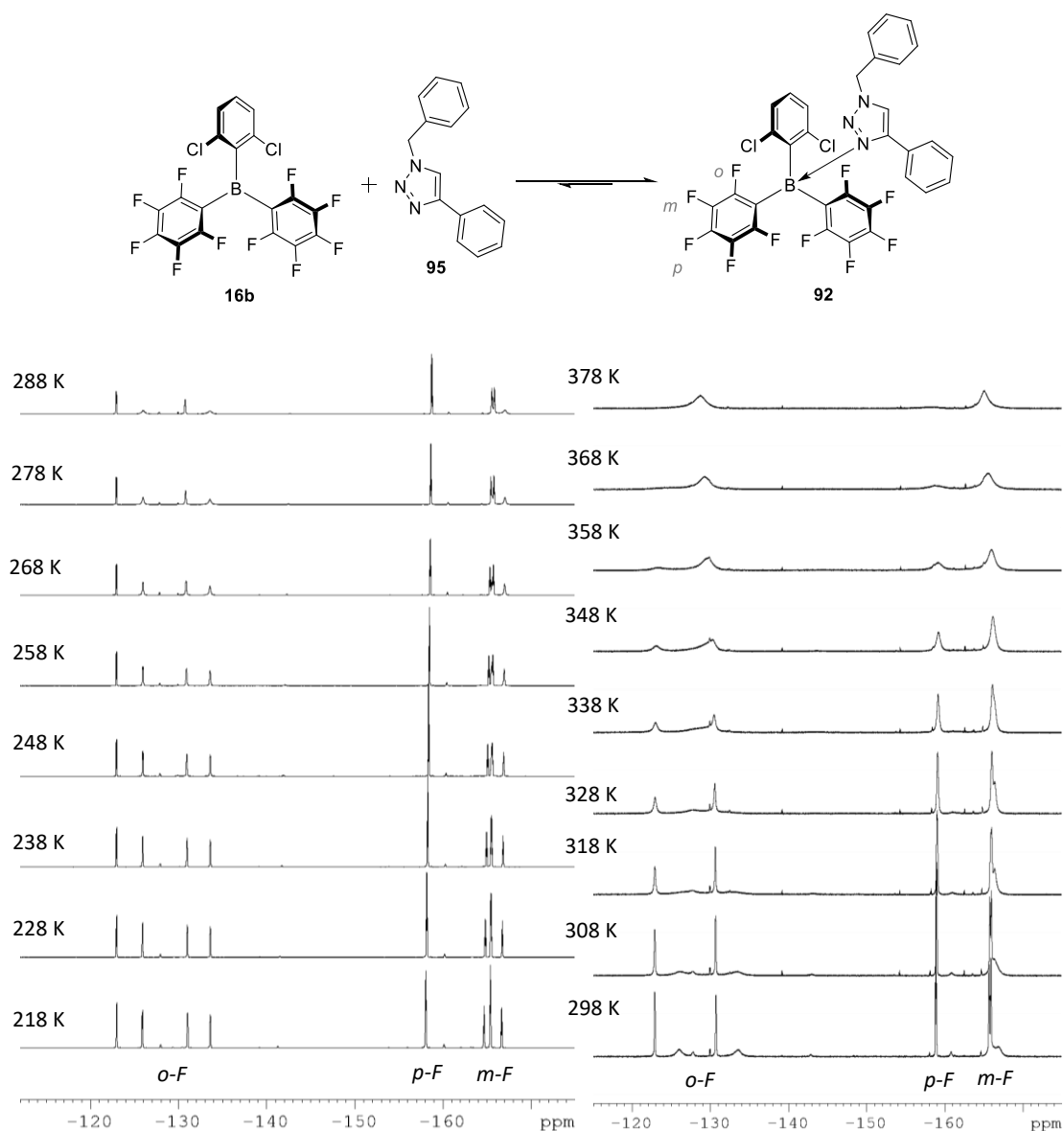


Figure 59. VT ^{19}F NMR spectra for equimolar **16b/95** in toluene- d_8 .

After analysing the VT NMR data, we found that our novel moisture tolerant system may not act as a thermally frustrated Lewis pair. Instead, like Stephan and co-workers' publications from 2018³¹⁴ and 2021³¹⁵ it is possible that we have formed a labile coordinated adduct, which could potentially engage in FLP chemistry from a

spectroscopically stable Lewis adduct. Our NMR spectroscopic data only supports the formation of a spectroscopically stable Lewis adduct. To determine whether our novel catalyst adducts **92** and **94** are capable of accessing FLP chemistry we set out to explore their reactivity with silanes and hydrogen.

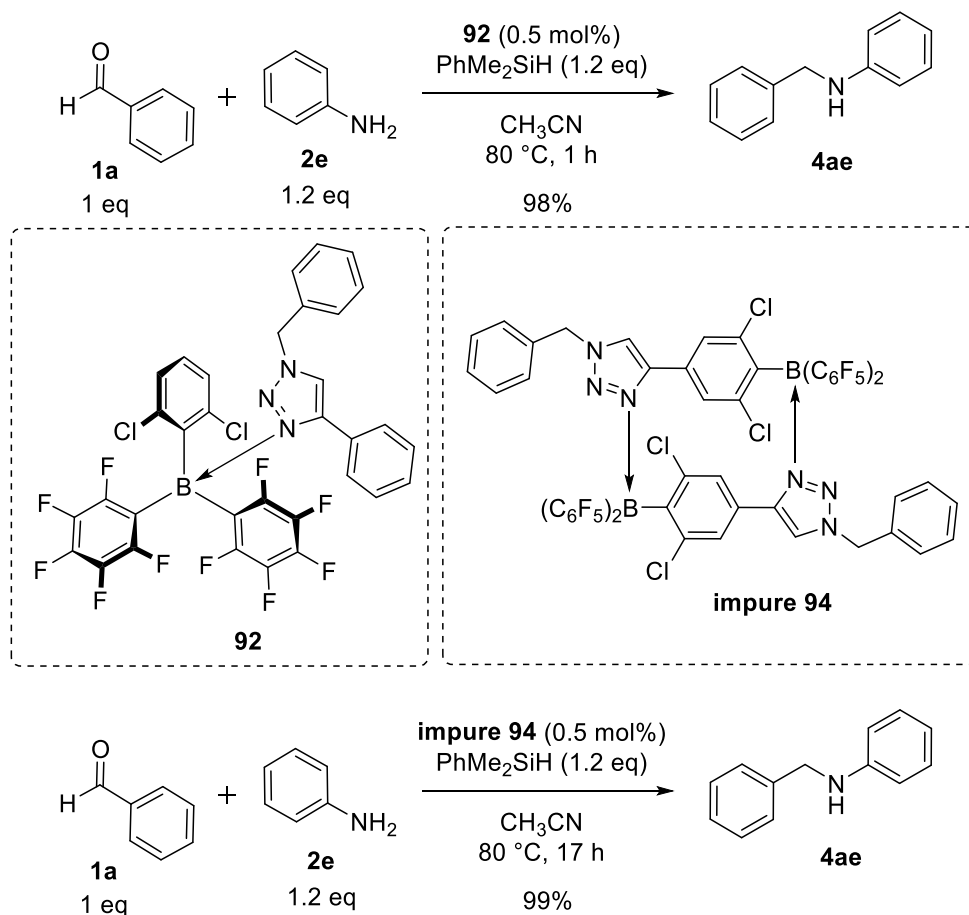
5.2.3 Preliminary FLP Reactivity of Novel Inter- /Intramolecular Adducts **92** and **94**

5.2.3.1 FLP Reactivity Using Silanes

Whilst our novel catalyst adducts **92** and **94** are stable classical Lewis adducts on the NMR timescale, we wanted to explore their ability to perform FLP chemistry. If the B-N coordination is labile then under reaction conditions the boranes empty p-orbital and triazoles lone pair would be available for FLP catalysis. If successful reactions occur, then our B-N adducts are proven to be labile not necessarily that the triazole unit is acting as the LB in the FLP system.

Our initial reactions explored the activation of silanes rather than hydrogen. Silanes were chosen as they are excellent hydride donors which are well established to perform reductive aminations with FLP systems (section 3.2.1).^{115,197,212} Due to such small amounts of material in the case of intramolecular **94**, we chose silanes as the easier starting point from which to test the lability of our adducts. As we had not observed this in the VT NMR spectra, we decided the best chance of successful FLP reactivity was to start with silanes before progressing to hydrogen.

We were extremely gratified to find that following conditions previously optimised for catalyst **16b**, (see section 3.2.1), both the intermolecular and intramolecular analogues **92** and **94** achieved excellent yields (98 and 99% respectively) with full conversion (Scheme 75). The intermolecular analogue **92** was able to achieve 95% yield in 30 minutes with 0.5 mol% catalyst loading and had achieved full conversion of benzaldehyde and 98% yield product within an hour.



Scheme 75. Preliminary FLP reactivity of novel labile B-N coordinated adducts **92** and

94.^{115,197,212}

Due to the complexity of the ^{19}F NMR spectrum in the intramolecular analogue **94** we could not be confident in the assignments and therefore, the quantity of the $\text{Ar}_2\text{B-OH}$. After our first pass synthesis of the intramolecular analogue monomer **76**, we only had enough compound for one reaction without repeating the synthetic route. We decided to weigh out the 0.5 mol% catalyst loading as if the catalyst was 100% pure and as a result, we were not surprised to find that the reductive amination proceeded more slowly than the intermolecular analogue. The yield reached only 50% after 2 hours and eventually 99% yield once left overnight. In this vein, it is also plausible that binding could be stronger in oligomers/dimers than the intermolecular analogue, and therefore, this could also be partially responsible for the slower reaction time.

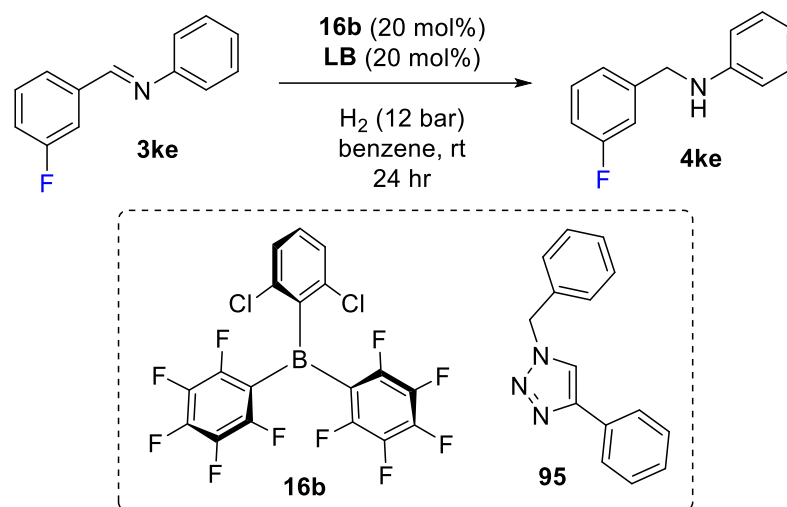
5.2.3.2 Reactivity Using Hydrogen

After the unsuccessful attempt to synthesise the novel intramolecular FLP-borane **76** for the second time, we decided to use the intermolecular adduct **92** to investigate the reactivity of the FLP-borane/triazole adduct with hydrogen. For the optimised batch reductive amination system, we had used THF as a solvent as discussed in section 3.2.3. Since THF competes as a Lewis base, we decided to test the ability of **92** to catalyse an imine hydrogenation in benzene, following the optimised system of Soós and co-workers (Table 20).⁶⁰

The Soós system has been optimised to use the sterically hindered bicyclic amine DABCO as the LB under relatively mild conditions (room temperature and 12 bar hydrogen pressure) for FLP hydrogenations. When reducing imine **3ke**, we observed a 99% yield under the optimised conditions using 20 mol% catalyst and DABCO (Table 20, Entry 3). We compared four LBs (imine starting material/amine product, lutidine, and pyridine) as well as our triazole **95** (Table 20, Entries 2 and 4 – 6).

We were not surprised to observe product **4ke** in 49% yield using no external LB (Entry 2), aware that imines starting materials can act as LBs in FLP-borane hydrogenation systems. We also noticed that as the steric hindrance of the LB decreased, so did the yield (99%, 74% and 47% yield for DABCO, lutidine and pyridine respectively). When using the triazole **95** (20 mol%) (thus forming intermolecular adduct **92 in situ**), we were gratified to achieve 91% yield, thus confirming that our novel FLP-borane system can access FLP chemistry with hydrogen despite the VT NMR spectra indicating full binding of the adduct.

Table 20. Preliminary FLP reactivity using novel labile intermolecular B-N adduct **92** for the catalytic reduction of imines using hydrogen.⁶⁰



Entry	BAR ₃	LB	Rxn time (hrs)	Yield* (%)
1**	none	none	24	0
2	16b	none	24	49
3	16b	DABCO	24	99
4	16b	Lutidine	24	74
5	16b	Pyridine	24	47
6	16b	95	24	91

*determined by ¹⁹F NMR spectroscopy. **blind/control reaction with no borane or LB.

5.5 Outlook and Conclusions

In summary, two new FLP systems have been identified. One is an intermolecular version that uses the moisture-tolerant FLP borane **16b** and triazole **95** and the other is a more complex intramolecular FLP system **94**, which has been synthesised once but never isolated in a pure form.

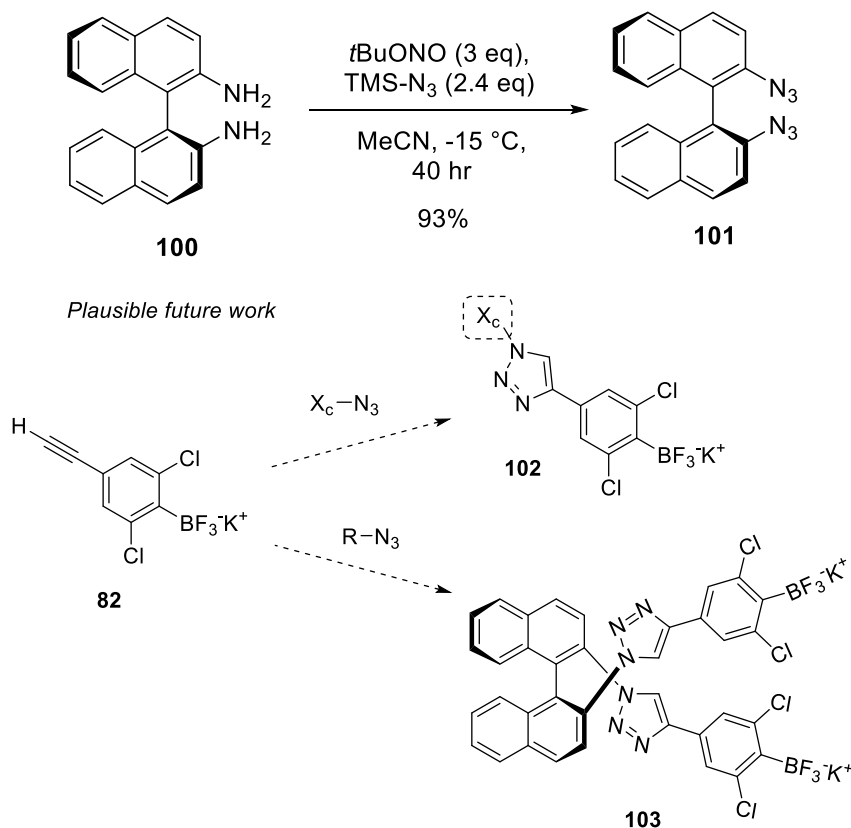
Due to the complexity of NMR spectroscopic analysis of the impure intramolecular FLP **94**, the novel intermolecular analogous FLP system **94** was created. This adduct was studied extensively by VT NMR spectroscopy, and the spectral similarities observed for

both intra- and intermolecular systems gave further evidence of the identity of the intramolecular borane **92**.

Through preliminary FLP reactivity testing both the intramolecular analogue **94** and intermolecular adduct **92** have been proven to possess FLP reactivity. Whilst the B-N adducts (**92** and **94**) were not labile spectroscopically both adducts were capable of catalysing reductive amination of benzaldehyde **1a** with aryl amine aniline **2e** using silanes, achieving 98% and 99% yield respectively, albeit the impure intramolecular catalyst **94** being significantly slower.

The intermolecular adduct **92** was also found to be an effective catalyst for imine reduction using hydrogen, achieving a 91% yield, comparable to the sterically hindered LB DABCO and significantly higher than yields obtained with the other LBs screened. This further broadens the potential scope of LBs capable of FLP type reactivity when paired with triaryl boranes, where the Lewis adduct equilibrium has not yet been observed.^{314,315} It serves as a good example of the importance of experimentally testing the reactivity of catalyst systems, regardless of spectroscopic evidence.

A synthetic pathway to produce other variations of intramolecular FLP system **94** has been partially optimised, with the potential to be adapted for the creation of a solid-supported FLP borane. The alkyne intermediate **82** has great potential to attach FLP borane groups to solid supports, creating heterogeneous boranes in the future. It could also be linked to various chiral scaffolds, or auxiliaries (X_c). For example, the use of alkyne **82** was envisaged for attachment to the (S)-BINAP diazide **101**,³¹⁶ in this project, but this was abandoned due to time constraints (Scheme 76). This approach could potentially impart the BINAP's chirality to both LA and LB, an approach said represent the future of asymmetric FLP catalysts.¹⁴⁹



*Scheme 76. Above. Synthesis of (S)-BINAP diazide **101** via Sandmeyer reaction with potential application as a chiral scaffold to impart chirality on the LA and LB involved.³¹⁶ Below. Plausible scope for CuAAC click reaction with key alkyne intermediate **82** to append to chiral scaffolds or auxiliaries.*

We believe it is important to compare inter- and intramolecular analogues of designed catalysts. This is a significant gap in the FLP field, as superior inter- versus intramolecular reactivity is often assumed or theoretically explored. Whilst the intramolecular FLP **94** (only 50% yield after 2 hour), relatively slower conversion can be attributed to its purity, we observed significantly faster reaction times using the intermolecular analogue **92** (98% yield after 1 hour). This is an area that should be further explored in future work for this project.

Finally, whilst we did not have access to sublimation equipment during this project, it should be noted that for any future work on the project, sublimation of crude materials might alleviate some of the purification issues observed and could be used for the purification of novel FLP-boranes.

Chapter Six: Conclusions

In this thesis three moisture tolerant FLP boranes have been synthesised and two of these (**16a/b**) were shown to perform as excellent catalysts for reductive aminations using silanes as well as hydrogen. Continuous flow chemistry has also been explored, as an alternative to classical batch hydrogenation conditions, for FLP-borane catalysed reductive aminations with limited success.

In chapter two, the synthesis of known moisture tolerant FLP-boranes was described. The purification of these boranes proved to be challenging and as a result, improvements were made to our own synthetic procedure to produce three pure moisture tolerant FLP-boranes on useful scale (10 mmol). In chapter three, the FLP-borane, $B(2,6\text{-Cl}_2\text{C}_6\text{F}_3)(\text{C}_6\text{F}_5)_2$ (**16b**) was found to be an effective catalyst for intermolecular reductive aminations using silanes. Conditions were found to perform reductive aminations using aryl and alkyl amines with aldehydes and ketones using **16b**. This led to the development of a novel intramolecular reductive amination of functionalised aminoketones for the synthesis of α -substituted pyrrolidines. Unfortunately, subsequent attempts to perform the reductive amination cyclisation using hydrogen were unsuccessful.

In chapter four, the use of continuous flow chemistry was employed as an alternative to the to classical batch hydrogenation conditions, for FLP-borane catalysed reductive aminations. The initial aim for this chapter was to develop a proof-of-concept reductive amination system using FLP-boranes as catalysts. Despite promising early results, it was ultimately discovered that metal leaching, due to previous work with the flow equipment, lead to inflated and nonreproducible results. It is noteworthy that results obtained after having identified the metal leaching issue (although not without their own issues) have shown higher catalytic activity when using FLP than without catalyst and as a result, provide a proof-of-concept for the reductive amination using hydrogen in flow. To the best of our knowledge this is the first example of such a reaction performed in flow using hydrogen.

Finally, in chapter five, a novel FLP system was discovered. This novel intramolecular FLP bears a borane and triazole functional group and was obtained via a route which initially aimed to be used for the synthesis of solid supported boranes. The synthesis of the

analogous intermolecular system **92** (triazole and borane moieties on separate molecules), the preliminary reactivity for both the inter- and intramolecular FLP system was explored. Gratifyingly despite appearing to be spectroscopically stable Lewis adducts, both inter- and intramolecular FLP systems were found to be excellent catalysts for simple reductive aminations using silanes. Moreover, the intermolecular analogue was found to be an effective catalyst for imine reductions in batch using hydrogen.

Despite clear progression there are avenues which could be explored for future developments on the foundations described in this thesis. Future work on FLP catalysed reductive aminations performed in continuous flow has clear potential for future improvement. If this work was to be repeated, new equipment should be used which has not been previously contaminated with metals. This equipment must be robust to THF, as whilst EtOAc appears to be an effective solvent for silanes, we have found that THF is a far superior solvent when using hydrogen.

Likewise, there is enormous potential for the further development of the intramolecular reductive amination cyclisation system. Future work should look to expand the substrate scope, including increasing/decreasing the ring size (4, 6, and 7-membered) and alternative ketone functionalisation such as (hetero)aryl and alkyl groups. Crucially, the system has enormous potential for asymmetric performance, future development of this system should focus upon adaptation of currently established asymmetric imine reductions using silanes to produce α -substituted cyclic amines in an enantioselective manner.

In conclusion, whilst a lot of avenues of FLP-catalysis have been explored, only limited success has been achieved with each of these avenues (chapters three, four and five). In hindsight, and from an outside perspective, it is clear that focusing on fewer of these avenues could have allowed for further progress in each of these areas. However, the somewhat broad structure of the work presented in this thesis was largely directed by the funding of this project.

For context, due to the style of funding I received from GISMO, we had no access to funds for consumables until working with Autichem Ltd. As a result, at the start of my PhD, 6-months was spent progressing a palladium catalysed hydroarylation system I had

worked on during my Masters by Research, as the necessary chemicals were available. Work on this project has continued in the group and has recently led to the preparation of a manuscript for publication. The work performed on the hydro arylation system has been discussed in appendix A. Once working with Autichem, significant focus was placed on the continuous flow project (chapter four and five), which transitioned us away from the preliminary work we were performing with silanes at the time.

Additionally, some of the broadness of this thesis has resulted from availability of equipment. Although the Parr reactor was available at the start of the project, we were only able use it from approximately halfway through my PhD because there was no clear policy for using hydrogen in the department. The approval of safety paperwork and requirement for external training delayed our access to this part of the project significantly. As a result, my FLP-borane catalysed reductive aminations were initially optimised and explored using silanes to gain experience with the chemistry.

Due to the equipment access, work was also carried out on a nickel-catalysed allylation system, which had been developed in the group. The research turned out to not be as trivial as first anticipated and as a result, the system required re-optimisation, substrate scope reproduction/expansion, a robustness screening, as well as exploration of the potential for enantioselective allylation. This work was carried out alongside my FLP research and has led to recent publication and the submitted manuscript has been included in appendix B.

To summarise this thesis has successfully explored the use of moisture tolerant FLP boranes to perform novel reductive aminations in batch using silanes as well as hydrogen. Whilst it is ultimately complex to draw many conclusions this thesis has also laid the foundations for the performance of FLP catalysed reductive amination in continuous flow using hydrogen.

Chapter Seven: Experimental Details and Characterising Data

7.1 General Methods

Sensitive and hygroscopic products were stored/handled in a MBraun UNIlab pro glovebox. Reagents were purchased from Sigma-Aldrich, Alfa Aesar, Fisher Scientific, Fluorochem, and Tokyo Chemical Industry UK, and were not purified further unless stated. Solvents were purchased anhydrous and stored over molecular sieves or dried over activated 3Å or 4Å MS in oven-dried J-Youngs tap round-bottom flasks (RBFs) for at least three days prior to use. Molecular sieves were activated by heating at 300 °C in a Carbolite ELF11/6B furnace for 24 hours following an adapted procedure by Lawton *et al.*³¹⁷ Thin layer chromatography was performed on aluminium sheets coated with Merck silica gel 60 F254 with visualisation using potassium permanganate solution, phosphomolybdic acid, and/or scrutinised under 254 nm UV light. Column chromatography was performed using Silica 60 (40-63 microns) supplied by Sigma-Aldrich or Fluorochem unless otherwise stated. H₂ was purchased from BOC (Hydrogen N4.5 (99.995% purity, Zero Grade H₂)).

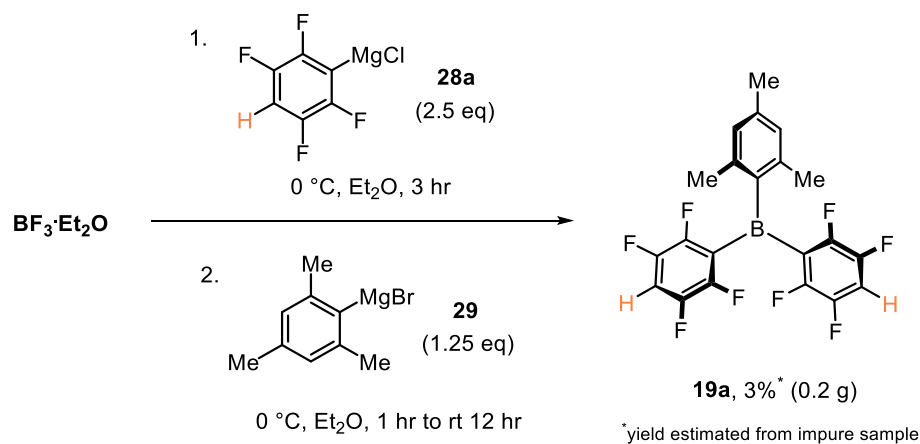
Nuclear magnetic resonance (NMR) spectroscopy was performed on a Bruker Avance 400 NMR spectrometer (¹H NMR at 400 MHz, ¹³C NMR at 100 MHz, ¹¹B at 128 MHz, ¹⁹F at 376 MHz) with the appropriate deuterated solvent, or in protonated solvents using solvent suppression experiments. Chemical shifts in ¹H, ¹³C, ¹¹B, and ¹⁹F NMR spectra are reported in parts per million (ppm, δ) relative to the deuterated solvent peak and reported as singlet (s), broad singlet (brs), doublet (d), triplet (t), quartet (q) and combinations thereof, or multiplet (m). Coupling constants (J) are quoted in Hz and are averaged between coupling partners and rounded to the nearest 0.1 Hz. Mass spectrometry (MS) was performed using a Shimadzu LCMS-IT-TOF instrument with electrospray ionisation in the positive mode. FT-IR data was acquired using Agilent Technologies Cary 630 FTIR instrument with wavenumbers being reported in cm⁻¹. Melting points were determined using a Gallenkamp melting point apparatus with in with a mercury thermometer.

All steps for the synthesis and purification of triaryl boranes (**16a/b**, **19a/b** and **76**) were performed using a Schlenk line. This includes evaporation of solvents, which were performed using a Oerlikon Leybold Trivac D4B vacuum pump as well as two external solvent traps submerged in liquid nitrogen (one between the reaction mixture glassware and the Schlenk line, and the primary trap between the Schlenk line and the vacuum pump) following a procedure reported by Borys.²⁰⁴ Batch reactions using hydrogen were performed using a Parr 4700 pressure vessel (45 mL volume) fitted with a rupture disc (maximum pressure 117 bar). The vessel was sealed by seating the Parr 4700 base in an A22AC3 bench socket and tightening the cap firmly with a 21AC4 box wrench. Once sealed the hydrogen cylinder was connected, and the Parr reactor was filled to the desired pressure (Figure 60). Reaction performed in continuous flow were carried out using a H-Cube[®] Mini Plus. All lab prepared and purchased Grignards were titrated before use in an oven-dried 10 mL crimp cap vial under an inert atmosphere of nitrogen using I₂ (accurately weighed (~80 mg)) dissolved in anhydrous THF (1 mL). The resulting dark red brown was vigorously stirred at room temperature and the respective Grignard reagent was added dropwise until the solution turns light yellow and then becomes colourless.



Figure 60. Parr 4700 pressure vessel setup.

7.2 Experimental Details for Chapter Two

7.2.1 Synthetic Route 1: FLP-borane Synthesis by Sequential Grignard Addition to $\text{BF}_3 \cdot \text{OEt}_2$ 

This procedure was adapted from a procedure reported by Soós *et al.*¹⁹⁸

In oven-dried glassware and under an inert atmosphere of nitrogen, an Et_2O solution of $\text{C}_6\text{F}_4\text{HMgCl}$ **28a** (2.5 eq), prepared according to the general procedure in section 7.2.2.3, was added dropwise to $\text{BF}_3 \cdot \text{OEt}_2$ (0.44 mL, 17.5 mmol, 1 eq) in anhydrous Et_2O (8 mL) at 0 °C. The reaction mixture was stirred at 0 °C for 3 hours then an Et_2O solution of $\text{C}_6\text{H}_2\text{Me}_3\text{MgBr}$ **29**, prepared according to the general procedure in section 7.2.2.3, was added dropwise to the reaction mixture at 0 °C. The reaction mixture was stirred at 0 °C for one hour, allowed to warm up gradually to room temperature, and stirred overnight. The next day, solvents were evaporated. The resulting brown solid was mixed with hexane (20 mL) warmed up and stirred vigorously. Hot decantation gave yellow solution that was filtered and transferred to an oven dried Schlenk flask. This process was repeated with hexane (2 x 20 mL). A white solid started to precipitate out from the combined hexane decantation's upon cooling. Concentration of the filtrate (to approx. to 10% of the volume) afforded further precipitation, the solids were cannula filtered off and washed with hexane. Drying under high vacuum produced crude **19a** (200 mg, 0.43 mmol, 3%, 92% purity) as a white solid.

This data matches data reported in literature.¹⁹⁸

^1H NMR (CH_2Cl_2 , 400 MHz) δ_{H} 6.65 (m, 2H), 6.34–6.26 (m, 2H), 2.12 (s, 3H), 2.09 (s, 6H).

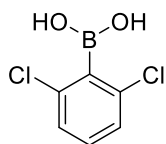
^{19}F NMR (CH_2Cl_2 , 376 MHz) δ_{F} –130.8 (m, 4F), –138.6 (m, 4F).

^{11}B NMR (CH_2Cl_2 , 128 MHz) δ_{B} 70.6 (brs).

7.2.2 Synthetic Route 2: FLP-borane Synthesis via Potassium Aryltrifluoroborate Salts (ArBF₃K)

7.2.2.1 Boronic Acid Synthesis

2,6-Dichlorophenyl boronic acid (**36**)⁶⁰



This procedure was adapted from a procedure reported by Soós *et al.*¹⁹⁰

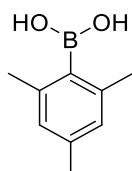
In oven-dried glassware and under an inert atmosphere of nitrogen, at $-78\text{ }^{\circ}\text{C}$, 2,6-dichlorobenzene (5.71 mL, 50.0 mmol, 1 eq) was added to a solution of ⁿBuLi (22 mL in hexanes, 2.5 M, 55.0 mmol, 1.1 eq) in anhydrous THF (70 mL). After a few minutes the 2-lithio-1,3-dichlorobenzene precipitated as a white solid from the solution. After 2 hours stirring at this temperature, trimethyl borate (12 mL, 108 mmol, 2.2 eq) was added to the mixture slowly. The mixture was slowly allowed to warm to room temperature and stirred overnight. The next day, aqueous HCl (1M, 70 mL) was added to the slurry at $0\text{ }^{\circ}\text{C}$ and the mixture was stirred at rt for two hours. Then the organic layer was separated, and the aqueous layer was extracted with Et₂O (3 x 50 mL). The combined organic layers were washed with brine (150 mL), dried over anhydrous MgSO₄, filtered off and evaporated to dryness. The resulting solid was triturated with hexane and dried. The product was obtained as a white solid (7.5 g, 39 mmol, 79%).

This data matches data reported in literature.⁶⁰

¹H NMR (DMSO-d₆, 400 MHz) δ_{H} 8.58 (s, 2H), 7.36-7.30 (m, 3H).

¹¹B-NMR (DMSO-d₆, 128 MHz) δ_{B} 27.7 (brs).

2,4,6-Trimethylphenyl boronic acid (**39**)⁶⁰



This procedure was adapted from a procedure reported by Soós *et al.*¹⁹⁰

In oven-dried glassware and under an inert atmosphere of nitrogen, a solution of mesityl bromide (7.65 mL, 50 mmol, 1 eq) and THF (25 mL) was added dropwise to activated

magnesium turnings (1.50 g, 60 mmol, 1.2 eq) in anhydrous THF (50 mL) and the reaction mixture was then stirred at reflux for 3 hours. After three hours the reaction mixture was cooled to $-78\text{ }^{\circ}\text{C}$, trimethyl borate (11.15 mL, 100 mmol, 2 eq) was added slowly, and then the reaction mixture was allowed to warm up to room temperature and stirred overnight. The next day, aqueous HCl (1M, 70 mL) was added to the slurry at $0\text{ }^{\circ}\text{C}$ and the mixture was stirred at rt for two hours. Then the organic layer was separated, and the aqueous layer was extracted with Et_2O (3 x 50 mL). The combined organic layers were washed with brine (150 mL), dried over anhydrous MgSO_4 , filtered off and evaporated to dryness. The resulting solid was triturated with hexane and dried. The product was obtained as a white solid (5.7 g, 34.8 mmol, 70%).

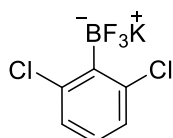
This data matches data reported in literature.⁶⁰

^1H NMR (DMSO- d_6 , 400 MHz) δ_{H} 8.03 (s, 2H), 6.74 (s, 1H), 6.73 (s, 1H), 2.23 (s, 6H), 2.20 (s, 3H).

^{11}B -NMR (DMSO- d_6 , 128 MHz) δ_{B} 30.6 (brs).

7.2.2.2 Potassium Aryltrifluoroborate Salt Synthesis

Potassium 2,6-dichlorophenyl trifluoroborate (**37**)^{60,190}



This procedure was adapted from a procedure reported by Soós *et al.*¹⁹⁰

KHF_2 (12.3 g, 157 mmol, 4 eq) was dissolved in DI water (40 mL). To the resulting solution was added, a solution of boric acid **36** (7.5 g, 39 mmol, 1 eq) in methanol (55 mL). The resulting suspension was stirred overnight. The next day, acetone (100 mL) was added to the suspension, decanted from the solid residue and evaporated to dryness. The resulting crude white solid was dried under vacuum. The crude white solid was dissolved in acetone (80 mL), solid residues were filtered off and the solute was evaporated to dryness. The resulting solid was then triturated with hexane (3 x 50 mL) and dried in a vacuum desiccator over phosphorus(V)-oxide for 3 days affording the product as a white solid (8.71 g, 34.4 mmol, 87%).

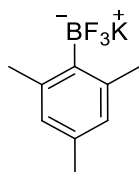
This data matches data reported in literature.⁶⁰

¹H NMR (DMSO-d₆, 400 MHz) δ_{H} 7.10 (d, J 7.8 Hz, 2H), 7.00 (dd, J 8.6 Hz, J 7.0 Hz, 1H).

¹⁹F NMR (DMSO-d₆, 376 MHz) δ_{F} -132.1 (dd, J 92.8 Hz, J 43.4 Hz, 3F).

¹¹B-NMR (DMSO-d₆, 128 MHz) δ_{B} 1.98 (m, J 47 Hz).

Potassium 2,4,6-trimethylphenyl trifluoroborate (**40**)¹⁹³



This procedure was adapted from a procedure reported by Soós *et al.*¹⁹⁰

KHF₂ (10.9 g, 139 mmol, 4 eq) was dissolved in DI water (40 mL). To the resulting solution was added, a solution of boronic acid **39** (7.5 g, 35 mmol, 1 eq) in methanol (50 mL). The resulting suspension was stirred overnight. The next day, acetone (100 mL) was added to the suspension, decanted from the solid residue and evaporated to dryness. The resulting crude white solid was dried under vacuum. The crude white solid was dissolved in acetone (80 mL), solid residues were filtered off and the solute was evaporated to dryness. The resulting solid was then triturated with hexane (3 x 50 mL) and dried in a vacuum desiccator over phosphorus(V)-oxide for 3 days affording the product as a white solid (6.25 g, 27.6 mmol, 80%).

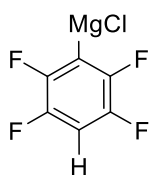
This data matches data reported in literature.¹⁹³

¹H NMR (DMSO-d₆, 400 MHz) δ_{H} 6.50 (s, 2H), 2.27 (s, 3H), 2.27 (s, 3H), 2.11 (s, 3H).

¹¹B-NMR (DMSO-d₆, 128 MHz) δ_{B} 3.73 (m, J 41 Hz).

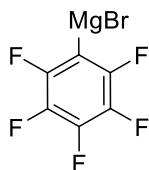
7.2.2.3 Preparation of Grignard Reagents

2,3,5,6-tetrafluorophenyl magnesium bromide (**28a**)



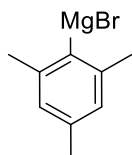
In oven-dried reflux apparatus and under inert atmosphere of nitrogen, $(C_6F_4H)MgCl$ **28a** was prepared from slow addition of *i*PrMgCl (2.5 eq, 2 M in Et₂O) to a solution of 2,3,5,6-tetrafluorophenylbromobenzene (2.5 eq) at 0 °C in Et₂O (1 M). The cloudy solution was then stirred for 2 hours at ambient temperature. The solution was titrated according to the general methods before use.

Perfluoro phenyl magnesium chloride (**28b**)



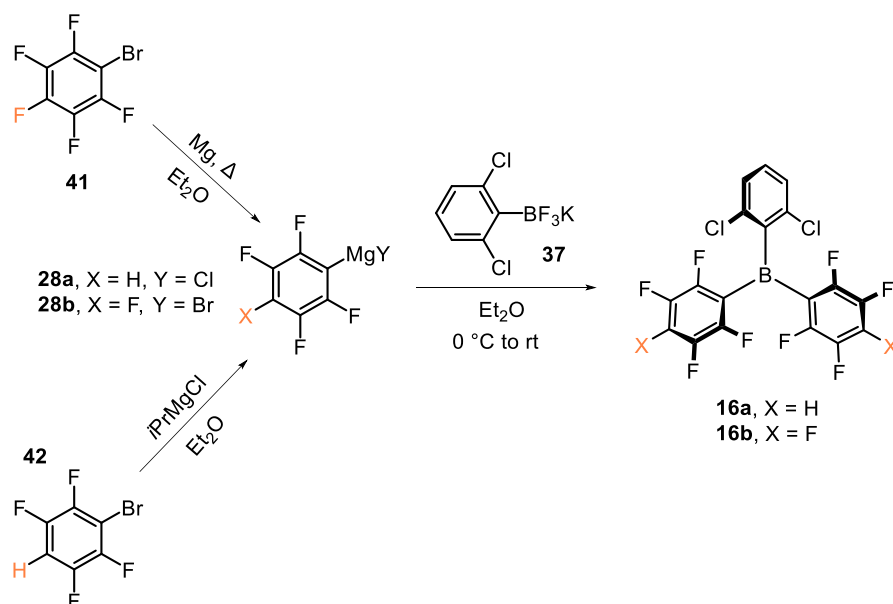
In oven-dried reflux apparatus and under inert atmosphere of nitrogen, $(C_6F_5)MgBr$ **28b** was prepared from the dropwise addition of a solution of perfluorobromobenzene (2.5 eq) in Et₂O (1M) to a suspension of activated magnesium turnings (3 eq) in Et₂O (2 M). After addition of the aryl bromide, the mixture was refluxed for 2 hours. The solution was then cooled to room and the solution was titrated according to the general methods before use.

Perfluoro phenyl magnesium bromide (**29**)



In oven-dried reflux apparatus and under inert atmosphere of nitrogen, MesMgBr **29** was prepared from the dropwise addition of 2-bromomesitylene (2.5 eq) in Et₂O (1M) to a suspension of activated magnesium turnings (3 eq) in Et₂O (2 M). After addition of the aryl bromide, the mixture was refluxed for 2 hours. The solution was then cooled to room and the solution was titrated according to the general methods before use.

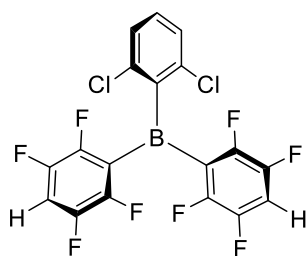
7.2.2.4 General Procedure 1: Synthesis of 2,6-dichlorophenyl Substituted Boranes



This procedure was adapted from a procedure reported by Soós *et al.*¹⁹⁰

In oven-dried reflux apparatus and under inert atmosphere of nitrogen, a solution of Grignard reagent (2.25 eq) in anhydrous Et₂O (prepared according to the procedures above) was cooled to 0 °C and added dropwise to a suspension of appropriate aryl-BF₃K salt (1 eq) in Et₂O (2.5 mL/mmol) at 0 °C. The resulting mixture was allowed to warm to rt and was stirred overnight. The next day the solvent was evaporated, and the solid residue was dried in vacuo at 80 °C for one hour. Then, the residue was extracted with hot toluene (5 mL/mmol) and the resulting suspension was filtered. The resulting solid residue was then extracted with hot toluene (2 x 2 mL/mmol) and the combined toluene extracts were evaporated to dryness. The residue was then washed with rt hexane (2 x 1 mL/mmol) and then dried under vacuum to yield the crude product. The crude product was then suspended in toluene (1 mL/mmol) overnight, the next day the supernatant solution was collected by syringe carefully ensuring that all insoluble solids were left behind. To the leftover solids, toluene (0.5 mL/mmol) was added and after the allowing the suspension to settle the supernatant solution was again collected by syringe. Combined supernatant solutions were then evaporated to dryness under reduced pressure yielding the desired triarylborane.

2,6-Dichlorophenylbis(tetrafluorophenyl)borane (**16a**)^{37,190}



16a was prepared according to general procedure 1 from potassium (2,6-dichlorophenyl) trifluoroborate (**37**) (10 mmol) and was isolated as a white solid (1.94 g, 4.26 mmol, 43% yield).

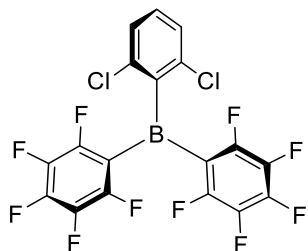
This data matches data reported in literature.³⁷

¹H NMR (CH₂Cl₂, 400 MHz) δ_H 7.32-7.24 (m, 5H).

¹⁹F NMR (CH₂Cl₂, 376 MHz) δ_F -129.4 (m, 4F), -139.2 (m, 4F).

¹¹B NMR (CH₂Cl₂, 128 MHz) δ_B 63.8 (brs).

2,6-Dichlorophenylbis(pentafluorophenyl)borane (**16b**)¹⁹²



16b was prepared according to general procedure 1 from potassium (2,6-dichlorophenyl) trifluoroborate (**37**) (10 mmol) and was isolated as an off-white solid (2.43 g, 4.94 mmol 49% yield).

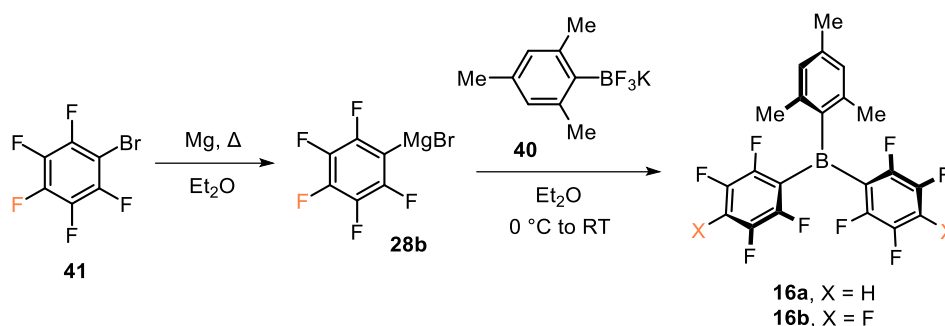
This data matches data reported in literature.¹⁹²

¹H NMR (CH₂Cl₂, 400 MHz) δ_H 7.39-7.31 (m, 3H).

¹⁹F NMR (CH₂Cl₂, 376 MHz) δ_F -127.9 (m, 4F), -144.5 (m, 2F), -161.7 (m, 4F).

¹¹B NMR (CH₂Cl₂, 128 MHz) δ_B 63.5 (brs).

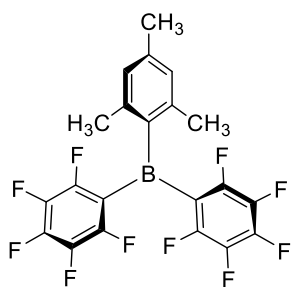
7.2.2.5 General Procedure 2: Synthesis of 2,4,6-Trimethylphenyl (Mesityl) Substituted Boranes



This procedure was adapted from a procedure reported by Jäckle *et al.*²¹³

In oven-dried reflux apparatus and under inert atmosphere of nitrogen, Grignard reagent (2.25 eq) in Et₂O was cooled to 0 °C and added dropwise to a suspension of appropriate aryl-BF₃K salt (1 eq) in Et₂O (2.5 mL/mmol) at 0 °C. The resulted mixture was allowed to warm to rt and stirred overnight. The next day the solvent was evaporated under reduced pressure, and the solid residue was dried in vacuo at 80 °C for one hour. The resulting solid was then suspended in 3:1 toluene-hexane (3 mL/mmol) (with sonication), after allowing the suspension to settle, the supernatant layer was removed by cannula filtration. The resulting solution was then evaporated in under vacuum to give an orange oil, which was left to stand. Recrystallisation of the crude material from hexane (2 mL/mmol) and a minimum amount of Et₂O at -70 °C yielded the desired triarylborane.

2,4,6-Trimethylphenylbis(pentafluorophenyl)borane (**19b**)^{198,213}



19b was prepared according to general procedure 2 from potassium (2,4,6-trimethylphenyl) trifluoroborate (**40**) (10 mmol) and was isolated as a white solid (1.10 g, 2.37 mmol, 24% yield).

This data matches data reported in literature.²¹³

$^1\text{H NMR}$ (CH_2Cl_2 , 400 MHz) δ_{H} 6.90 (s, 2H), 2.35 (s, 3H), 2.13 (s, 6H).

$^{19}\text{F NMR}$ (CH_2Cl_2 , 376 MHz) δ_{F} -123.4 (m, 4F), -146.5 (m, 2F), -161.6 (m, 4F).

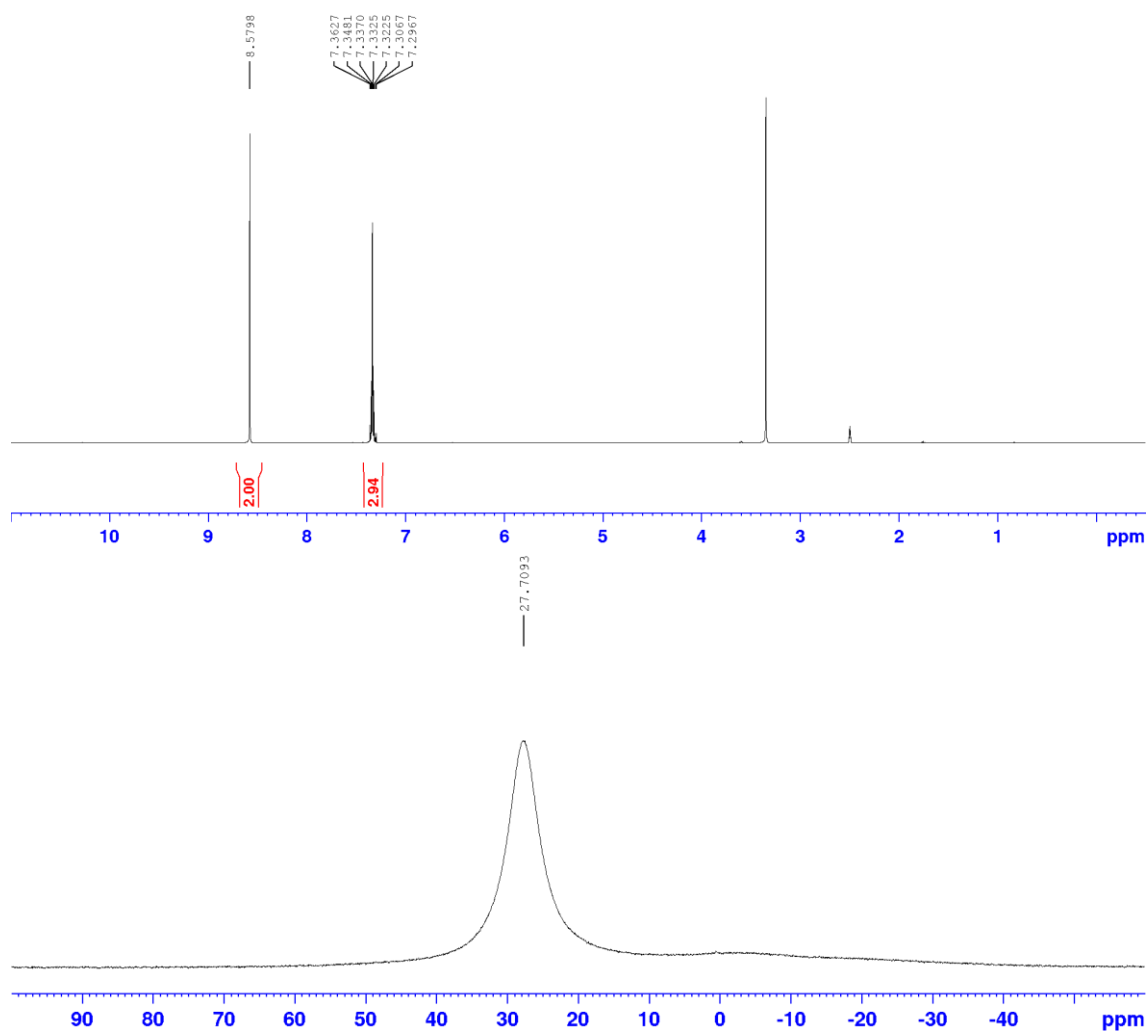
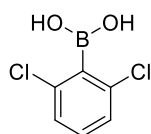
$^{11}\text{B NMR}$ (CH_2Cl_2 , 128 MHz) δ_{B} 68.8 (brs).

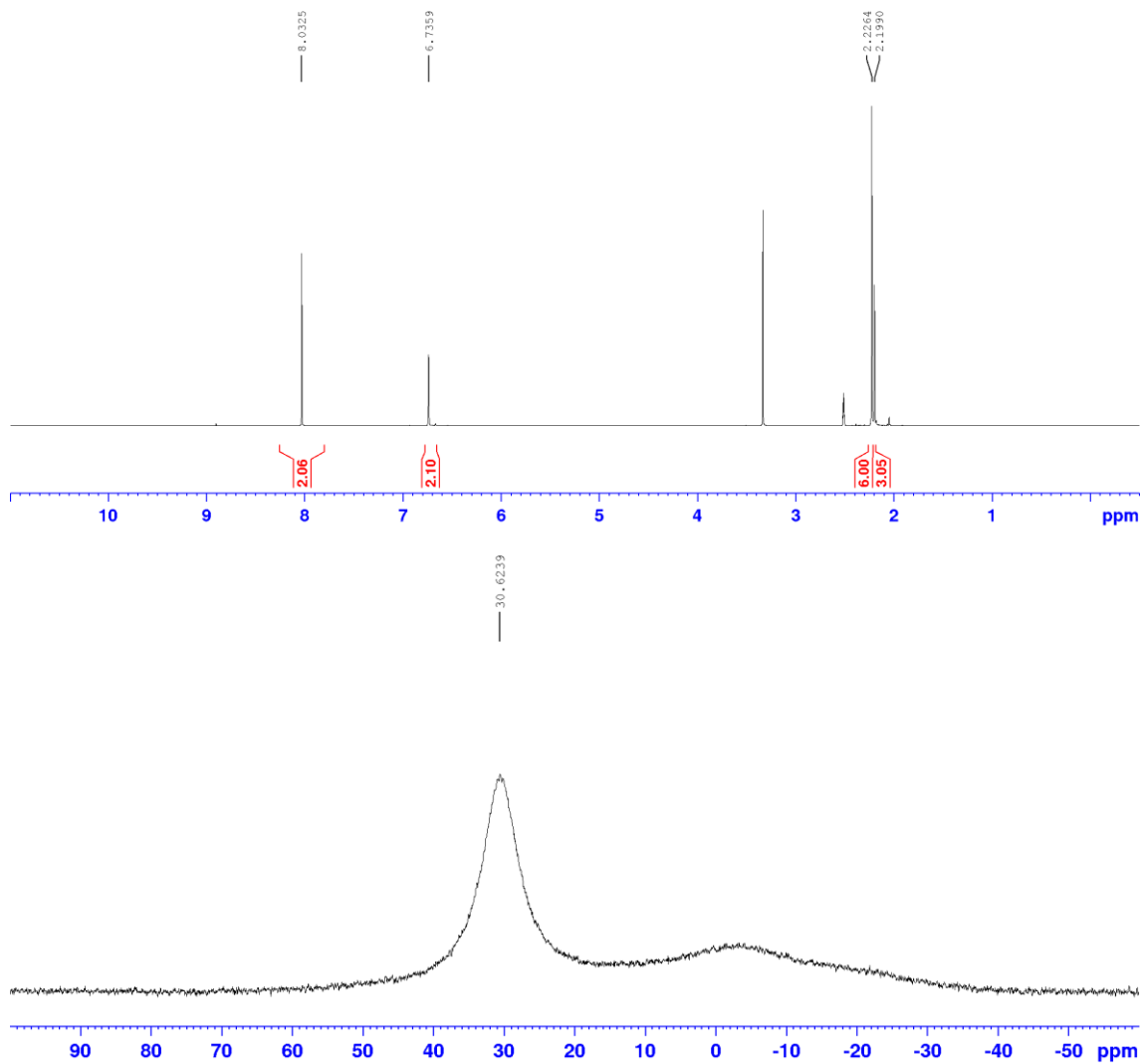
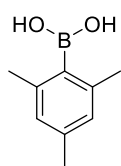
7.2.3 NMR Spectra

7.2.3.1 NMR Spectra of Synthesised Boronic Acid, Potassium Aryltrifluoroborate Salt

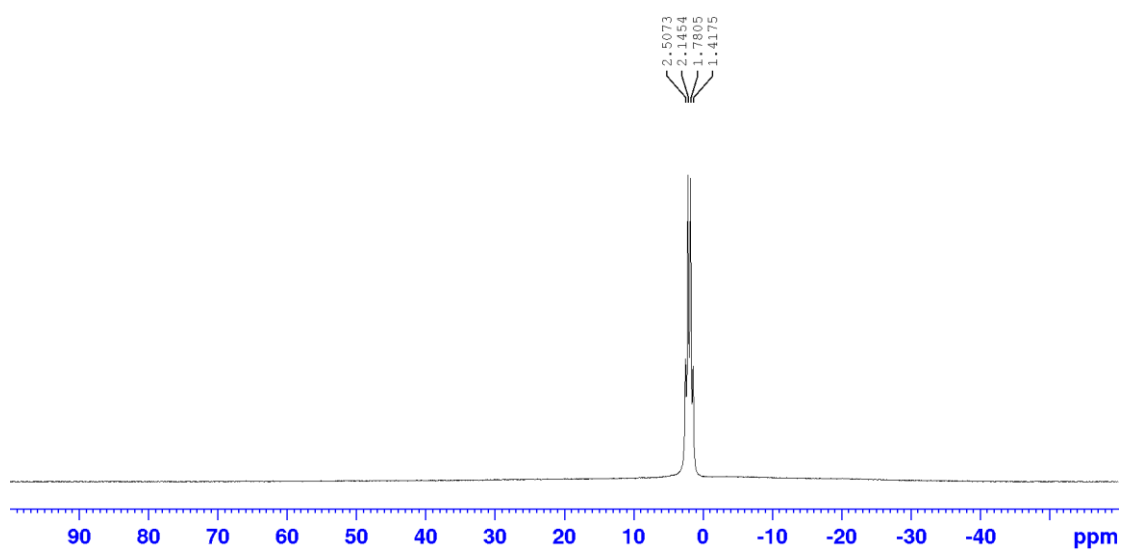
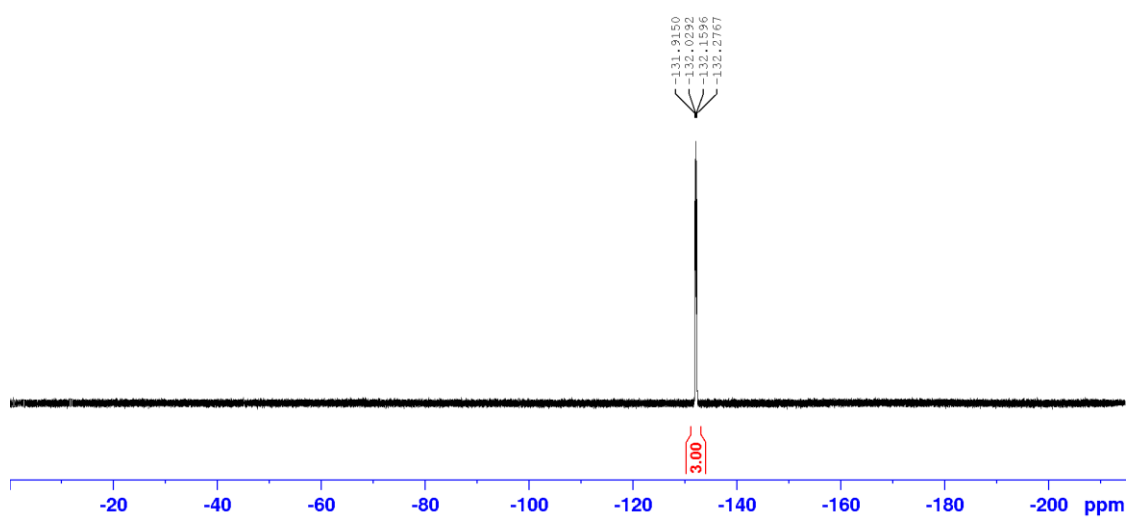
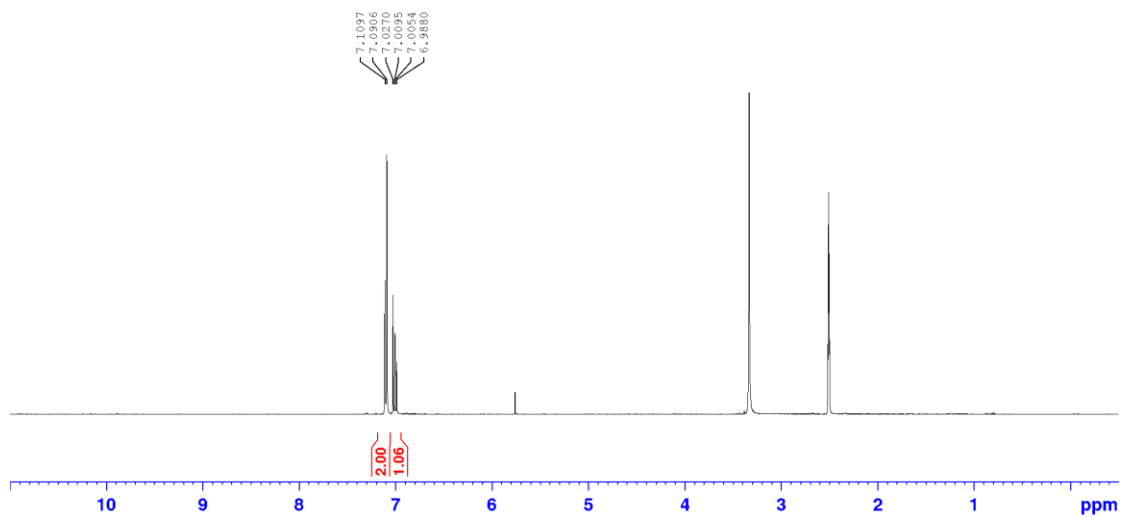
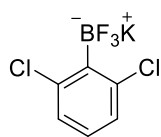
Intermediates and Triaryl Boranes

2,6-Dichlorophenyl boronic acid (**36**)

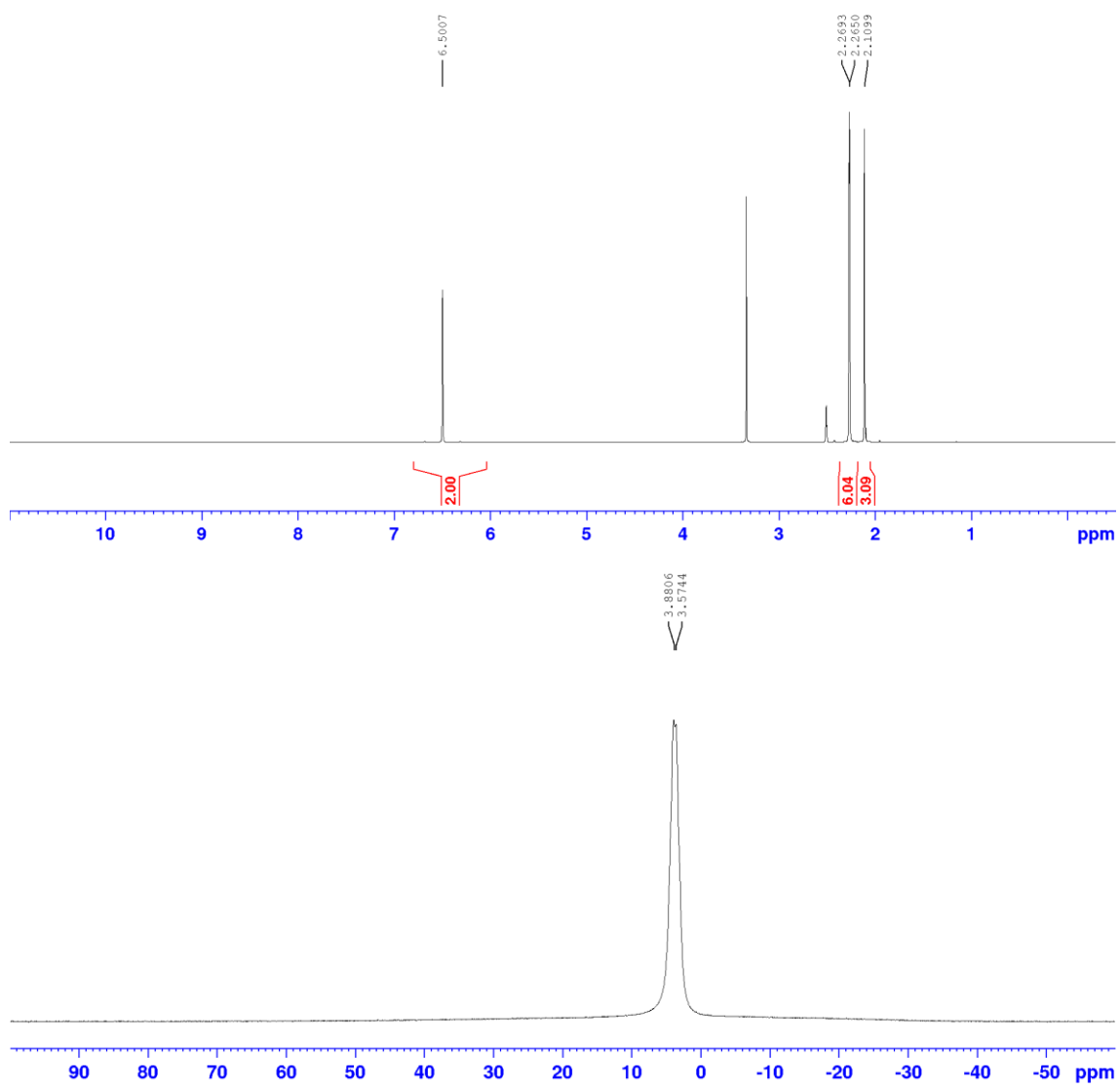
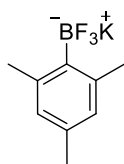


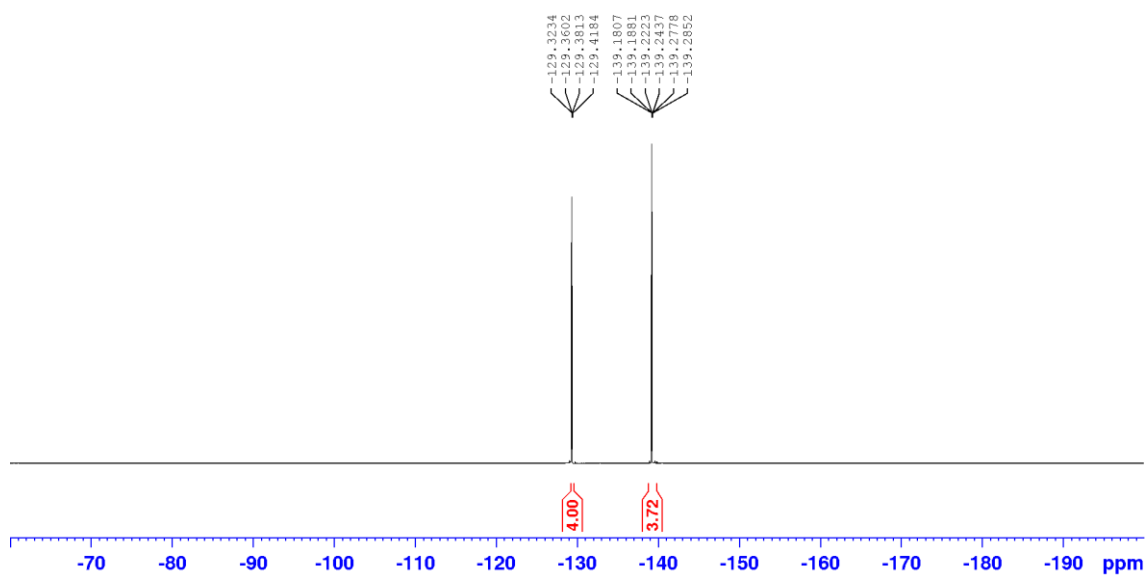
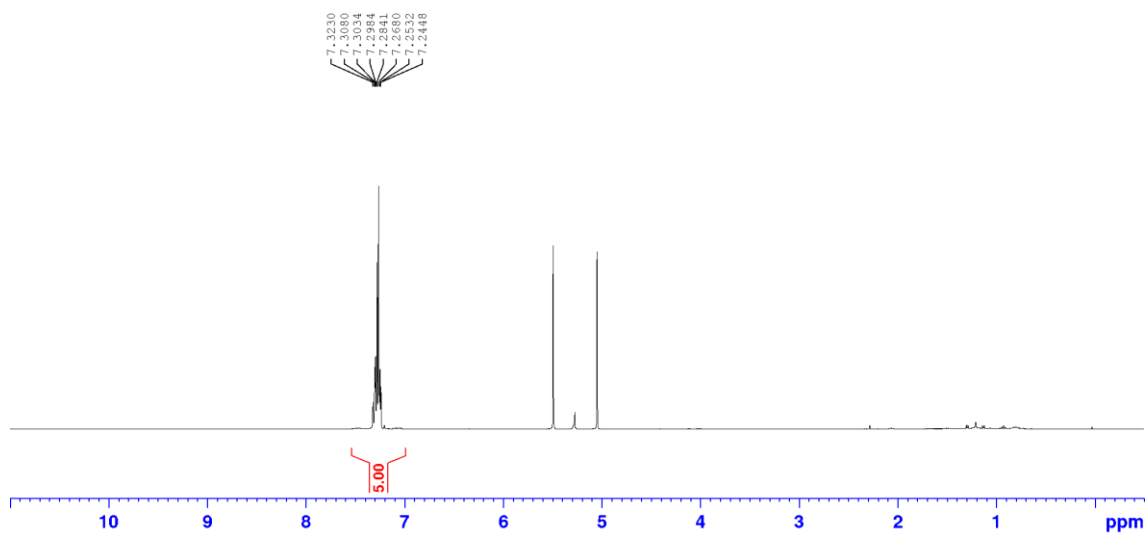
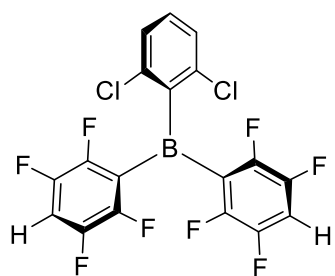
2,4,6-Trimethylphenyl boronic acid (**39**)

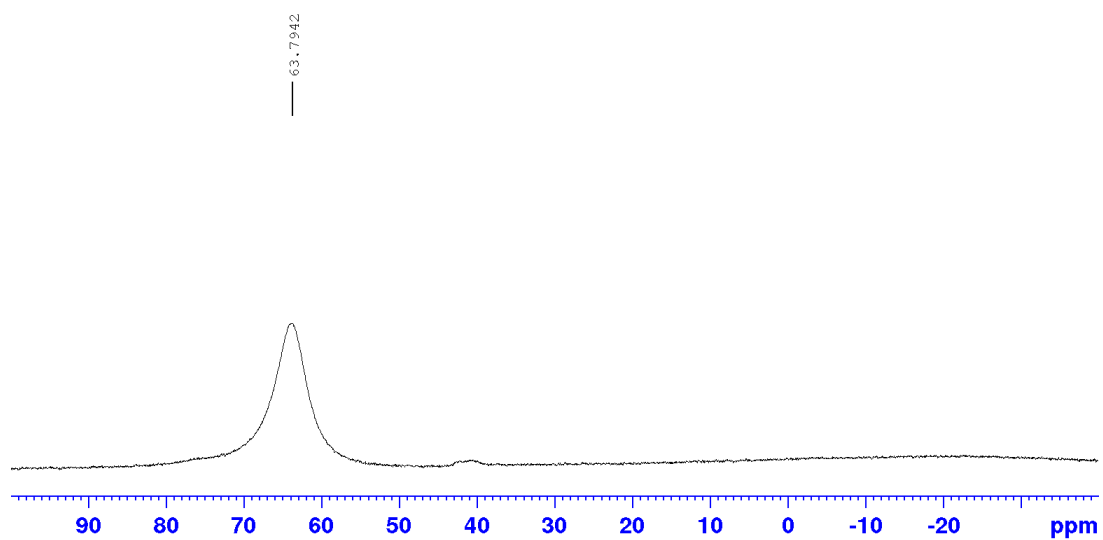
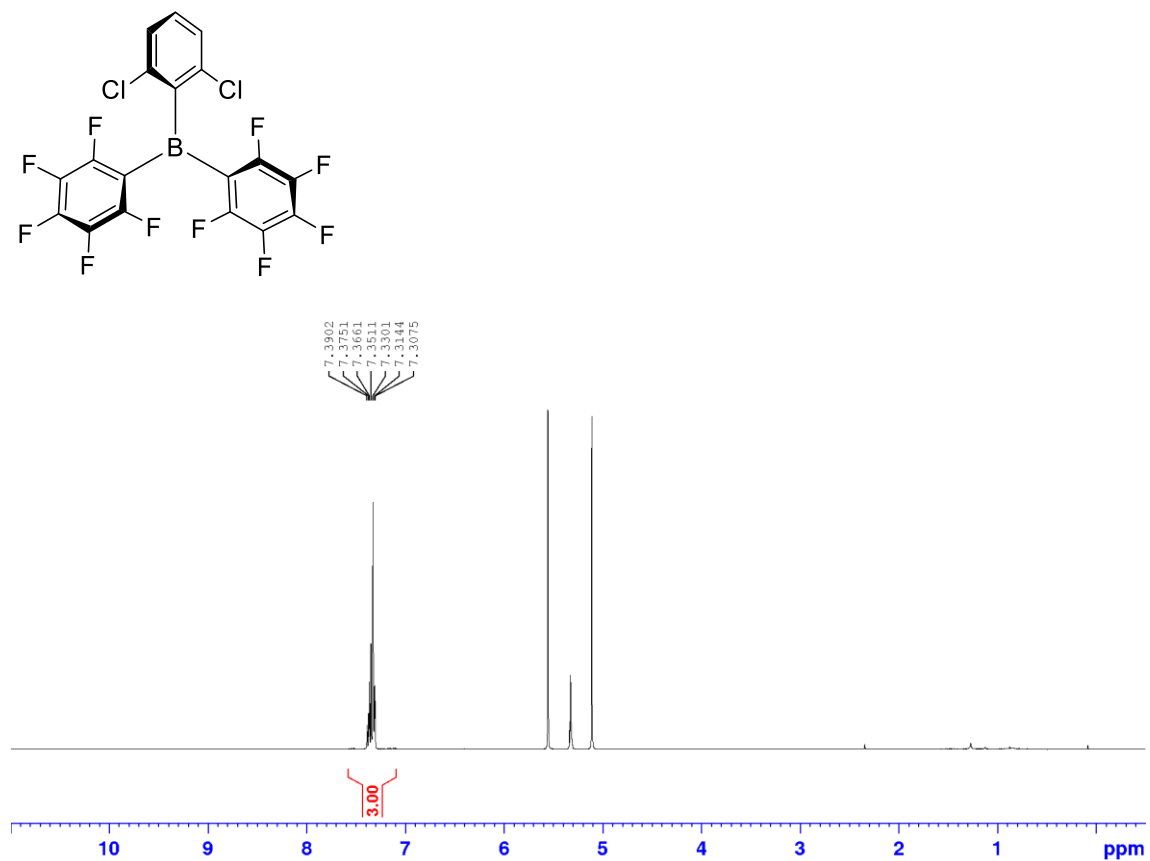
Potassium 2,6-dichlorophenyl trifluoroborate (37)

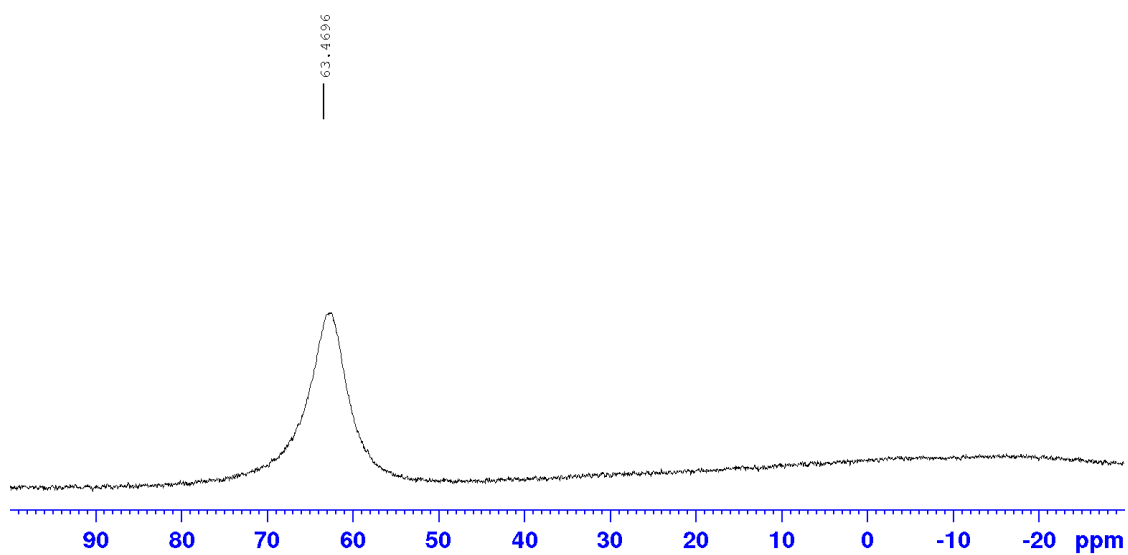
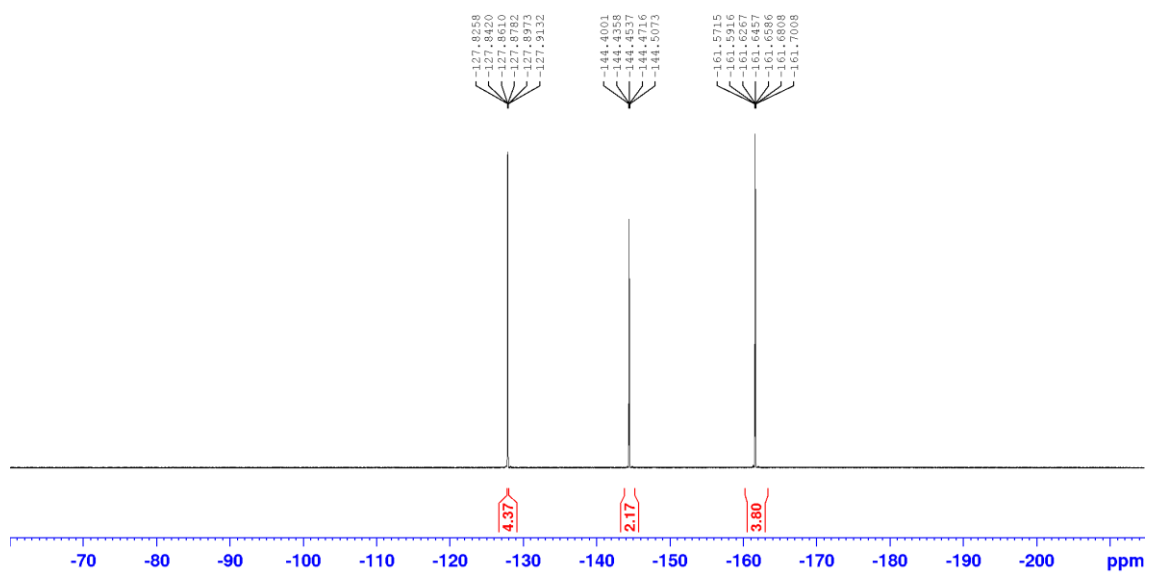


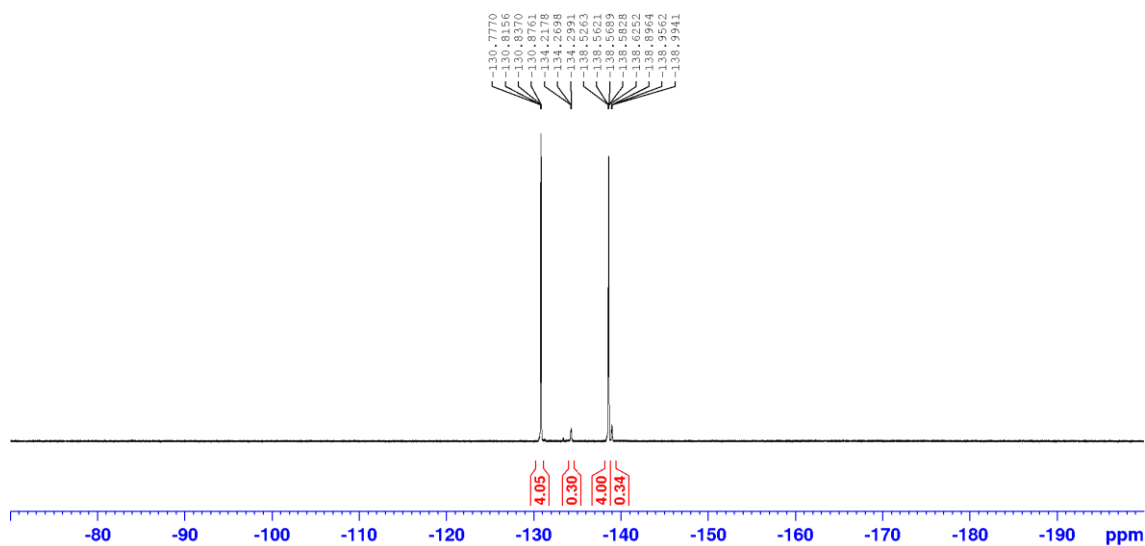
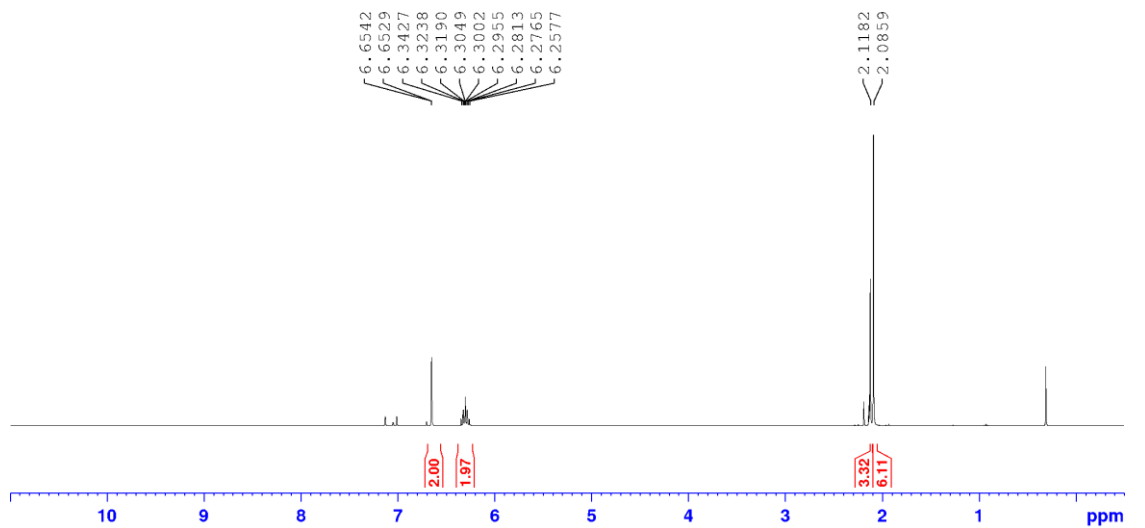
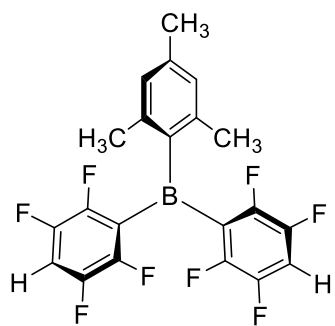
Potassium 2,4,6-trimethylphenyl trifluoroborate (40)

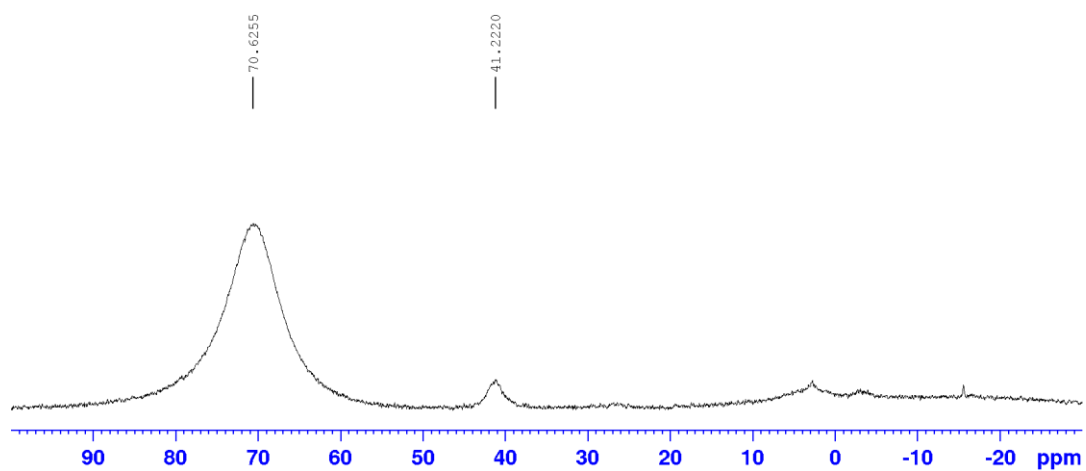
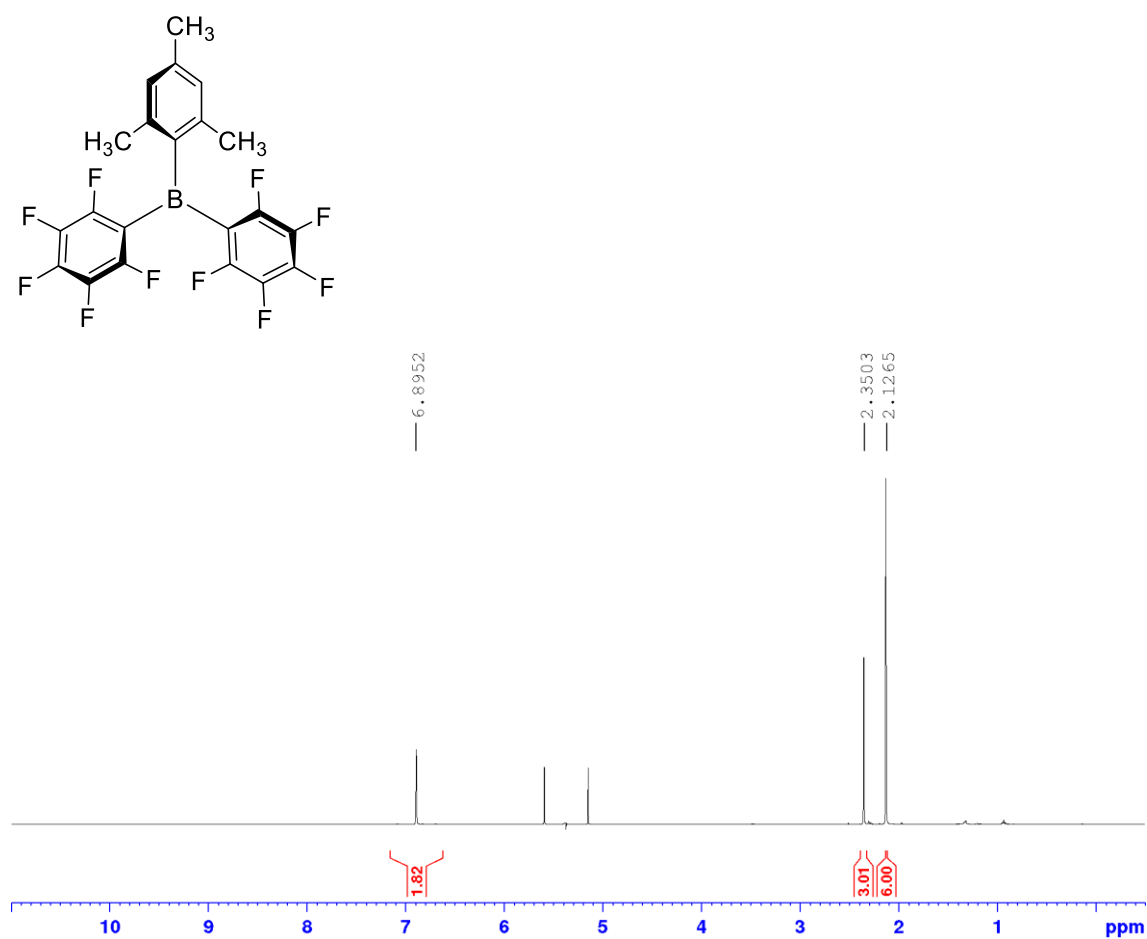


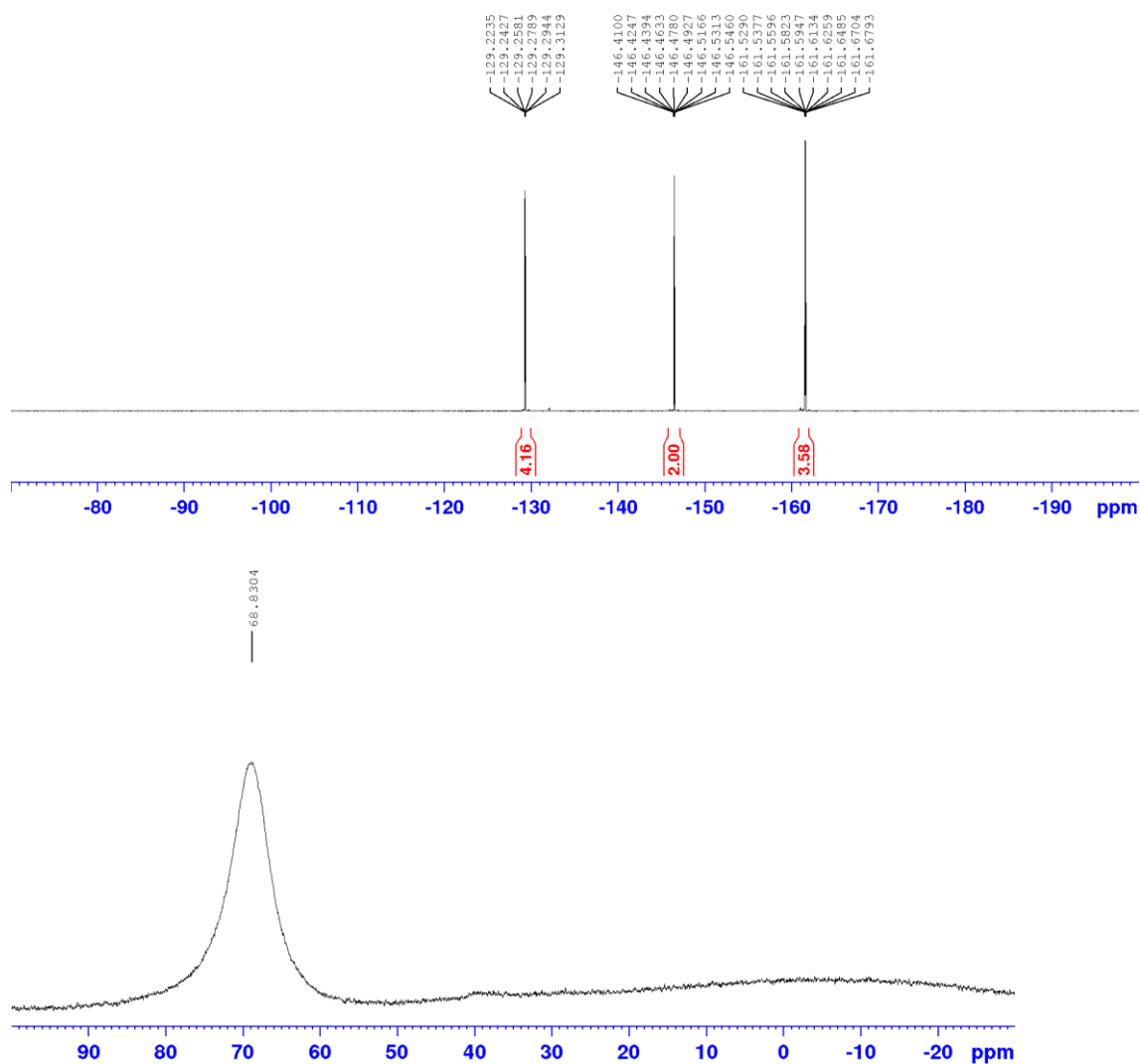
2,6-Dichlorophenylbis(tetrafluorophenyl)borane (**16a**)

2,6-Dichlorophenylbis(pentafluorophenyl)borane (**16b**)



2,4,6-Trimethylphenylbis(tetrafluorophenyl)borane (**19a**)

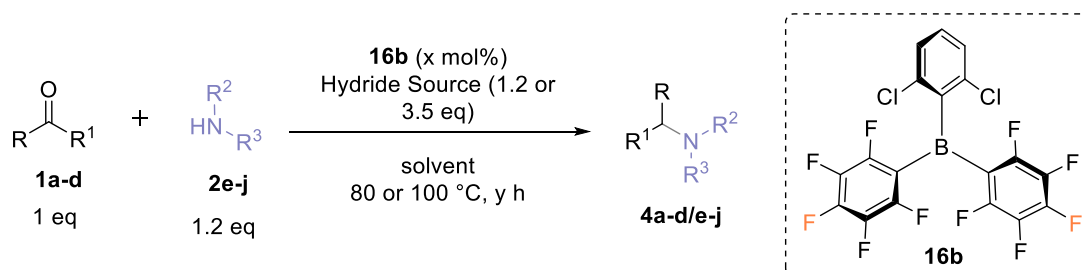
2,4,6-Trimethylphenylbis(pentafluorophenyl)borane (**19b**)



7.3 Experimental Details for Chapter Three

7.3.1 General Procedures

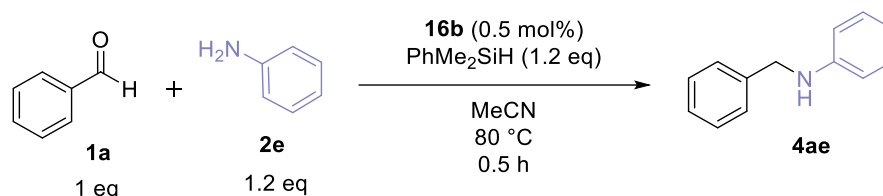
7.3.1.1 General Procedure 3: Batch Reductive Aminations with Silanes



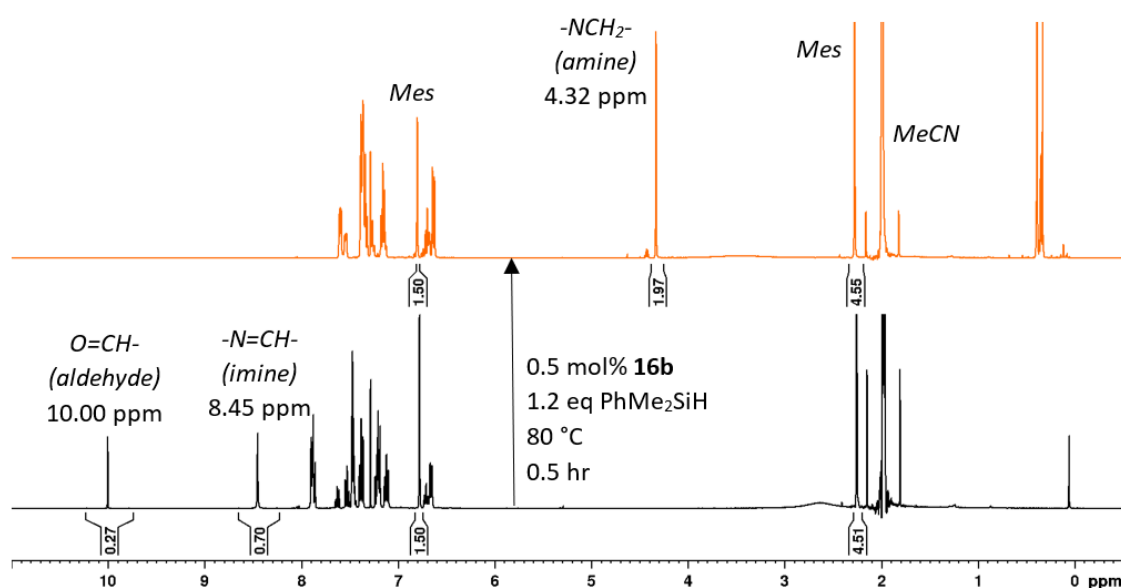
To an oven-dried 10 mL crimp cap vial open to the air were added sequentially amine **2e-j** (1.2 eq), carbonyl **1a-d** (1.0 eq), and mesitylene (0.5 eq, internal standard) in solvent

(0.75 mL/mmol of carbonyl). To this mixture, **16b** dissolved in solvent (50 mL/mmol of **16b**) was added. At this point, a 50 μ L aliquot was taken in CDCl_3 (0.5 mL) and analysed by ^1H NMR spectroscopy (initial imine/carbonyl/mesitylene ratio). Finally, hydride source was loaded, and the vial was sealed. The reaction mixture was stirred at temperatures specified in chapter three (see Table 1, Table 2, Table 3, Table 4, Scheme 43 and Scheme 44) (80 $^\circ\text{C}$ or 100 $^\circ\text{C}$) for 0.5 to 17 hours. The product was purified by flash silica gel column chromatography or alternatively the yields were determined by quantitative ^1H NMR spectroscopy; either by relative integration of product and starting material resonances (where no other species were observed); or by integration of an internal standard (mesitylene).

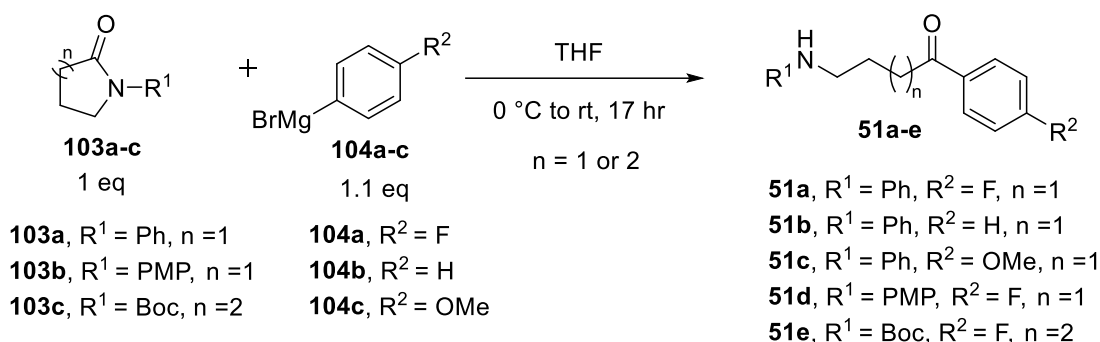
Typical ^1H NMR Spectroscopic Yield Determination



Initial ^1H NMR aliquot of the crude reaction mixture before addition of dimethylphenylsilane (bottom; black) and ^1H NMR aliquot of the crude reaction mixture post reaction (top; orange). The determination of the NMR spectroscopic yields was based on the benzylic protons α to the N on the product (d, $\delta \sim 4.32$ ppm) (top).



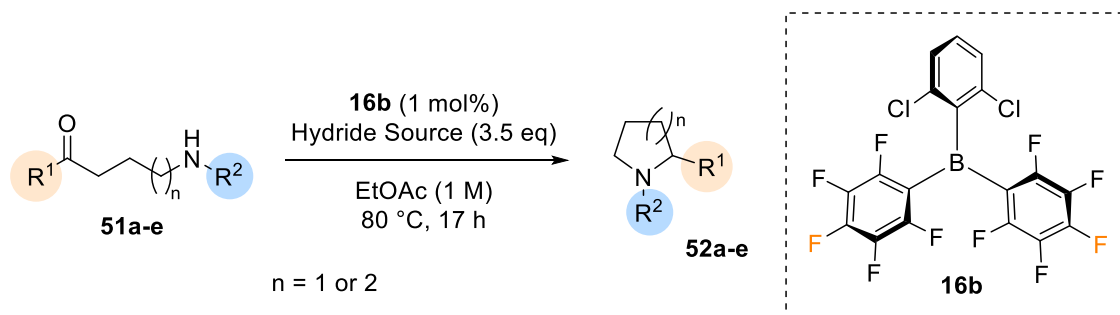
7.3.1.2 General Procedure 4: Synthesis of Amino Ketones



This procedure was adapted from a procedure reported by Watile *et al.*²²⁸

To oven-dried glassware and under an atmosphere of nitrogen was added *N*-aryl-2-pyrrolidinones/piperidinones **103a-c** (10 mmol, 1 eq) and anhydrous THF (20 mL). The solution was cooled to 0 °C and bought aryl magnesium bromide **104a-c** (1.1 eq) was added dropwise. The reaction was allowed to attain room temperature and stirred at this temperature for 17 hours. After 17 hours the reaction was quenched with aqueous saturated NH₄Cl solution (30 mL) and extracted with Et₂O (3 × 50 mL). The combined organic layers were dried over MgSO₄, filtered, and evaporated under reduced pressure. The product was purified by flash silica gel column chromatography (DCM to 99:1 DCM:EtOAc), unless otherwise stated.

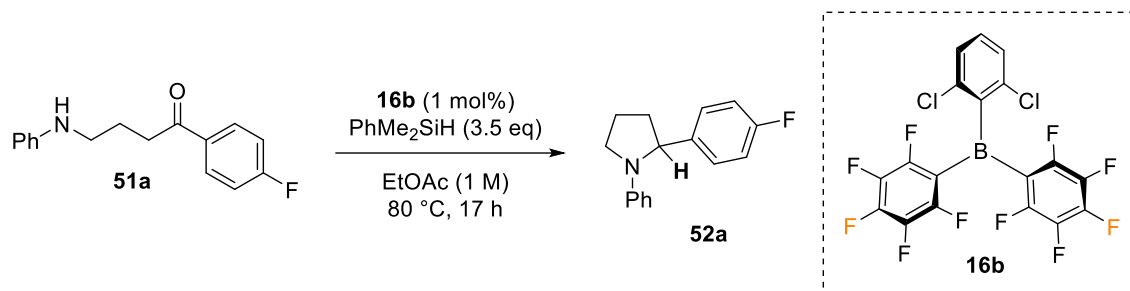
7.3.1.2 General Procedure 5: Intramolecular Reductive Amination Cyclisation of Amino Ketones



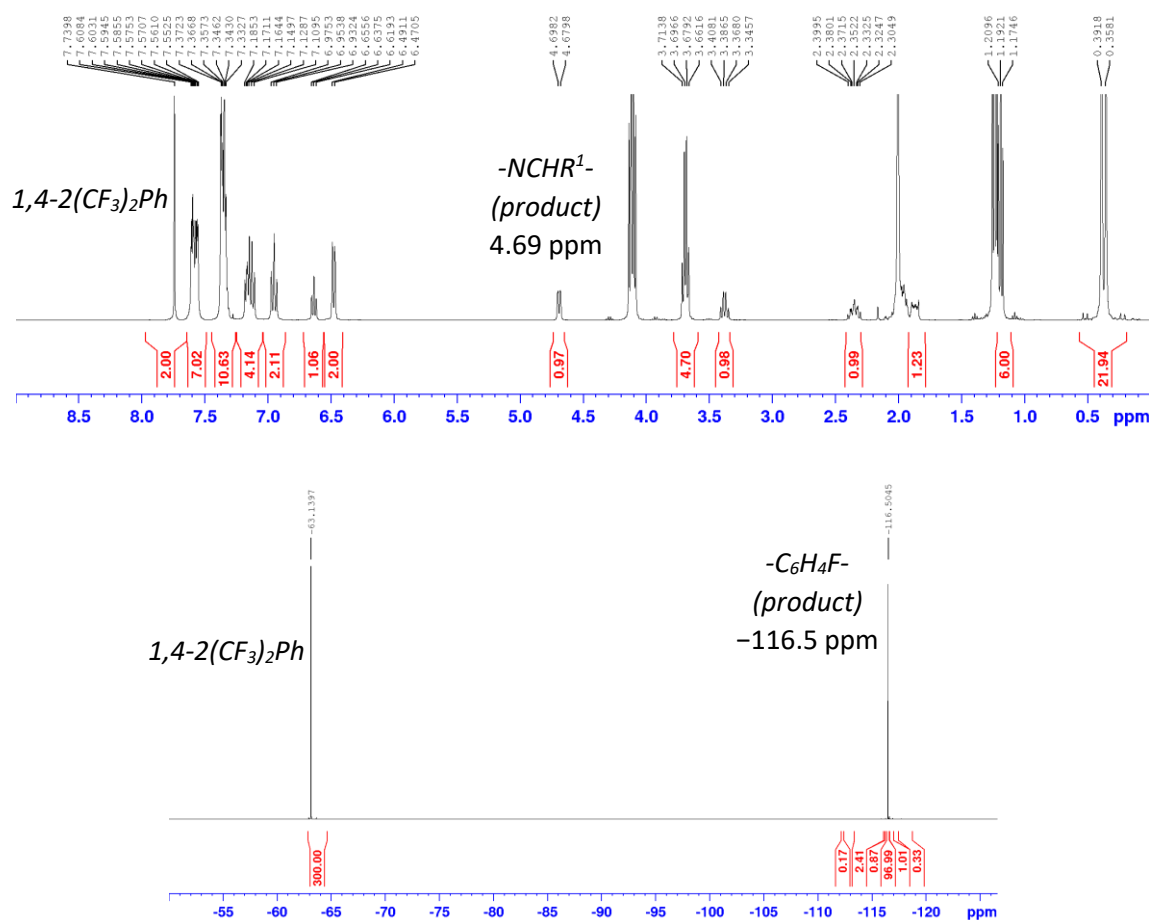
To an oven-dried 10 mL crimp cap vial open to the air were added sequentially amino ketone **51a-e** (0.2 mmol, 1.0 eq), 1,4-bis(trifluoromethyl)benzene (16 μL, 0.1 mmol, 0.5 eq, internal standard) and **16b** (1.0 mg, 2 μmol, 0.01 eq, 1 mol%) dissolved in anhydrous EtOAc (0.2 mL). To this mixture, hydride source (3.5 eq) was added, and the vial was

sealed. The reaction mixture was stirred at 80 °C for 17 hours. The yields were determined by quantitative ^1H and /or ^{19}F NMR spectrum through use of an internal standard {1,4-bis[trifluoromethyl]benzene [1,4-2(CF₃)₂Ph]}, unless otherwise stated.

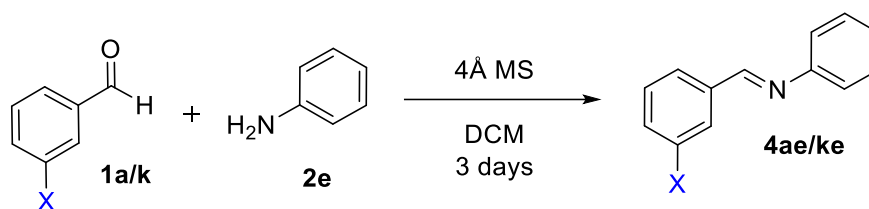
Typical $^1\text{H}/^{19}\text{F}$ NMR Spectroscopic Yield Determination



The determination of the NMR spectroscopic yields was based on the ^{19}F NMR spectrum where possible (bottom) or in the ^1H NMR spectrum using the chiral 2-pyrroldine proton α to the N on the product (dd, $\delta \sim 4.69$ ppm) (top).



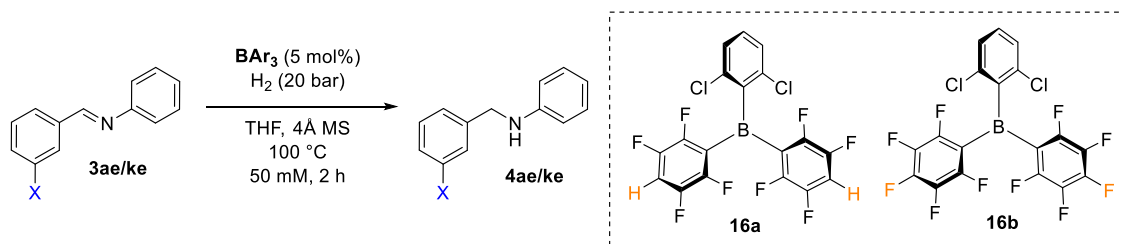
7.3.1.3 General Procedure 6: Preparation of Imines



To an oven-dried 10 mL crimp cap vial were added sequentially aldehyde (5 mmol), aniline (5 mmol) and 4 Å molecular sieves (~1 g) in CH₂Cl₂ (15 mL). The reaction mixture was left at ambient temperature for 3 days. After 3 days the reaction mixture was filtered and evaporated under reduced pressure to yield the desired imine.

7.3.1.4 General Procedure 7: Batch Reductions with Hydrogen

Procedure A: Glovebox



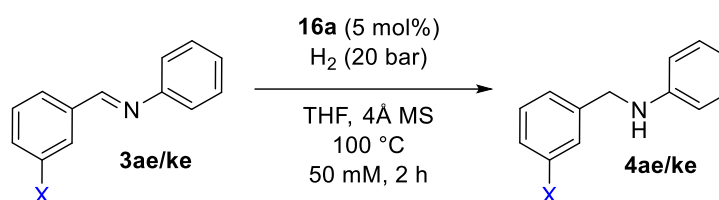
In a glovebox to an oven dried glass vial were added sequentially imine **3ae** or **3ke** (0.1 mmol, 1 eq), **BAr**₃ (5 μmol, 0.05 eq, 5 mol%) (see Table 10), 4 Å molecular sieves (25 mg), and anhydrous THF (2 mL). The vial was placed in a 30 mL Parr pressure vessel. Once sealed, the vessel was removed from the glovebox and pressurised with H₂ (20 bar). The reaction mixture was stirred at 100 °C for 2 hours. After 2 hours the reaction mixture was then cooled to room temperature, degassed and an aliquot of the reaction mixture (0.5 mL) was taken and analysed by quantitative ¹H and ¹⁹F NMR spectroscopy. The yields were determined by relative integration of product and starting material resonances or by integration of an internal standard (mesitylene when X = H).

Procedure B: Fume hood

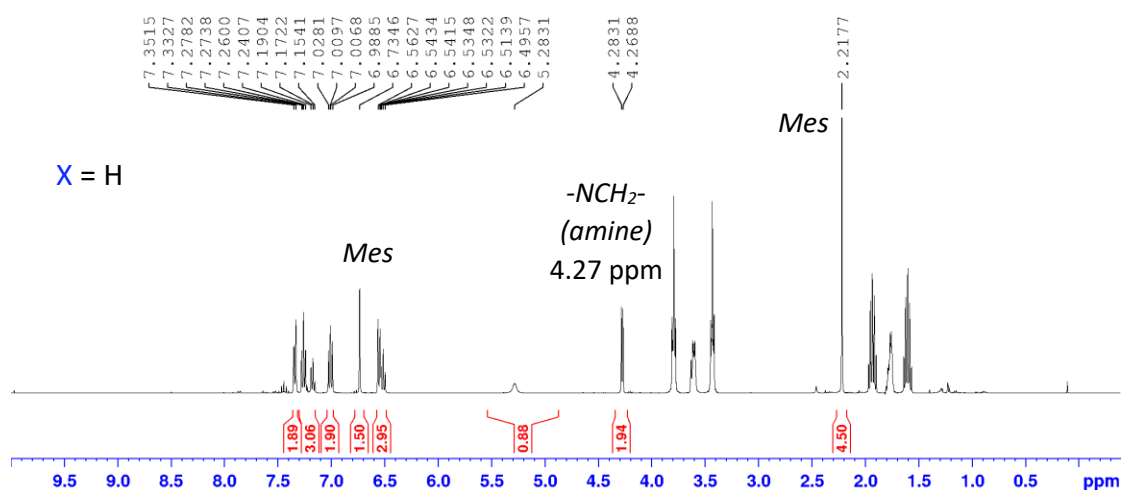
To an oven dried glass vial was added sequentially imine **3ae** or **3ke** (50 μmol, 1 eq), **BAr**₃ (2.5 μmol, 0.05 eq, 5 mol%), 4 Å molecular sieves (10 mg) (if necessary; see Table

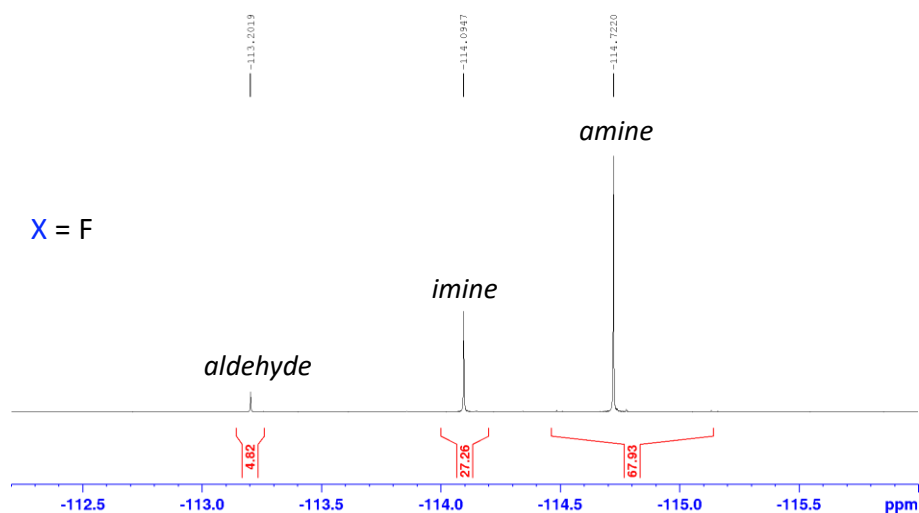
11), and anhydrous THF (1 mL). The vial was placed in a 30 mL Parr pressure vessel flushed with argon. The pressure vessel remained under argon for 2 minutes before the vessel was sealed. Once sealed, the reaction mixture was and pressurised with H₂ (20 bar) and heated at 100 °C for 2 hours. After 2 hours the reaction mixture was then cooled to room temperature, degassed and an aliquot of the reaction mixture (0.5 mL) was taken and analysed by quantitative ¹H and ¹⁹F NMR spectroscopy. The yields were determined by relative integration of product and starting material resonances or by integration of an internal standard (mesitylene when X = H).

Typical ¹H/¹⁹F NMR Spectroscopic Yield Determination

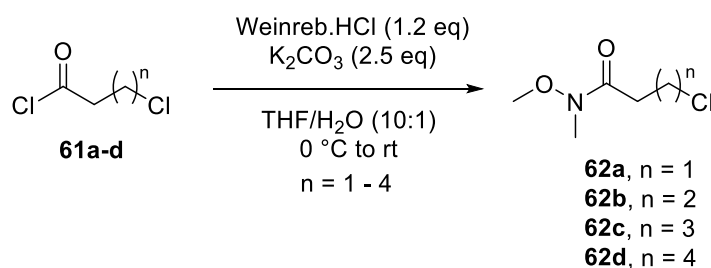


The determination of the NMR spectroscopic yields was based on the ¹⁹F NMR spectrum where possible (bottom, X = F) or in the ¹H NMR spectrum using the benzylic protons α to the N on the product (d, δ ~ 4.28 ppm) (top).





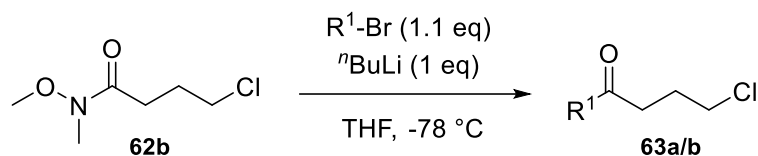
7.3.1.5 General Procedure 8: Synthesis of Weinreb amides



This procedure was adapted from a procedure reported by Lautens *et al.*³¹⁸

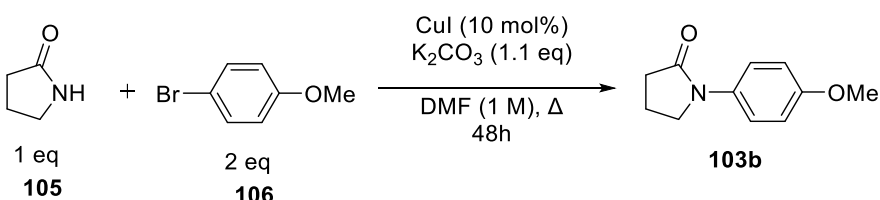
N,O-Dimethylhydroxylamine hydrochloride (1.2 eq) was dissolved in THF/water (10:1, 33 mL). K_2CO_3 (2.0 eq) was added, and the mixture cooled to 0 °C. The acid chloride **61a-d** (1 eq) was added at 0 °C then the mixture allowed to warm to room temperature and stirred overnight. The reaction was quenched with H_2O (3.3 mL/mmol) and diluted with EtOAc (4 mL/mmol). The aqueous layer was extracted with EtOAc (2 x 4 mL/mmol), and the combined organic layer was washed once with H_2O (4 mL/mmol), dried over MgSO_4 , filtered and evaporated under reduced pressure. The product **62a-d** was continued into the next step in the synthesis without need for further purification.

7.3.1.6 General Procedure 9: Synthesis of Functionalised Ketones from Weinreb amides



This procedure was adapted from a procedure reported by Lautens *et al.*³¹⁸

The Weinreb amide **62b** was dissolved in a minimal amount of THF and added dropwise to a solution of aryl bromide (1.5 eq) dissolved in THF (5 mL/mmol) and cooled to $-78\text{ }^\circ\text{C}$. At $-78\text{ }^\circ\text{C}$ $n\text{BuLi}$ (1.6 M in hexanes, 1 eq) was added dropwise and the reaction was stirred at $-78\text{ }^\circ\text{C}$ for 2 hours. After 2 hours the mixture was quenched with H_2O (5 mL/mmol) and diluted with EtOAc (5 mL/mmol). The aqueous layer was extracted with EtOAc (2 x 5 mL/mmol), and the combined organic layer was washed once with H_2O (4 mL/mmol), dried over MgSO_4 , filtered and evaporated under reduced pressure. The product (**63a** or **63b**) was purified by flash silica gel column chromatography (25:1 hexane:EtOAc) unless otherwise stated.

7.3.2 Synthesis of *N*-(*para*-Methoxyphenyl) Pyrrolidinone (**103b**)²²⁸

This procedure was adapted from a procedure reported by Watile *et al.*²²⁸

2-Pyrrolidinone **105** (3.4 g, 40 mmol, 1 eq), 4-bromo anisole **106** (10 mL, 14.96 g, 80 mmol, 2 eq), anhydrous K_2CO_3 (6.08 g, 44 mmol, 1.1 eq) and CuI (0.76 g, 4 mmol, 0.1 eq, 10 mol%) were dissolved in anhydrous DMF (40 mL). The reaction mixture was heated at reflux for 48 hours. After 48 hours, the reaction mixture was cooled to room temperature. Aqueous saturated NH_4Cl solution (60 mL) was added, and the resulting mixture was stirred for 15 minutes at room temperature. The mixture was extracted with EtOAc (4 x 50 mL). The combined organic layers were washed with brine (1 x 50 mL), dried over MgSO_4 , filtered and evaporated under reduced pressure. The product was

purified by recrystallisation with minimal EtOAc and subsequent dilution with hexane as a pale brown solid (3.86 g, 20.2 mmol, 50%).

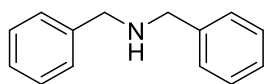
This data matches data reported in literature.²²⁸

¹H NMR (CDCl₃, 400 MHz) δ_{H} 7.53-7.49 (m, 2H), 3.85 (t, J 7.0 Hz, 2H), 3.82 (s, 3H), 2.61 (t, J 7.0 Hz, 2H), 2.21-2.14 (m, 2H).

7.3.3 Compound Characterisation Data

7.3.3.1 Batch Reductive Aminations with Silanes

Dibenzylamine (**4ag**)³⁴



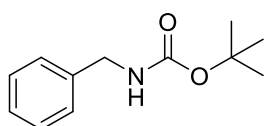
According to general procedure 3, benzaldehyde (**1a**, 41 μ L, 42 mg, 0.4 mmol) and benzylamine (**2g**, 52 μ L, 51 mg, 0.48 mmol)

and dimethylphenylsilane (0.21 mL, 1.4 mmol, 3.5 eq) were heated at 100 °C. The product (**4ag**) was purified by flash silica gel column chromatography (9:1 hexane:EtOAc) and isolated as a yellow oil (73 mg, 0.32 mmol, 93%).

This data matches data reported in literature.³⁴

¹H NMR (CDCl₃, 400 MHz) δ_{H} 7.37-7.24 (m, 10H), 3.82 (s, 4H).

N-Boc benzylamine (**4ah**)³¹⁹



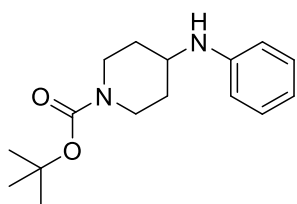
According to general procedure 3, benzaldehyde (**1a**, 41 μ L, 42 mg, 0.4 mmol) and *tert*-Butylcarbamate (**2h**, 56 mg, 0.48 mmol) and dimethylphenylsilane (0.21 mL, 1.4 mmol, 3.5 eq) were

heated at 100 °C. The product (**4ah**) was purified by flash silica gel column chromatography (9:1 to 8:2 hexane:EtOAc) and isolated as a colourless oil (12 mg, 0.06 mmol, 14%).

This data matches data reported in literature.³¹⁹

¹H NMR (CDCl₃, 400 MHz) δ_{H} 7.31-7.27 (m, 5H), 4.85 (brs, 1H), 4.34 (d, J 5.6 Hz, 2H) 1.49 (s, 9H).

1-*N*-Boc-4-phenylaminopiperidine (**4ce**)³²⁰

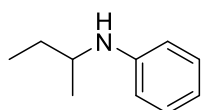


According to general procedure 3, *N*-Boc-piperidin-4-one (**1c**, 80 mg, 0.4 mmol) and aniline (**2e**, 44 μ L, 45 mg, 0.48 mmol) and dimethylphenylsilane (0.21 mL, 1.4 mmol, 3.5 eq) were heated at 100 °C. The product (**4ce**) was purified by flash silica gel column chromatography (8:2 hexane:EtOAc) and isolated as a pale yellow solid (28 mg, 0.1 mmol, 26%).

This data matches data reported in literature.³²⁰

¹H NMR (CDCl₃, 400 MHz) δ_{H} 7.19 (t, J 7.9 Hz, 2H), 6.72 (t, J 7.3 Hz, 1H), 6.63 (d, J 7.9 Hz, 2H), 4.06 (bs, 2H), 3.53 (s, 1H), 3.45 (tt, J 10.2, 3.9 Hz, 1H), 2.95 (t, J 12.1 Hz, 2H), 2.06 (d, J 11.7 Hz, 2H), 1.49 (s, 9H), 1.40-1.28 (m, 2H).

N-*sec*-Butylaniline (**4de**)³²¹

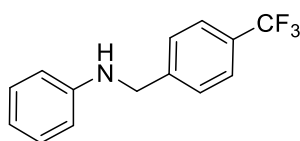


According to general procedure 3, 2-butanone (**1d**, 36 μ L, 29 mg, 0.4 mmol) and aniline (**2e**, 44 μ L, 45 mg, 0.48 mmol) and dimethylphenylsilane (0.21 mL, 1.4 mmol, 3.5 eq) were heated at 100 °C. The product (**4de**) was purified by flash silica gel column chromatography (9:1 hexane:EtOAc) and isolated as a yellow oil (21 mg, 0.14 mmol, 35%).

This data matches data reported in literature.³²¹

¹H NMR (CDCl₃, 400 MHz) δ_{H} 7.22-7.17 (m, 2H), 6.71-6.67 (m, 1H), 6.62-6.59 (m, 2H), 3.47-3.40 (m, 2H), 1.69-1.59 (m, 1H), 1.56-1.45 (m, 1H), 1.21 (d, J 6.2 Hz, 3H), 0.97 (t, J 7.4 Hz, 3H).

N-4-(Trifluoromethyl)benzyl)benzenamine (**49**)³⁷



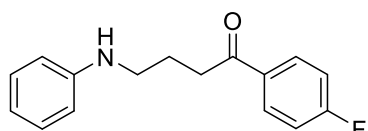
According to general procedure 3, 2-methyl-*N*-[4-(trifluoromethyl)benzylidene] propane-2-sulfonamide (**47**, 0.139 g, 0.5 mmol) and aniline (**2e**, 46 μ L, 47 mg, 0.5 mmol) and dimethylphenylsilane (0.27 mL, 1.75 mmol, 3.5 eq) were heated at 100 °C. The product (**49**) was purified by flash silica gel column chromatography (9:1 to 8:2 hexane:EtOAc) and isolated as a yellow oil (0.116 g, 0.46 mmol, 92%).

This data matches data reported in literature.³⁷

$^1\text{H NMR}$ (CDCl_3 , 400 MHz) δ_{H} 7.22-7.17 (m, 2H), 6.71-6.67 (m, 1H), 6.62-6.59 (m, 2H), 3.47-3.40 (m, 2H), 1.69-1.59 (m, 1H), 1.56-1.45 (m, 1H), 1.21 (d, J 6.2 Hz, 3H), 0.97 (t, J 7.4 Hz, 3H).

7.3.3.2 Synthesis of Amino Ketones

1-(4-Fluorophenyl)-4-(phenylamino)butan-1-one (**51a**)²²⁸

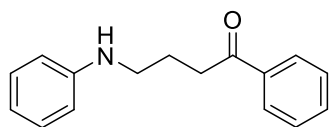


According to general procedure 4, *N*-phenyl-2-pyrrolidinone (1.61 g, 10 mmol, 1 eq) and 4-fluorophenyl magnesium bromide (0.58 M in THF, 19 mL, 11 mmol, 1.1 eq) were stirred at room temperature for 17 hours. The product (**51a**) was purified according to general procedure 4 by flash silica gel column chromatography as an off-white solid (1.74 g, 6.8 mmol, 68%).

This data matches data reported in literature.²²⁸

$^1\text{H NMR}$ (CDCl_3 , 400 MHz) δ_{H} 8.03-7.99 (m, 2H), 7.23-7.12 (m, 4H), 6.75-6.71 (m, 1H), 6.66-6.63 (m, 2H), 3.77 (brs, 1H), 3.26 (t, J 6.9 Hz, 2H), 3.11 (t, J 6.9 Hz, 2H), 2.11 (quintet, J 6.9 Hz, 2H).

1-(Phenyl)-4-(phenylamino)butan-1-one (**51b**)²²⁹

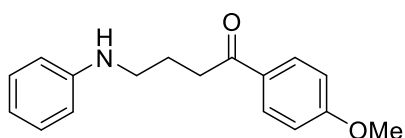


According to general procedure 4, *N*-phenyl-2-pyrrolidinone (1.61 g, 10 mmol, 1.0 eq) and phenyl magnesium bromide (2.67 M in THF, 4.12 mL, 11 mmol, 1.1 eq) were stirred at room temperature for 17 hours. The product (**51b**) was purified according to general procedure 4 by flash silica gel column chromatography and isolated as an off-white solid (1.59 g, 6.6 mmol, 66%).

This data matches data reported in literature.²²⁹

$^1\text{H NMR}$ (CDCl_3 , 400 MHz) δ_{H} 8.01-7.98 (m, 2H), 7.61-7.57 (m, 1H), 7.51-7.47 (m, 2H), 7.23-7.18 (m, 2H), 6.75-6.71 (m, 1H), 6.67-6.64 (m, 2H), 3.79 (brs, 1H), 3.26 (t, J 6.9 Hz, 2H), 3.15 (t, J 6.9 Hz, 2H), 2.12 (quintet, J 6.9 Hz, 2H).

1-(4-Methoxyphenyl)-4-(phenylamino)butan-1-one (**51c**)²²⁹

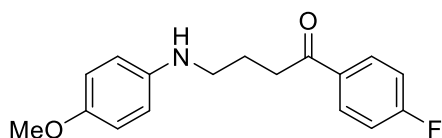


According to general procedure 4, *N*-phenyl-2-pyrrolidinone (1.61 g, 10 mmol, 1 eq) and 4-methoxyphenyl magnesium bromide (0.75 M in THF, 14.7 mL, 11 mmol, 1.1 eq) were stirred at room temperature for 17 hours. The product (**51c**) was purified according to general procedure 4 by flash silica gel column chromatography and isolated as an off-white solid (1.47 g, 5.5 mmol, 55%).

This data matches data reported in literature.²²⁹

¹H NMR (CDCl₃, 400 MHz) δ_H 7.99-7.95 (m, 2H), 7.21-7.17 (m, 2H), 6.97-6.94 (m, 2H), 6.73-6.70 (m, 1H), 6.66-6.63 (m, 2H), 3.89 (s, 3H), 3.80 (brs, 1H), 3.25 (t, J 6.9 Hz, 2H), 3.09 (t, J 6.9 Hz, 2H), 2.10 (quintet, J 6.9 Hz, 2H).

1-(4-Fluorophenyl)-4-((4-methoxyphenyl)amino)butan-1-one (**51d**)²²⁸

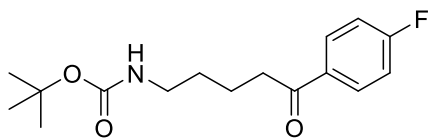


According to general procedure 4, *N*-(*para*-methoxyphenyl)pyrrolidinone (1.91 g, 10 mmol, 1 eq) and 4-fluorophenyl magnesium bromide (0.7 M in THF, 16 mL, 11 mmol, 1.1 eq) were stirred at room temperature for 17 hours. The product (**51d**) was purified by recrystallisation (using minimal EtOAc and subsequent dilution with hexane) and isolated as a pale brown solid (1.26 g, 4.4 mmol, 44%).

This data matches data reported in literature.²²⁸

¹H NMR (CDCl₃, 400 MHz) δ_H 8.03-7.99 (m, 2H), 7.14-7.12 (m, 2H), 6.82-6.78 (m, 2H), 6.63-6.59 (m, 2H), 6.63-6.59 (m, 2H), 3.77 (s, 3H), 3.46 (brs, 1H), 3.21 (t, J 6.8 Hz, 2H), 3.11 (t, J 6.8 Hz, 2H), 2.09 (quintet, J 6.8 Hz, 2H).

1-(4-Fluorophenyl)-5-(Boc-amino)pentan-1-one (**51e**)³²²



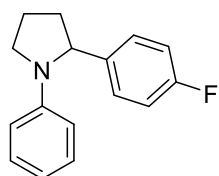
According to general procedure 4, *N*-Boc-2-piperidinone (1 g, 5 mmol, 1 eq) and 4-fluorophenyl magnesium bromide (0.7 M in THF, 8 mL, 5.5 mmol, 1.1 eq) were stirred at room temperature for 17 hours. The product (**51e**) was purified by recrystallisation (using minimal EtOAc and subsequent dilution with hexane) and isolated as a pale brown solid (0.4 g, 1.4 mmol, 27%).

This data matches data reported in literature.³²²

$^1\text{H NMR}$ (CDCl_3 , 400 MHz) δ_{H} 8.02-7.99 (m, 2H), 7.18-7.12 (m, 2H), 4.62 (brs, 1H), 3.21-3.16 (m, 2H), 2.99 (t, J 7.0 Hz, 2H), 1.79 (quintet, J 6.8 Hz, 2H), 1.63-1.56 (m, 2H), 1.46 (s, 3H).

7.3.3.3 Intramolecular Reductive Amination Cyclisation

N-Phenyl-2-(4-fluorophenyl)-pyrrolidine (**52a**)²²⁹



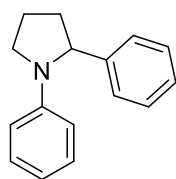
According to general procedure 5, 1-(4-fluorophenyl)-4-(phenylamino)butan-1-one **51a** (52 mg, 0.2 mmol, 1 eq), **16b** (1.0 mg, 2 μmol , 0.01 eq, 1 mol%) and dimethylphenylsilane (0.11 mL, 0.7 mmol, 3.5 eq) were stirred at room temperature for 17 hours. were heated at 100 °C. The product (**52a**) was estimated by ^1H and ^{19}F NMR spectroscopy according to general procedure 5 (96%). The product was also purified by flash silica gel column chromatography (hexane) and isolated pure as a pale-yellow oil (10 mg, 0.04 mmol, 21%).

This data matches data reported in literature.²²⁹

$^1\text{H NMR}$ (CDCl_3 , 400 MHz) δ_{H} 7.29-7.23 (m, 4H), 7.09-7.05 (m, 2H), 6.75 (t, J 7.2 Hz, 1H), 6.58 (d, J 8.3 Hz, 2H) 4.80 (dd, J 8.1, 1.4 Hz, 1H), 3.82-3.77 (m, 1H), 3.52-3.46 (m, 1H), 2.51-2.41 (m, 1H), 2.13-1.97 (m, 3H).

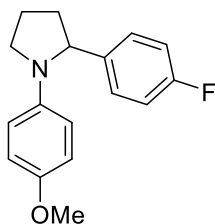
Title compound **52a** was also isolated with the ethoxydimethylphenylsilane **58** impurity as a clear oil (56 mg, 61% yield, 53% purity).

N-Phenyl-2-(4-fluorophenyl)-pyrrolidine (**52b**)²²⁹



According to general procedure 5, 1-(phenyl)-4-(phenylamino)butan-1-one **51b** (48 mg, 0.2 mmol, 1 eq), **16b** (1.0 mg, 0.002 mmol, 0.01 eq, 1 mol%) and dimethylphenylsilane (0.11 mL, 0.7 mmol, 3.5 eq) were stirred at room temperature for 17 hours. were heated at 100 °C. The product (**52a**) was estimated by ^1H according to general procedure 5 (93%).

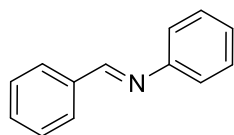
Whilst **52b** was not isolated the crude NMR spectroscopic data matches data reported in literature.²²⁹

N-Phenyl-2-(4-fluorophenyl)-pyrrolidine (**52d**)²²⁸

According to general procedure 5, 1-(4-fluorophenyl)-4-((4-methoxyphenyl)amino)butan-1-one **51d** (57 mg, 0.2 mmol, 1 eq), **16b** (1.0 mg, 0.002 mmol, 0.01 eq, 1 mol%) and dimethylphenylsilane (0.11 mL, 0.7 mmol, 3.5 eq) were stirred at room temperature for 17 hours. were heated at 100 °C. The product (**52a**) was estimated by ¹H and ¹⁹F NMR according to general procedure 5 (48%).

Whilst **52d** was not isolated the crude NMR spectroscopic data matches data reported in literature.²²⁸

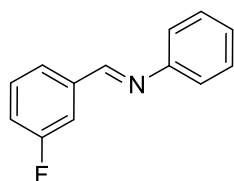
7.3.3.4 Imines Prepared for Reductions

N-(Benzylidene)aniline (**3ae**)³²⁴

3ae was prepared according to general procedure 5 from benzaldehyde (**1a**, 0.51 mL, 0.53 g, 5 mmol) and aniline (**2e**, 455 μL, 0.47 g, 5 mmol) and was isolated as a yellow oil (0.82 g, 4.5 mmol, 90%).

This data matches data reported in literature.³²⁴

¹H NMR (CDCl₃, 400 MHz) δ_H 8.49 (s, 1H), 7.95-7.93 (m, 2H), 7.52-7.50 (m, 3H), 7.45-7.41 (m, 2H), 7.28-7.24 (m, 3H).

N-(3-Fluorobenzylidene)aniline (**3ke**)³²⁵

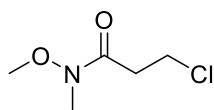
3ke was prepared according to general procedure 5 from 3-F benzaldehyde (**1k**, 0.53 mL, 0.62 g, 5 mmol) and aniline (**2e**, 455 μL, 0.47 g, 5 mmol) and was isolated as a yellow oil (0.92 g, 4.62 mmol, 92%).

This data matches data reported in literature.³²⁵

¹H NMR (CDCl₃, 400 MHz) δ_H 8.47 (s, 1H), 7.72-7.66 (m, 2H), 7.50-7.42 (m, 3H), 7.31-7.19 (m, 4H).

¹⁹F NMR (CDCl₃, 376 MHz) δ_F -112.7 (s, 1F).

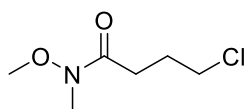
7.3.3.5 Weinreb amides

3-Chloro-*N*-methoxy-*N*-methylpropanamide (**62a**)³²⁶

In oven dried glassware crude 3-chloropropionyl chloride was prepared from refluxing 3-chloropropanoic acid (1.09 g, 10.4 mmol) in SOCl_2 (0.76 mL, 10.4 mmol) and DCM (50 mL) for 2 hours. After 2 hours the solvent was removed under vacuum. The crude acid chloride was carried on into the next step without further purification. **62a** was prepared according to general procedure 8 from crude 3-chloropropionyl chloride (1.27 g, 10 mmol) and *N,O*-dimethylhydroxylamine hydrochloride (1.17 g, 12 mmol) and was isolated as a pale yellow oil (1.15 g, 7.59 mmol, 76%).

This data matches data reported in literature.³²⁶

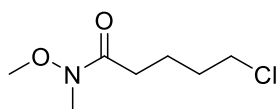
¹H NMR (CDCl_3 , 400 MHz) δ_{H} 3.81 (t, J 6.9 Hz, 2H), 3.71 (s, 3H), 3.21 (s, 3H), 2.92 (t, J 6.9 Hz, 2H).

4-Chloro-*N*-methoxy-*N*-methylbutanamide (**62b**)³²⁶

62b was prepared according to general procedure 8 from crude 4-chloro butyryl chloride (1.12 mL, 1.41 g, 10 mmol) and *N,O*-dimethylhydroxylamine hydrochloride (1.17 g, 12 mmol) and was isolated as a pale yellow oil (1.6 g, 9.7 mmol, 97%).

This data matches data reported in literature.³²⁶

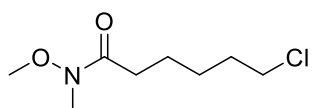
¹H NMR (CDCl_3 , 400 MHz) δ_{H} 3.72 (s, 3H), 3.65 (t, J 6.3 Hz, 2H), 3.20 (s, 3H), 2.64 (t, J 7.0 Hz, 2H), 2.12 (quintet, J 6.5 Hz, 2H).

5-Chloro-*N*-methoxy-*N*-methylpentanamide (**62c**)³²⁷

62c was prepared according to general procedure 8 from crude 4-chloro valeryl chloride (1.29 mL, 1.55 g, 10 mmol) and *N,O*-dimethylhydroxylamine hydrochloride (1.17 g, 12 mmol) and was isolated as a pale yellow/orange oil (1.72 g, 9.6 mmol, 96%).

This data matches data reported in literature.³²⁷

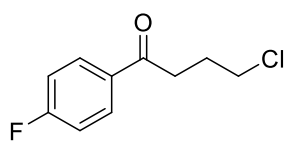
¹H NMR (CDCl_3 , 400 MHz) δ_{H} 3.69 (s, 3H), 3.57 (t, J 6.6 Hz, 2H), 3.19 (s, 3H), 2.47 (t, J 6.6 Hz, 2H), 1.82-1.75 (m, 4H).

6-Chloro-*N*-methoxy-*N*-methylhexanamide (**62d**)

62d was prepared according to general procedure 8 from crude 6-chloro hexanoyl chloride (1.0 g, 5.9 mmol) and *N*,*O*-dimethylhydroxylamine hydrochloride (0.7 g, 7.1 mmol) and was isolated as a pale yellow oil (1.12 g, 5.78 mmol, 98%).

$^1\text{H NMR}$ (CDCl_3 , 400 MHz) δ_{H} 3.68 (s, 3H), 3.54 (t, J 6.6 Hz, 2H), 3.17 (s, 3H), 2.44 (t, J 6.6 Hz, 2H), 1.84-1.77 (m, 2H), 1.70-1.62 (m, 2H), 1.53-1.45 (m, 2H).

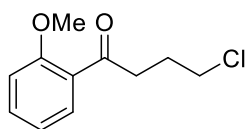
7.3.3.6 Chloro-alkyl substituted ketones

4-Chloro-1-(4-fluorophenyl)-1-butanone (**63a**)³²⁸

63a was prepared according to general procedure 9 from 4-chloro-*N*-methoxy-*N*-methylbutanamide **62b** (0.9 g, 5 mmol) and 4-fluorobromobenzene (0.61 mL, 0.96 g, 5.5 mmol). The product (**63a**) was purified according to general procedure 4 by flash silica gel column chromatography and isolated as a clear oil (0.42 g, 1.96 mmol, 39%).

This data matches data reported in literature.³²⁸

$^1\text{H NMR}$ (CDCl_3 , 400 MHz) δ_{H} 8.03-7.98 (m, 2H), 7.18-7.12 (m, 2H), 3.60 (t, J 6.2 Hz, 2H), 3.00 (t, J 6.8 Hz, 2H), 1.95-1.85 (m, 4H).

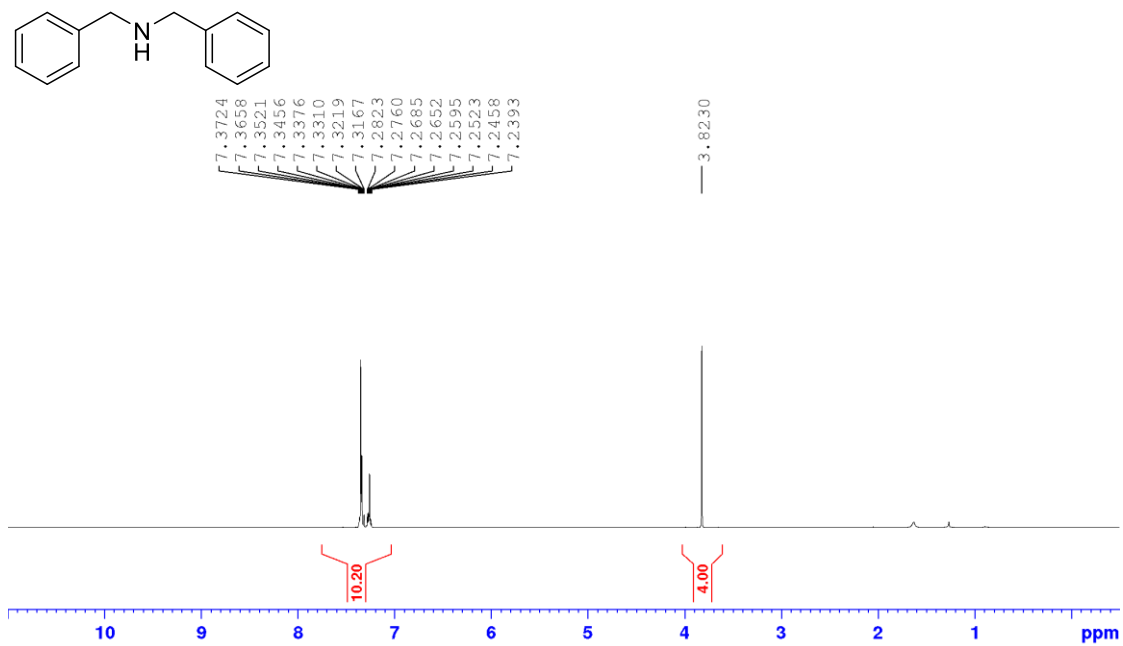
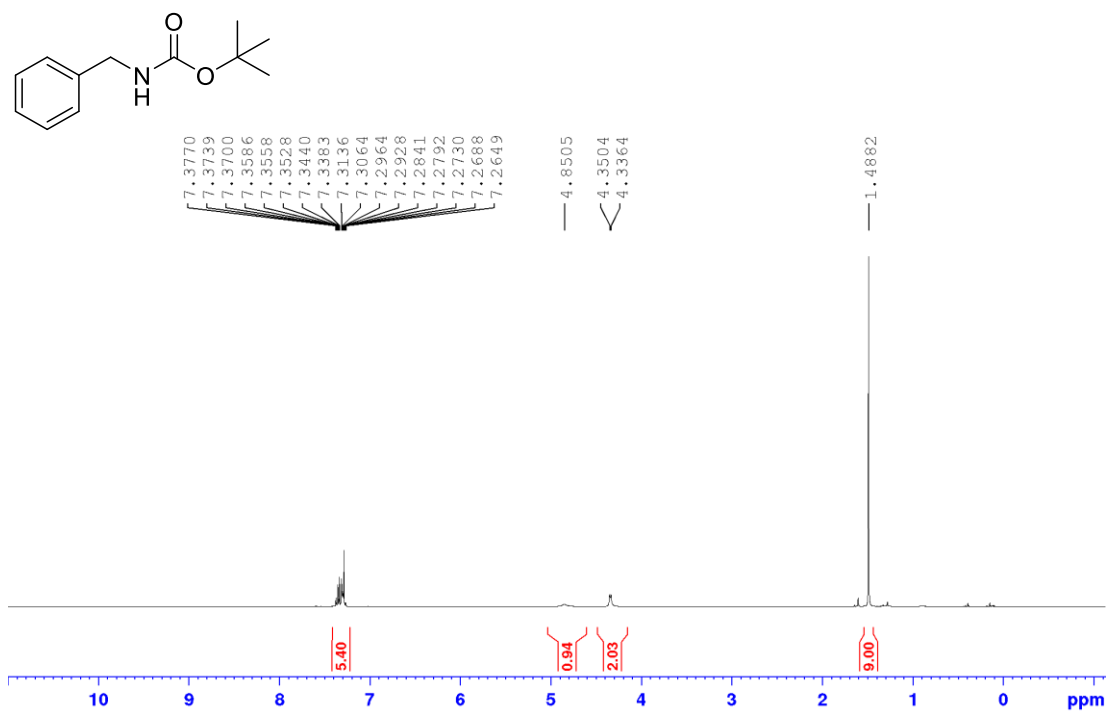
4-Chloro-1-(2-methoxyphenyl)-1-butanone (**63b**)³²⁹

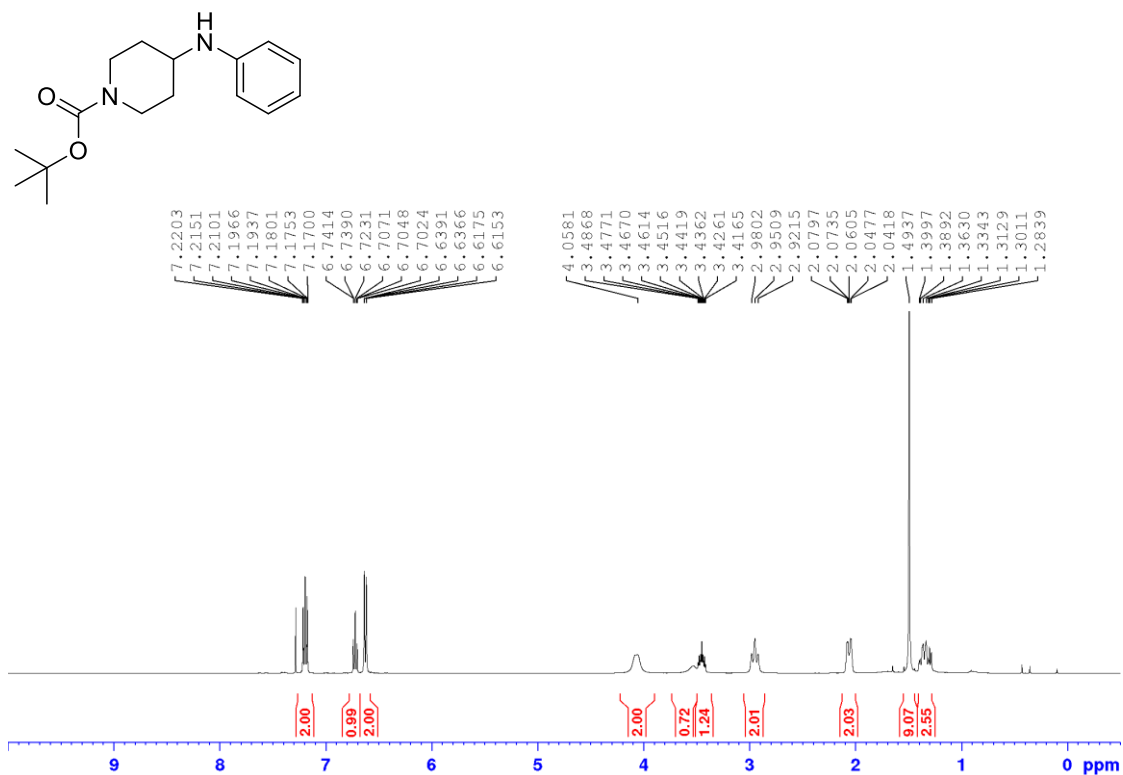
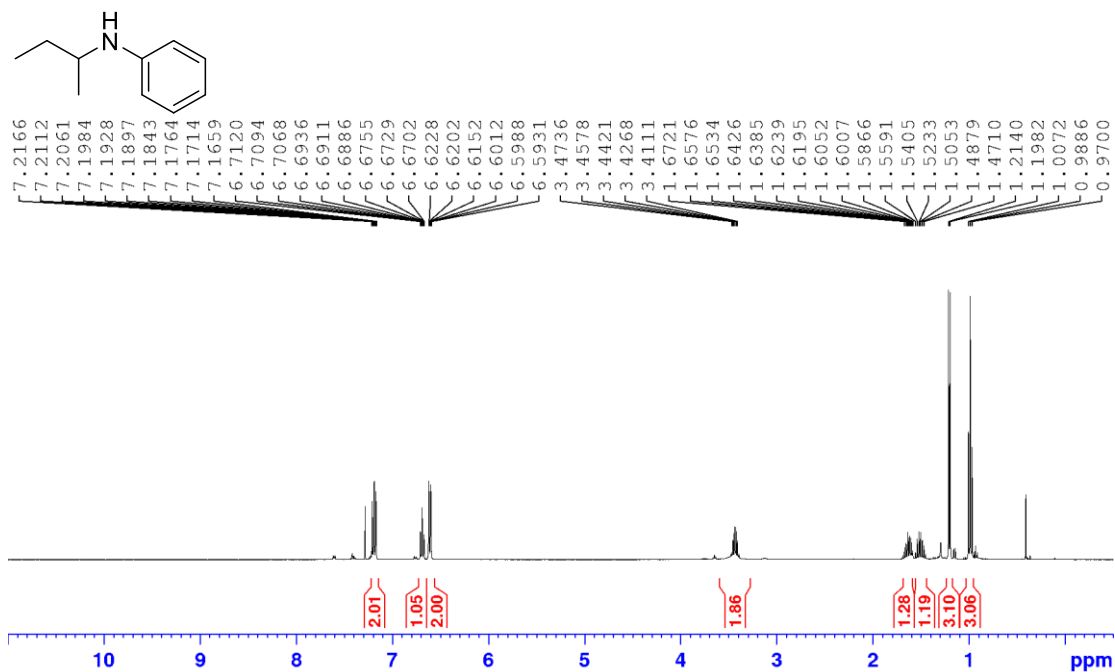
63b was prepared according to general procedure 9 from 4-chloro-*N*-methoxy-*N*-methylbutanamide **62b** (0.5 g, 3 mmol) and 2-bromoanisole (0.41 mL, 0.62 g, 3.3 mmol). The product (**63b**) was purified according to general procedure 4 by flash silica gel column chromatography and isolated as a clear oil (0.2 g, 0.94 mmol, 28%).

This data matches data reported in literature.³²⁹

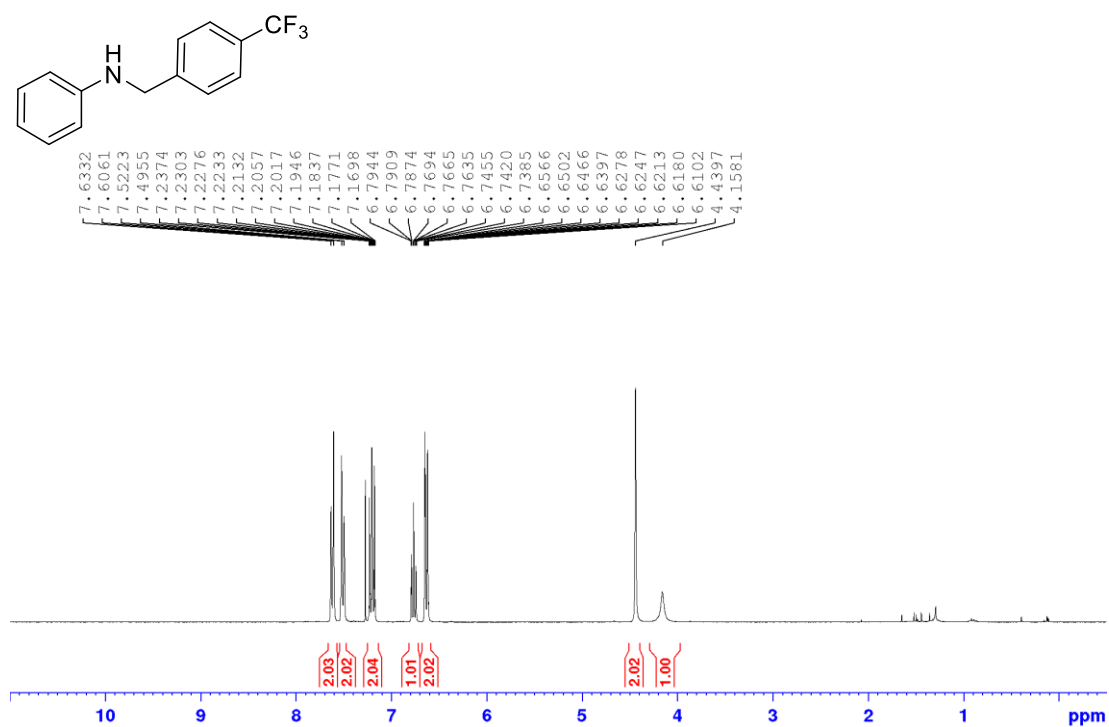
$^1\text{H NMR}$ (CDCl_3 , 400 MHz) δ_{H} 7.72 (dd, J 7.7, 1.8 Hz, 1H), 7.49 (ddd, J 8.4, 7.3, 1.9 Hz, 1H), 7.05-6.98 (m, 2H), 3.94 (s, 3H), 3.67 (t, J 6.3 Hz, 2H), 3.19 (t, J 6.8 Hz, 2H), 2.21 (quintet, J 6.6 Hz, 2H).

7.3.3.7 NMR Spectra of Batch Reductive Aminations with Silanes

Dibenzylamine (**4ag**)*N*-Boc benzylamine (**4ah**)

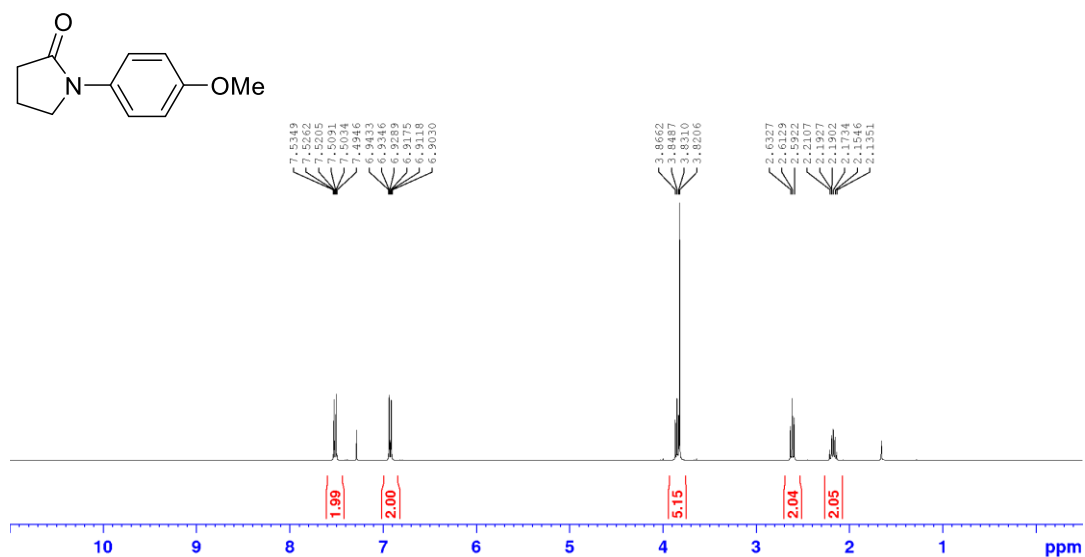
1-*N*-Boc-4-phenylaminopiperidine (**4ce**)*N*-*sec*-Butylaniline (**4de**)

***N*-(4-(Trifluoromethyl)benzyl)benzenamine (49)**

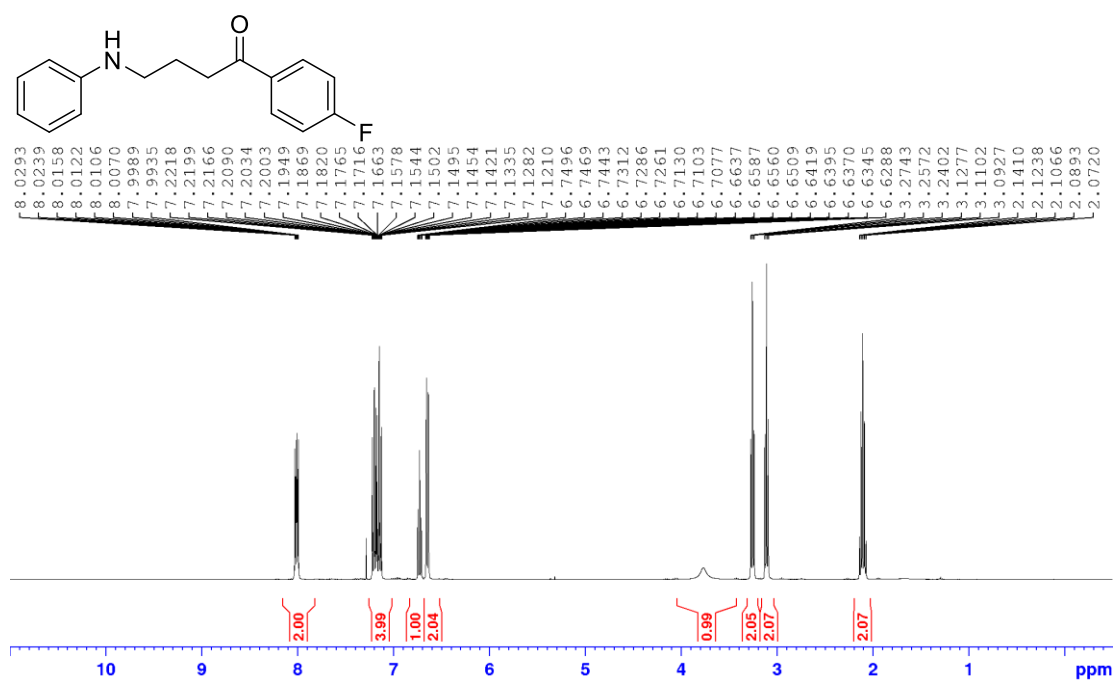


7.3.3.8 NMR Spectra of Amino Ketones and Amino Ketone Starting Materials

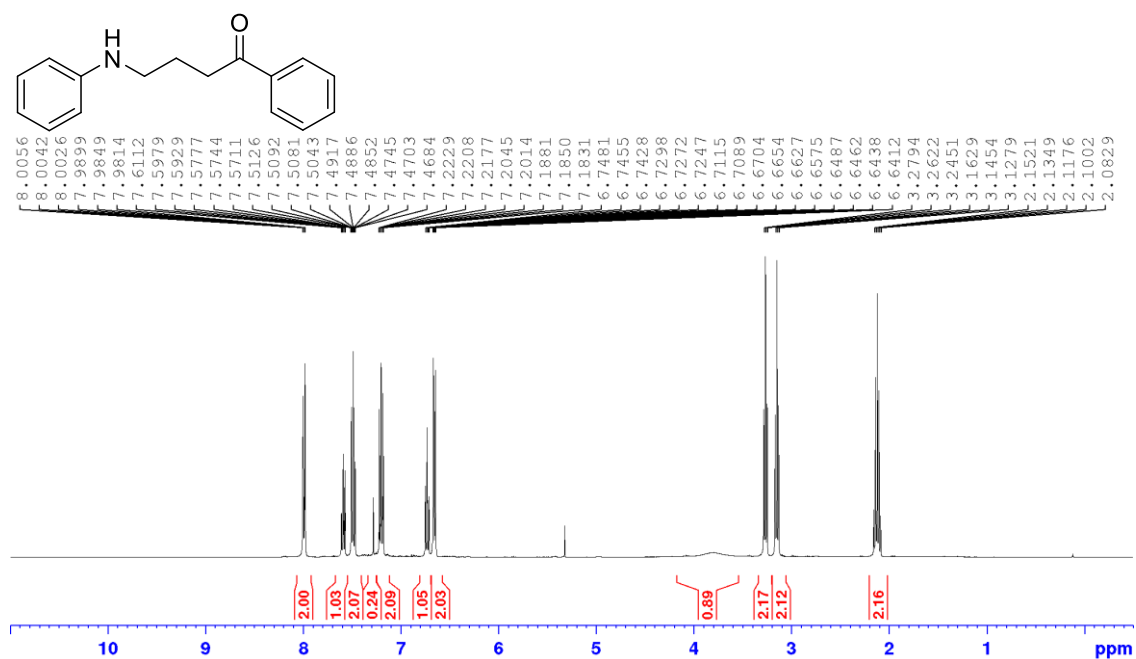
***N*-(*para*-Methoxyphenyl)pyrrolidinone (103b)**

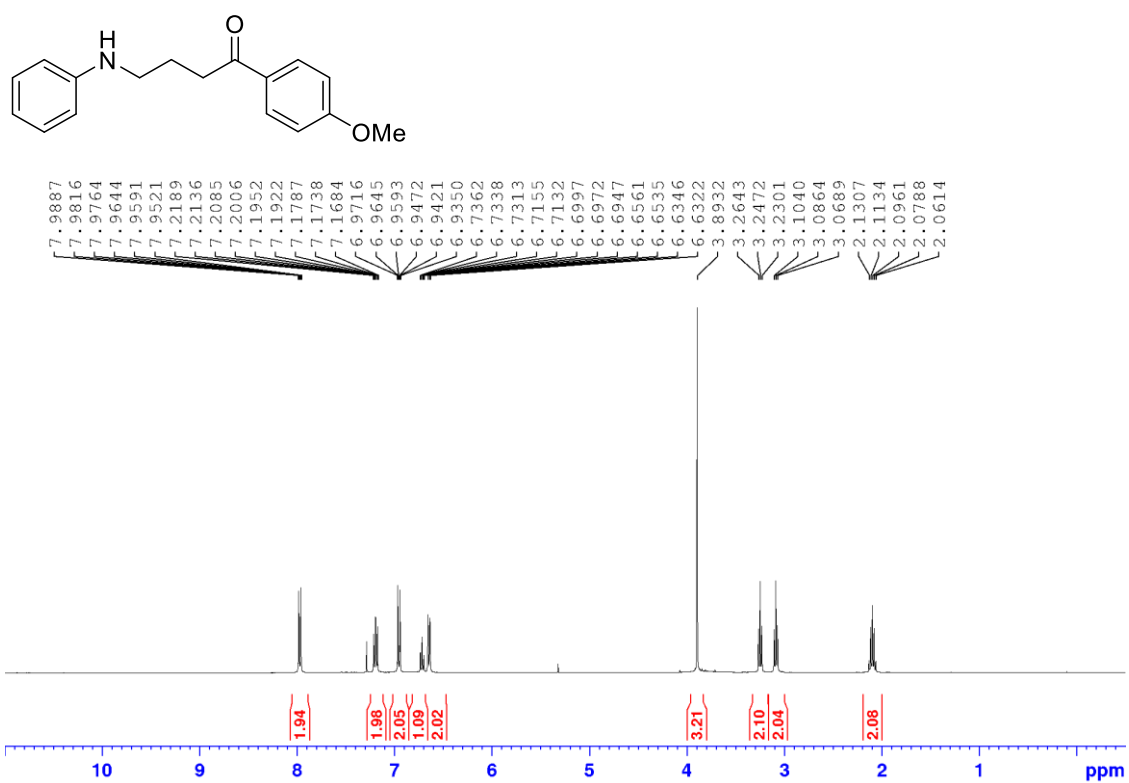
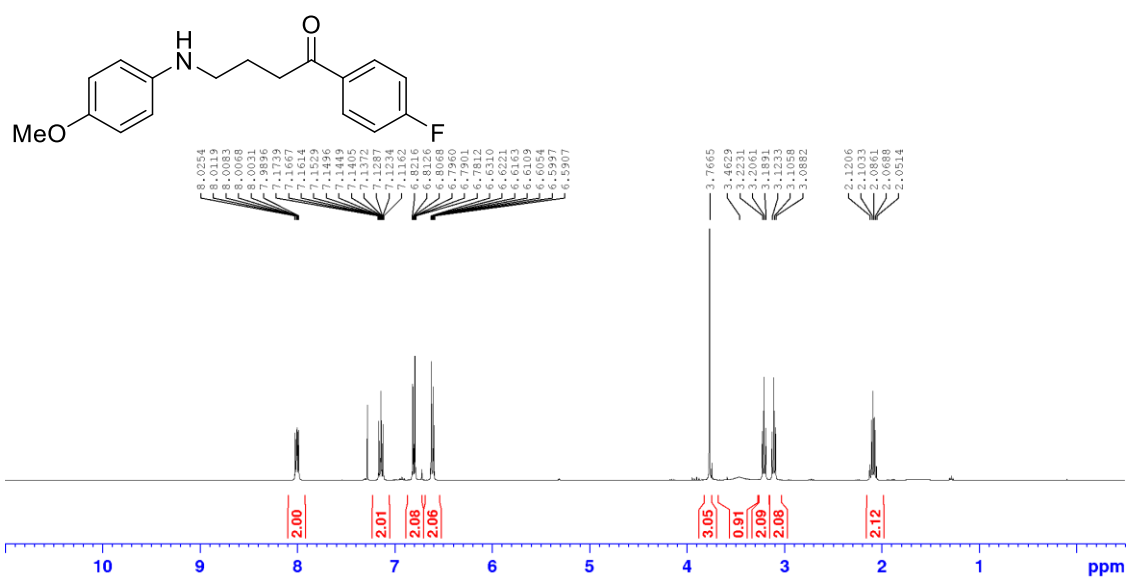


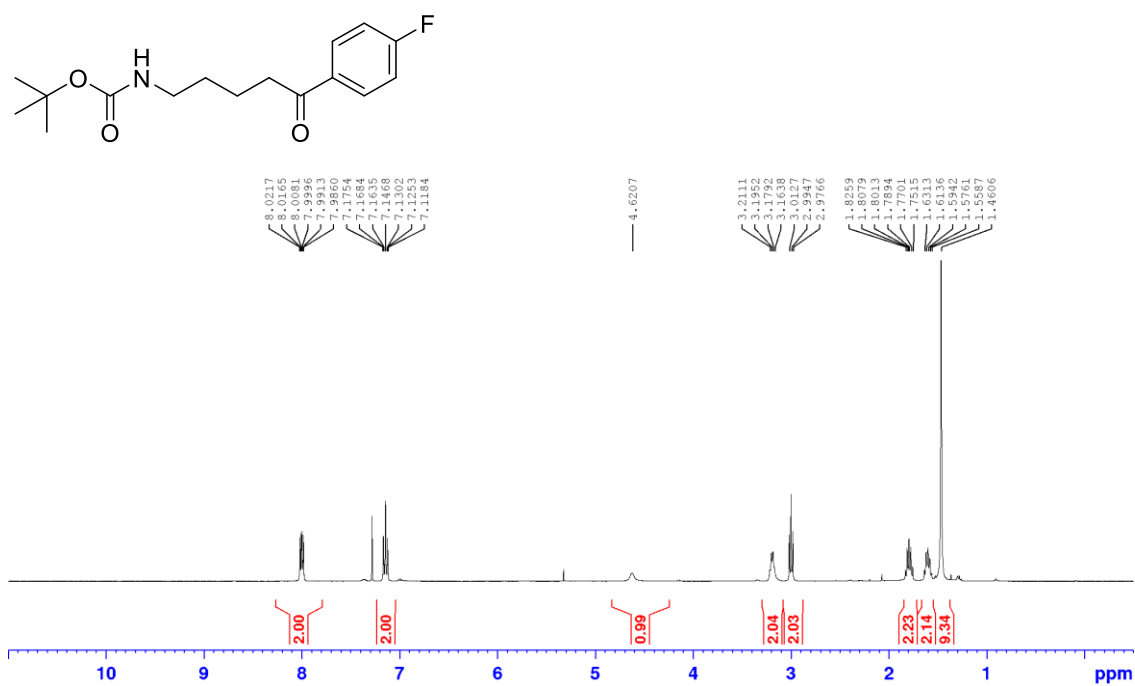
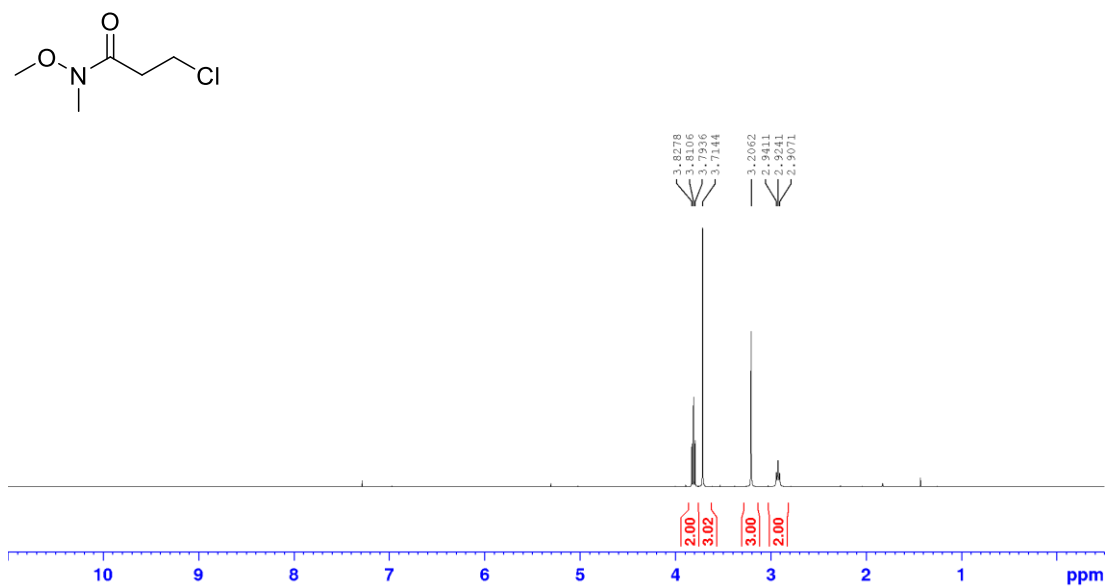
1-(4-Fluorophenyl)-4-(phenylamino)butan-1-one (51a)

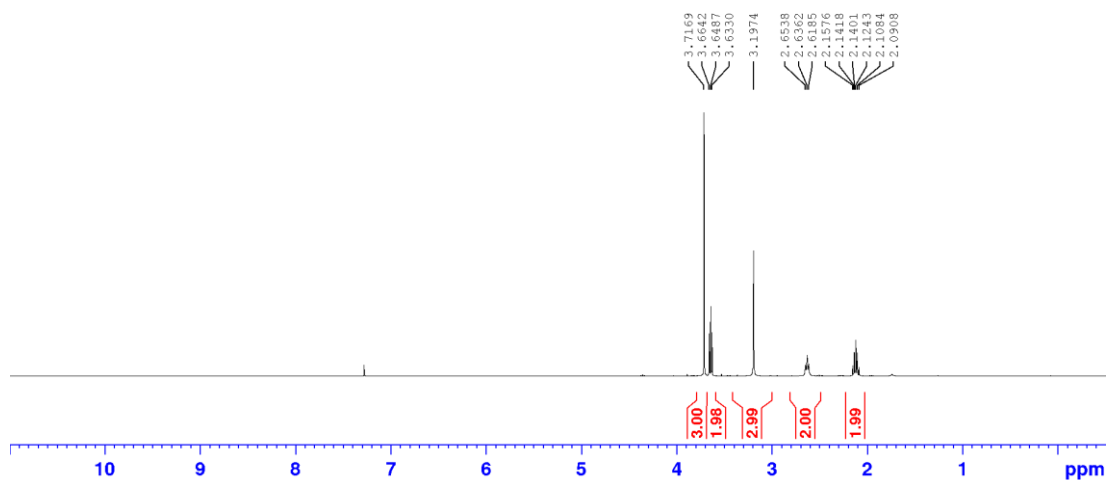
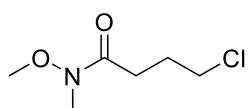
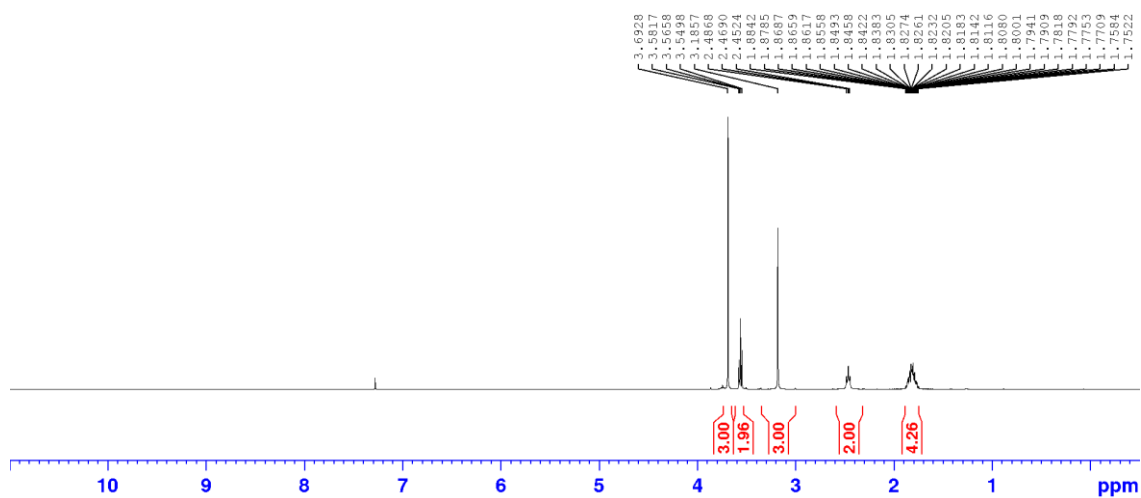
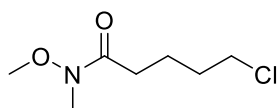


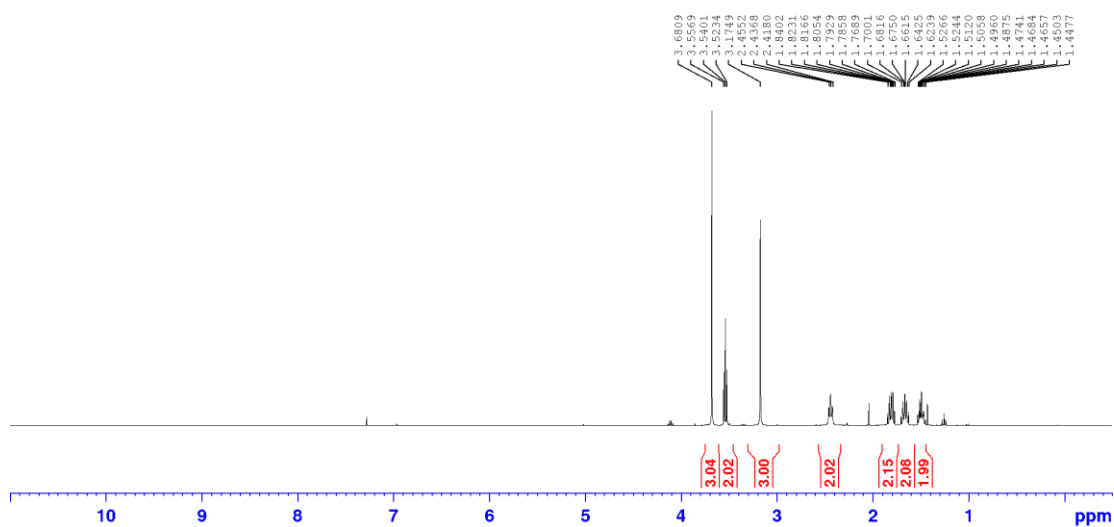
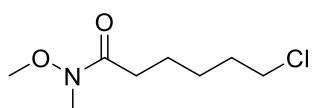
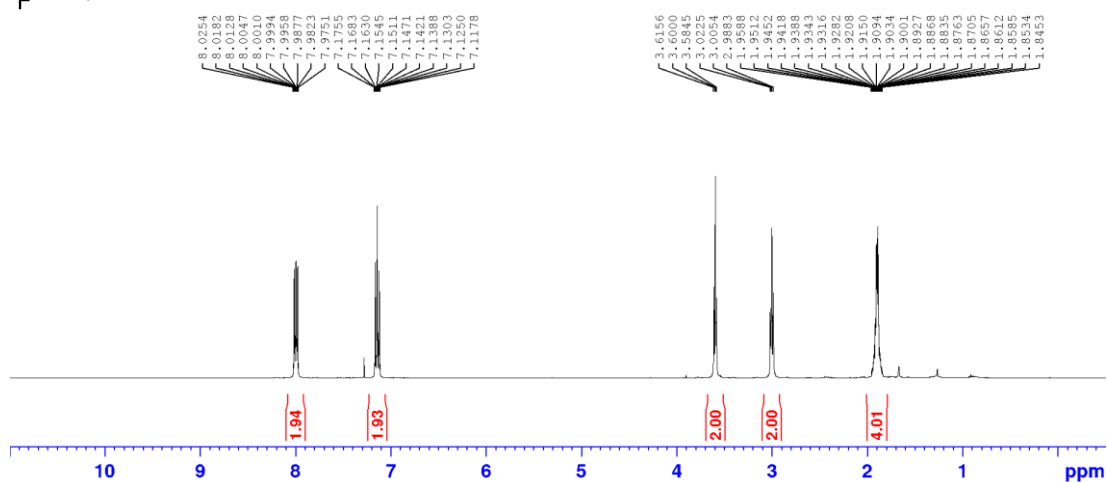
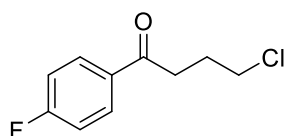
1-(Phenyl)-4-(phenylamino)butan-1-one (51b)

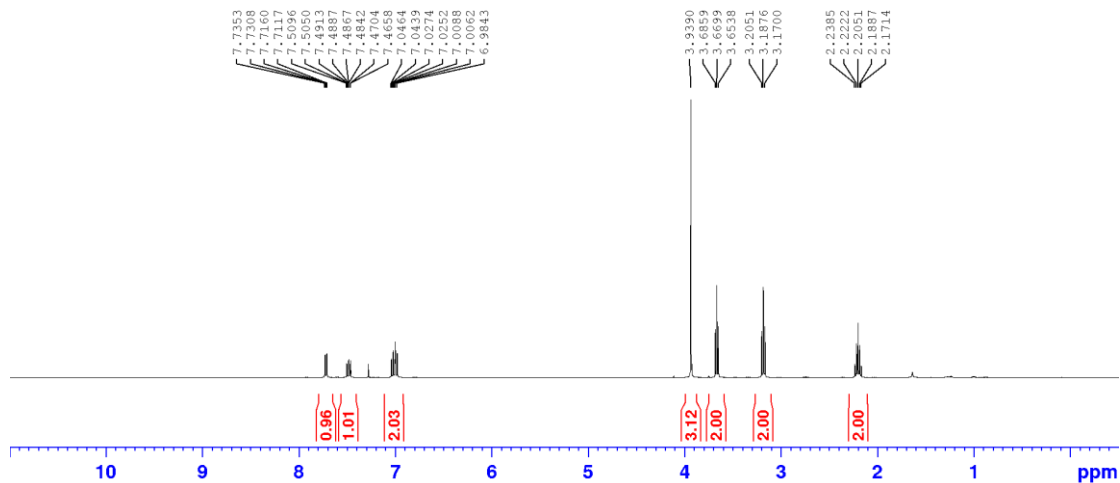
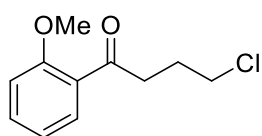


1-(4-Methoxyphenyl)-4-(phenylamino)butan-1-one (**51c**)1-(4-Fluorophenyl)-4-((4-methoxyphenyl)amino)butan-1-one (**51d**)

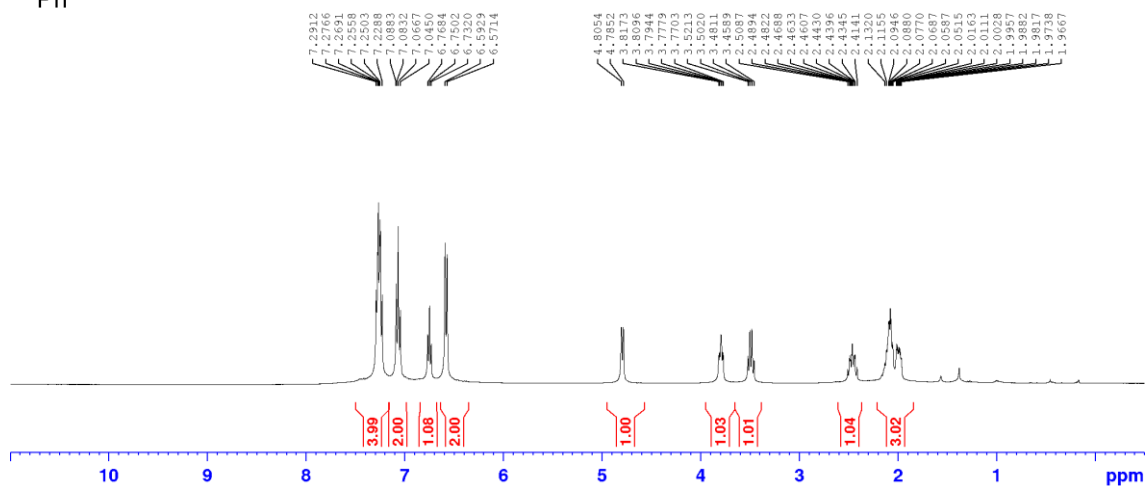
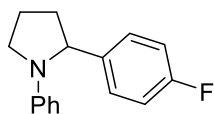
1-(4-Fluorophenyl)-5-(Boc-amino)pentan-1-one (**51e**)3-Chloro-N-methoxy-N-methylpropanamide (**62a**)

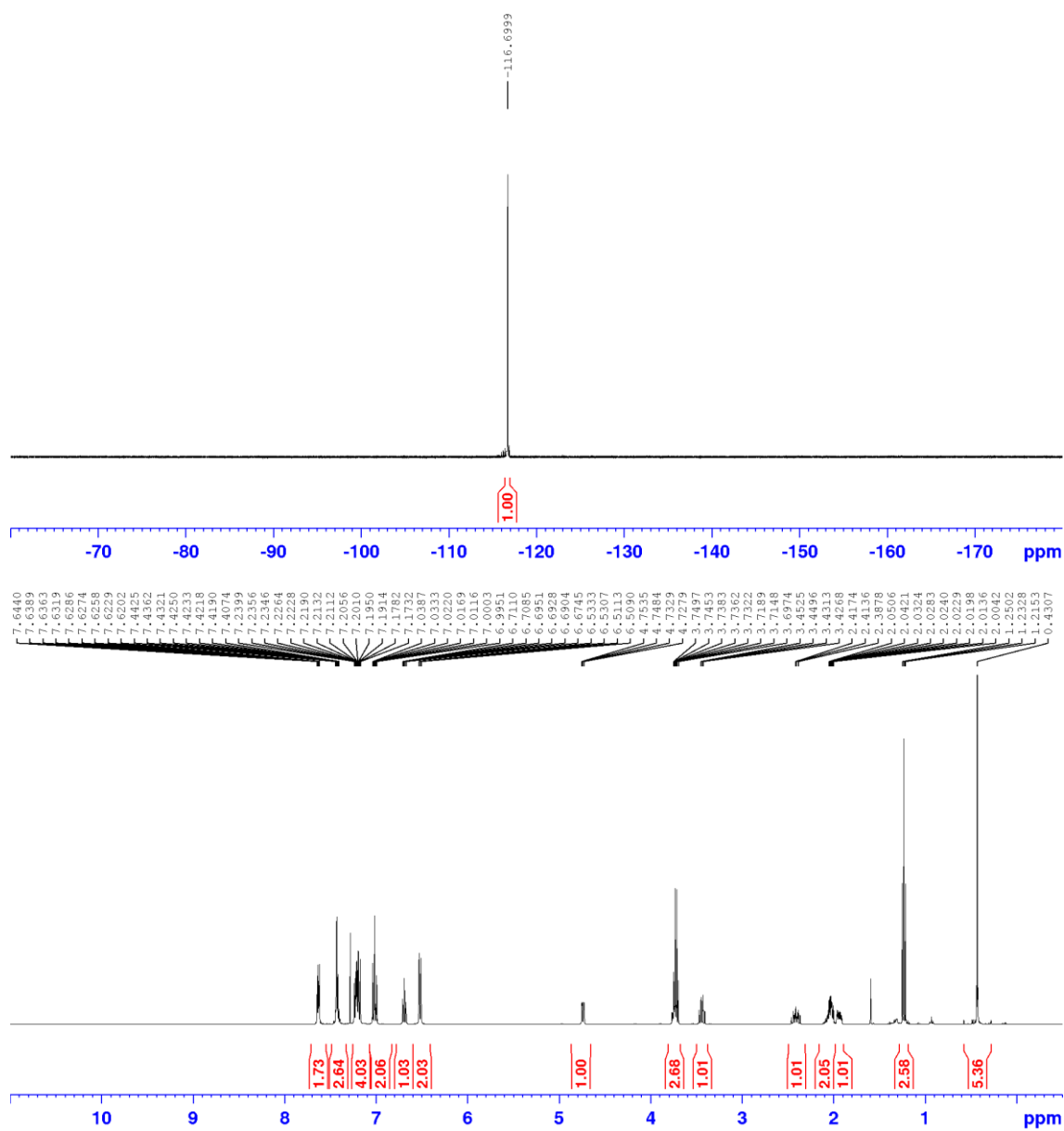
4-Chloro-*N*-methoxy-*N*-methylbutanamide (**62b**)5-Chloro-*N*-methoxy-*N*-methylpentanamide (**62c**)

6-Chloro-*N*-methoxy-*N*-methylhexanamide (**62d**)4-Chloro-1-(4-fluorophenyl)-1-butanone (**63a**)

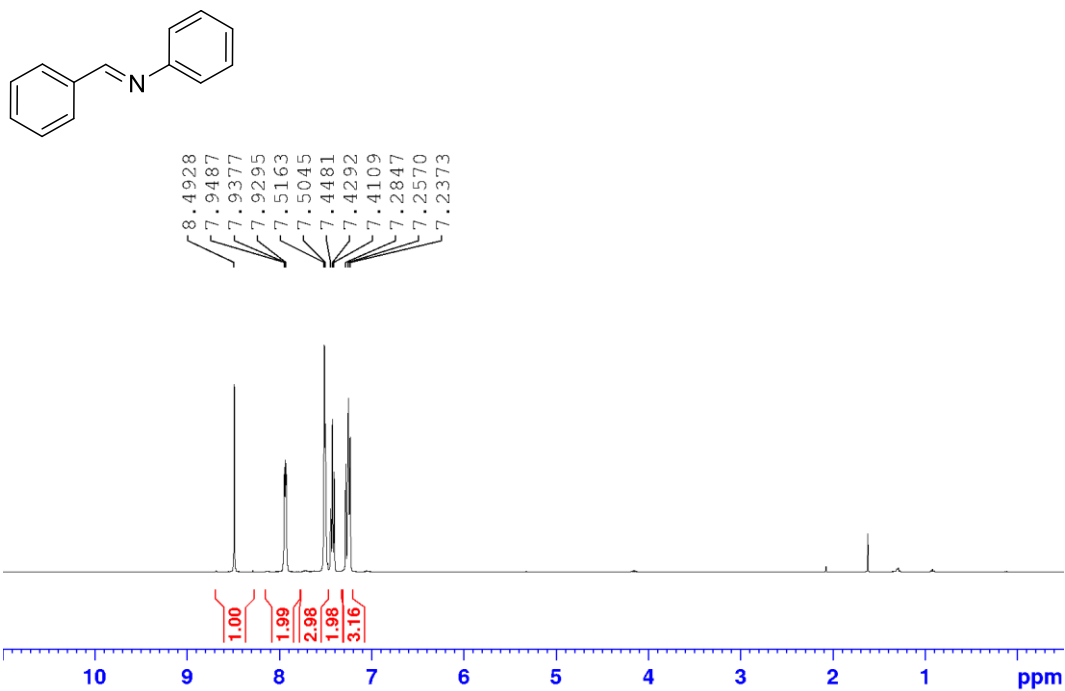
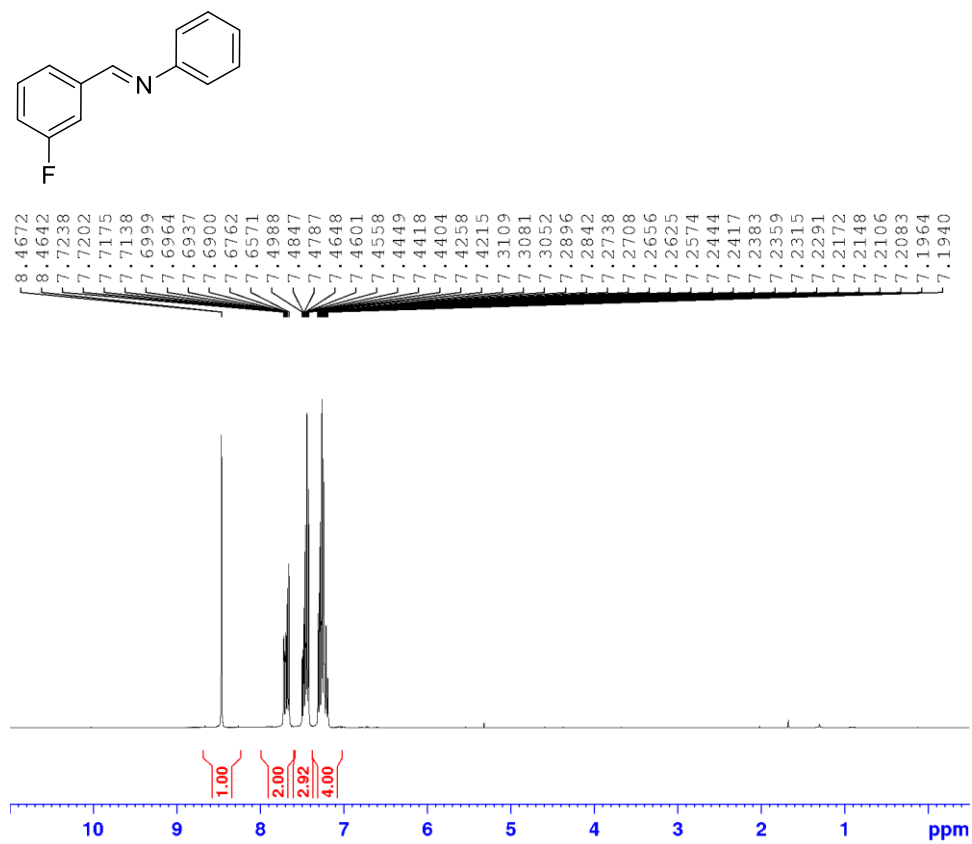
4-Chloro-1-(2-methoxyphenyl)-1-butanone (**63b**)

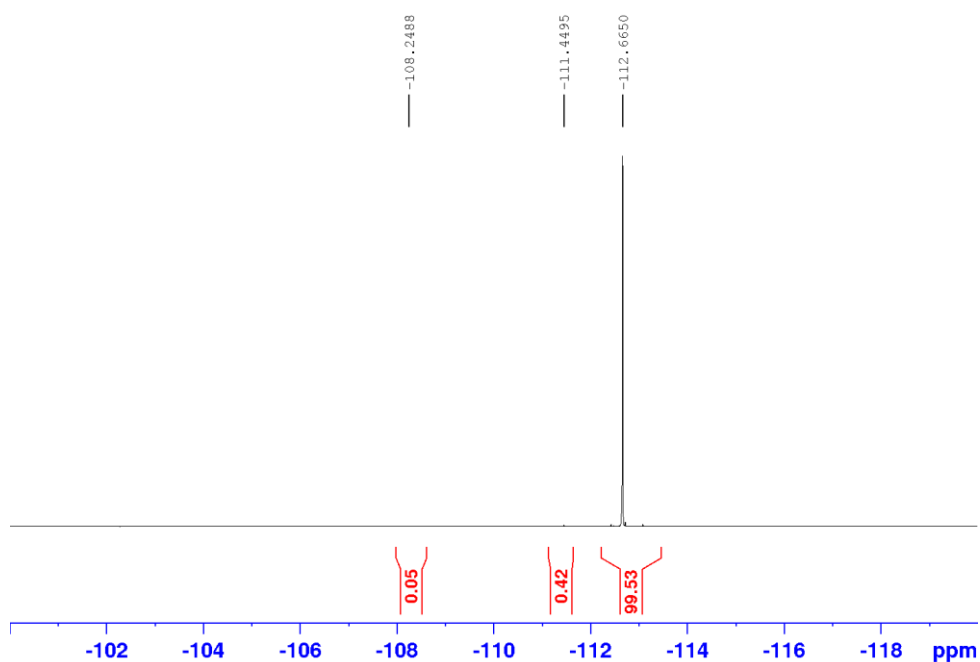
7.3.3.9 NMR Spectra Amino Ketones Intramolecular Reductive Amination Cyclisation

N-Phenyl-2-(4-fluorophenyl)-pyrrolidine (**52a**)



7.3.3.10 NMR Spectra of Imines

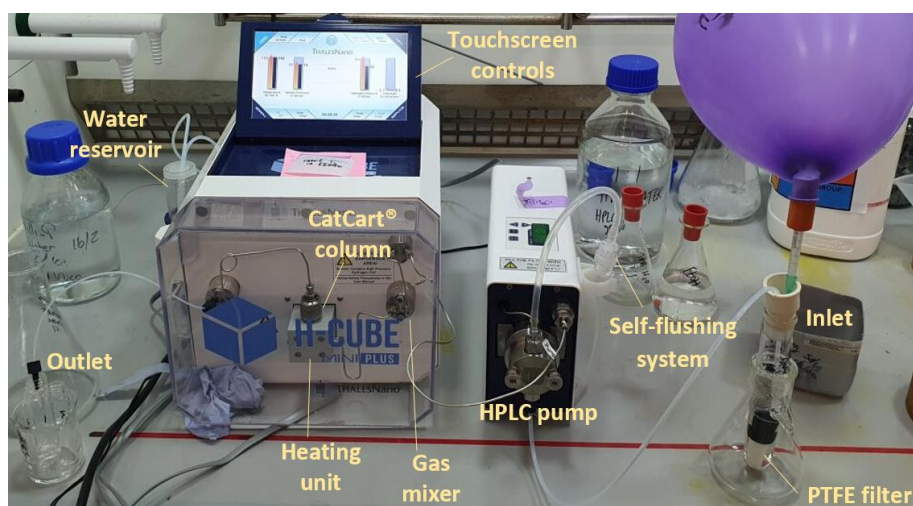
N-(Benzylidene)aniline (**3ae**)***N***-(3-Fluorobenzylidene)aniline (**3ke**)



7.4 Experimental Details for Chapter Four

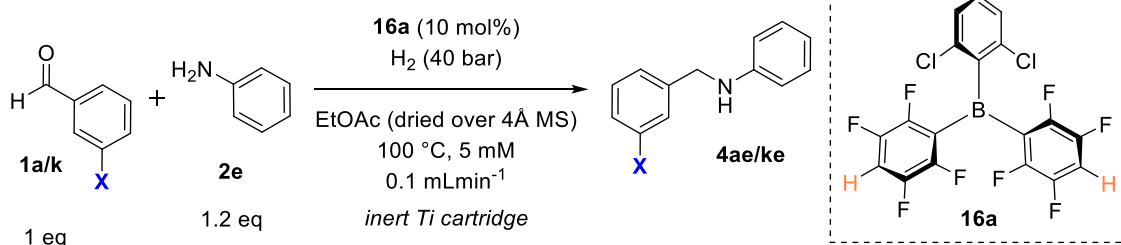
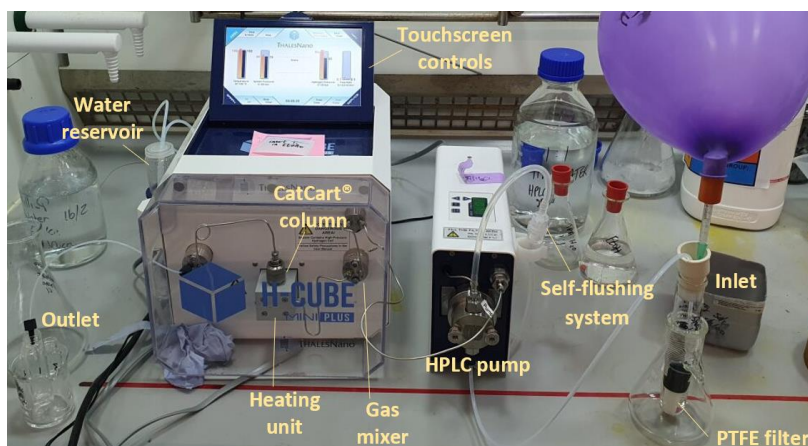
7.4.1 General Procedures

7.4.1.1 General Procedure 10: Equilibration of H-cube®



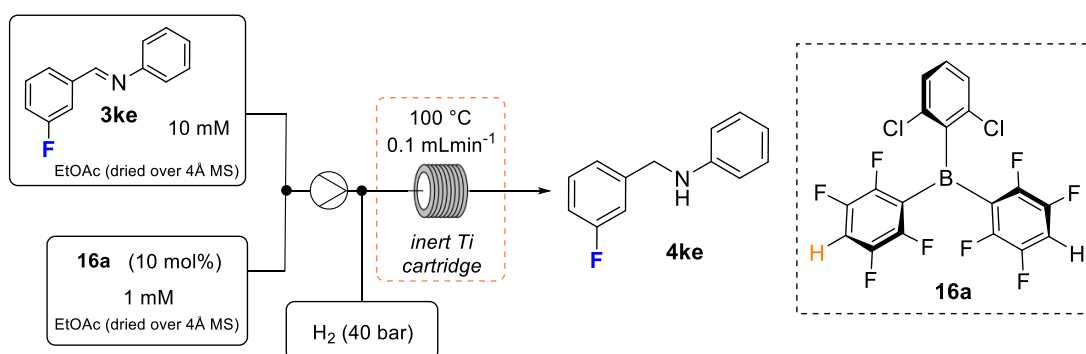
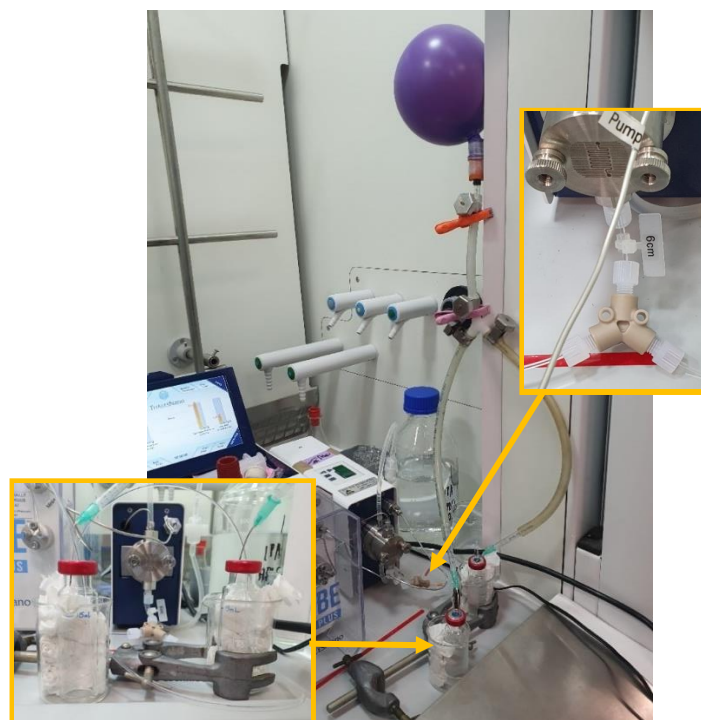
The reaction parameters (temperature, flow rate and H₂ pressure) were selected on the H-Cube®, fitted with the inert titanium CatCart®. Then, the desired solvent was pumped through the system until the instrument had equilibrated at the desired reaction parameters and that EtOH (H-Cube® storage solvent) could not be detected in the aliquots of solvent pumped out of the H-Cube®.

7.4.1.2 General Procedure 11: Reductive Amination Setup in Continuous Flow with One Stock Solution using the PTFE filter inlet



To an oven dried Schlenk tube and under an atmosphere of argon were added sequentially aniline (11 μL , 0.12 mmol, 1.2 eq), aldehyde **1a** or **k** (0.1 mmol, 1 eq) and anhydrous EtOAc (19 mL). To this mixture, a solution of **16a** (4.55 mg, 0.01 mmol, 0.1 eq, 10 mol%), prepared from the addition of anhydrous EtOAc (1 mL) to pre-weighed catalyst, was added and the reaction mixture was stirred at room temperature for 2 minutes. After equilibration of the H-cube[®] to the desired parameters, the sample inlet line fitted with the PTFE filter was inserted into the oven dried Schlenk tube containing the reaction mixture, which was immediately stoppered using a pierced Suba seal (shown in the above image) and placed under an inert atmosphere of argon. The reaction progress was monitored by collection of separate solutions at given time intervals (40 – 60, 60 – 80, and 80 – 100 minutes). The yields were determined from aliquots taken from solution 1 (40 – 60 minutes unless otherwise stated in Table 13, Table 14, Figure 37, Figure 40, Scheme 54 and Scheme 55) using quantitative ¹H and ¹⁹F NMR spectroscopic data, by relative integration of product and starting material resonances.

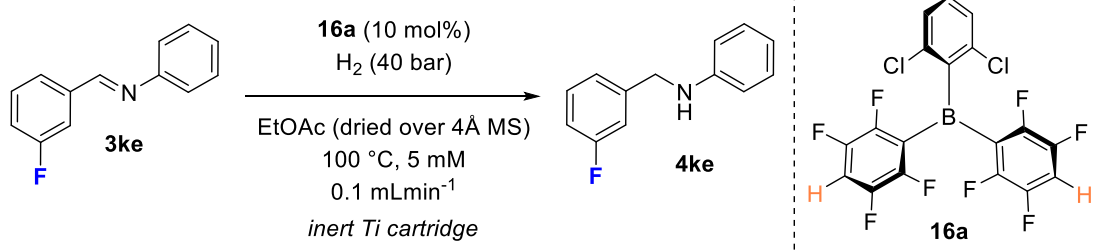
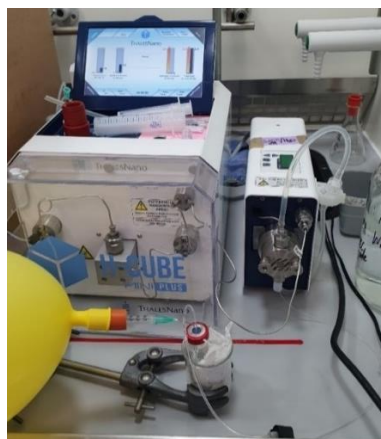
7.4.1.3 General Procedure 12: Anhydrous Reduction Setup using Two Stock Solutions in Continuous Flow using Hydrogen



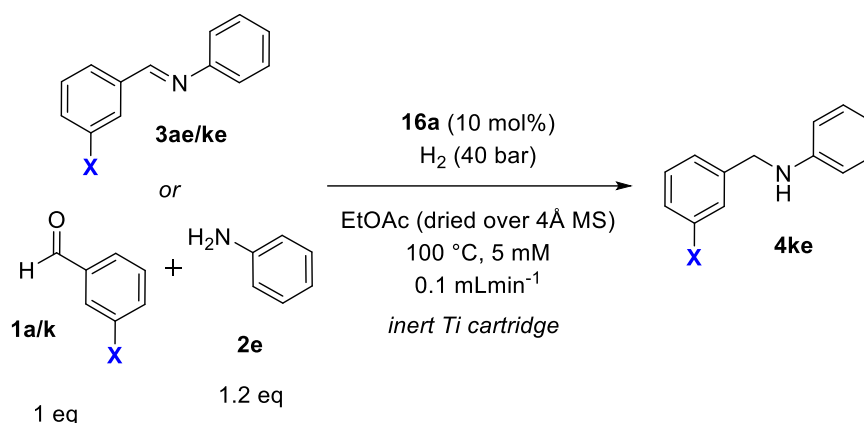
To an oven dried Schlenk tube and under an atmosphere of argon was added *N*-(3-fluorobenzylidene)aniline (50 mg, 0.25 mmol, 1 eq) and anhydrous EtOAc (25 mL) (Reaction mixture 1 (10 mM)). To another oven dried Schlenk tube and under an atmosphere of argon was added **16a** (11.4 mg, 0.025 mmol, 0.1 eq, 10 mol%) and anhydrous EtOAc (25 mL) (Reaction mixture 2 (1 mM)). The H-Cube[®] was set up with two sealed oven dried 10 mL crimp cap vials as inlets under an inert atmosphere of argon (see image above). After equilibration, according to general procedure 10, the two reaction mixtures were simultaneously transferred to the two 10 mL crimp cap vial inlets and placed under an inert atmosphere of argon. The reaction was monitored by aliquots

of the crude reaction mixture (0.5 mL) taken at given time intervals (see Figure 43) and analysed by quantitative ^1H and ^{19}F NMR spectroscopy. The yields were determined from each aliquot by quantitative ^{19}F NMR spectrum integration by relative integration of product and starting material resonances.

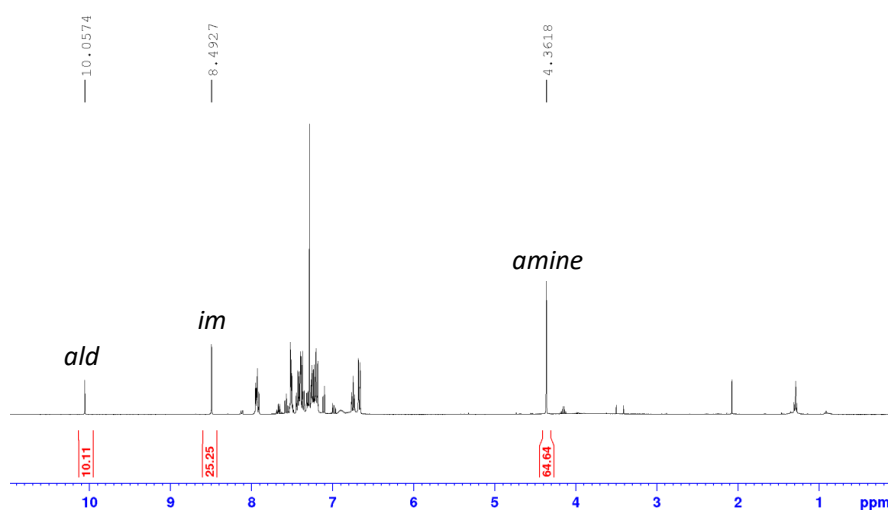
7.4.1.4 General Procedure 13: Anhydrous Reduction Setup in Continuous Flow using a Single Stock Solution

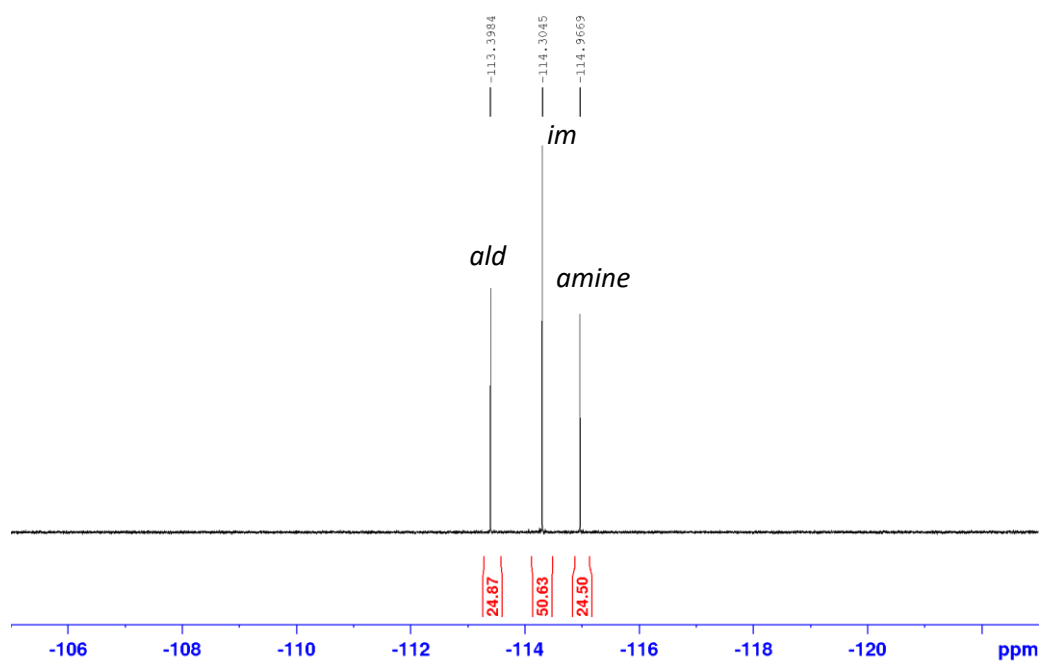
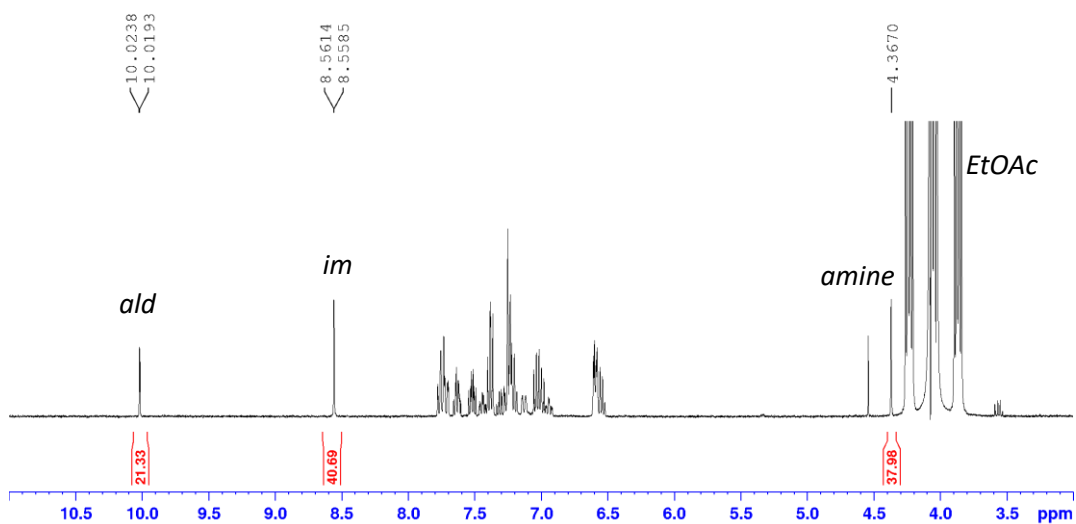


To an oven dried Schlenk tube and under an atmosphere of argon were added sequentially *N*-(3-fluorobenzylidene)aniline (20 mg, 0.1 mmol, 1 eq), **16a** (2.3 mg, 5 μmol , 0.05 eq, 5 mol%) and anhydrous EtOAc (17.5 mL). The reaction parameters (100 $^\circ\text{C}$, 0.1 mLmin $^{-1}$, and 40 bar H $_2$ pressure) were selected on the H-Cube $^\circ$, fitted with the inert titanium CatCart $^\circ$ and set up with an oven dried 10 mL crimp cap vial as inlet under an inert atmosphere of argon (see image above Figure 44). After equilibration, according to general procedure 10, the reaction mixture was transferred to the 10 mL crimp cap vial inlet under an inert atmosphere of argon. The reaction was monitored by aliquots of the crude reaction mixture (0.5 mL), one combined aliquot (20 – 60 minutes, 4 mL) was collected and analysed by quantitative ^1H and ^{19}F NMR spectroscopy. The yields were determined from each aliquot by quantitative ^{19}F NMR spectrum integration by relative integration of product and starting material resonances.

7.4.1.5 Typical $^1\text{H}/^{19}\text{F}$ NMR Spectroscopic Yield Determination

During the preliminary results ($X = \text{H}$) aliquots were taken and volatiles were removed under vacuum before an NMR sample was prepared in CDCl_3 . The determination of the yields was based ^1H NMR spectrum using the benzylic protons α to the N on the product (d, $\delta \sim 4.36$ ppm) (top). Alternatively, for the solvent optimisation ($X = \text{F}$) and thereafter the reaction were monitored by aliquots of the crude reaction mixture (0.5 mL), and yields were determined from each aliquot by quantitative ^1H and ^{19}F NMR spectroscopy. The determination of the yields was based on the ^1H NMR spectrum using the benzylic protons α to the N on the product (d, $\delta \sim 4.37$ ppm) (middle) or ^{19}F NMR spectrum (bottom, $X = \text{F}$).

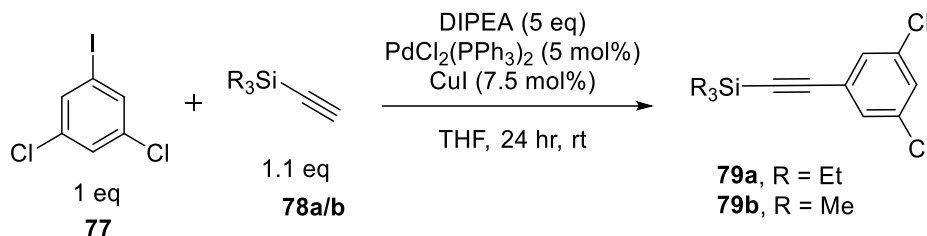




7.5 Experimental Details for Chapter Five

7.5.1 General Procedures

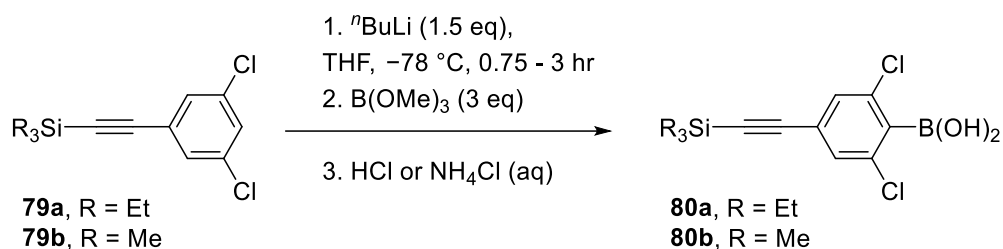
7.5.1.1 General Procedure 14: Sonogashira Cross-Coupling



This procedure was adapted from a procedure reported by Dichtel *et al.*²⁸⁸

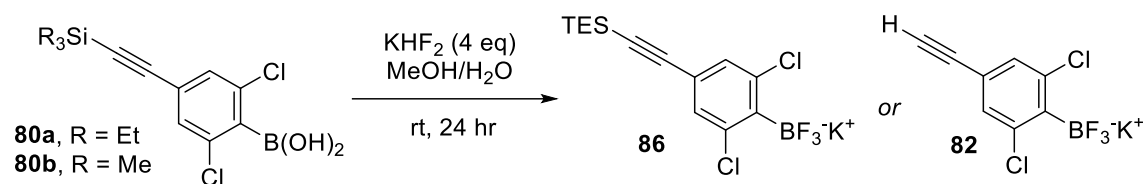
To oven dried glassware and under an atmosphere of nitrogen were added 3,5-dichloroiodobenzene **77** (1 eq), THF (0.3 M) and diisopropylamine (5 eq). The resulting solution was sparged with nitrogen whilst stirring for 20 minutes at room temperature. To the resulting solution $\text{PdCl}_2(\text{PPh}_3)_2$ (2.11 g, 3 mmol, 0.05 eq, 5 mol%) and CuI (0.86 g, 4.5 mmol, 0.075 eq, 7.5 mol%) were then added and the resulting suspension was sparged with nitrogen for 10 minutes at room temperature. To the resulting solution triethylsilylacetylene (**78a**) or trimethylsilylacetylene (**78b**) (1.1 eq) was added. The mixture was stirred at room temperature for 24 hours. After 24 hours, the reaction mixture diluted with CH_2Cl_2 (4 mL per mmol of **77**). The resulting mixture was washed with saturated aqueous NH_4Cl (4 mL per mmol of **77**), saturated aqueous NaHCO_3 (4 mL per mmol of **77**). The organic layer was dried over MgSO_4 , filtered, and evaporated under reduced pressure. The product was purified by flash silica gel column chromatography (hexanes) to afford the crude product **79a** or **79b** with respective homo-coupled diTMS/TES-diacetylene as a clear colourless oil. The crude product was used in the next synthetic step without any further purification.

7.5.1.2 General Procedure 15: Boronic Acid Formation



This procedure was adapted from a procedure reported by Lee *et al.*²⁸⁹

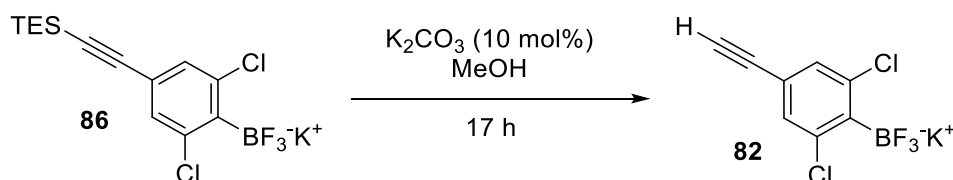
To oven dried glassware and under an atmosphere of nitrogen were added **79a** or **79b** (1 eq) and THF (0.1 M). The solution was cooled to $-78\text{ }^\circ\text{C}$ and ${}^n\text{BuLi}$ (1.6 M in hexanes, 1.5 eq) was added slowly; after complete addition, the reaction mixture was stirred for 0.75 to 3 hours (see Table 18) at $-78\text{ }^\circ\text{C}$. After cooling once again to $-78\text{ }^\circ\text{C}$, trimethylborate (3 eq) was added slowly to the mixture. After stirring for 1 hour, the reaction was slowly allowed to warm up to room temperature and stirred for a further 12 hours. Then, the reaction was quenched with aqueous 1M HCl or saturated aqueous NH_4Cl (6 mL per mmol of **79a/b**) and extracted with DCM (3 x 5 mL per mmol of **79a/b**). The combined organic layers were dried with MgSO_4 , and the solvent was removed under reduced pressure to afford the crude product. The crude product was dissolved in Et_2O , and the resulting organic layer was washed with water (3 x 2 mL per mmol of **79a/b**). The organic layer was dried with MgSO_4 , and the solvent was removed under reduced pressure to afford the crude product, which was used in the next synthetic step without any further purification, unless otherwise stated.

7.5.1.3 General Procedure 16: Potassium Aryltrifluoroborate Salt Formation^{189,190}

This procedure was adapted from a procedure reported by Soós *et al.*¹⁹⁰

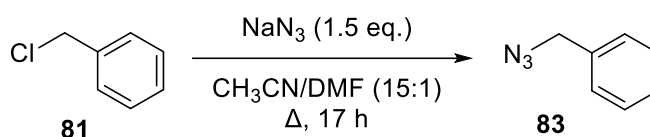
KHF₂ (4 eq) was dissolved in DI water (1 mL/mmol of KHF₂). To the resulting solution was added, a solution of boronic acid **80a** or **80b** (1 eq) in methanol (7 mL/mmol of **80a/b**). The resulting suspension was stirred overnight. The next day, acetone (10 mL/mmol of **80a/b**) was added to the suspension, decanted from the solid residue and evaporated to dryness. The resulted crude white solid was dried on rotary evaporator on 60 °C for two hours. The crude white solid was dissolved in acetone (6 mL/mmol of **80a/b**), filtered off and evaporated to dryness. The resulting solid was triturated with hexane (3 x 5 mL/mmol of **80a/b**) and dried in a vacuum desiccator over phosphorus(V)-oxide for 3 days, unless otherwise stated, affording the products (**86** or **82**) were obtained as white solids.

7.5.1.4 General Procedure 17: TES Deprotection



This procedure was adapted from a procedure reported by López *et al.*²⁹³

86 (1 eq) dissolved in MeOH (10 mL/mmol of **86**) and K₂CO₃ (0.1 eq, 10 mol%) was added. The mixture was stirred at room temperature for 17 hours. After 17 hours, the solvent was removed under reduced pressure. The resulting residue was triturated with hexane (6 mL/mmol of **86**), filtered and washed again with heptane (3 x 6 mL/mmol of **86**) to yield the crude product. The crude solid was purified by dissolution in a minimal amount of acetone and precipitation with Et₂O to obtain the desired pure compound (**82**) as a white solid.

7.5.1.5 Synthesis of Benzyl Azide (**83**)

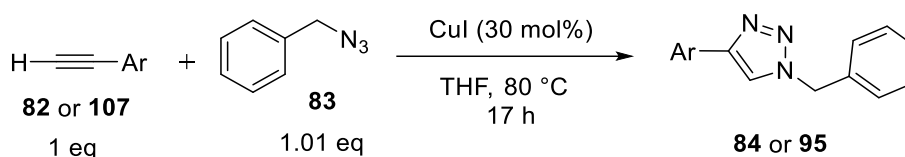
This procedure was adapted from a procedure reported by Boechat *et al.*³³⁰

Benzyl chloride **81** (2.32 mL, 2.53 g, 20 mmol, 1 eq) and NaN₃ (1.95 g, 30 mmol, 1.5 eq) were reacted in MeCN and DMF (15:1, 120 mL). The reaction mixture was stirred under reflux for 17 hours. After 17 hours the reaction mixture was diluted with water (6 mL/mmol of Benzyl chloride) and extracted with DCM (60 mL). The combined organic layers were washed with water (60 mL), dried over MgSO₄, filtered and evaporated under reduced pressure. The product was isolated as a yellow oil (2.39 g, 17.9 mmol, 90%).

This data matches data reported in literature.³³⁰

¹H NMR (CDCl₃, 400 MHz) δ_H 7.45-7.34 (m, 5H), 4.37 (s, 2H).

7.5.1.6 General Procedure 18: Click Reaction



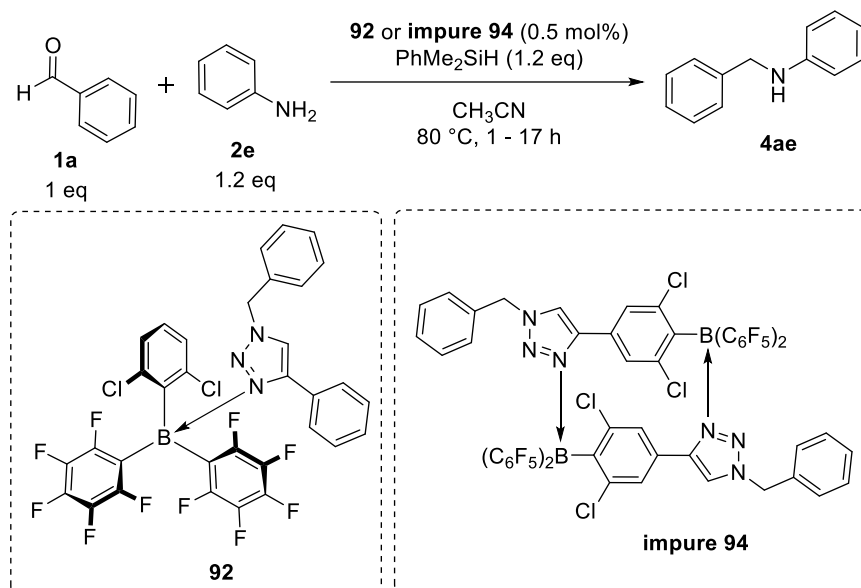
This procedure was adapted from a procedure reported by Molander *et al.*²⁹⁵

To an oven-dried 20 mL crimp cap vial were added sequentially terminal alkyne **82** or **107** (1 eq), benzyl azide (**83**) (1.01 eq), CuI (0.3 eq, 30 mol%) and anhydrous THF (2 mL/mmol of **82** or **107**). The vial was then sealed, and the mixture stirred at 80 °C for 17 hours. After 17 hours and the solvent was removed under reduced pressure. The resulting solid was dissolved in acetone (5 mL/mmol of **82** or **107**) and filtered through Celite. The resulting filtrate was evaporated under reduced pressure. The resulting solid was purified by dissolution in a minimal amount of acetone and precipitation with Et₂O to obtain the desired pure compound **84** or **95** as a solid, unless otherwise stated.

7.5.2 Preliminary FLP Reactivity of Novel Inter-/Intramolecular FLPs **92** and **94**

7.5.2.1 Silanes

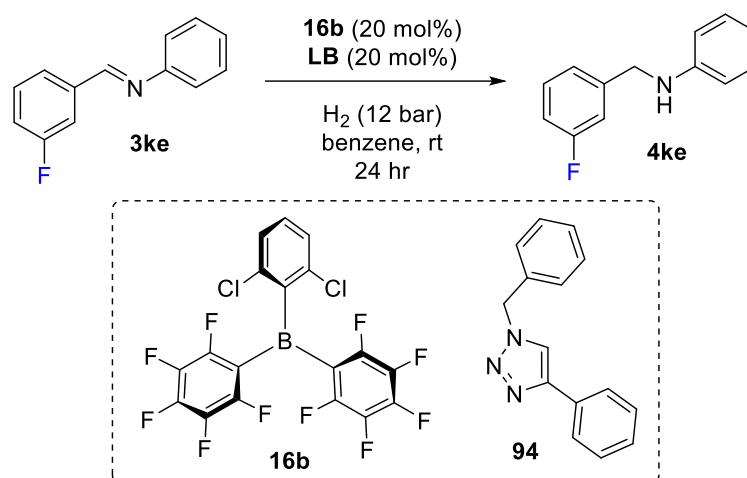
7.5.2.1.1 General Procedure 19: Batch Reductive Aminations with Novel Inter-/Intramolecular FLPs using Hydrogen



To an oven-dried 10 mL crimp cap vial open to the air were added sequentially aniline **2e** (1.2 eq), benzaldehyde **1a** (1.0 eq), and mesitylene (0.5 eq, internal standard) in anhydrous MeCN (0.75 mL/mmol of benzaldehyde). To this mixture, **92** or **impure 94** (0.5 mol%) in anhydrous MeCN (50 mL/mmol of **92** or **impure 94**). Finally, dimethylphenylsilane (1.2 eq) was added and the vial was sealed. The reaction mixture was stirred at $80\text{ }^\circ\text{C}$ for 1 or 17 hours (see Scheme 75). The yields were determined by ^1H NMR spectrum integration by integration of an internal standard (mesitylene).

7.5.2.2 Hydrogen

7.5.2.2.1 General Procedure 20: Batch Reductions with Novel Inter-/Intramolecular FLPs using Hydrogen



This procedure was adapted from a procedure reported by Soós *et al.*⁶⁰

To an oven dried glass vial were added sequentially *N*-(3-fluorobenzylidene)aniline (**3ke**) (20 mg, 0.1 mmol, 1 eq), **16b** (9.8 mg, 0.02 mmol, 0.2 eq, 20 mol%), Lewis base (0.2 eq, 20 mol%, see Table 20), and anhydrous benzene-d₆ (0.5 mL). The vial was placed in a 30 mL Parr pressure vessel flushed with argon. The pressure vessel remained under argon for 2 minutes before the vessel was sealed. Once sealed, the reaction mixture was and pressurised with H₂ (12 bar) and kept at room temperature for 24 hours. After 24 hours the reaction mixture was degassed, and an aliquot of the reaction mixture (0.5 mL) was taken and analysed by quantitative ¹H and ¹⁹F NMR spectroscopy. The yields were determined the same general procedure 7 (X = F); by relative integration of product and starting material resonances.

7.5.3 Synthesis of Diazide **100** for Potential Future Asymmetric FLP Borane Scaffold



This procedure was adapted from a procedure reported by Elsevier *et al.*³¹⁶

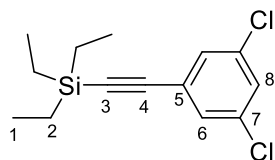
A solution of (*S*)-1,1'-binaphthyl-2,2'-diamine (2.84 g, 10 mmol, 1.0 eq) in MeCN (50 mL) was cooled to 0 °C, after which *t*butyl nitrite (3.6 mL, 30 mmol, 3.0 eq) was added. Trimethylsilyl azide (3.2 mL, 24 mmol, 2.4 eq) was added to this solution, which resulted in a colour change from brown to bright red. This solution was stirred at -15 °C for 40 h, whereafter the solution was filtered, the solvents were evaporated. The product was purified by flash silica gel column chromatography (hexane to 10:1 hexane:EtOAc) the yield the product **101** as an orange solid (3.13 g, 9.3 mmol, 93 % yield).

This data matches data reported in literature.³¹⁶

¹H NMR (DMSO-*d*₆, 400 MHz) δ_{H} 8.20 (d, J 9.0 Hz, 2H), 8.05 (d, J 8.2 Hz, 2H), 7.66 (d, J 8.7 Hz, 2H), 7.49-7.45 (m, 2H), 7.34-7.32 (m, 2H), 6.93 (d, J 8.2 Hz, 2H).

7.5.4 Compound Characterisation Data

7.5.4.1 Sonogashira Cross-Coupling

1-[(Trimethylsilyl)ethynyl]-3,5-dichlorobenzene (**79a**)

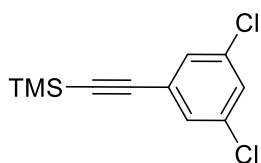
According to general procedure 14, 3,5-dichloro iodobenzene (16.37 g, 60 mmol, 1 eq) and triethylacetylene (12.9 mL, 10.10 g, 72 mmol, 1.1 eq) were reacted to give the title compound **79a** (isolated with the homo-coupled diTES-diacetylene impurity) as a clear colourless oil (17.47 g, 96% yield, 94% purity). The crude product was used in the next synthetic step without any further purification.

$^1\text{H NMR}$ (CDCl_3 , 400 MHz) δ_{H} 7.34 (d, J 1.9 Hz, 2H, **H6**), 7.30 (t, J 1.9 Hz, 1H, **H8**), 1.06-0.98 (m, 9H, **H1**), 0.71-0.62 (m, 6H, **H2**).

$^{13}\text{C NMR}$ (CDCl_3 , 100 MHz) δ_{C} 134.8 (**C7**), 130.2 (**C6**), 128.7 (**C8**), 126.1 (**C5**), 103.2 (**C3**), 95.0 (**C4**), 7.4 (**C2**), 4.3 (**C1**).

$\text{IR } \nu_{\text{max}}$ (thin film, cm^{-1}): 2954, 2874, 2134, 2063, 1554, 919.

*A MS should have been run; however, we no longer have compound **79a**. All of compound **79a** was used in subsequent steps to form **82** and **76**, which have been fully assigned, and therefore, we are confident that **79a** was the desired compound.*

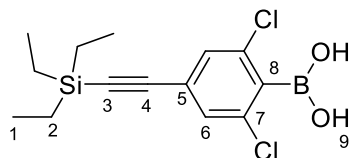
1-[(Trimethylsilyl)ethynyl]-3,5-dichlorobenzene (**79b**)²⁸⁸

According to general procedure 14, 3,5-dichloro iodobenzene (11.23 g, 41.15 mmol, 1 eq) and trimethylsilylacetylene (7.12 mL, 51.5 mmol, 1.1 eq) were reacted to give the title compound **79b** (isolated with the homo-coupled diTMS-diacetylene impurity) as a clear colourless oil (10.32 g, 99% yield, 96.5% purity). The crude product was used in the next synthetic step without any further purification.

This data matches data reported in literature.²⁸⁸

$^1\text{H NMR}$ (DMSO-d_6 , 400 MHz) δ_{H} 7.65 (t, J 1.9 Hz, 1H), 7.50 (d, J 1.9 Hz, 2H), 0.24 (s, 9H).

7.5.4.2 Boronic Acid Formation

(4-[(Triethylsilyl)ethynyl]-2,6-dichlorophenyl)boronic acid (**80a**)

According to general procedure 15, to a solution of 1-[(triethylsilyl)ethynyl]-3,5-dichlorobenzene (**79a**) (1.43 g, 5 mmol, 1 eq) was added n BuLi (1.6 M in hexane, 4.7 mL, 7.5 mmol) at -78°C . After 45 minutes trimethyl borate (2.3 mL, 2.08 g, 20 mmol, 4 eq) was added and the mixture was stirred at room temperature for 24 hours. The title compound was isolated once as an off white solid (0.4 g, 1.2 mmol, 24%) but otherwise carried on without further purification.

$^1\text{H NMR}$ (DMSO- d_6 , 400 MHz) δ_{H} 8.68 (s, 2H, **H9**), 7.44 (s, 2H, **H6**), 1.01 (t, J 7.9 Hz, 9H, **H1**), 0.67 (q, J 7.9 Hz, 6H, **H2**).

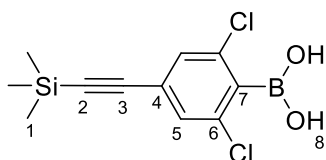
$^{13}\text{C NMR}$ (DMSO- d_6 , 100 MHz) δ_{C} 136.4 (**C7**), 129.8 (**C6**), 124.8 (**C5**), 103.9 (**C4**), 94.7 (**C3**), 7.8 (**C2**), 4.2 (**C1**). A signal of the ipso-carbon (**C8**) with respect to the boron atom was not identified.

$^{11}\text{B-NMR}$ (DMSO- d_6 , 128 MHz) δ_{B} 28.0.

IR ν_{max} (solid, cm^{-1}): 3207, 2956, 2134, 1353, 839.

m.p. 100 – 102 $^{\circ}\text{C}$

*A MS should have been run; however, we no longer have compound **80a**. All of compound **80a** was used in subsequent steps to form **82** and **76**, which have been fully assigned, and therefore, we are confident that **80a** was the desired compound.*

(4-[(Trimethylsilyl)ethynyl]-2,6-dichlorophenyl)boronic acid (**80b**)

According to general procedure 15, to a solution of 1-[(trimethylsilyl)ethynyl]-3,5-dichlorobenzene (**79b**) (3.12 g, 12.8 mmol, 1 eq) was added n BuLi (1.6 M in hexane, 11.3 mL, 18 mmol) at -78°C . After 45 minutes trimethyl borate (4 mL, 3.75 g, 36 mmol, 3 eq)

was added and the mixture was stirred at room temperature for 24 hours. The title compound was isolated as a white solid (4.42 g, 15.4 mmol, 64%).

$^1\text{H NMR}$ (DMSO- d_6 , 400 MHz) δ_{H} 8.69 (s, 2H, **H8**), 7.45 (s, 2H, **H5**), 0.24 (s, 9H, **H1**).

$^{13}\text{C NMR}$ (DMSO- d_6 , 100 MHz) δ_{C} 140.3 (**C7**), 136.4 (**C6**), 129.7 (**C5**), 124.7 (**C4**), 102.6 (**C3**), 97.4 (**C2**), 0.2 (**C1**).

$^{11}\text{B-NMR}$ (DMSO- d_6 , 128 MHz) δ_{B} 28.5.

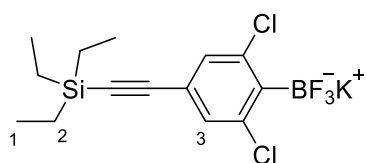
IR ν_{max} (solid, cm^{-1}): 3207, 2956, 2134, 1353, 839.

m.p. 169 – 171 °C

HRMS (ESI) m/z $[\text{M-H}]^-$ calculated for $\text{C}_{11}\text{H}_{12}\text{BCl}_2\text{O}_2\text{Si}$: 285.0082, found: 285.0063.

7.5.4.3 Potassium Aryltrifluoroborate Salt Formation

Potassium(4-[(Triethylsilyl)ethynyl]-2,6-dichlorophenyl)trifluoroborate (**86**)



According to general procedure 16, (4-[(triethylsilyl)ethynyl]-2,6-dichlorophenyl)boronic acid (**80a**) (2.18 g, 6.62 mmol, 1 eq) was stirred with KHF_2 (2.07 g, 26.5 mmol, 4 eq) at room temperature for 24 hours. The title compound was isolated as a white solid (2.0 g, 5.1 mmol, 77%).

$^1\text{H NMR}$ (DMSO- d_6 , 400 MHz) δ_{H} 7.16 (s, 2H, **H3**), 0.99 (t, J 7.9 Hz, 9H, **H1**), 0.64 (q, J 7.9 Hz, 6H, **H2**).

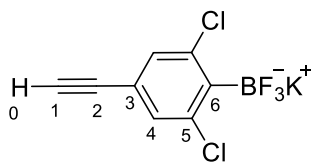
$^{19}\text{F-NMR}$ (DMSO- d_6 , 282 MHz) δ_{F} -132.4 (brs, 3F).

$^{11}\text{B-NMR}$ (DMSO- d_6 , 128 MHz) δ_{B} 1.94 (brs).

$^{13}\text{C NMR}$, *IR* and *MS* should have been run; however, we no longer have compound **86**. All of compound **86** was used in subsequent steps to form **82** and **76**, which have been fully assigned, and therefore, we are confident that **86** was the desired compound.

7.5.4.4 TES Deprotection/ Potassium Aryltrifluoroborate Salt Formation with TMS-protecting group

Potassium(4-(ethynyl)-2,6-dichlorophenyl)trifluoroborate (**82**)



TES Deprotection: According to general procedure 17, potassium 4-[(triethylsilyl)ethynyl]-2,6-dichlorophenyl trifluoroborate (**86**) (1.95 g, 4.98 mmol, 1 eq) and K_2CO_3 (70 mg, 0.5 mmol, 0.1 eq, 10 mol%) were stirred at room temperature for 17 hours. The title compound was isolated as a white solid (0.69 g, 2.5 mmol, 50%).

or

ArBF₃K salt formation with TMS-protecting group: According to general procedure 16, 4-[(trimethylsilyl)ethynyl]-2,6-dichlorophenyl boronic acid (**80b**) (2.01 g, 7 mmol, 1 eq) was stirred with KHF₂ (2.34 g, 28 mmol, 4 eq) at room temperature for 24 hours. The title compound was isolated as a white solid (1.74 g, 6.3 mmol, 90%).

¹H NMR (DMSO-d₆, 400 MHz) δ_H 7.20 (s, 2H, **H4**), 4.22 (s, 1H, **H0**).

¹³C NMR (DMSO-d₆, 100 MHz) δ_C 139.8 (**C5**), 130.9 (**C5**), 121.4 (**C3**), 81.9 (**C1**), 82.1 (**C2**).

A signal of the ipso-carbon (**C6**) with respect to the boron atom was not identified.

¹⁹F-NMR (DMSO-d₆, 282 MHz) δ_F -132.3 (m, 3F).

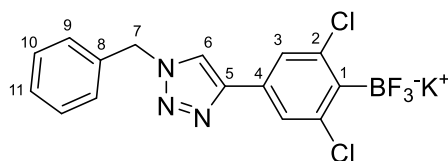
¹¹B-NMR (DMSO-d₆, 128 MHz) δ_B 1.82.

IR ν_{max} (solid, cm⁻¹): 3291, 1513, 1364, 1167, 1079, 951.

HRMS (ESI) *m/z* [M-K]⁻ calculated for C₈H₃BCl₂F₃: 236.9662, found: 236.9661.

7.5.4.5 Click Reaction

Potassium(4-(1-benzyl-1H-1,2,3-triazol-4-yl)-2,6-dichlorophenyl)trifluoroborate (**84**)



According to general procedure 18, terminal alkyne **82** (1.74 g, 6.28 mmol, 1 eq) and benzyl azide (0.85 g, 6.35 mmol, 1 eq) were heated at 80 °C. The title compound was isolated as a white solid (2.33 g, 90%).

$^1\text{H NMR}$ (DMSO- d_6 , 400 MHz) δ_{H} 8.72 (s, 1H, **H6**), 7.61 (s, 2H, **H3**), 7.33-7.42 (m, 5H, **H9-11**), 5.62 (s, 2H, **H7**).

$^{13}\text{C NMR}$ (DMSO- d_6 , 100 MHz) δ_{C} 145.3 (**C5**), 140.3 (**C2**), 136.3 (**C8**), 130.5 (**C4**), 129.3 (**C10**), 128.7 (**C11**), 128.5 (**C9**), 124.7 (**C3**), 122.5 (**C6**), 53.6 (**C7**). A signal of the ipso-carbon (**C1**) with respect to the boron atom was not identified.

$^{19}\text{F NMR}$ (DMSO- d_6 , 376 MHz) δ_{F} -132.3 (m, 3F).

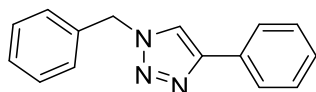
$^{11}\text{B NMR}$ (DMSO- d_6 , 128 MHz) δ_{B} 2.00 (brs).

$\text{IR } \nu_{\text{max}}$ (solid, cm^{-1}): 1605, 1374, 1165, 1075, 934.

m.p. 290 – 292 °C

HRMS (ESI) m/z [M-K] $^-$ calculated for $\text{C}_{15}\text{H}_{10}\text{BCl}_2\text{F}_3\text{N}_3$: 370.0302, found: 370.0305.

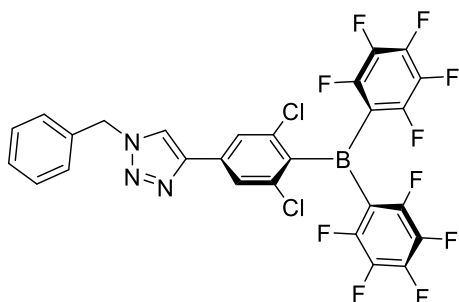
4-Phenyl-1-(benzyl)-1H-1,2,3-triazole (**95**)³³¹



According to general procedure 18, phenyl acetylene (0.88 mL, 0.82 g, 8 mmol, 1 eq) and benzyl azide (1.07 g, 8 mmol, 1 eq) were heated at 80 °C. The product (**95**) was purified by flash silica gel column chromatography (8:2 to 7:3 hexane:EtOAc) as a white solid (1.69 g, 7.2 mmol, 90%).

This data matches data reported in literature.³³¹

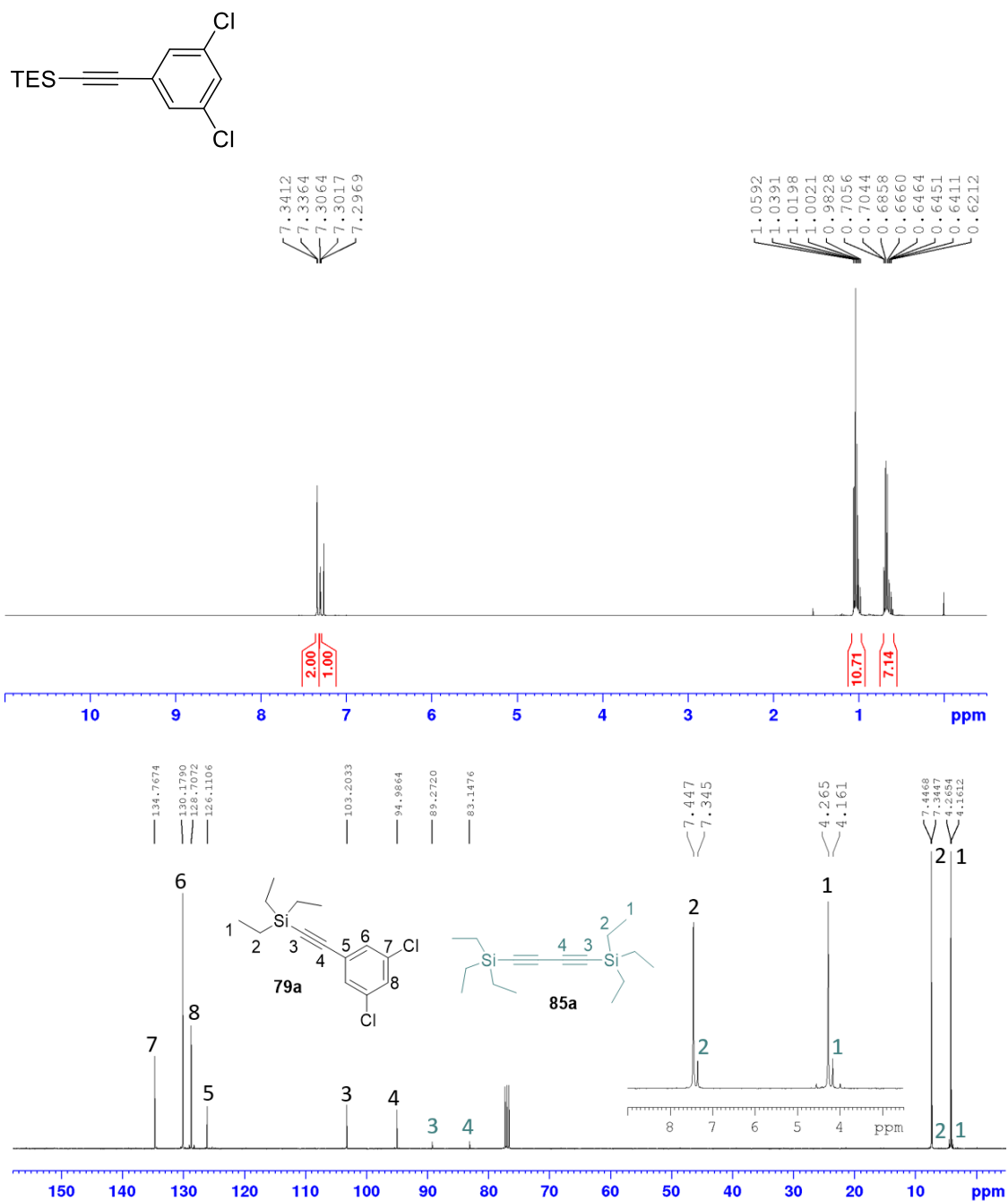
$^1\text{H NMR}$ (CDCl_3 , 400 MHz) δ_{H} 7.84-7.81 (m, 2H), 7.68 (s, 1H), 7.44-7.38 (m, 5H), 7.36-7.31 (m, 3H), 5.60 (s, 2H).

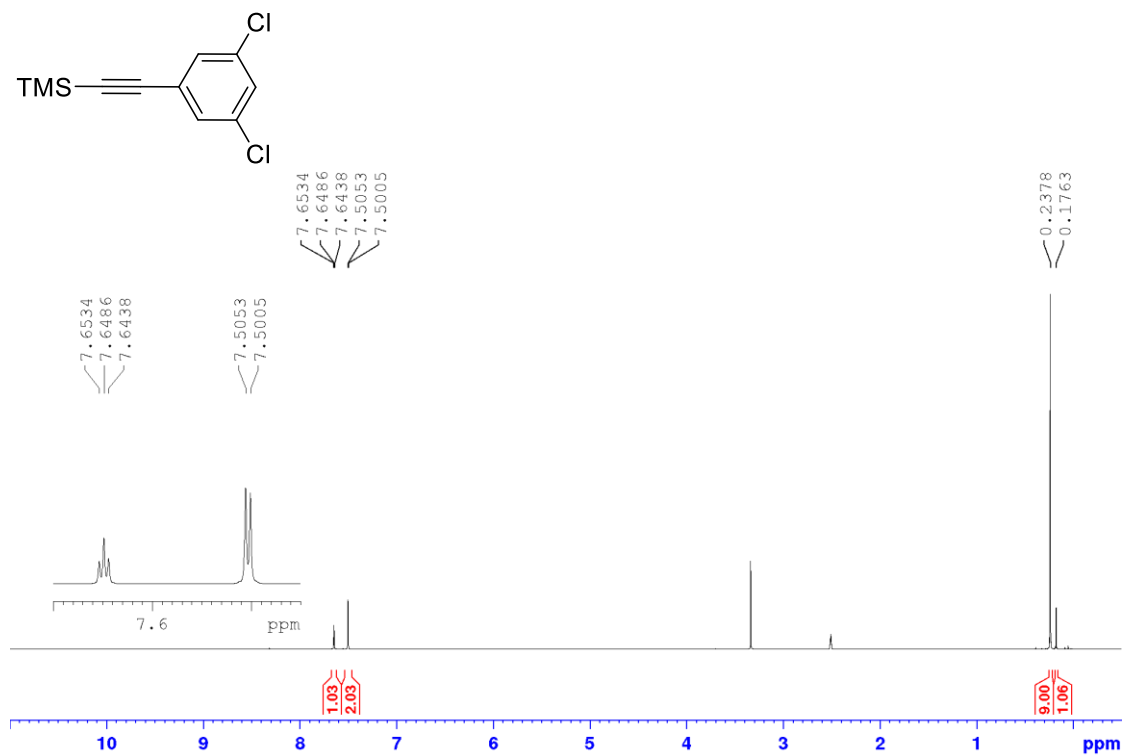
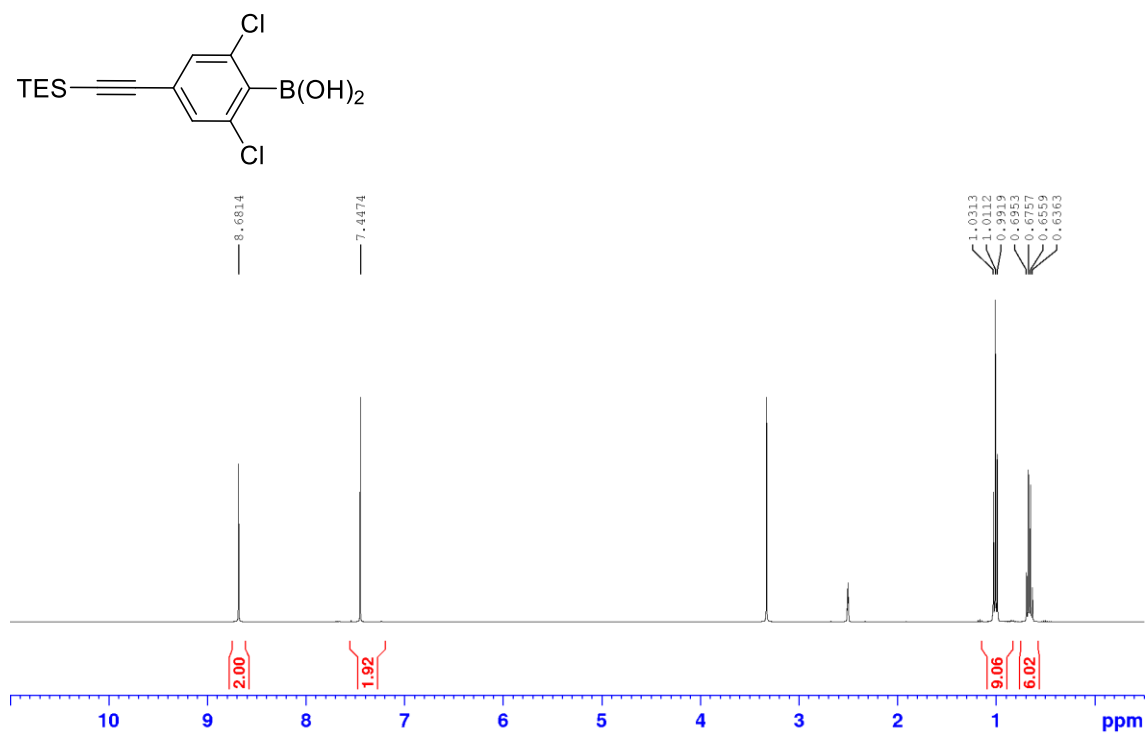
7.5.4.5 Attempted Synthesis of Target Triaryl Borane **76**4-(4-(1-Benzyl-1*H*-1,2,3-triazol-4-yl)-2,6-dichlorophenyl)bis(tetrafluorophenyl)borane (**76**)

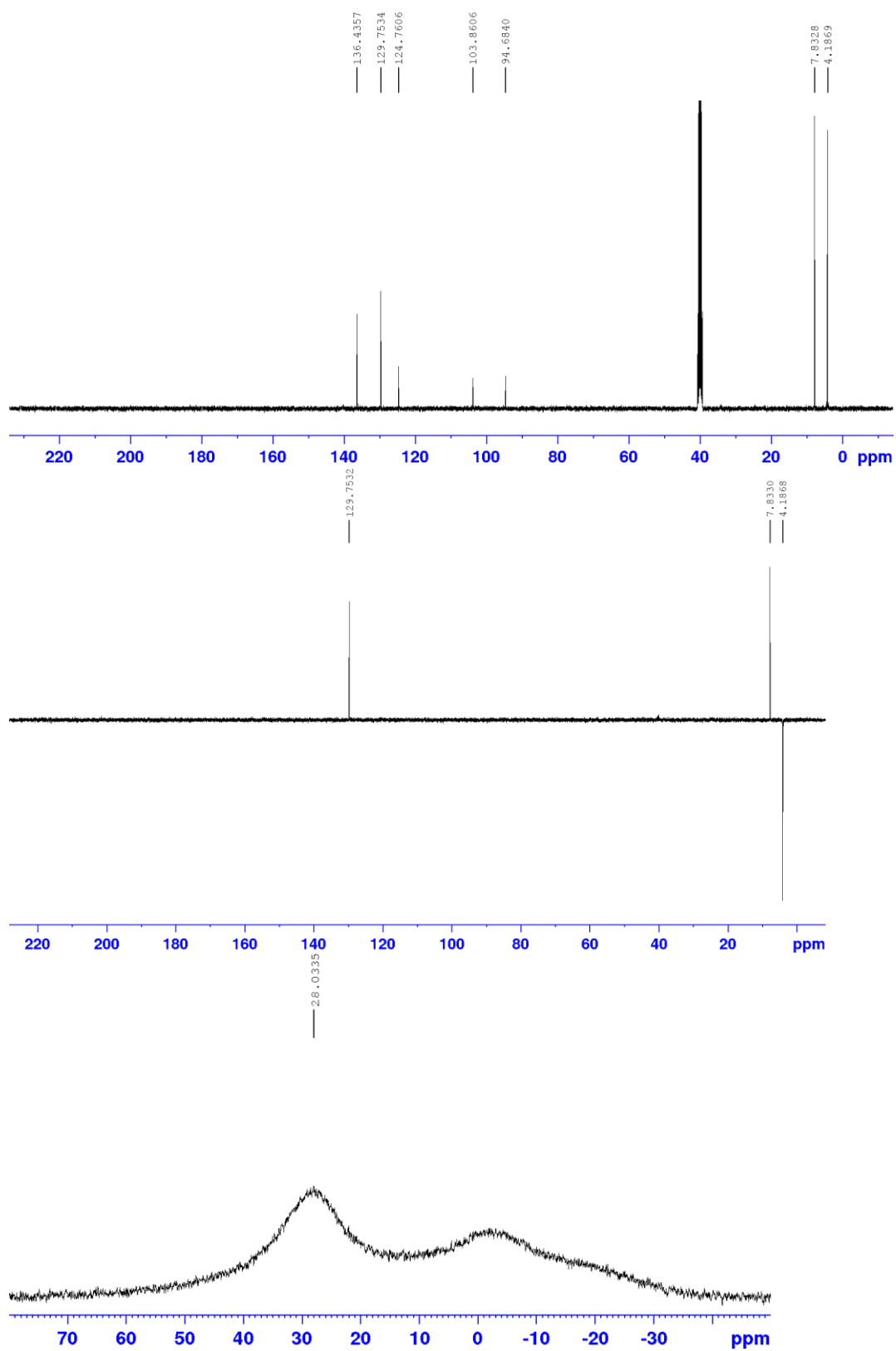
76 was prepared according to general procedure 1 from Potassium(4-(1-benzyl-1*H*-1,2,3-triazol-4-yl)-2,6-dichlorophenyl)trifluoroborate (**34**) (0.55 g, 1.34 mmol) and was isolated impure as a beige solid (86 mg, unknown yield due to complexity of the NMR spectrum) *To aid in determining if **76** had been successfully synthesis and intermolecular adduct **92** was synthesised for comparison, which revealed similarly complex NMR spectrum. The NMR spectrum for **76** is shown in the next section 7.5.4.6 and the intermolecular adduct **92** is discussed in detail in section 7.5.5).*

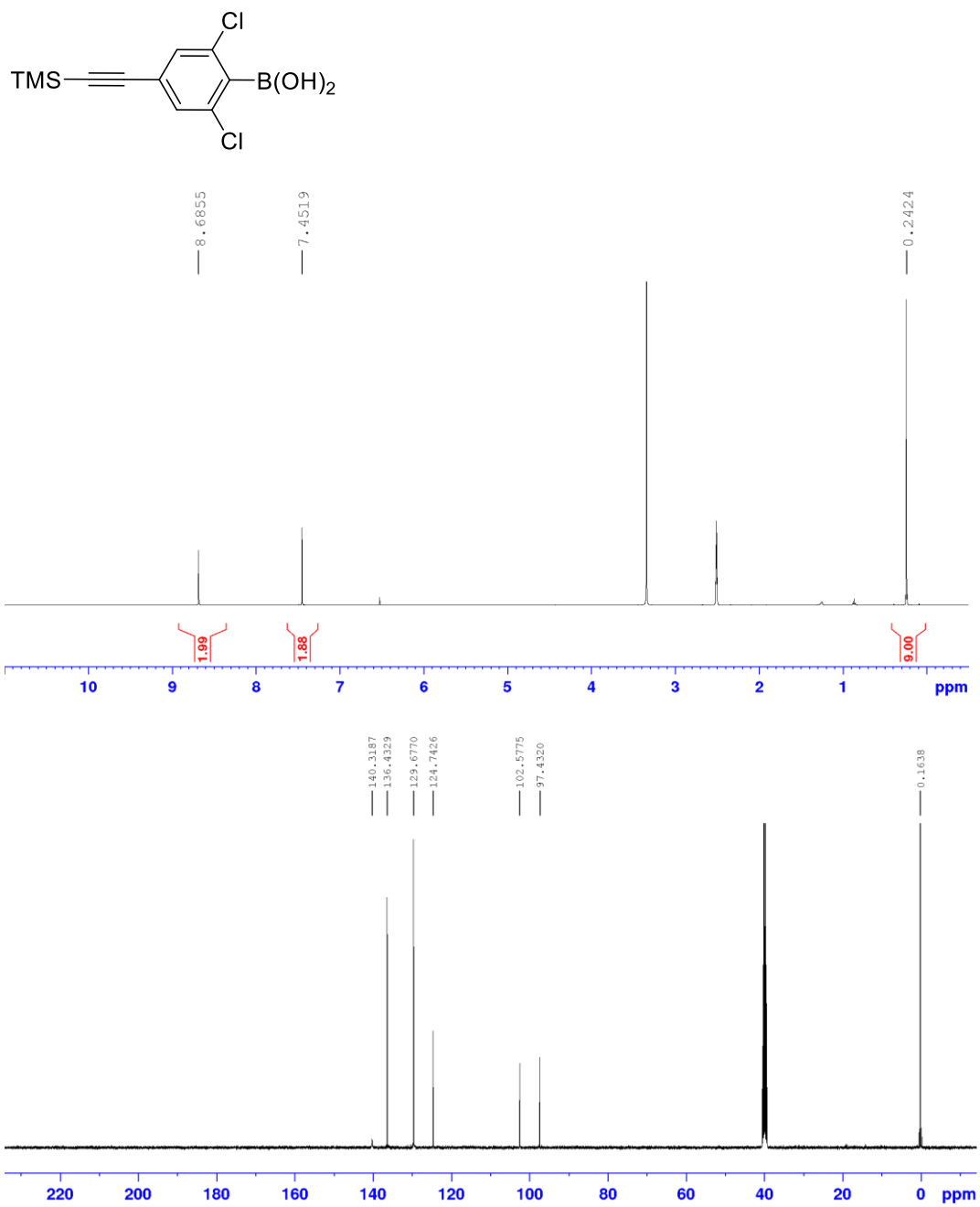
A MS had been submitted; however, the result has been delayed due to complications with the Lancaster University Chemistry Department mass spectrometer resulting in the MS being outsourced to another institute.

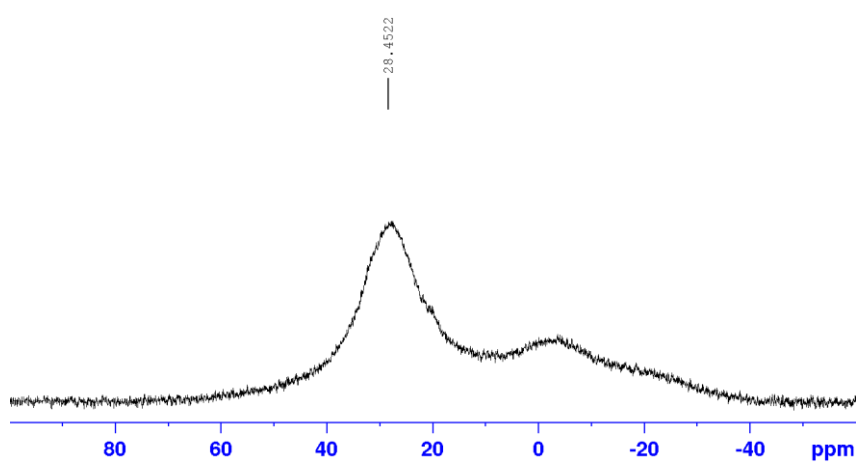
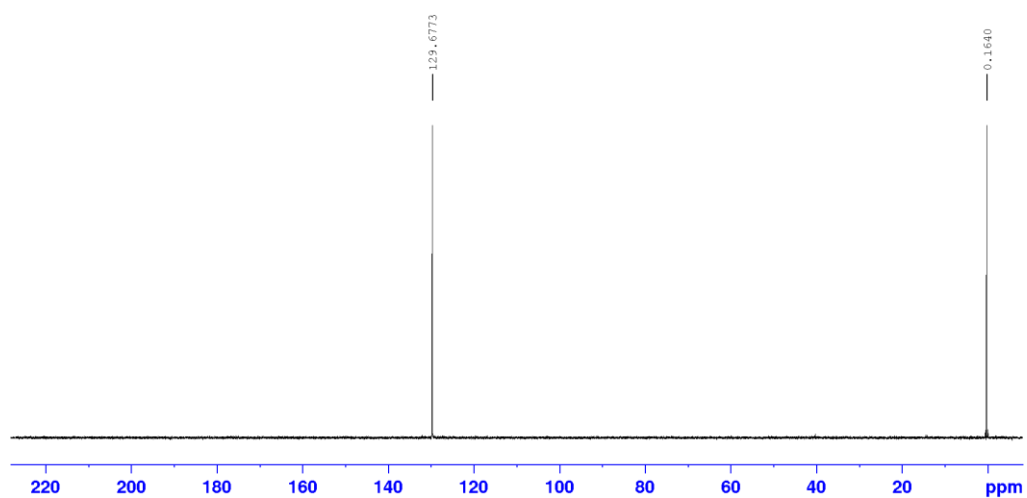
7.5.4.6 NMR Spectra

1-[(Trimethylsilyl)ethynyl]-3,5-dichlorobenzene (**79a**)

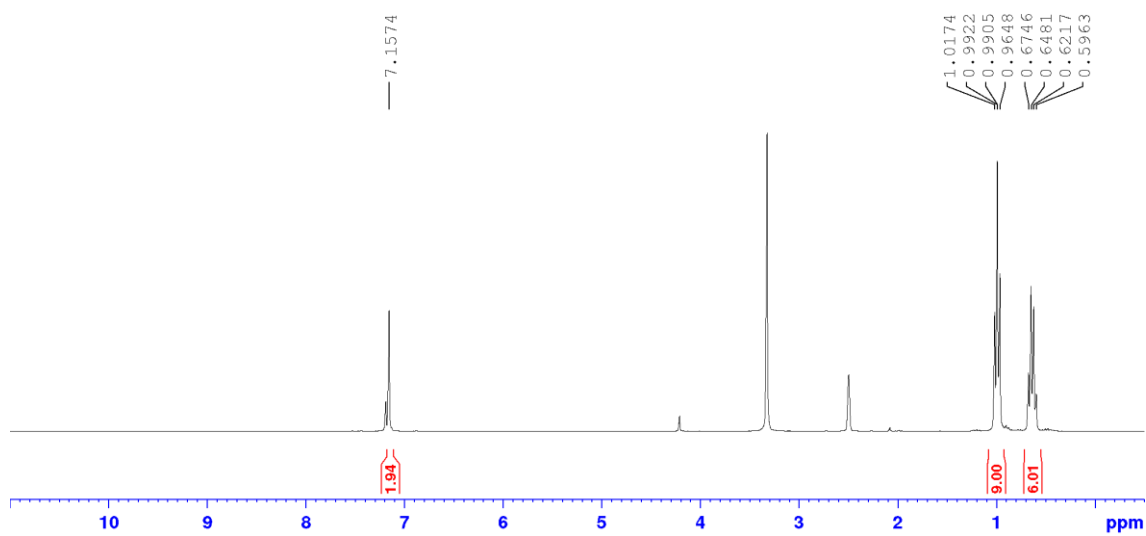
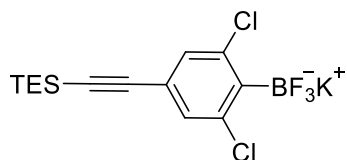
1-[(Trimethylsilyl)ethynyl]-3,5-dichlorobenzene (**79b**)(4-[(Triethylsilyl)ethynyl]-2,6-dichlorophenyl)boronic acid (**80a**)

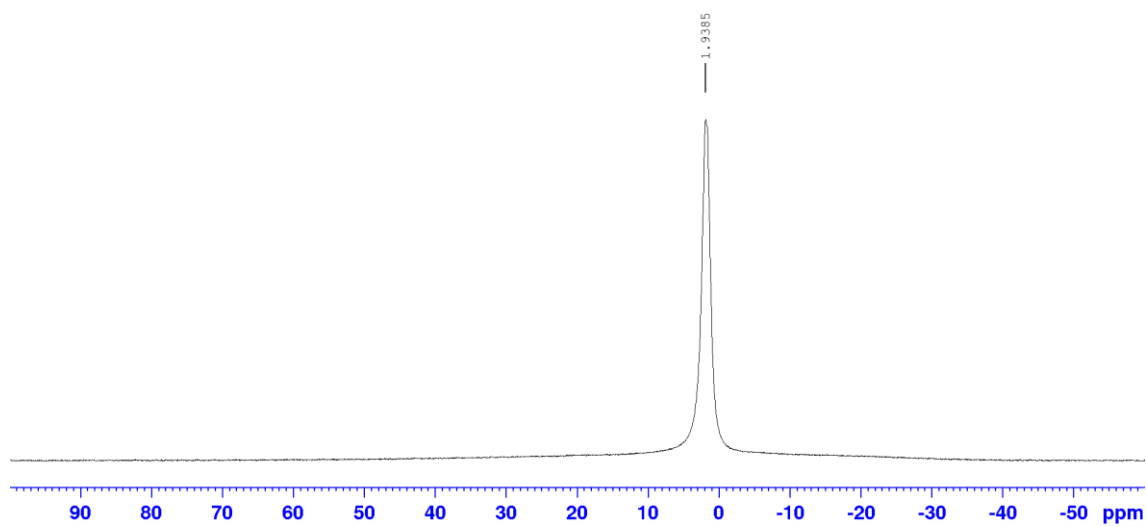
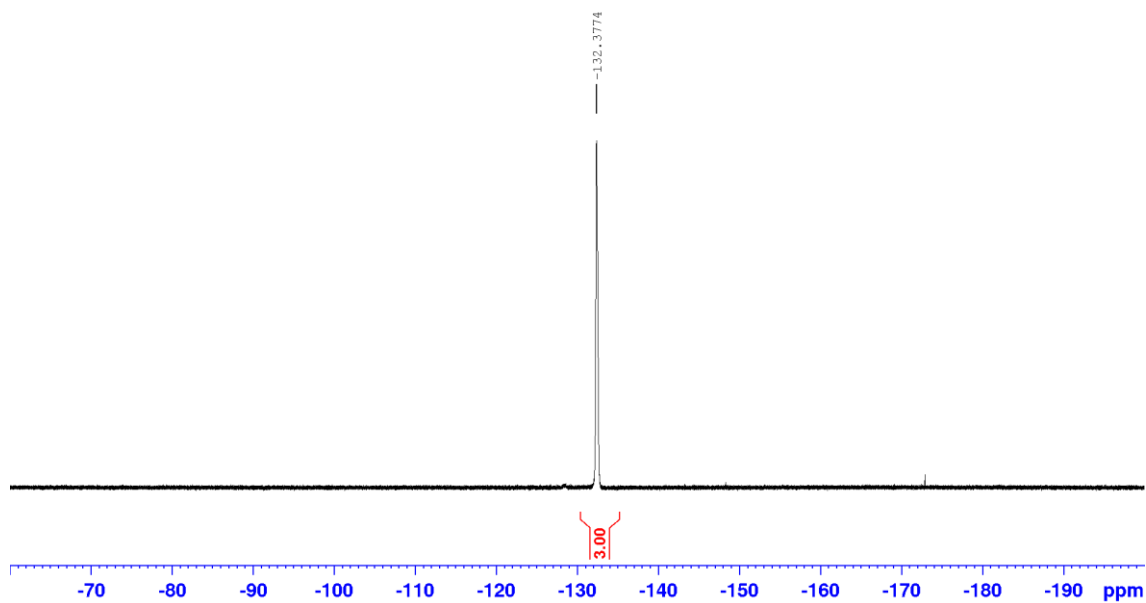


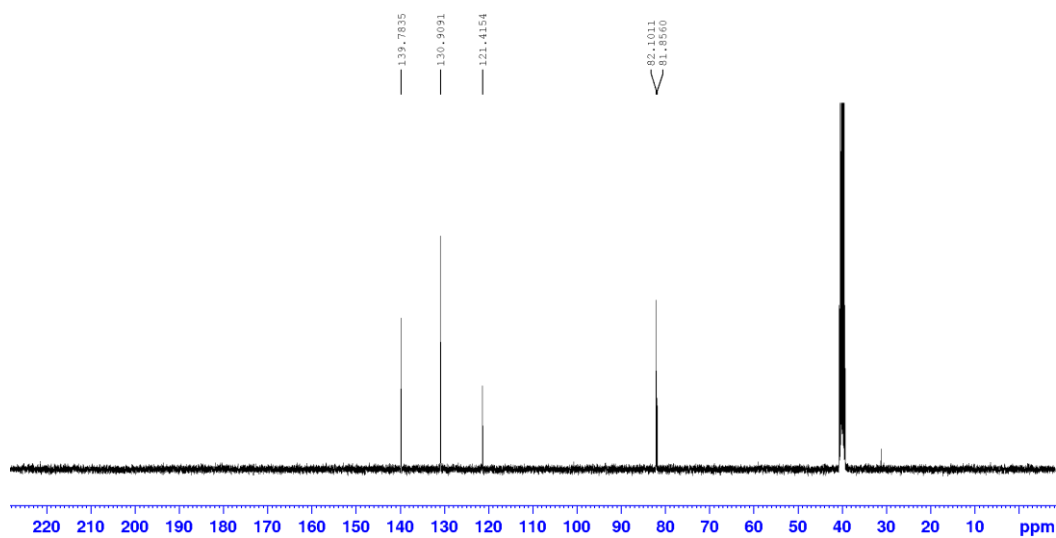
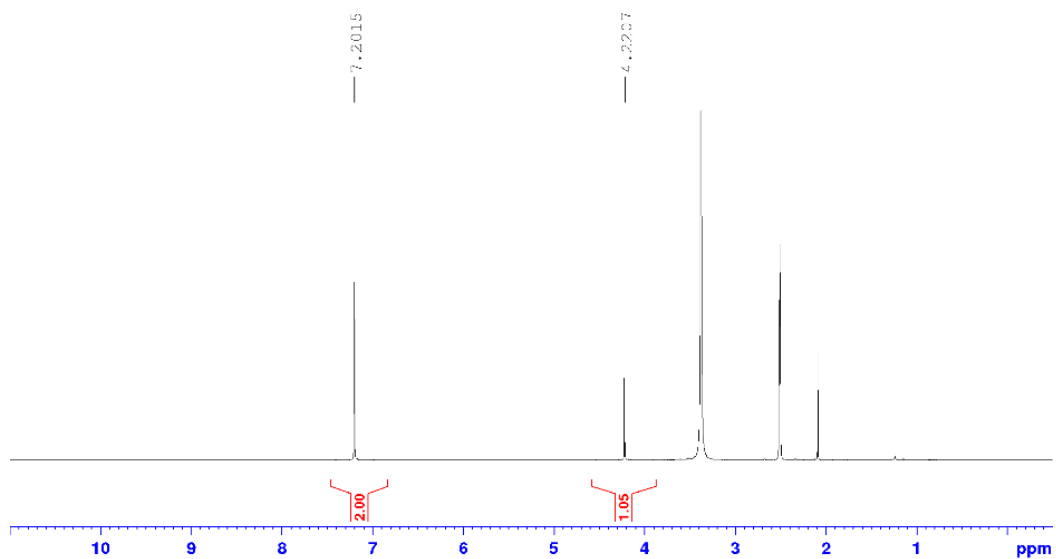
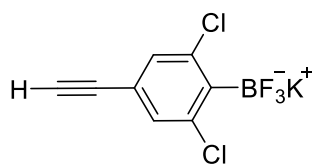
4-[(Trimethylsilyl)ethynyl]-2,6-dichlorophenyl boronic acid (**80b**)

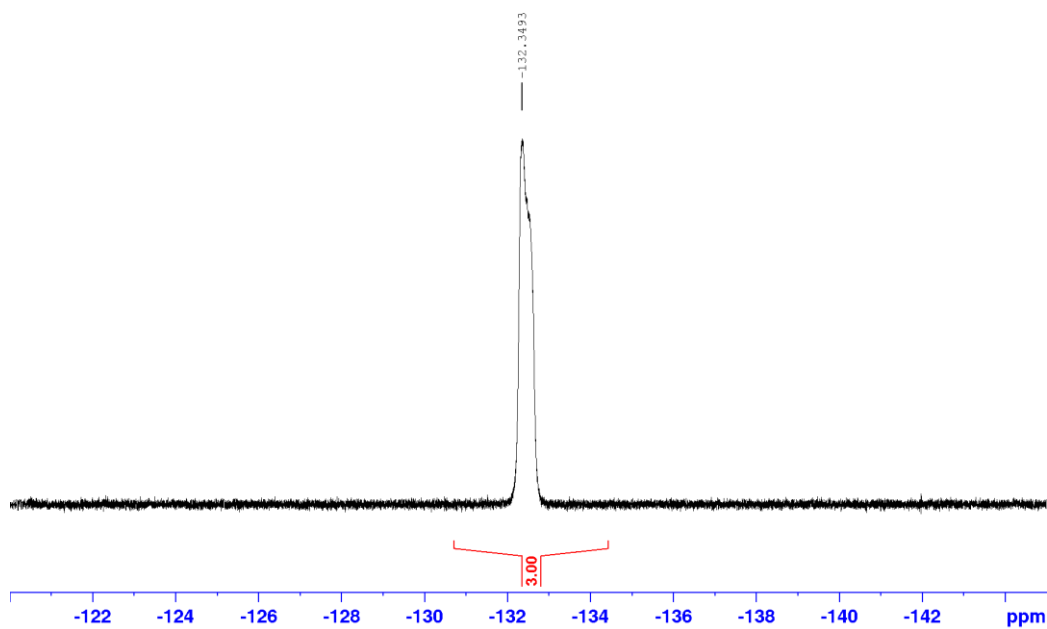
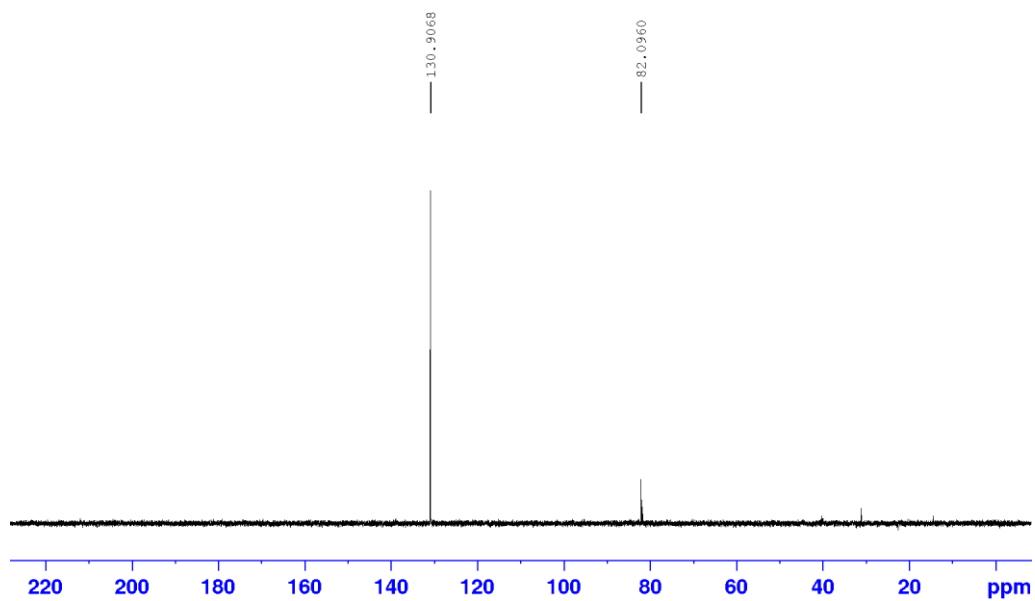


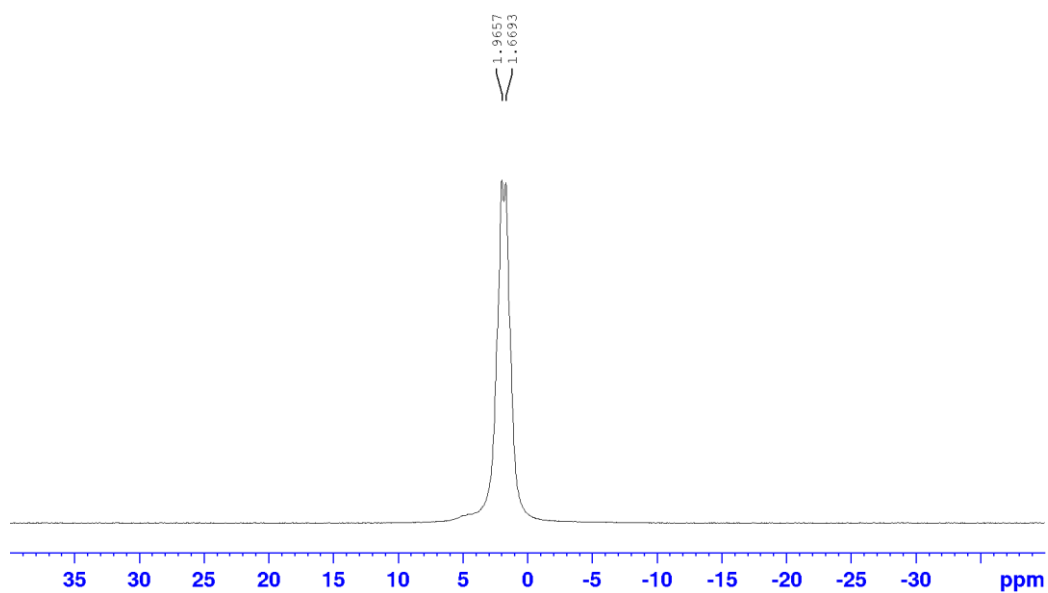
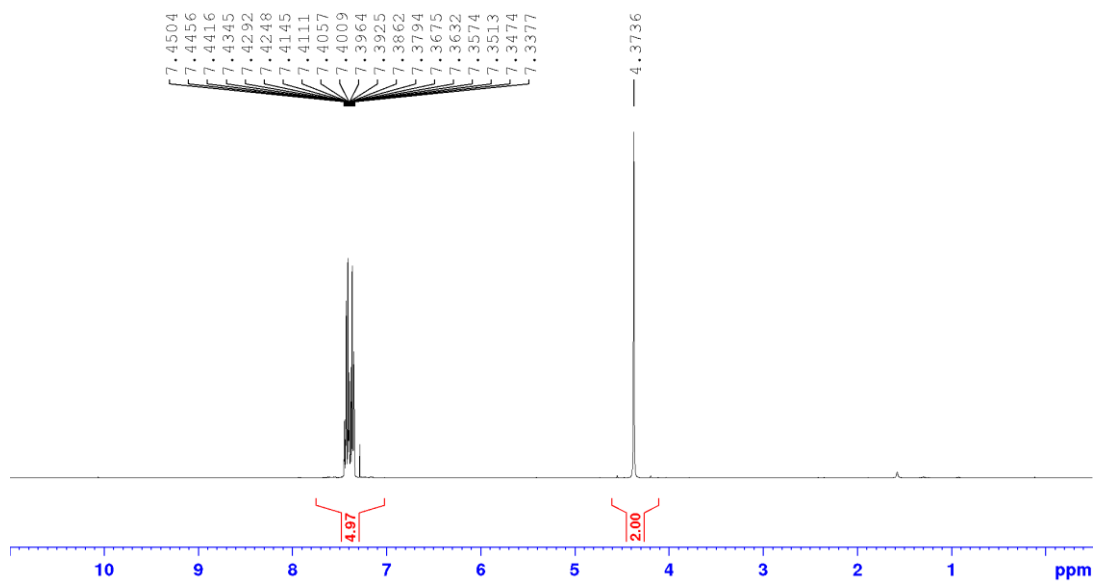
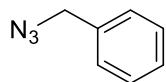
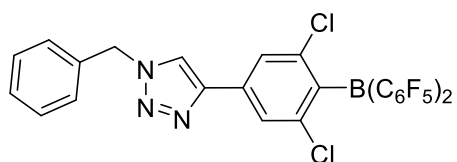
Potassium 4-[(triethylsilyl)ethynyl]-2,6-dichlorophenyl trifluoroborate (**86**)

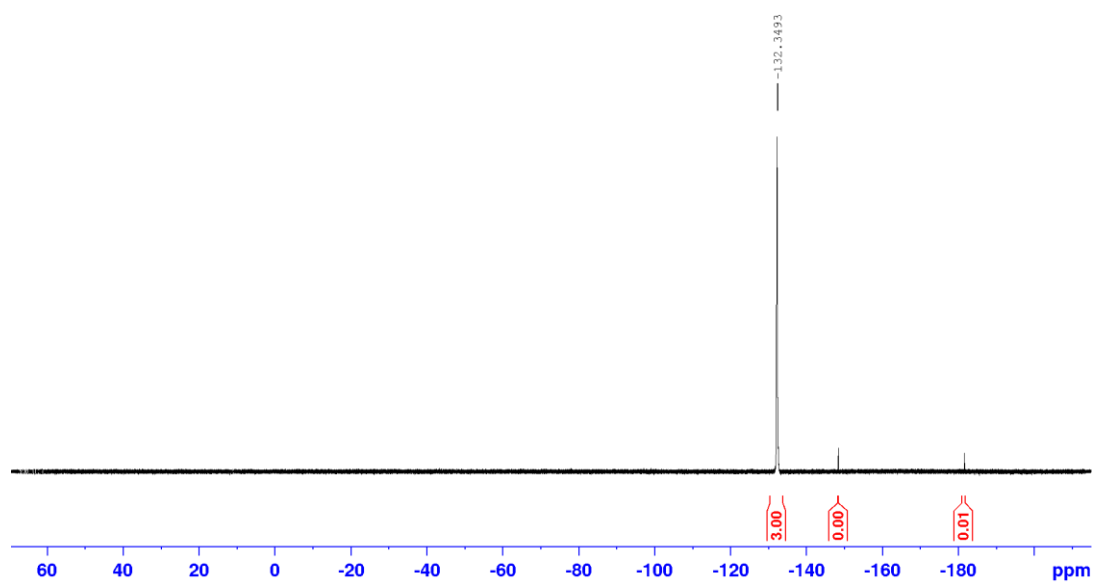
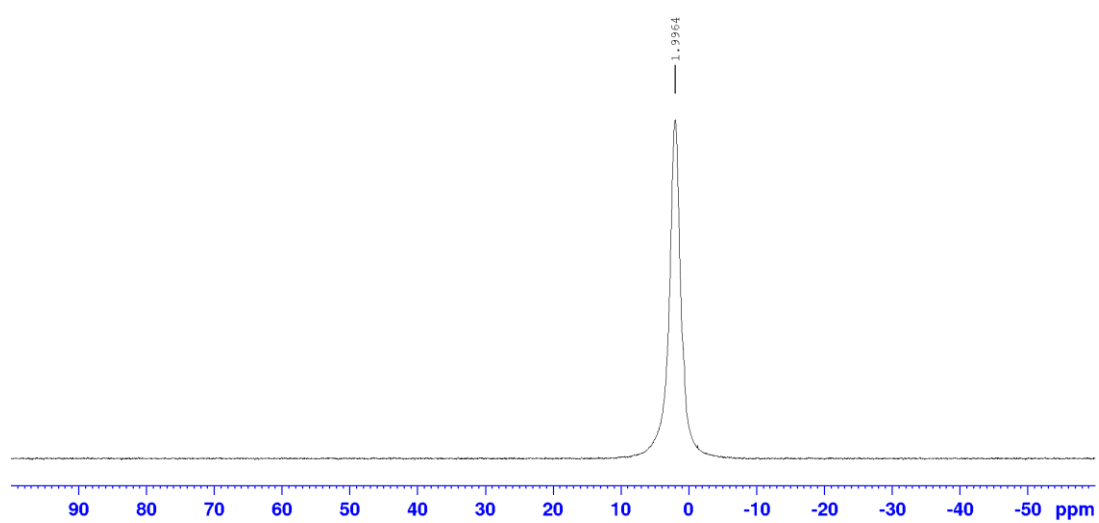
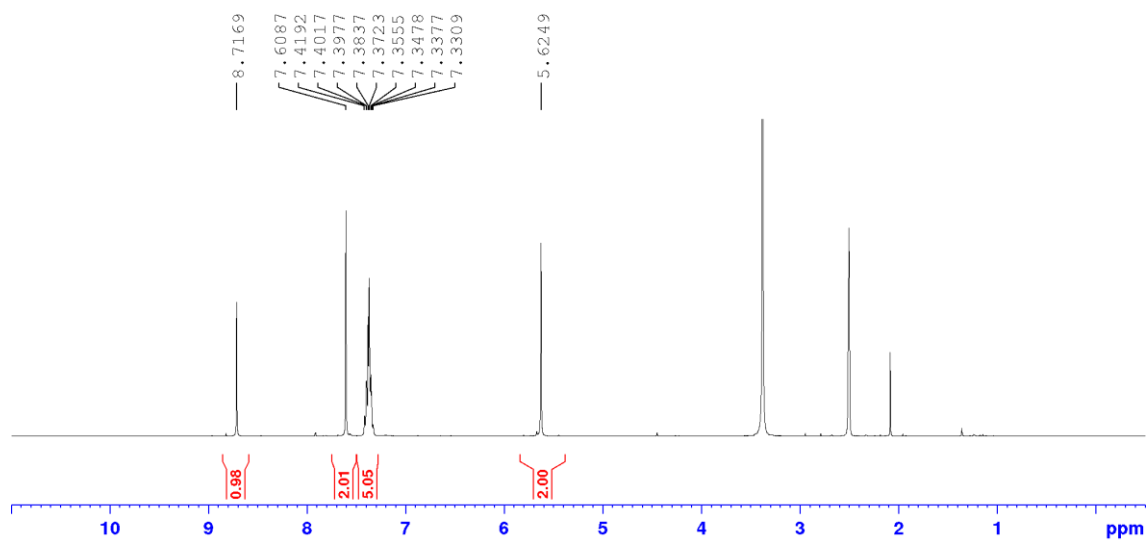


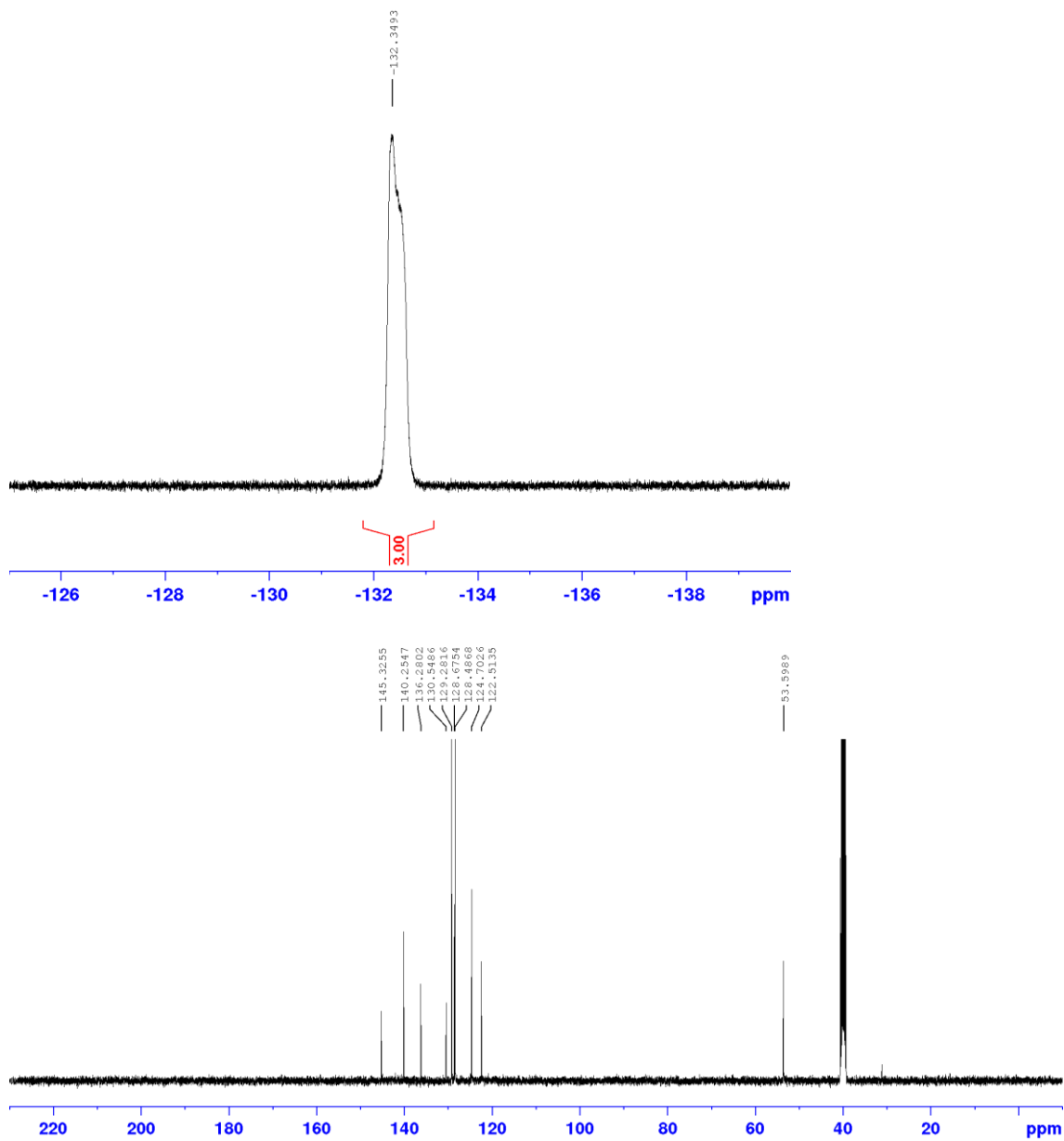


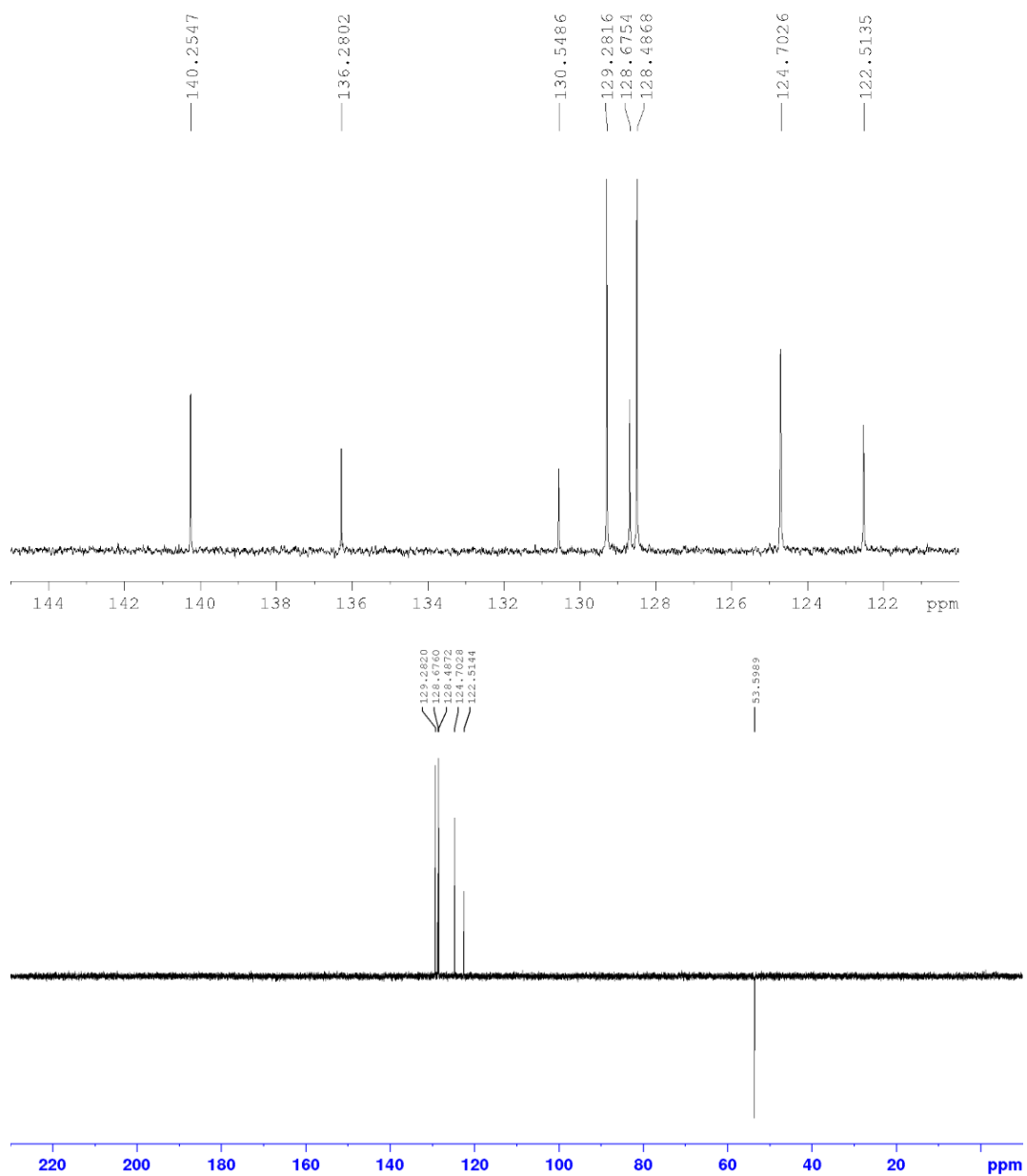
Potassium(4-(ethynyl)-2,6-dichlorophenyl)trifluoroborate (**82**)



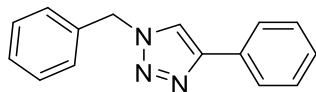
Benzyl azide (**83**)Potassium(4-(1-benzyl-1*H*-1,2,3-triazol-4-yl)-2,6-dichlorophenyl)trifluoroborate (**84**)

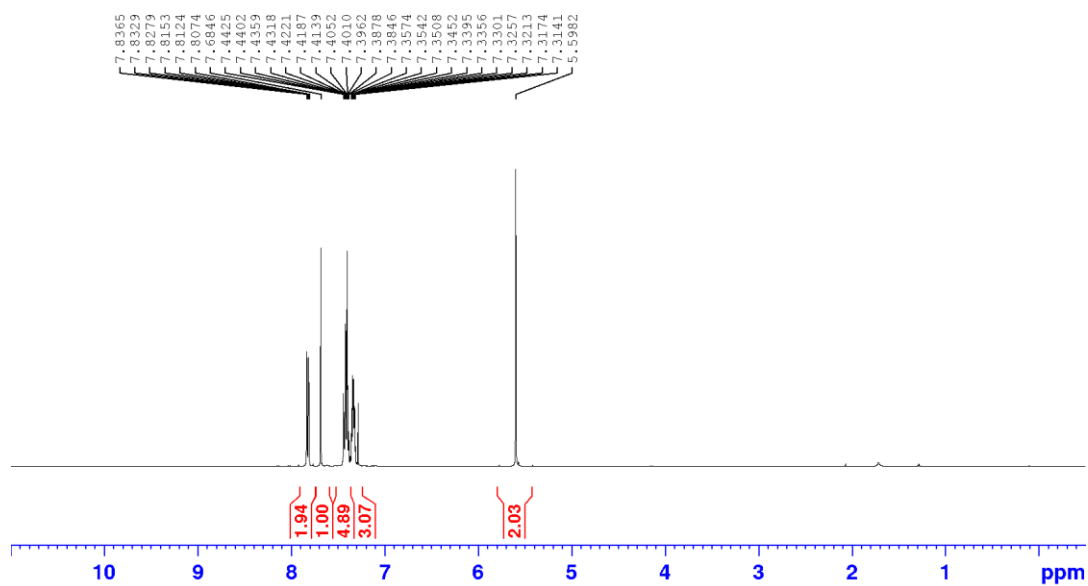
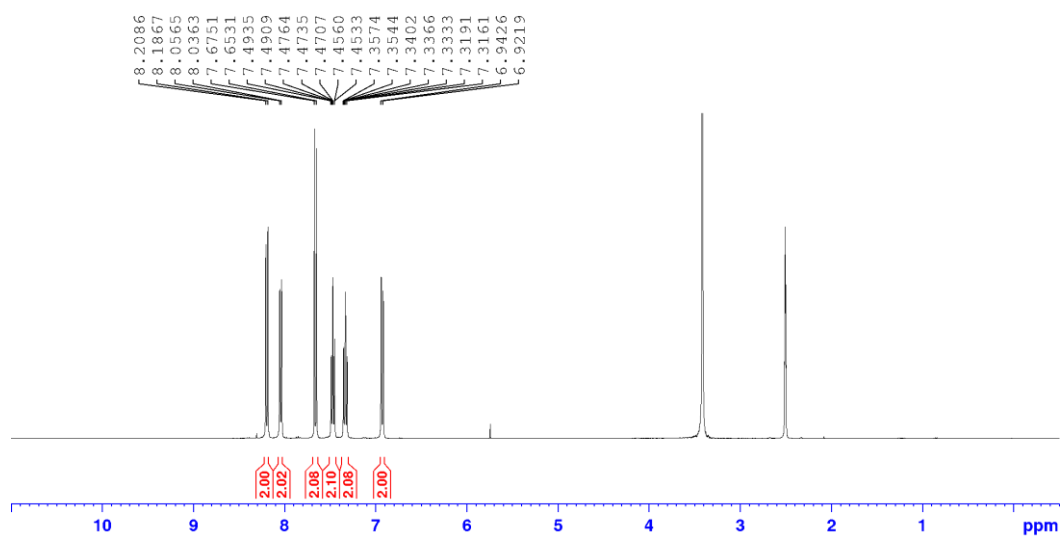
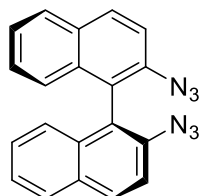




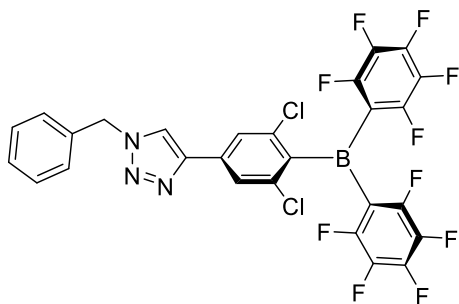


4-phenyl-1-(benzyl)-1H-1,2,3-triazole (95)

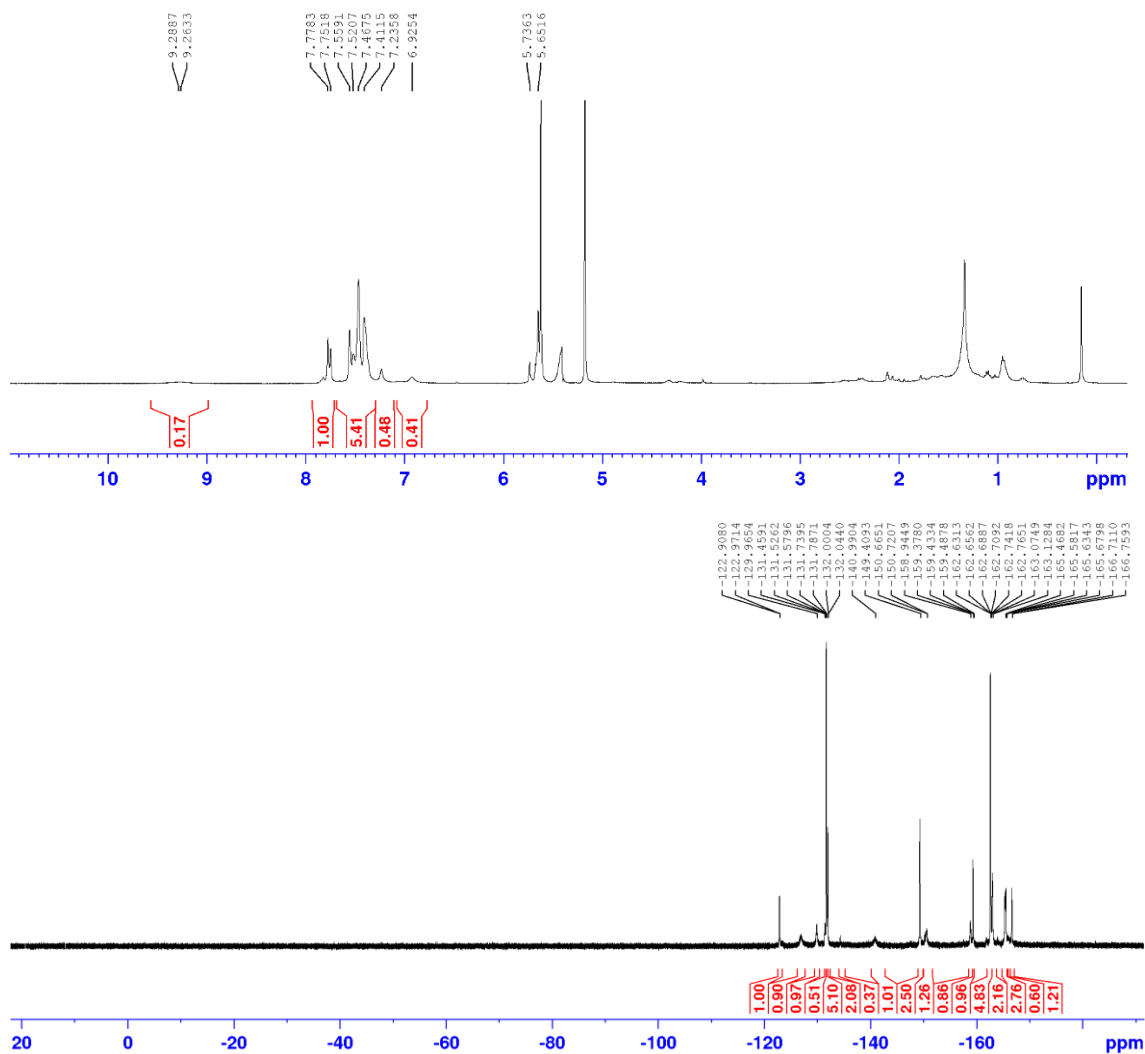


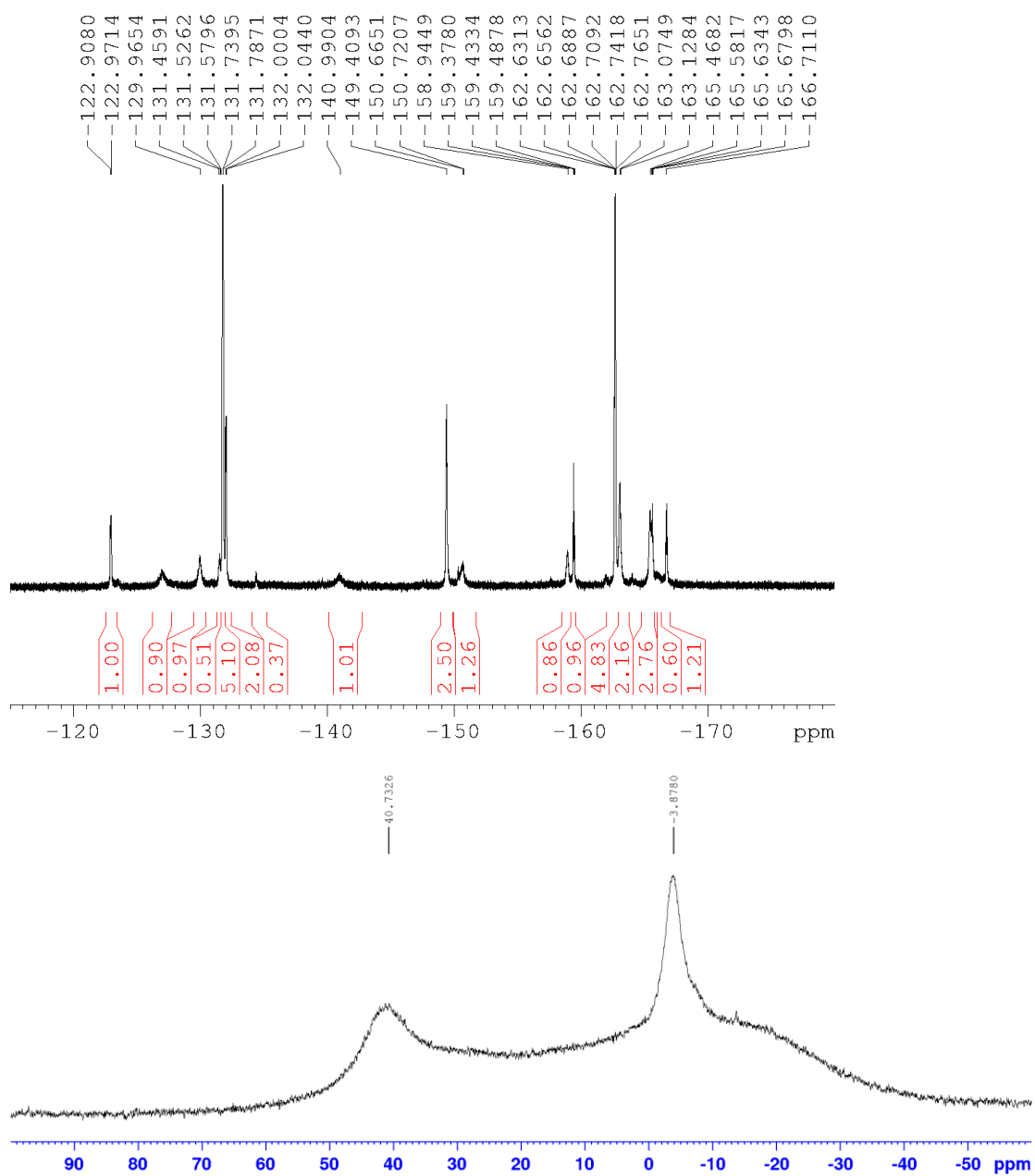
(S)-1,1'-Binaphthyl 2,2'-diazide (**101**)

4-(4-(1-Benzyl-1H-1,2,3-triazol-4-yl)-2,6-dichlorophenylbis(tetrafluorophenyl)borane
(76)



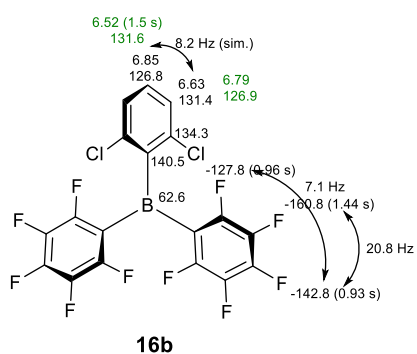
Complex mixture, unassignable and impure.



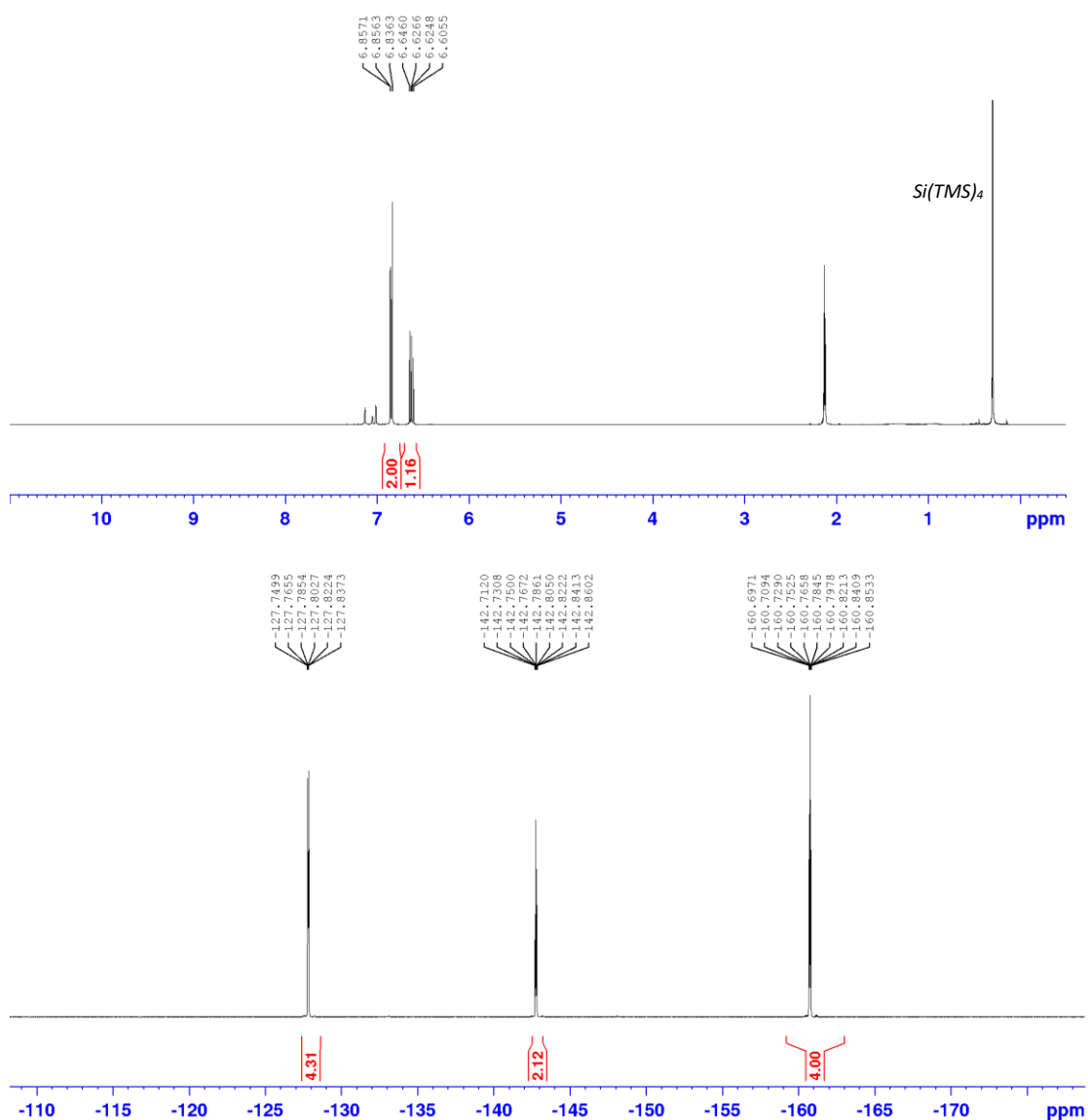


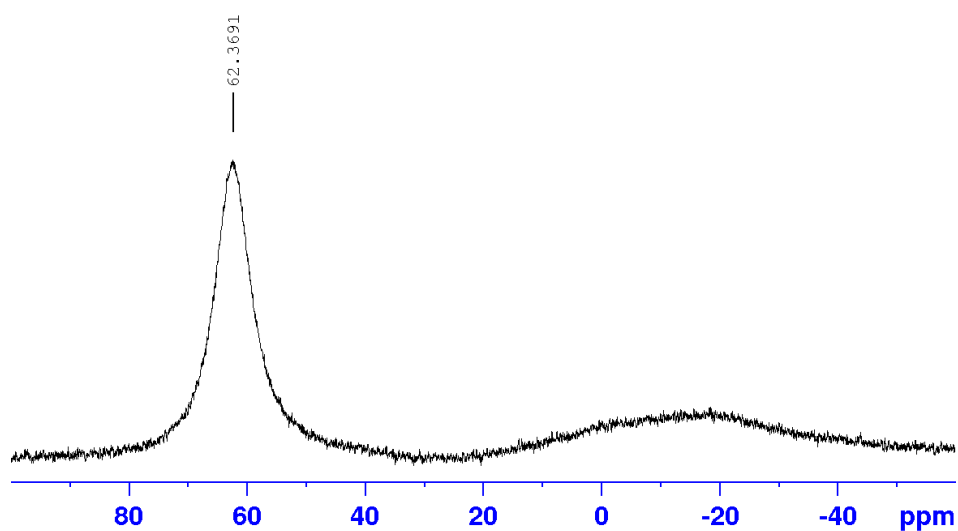
7.5.5 Intermolecular FLP **92** Characterisation and VT NMR Spectroscopy

Inside a glovebox, an oven-dried NMR tube fitted with a J. Young's valve was loaded with borane **16b** and/or triazole **95** in toluene- d_8 (0.6 mL, 68 mM). For full characterisation, free borane **16b** and triazole **95** were also individually analysed by VT NMR spectroscopy. Various ratios of borane:triazole were also prepared to monitor effect on the adduct **92** as well as to identify the 'free' borane (**16b**) or triazole (**95**). These ratios included nominally 1:1 **16b:95** (determined by ^{19}F NMR spectrum integration to be 1.03:1), excess borane 1.3:1 **16b:95**, and excess triazole 1:1.5 **16b:95**. All VT NMR spectroscopic experiments were performed by Dr Geoffrey Akien with assistance from myself. Some ^1H NMR spectra contain a $\text{Si}(\text{TMS})_4$ resonance (~ 0.3 ppm), this is because some DOSY NMR spectroscopic experiments were attempted to monitor the adduct binding, using $\text{Si}(\text{TMS})_4$ as an internal standard. Unfortunately, these were unsuccessful, and therefore are not discussed here however, the resonance will still be present in select spectra.

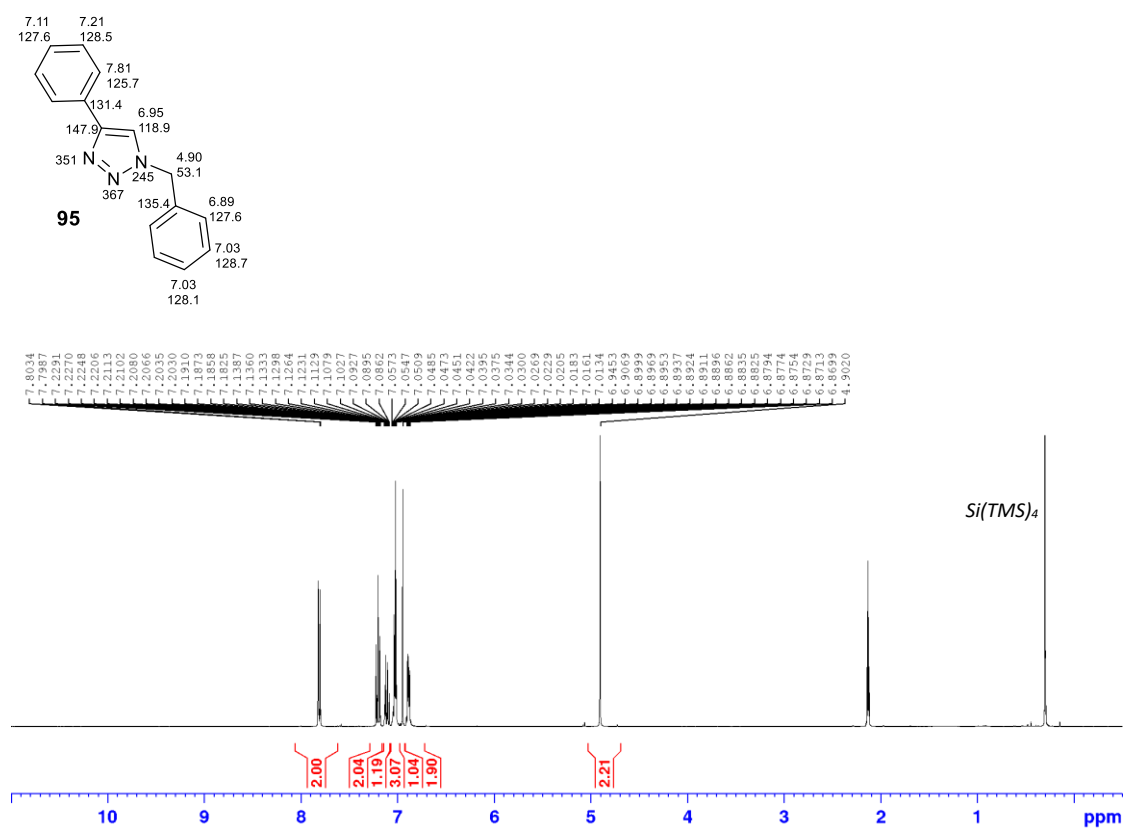
16b in toluene-d₈

(p coupling assignment verified with homodecoupling)

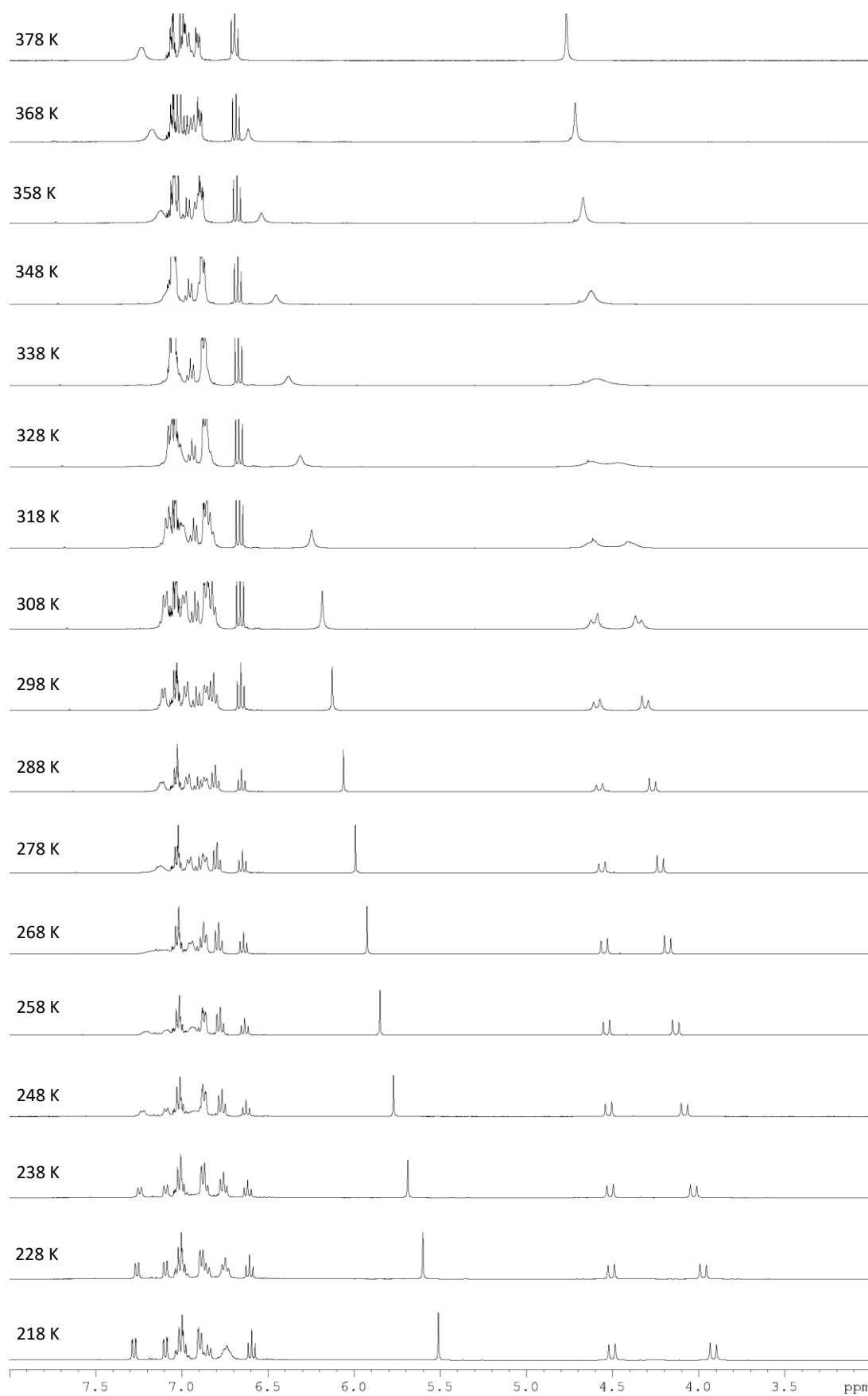
298 K
228 K



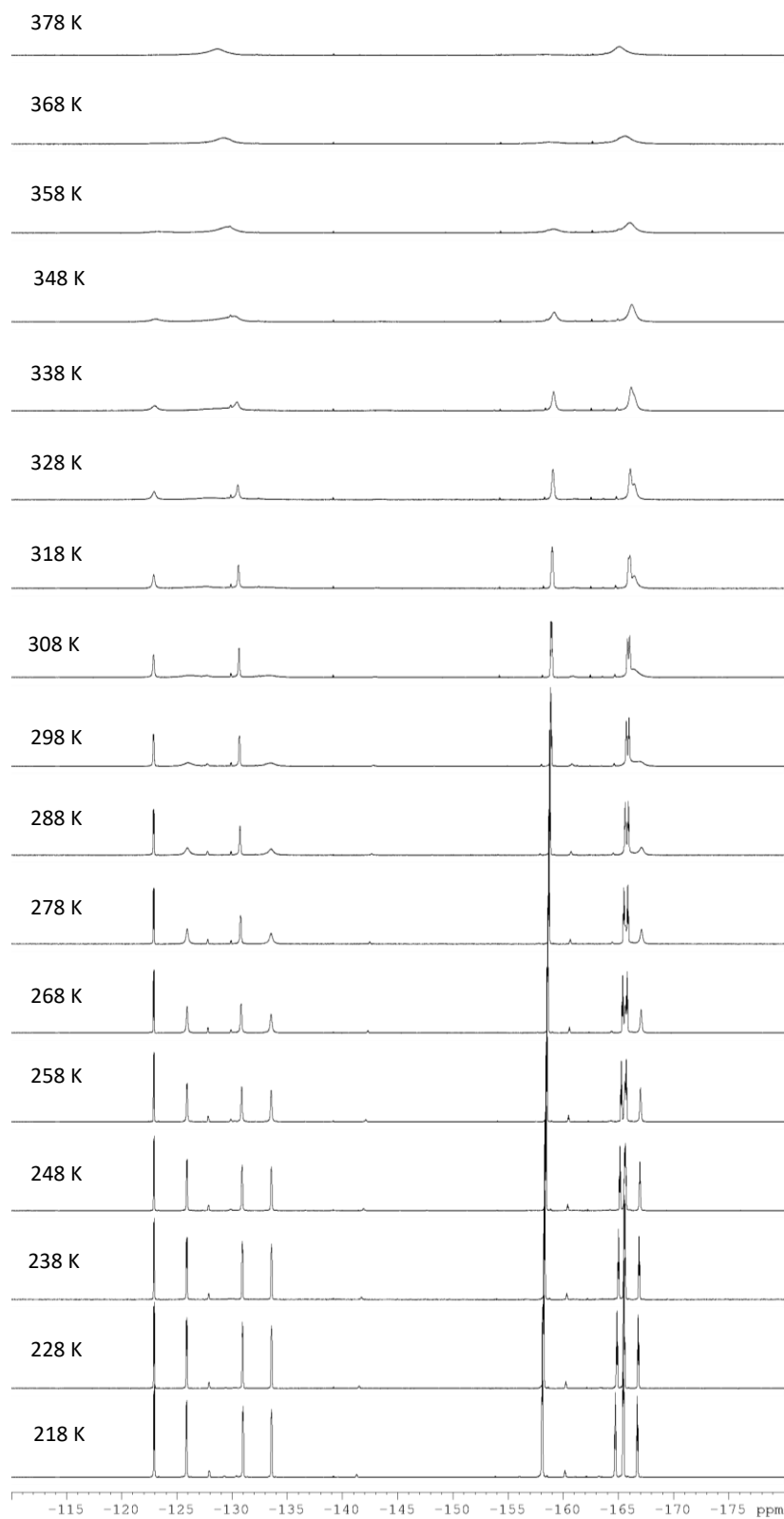
95 in toluene-d₈



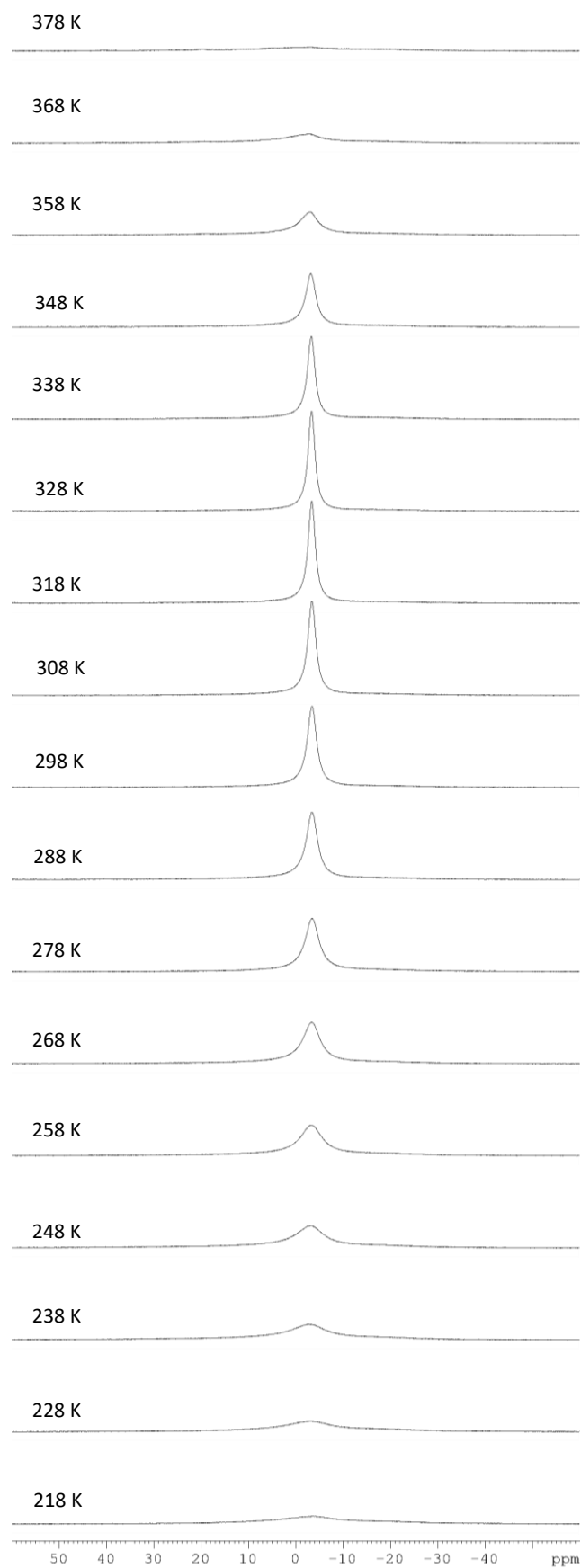
VT ^1H NMR spectra for a stoichiometric mixture of **16b** and **95** in toluene- d_8



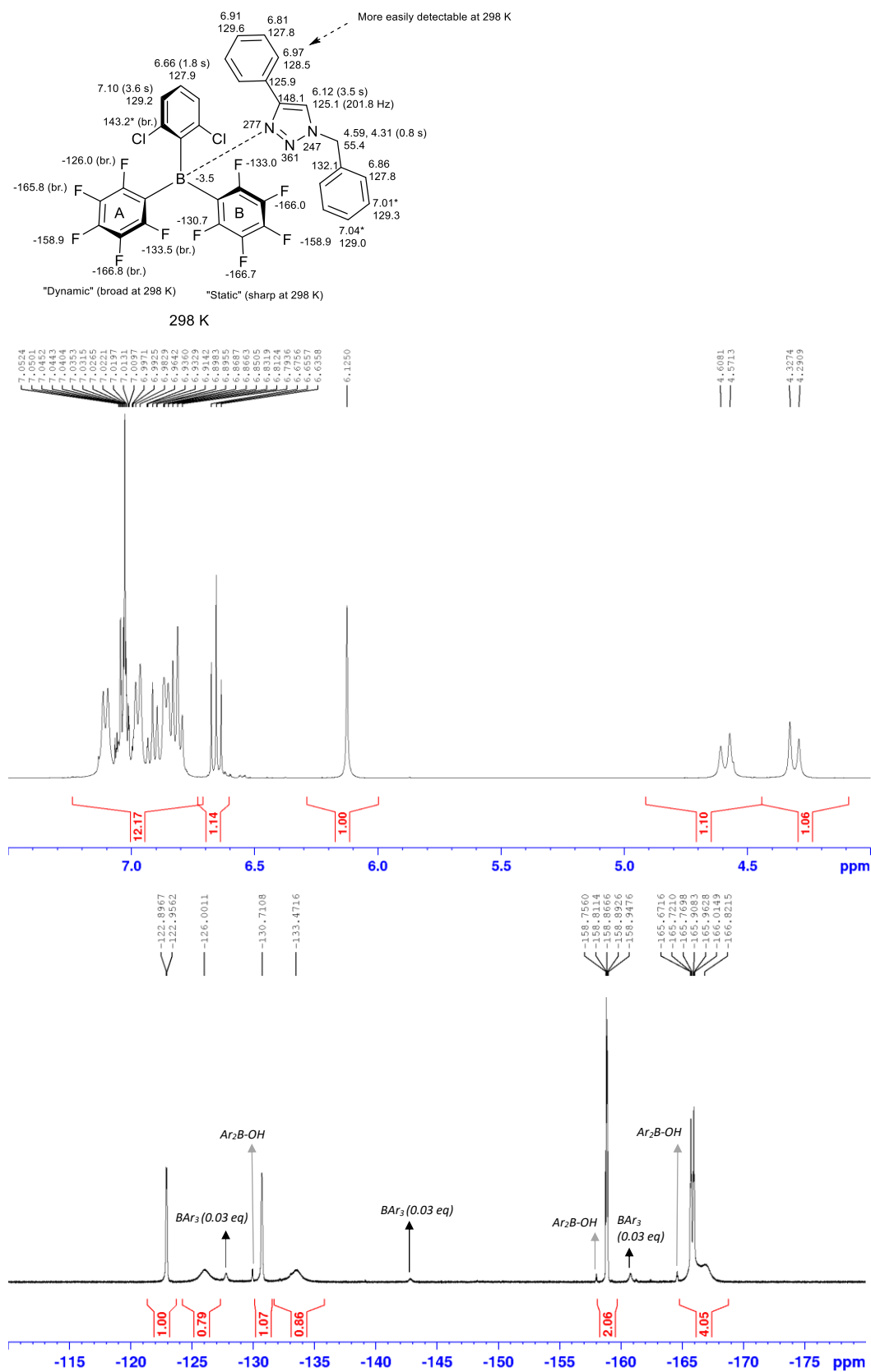
VT ^{19}F NMR spectra for a stoichiometric mixture of **16b** and **95** in toluene- d_8



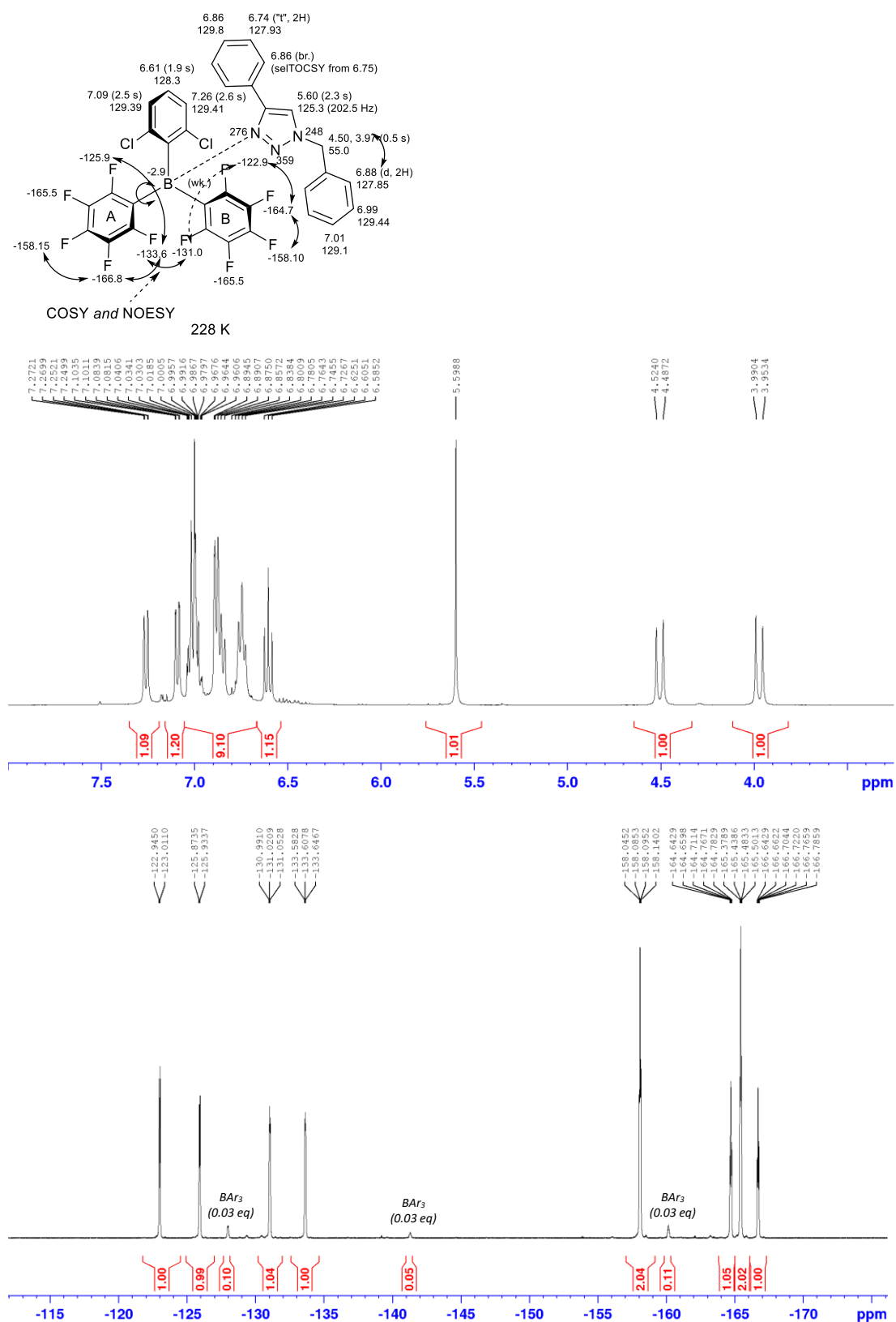
VT ^{11}B NMR spectra for a stoichiometric mixture of **16b** and **95** in toluene- d_8



^1H and ^{19}F NMR spectra for a stoichiometric mixture of **16b** and **95** in toluene- d_8 (298 K)



^1H and ^{19}F NMR spectra for a stoichiometric mixture of **16b** and **95** in toluene- d_8 (228 K)



References

- 1 Greater Innovation for Smarter Materials Optimisation (GISMO), <https://www.smarter-materials.org.uk/>, (Accessed 22nd June 2024).
- 2 H. U. Blaser, *Top. Catal.*, 2010, **53**, 997–1001.
- 3 J. W. Thomson, J. A. Hatnean, J. J. Hastie, A. Pasternak, D. W. Stephan and P. A. Chase, *Org. Process. Res. Dev.*, 2013, **17**, 1287–1292.
- 4 H. C. Brown and P. V. Ramachandran, Sixty Years of Hydride Reductions, *ACS Symposium Series*, 1996, chp 1, 1–30.
- 5 P. I. Dalko and L. Moisan, *Angew. Chem. Int. Ed.*, 2004, **43**, 5138–5175.
- 6 P. Sabatier, *Ind. Eng. Chem.*, 1926, **18**, 1005–1008.
- 7 W. S. Knowles, *Adv. Synth. Catal.*, 2003, **345**, 3–13.
- 8 R. Noyori, *Adv. Synth. Catal.*, 2003, **345**, 15–32.
- 9 J. Lam, K. M. Szkop, E. Mosaferi and D. W. Stephan, *Chem. Soc. Rev.*, 2019, **48**, 3592–3612.
- 10 D. W. Stephan, *Science*, 2016, **354**, 1248–1257.
- 11 S. Gomez, J. A. Peters and T. Maschmeyer, *Adv. Synth. Catal.*, 2002, **344**, 1037–1057.
- 12 K. Murugesan, T. Senthamarai, V. G. Chandrashekhar, K. Natte, P. C. J. Kamer, M. Beller and R. V. Jagadeesh, *Chem. Soc. Rev.*, 2020, **49**, 6273–6328.
- 13 N. A. McGrath, M. Brichacek and J. T. Njardarson, *J. Chem. Educ.*, 2010, **87**, 1348–1349.
- 14 E. A. Mitchell, A. Peschiulli, N. Lefevre, L. Meerpoel and B. U. W. Maes, *Chem. Eur. J.*, 2012, **18**, 10092–10142.
- 15 X. Fang and C. J. Wang, *Org. Biomol. Chem.*, 2018, **16**, 2591–2601.
- 16 J. Shearer, J. L. Castro, A. D. G. Lawson, M. MacCoss and R. D. Taylor, *J. Med. Chem.*, 2022, **65**, 8699–8712.
- 17 J. R. Lewis, *Nat. Prod. Rep.*, 2001, **18**, 95–128.
- 18 D. P. Affron and J. A. Bull, *Eur. J. Org. Chem.*, 2016, **2016**, 139–149.
- 19 A. Nadin, C. Hattotuwigama and I. Churcher, *Angew. Chem. Int. Ed.*, 2012, **51**, 1114–1122.
- 20 Z. Wang, S. Luo, S. Zhang, W. L. Yang, Y. Z. Liu, H. Li, X. Luo and W. P. Deng, *Chem. - Eur. J.*, 2013, **19**, 6739–6745.
- 21 K. Natte, H. Neumann, R. V. Jagadeesh and M. Beller, *Nat. Commun.*, 2017, **8**, 1–9.
- 22 R. V. Jagadeesh, K. Murugesan, A. S. Alshammari, H. Neumann, M.-M. Pohl, J. Radnik and M. Beller, *Science*, 2017, **358**, 326–332.

- 23 Z. Wu, W. Wang, H. Guo, G. Gao, H. Huang and M. Chang, *Nat. Commun.*, 2022, **13**, 1–9.
- 24 A. F. Abdel-Magid, K. G. Carson, B. D. Harris, C. A. Maryanoff and R. D. Shah, *J. Org. Chem.*, 1996, **61**, 3849–3862
- 25 M. Chatterjee, T. Ishizaka and H. Kawanami, *Green. Chem.*, 2016, **18**, 487–496.
- 26 K. Murugesan, T. Senthamarai, V. G. Chandrashekar, K. Natte, P. C. J. Kamer, M. Beller and R. V. Jagadeesh, *Chem. Soc. Rev.*, 2020, **49**, 6273–6328.
- 27 T. Zell and R. Langer, *ChemCatChem*, 2018, **10**, 1930–1940.
- 28 V. Fasano and M. J. Ingleson, *Chem. Eur. J.*, 2017, **23**, 2217–2224.
- 29 V. Fasano, J. E. Radcliffe and M. J. Ingleson, *ACS Catal.*, 2016, **6**, 1793–1798.
- 30 É. Dorkó, M. Szabó, B. Kótai, I. Pápai, A. Domján and T. Soós, *Angew. Chem. Int. Ed.*, 2017, **129**, 9640–9644.
- 31 F. Vidal, J. McQuade, R. Lalancette and F. Jäkle, *J. Am. Chem. Soc.*, 2020, **142**, 14427–14431.
- 32 H. Zhou, W. Zhao, T. Zhang, H. Guo, H. Huang and M. Chang, *Synthesis*, 2019, **51**, 2713–2719.
- 33 Y. Hoshimoto and S. Ogoshi, *ACS Catal.*, 2019, **9**, 5439–5444.
- 34 V. Fasano and M. J. Ingleson, *Chem. Eur. J.*, 2017, **23**, 2217–2224.
- 35 Z. Pan, L. Shen, D. Song, Z. Xie, F. Ling and W. Zhong, *Am. J. Org. Chem.*, 2018, **83**, 11502–11509.
- 36 X. Feng and H. Du, *Tetrahedron Lett.*, 2014, **55**, 6959–6964.
- 37 Y. Hoshimoto, T. Kinoshita, S. Hazra, M. Ohashi and S. Ogoshi, *J Am Chem Soc*, 2018, **140**, 7292–7300.
- 38 N. Wright, *Chemicals Northwest, Elements Autumn*, 2021, 12.
- 39 Y. Shaalan, L. Boulton and C. Jamieson, *Org. Process Res. Dev.*, 2020, **24**, 2745–2751.
- 40 H. Zhou, W. Zhao, T. Zhang, H. Guo, H. Huang and M. Chang, *Synthesis*, 2019, **51**, 2713–2719.
- 41 H. C. Brown and R. M. Adams, *J. Am. Chem. Soc.*, 1942, **64**, 2557–2563.
- 42 W. Tochtermann, *Angew. Chem. Int. Ed.*, 1966, **5**, 351–371.
- 43 G. Wittig and E. Benz, *Chem. Ber.*, 1959, **92**, 1999–2013.
- 44 G. C. Welch, R. R. San Juan, J. D. Masuda and D. W. Stephan, *Science*, 2006, **314**, 1124–1126.
- 45 D. J. Scott, M. J. Fuchter and A. E. Ashley, *Chem. Soc. Rev.*, 2017, **46**, 5689–5700.
- 46 P. A. Chase, G. C. Welch, T. Jurca and D. W. Stephan, *Angew. Chem. Int. Ed.*, 2007, **46**, 8050–8053.

- 47 G. C. Welch, L. Cabrera, P. A. Chase, E. Hollink, J. D. Masuda, P. Wei and D. W. Stephan, *Dalton Trans.*, 2006, **31**, 3407–3414.
- 48 G. C. Welch and D. W. Stephan, *J. Am. Chem. Soc.*, 2007, **129**, 1880–1881.
- 49 T. Özgün, K. Y. Ye, C. G. Daniliuc, B. Wibbeling, L. Liu, S. Grimme, G. Kehr and G. Erker, *Chem. Eur. J.*, 2016, **22**, 5988–5995.
- 50 Z. Mo, E. L. Kolychev, A. Rit, J. Campos, H. Niu and S. Aldridge, *J. Am. Chem. Soc.*, 2015, **137**, 12227–12230.
- 51 J. C. Slootweg and A. R. Jupp, *Frustrated Lewis Pairs*, Springer US, 2021.
- 52 D. J. Scott, M. J. Fuchter and A. E. Ashley, *Chem. Soc. Rev.*, 2017, **46**, 5689–5700.
- 53 S. A. Weicker and D. W. Stephan, *Bull. Chem. Soc. Jpn.*, 2015, **88**, 1003–1016.
- 54 P. Sarkar, S. Das and S. K. Pati, *Chem. Asian J.*, 2022, **17**, DOI: 10.1002/asia.202200148.
- 55 J. M. Farrell, R. T. Posaratnanathan and D. W. Stephan, *Chem. Sci.*, 2015, **6**, 2010–2015.
- 56 G. Ménard and D. W. Stephan, *Angew. Chem. Int. Ed.*, 2012, **51**, 8272–8275.
- 57 T. J. Herrington, B. J. Ward, L. R. Doyle, J. McDermott, A. J. P. White, P. A. Hunt and A. E. Ashley, *Chem. Commun.*, 2014, **50**, 12753–12756.
- 58 S. Freitag, K. M. Krebs, J. Henning, J. Hirdler, H. Schubert and L. Wesemann, *Organometallics*, 2013, **32**, 6785–6791.
- 59 C. Caputo, L. Hounjet, R. Dobrovetsky and D. Stephan, *Science*, 2013, **341**, 1374–1377.
- 60 É. Dorkó, B. Kótai, T. Földes, Á. Gyömöre, I. Pápai and T. Soós, *J. Organomet. Chem.*, 2017, **847**, 258–262.
- 61 S. J. Geier and D. W. Stephan, *J. Am. Chem. Soc.*, 2009, **131**, 3476–3477.
- 62 D. J. Scott, T. R. Simmons, E. J. Lawrence, G. G. Wildgoose, M. J. Fuchter and A. E. Ashley, *ACS Catal.*, 2015, **5**, 5540–5544.
- 63 Y. Hoshimoto, T. Kinoshita, M. Ohashi and S. Ogoshi, *Angew. Chem. Int. Ed.*, 2015, **127**, 11832–11837.
- 64 J. C. Slootweg, A. R. Jupp Editors, P. W. N. M. Van Leeuwen, C. Claver and N. Turner, *Frustrated Lewis Pairs*, Springer, 2021.
- 65 C. M. Mömning, E. Otten, G. Kehr, R. Fröhlich, S. Grimme, D. W. Stephan and G. Erker, *Angew. Chem. Int. Ed.*, 2009, **48**, 6643–6646.
- 66 Z. Mo, E. L. Kolychev, A. Rit, J. Campos, H. Niu and S. Aldridge, *J. Am. Chem. Soc.*, 2015, **137**, 12227–12230.
- 67 M. Sajid, A. Klose, B. Birkmann, L. Liang, B. Schirmer, T. Wiegand, H. Eckert, A. J. Lough, R. Fröhlich, C. G. Daniliuc, S. Grimme, D. W. Stephan, G. Kehr and G. Erker, *Chem. Sci.*, 2013, **4**, 213–219.

- 68 W. Nie, H. F. T. Klare, M. Oestreich, R. Fröhlich, G. Kehr and G. Erker, *Zeitschrift für Naturforschung B*, 2012, **67**, 987–994.
- 69 G. C. Welch, J. D. Masuda and D. W. Stephan, *Inorg. Chem.*, 2006, **45**, 478–480.
- 70 M. A. Dureen, C. C. Brown and D. W. Stephan, *Organometallics*, 2010, **29**, 6594–6607.
- 71 D. J. Scott, *Next Generation 'Frustrated Lewis Pairs'*, Imperial College London, 2016.
- 72 T. A. Rokob, A. Hamza, A. Stirling, T. Soós and I. Pápai, *Angew. Chem. Int. Ed.*, 2008, **47**, 2435–2438.
- 73 A. R. Jupp, *Dalton Trans.*, 2022, **51**, 10681–10689.
- 74 J. Paradies, *Cooperative H₂ Activation by Borane-Derived Frustrated Lewis Pairs*, 2015, chp 9, 263–294.
- 75 L. L. Zeonjuk, N. Vankova, A. Mavrandonakis, T. Heine, G. V. Röschenhaler and J. Eicher, *Chem. Eur. J.*, 2013, **19**, 17413–17424.
- 76 L. L. Zeonjuk, P. S. Petkov, T. Heine, G. V. Röschenhaler, J. Eicher and N. Vankova, *Phys. Chem. Chem. Phys.*, 2015, **17**, 10687–10698.
- 77 J. Paradies, *Acc. Chem. Res.*, 2023, **56**, 821–834.
- 78 T. A. Rokob, A. Hamza, A. Stirling and I. Pápai, *J. Am. Chem. Soc.*, 2009, **131**, 2029–2036.
- 79 S. Grimme, H. Kruse, L. Goerigk and G. Erker, *Angew. Chem. Int. Ed.*, 2010, **49**, 1402–1405.
- 80 S. Tussing, L. Greb, S. Tamke, B. Schirmer, C. Muhle-goll, B. Luy and J. Paradies, *Chem. Eur. J.*, 2015, **21**, 8056–8059.
- 81 S. Tussing, K. Kaupmees and J. Paradies, *Chem. Eur. J.*, 2016, **22**, 7422–7426.
- 82 J. Paradies, *Coord. Chem. Rev.*, 2019, **380**, 170–183.
- 83 A. R. Jupp and D. W. Stephan, *Trends Chem.*, 2019, **1**, 35–48.
- 84 W. E. Piers, A. J. V. Marwitz and L. G. Mercier, *Inorg. Chem.*, 2011, **50**, 12252–12262.
- 85 L. (Leo) Liu, L. L. Cao, Y. Shao, G. Ménard and D. W. Stephan, *Chem.*, 2017, **3**, 259–267.
- 86 F. Holtrop, A. R. Jupp, B. J. Kooij, N. P. van Leest, B. de Bruin and J. C. Slootweg, *Angew. Chem. Int. Ed.*, 2020, **132**, 22394–22400.
- 87 F. Holtrop, A. R. Jupp, N. P. van Leest, M. Paradiz Dominguez, R. M. Williams, A. M. Brouwer, B. de Bruin, A. W. Ehlers and J. C. Slootweg, *Chem. Eur. J.*, 2020, **26**, 9005–9011.
- 88 W. E. Piers and T. Chivers, *Chem. Soc. Rev.*, 1997, **26**, 345–354.
- 89 A. R. Siedle, R. A. Newmark, W. M. Lamanna and J. C. Huffman, *Organometallics*, 1993, **12**, 1491–1492.
- 90 M. G. Guerzoni, A. Dasgupta, E. Richards and R. L. Melen, *Chem. Catalysis*, 2022, **2**, 2865–2875.

- 91 N. Lewis, G., *Valence and the structure of atoms and molecules*, Chemical Catalog. Company, 1923.
- 92 U. Mayer, V. Gutmann and W. Gerger, *Monatsh. Chem.*, 1975, **106**, 1235–1257.
- 93 M. A. Beckett, G. C. Strickland, J. R. Holland and K. S. Varma, *Polymer*, 1996, **37**, 4629–4631.
- 94 J. L. Carden, A. Dasgupta and R. L. Melen, *Chem. Soc. Rev.*, 2020, **49**, 1706–1725.
- 95 R. F. Childs, D. L. Mulholland and A. Nixon, *Can. J. Chem.*, 1982, **60**, 801–808.
- 96 I. B. Sivaev and V. I. Bregadze, *Coord. Chem. Rev.*, 2014, **270–271**, 75–88.
- 97 J. Paradies and S. Tussing, *Frustrated Lewis pair-catalyzed reductions using molecular hydrogen*, 2019, chp 7, 167-225.
- 98 M. A. Beckett, D. S. Brassington, S. J. Coles and M. B. Hursthouse, *Inorg. Chem. Commun.*, 2000, **3**, 530–533.
- 99 J. A. Nicasio, S. Steinberg, B. Inés and M. Alcarazo, *Chem. Eur. J.*, 2013, **19**, 11016–11020.
- 100 É. Dorkó, M. Szabó, B. Kótai, I. Pápai, A. Domján and T. Soós, *Angew. Chem. Int. Ed.*, 2017, **56**, 9512–9516.
- 101 A. E. Ashley, T. J. Herrington, G. G. Wildgoose, H. Zaher, A. L. Thompson, N. H. Rees, T. Krämer and D. Öhare, *J. Am. Chem. Soc.*, 2011, **133**, 14727–14740.
- 102 M. Ullrich, A. J. Lough and D. W. Stephan, *J. Am. Chem. Soc.*, 2009, **131**, 52–53.
- 103 Z. Lu, Z. Cheng, Z. Chen, L. Weng, Z. H. Li and H. Wang, *Angew. Chem. Int. Ed.*, 2011, **50**, 12227–12231.
- 104 S. C. Binding, H. Zaher, F. Mark Chadwick and D. O’Hare, *Dalton Trans.*, 2012, **41**, 9061–9066.
- 105 S. Das and S. K. Pati, *Chem. Eur. J.*, 2017, **23**, 1078–1085.
- 106 M. Heshmat and T. Privalov, *J. Phys. Chem. A*, 2018, **122**, 5098–5106.
- 107 É. Dorkó, B. Kótai, T. Földes, Á. Gyömöre, I. Pápai and T. Soós, *J. Organomet. Chem.*, 2017, **847**, 258–262.
- 108 M. V. Metz, D. J. Schwartz, C. L. Stern, P. N. Nickias and T. J. Marks, *Angew. Chem. Int. Ed.*, 2000, **39**, 1312–1316.
- 109 M. V. Metz, D. J. Schwartz, C. L. Stern, T. J. Marks and P. N. Nickias, *Organometallics*, 2002, **21**, 4159–4168.
- 110 D. W. Stephan and G. Erker, *Angew. Chem. Int. Ed.*, 2015, **54**, 6400–6441.
- 111 S. A. Weicker and D. W. Stephan, *Bull. Chem. Soc. Jpn.*, 2015, **88**, 1003–1016.
- 112 D. W. Stephan and G. Erker, *Angew. Chem. Int. Ed.*, 2010, **49**, 46–76.
- 113 J. Paradies, *SynLett.*, 2013, **24**, 777–780.

- 114 L. Köring, N. A. Sitte, M. Bursch, S. Grimme and J. Paradies, *Chem - Eur J*, 2021, **27**, 14179–14183.
- 115 V. Fasano, J. E. Radcliffe and M. J. Ingleson, *ACS Catal.*, 2016, **6**, 1793–1798.
- 116 P. Spies, S. Schwendemann, S. Lange, G. Kehr, R. Fröhlich and G. Erker, *Angew. Chem. Int. Ed.*, 2008, **47**, 7543–7546.
- 117 T. A. Rokob, A. Hamza, A. Stirling and I. Pápai, *J. Am. Chem. Soc.*, 2009, **131**, 2029–2036.
- 118 D. Chen and J. Klankermayer, *Chem. Commun.*, 2008, 2130–2131.
- 119 M. Mewald and M. Oestreich, *Chem. Eur. J.*, 2012, **18**, 14079–14084.
- 120 É. Dorkó, M. Szabó, B. Kótai, I. Pápai, A. Domján and T. Soós, *Angew. Chem. Int. Ed.*, 2017, **56**, 9512–9516.
- 121 M. Bakos, Á. Gyömöre, A. Domján and T. Soós, *Angew. Chem. Int. Ed.*, 2017, **56**, 5217–5221.
- 122 V. Fasano, J. E. Radcliffe and M. J. Ingleson, *ACS Catal.*, 2016, **6**, 1793–1798.
- 123 V. Fasano and M. J. Ingleson, *Synthesis*, 2018, **50**, 1783–1795.
- 124 Y. Hoshimoto, T. Kinoshita, S. Hazra, M. Ohashi and S. Ogoshi, *J. Am. Chem. Soc.*, 2018, **140**, 7292–7300.
- 125 Y. Hoshimoto, S. Ogoshi, Y. Hisata, T. Washio and S. Takizawa, *ChemRxiv*, 2023, preprint, DOI: 10.26434/chemrxiv-2023-3mwbd.
- 126 K. Murugesan, T. Senthamarai, V. G. Chandrashekhar, K. Natte, P. C. J. Kamer, M. Beller and R. V. Jagadeesh, *Chem. Soc. Rev.*, 2020, **49**, 6273–6328.
- 127 V. Fasano and M. J. Ingleson, *Synthesis*, 2018, **50**, 1783–1795.
- 128 É. Dorkó, B. Kótai, T. Földes, Á. Gyömöre, I. Pápai and T. Soós, *J. Organomet. Chem.*, 2017, **847**, 258–262.
- 129 T. Mahdi and D. W. Stephan, *Angew. Chem. Int. Ed.*, 2015, **54**, 8511–8514.
- 130 H. Yamamoto et al., US 2011/0245223 A1, 2011.
- 131 C. Bergquist, B. M. Bridgewater, C. J. Harlan, J. R. Norton, R. A. Friesner and G. Parkin, *J. Am. Chem. Soc.*, 2000, **122**, 10581–10590.
- 132 D. J. Scott, T. R. Simmons, E. J. Lawrence, G. G. Wildgoose, M. J. Fuchter and A. E. Ashley, *ACS Catal.*, 2015, **5**, 5540–5544.
- 133 M. Bakos, Z. Dobi, D. Fegyverneki, Á. Gyömöre, I. Fernández and T. Soós, *ACS Sustain. Chem. Eng.*, 2018, **6**, 10869–10875.
- 134 Á. Gyömöre, M. Bakos, T. Földes, I. Pápai, A. Domján and T. Soós, *ACS Catal.*, 2015, **5**, 5366–5372.
- 135 T. Mahdi and D. W. Stephan, *J. Am. Chem. Soc.*, 2014, **136**, 15809–15812.
- 136 D. J. Scott, M. J. Fuchter and A. E. Ashley, *J. Am. Chem. Soc.*, 2014, **136**, 15813–15816.

- 137 R. H. Morris, *Chem. Rev.*, 2016, **116**, 8588–8654.
- 138 D. J. Scott, T. R. Simmons, E. J. Lawrence, G. G. Wildgoose, M. J. Fuchter and A. E. Ashley, *ACS Catal.*, 2015, **5**, 5540–5544.
- 139 G. Erös, K. Nagy, H. Mehdi, I. Pápai, P. Nagy, P. Király, G. Tárkányi and T. Soós, *Chem. Eur. J.*, 2012, **18**, 574–585.
- 140 G. Eros, H. Mehdi, I. Pápai, T. A. Rokob, P. Király, G. Tárkányi and T. Soós, *Angew. Chem. Int. Ed.*, 2010, **49**, 6559–6563.
- 141 W. S. Knowles, *Adv. Synth. Catal.*, 2003, **345**, 3–13.
- 142 H. U. Blaser, H. P. Buser, K. Coers, R. Hanreich, H. P. Jalett., E. Jelsch, B. Pugin, H. D. Schneider, F. Spindler and A. Wegmann, *Chimia*, 1999, **53**, 275–280.
- 143 H. P. Meyer, A. Kiener, R. Imwinkelried and N. Shaw, *Chimia*, 1997, **51**, 287–289.
- 144 H. U. Blaser, F. Spindler and M. Studer, *Appl. Catal. A Gen.*, 2001, **221**, 119–143.
- 145 X. Feng and H. Du, *Tetrahedron Lett.*, 2014, **55**, 6959–6964.
- 146 L. Shi and Y. G. Zhou, *ChemCatChem*, 2015, **7**, 54–56.
- 147 X. Feng, W. Meng and H. Du, *Chem. Soc. Rev.*, 2023, **52**, 8580–8598.
- 148 X. Feng, W. Meng and H. Du, *Chem. Soc. Rev.*, 2023, **52**, 8580–8598.
- 149 M. G. Guerzoni, A. Dasgupta, E. Richards and R. L. Melen, *Chem. Catalysis*, 2022, **2**, 2865–2875.
- 150 D. Chen and J. Klankermayer, *Chem. Commun.*, 2008, 2130–2131.
- 151 Y. Liu and H. Du, *J. Am. Chem. Soc.*, 2013, **135**, 6810–6813.
- 152 S. Wei and H. Du, *J. Am. Chem. Soc.*, 2014, **136**, 12261–12264.
- 153 X. Wang, G. Kehr, C. G. Daniliuc and G. Erker, *J. Am. Chem. Soc.*, 2014, **136**, 3293–3303.
- 154 K. Y. Ye, X. Wang, C. G. Daniliuc, G. Kehr and G. Erker, *Eur. J. Inorg. Chem.*, 2017, **2**, 368–371.
- 155 M. Lindqvist, K. Borre, K. Axenov, B. Kótai, M. Nieger, M. Leskelä, I. Pápai and T. Repo, *J. Am. Chem. Soc.*, 2015, **137**, 4038–4041.
- 156 B. Gao, X. Feng, W. Meng and H. Du, *Angew. Chem. Int. Ed.*, 2020, **59**, 4498–4504.
- 157 Z. Pan, L. Shen, D. Song, Z. Xie, F. Ling and W. Zhong, *Am. J. Org. Chem.*, 2018, **83**, 11502–11509.
- 158 P. J. Cossar, L. Hizartzidis, M. I. Simone, A. McCluskey and C. P. Gordon, *Org. Biomol. Chem.*, 2015, **13**, 7119–7130.
- 159 M. Baumann, T. S. Moody, M. Smyth and S. Wharry, *Org. Process Res. Dev.*, 2020, **24**, 1802–1813.

- 160 M. B. Plutschack, B. Pieber, K. Gilmore and P. H. Seeberger, *Chem. Rev.*, 2017, **117**, 11796–11893.
- 161 M. Guidi, P. H. Seeberger and K. Gilmore, *Chem. Soc. Rev.*, 2020, **49**, 8910–8932.
- 162 J. Britton and C. L. Raston, *Chem. Soc. Rev.*, 2017, **46**, 1250–1271.
- 163 J. Madarász, G. Farkas, S. Balogh, Á. Szöllosy, J. Kovács, F. Darvas, L. Üрге and J. Bakos, *J. Flow Chem.*, 2011, **1**, 62–67.
- 164 S. Kobayashi, *Chem. Asian J.*, 2016, **11**, 425–436.
- 165 K. H. Hopmann and A. Bayer, *Coord. Chem. Rev.*, 2014, **268**, 59–82.
- 166 Q. Li, C. J. Hou, X. N. Liu, D. Z. Huang, Y. J. Liu, R. F. Yang and X. P. Hu, *RSC Adv.*, 2015, **5**, 13702–13708.
- 167 S. Zhou, S. Fleischer, K. Junge and M. Beller, *Angew. Chem. Int. Ed.*, 2011, **50**, 5120–5124.
- 168 M. Irfan, T. N. Glasnov and C. O. Kappe, *ChemSusChem*, 2011, **4**, 300–316.
- 169 T. Yu, J. Jiao, P. Song, W. Nie, C. Yi, Q. Zhang and P. Li, *ChemSusChem*, 2020, **13**, 2876–2893.
- 170 C. J. Mallia and I. R. Baxendale, *Org. Process Res. Dev.*, 2016, **20**, 327–360.
- 171 B. Gutmann, D. Cantillo and C. O. Kappe, *Angew. Chem. Int. Ed.*, 2015, **54**, 6688–6728.
- 172 S. Kobayashi, *Chem. Asian J.*, 2016, **11**, 425–436.
- 173 K. S. Elvira, X. C. I Solvas, R. C. R. Wootton and A. J. Demello, *Nat. Chem.*, 2013, **5**, 905–915.
- 174 D. Cantillo and C. O. Kappe, *ChemCatChem*, 2015, **6**, 3286–3305.
- 175 M. Irfan, T. N. Glasnov and C. O. Kappe, *ChemSusChem*, 2011, **4**, 300–316.
- 176 T. Yu, J. Jiao, P. Song, W. Nie, C. Yi, Q. Zhang and P. Li, *ChemSusChem*, 2020, **13**, 2876–2893.
- 177 Z. Amara, M. Poliakoff, R. Duque, D. Geier, G. Franciò, C. M. Gordon, R. E. Meadows, R. Woodward and W. Leitner, *Org. Process Res. Dev.*, 2016, **20**, 1321–1327.
- 178 N. Sugisawa, H. Nakamura and S. Fuse, *Catalysts*, 2020, **10**, 1321.
- 179 P. Ji, X. Feng, P. Oliveres, Z. Li, A. Murakami, C. Wang and W. Lin, *J. Am. Chem. Soc.*, 2019, **141**, 14878–14888.
- 180 K. Omoregbee, K. N. H. Luc, A. H. Dinh and T. V. Nguyen, *J. Flow Chem.*, 2020, **10**, 161–166.
- 181 M. K. Jackl, L. Legnani, B. Morandi and J. W. Bode, *Org. Lett.*, 2017, **19**, 4696–4699.
- 182 D. Voicu, M. Abolhasani, R. Choueiri, G. Lestari, C. Seiler, G. Menard, J. Greener, A. Guenther, D. W. Stephan and E. Kumacheva, *J. Am. Chem. Soc.*, 2014, **136**, 3875–3880.

- 183 D. Voicu, D. W. Stephan and E. Kumacheva, *ChemSusChem*, 2015, **8**, 4202–4208.
- 184 L. C. Wilkins, J. L. Howard, S. Burger, L. Frenzel-Beyme, D. L. Browne and R. L. Melen, *Adv. Synth. Catal.*, 2017, **359**, 2580–2584.
- 185 A. R. Jupp and D. W. Stephan, *Trends Chem.*, 2019, **1**, 35–48.
- 186 D. Voicu, M. Abolhasani, R. Choueiri, G. Lestari, C. Seiler, G. Menard, J. Greener, A. Guenther, D. W. Stephan and E. Kumacheva, *J. Am. Chem. Soc.*, 2014, **136**, 3875–3880.
- 187 D. Voicu, D. W. Stephan and E. Kumacheva, *ChemSusChem*, 2015, **8**, 4202–4208.
- 188 J. L. Carden, *Enabling technologies to access new materials using frustrated Lewis pairs*, Cardiff University, 2021.
- 189 É. Dorkó, M. Szabó, B. Kótai, I. Pápai, A. Domján and T. Soós, *Angew. Chem. Int. Ed.*, 2017, **56**, 9512–9516.
- 190 Á. Gyömöre, M. Bakos, T. Földes, I. Pápai, A. Domján and T. Soós, *ACS Catal.*, 2015, **5**, 5366–5372.
- 191 É. Dorkó, M. Szabó, B. Kótai, I. Pápai, A. Domján and T. Soós, *Angew. Chem. Int. Ed.*, 2017, **129**, 9640–9644.
- 192 M. Bakos, Z. Dobi, D. Fegyverneki, Á. Gyömöre, I. Fernández and T. Soós, *ACS Sustain. Chem. Eng.*, 2018, **6**, 10869–10875.
- 193 É. Dorkó, B. Kótai, T. Földes, Á. Gyömöre, I. Pápai and T. Soós, *J. Organomet. Chem.*, 2017, **847**, 258–262.
- 194 T. Mahdi and D. W. Stephan, *J. Am. Chem. Soc.*, 2014, **136**, 15809–15812.
- 195 V. Fasano, J. H. W. LaFortune, J. M. Bayne, M. J. Ingleson and D. W. Stephan, *Chem. Commun.*, 2018, **54**, 662–665.
- 196 J. W. Thomson, J. A. Hatnean, J. J. Hastie, A. Pasternak, D. W. Stephan and P. A. Chase, *Org. Process Res. Dev.*, 2013, **17**, 1287–1292.
- 197 V. Fasano and M. J. Ingleson, *Synthesis*, 2018, **50**, 1783–1795.
- 198 G. Erös, K. Nagy, H. Mehdi, I. Pápai, P. Nagy, P. Király, G. Tárkányi and T. Soós, *Chem. Eur. J.*, 2012, **18**, 574–585.
- 199 A. Michaelis and H. V. Soden, *Liebigs Ann. Chem.*, 1885, **229**, 295–334.
- 200 S. M. Berger, M. Ferger and T. B. Marder, *Chem. Eur. J.*, 2021, **27**, 7043–7058.
- 201 J. L. Carden, A. Dasgupta and R. L. Melen, *Chem. Soc. Rev.*, 2020, **49**, 1706–1725.
- 202 S. M. Berger, M. Ferger and T. B. Marder, *Chem. Eur. J.*, 2021, **27**, 7043–7058.
- 203 Y. Hoshimoto, S. Ogoshi, Y. Hisata, T. Washio and S. Takizawa, *ChemRxiv*, 2023, preprint, DOI: 10.26434/chemrxiv-2023-3mwbd.
- 204 A. M. Borys, *Organometallics*, 2023, **42**, 182–196.

- 205 A. E. Ashley, T. J. Herrington, G. G. Wildgoose, H. Zaher, A. L. Thompson, N. H. Rees, T. Krämer and D. Öhare, *J. Am. Chem. Soc.*, 2011, **133**, 14727–14740.
- 206 D. Fegyverneki, N. Kolozsvári, D. Molnár, O. Egyed, T. Holczbauer and T. Soós, *Chem. Eur. J.*, 2019, **25**, 2179–2183.
- 207 R. D. Chambers, H. C. Clark, C. J. Willis Yol, B. R. D Chambers and C. J. Willis, *J. Am. Chem. Soc.*, **82**, 5298–5301.
- 208 G. A. Molander and N. Ellis, *Acc. Chem. Res.*, 2007, **40**, 275–286.
- 209 M. Ferger, S. M. Berger, F. Rauch, M. Schönitz, J. Rühle, J. Krebs, A. Friedrich and T. B. Marder, *Chem. Eur. J.*, 2021, **27**, 9094–9101.
- 210 L. Wu and K. Burgess, *Chem. Commun.*, 2008, **40**, 4933–4935.
- 211 E. V Rumyantsev, Y. S. Marfin and E. V Antina, *Russ. Chem. Bull.*, **59**, 1890–1895.
- 212 F. Vidal, J. McQuade, R. Lalancette and F. Jäkle, *J. Am. Chem. Soc.*, 2020, **142**, 14427–14431.
- 213 S. A. Cummings, M. Iimura, C. J. Harlan, R. J. Kwaan, I. Vu Trieu, J. R. Norton, B. M. Bridgewater, F. Jäkle, A. Sundararaman and M. Tilset, *Organometallics*, 2006, **25**, 1565–1568.
- 214 S. D. Roughley and A. M. Jordan, *J. Med. Chem.*, 2011, **54**, 3451–3479.
- 215 O. I. Afanasyev, E. Kuchuk, D. L. Usanov and D. Chusov, *Chem. Rev.*, 2019, **119**, 11857–11911.
- 216 G. Eros, H. Mehdi, I. Pápai, T. A. Rokob, P. Király, G. Tárkányi and T. Soós, *Angew. Chem. Int. Ed.*, 2010, **49**, 6559–6563.
- 217 J. A. Mendes, P. R. R. Costa, M. Yus, F. Foubelo and C. D. Buarque, *Beilstein J. Org. Chem.*, 2021, **17**, 1096–1140.
- 218 M. D. Visco, J. T. Reeves, M. A. Marsini, I. Volchkov, C. A. Busacca, A. E. Mattson and C. H. Senanayake, *Tetrahedron Lett.*, 2016, **57**, 1903–1905.
- 219 L. Jiang, P. Zhou, Z. Zhang, S. Jin and Q. Chi, *Ind. Eng. Chem. Res.*, 2017, **56**, 12556–12565.
- 220 Y. Zhang, Q. Yan, G. Zi and G. Hou, *Org. Lett.*, 2017, **19**, 4215–4218.
- 221 C. Yin, R. Zhang, Y. Pan, S. Gao, X. Ding, S. T. Bai, Q. Lang and X. Zhang, *Am. J. Org. Chem.*, 2024, **89**, 527–533.
- 222 T. Wang, H. Xu, J. He and Y. Zhang, *Tetrahedron*, 2020, **76**, 131394.
- 223 M. C. Fu, R. Shang, W. M. Cheng and Y. Fu, *Angew. Chem. Int. Ed.*, 2015, **54**, 9042–9046.
- 224 T. Mahdi and D. W. Stephan, *Chem. Eur. J.*, 2015, **21**, 11134–11142.
- 225 C. M. Alder, J. D. Hayler, R. K. Henderson, A. M. Redman, L. Shukla, L. E. Shuster and H. F. Sneddon, *Green Chem.*, 2016, **18**, 3879–3890.

- 226 Z. Luo, S. Wan, Y. Pan, Z. Yao, X. Zhang, B. Li, J. Li, L. Xu and Q. H. Fan, *Asian J. Org. Chem.*, 2022, **11**, 3–9.
- 227 Z. Luo, Y. Pan, Z. Yao, J. Yang, X. Zhang, X. Liu, L. Xu and Q. H. Fan, *Green Chem.*, 2021, **23**, 5205–5211.
- 228 A. Bunrit, P. Srifá, T. Rukkijakan, C. Dahlstrand, G. Huang, S. Biswas, R. A. Watile and J. S. M. Samec, *ACS Catal.*, 2020, **10**, 1344–1352.
- 229 A. Bunrit, C. Dahlstrand, S. K. Olsson, P. Srifá, G. Huang, A. Orthaber, P. J. R. Sjöberg, S. Biswas, F. Himo and J. S. M. Samec, *J. Am. Chem. Soc.*, 2015, **137**, 4646–4649.
- 230 T. Ma, H. Y. Zhang, G. Yin, J. Zhao and Y. Zhang, *J. Flow Chem.*, 2018, **8**, 35–43.
- 231 C. B. Pollard and D. C. Young, *J. Org. Chem.*, 1951, **16**, 661–672.
- 232 G. Li, Y. Liang and J. C. Antilla, *J. Am. Chem. Soc.*, 2007, **129**, 5830–5831.
- 233 S. Xu, J. S. Boschen, A. Biswas, T. Kobayashi, M. Pruski, T. L. Windus and A. D. Sadow, *Dalton Trans.*, 2015, **44**, 15897–15904.
- 234 G. L. Beutner, M. S. Bultman, B. M. Cohen, J. Fan, J. Marshall and C. Sfougataki, *Org. Process Res. Dev.*, 2019, **23**, 2050–2056.
- 235 B. Gao, X. Feng, W. Meng and H. Du, *Angew. Chem. Int. Ed.*, 2020, **132**, 4528–4534.
- 236 J. Chen, B. Gao, X. Feng, W. Meng and H. Du, *Org. Lett.*, 2021, **23**, 8565–8569.
- 237 X. Zhu and H. Du, *Org. Biomol. Chem.*, 2015, **13**, 1013–1016.
- 238 Y. Shaalan, L. Boulton and C. Jamieson, *Org. Process Res. Dev.*, 2020, **24**, 2745–2751.
- 239 C. Pratley, Y. Shaalan, L. Boulton, C. Jamieson, J. A. Murphy and L. J. Edwards, *Org. Process Res. Dev.*, 2024, **28**, 1725–1733.
- 240 M. C. Bryan, D. Wernick, C. D. Hein, J. V. Petersen, J. W. Eschelbach and E. M. Doherty, *Beilstein J. Org. Chem.*, 2011, **7**, 1141–1149.
- 241 D. Rodríguez-Padrón, A. Perosa, L. Longo, R. Luque and M. Selva, *ChemSusChem*, 2022, **15**, DOI: 10.1002/cssc.202200503.
- 242 J. M. Tukacs, R. V. Jones, F. Darvas, G. Dibó, G. Lezsák and L. T. Mika, *RSC Adv.*, 2013, **3**, 16283–16287.
- 243 B. Poznansky, S. E. Cleary, L. A. Thompson, H. A. Reeve and K. A. Vincent, *Front. in Chem. Eng.*, 2021, **3**, 1–11.
- 244 L. C. Wilkins, J. L. Howard, S. Burger, L. Frenzel-Beyme, D. L. Browne and R. L. Melen, *Adv. Synth. Catal.*, 2017, **359**, 2580–2584.
- 245 T. Glasnov, *Continuous-Flow Chemistry in the Research Laboratory: Modern Organic Chemistry in Dedicated Reactors at the Dawn of the 21st Century*, Springer, 2016.
- 246 I. Kovacs, R. V. Jones, K. Niesz, C. Csajagi, B. Borcsek, F. Darvas and L. Urge, *J. Lab. Autom.*, 2007, **12**, 284–290.

- 247 C. M. Alder, J. D. Hayler, R. K. Henderson, A. M. Redman, L. Shukla, L. E. Shuster and H. F. Sneddon, *Green Chem.*, 2016, **18**, 3879–3890.
- 248 A. Jordan, C. G. J. Hall, L. R. Thorp and H. F. Sneddon, *Chem. Rev.*, 2022, **122**, 6749–6794.
- 249 J. Qiu and J. Albrecht, *Org. Process Res. Dev.*, 2018, **22**, 829–835.
- 250 F. P. Byrne, S. Jin, G. Paggiola, T. H. M. Petchey, J. H. Clark, T. J. Farmer, A. J. Hunt, C. Robert McElroy and J. Sherwood, *Sustainable Chem. Processes*, 2016, **4**, 1–24.
- 251 G. F. Pauli, B. U. Jaki and D. C. Lankin, *J. Nat. Prod.*, 2005, **68**, 133–149.
- 252 D. J. Scott, M. J. Fuchter and A. E. Ashley, *Angew. Chem. Int. Ed.*, 2014, **53**, 10218–10222.
- 253 W. L. F. Armarego and C. L. L. Chai, *Purification of Laboratory Chemicals*, Elsevier, 2013.
- 254 A. Lazzarini, R. Colaiezzi, F. Gabriele and M. Crucianelli, *Materials*, 2021, **14**, 1–44.
- 255 C. G. Frost and L. Mutton, *Green Chem.*, 2010, **12**, 1687–1703.
- 256 R. Munirathinam, J. Huskens and W. Verboom, *Adv. Synth. Catal.*, 2015, **357**, 1093–1123.
- 257 Y. Ma, S. Zhang, C. R. Chang, Z. Q. Huang, J. C. Ho and Y. Qu, *Chem. Soc. Rev.*, 2018, **47**, 5541–5553.
- 258 J. Garcia-Sanchez and V. Baldovino-Medrano, *Ind. Eng. Chem. Res.*, 2023, **62**, 7769–7838.
- 259 J. Y. Xing, J. C. Buffet, N. H. Rees, P. Nørby and D. O’Hare, *Chem. Commun.*, 2016, **52**, 10478–10481.
- 260 M. Trunk, J. F. Teichert and A. Thomas, *J. Am. Chem. Soc.*, 2017, **139**, 3615–3618.
- 261 A. Willms, H. Schumacher, T. Tabassum, L. Qi, S. L. Scott, P. J. C. Hausoul and M. Rose, *ChemCatChem*, 2018, **10**, 1835–1843.
- 262 A. Willms, H. Schumacher, T. Tabassum, L. Qi, S. L. Scott, P. J. C. Hausoul and M. Rose, *ChemCatChem*, 2018, **10**, 1835–1843.
- 263 J. Ye and J. K. Johnson, *ACS Catal.*, 2015, **5**, 2921–2928.
- 264 J. Ye, B. Y. Yeh, R. A. Reynolds and J. K. Johnson, *Mol. Simul.*, 2017, **43**, 821–827.
- 265 B. Luo, R. Sang, L. Lin and L. Xu, *Catal. Sci. Technol.*, 2019, **9**, 65–69.
- 266 D. W. Stephan, *Chem.*, 2018, **4**, 2483–2485.
- 267 Z. Niu, W. D. C. Bhagya Gunatilleke, Q. Sun, P. C. Lan, J. Perman, J. G. Ma, Y. Cheng, B. Aguila and S. Ma, *Chem.*, 2018, **4**, 2587–2599.
- 268 M. Wang, F. Nudelman, R. R. Matthes and M. P. Shaver, *J. Am. Chem. Soc.*, 2017, **139**, 14232–14236.
- 269 Y. Ma, S. Zhang, C. R. Chang, Z. Q. Huang, J. C. Ho and Y. Qu, *Chem. Soc. Rev.*, 2018, **47**, 5541–5553.

- 270 M. Wang, M. Shanmugam, E. J. L. McInnes and M. P. Shaver, *J. Am. Chem. Soc.*, 2023, **145**, 24294–24301.
- 271 W. Y. Sung, M. H. Park, J. H. Park, M. Eo, M. S. Yu, Y. Do and M. H. Lee, *Polymer*, 2012, **53**, 1857–1863.
- 272 L. Chen, R. Liu and Q. Yan, *Angew. Chem. Int. Ed.*, 2018, **130**, 9480–9484.
- 273 B. Robert and B. Merrifield, *Angew. Chem. Int. Ed.*, 1985, **24**, 799–810.
- 274 R. Merrifield, *J. Am. Chem. Soc.*, 1963, **14**, 2149–2154.
- 275 F. Zaragoza and S. V. Petersen, *Tetrahedron*, 1996, **52**, 10823–10826.
- 276 V. V. Rostovtsev, L. G. Green, V. V. Fokin and K. B. Sharpless, *Angew. Chem. Int. Ed.*, 2002, **41**, 2596–2599.
- 277 C. W. Tornøe, C. Christensen and M. Meldal, *Am. J. Org. Chem.*, 2002, **67**, 3057–3064.
- 278 J. Tulla-Puche and F. Albericio, *The power of functional resins in organic synthesis*, John Wiley & Sons, 2008.
- 279 V. Castro, H. Rodríguez and F. Albericio, *ACS Comb. Sci.*, 2016, **18**, 1–14.
- 280 G. C. Tron, T. Pirali, R. A. Billington, P. L. Canonico, G. Sorba and A. A. Genazzani, *Med. Res. Rev.*, 2008, **28**, 278–308.
- 281 H. Kolb and B. Sharpless, *Drug Discov. Today*, 2003, **8**, 1128–1137.
- 282 H. C. Kolb, M. G. Finn and K. B. Sharpless, *Angew. Chem. Int. Ed.*, 2001, **40**, 2004–2021.
- 283 C. Rodríguez-Esrich and M. A. Pericàs, *Chem. Rec.*, 2019, **19**, 1872–1890.
- 284 Ž. Ban, Z. Karačić, S. Tomić, H. Amini, T. B. Marder and I. Piantanida, *Molecules*, 2021, **26**, 1–18.
- 285 J. Yoshino, S. Konishi, R. Kanno, N. Hayashi and H. Higuchi, *Eur. J. Org. Chem.*, 2019, **2019**, 6117–6121.
- 286 S. Arseniyadis, A. Wagner and C. Mioskowski, *Tetrahedron Lett.*, 2002, **43**, 9717–9719.
- 287 X. Creary, K. Chormanski, G. Peirats and C. Renneburg, *Am. J. Org. Chem.*, 2017, **82**, 5720–5730.
- 288 D. Lehnherr, J. M. Alzola, E. B. Lobkovsky and W. R. Dichtel, *Chem. Eur. J.* 2015, **21**, 18122–18127.
- 289 M. Kim, S. Im, C. H. Ryu, S. H. Lee, J. H. Hong and K. M. Lee, *Dalton Trans.*, 2021, **50**, 3207–3215.
- 290 N. K. Lee, S. Y. Yun, P. Mamidipalli, R. M. Salzman, D. Lee, T. Zhou and Y. Xia, *J. Am. Chem. Soc.*, 2014, **136**, 4363–4368.
- 291 R. A. Batey and T. D. Quach, *Tetrahedron Lett.*, 2001, **42**, 9099–9103.
- 292 G. L. Larson, *Synthesis*, 2018, **50**, 2433–2462.

- 293 S. López, F. Fernández-Trillo, L. Castedo and C. Saá, *Org. Lett.*, 2003, **5**, 3725–3728.
- 294 N. H. Evans, C. E. Gell and M. J. G. Peach, *Org. Biomol. Chem.*, 2016, **14**, 7972–7981.
- 295 G. A. Molander and J. Ham, *Org. Lett.*, 2006, **8**, 2767–2770.
- 296 T. Maki, K. Ishihara and H. Yamamoto, *Org. Lett.*, 2006, **8**, 1431–1434.
- 297 A. J. J. Lennox and G. C. Lloyd-Jones, *J. Am. Chem. Soc.*, 2012, **134**, 7431–7441.
- 298 R. Ting, C. W. Harwig, J. Lo, Y. Li, M. J. Adam, T. J. Ruth and D. M. Petrin, *Am. J. Org. Chem.*, 2008, **73**, 4662–4670.
- 299 G. Eaton, *J. Chem. Educ.*, 1969, **46**, 547.
- 300 F. Focante, P. Mercandelli, A. Sironi and L. Resconi, *Coord. Chem. Rev.*, 2006, **250**, 170–188.
- 301 S. Schwendemann, R. Fröhlich, G. Kehr and G. Erker, *Chem. Sci.*, 2011, **2**, 1842–1849.
- 302 X. Wang, G. Kehr, C. G. Daniliuc and G. Erker, *J. Am. Chem. Soc.*, 2014, **136**, 3293–3303.
- 303 J. Chen, R. A. Lalancette and F. Jäkle, *Chem. Eur. J.*, 2014, **20**, 9120–9129.
- 304 Y. L. Rao, T. Kusamoto, R. Sakamoto, H. Nishihara and S. Wang, *Organometallics*, 2014, **33**, 1787–1793.
- 305 S. Schraff, Y. Sun and F. Pammer, *J. Mater. Chem. C Mater.*, 2017, **5**, 1730–1741.
- 306 J. Merz, J. Fink, A. Friedrich, I. Krummenacher, H. H. Al Mamari, S. Lorenzen, M. Haehnel, A. Eichhorn, M. Moos, M. Holzapfel, H. Braunschweig, C. Lambert, A. Steffen, L. Ji and T. B. Marder, *Chem. Eur. J.*, 2017, **23**, 13164–13180.
- 307 T. Eicher, S. Hauptmann and A. Speicher, *The chemistry of heterocycles: structure, reactions, syntheses, and applications*, John Wiley & Sons, 2013.
- 308 R. J. Mayer, N. Hampel and A. R. Ofial, *Chem. Eur. J.*, 2021, **27**, 4070–4080.
- 309 A. Massey, *J. Organomet. Chem.*, 1966, **5**, 218–225.
- 310 A. D. Horton and J. De With, *Chem. Commun.*, 1996, **11**, 1375–1376.
- 311 A. D. Horton, J. De With, A. J. Van Der Linden and H. Van De Weg, *Organometallics*, 1996, **15**, 2672–2674.
- 312 D. B. G. Berry, I. Clegg, A. Codina, C. L. Lyall, J. P. Lowe and U. Hintermair, *React. Chem. Eng.*, 2022, **7**, 2009–2024.
- 313 T. Beringhelli, D. Donghi, D. Maggioni and G. D'Alfonso, *Coord. Chem. Rev.*, 2008, **252**, 2292–2313.
- 314 T. C. Johnstone, G. N. J. H. Wee and D. W. Stephan, *Angew. Chem. Int. Ed.*, 2018, **130**, 5983–5986.
- 315 Y. Zhao, D. Mandal, J. Guo, Y. Wu and D. W. Stephan, *Chem. Commun.*, 2021, **57**, 7758–7761.

- 316 S. N. Sluijter, L. J. Jongkind and C. J. Elsevier, *Eur. J. Inorg. Chem.*, 2015, **2015**, 2948–2955.
- 317 D. B. G. Williams and M. Lawton, *Am. J. Org. Chem.*, 2010, **75**, 8351–8354.
- 318 A. Torelli, A. Whyte, I. Polishchuk, J. Bajohr and M. Lautens, *Org. Lett.*, 2020, **22**, 7915–7919.
- 319 T. Mita, J. Chen, M. Sugawara and Y. Sato, *Angew. Chem. Int. Ed.*, 2011, **50**, 1393–1396.
- 320 P. V. Kattamuri, J. Yin, S. Siriwongsup, D. H. Kwon, D. H. Ess, Q. Li, G. Li, M. Yousufuddin, P. F. Richardson, S. C. Sutton and L. Kürti, *J. Am. Chem. Soc.*, 2017, **139**, 11184–11196.
- 321 T. J. Barker and E. R. Jarvo, *Angew. Chem. Int. Ed.*, 2011, **50**, 8325–8328.
- 322 S. Hussain, F. Leipold, H. Man, E. Wells, S. P. France, K. R. Mulholland, G. Grogan and N. J. Turner, *ChemCatChem*, 2015, **7**, 579–583.
- 323 T. Mitsudome, Y. Yamamoto, A. Noujima, T. Mizugaki, K. Jitsukawa and K. Kaneda, *Chem. Eur. J.*, 2013, **19**, 14398–14402.
- 324 C. Wang, K. Huang, J. Wang, H. Wang, L. Liu, W. Chang and J. Li, *Adv. Synth. Catal.*, 2015, **357**, 2795–2802.
- 325 Y. Zhang, F. Lu, H. Y. Zhang and J. Zhao, *Catal. Letters*, 2017, **147**, 20–28.
- 326 M. Rui, G. Rossino, S. Coniglio, S. Monteleone, A. Scuteri, A. Malacrida, D. Rossi, L. Catenacci, M. Sorrenti, M. Paolillo, D. Curti, L. Venturini, D. Schepmann, B. Wünsch, K. R. Liedl, G. CavaLett.i, V. Pace, E. Urban and S. Collina, *Eur. J. Med. Chem.*, 2018, **158**, 353–370.
- 327 J. A. Murphy, A. G. J. Commeureuc, T. N. Snaddon, T. M. McGuire, T. A. Khan, K. Hisler, M. L. Dewis and R. Carling, *Org. Lett.*, 2005, **7**, 1427–1429.
- 328 X. Zhang and D. W. C. MacMillan, *J. Am. Chem. Soc.*, 2017, **139**, 11353–11356.
- 329 L. Huan and C. Zhu, *Org. Chem. Front.*, 2016, **3**, 1467–1471.
- 330 M. De Lourdes G. Ferreira, L. C. S. Pinheiro, O. A. Santos-Filho, M. D. S. Peçanha, C. Q. Sacramento, V. Machado, V. F. Ferreira, T. M. L. Souza and N. Boechat, *Med. Chem. Res.*, 2014, **23**, 1501–1511.
- 331 D. Wang, N. Li, M. Zhao, W. Shi, C. Ma and B. Chen, *Green Chem.*, 2010, **12**, 2120–2123.
- 332 E. A. Mitchell, A. Peschiulli, N. Lefevre, L. Meerpoel and B. U. W. Maes, *Chem. Eur. J.*, 2012, **18**, 10092–10142.
- 333 J. R. Lewis, *Nat. Prod. Rep.*, 2001, **18**, 95–128.
- 334 X. Fang and C. J. Wang, *Org. Biomol. Chem.*, 2018, **16**, 2591–2601.
- 335 D. P. Affron and J. A. Bull, *Eur. J. Org. Chem.*, 2016, **2016**, 139–149.
- 336 A. Nadin, C. Hattotuagama and I. Churcher, *Angew. Chem. Int. Ed.*, 2012, **51**, 1114–1122.

- 337 J. B. Sweeney, J. Doucet and B. Thapa, *iScience*, 2018, **9**, 328–336.
- 338 H. Yamamoto et al., US 2011/0245223 A1, 2011.
- 339 M. P. Seller, J. Nozulak, US 7012085 B2, 2006.
- 340 Q. Lang, G. Gu, Y. Cheng, Q. Yin and X. Zhang, *ACS Catal.*, 2018, **8**, 4824–4828.
- 341 R. Shintani, W. L. Duan, T. Nagano, A. Okada and T. Hayashi, *Angew. Chem. Int. Ed.*, 2005, **44**, 4611–4614.
- 342 B. Su, M. Deng and Q. Wang, *Adv. Synth. Catal.*, 2014, **356**, 977–981.
- 343 O. Takae and S. Haruyo, JP2001278857A, 2001, 1–4.

Appendices

Appendix A Palladium-catalysed Hydro arylation for the Synthesis of 3-aryl Pyrrolidines

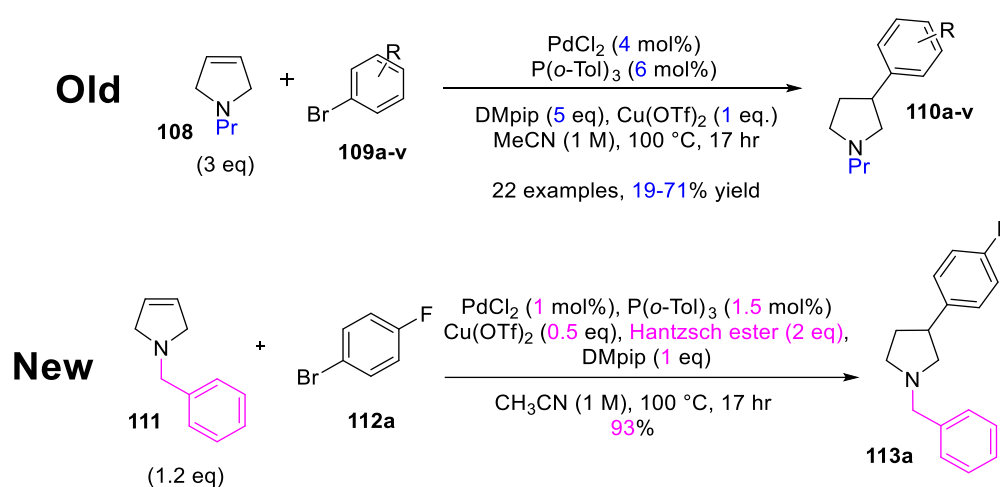
A.1 Introduction and Previous Work

Saturated cyclic amines are important structural motifs in natural products, with the most prominent being 5- and 6-membered systems.³³² Saturated heterocycles; nitrogen-containing rings are crucial components across a range of biologically active compounds featuring greatly in pharmaceuticals.³³³ Pyrrolidines in particular have inspired extensive studies as an important template in drug discovery.³³⁴

More recently, the use of pyrrolidines in medicinal chemistry has led to calls for increased saturation and more 3-dimensional characteristics in drug-like compounds.³³⁵ These chiral pyrrolidines play a crucial role as both building blocks for auxiliaries as well as key structures in biologically active substances and it is proposed that the increased fraction of sp³ centres will afford more successful drug candidates.³³⁶ As part of my Masters by research project, I set out to further optimise a reductive Heck system, previously developed by Doulcet *et al.* My goals were to improve yields, lower catalytic loading and create a library of novel 3-substituted pyrrolidines with scope for further molecular diversity.

Work by Doulcet *et al.* developed a reductive Heck system, to produce a range of 3-arylated *N*-propyl pyrrolidines and importantly this method was shown to apply to *N*-benzyl pyrrolines (Scheme 77).³³⁷ This work used a large excess (3 eq) of the *N*-propyl/*N*-benzyl pyrroline starting materials to act as a sacrificial hydride source. It was then proposed that the use of an external hydride source, as previously mentioned, should allow for the reduction of excess 3-pyrroline (**108**) and could provide significant improvement in the reaction. Upon screening a select number of known reductive Heck hydride sources, it was determined that the most successful hydride source was

Hantzsch ester. During the my Masters by research project I studied the system to create a new set of optimised conditions providing **113a** in excellent yield (Scheme 77), while reducing the waste generated (low Pd loading, sub stoichiometric amounts of copper additive, and a lower excess of pyrroline) and making the reaction more economically viable. The best-optimised conditions for this reductive Heck system were then progressed into the next stages of the project for the screening of aryl bromides. The movement away from the propyl-protecting group to the benzyl also provided easy access to the deprotected *N*-H pyrrolidine analogues through facile deprotection via hydrogenation.



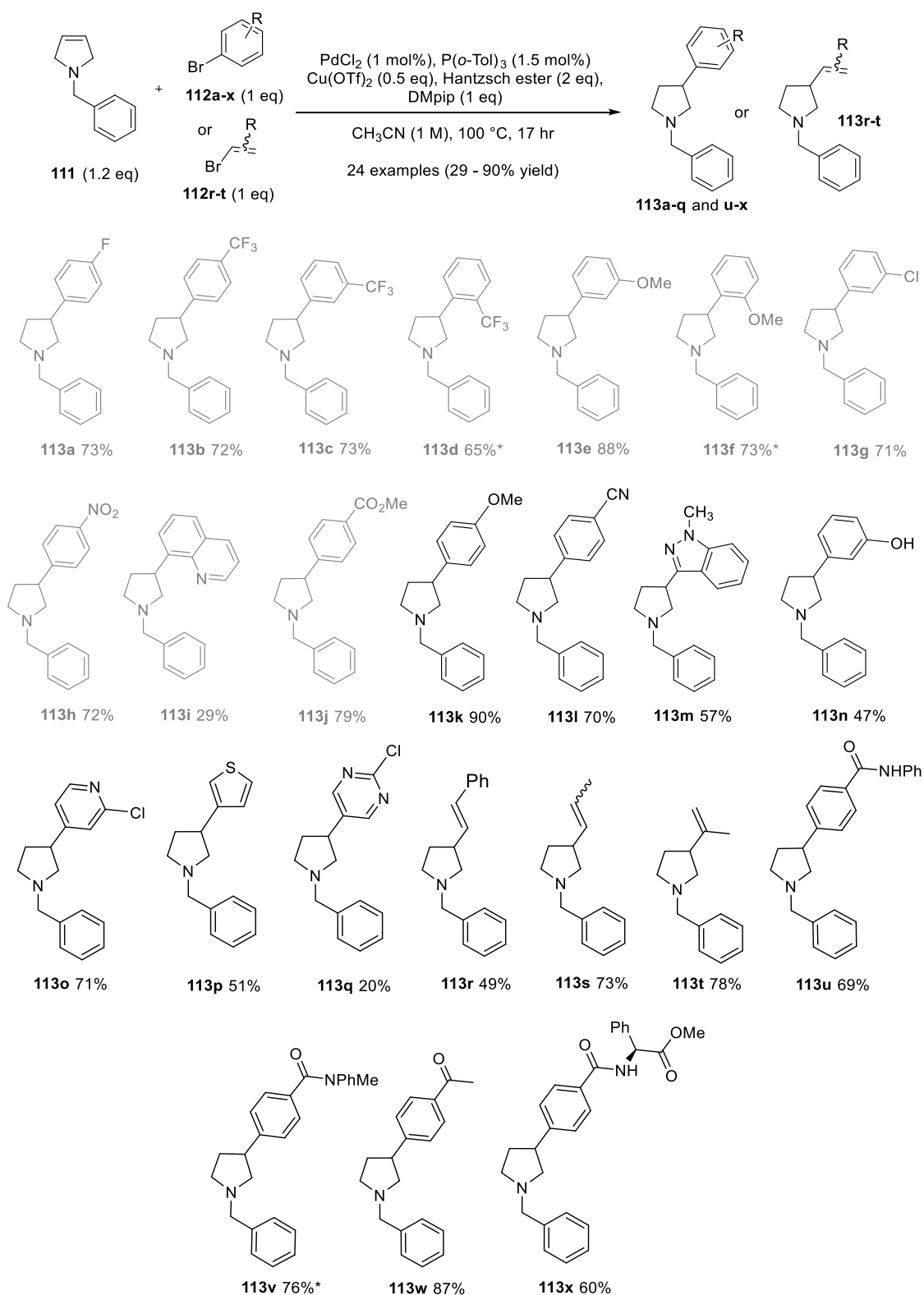
Scheme 77. **Old.** Optimised conditions from Sweeney group paper to make 3-substituted propyl pyrrolidines and **New.** Optimised conditions from the previous project using an external hydride source and yield determined by ^{19}F NMR spectroscopic analysis.³³⁷

A.2 Results and Discussion

A.2.2 Substrate Scope Expansion

Only 10 compounds were initially screened (in my masters), as shown in grey (Scheme 78), this has now been expanded, adding 14 extra novel compounds to the library. The scope of the reaction was first assessed by exploring the electronic and steric effects of substituents on aryl bromide starting materials. For this ortho, meta and para bromobenzotrifluoride and bromoanisole were reacted with *N*-benzyl pyrroline (**111**). Ortho-substituents and strong electronically donating groups were thought to have the

worst yield, as theoretically they would hinder/slow the oxidative addition. The synthesis of compounds (**113b-f** and **k**) showed that electronic effects had little influence on the reaction outcome whether the aryl bromide was substituted with either an electron-withdrawing or donating group, obtaining good to excellent isolated yields (65 – 90%). Although ortho methoxy and trifluoromethyl **113d** and **f** could not be isolated purely, their determined NMR spectroscopic yields (65% and 73% respectively) demonstrate the compatibility of sterically hindered ortho-substituted aryl-bromides, although as expected, these are slightly less successful than their meta and para-analogues. The screening sample of chemical functionalities showed overall very good compatibility with ether, nitro, nitrile, ester, amide and halide functional groups **113a-h** and **j** (60 – 90% yield). Unfortunately, the quinoline and 2-chloro pyrimidine substituted products, **113i** and **q** were isolated in poor yield (29% and 20% respectively), which would be expected to suffer from chelation of the nitrogen to the palladium catalyst as well as, for the quinoline, some steric hindrance. Similarly following in this trend of available heteroatom chelation hindering successful conversion are the isolated yields of indazole, furan and alcohol-substituted products, **113m**, **p** and **n**, which were obtained in moderate yields (47 – 57% yield). We were extremely gratified to find that our system applied to alkenyl bromides **112r-t**. This opens a completely new avenue for molecular diversification in future library synthesis. We were also pleased to see that the alkenyl-substituted products also progressed with moderate to good yields (49 – 78%).



Scheme 78. Screening of (hetero)aryl and alkenyl bromides showing isolated yield after purification (Previously screened compounds (grey), newly synthesised compounds (black)).

A.2.3 Application to Drug Compound Synthesis

HSD-1 inhibitor (**114**)³³⁸ (Figure 61). The α -adrenoceptor antagonist **115**, developed by Novartis in 2006³³⁹, was synthesised as a racemic mixture and without a specified enantiomer given for the drug. However, as enantiopure compounds have since been synthesised^{340,341}, work to make our reaction asymmetric, or to separate the two enantiomers is a target for future study. Nevertheless, we devised a plausible synthetic route (Scheme 79) which currently has led to the synthesis of the 3-pyrroline drug compound intermediate **120**.^{342,343} This drug intermediate pyrroline (**120**) when reacted with *ortho*-bromoanisole in our optimised reductive Heck system did not successfully produce the α -2-adrenoceptor antagonist drug (Scheme 80). Rather than being incorporated into the pyrroline synthesis this drug compound will be accessible via reductive amination using the respective aldehyde and 3-substituted pyrrolidine **113f** after benzyl deprotection.

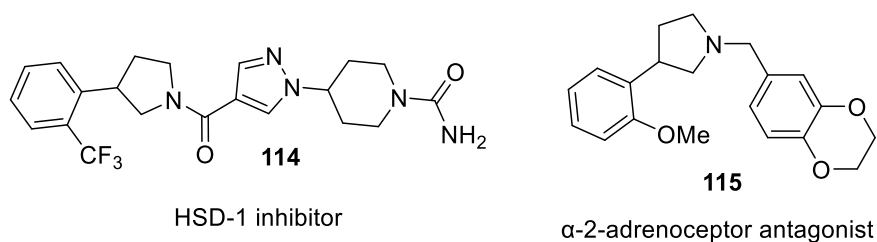
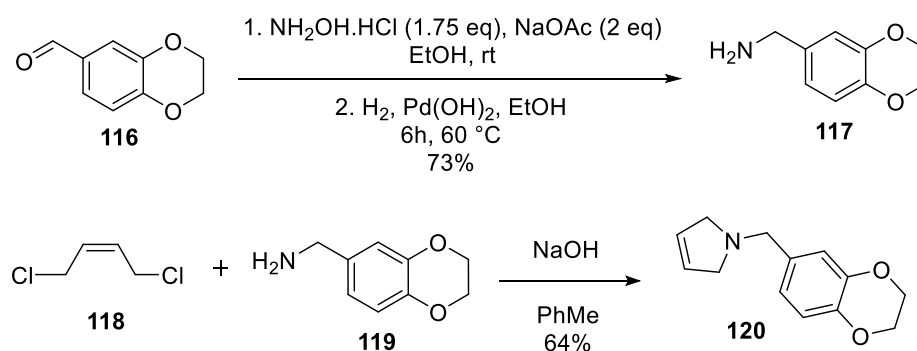
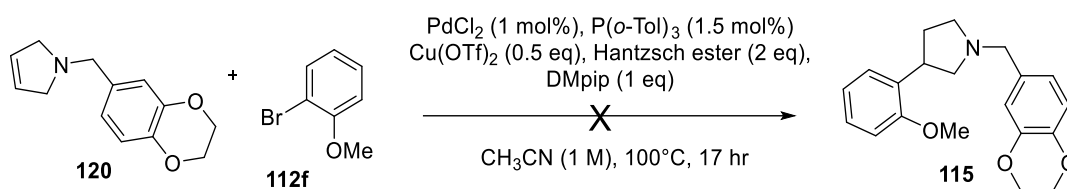


Figure 61. Biologically active compounds, which are synthetically attainable through this project.³³⁸⁻³⁴¹



Scheme 79. Synthetic route to produce the α -2-adrenoceptor antagonist pyrroline intermediate.^{342,343}



*Scheme 80. Application of drug compound intermediate **120** in our optimised reductive Heck system to produce biologically active α -2-adrenoceptor antagonist (**115**).*

A.3 Outlook and Conclusion

In conclusion, the project has successfully taken an established set of optimised conditions for the reductive Heck reaction of *N*-benzyl pyrrolidine with (hetero)aryl bromides. The substrate scope has been significantly expanded to provide a small library of racemic chiral pyrrolidines (from 10 to 24 examples with good to excellent yields of 65 – 90%, 5 examples with moderate yields of 49 – 60%, and 2 examples with poor yield 20% and 29%). Importantly the substrate scope has been expanded to include alkenyl bromides, with the potential for diverse expansion in future work.

This project has also provided potential synthetic routes to two biologically active drug compounds. Unfortunately, whilst the incorporation of the drug intermediates into our pyrrolidine synthesis was not successful in our system, both drug compounds are still accessible by reductive amination using the respective analogues after benzyl deprotection.

Our findings have raised additional questions that would be of extreme interest for future studies. It is important to examine the roles of the Hantzsch ester and Cu(OTf)₂ in the reaction mechanism. This project has been subject to successful further work within the group, resulting in the preparation of a manuscript for submission. The additional work that has been done has answered many of the questions I had about the reaction mechanism. The work presented here has laid the foundations for further research and expansion of the substrate scope in several areas for the group to continue their projects.

Appendix B C-C Bond Formation by Dual Pyrrolidine and Nickel Catalysis: Allylation of Ketones by Allylic Alcohols

At the time of writing, our communication manuscript has been accepted to *Advanced Synthesis & Catalysis*. It is reproduced here without modification from the submitted manuscript.

DOI: 10.1002/adsc.202((will be filled in by the editorial staff))

C-C Bond Formation by Dual Pyrrolidine and Nickel Catalysis: Allylation of Ketones by Allylic Alcohols

Noah Wright,^a Bara Townsend,^a Steven Nicholson,^a Joshua Robinson,^a Geoffrey Akien,^a Anthony K. Ball,^a Joseph B. Sweeney^{b*} and Julien Doulcet^{a*}

^a Department of Chemistry, Lancaster University, Lancaster, LA1 4YB, United Kingdom

E-mail: j.doucet@lancaster.ac.uk

^b Faculty Hub, Chadwick Building, University of Liverpool, Liverpool L69 7ZL, United Kingdom

E-mail: j.sweeney2@liverpool.ac.uk

Received: ((will be filled in by the editorial staff))

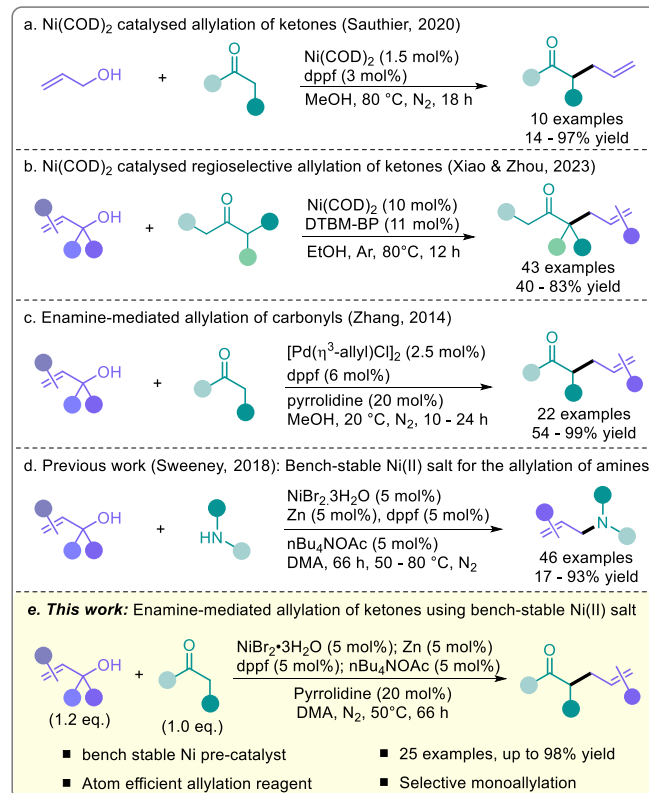
Abstract. Whilst catalytic ketone allylation using palladium(0) is well-precedented, nickel(0)-catalysed equivalents of such reactions remain scarce. We report here the first nickel-catalysed allylation of ketones which uses an easily handled and inexpensive bench-stable Ni(II) pre-catalyst. This method avoids generation of stoichiometric by-products via the use of readily available allyl alcohols, rather than the esters or related derivatives which are often used in such transformations. Under the optimised conditions, 25 monoallylated ketones were obtained with yields up to 98% and with high selectivity for the linear (*E*)-isomers.

Keywords: Allylation; C-C coupling; Ketone; Nickel; Sustainable catalysis

The use of metal catalysts in carbon-carbon bond-forming reactions is an indispensable modern paradigm, and within this broad and widely used class of reaction, allyl transfer processes occupy a special place, as the first reported examples of practical methodology.^[1] Though palladium catalysis has traditionally dominated the area, a diverse range of metal catalysts are now powerful effectors for catalytic allylation processes.^[2] Alongside methodical variation in the metallic component of catalytic allylations, broadening of the chemical nature of the allyl donors has also received much attention: traditionally, allylic halides, esters and carbonates were used in the reactions, but several non-activated allyl donors have now been shown to be highly effective in metal-catalysed allylation reactions.^[3] In particular, allyl alcohols have received increasing interest^[4] since their use in allylation reactions would generate water as the sole by-product, lowering the costs and environmental burden caused by the creation of stoichiometric amounts of waste in the case of other allyl donors.^[5]

In addition to the use of simpler reagents and ‘cleaner’ processes for catalytic allylation, the nature of the metal catalysts used has also been of considerable recent interest, especially from the

perspective of sustainability and Earth-abundance. An example of this focus is the replacement of palladium by nickel^[6] in catalytic C-C bond-forming transformations, which is considered desirable and advantageous due both to the economic advantages in using nickel, and the inherent chemical differences in character of nickel(0), which facilitates novel opportunities for catalytic bond-formation via chemical processes not available to less Earth-abundant, and economically less sustainable metals.^[7] Weighing against these advantages, the major



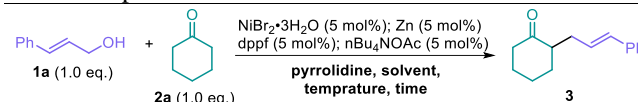
Scheme 1. Allyl alcohol donors in catalytic allylation strategies.

disadvantage of the use of nickel in catalytic manifolds as an alternative to palladium is the relative

complication in accessing and handling nickel(0) complexes: the most widely used catalytic nickel complex, Ni(COD)₂, is air-sensitive, demanding special handling protocols (most often by use of a glove-box), which still limits the appeal and applicability of Ni(0)-catalysed processes. There has, therefore, been intense interest in the development and use of alternatives to Ni-COD complexes, and several elegant Ni(0) pre-catalyst systems aiming to address this challenge have been developed.^[8] Main group metals (typically Zn^[9] or Mn^[10]) have been used *in situ*, as reducing agents, to convert Ni(II) into catalytically active Ni(0) complexes, most often using super-stoichiometric amounts of the reductant. As an adjunct to other reported methods, we have previously disclosed a novel 'totally catalytic' combination, and have demonstrated the method's utility in both C-allylation and N-allylation using allyl alcohols, on gram-scale, to deliver industrially and biologically relevant products (Scheme 1d).^[11]

The use of nickel catalysis for ketone allylation is scarcely reported in the literature and has relied exclusively on the use of air-sensitive Ni(COD)₂ (Scheme 1a & 1b),^[12] and so, we sought to develop a method using our totally catalytic nickel system to enable such a transformation. Enamine nucleophiles have been shown to be very effective in promoting allylic alkylation reactions (e.g. Scheme 1c),^[13] so we envisaged a dual enamine-Ni(0) catalytic protocol, anticipating allylation of ketones by allyl alcohols in the presence of a secondary amine co-catalyst. We report here the successful realisation of our ambition, and describe the first method which uses a bench-stable Ni(II) pre-catalyst to effectively promote the allylation of ketones using allyl alcohols (Scheme 1e).

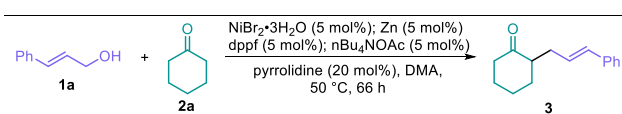
Starting with pyrrolidine as an exemplar amine co-catalyst, our studies began with a screening of ligands and solvents under various stoichiometries using the standard Ni(0) conditions we previously reported (Table 1). Our first results (Table 1, entry 1-3), indicated that the totally catalytic system was suitable for the allylation of cyclohexanone (**2a**) with compound **3** obtained in good yield; we were particularly pleased to observe that there was no sign of the potential and competing *N*-allylation process^[11b] and *N*-cinnamyl pyrrolidine was not observed in the crude product mixture. With regard to ligand choice, dppb was unsatisfactory (Table 1, entry 7), and whilst solvent variation (Table 1, entries 8 – 13) was ineffective, change in pyrrolidine stoichiometry (Table 1, entry 15) improved the process, delivering **3** in 93% yield; the latter observation supports the assumption that an enamine intermediate was involved in the process (see also SI, scheme S3). Alternatives to pyrrolidine were not productive (e.g., Table 1, entry 18), with **3** obtained in low yield, and high yields of *N*-allylation observed (92%). A range of control reactions (Table 1, entries 19 – 23) clearly demonstrated that all components of the catalytic system are required for the reaction to proceed effectively.

Table 1. Optimisation of reaction conditions


Entry	Ligand	Solvent	Pyrrolidine (mol%)	Temp /°C	Time (h)	3 yield [%] ^[a]
1	dppf	DMA	20	50	18	38
2	dppf	DMA	20	50	48	53
3	dppf	DMA	20	50	66	76
4	dppf	DMA	20	80	18	50
5	dppf	DMA	20	80	48	77
6	dppf	DMA	20	25	18	14
7	dppb	DMA	20	50	66	0
8	dppf	DMF	20	50	66	75
9	dppf	MeOH	20	50	66	0
10	dppf	THF	20	50	66	6
11	dppf	DCE	20	50	66	17
12	dppf	Toluene	20	50	66	16
13	dppf	NMP	20	50	66	57
14	dppf	DMA	10	50	66	58
15	dppf	DMA	40	50	66	93
16	dppf	DMA	20	50	66	15 ^[b]
17	dppf	DMA	20	50	66	0 ^[c]
18	dppf	DMA	20	50	66	7 ^[d]
19	dppf	DMA	0	50	66	0
20	dppf	DMA	20	50	66	21 ^[e]
21	dppf	DMA	20	50	66	0 ^[f]
22	dppf	DMA	20	50	66	0 ^[g]
23	-	DMA	20	50	66	0

[a] Determined from ¹H NMR. [b] Using Ni(OAc)₂·4H₂O (0.05 mmol). [c] Using Ni(OH)₂ (0.05 mmol). [d] Using morpholine (20 mol%) instead of pyrrolidine. [e] Without nBu₄NOAc. [f] Reaction without NiBr₂·3H₂O. [g] Reaction without zinc.

Considering the multiple sites for allylation present in the substrate ketone, and potential allylation of the amine co-catalyst, we next examined variation in reagent stoichiometry. We were subsequently pleased to observe that using only a slight deviation from 1:1 stoichiometry was necessary for maximum yield (Table 2, entry 6); it is noteworthy that even with high loadings of either allyl donor (entry 1) or ketone (entry 11), acceptable yields of monoallylated product were still obtained.

Table 2. Optimisation of stoichiometry


Entry	1a (mmol)	2a (mmol)	3 yield [%] ^[a]
1	5	1	73
2	4	1	96
3	3	1	93
4	2	1	99
5	1.5	1	95
6	1.2	1	93 (93^[b])
7	1	1	76 (75 ^[b])
8	1	2	82
9	1	3	81
10	1	4	80
11	1	5	84

[a] Determined from ¹H NMR. [b] Isolated yield.

A range of ketones gave allylated products **15-25** (Table 3, entries 14 – 24); notably allylation of indanone required elevated temperature (80 °C) (likely due to increased steric bulk at C–2), and 2-substituted cyclopentanones and cyclohexanones reacted sluggishly even at elevated temperatures (see SI, Scheme S2), in agreement with the previously reported reactions of this ketone class.^[13c] Diketone **2i** provided product **22** in moderate yield due to competitive diallylation. Moving away from 5- or 6-membered rings proved more difficult, cycloheptanone **2k** gave product **24** in low 16% yield and cyclobutanone was unreactive. Finally, acetone (**2l**) was successfully reacted, albeit providing product **25** in only 20% yield, while other acyclic ketones like acetophenone were found to be unreactive (even as the performed enamine, see SI, scheme S4).

Table 4. Robustness screening.

Entry	Additive	Yield of 3 (%) ^[a]	Additive remaining (%) ^[a]	1a remaining (%) ^[a]
1	None	97	-	13
2 ^[b]		8	ND ^[c]	ND
3		22	ND ^[c]	60
4		8	100	78
5		38	100	48
6		21	94	59
7		59	100	30
8		51	83	40
9		25	81 ^[d]	61
10	H ₂ O	42	-	31

[a] Determined from ¹H NMR using mesitylene as a standard. [b] 10 mol% additive used. [c] Could not be clearly identified in ¹H NMR. [d] Broad signals in ¹H NMR attributed to pyridine.

Robustness screening, popularised by Glorius in the past decade,^[14] has proven to be an effective way to further demonstrate the scope of a reaction without requiring the synthesis of complex starting materials, and a recent report by Nelson *et al.*^[15] on Ni-catalysed Suzuki-Miyaura cross-coupling reactions disclosed that many functional groups can poison the Ni(0) catalyst. Some of the results obtained during the reagent screening (such as the lack of reaction using 4-chlorocinnamyl alcohol or acetophenone, SI scheme S1 & S2) induced us to verify whether the

trends previously observed by Nelson would apply to our catalytic system (Table 4). Aryl chlorides were found to inhibit the reaction strongly (Table 4, entries 2 and 3) providing an explanation for the lack of reactivity of 4-chlorocinnamyl alcohol previously observed. In a similar reactivity pattern to that observed by Nelson, we found that both amines and carbonyl containing compounds (Table 4, entries 4-9) also inhibited the reaction strongly; it is notable that acetophenone (Table 4, entry 4), which did not react with cinnamyl alcohol (SI, scheme S2) was one of the strongest inhibitors for the reaction. Finally, the addition of one equivalent of water affected the reaction adversely (Table 4, entry 10), suggesting that use of anhydrous solvent is preferable.

In summary, we have described a practical, scalable method for executing nickel-catalysed α -allylation of ketones using readily available, inexpensive catalysts and reagents. The use of allyl alcohols as substrates, and a bench-stable Ni(II) salt as a pre-catalyst offers significant practical advantages. The scope of the reaction has been established by screening several allyl alcohols (> 20) and carbonyls (> 20) as well as performing a robustness screening. The substrate screening confirmed reactivity trends observed in other allylation reports using allyl alcohols^[13b-c] and the robustness screening highlighted that Ni(0) poisoning, which was previously observed for Ni(0) catalysed Suzuki-Miyaura cross-coupling reactions,^[15] affect our catalytic system in this allylation reaction too.

Experimental Section

General procedure for the Ni-catalysed allylation of ketones: To an oven-dried 10-mL crimp cap vial flushed with nitrogen were added sequentially NiBr₂·3H₂O (14 mg, 0.05 mmol, 0.05 eq.), Zn powder (3.2 mg, 0.05 mmol, 0.05 eq.), dppf (28 mg, 0.05 mmol, 0.05 eq.) and ⁿBu₄NOAc (15 mg, 0.05 mmol, 0.05 eq.). The vial was then sealed and further flushed with nitrogen. Anhydrous DMA (2.0 mL) was then added to the reaction vial and the resulting stirring suspension was sparged with nitrogen at room temperature for 15 minutes. To the resulting solution, alcohol **1** (1.2 mmol, 1.2 eq.), ketone **2** (1 mmol, 1 eq.) and pyrrolidine (16.5 μ L, 0.2 mmol, 0.2 eq.) were added sequentially. The reaction mixture was then stirred at 50 °C for 66 hours unless otherwise stated. After 66 hours, the reaction vessel was cooled to room temperature before diluting the reaction mixture with DCM (20 mL). The resulting mixture was washed with saturated sodium bicarbonate solution (20 mL) and the aqueous layer was further extracted with DCM (2 x 20 mL). The combined organic layers were dried with MgSO₄, filtered and evaporated under reduced pressure. The product was purified by flash silica gel column chromatography (heptane 100% to 95:5 to 9:1 heptane:EtOAc, v/v), unless otherwise stated.

Acknowledgements

We thank Lancaster University for funding.

References

- [1] (a) J. Tsuji, H. Takahashi, A. Morikawa, *Tetrahedron Lett.* **1965**, 6, 4387. (b) B. M. Trost, T. J. Fullerton, *J. Am. Chem. Soc.* **1973**, 95, 292. (c) B.M. Trost, D. L. Van Vranken, *Chem. Rev.* **1996**, 96, 395. (d) B. M. Trost, M. L. Crawley, *Chem. Rev.* **2003**, 103, 2921. (e) J. Tsuji, *Palladium Reagents Catalysts: New Perspectives for the 21st Century*, Wiley, **2004**.
- [2] (a) Z. Lu, S. Ma, *Angew. Chem. Int. Ed.* **2008**, 47, 258. (b) J. D. Weaver, A. Recio, A. J. Grenning, J. A. Tunge, *Chem. Rev.* **2011**, 111, 1846. (c) N. Kumar Mishra, S. Sharma, J. Park, S. Han, I. S. Kim, *ACS Catal.* **2017**, 7, 2821. (d) Q. Cheng, H.-F. Tu, C. Zheng, J.-P. Qu, G. Helmchen, S.-L. You, *Chem. Rev.* **2019**, 119, 1855. (e) O. Pàmies, J. Margalef, S. Cañellas, J. James, E. Judge, P. J. Guiry, C. Moberg, J.-E. Bäckvall, A. Pfaltz, M. A. Pericàs, M. Diéguez, *Chem. Rev.* **2021**, 121, 4373. (f) L. Süsse, B.M. Stoltz, *Chem. Rev.* **2021**, 121, 4084. (g) M. Pareek, R.B. Sunoj, *Chem. Sci.* **2021**, 12, 2527. (h) R. Shibuya, L. Lin, Y. Nakahara, K. Mashima, T. Ohshima, *Angew. Chem. Int. Ed.* **2014**, 53, 4377. (i) A. Béthegnies, A. Saint Pol, B. Mouhsine, C. Dumont, M. Sauthier, *Molecular Catalysis* **2024**, 556, 113909.
- [3] N. A. Butt, W. Zhang, *Chem. Soc. Rev.* **2015**, 44, 7929.
- [4] B. Sundararaju, M. Achard, C. Bruneau, *Chem. Soc. Rev.* **2012**, 41, 4467.
- [5] (a) D. J. C. Constable, P. J. Dunn, J. D. Hayler, G. R. Humphrey, J. L. Leazer Jr, R. J. Linderman, K. Lorenz, J. Manley, B. A. Pearlman, A. Wells, A. Zaks, T. Y. Zhang, *Green Chem.* **2007**, 9, 411. (b) S. Bhattacharya, B. Basu, *Physical Sciences Reviews*, **2023**, 8, 4527.
- [6] V. P. Ananikov, *ACS Catal.* **2015**, 5, 1964.
- [7] A. Y. Chan, I. B. Perry, N. B. Bissonnette, B. F. Buksh, G. A. Edwards, L. I. Frye, O. L. Garry, M. N. Lavagnino, B. X. Li, Y. Liang, E. Mao, A. Millet, J. V. Oakley, N. L. Reed, H. A. Sakai, C. P. Seath, D. W. C. MacMillan, *Chem. Rev.* **2022**, 122, 1485.
- [8] (a) R. A. Kelly, N. M. Scott, S. Díez-González, E. D. Stevens, S. P. Nolan, *Organometallics* **2005**, 24, 3442. (b) C. Chen, L. – M. Yang, *J. Org. Chem.* **2007**, 72, 6324. (c) S. Ge, J. F. Hartwig, *Angew. Chem. Int. Ed.* **2012**, 51, 12837. (d) E. A. Standley, T. F. Jamison, *J. Am. Chem. Soc.* **2013**, 135, 1585. (e) E. A. Standley, S. J. Smith, P. Müller, T. F. Jamison, *Organometallics* **2014**, 33, 2012. (f) N. H. Park, G. Teverovskiy, S. L. Buchwald, *Org. Lett.* **2014**, 16, 220. (g) R. L. Jezorek, N. Zhang, P. Leowanawat, M. H. Bunner, N. Gutsche, A. K. R. Pesti, J. T. Olsen, V. Percec, *Org. Lett.* **2014**, 16, 6326. (h) J. Magano, S. Monfette, *ACS Catal.* **2015**, 5, 3120. (i) J. D. Shields, E. E.; Gray, A. G.; Doyle, *Org. Lett.* **2015**, 17, 2166. (j) L. Nattmann, J. Cornella, *Organometallics* **2020**, 39, 3295. (k) V. T. Tran, Z. Q. Li, O. Apolinar, J. Derosa, M. V. Joannou, S. R. Wisniewski, M. D. Eastgate, K. M. Engle, *Angew. Chem. Int. Ed.* **2020**, 59, 7409.
- [9] For a recent example see: J. An, X. Zhou, Y. Zhang, Z. Ye, Q. Guo, H. Song, Z. Song, X.-Y. Liu, Y. Qin, *Org. Chem. Front.*, **2023**, 10, 1897.
- [10] For a recent example see: L. Su, G. Ma, Y. Song, H. Gong, *Org. Lett.* **2021**, 23, 2493–2497.
- [11] (a) J. B. Sweeney, A. K. Ball, L. J. Smith, *Chem. Eur. J.* **2018**, 24, 7354. (b) J. B. Sweeney, A. K. Ball, P. A. Lawrence, M. C. Sinclair, L. J. Smith, *Angew. Chem. Int. Ed.* **2018**, 57, 10202.
- [12] (a) B. Mouhsine, A. Karim, C. Dumont, M. Sauthier, *Green Chem.* **2020**, 22, 950. (b) M.-M. Li, T. Zhang, L. Cheng, W.-G. Xiao, J.-T. Ma, L.-J. Xiao, Q.-L. Zhou, *Nat Commun* **2023**, 14, 3326.
- [13] (a) N.A. Butt, G. Yang, W. Zhang, *Chem. Rec.* **2016**, 16, 2687. (b) X. Huo, G. Yang, D. Liu, Y. Liu, I. D. Gridnev, W. Zhang, *Angew. Chem. Int. Ed.* **2014**, 53, 6776. (c) I. Usui, S. Schmidt, B. Breit, *Org. Lett.* **2009**, 11, 1453.
- [14] K. D. Collins, F. Glorius, *Nature Chem.* **2013**, 5, 597.
- [15] (a) A. K. Cooper, D. K. Leonard, S. Bajo, P. M. Burton, D. J. Nelson, *Chem. Sci.* **2020**, 11, 1905. (b) A. K. Cooper, P. M. Burton, D. J. Nelson, *Synthesis* **2020**, 52, 565.